VOL. 667 NOS. 1 + 2 APRIL 29, 1994
COMPLETE IN ONE ISSUE

JOURNAL OF CHROMATOGRAPHY A

INCLUDING ELECTROPHORESIS AND OTHER SEPARATION METHODS

ELSEVIER

JOURNAL OF CHROMATOGRAPHY A

INCLUDING ELECTROPHORESIS AND OTHER SEPARATION METHODS

Scope. The *Journal of Chromatography A* publishes papers on all aspects of **chromatography, electrophoresis** and related methods. Contributions consist mainly of research papers dealing with chromatographic theory, instrumental developments and their applications. In the *Symposium volumes*, which are under separate editorship, proceedings of symposia on chromatography, electrophoresis and related methods are published. *Journal of Chromatography B: Biomedical Applications* —This journal, which is under separate editorship, deals with the following aspects: developments in and applications of chromatographic and electrophoretic techniques related to clinical diagnosis or alterations during medical treatment; screening and profiling of body fluids or tissues related to the analysis of active substances and to metabolic disorders; drug level monitoring and pharmacokinetic studies; clinical toxicology; forensic medicine; veterinary medicine; occupational medicine; results from basic medical research with direct consequences in clinical practice.

Submission of Papers. The preferred medium of submission is on disk with accompanying manuscript (see *Electronic manuscripts* in the Instructions to Authors, which can be obtained from the publisher, Elsevier Science B.V., P.O. Box 330, 1000 AH Amsterdam, Netherlands). Manuscripts (in English; *four* copies are required) should be submitted to: Editorial Office of *Journal of Chromatography A*, P.O. Box 681, 1000 AR Amsterdam, Netherlands, Telefax (+31-20) 5862 304, or to: The Editor of *Journal of Chromatography B: Biomedical Applications*, P.O. Box 681, 1000 AR Amsterdam, Netherlands. Review articles are invited or proposed in writing to the Editors who welcome suggestions for subjects. An outline of the proposed review should first be forwarded to the Editors for preliminary discussion prior to preparation. Submission of an article is understood to imply that the article is original and unpublished and is not being considered for publication elsewhere. For copyright regulations, see below.

Publication information. *Journal of Chromatography A* (ISSN 0021-9673): for 1994 Vols. 652–682 are scheduled for publication. *Journal of Chromatography B: Biomedical Applications* (ISSN 0378-4347): for 1994 Vols. 652–662 are scheduled for publication. Subscription prices for *Journal of Chromatography A*, *Journal of Chromatography B: Biomedical Applications* or a combined subscription are available upon request from the publisher. Subscriptions are accepted on a prepaid basis only and are entered on a calendar year basis. Issues are sent by surface mail except to the following countries where air delivery via SAL is ensured: Argentina, Australia, Brazil, Canada, China, Hong Kong, India, Israel, Japan, Malaysia, Mexico, New Zealand, Pakistan, Singapore, South Africa, South Korea, Taiwan, Thailand, USA. For all other countries airmail rates are available upon request. Claims for missing issues must be made within six months of our publication (mailing) date. Please address all your requests regarding orders and subscription queries to: Elsevier Science B.V., Journal Department, P.O. Box 211, 1000 AE Amsterdam, Netherlands. Tel.: (+31-20) 5803 642; Fax: (+31-20) 5803 598. Customers in the USA and Canada wishing information on this and other Elsevier journals, please contact Journal Information Center, Elsevier Science Inc., 655 Avenue of the Americas, New York, NY 10010, USA, Tel. (+1-212) 633 3750, Telefax (+1-212) 633 3764.

Abstracts/Contents Lists published in Analytical Abstracts, Biochemical Abstracts, Biological Abstracts, Chemical Abstracts, Chemical Titles, Chromatography Abstracts, Current Awareness in Biological Sciences (CABS), Current Contents/Life Sciences, Current Contents/Physical, Chemical & Earth Sciences, Deep-Sea Research/Part B: Oceanographic Literature Review, Excerpta Medica, Index Medicus, Mass Spectrometry Bulletin, PASCAL-CNRS, Referativnyi Zhurnal, Research Alert and Science Citation Index.

US Mailing Notice. *Journal of Chromatography A* (ISSN 0021-9673) is published weekly (total 52 issues) by Elsevier Science B.V., (Sara Burgerhartstraat 25, P.O. Box 211, 1000 AE Amsterdam, Netherlands). Annual subscription price in the USA US$ 4994.00 (US$ price valid in North, Central and South America only) including air speed delivery. Second class postage paid at Jamaica, NY 11431. **USA POSTMASTERS**: Send address changes to *Journal of Chromatography A*, Publications Expediting, Inc., 200 Meacham Avenue, Elmont, NY 11003. Airfreight and mailing in the USA by Publications Expediting.

See inside back cover for Publication Schedule, Information for Authors and information on Advertisements.

0021-9673/94/$07.00

Printed in the Netherlands

VOL. 667, NOS. 1 + 2 JOURNAL OF CHROMATOGRAPHY A APRIL 29, 1994

CONTENTS

(Abstracts/Contents Lists published in Analytical Abstracts, Biochemical Abstracts, Biological Abstracts, Chemical Abstracts, Chemical Titles, Chromatography Abstracts, Current Awareness in Biological Sciences (CABS), Current Contents/Life Sciences, Current Contents/Physical, Chemical & Earth Sciences, Deep-Sea Research/Part B: Oceanographic Literature Review, Excerpta Medica, Index Medicus, Mass Spectrometry Bulletin, PASCAL-CNRS, Referativnyi Zhurnal, Research Alert and Science Citation Index)

REGULAR PAPERS

Column Liquid Chromatography

(Continued overleaf)

Contents (continued)

(Continued overleaf)

SHORT COMMUNICATIONS

Column Liquid Chromatography

Gas Chromatography

Supercritical Fluid Chromatography

Planar Chromatography

Electrophoresis

JOURNAL OF CHROMATOGRAPHY A

VOL. 667 (1994)

JOURNAL OF CHROMATOGRAPHY A

INCLUDING ELECTROPHORESIS AND OTHER SEPARATION METHODS

ELSEVIER

AMSTERDAM — LONDON — NEW YORK — TOKYO

0021-9673/94/$07.00

Printed in the Netherlands

ELSEVIER

Journal of Chromatography A, 667 (1994) 1–9

JOURNAL OF CHROMATOGRAPHY A

Reproducibility of physical characteristics, protein immobilization and chromatographic performance of 3M Emphaze Biosupport Medium AB 1☆

Peter R. Johnson*,[a], Niki J. Stern[b], Philip D. Eitzman[b], Jerald K. Rasmussen[b], Dean S. Milbrath[b], Raymond M. Gleason[b], Ralph E. Hogancamp[b]

[a]*3M Company, 3M Pharmaceuticals, 3M Center-270-4S-02, St. Paul, MN 55144-1000, USA*

[b]*3M Company, Bioapplications Group, 3M Center-260-6B-16, St. Paul, MN 55144-1000, USA*

(First received June 15th, 1993; revised manuscript received November 4th, 1993)

Abstract

3M Emphaze Biosupport Medium AB 1, a polymeric azlactone-functional support, provides for rapid and efficient coupling of proteins for uses such as affinity chromatography. The support is easy to use, with no preactivation or additional reagents required. It rapidly immobilizes proteins from solutions between pH 4 and 11.

Materials used in chromatographic processes need to be reproducible, in order to provide uniform performance. The following characteristics have been monitored in order to evaluate the reproducibility of Emphaze Biosupport Medium: particle size distribution, pore size distribution, surface area, bed volume, protein exclusion limits, pressure and flow performance, protein coupling and affinity performance.

1. Introduction

The development of 3M Emphaze Biosupport Medium AB 1 began in the mid-1980s when a group of synthetic chemists and biochemists at 3M began to collaborate on the use of azlactone-based polymers for covalently coupling biomolecules to polymeric supports [1–6]. The azlactone chemistry provides a stable reactive group for easy and versatile coupling of nucleophilic molecules, as illustrated in Fig. 1.

The initial developmental work with azlactone media focused on the reactive azlactone chemistry, and the evaluation of immobilized biomolecules [7–12]. The next step was to incorporate this reactive azlactone chemistry into a robust support which was suitable for chromatographic applications. The final stage of development

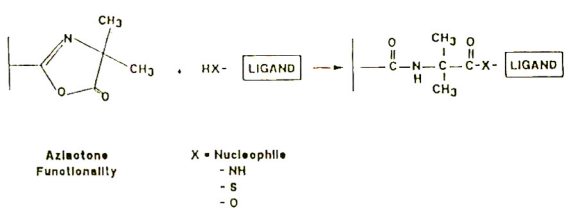

Fig. 1. Azlactone reaction chemistry, the covalent coupling of a nucleophile to vinyldimethylazlactone.

* Corresponding author.

Presented at the *10th International Symposium on Preparative Chromatography, Arlington, VA, June 14–16, 1993.* The majority of the papers presented at this symposium were published in *J. Chromatogr. A*, Vol. 658, No. 2 (1994).

0021-9673/94/$07.00
SSDI 0021-9673(93)E1202-B

involved scaling-up the synthetic steps to obtain a manufacturing process which produced uniform, fully functional product with each lot.

This product, 3M Emphaze Biosupport Medium AB 1, is a porous co-polymer of vinyldimethylazlactone and methylenebisacrylamide. The support is spherical, with an average bead diameter of 60 μm, as illustrated in Fig. 2. Emphaze AB 1 is supplied in a stable, dry form. Coupling of biomolecules is accomplished by addition of dry AB 1 to a solution which contains the biomolecule. As the beads swell in this solution, the covalent binding of biomolecules occurs. Typically the coupling reaction is complete within one hour, and the hydrated volume is approximately 8 ml of support per gram of dry media. Emphaze AB 1 contains over 30 μmol of reactive sites per ml of support, and can couple over 35 mg of protein per ml of swollen gel.

Emphaze AB 1 is stable in both aqueous and non-aqueous solutions, and buffer or solvent switching causes negligible, if any, changes in volume to occur. This feature permits elution and cleaning of the support with harsh solutions, the coupling of hydrophobic ligands in non-aqueous solvents, and also non-aqueous immobilized enzyme work.

This article focuses on the final stage of product development, and describes the physical and biochemical properties of Emphaze AB 1 which were evaluated in order to demonstrate the run-to-run uniformity of the manufacturing process.

Fig. 2. Photomicrograph of 3M Emphaze Biosupport Medium AB 1.

2. Experimental

2.1. Materials

Stationary phases

Twenty seven different lots of 3M Emphaze Biosupport Media AB 1 (3M Company, St. Paul, MN, USA) were used as sample media for the following series of physical and chemical analyses.

Chemicals and solvents

Sodium chloride, monobasic and dibasic sodium phosphate, boric acid, D(+)-glucosamine hydrochloride, 2-(N-cyclohexylamino)ethanesulfonic acid (CHES) buffer, sodium dodecyl sulfate (SDS), ethanolamine, guanidine hydrochloride, cytochrome *c*, lysozyme, horse heart myoglobin, carbonic anhydrase, ovalbumin, fetuin, bovine serum albumin, alkaline phosphatase, human immunoglobulin, catalase, apoferritin, thyroglobulin, blue dextran (M_r 2 000 000), and λ phage DNA (M_r 30 000 000) were purchased from Sigma (St. Louis, MO, USA). "BCA" reagent for colorimetric protein analysis was obtained from Pierce (Rockford, IL, USA). Potassium chloride was obtained from J.T. Baker (Phillipsburg, NJ, USA). Trisodium citrate, sodium sulfate and sodium pyrophosphate were obtained from Mallinckrodt (Paris, KY, USA). Sodium hydroxide was obtained from EM Science (Gibbstown, NJ, USA). Sodium nitrite was obtained from Matheson, Coleman & Bell (Norwood, OH, USA). Recombinant Protein A was purchased from Repligen (Cambridge, MA, USA). Tissue culture fluid consisted of ATCC HB-124 DB9G8 (murine anti-insulin IgG_{2ak}) cultured in 10% fetal calf serum with 90% RPMI-1640 (Gibco, Grand Island, NY, USA). Liquid nitrogen was obtained from Oxygen Services (St. Paul, MN, USA). A Barnstead water-treatment system (Dubuque, IA, USA) produced ultra-pure water.

2.2. Equipment

Particle size measurements were performed with a Coulter LS-100 light-scattering particle size analyzer (Hialeah, FL, USA), which was equipped with a hazardous fluid module. A Micromeretics ASAP-2400 porosimeter (Norcross, GA, USA) was used to obtain pore size and surface area measurements. Graduated centrifuge tubes (15 ml, part 25319-15, Corning, Corning, NY, USA) and a tabletop centrifuge (Beckman Model TJ-6, Palo Alto, CA, USA) were used in determining hydration volumes. Flow parameters were measured with a system which was controlled and monitored by a Vectra ES-12 personal computer (Hewlett-Packard, Avondale, PA, USA). The other system components included a Model QV-0 Lab Pump (Fluid Metering, Oyster Bay, NY, USA) which was able to operate at flow-rates between 4 and 40 ml/min, a 0 to 1.3 MPa pressure transducer (Model PX941-200GI; Omega Engineering, Stamford, CT, USA), a Model DAS-8/AO data acquisition and control interface board (Keithly MetraByte, Taunton, MA, USA), and a 10 cm × 1 cm Waters AP-1 glass column (Milford, MA, USA).

Exclusion volume measurements were made with an HPLC system which consisted of the following components: a Spectra-Physics Model SP8750 pump (San Jose, CA, USA), a Spectra-Physics Model SP8780XR autosampler, a Kratos Spectroflow 757 UV monitor (Ramsey, NJ, USA), a Spectra-Physics Model SP4270 integrator and Spectra-Physics Spectra Station software. Polyether ether ketone (PEEK) columns (150 × 4.6 mm) were obtained from Alltech (Deerfield, IL, USA). The protein coupling analyses employed a Hewlett-Packard Model 8452A diode array spectrophotometer for absorbance measurements. Hema-Tek rocker plates were obtained from Miles (Elkhart, IN, USA), Labquake rotary mixers were obtained from Labindustries (Berkeley, CA, USA) and Vortex Genie-2 mixers were obtained from Scientific Industries (Bohemia, NY, USA). Tissue culture fluid was cultured in an Acusyst-P hollow fiber reactor (Endotronics, Minneapolis, MN, USA) and filtered through a 0.45-μm Pellicon cassette (Millipore, Milford, MA, USA). Affinity chromatography was performed on a Waters Delta Prep 3000 liquid chromatograph, which was controlled by Waters Maxima software. Polyacrylamide gel electrophoresis was performed with a Model PS 2500 power supply and model SE 250 gel apparatus (both from Hoefer Scientific, San Francisco, CA, USA), 10–20% gradient gels (Daiichi Pure Chemicals, Tokyo, Japan), and PRO Blue Stain (Integrated Separation Systems, Natick, MA, USA).

2.3. Procedures

Measurement of particle size

Prior to the analysis of samples, a control sample of garnet particles with an average diameter of 15 μm (Coulter LS Control G15) was analyzed to verify proper instrument operation. Analyses of hydrated Emphaze AB 1 samples were conducted by adding sufficient sample (20%, v/v, in filtered water) to produce 8 to 12% obscuration of incident laser light. The resulting diffraction pattern was analyzed to obtain a particle size distribution using a mathematical model which accounted for the refractive indices of the suspending fluid and the particles.

Measurement of pore size and surface area

To prepare samples for porosimetry measurements, 150 to 200 mg of Emphaze AB 1 dry beads were evacuated on the degas manifold of the ASAP 2400 at 100°C and less than 10 Mtorr (1 Torr = 133.322 Pa), until the instrument detected no further removal of volatiles. Samples were then transferred to the analysis manifold for automated measurement of the adsorption and desorption isotherms using nitrogen gas.

Measurement of hydration volume

Approximately 250 mg of Emphaze AB 1 dry beads were hydrated in calibrated, graduated centrifuge tubes by the addition of 10 ml of phosphate-buffered saline (PBS: 150 m*M* sodium chloride, 25 m*M* sodium phosphate) pH 7.4, and then mixing for 60 min on a rocker plate or rotary mixer. The beads were settled by centrifu-

gation at 1330 *g* for 90 min, and the bed volume in the graduated centrifuge tube was noted. The hydration volume for the sample is obtained by dividing this bed volume by the sample mass.

Measurement of flow parameters

Samples were prepared for analysis by hydration of 1.2–1.5 g of Emphaze AB 1 in 20 ml of PBS, pH 7.5. After mixing the bead slurry on a rocker plate for 30 min, the sample was centrifuged at 1330 *g* for 10 min. The volume of supernatant was then adjusted to obtain a 75% (v/v) slurry concentration. The Waters AP-1 column was primed with 1 ml of buffer, and then 11 ml of bead slurry was added to the column through the attached packing adapter. Buffer was allowed to flow from the column until the packing adapter was empty. Flow was then stopped, and the slurry was allowed to settle for 30 min. The column inlet assembly was then installed, and the inlet frit was carefully positioned at the level of the settled beads. The system was then operated at a flow-rate of 4 ml/min (306 cm/h) for 5 min to pack the bed further, and the inlet was again adjusted to the level of the settled beads. The analysis program was then initiated. The flow-rate was varied from 4 to 40 ml/min (306 to 3056 cm/h), in 4 ml/min increments, for 5 min per increment. The system pressure was monitored continuously.

Size-exclusion chromatography

A hydrophilic stationary phase for size-exclusion chromatography was prepared by coupling glucosamine to samples of Emphaze AB 1 Biosupport Media. Emphaze beads (0.8 to 0.9 g) were added to a buffered glucosamine solution (20 mg/ml of glucosamine hydrochloride, 1.2 *M* sodium sulfate, 50 m*M* sodium pyrophosphate at pH 8.5). The slurry was dispersed by vortex mixing, then mixed at room temperature overnight on a rocker plate. The derivatized Emphaze beads were then rinsed twice with four bed volumes of PBS, pH 7.4, and finally slurry packed into PEEK columns (150 × 4.6 mm) for exclusion volume analyses. The mobile phase (100 m*M* sodium sulfate, 50 m*M* sodium phosphate, 50 m*M* boric acid at pH 7.0) was also used to prepare 1 mg/ml solutions of the size exclusion solutes: sodium nitrite, cytochrome *c*, lysozyme, myoglobin, carbonic anhydrase, ovalbumin, fetuin, bovine serum albumin, alkaline phosphatase, human immunoglobulin, catalase, apoferritin, thyroglobulin, blue dextran, and λ phage DNA (50 μg/ml). The flow-rate for size-exclusion analysis was 0.25 ml/min. The size-exclusion solutes were injected individually, in order to avoid merged peaks. A composite chromatogram of four size-exclusion test solutes is shown in Fig. 3. The large particle size, as well as some non-specific interactions, have caused considerable band broadening.

The elution volume for sodium nitrite represented the total permeable volume, V_P, and the elution volume for λ phage DNA represented the total exclusion volume, V_E. The pore volume of the packed column, V_{pore}, is the difference between the total permeable volume and the total exclusion volume. The accessible pore volume for a given solute, V_{solute}, is the difference between the solute's retention volume, V_R, and the exclusion volume. The percentage of the pore volume which is accessible to a given solute was calculated as follows:

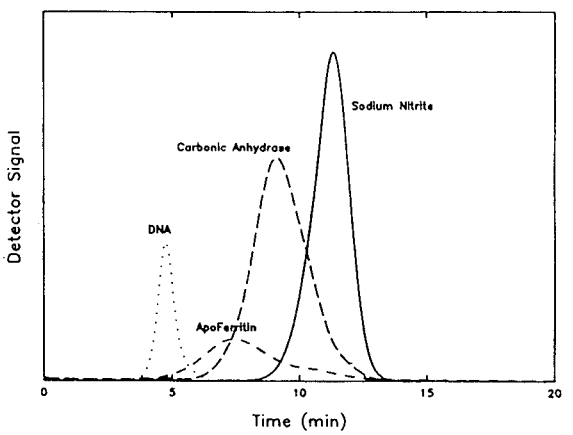

Fig. 3. A composite chromatogram for four size-exclusion reference solutes.

$$\text{Solute accessibility } (\%) = 100(V_{\text{solute}}/V_{\text{pore}})$$
$$= 100[(V_R - V_E)/(V_P - V_E)]$$

since elution volume = elution time (t) × flow-rate, then dividing the numerator and denominator by flow-rate transforms the above formula to:

$$\text{Solute accessibility } (\%) = \frac{(t_R - t_{DNA})}{(t_{\text{nitrite}} - t_{DNA})} \cdot 100$$
$$= 100K_{av}$$

This relationship was then used to evaluate the exclusion limits and permeability of the Emphaze media by size-exclusion chromatography.

Measurement of protein coupling

Emphaze AB 1 samples (28–32 mg) were hydrated with 3 ml of myoglobin reagent solution (5 mg/ml myoglobin, 1.0 *M* sodium citrate, 0.1 *M* CHES, pH 9.0) and then mixed on a rocker plate or rotary mixer at room temperature for 60 to 70 min. A 5-ml volume of 1% (w/w) SDS was then added to the sample tube, and the mixing was continued for an additional 30 min to remove non-specifically bound myoglobin. The slurry was centrifuged at 1330 *g* for 5 min to settle the beads, and the supernatant was sampled for spectrophotometric measurement at 532 nm (A_{super}). The spectrophotometer was blanked with respect to a solution which contained citrate–CHES buffer (3 ml) plus 1% SDS (5 ml). The absorbance of a myoglobin reference solution (A_{ref}), which contained 3 ml of myoglobin reagent solution and 5 ml of 1% SDS, represented the amount of myoglobin available for coupling. The difference between the reference and supernatant absorbances was proportional to the amount of myoglobin coupled to the bead sample, as follows:

$$B\ (\text{mg/g}) = (A_{\text{ref}} - A_{\text{super}})CV/[WA_{\text{ref}}]$$

where B is the amount of myoglobin coupled, C is the concentration of the myoglobin reference solution, V is the amount of myoglobin reagent solution per sample and W is the sample mass.

Purification of IgG by affinity chromatography

An affinity support for the purification of murine IgG from tissue culture fluid was prepared by coupling recombinant Protein A to 3M Emphaze Biosupport Medium AB 1. Emphaze beads (18.72 g) were added to a 1-l bottle which contained 555 ml of a buffered Protein A solution (2.03 mg/ml of Protein A, 0.85 *M* sodium citrate, 100 m*M* 3-(N-morpholino)propanesulfonic acid (MOPS) at pH 7.5). The bottle was then rocked for 1 h at room temperature. After the coupling reaction, the slurry was filtered on a glass fritted Buchner funnel, porosity D, and the filtrate was used to determine the amount of Protein A that was coupled to the Emphaze media. The Protein A beads were then resuspended in 600 ml of quenching solution (1.0 *M* ethanolamine, 25 m*M* sodium pyrophosphate, pH 7.5), rocked for 5 h, filtered as above, then resuspended in 400 ml of PBS for 20 min. The washing was completed by filtering the PBS from the slurry and then gradually rinsing the filtercake with 1.8 l of PBS. The washed Protein A beads were then slurried in PBS and stored at 5°C before use. The BCA colorimetric protein assay was used to determine the amount of Protein A which was coupled to Emphaze AB 1, based upon the difference in Protein A concentration between the initial and filtrate solutions. The affinity support contained 7.7 mg of Protein A per ml of media. A 1-ml volume of the Emphaze–Protein A support was then slurry packed into a Waters AP-1 glass column (1.0 cm I.D.) to a final bed height of 1.3 cm.

The isolation of murine IgG was begun after equilibrating the affinity column with PBS. The column was loaded at 1 ml/min (76 cm/h) with 25 ml of filtered (0.45 μm) tissue culture fluid which contained murine IgG. The affinity column was then washed, eluted, cleaned and reequilibrated at 3 ml/min (229 cm/h). The wash and reequilibration buffer was PBS, pH 7.2. The elution buffer was 100 m*M* sodium citrate, pH 2.5, and the cleaning buffer was 3.0 *M* guanidine hydrochloride, 20 m*M* sodium phosphate, pH 7.2. The eluted IgG was quantified by spectrophotometric analysis at 280 nm, and its purity

was confirmed by polyacrylamide gel electrophoresis.

3. Results and discussion

3.1. Particle size

Typical particle size distributions for seven lots of Emphaze AB 1, as measured by the light-scattering particle size analyzer, are illustrated in Fig. 4. A photomicrograph of representative Emphaze AB 1 medium is presented in Fig. 2. The average particle diameter was 62 μm, and 85% of the particles ranged in diameter from 45 to 81 μm. The reproducibility of these three particle size parameters for 27 production lots of Emphaze AB 1 is summarized in Fig. 5. The relative standard deviation (R.S.D.) for the average particle size measurement was 2.0%, and the R.S.D.s for the 5th and 90th percentiles were 1.7 and 3.5%, respectively.

3.2. Pore size and exclusion volumes

A typical pore size distribution for dry Emphaze AB 1 beads, as measured by nitrogen porosimetry, is shown in Fig. 6. The cumulative pore distribution data, shown in Fig. 7, indicates that over 70% of the pore volume for Emphaze

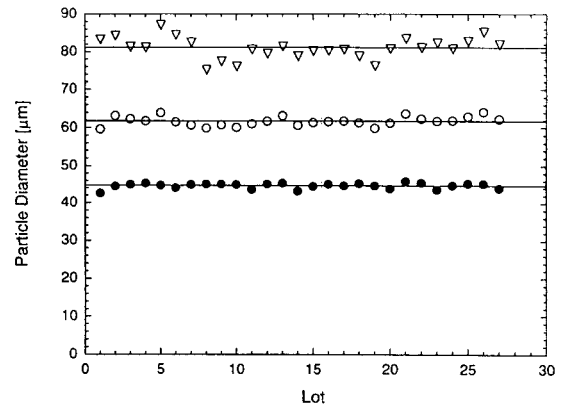

Fig. 5. Lot-to-lot reproducibility of particle size parameters: ▽ = 90th percentile; ○ = mean diameter; ● = 5th percentile.

AB 1 is within pores that have pore diameters greater than 300 Å.

Since the dry support swells approximately twofold upon hydration, the accessible pore volume of the hydrated media may be somewhat different from that of the dry support. Size-exclusion chromatography was performed with Emphaze AB 1 media in order to obtain a practical perspective of the porous structure of hydrated support. The size-exclusion data in Fig. 8 shows that apoferritin, a protein with a molecular mass of 443 000, had access to 40% of the bead pore volume. IgG, with a molecular mass of 150 000, had access to 57% of the bead pore

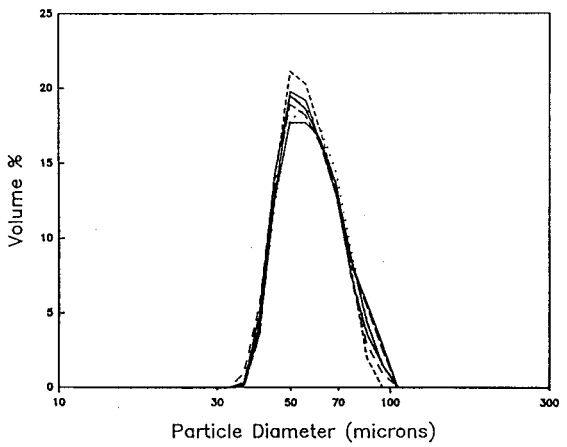

Fig. 4. Particle size distribution (of seven lots) for 3M Emphaze Biosupport Medium AB 1.

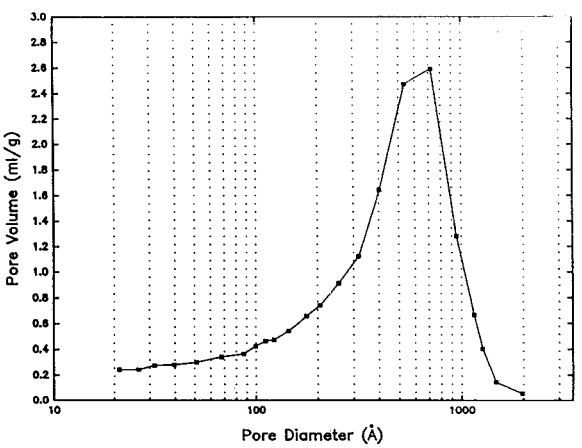

Fig. 6. Desorption pore size distribution for 3M Emphaze Biosupport Medium AB 1.

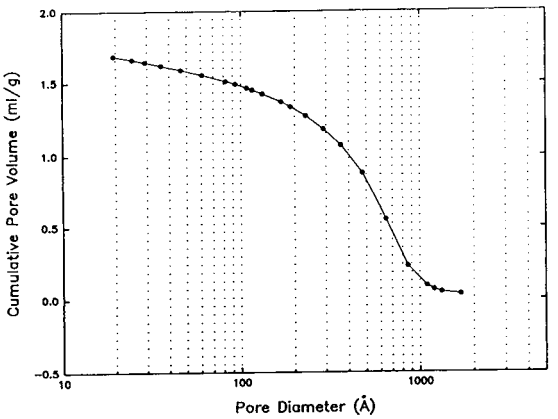

Fig. 7. Cumulative pore volume distribution for 3M Emphaze Biosupport Medium AB 1.

volume, and carbonic anhydrase, with a molecular mass of 29 000, had access to 73% of the bead pore volume. The values for the mean pore diameter for 27 lots of dry Emphaze AB 1 are reported in Fig. 9. The R.S.D. for the mean pore diameter was 4.6%. The mean pore diameter of 190 Å is less than the pore diameter which represents the greatest pore volume (700 Å, from Fig. 6), because calculation of the mean pore value is influenced by the relatively large

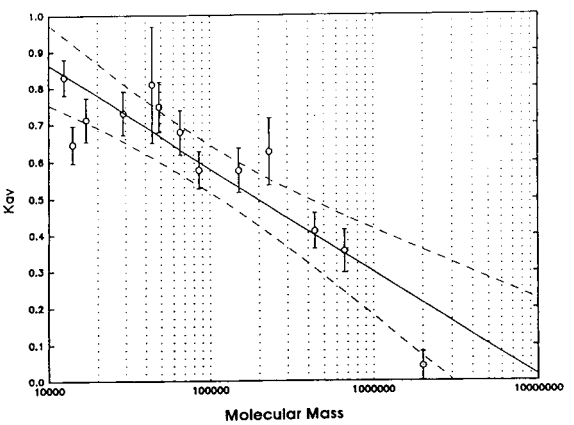

Fig. 8. Size-exclusion performance for proteins (molecular mass): cytochrome *c* (12 400), lysozyme (14 000), myoglobin (16 900), carbonic anhydrase (29 000), ovalbumin (44 000), fetuin (48 700), bovine serum albumin (66 000), alkaline phosphatase (86 000), human immunoglobulin (150 000), catalase (232 000), apoferritin (440 000), thyroglobulin (670 000), blue dextran (2 000 000), λ phage DNA (30 000 000).

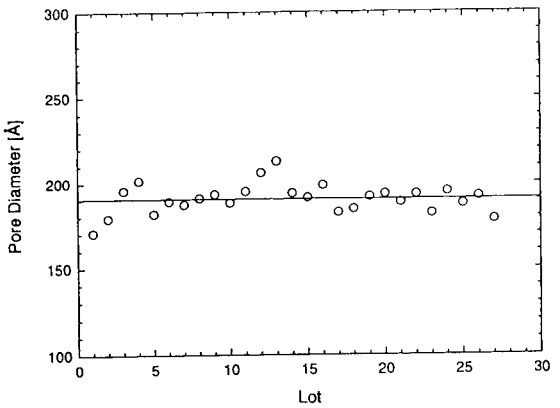

Fig. 9. Lot-to-lot reproducibility of pore diameter.

population of small diameter pores which contribute very little to the total pore volume. Also note that average pore size values which are obtained by nitrogen porosimetry are typically smaller than those from mercury porosimetry. This is because nitrogen is smaller than mercury, and thus it can obtain data from smaller pores.

3.3. Surface area

A typical surface area distribution for dry Emphaze AB 1 media is presented in Fig. 10. This graph displays the cumulative pore surface area as a function of pore diameter. Approximately 25% of the total surface area is contained in pores having diameters greater than 300 Å,

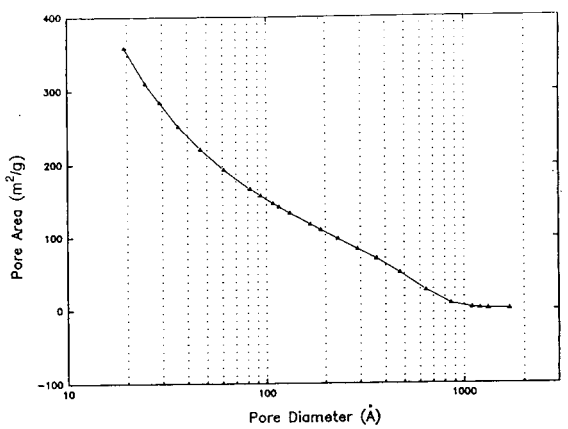

Fig. 10. Cumulative desorption pore surface area distribution.

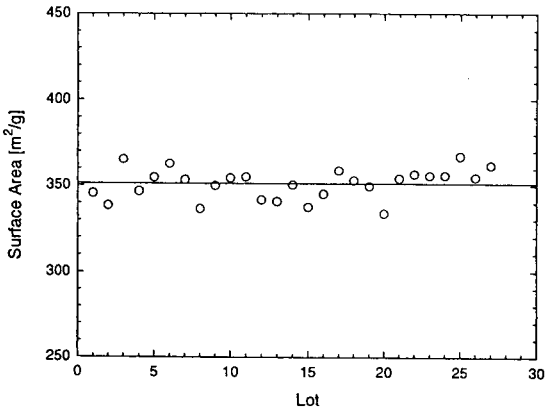

Fig. 11. Lot-to-lot reproducibility of surface area.

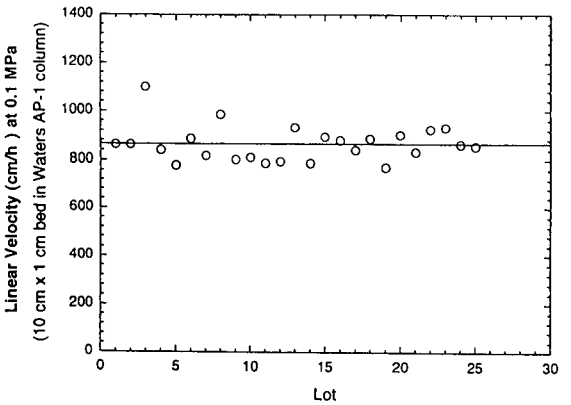

Fig. 13. Lot-to-lot reproducibility of flow-rate at 0.1 MPa.

and 41% of the total surface area is contained in pores having diameters greater than 100 Å. The reproducibility of bead surface area for Emphaze AB 1 medium is summarized in Fig. 11. For 27 production runs the mean surface area was 351 m^2/g, with an R.S.D. of 2.5%.

3.4. Hydration volume

The reproducibility of hydration volume values for Emphaze AB 1 media is displayed in Fig. 12. The mean hydration volume for 27 production runs was 8.3 ml per gram of dry media. This value varied by 3.3% over these bead lots.

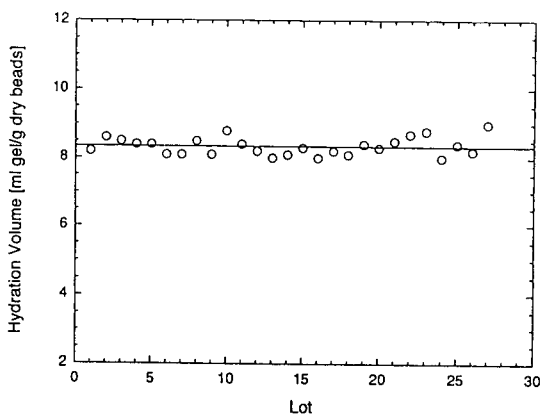

Fig. 12. Lot-to-lot reproducibility of hydration volume.

3.5. Flow parameters

The reproducibility of flow-rate at 0.1 MPa is reported in Fig. 13. For 27 production lots of beads the flow-rate at 0.1 MPa averaged 865 cm/h, with an R.S.D. of 8.5%.

3.6. Protein coupling

The reproducibility of protein coupling performance by Emphaze AB 1 was evaluated with myoglobin, a reasonably priced protein with a visible color to facilitate a protein coupling assay. The Emphaze AB 1 samples were challenged with a sufficient amount of myoglobin to attain a 50% coupling efficiency of the myoglobin. For eight production runs, myoglobin coupling performance averaged 30 mg of myoglobin per ml of media, with a lot-to-lot (R.S.D.) of 7.9%, as shown in Fig. 14.

3.7. Purification of IgG from ascites by Protein A affinity chromatography: reproducibility of separations using Protein A-modified Emphaze AB 1

A single column which contained Protein A-modified Emphaze AB 1 was used to isolate murine IgG from tissue culture media, and the affinity support was then cleaned with 3.0 *M* guanidine hydrochloride after each separation.

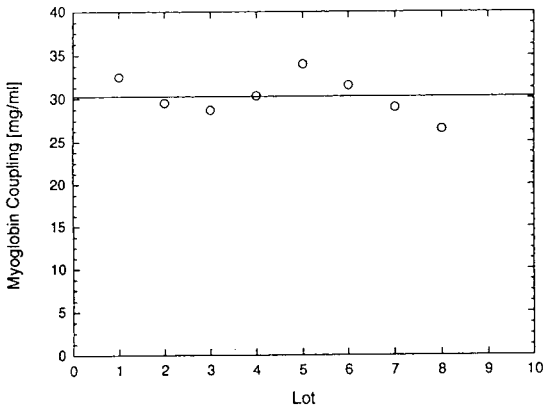

Fig. 14. Lot-to-lot reproducibility of protein coupling performance.

Fig. 15 summarizes the performance of this affinity support over 139 purification cycles. The lot-to-lot R.S.D. was 5.2%, and the Protein A-modified Emphaze AB 1 media retained 99% of its specific binding capacity after 139 cycles.

4. Conclusions

The physical and biochemical performance characteristics for 27 production lots of 3M Emphaze Biosupport Medium AB 1 were monitored in order to evaluate the reproducibility of manufacturing this chromatographic support. The physical attributes, such as particle size distribution, pore size distribution, surface area, hydration volume, and flow-rate at 0.1 MPa, as well as the biochemical attributes, such as protein coupling and affinity purifications, all exhibited excellent lot-to-lot reproducibility, with R.S.D.s ranging from 1.7 to 8.5% for these parameters.

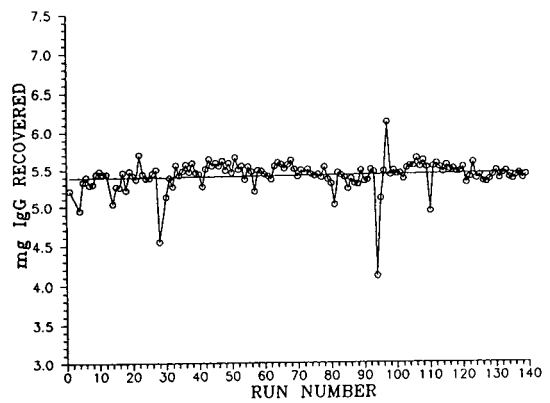

Fig. 15. Run-to-run reproducibility of IgG purification by protein A-modified Emphaze AB 1. O——O = Concentration by A_{280}.

5. References

[1] S.M. Heilmann, J.K. Rasmussen, L.R. Krepski, D.S. Milbrath and P.L. Coleman, *U.S. Pat.*, 4 737 560 (April 12, 1988).

[2] S.M. Heilmann, J.K. Rasmussen, L.R. Krepski, D.S. Milbrath and P.L. Coleman, *U.S. Pat.*, 4 871 824 (October, 1989).

[3] S.M. Heilmann, J.K. Rasmussen, L.R. Krepski, D.S. Milbrath and P.L. Coleman, *Eur. Pat. Publ.*, O 392 735 A2.

[4] J.K. Rasmussen, S.M. Heilmann, L.R. Krepski, H.K. Smith II, M.M. Walker, D.S. Stauffer, D.S. Milbrath and P.L. Coleman, *Polym. Prepr. (Am. Chem. Soc., Div. Polym. Chem.)*, 31 (1990) 442–443.

[5] J.K. Rasmussen, S.M. Heilmann, L.R. Krepski, K.M. Jensen, J. Mickelson and K. Johnson, *React. Polym.*, 16 (1991/1992) 199–212.

[6] J.K. Rasmussen, J.I. Hembre, N.I. Koski, D.S. Milbrath, P.L. Coleman, M.M. Walker, D.S. Stauffer, S.M. Heilmann, L.R. Krepski, H.K. Smith II, R.J. Loer, S.A. Van Keuren, Z.A. Calubayan, W.T. Conway, W.J. Johnson, R.J. Rossiter and D.A. Swenson, *Makromol. Chem., Macromol. Symp.*, 54/55 (1992) 535–550.

[7] P.L. Coleman, M.M. Walker, S.M. Heilmann, L.R. Krepski, J.R. Rasmussen and K.M. Jensen, *FASEB J.*, 2 (1988) A1770, No. 8563.

[8] D.S. Milbrath, P.L. Coleman, M.M. Walker, S.M. Heilmann, J.K. Rasmussen and L.R. Krepski, *Abstr. Pap. —Am. Chem. Soc.*, 198th (1989) MBT Division, Section C, paper 19, MBTD 21; MBTD Newsletter, *Fermentor*, 9/12 (1989) 51.

[9] P.L. Coleman, D.S. Milbrath, M.M. Walker, S.M. Heilmann and L.R. Krepski, *J. Cell Biochem.*, 44 (1990) 19.

[10] P.L. Coleman, M.M. Walker, D.S. Milbrath and D.S. Stauffer, *J. Chromatogr.*, 512 (1990) 345–363.

[11] D.S. Milbrath, P.L. Coleman, M.M. Walker and D.S. Stauffer, *Extended Abstracts of the Annual Meeting, Chicago*, American Institute of Chemical Engineers, New York, 1990, paper 104E.

[12] P.L. Coleman, M.M. Walkers, C.L. Reese and D.S. Milbrath, *FASEB J.*, 5 (1991) A805, No. 2528.

ELSEVIER

Journal of Chromatography A, 667 (1994) 11–17

JOURNAL OF CHROMATOGRAPHY A

6,6′-Dinitrobiphenyl-2,2′-dicarboxylic acid ionically bonded to aminopropyl silica: new axially chiral phase of C_2 symmetry for high-performance liquid chromatographic separation of enantiomeric amino alcohol derivatives

Miloš Tichý*, Jana Holanová, Jiří Závada

Institute of Organic Chemistry and Biochemistry, Academy of Sciences of the Czech Republic, 166 10 Prague 6, Czech Republic

(First received October 18th, 1993; revised manuscript received November 9th, 1993)

Abstract

(*R*)-(+)-6,6′-Dinitrobiphenyl-2,2′-dicarboxylic acid, ionically bonded to 3-aminopropylsilanized silica (CSP 1), is the first ionically bonded axially chiral phase of C_2 symmetry. The phase is specifically efficient for the separation of a wide range of enantiomeric vicinal benzamido alcohols, whether open-chain, cyclic or polycyclic. To assess the steric and polar effects of the 6,6′-substituents, the performance of CSP 1 is compared with that of the analogous (but less effective) phase CSP 2, based on (*S*)-(+)-6,6′-dimethylbiphenyl-2,2′-dicarboxylic acid. Some conclusions about the relation between the separation effectivity and the analyte structure, as well as about the factors involved in the chiral recognition process, are given.

1. Introduction

During the last decade the preparation and use of chiral stationary phases has represented a very progressive trend in analytical as well as preparative organic chemistry, thanks particularly to the pioneering work of Pirkle and Pochapsky [1] who, using a simple rationale, succeeded in making more or less "tailor-made" chiral stationary phases of wide applicability and good accessibility.

Most chiral stationary phases (CSPs) described so far are based on systems whose asymmetry is derived from one or more *centres* of chirality (*i.e.* asymmetric atoms). Interestingly, only very few chiral phases based on other kinds of chirality (*e.g.* helical or axial) have been examined, in spite of their considerable separation potential. Systems possessing a C_2 symmetry axis offer a special promise for chiral recognition (and separation of the enantiomers) because in this particular case the number of possible competing diastereoisomeric situations in the interaction of the analyte with the phase is strongly reduced (for a discussion and review see ref. 2). To our knowledge, only three C_2 symmetrical chiral stationary phases have been described [3–5] so

* Corresponding author.

0021-9673/94/$07.00
SSDI 0021-9673(93)E0021-L

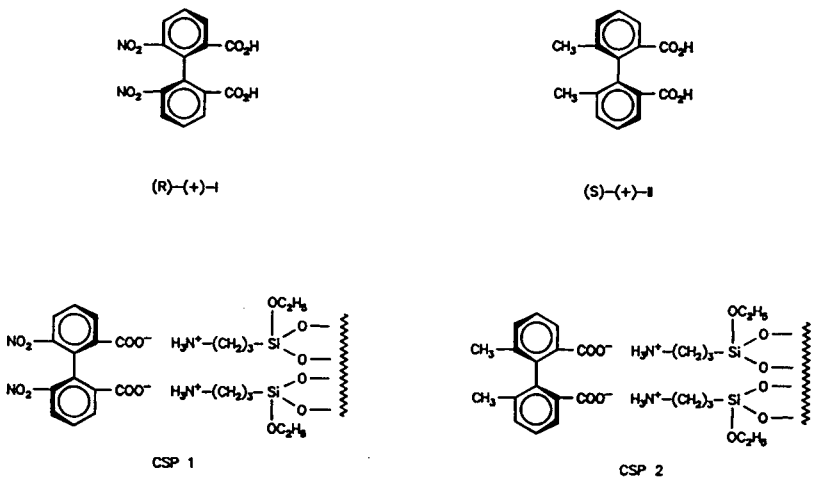

Fig. 1. Structure of (*R*)-(+)-**I**, (*S*)-(+)-**II**, CSP 1 and CSP 2.

far (separating helicenes [3], heterocyclic systems [4] and amines [5])[a].

In this communication we present results obtained with CSPs based on simple biphenyl compounds of C_2 symmetry, (*R*)-(+)-6,6′-dinitrobiphenyl-2,2′-dicarboxylic acid [(*R*)-(+)-I] and (*S*)-(+)-6,6′-dimethylbiphenyl-2,2′-dicarboxylic acid [(*S*)-(+)-II] (Fig. 1), in the separation of benzoyl derivatives of vicinal amino alcohols.

2. Experimental

2.1. General

Liquid chromatography was carried out using a Varian 2510 pump, a Varian 2550 UV detector (detection at 254 nm) and a polarimetric detector (Chiralizer, Knauer).

Analyses were performed on 250 × 4 mm stainless-steel columns (slurry-packed in the usual manner) with 10% 2-propanol in heptane as the mobile phase (flow-rate 0.5 ml/min). Sample solutions (about 1 mg/ml) were introduced via a 20-μl loop. Hold-up times were determined using 1,3,5-tri-*tert.*-butylbenzene.

2.2. Materials

(*R*)-(+)-6′6′-Dinitrobiphenyl-2,2-dicarboxylic acid [(*R*)-**I**] and (*S*)-(+)-6′,6′-dimethylbiphenyl-2,2-dicarboxylic acid [(*S*)-**II**] were prepared and resolved as described previously [12–14]; (*R*)-**I**: m.p. 231–233°C, $[\alpha]_D^{20}$ + 130.1° (*c* 0.5, methanol) reported [13]: m.p. 229–230.5°C and $[\alpha]_D^{20}$ + 127° (*c* 2.4, methanol); (*S*)-**II**: m.p. 212–214°C, $[\alpha]_D^{20}$ + 21.1° (*c* 1.0, methanol) reported [14] m.p. 213–214°C and $[\alpha]_D$ + 22.1° (*c* 1.0 methanol). 3-Aminopropylsilanized silica was a Tessek product (Separon SGX-NH_2, 7 μm, 1.48 mmol NH_2/g, based on nitrogen analysis). The benzamido and *p*-nitrobenzamido alcohols were mostly available from our previous studies; the pertinent references concerning their preparation and/or physicochemical properties are as follows: compounds **1a**, **1b**, **2b** [15], **2a** [16], **3a–7a**, **10a**, **11a** [17], **8a**, **9a** [18], **12a**, *cis*-**28a** [19], **13a**, **14a** [20], **15b**, **16b**, **16c**, **17a** [21], **18a**, **18g** [22], **19a**, **21a** [23], **19b**, **20b**, **21b**, **22b**, **29a**, **30b**, **32a** [24], **23a**, **24b** [25], **25a**, **26a**, **27a** [26], *trans*-**28a** [27], **30a** [28].

The benzamido acetates were prepared by treating the corresponding benzamido alcohols

[a] Few other CSPs [6–11], derived from axially chiral 2,2′-disubstituted 1,1′-binaphthyls but attached to the support by only one of the naphthalene rings, have been described. These, however, do not possess C_2 symmetry and thus do not offer the advantage of reducing the number of competing diastereoisomeric situations.

with acetic anhydride in pyridine at room temperature overnight.

2.3. Preparation of stationary phases

A solution of the appropriate acid (2.3 mmol) in methanol (15 ml) was mixed with a slurry of Separon SGX-NH_2 (3.0 g, 4.44 mmol) in methanol (10 ml). The mixture was shaken intermittently for 1 day at room temperature, filtered, and the adsorbent was washed with methanol, acetone, ether and pentane (70 ml each) and dried at 50–60°C *in vacuo*. The washings were evaporated and the recovered unreacted acid was accurately weighed. The amount of acid retained on the adsorbent was obtained by subtracting the weight of the recovered acid from that originally applied. For CSP 1 the content of (*R*)-**I** was 0.46 mmol/g; for CSP 2 the content of (*S*)-**II** was 0.47 mmol/g.

3. Results and discussion

The ionic stationary phases CSP 1 and CSP 2 (Fig. 1) were prepared by simple treatment of 3-aminopropylsilanized silica with solutions of acids (*R*)-**I** and (*S*)-**II**, respectively, packing the columns and washing with 10% 2-propanol in heptane until the baseline was steady. No leaching, substantial change in retention times or loss of effectivity of the columns was observed during 8 months' daily performance using mostly 10% 2-propanol in heptane as the mobile phase[a] (see Table 1).

Since the sorbent retained less than 0.5 equivalents of the acids per equivalent of the NH_2 groups originally present, we suppose that both the carboxyl groups are ionically bonded to the neighbouring amino groups as depicted in Fig. 1 and that the whole system therefore meets the requirements of C_2 symmetry.

The acids (*R*)-**I** and (*S*)-**II** represent a pair of compounds in which the groups in positions 6 and 6′ differ much in polarity: this should give some information about the polar and steric factors involved in the chiral recognition in the studied biphenyl system. The fact that the acids I and II differ in their absolute configuration (different arrangement about the chiral axis) is of course immaterial. We have found that CSP 1 specifically resolves benzamido derivatives of vicinal amino alcohols.

There are only scattered reports on chiral separation of amino alcohols [30–39], mostly with emphasis on β-blockers. No systematic study has been described so far concerning this important group of compounds.

Having a large collection of model vicinal amino alcohols and their derivatives, we were able to investigate in more detail the relation between structure of the analytes and their separation behaviour. Compounds analysed on the phases CSP 1 and CSP 2 are listed in Fig. 2 and the HPLC analytical results are given in Table 1.

The phase CSP 1 resolves benzoyl derivatives of vicinal amino alcohols, irrespective of whether they are acyclic (*threo* or *erythro*) or cyclic (*trans* or *cis*, common or large rings), the resolution being invariably much better than on CSP 2. Under the same conditions, *p*-nitrobenzamido derivatives have a longer retention time and are somewhat better separated than the benzamido derivatives. In the cyclic series, *trans*-isomers of compounds with smaller rings have greater α-values than the *cis*-isomers; this difference decreases with increasing ring size. For many of the cyclic benzamido alcohols investigated baseline separation was achieved. As expected, the elution time becomes shorter with increasing ring size.

In the case of a mixture of *cis*- and *trans*-2-aminocyclohexanol derivatives (**2a**) it is possible to separate both diastereoisomers into enantiomers simultaneously in one single analysis, the chromatogram containing two doublets owing to

[a] The acid I is known to be completely optically stable at room temperature. Its racemization, together with decomposition, is reported [29] to take place only under drastic conditions (140–160°C) in a strongly alkaline medium. No data on racemization of the acid II are available, nevertheless the fact that over 8 months the performance (retention times and separation coefficients) of the CSPs remained unchanged shows that at room temperature both the CSPs are stable in all respects.

Table 1
Chromatographic data for separation of enantiomeric benzamido alcohols on CSP 1 and CSP 2

Compound	CSP 1		CSP 2	
	k_1' (sign)	α	k_1' (sign)	α
cis-**1a**	4.12 (+)	1.09		
trans-**1a**	9.00 (−)	1.14 (B)		
trans-**1d**	8.12 (+)	1.18 (B)	4.75 (−)	1.18
trans-**1e**	5.50	1.0[a]		
cis-**2a**	4.12 (+)	1.15	2.25	1.0
cis-**2b**	6.50 (+)	1.27 (B)	4.62	1.0[a]
cis-**2e**	8.75	1.0[a]	1.87	1.0[a]
trans-**2a**	6.12 (−)[b]	1.36 (B)	2.62 (+)[c]	1.24
	5.75 (−)	1.35 (B)[d]	2.87 (+)	1.26[d]
trans-**2b**	9.37 (−)	1.50 (B)		
trans-**2e**	3.25	1.0[a]	0.87	1.0[a]
			1.75[e]	1.0[a]
trans-**2f**	2.12	1.0[a]		
cis-**3a**	4.12 (+)	1.15		
cis-**4a**	3.62 (+)	1.12		
trans-**4a**	4.25 (+)	1.35 (B)		
trans-**5a**	3.37 (+)	1.22 (B)		
cis-**6a**	3.12 (+)	1.12 (B)	1.62 (−)	1.15
trans-**6a**	3.12	1.24 (B)	1.75	1.0[a]
cis-**7a**	2.75 (+)	1.14 (B)	1.50 (−)	1.08
trans-**7a**	2.87 (+)	1.22 (B)	1.62	1.0[a]
cis-**8a**	2.50 (+)	1.20 (B)		
trans-**8a**	2.62 (+)	1.18 (B)		
trans-**9a**	2.62 (+)	1.14 (B)		
cis-**10a**	2.25 (+)	1.11 (B)		
trans-**10a**	2.37 (+)	1.21 (B)	1.12	1.0[a]
cis-**11a**	2.00 (+)	1.12		
trans-**11a**	1.87 (+)	1.20		
cis-**12a**	1.50 (+)	1.17	0.75	1.0[a]
			2.25[e]	1.0[a]
trans-**12a**	1.50 (+)	1.17	0.75	1.0[a]
			2.25[e]	1.0[a]
trans-**13a**	2.87 (−)	1.13	1.37	1.0[a]
cis-**14a**	2.50 (+)	1.10	1.25	1.0[a]
			3.62[e]	1.0[a]
trans-**14a**	2.37 (+)	1.05	1.25	1.0[a]
			3.75[e]	1.0[a]
erythro-**15b**	9.62 (+)	1.16 (B)	7.00	1.0[a]
threo-**16b**	3.12 (+)	1.16 (B)	2.12	1.0[a]
erythro-**16b**	3.12 (+)	1.24 (B)	1.87	1.0[a]
erythro-**16c**	1.25 (+)	1.20 (B)		
threo-**17a**	2.12	1.0[a]	1.12	1.0[a]
erythro-**17a**	2.00	1.0[a]		
threo-**18a**	8.12 (−)	1.17 (B)	3.50 (+)	1.07
erythro-**18a**	5.25 (−)	1.12	2.62	1.0[a]
threo-**18e**	5.00	1.0[a]		
erythro-**18e**	8.75	1.0[a]		
erythro-**18g**[f]	9.50	1.0[a]		
19a	2.50 (+)	1.10	1.50	1.0[a]
19b	3.75 (+)	1.23 (B)	2.75	1.0[a]

Table 1 *(continued)*

Compound	CSP 1		CSP 2	
	k_1' (sign)	α	k_1' (sign)	α
20b	5.25 (−)	2.05 (B)	2.62 (+)	1.24 (B)
20e	15.75	1.0[a]		
21a	4.87 (−)	1.05	1.50	1.0[a]
21b	11.87 (−)	1.07	4.62 (−)	1.05
22b	6.00 (−)	1.52 (B)	3.37 (+)	1.18
23a	2.87	1.0[a]		
24b	5.00 (+)	1.55 (B)	2.50	1.0[a]
25a	3.75	1.0[a]	1.75	1.0[a]
26a	7.62 (+)	1.15 (B)	3.12 (−)	1.08
27a	7.75	1.0[a]	2.12 (−)	1.11
cis-**28a**	3.25	1.0[a]	1.87	1.0[a]
trans-**28a**	8.37 (+)	1.10 (B)	3.25	1.0[a]
trans-**28e**	3.62	1.0[a]	1.00	1.0[a]
29a	4.25 (−)	1.26	1.75 (+)	1.21
30a	5.87	1.0[a]		
30b	14.62	1.0[a]		
31a	3.50 (−)	1.32 (B)	1.75 (+)	1.21

Mobile phase: 10% 2-propanol in *n*-heptane, flow-rate 0.5 ml/min. The capacity factor (k_1') refers to the first enantiomer eluted (its sign of rotation is given in parentheses), and the separation factor (α) is the ratio of capacity factors of the enantiomers (B denotes baseline separation). No attempts were made to optimize the analytical conditions for the individual compounds.

[a] No separation.

[b] (1*R*)-*trans*-2-Benzamidocyclohexanol.

[c] (1*S*)-*trans*-2-Benzamidocyclohexanol.

[d] Measured after 8 months of performance.

[e] Mobile phase: 5% 2-propanol in *n*-heptane.

[f] (+/−)-N-Benzoylephedrine.

separated enantiomers of the *cis*- and *trans*-isomer (Fig. 3).

The effect of conformation on the separation behaviour can be followed by comparison of compounds **19–32**, which have fixed geometry and exist in one conformation. As can be seen, on CSP 1 the diequatorial *trans*-isomers **22b**, **24b**, **29a** and **32a** are well separated, whereas the *trans*-diaxial isomers (**21a**, **21b**, **23a**, **30a**, **30b**) are separated poorly, if at all. Also, the twistane *trans*-isomer (**27a**), in which the dihedral angle between the functional groups is 150°, is not separated on CSP 1, whereas with the *trans*-90° isomer (**26a**) we observed a baseline separation. Interestingly, the generally less effective CSP 2 separates not only the twistane derivative (**26a**) but also the isomer (**27a**), being thus complementary to CSP 1. The bicyclo[2.2.2]octane derivative *trans*-**28a** (dihedral angle 120°) is baseline separated on CSP 1, whereas the epimeric *cis*-**28a** (about 0°) shows only an inflex (neither of them was separated on CSP 2). No separation was observed for the twistane *cis*-isomer (**25a**) with 30° dihedral angle. On the other hand, the *tert.*-butylcyclohexane *cis*-derivatives (**19b** and **20b**) (with approximately 60° dihedral angle) are separated completely. Summing up, CSP 1 resolved all benzamido alcohols of our set that have dihedral angles from about 60° to about 120°.

The elution order of enantiomers separated on CSP 1 is reversed (with the exception of **21b**) as compared with the order observed on CSP 2 (which is of opposite chirality). This suggests the same type of chiral recognition on both columns, which in the case of CSP 1 is apparently enhanced by polar operation of the nitro groups.

The analytes have two potential hydrogen

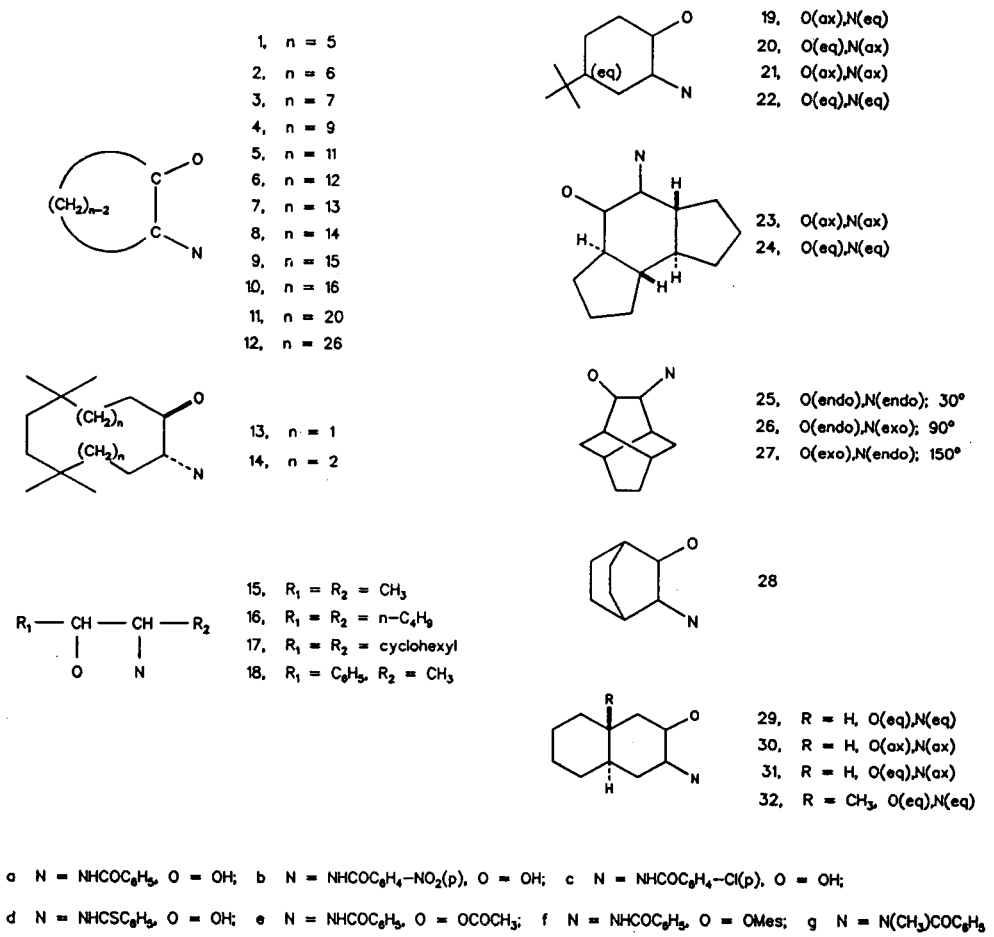

Fig. 2. Amino alcohol derivatives studied.

bonding sites —the hydroxy and the benzamido groups— which can play an important role in chiral recognition. In order to assess the importance of hydrogen bonding between the CSP and the hydroxyl group in the analyte, we converted some of the benzamides into benzamido acetates (*trans*-**1e**, *cis*- and *trans*-**2e**, *threo*- and *erythro*-**18e**, **20e**, *trans*-**28e**, **29e**). None of them was separated on CSP 1 or CSP 2. The same result was obtained with the mesylate *trans*-**2f**. Evidently, the presence of a free hydroxyl group is essential for separation. The inseparability of racemic N-benzoylephedrine (*erythro*-**18g**) indicates that the presence of a hydrogen on the amidic nitrogen atom is equally important.

Although it would be at present premature to draw any conclusions about the mechanism of chiral recognition on the CSPs described, it is evident that CSP 1 represents a wide-ranging chiral phase for separation of vicinal benzamido alcohols of various structural types. Further investigation in the direction of separator systems based on C_2 symmetry may thus be fruitful and is under way.

4. Acknowledgements

Financial support from the Grant Agency of the Academy of Sciences of the Czech Republic (Reg. No. 45505), as well as the Grant Agency

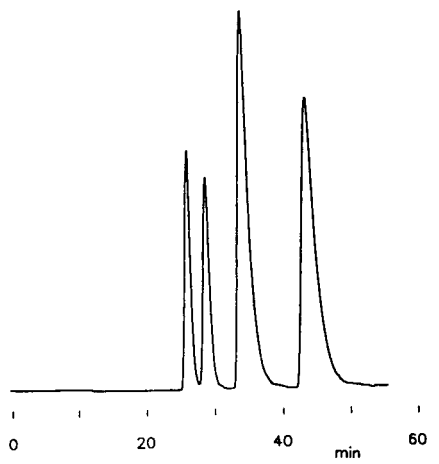

Fig. 3. Simultaneous separation of enantiomers of *cis*- and *trans*-2-benzamidocyclohexanols (*cis*- and *trans*-**2a**) on CSP 1. For chromatographic conditions see Table 1.

of the Czech Republic (Reg. No. 203/93/0059) is gratefully acknowledged.

5. References

[1] W.H. Pirkle and T.C. Pochapsky, *Chem. Rev.*, 89 (1989) 347.
[2] J.K. Whitesell, *Chem. Rev.*, 89 (1989) 1581.
[3] F. Mikes and G. Boshart, *J. Chromatogr.*, 149 (1978) 455.
[4] B. Feibush, A. Figueroa, R. Charles, K.D. Onan, P. Feibush and B.L. Karger, *J. Am. Chem. Soc.*, 108 (1986) 3310.
[5] T. Shinbo, T. Yamaguchi, K. Nishimura and M. Sugiura, *J. Chromatogr.*, 405 (1987) 145.
[6] L.R. Sousa, G.D.Y. Sogah, D.H. Hoffmann and D.J. Cram, *J. Am. Chem. Soc.*, 100 (1978) 4569.
[7] G.D.Y. Sogah and D.J. Cram, *J. Am. Chem. Soc.*, 101 (1979) 3035.
[8] J. Yamashita, T. Numakura, H. Kita, T. Suzuki, S. Oi, S.S. Miyano, H. Hashimoto and N. Takai, *J. Chromatogr.*, 403 (1987) 275.
[9] S. Oi, M. Shijo, J. Yamashita and S. Miyano, *Chem. Lett.*, (1988) 1545.
[10] J. Yamashita, H. Satoh, S. Oi, T. Suzuki, S. Miyano and N. Takai, *J. Chromatogr.*, 464 (1989) 411.
[11] S. Oi, M. Shijo, H. Tanaka, S. Miyano and J. Yamashita, *J. Chromatogr.*, 645 (1993) 17.
[12] A.V. Ingersoll and J.R. Little, *J. Am. Chem. Soc.*, 56 (1934) 2123.
[13] M. Siegel and K. Mislow, *J. Am. Chem. Soc.*, 80 (1958) 473.
[14] S. Kanoh, H. Muramoto, N. Kobayashi, M. Motoi and H. Suda, *Bull. Chem. Soc. Jpn.*, 60 (1987) 3659.
[15] E.G. McCasland and D.A. Smith, *J. Am. Chem. Soc.*, 72 (1950) 2190.
[16] E.G. McCasland, R.K. Clark and H.E. Carter, *J. Am. Chem. Soc.*, 71 (1949) 637.
[17] J. Sicher and M. Svoboda, *Collect. Czech. Chem. Commun.*, 23 (1958) 1252.
[18] M. Svoboda, M. Tichý and J. Sicher, *Collect. Czech. Chem. Commun.*, 23 (1958) 1958.
[19] M. Svoboda and J. Sicher, *Collect. Czech. Chem. Commun.*, 30 (1965) 2948.
[20] J. Sicher and M. Svoboda, unpublished results.
[21] M. Pánková and J. Sicher, *Collect. Czech. Chem. Commun.*, 30 (1965) 388.
[22] G. Fodor, V. Bruckner, J. Kiss and G. Ohegyi, *J. Org. Chem.*, 14 (1949) 337.
[23] J. Sicher, F. Šipoš and M. Tichý, *Collect. Czech. Chem. Commun.*, 26 (1961) 847.
[24] M. Pánková and M. Tichý, *Collect. Czech. Chem. Commun.*, 40 (1975) 634.
[25] M. Tichý and M. Pánková, *Collect. Czech. Chem. Commun.*, 40 (1975) 647.
[26] M. Tichý and L. Kniežo, *Collect. Czech. Chem. Commun.*, 43 (1978) 2154.
[27] J. Sicher, M. Tichý, F. Šipoš, M. Svoboda and J. Jonáš, *Coll. Czech. Chem. Commun.*, 29 (1964) 1561.
[28] R. Wylde and C. Atard, *Bull. Soc. Chim. Fr.*, (1972) 2799.
[29] R. Kuhn and O. Albrecht, *Ann.*, 455 (1927) 272.
[30] W.H. Pirkle, D.W. House and J.M. Finn, *J. Chromatogr.*, 192 (1980) 143.
[31] W.H. Pirkle, J.M. Finn, J.L. Schreiner and B.C. Hamper, *J. Am. Chem. Soc.*, 103 (1981) 3964.
[32] I.W. Wainer, T.D. Doyle, Z. Hamidzaden and M. Aldridge, *J. Chromatogr.*, 261 (1983) 123.
[33] W.H. Pirkle and C.J. Welch, *J. Org. Chem.*, 49 (1984) 138.
[34] W.H. Pirkle, M.H. Hyun and B. Bank, *J. Chromatogr.*, 316 (1984) 585.
[35] W.H. Pirkle, T.C. Pochapsky, G.S. Mahler, D.E. Corey, D.S. Reno and D.M. Alessi, *J. Org. Chem.*, 51 (1986) 4991.
[36] F. Gasparrini, D. Misiti, C. Villani and F. La Torre, *J. Chromatogr.*, 539 (1991) 25.
[37] W.H. Pirkle and J.A. Burke, *J. Chromatogr.*, 557 (1991) 173.
[38] B. Gallinella, F. La Torre, R. Cirilli and C. Villani, *J. Chromatogr.*, 639 (1993) 193.
[39] A. Dobashi, Y. Dobashi, K. Kinoshita and S. Hara, *Anal. Chem.*, 60 (1988) 1985.

ELSEVIER

Journal of Chromatography A, 667 (1994) 19–28

JOURNAL OF CHROMATOGRAPHY A

Effect of mobile phase composition on the enantioselectivity of chromatographic separation on a quinine-bonded silica stationary phase

P.N. Nesterenko*[,a], V.V. Krotov[b], S.M. Staroverov[b]

[a]*Department of Analytical Chemistry, Lomonosov State University, Leninskie Gory, 119899 Moscow, Russian Federation*
[b]*JV BioChemMack, Lomonosov State University, Leninskie Gory, 119899 Moscow, Russian Federation*

(First received August 18th, 1992; revised manuscript received December 10th, 1993)

Abstract

The effect of the nature and of the composition eluent on the enantiomer separation of 2,2,2-trifluoro-1-(9-anthryl)ethanol (TFAE) on a chiral stationary phase under HPLC conditions was studied. A series of solvents with different properties were examined as the mobile phase. The best enantioselectivity was achieved with pure benzene, methylene chloride and carbon tetrachloride. The results obtained are discussed in accordance with the three-point interaction model and solvatochromic parameters of the solvents. It is shown that the selectivity of enantiomer separation depends mainly on the hydrogen-accepting ability and dipolarity–polarizability parameters of the solvent. A simplified model of the retention and separation of TFAE enantiomers is proposed.

1. Introduction

Over the last decade there has been a considerable increase in the number of publications dedicated to enantiomer separations by HPLC with chiral stationary phases (CSPs). For enantiomer separation there should be at least a three-point interaction between the chiral bonded selector and the molecule of an optically active sample compound. These conditions are provided with different silica surface modifiers [1,2]. The development of new stationary phases remains the main way to improve the enantioselectivity of chromatographic separations [3–5]. In our opinion, however, the resources of already developed CSPs have not been exhausted and can be improved by optimization of the mobile phase composition.

A number of workers have attempted to find relationships between enantioselectivity and composition of achiral mobile phase in chiral phase liquid chromatography [6–9]. Most of the work has involved binary or tertiary solvent systems. Generally, these studies were concerned with elucidating the influence of polar additives to mobile phase on the enantioselectivity of separation. Siret *et al.* [7] found a unique reversal of the elution order of enantiomers on changing from hexane–2-propanol to hexane–chloroform or hexane–methylene chloride mobile phases. A similar result was observed by Pirkle *et al.* [9] but for normal- and reversed-phase modes. However, the effect of the nature of the organic solvent used as a single-solvent mobile phase on the separation of enan-

* Corresponding author.

0021-9673/94/$07.00
SSDI 0021-9673(93)E1296-C

tiomers has not been investigated. In this study we considered both the influence of polar additives in the mobile phase and the nature of the organic solvent on the enantioselectivity of separation of (*R*,*S*)-2,2,2-trifluoro-1-(9-anthryl)ethanol [(*R*,*S*)-TFAE] on a quinine-bonded chiral stationary phase (CSP).

2. Experimental

The measurements were carried out with a liquid chromatographic system composed of a Beckman (Berkeley, CA, USA) Model 114M pump, a Rheodyne (Cotati, CA, USA) Model 7125 injection valve with a 20-μl loop and a Uvicord S 2238 UV detector (LKB, Bromma, Sweden) with 254- and 365-nm interference filters. The stainless-steel column (250 × 4.0 mm I.D.) was slurry packed with quinine-bonded silica. The CSP with bonded quinine was prepared by modification of the surface of silica (Silasorb Si 300, 5 μm; Lachema, Brno, Czech Republic) with the triethoxysilyl derivative of quinine:

$$\equiv Si{-}OH + (C_2H_5O)_3Si(CH_2)_2Quin \longrightarrow \equiv Si{-}O{-}\underset{\displaystyle |}{\overset{\displaystyle |}{Si}}(CH_2)_2Quin$$

where Quin =

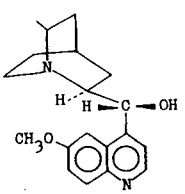

A 10-g amount of silica dried under vacuum at 200°C was treated with the triethoxysilyl derivative of quinine in 100 ml of dry toluene at 100°C for 10 h. The modified silica was washed with benzene, diethyl ether, ethanol and acetone. The sample contained 5.6% C, which corresponds to 0.5 mmol/m^2 of bonded quinine molecules. Part of the prepared CSP was treated with trimethylchlorosilane for end-capping residual silanol groups.

Optically pure (*S*)- and (*R*)-TFAE isomers were purchased from Aldrich (Milwaukee, WI, USA). Chromatographic-grade hexane, 2-propanol, methylene chloride, carbon tetrachloride and chloroform (J.T. Baker) and purified benzene, toluene, *o*-, *m*- and *p*-xylene, bromobenzene, benzonitrile and 1,1-dichlorethane were used for mobile phase preparation. The elution order of enantiomers was determined on the retention of pure (*S*)- and (*R*)-TFAE.

3. Results and discussion

Among the most useful CSPs are the "brush-type" phases, which consist of a silica matrix with covalently bonded chiral groups. Most "brush-type" CSPs contains at least three functional groups required for chiral recognition in accordance with Dalgliesh's work [10]. For quinine this concept is applicable. Quinine and TFAE provide a hydroxyl group within the molecules suitable for intermolecular hydrogen bonding, and they contain aromatic fragments for π–π interactions. These interactions combined with steric hindrance are responsible for the separation of optical isomers of arylalkylcarbinols and binaphthols with quinine-type CSPs [11–15].

3.1. Role of the structure of arylalkylcarbinols on retention and enantioselectivity of separation

Arylalkylcarbinols are the most often investigated substrates for optical resolution with quinine CSPs. The following conclusions have been drawn regarding the retention and separation of optical isomers of these compounds. First, it has been observed that steric hindrance of the alkyl group on the assymmetric centre is important for obtaining a good separation factor [11,14]. However, the volume of CF_3, CH_3 and C_2H_5 substituents on the chiral centre of alkylphenylcarbinols can be calculated to be insufficient for the appearance of steric hindrance by interaction with quinine residues. There was no visible resolution for the corresponding racemic alkylphenylcarbinols on this chiral phase [14]. Second, it has been shown that

the donor–acceptor properties of substituents of the phenyl rings play an important role. With decreasing electron-donating ability of a *para* substituent on the phenyl ring of carbinols [4-CH_3 >unsubstituted > 4-Cl > 4-$(CH_3)_2N$ > 4-CF_3 > 3, 4-Cl_2] the capacity factor for the first eluted enantiomer increases from 2.3 to 6.8. At the same time, the enantioselectivity of separation is slightly changed from 1.05 to 1.10 [14]. The replacement of a methyl group with a trifluoromethyl group adjacent to the chiral centre of carbinols causes an increase in the α and k' values. As concluded, the hydrogen bond between the C_9-OH group of the bonded quinine with the OH group of arylalkylcarbinols remains a strong interaction that defines the enantioselectivity of separation.

3.2. Chiral recognition model of bonded quinine to 2,2,2-trifluoro-1-(9-anthryl)ethanol

TFAE was chosen for this study because it is a well investigated compound; it meets many requirements for multi-point interactions of selector and selectand and has been separated with α values between 1.1 and 1.17 using three chiral stationary phases containing quinine residues covalently attached to the silica surface via different routes as a chiral selector [11,12,15]. The absorption maximum of TFAE at 320–360 nm allows mobile phase solvents that are UV absorbing up to 280 nm or higher to be used.

It can be assumed that the retention mechanism of TFAE on quinine CSPs is similar to that for polar compounds on amino-bonded stationary phases in normal-phase LC. There are three models, proposed by Snyder and Shunk [16], Scott and Kucera [17] and Hennion *et al.* [18], which are applicable for the description of retention on polar amino-bonded phases. For the correct choice one should consider the main types of interaction of TFAE isomers with a quinine CPS:

(1) Usually, a "one-to-one" interaction of the solute (TFAE) with the quinine moiety of a "brush-type" CSP is considered for chiral recognition.

(2) A TFAE molecule can displace any number of preadsorbed solvent molecules. However, with separated enantiomers the distinction in retention and enantioselectivity of separation is defined by displacement of different numbers of solvent molecules that interact with definite functional group(s) near the asymmetric centre of the CSP. The C_9-OH group of bonded quinine would be one of them.

(3) The interaction between TFAE and solvent molecules can contribute to k'. This interaction may be of some importance for α if related to group(s) which is (are) responsible for chiral recognition (*e.g.*, the OH group in the TFAE molecule).

The above statements are generally satisfactory for the model proposed by Hennion *et al.* [18] for the retention of polar solutes on amino-bonded phases. This model can be used for a description of the retention of TFAE on a quinine CSP with hexane–2-propanol mixtures as mobile phase.

For one of enantiomers of TFAE one can propose that the formation of a hydrogen bond between the C_9-OH group of the quinine residue and the OH group of TFAE leads to displacement of at least one additional molecule of preadsorbed 2-propanol in comparison with its optical antipode. This leads to a dependence of enantioselectivity α on the nature of the mobile phase.

3.3. Influence of the nature of the mobile phase

Several mobile phases have been used for the separation of TFAE enantiomers on quinine CSPs, *e.g.*, hexane–2-propanol [11,13,15], methylene chloride, acetonitrile–methylene chloride [12] and benzene [15], and different separation factors were obtained. In order to evaluate this effect we studied the influence of the nature of the mobile phase on the enantioselectivity of separation by using binary and single-solvent mobile phases.

Binary mobile phases

In the first step, different binary solvent systems consisting of hexane, benzene, carbon tetrachloride, toluene and *o*-, *m*- and *p*-xylene and with various contents of 2-propanol and

methanol were studied as mobile phases. It was found (Table 1) that an increase in the alcohol content led in all instances to a decrease in the retention times of the TFAE isomers and in enantioselectivity (Figs. 1 and 2). These results confirm that hydrogen bonding between the quinine CSP and TFAE is a determining factor for enantioselectivity in aprotic solvents. According to this, a different number of polar solvent molecules may be displaced from quinine residues during the formation of surface diastereomeric complexes.

As shown in Fig. 3, the plots of log α *versus* content of 2-propanol for different bulk solvents are not straight and are closely related to the curve for titration of quinine groups by 2-propanol in hexane. Fig. 3 shows only one region (−log [IP] from 2 to 2.8–3.0) that is approximately linear. In this region the hydrogen-bonding interactions between the solute and quinine became stronger with decrease in the 2-propanol content. A further decreasing in the polar solvent content should lead to a convex curve owing to the growing contribution to hydrogen bonding interactions of traces of water present in the organic solvent. The enantioselectivity for pure bulk solvents is dependent on their water content. For high concentrations of 2-propanol (2–5%) the curve is concave. This may be connected with self-association of 2-propanol molecules in the mobile phase and stabilization of the quinine–2-propanol associate.

A similar dependence (Fig. 3) was obtained for (*R*, *S*)-β,β-binaphthol and hexane–2-propanol mobile phases with various contents of the polar constituent. It should be mentioned that in accordance with NMR investigations [19], the hydrogen bonding is the dominant interaction in the chiral recognition of β,β-binaphthol with bonded quinine.

Dobashi *et al.* [8] investigated the retention mechanism and the role of hydrogen bonding in the separation of enantiomers of *N*-acetyl-D,L-leucine O-methyl ester on a diamide-bonded L-valine chiral stationary phase. The calculated values of log α for hexane–2-propanol mobile phases show a similar dependence (Fig. 3) as obtained for TFAE and β,β-binaphthol with quinine CSPs. The chiral recognition of the diamide CSP–*N*-acetyl-D,L-leucine O-methyl ester is connected with stronger hydrogen-bonding interactions than for the TFAE–quinine CSP system, so the "titration curve" of log α *versus* N_{IP} was observed at higher concentrations of 2-propanol in hexane. It should be noted that the hydrogen bonding was also the main interaction for the diamide-bonded L-valine CSP.

On replacement of hexane with other nonpolar organic solvents, *e.g.*, benzene or carbon tetrachloride, the character of the log α–N_{IP} relationship does not change significantly (Fig. 3). A similar dependence of log α as a function of 2-propanol content was obtained.

The nature of the polar additive to the mobile phases remains important. Stuurman *et al.* [12] investigated the influence of the type of alcohol and water as polar additives to the mobile phase on the retention and separation of TFAE. There was no significant difference between 2-propanol, *tert.*-butanol and 1-pentanol, and a slight decrease of retention and selectivity was noted for methanol as additive. The influence of water was the same as for the addition of alcohols. The author's conclusion [12] about the weak competition of polar additives (alcohols, water) with (*R*)- and (*S*)-TFAE for interaction sites of quinine residues is not, however, in good agreement with our results.

Single-solvent mobile phases

One could propose that the separation factor α should be increased significantly when pure aprotic solvents are used as mobile phases. Therefore, it was of interest to compare the effects of pure solvents with different properties and polarities on chiral recognition and enantioselectivity. Different solvents were investigated as mobile phases for the separation of (*R*)- and (*S*)-TFAE on the quinine-bonded CSP. The characteristics of the chosen solvents are summarized in Table 2.

The data in Table 3 show enantioselectivity for (*R*,*S*)-TFAE, confirming the supposition that the hydrogen donor–acceptor ability of a pure solvent is an important part of chiral recognition with a quinine CSP. The retention times of the

Table 1
Influence of 2-propanol content on retention and separation of (*S*)- and (*R*)-TFAE

Solvent	2-Propanol content (%, v/v)	k'_1	$1/k'_1$	α
Hexane	0.5	17.99 (13.96)[a]	0.06 (0.07)	1.10 (1.10)
	1.0	8.01 (6.33)	0.13 (0.16)	1.08 (1.06)
	2.5	3.93 (2.29)	0.26 (0.44)	1.07 (1.04)
	5.0	1.72 (1.23)	0.58 (0.81)	1.06 (1.03)
	10.0	0.87 (0.62)	1.14 (1.61)	1.03 (1.02)
	20.0	0.58	1.73	–[b]
Benzene	0	2.80	0.36	1.46
	0.1	2.67	0.37	1.42
	0.2	1.57	0.64	1.35
	0.4	1.21	0.83	1.24
	0.5	1.13	0.89	1.25
	1.0	0.96	1.02	1.23
	2.0	0.57	1.75	1.20
Toluene	0	1.36	0.74	1.28
	0.2	1.03	0.97	1.23
	1.0	0.86	1.16	1.17
o-Xylene	0	1.74	0.57	1.26
	0.2	1.10	0.91	1.20
m-Xylene	0	2.00	0.50	1.35
	0.2	1.22	0.85	1.25
	1.0	0.88	1.14	1.22
p-Xylene	0	1.44	0.69	1.26
	0.2	1.22	0.82	1.22
	1.0	0.88	1.14	1.18
Bromobenzene	0.2	1.17	0.86	1.10
Carbon tetrachloride	0	15.04	0.07	1.53
	0.1	14.21	0.07	1.39
	0.2	8.56	0.12	1.28
	0.4	4.69	0.27	1.19
	1.0	1.89	0.52	1.13
	2.0	0.93	1.07	1.09
	5.0	0.49	2.04	1.0
Carbon tetrachloride	0.1[c]	14.36	0.07	1.32
	0.2	10.72	0.09	1.22
	0.5	4.78	0.21	1.09
	1.0	2.31	0.43	1.04

[a]Data obtained with undried hexane.
[b]No resolution of peaks.
[c]Methanol was used as a polar component.

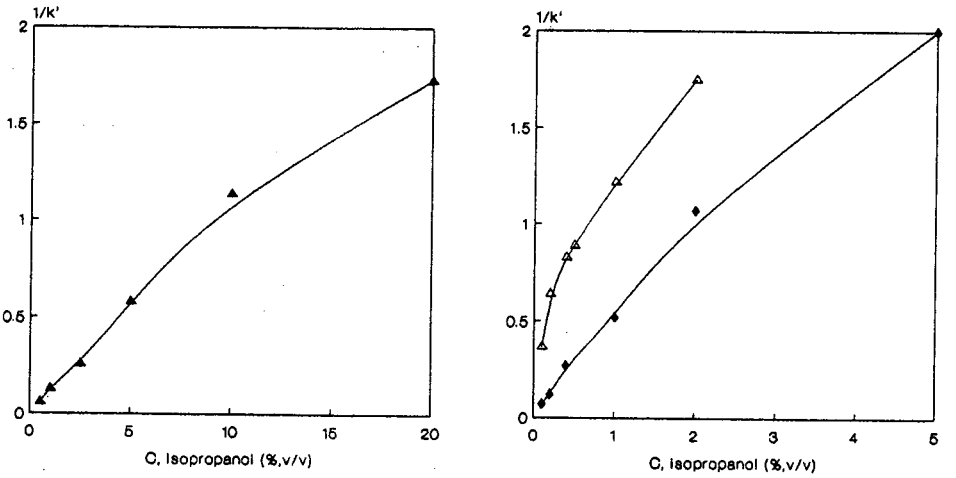

Fig. 1. Plot of $1/k'_1$ of (*R*)-TFAE *versus* concentration of 2-propanol in (▲) hexane, (△) benzene and (◆) carbon tetrachloride.

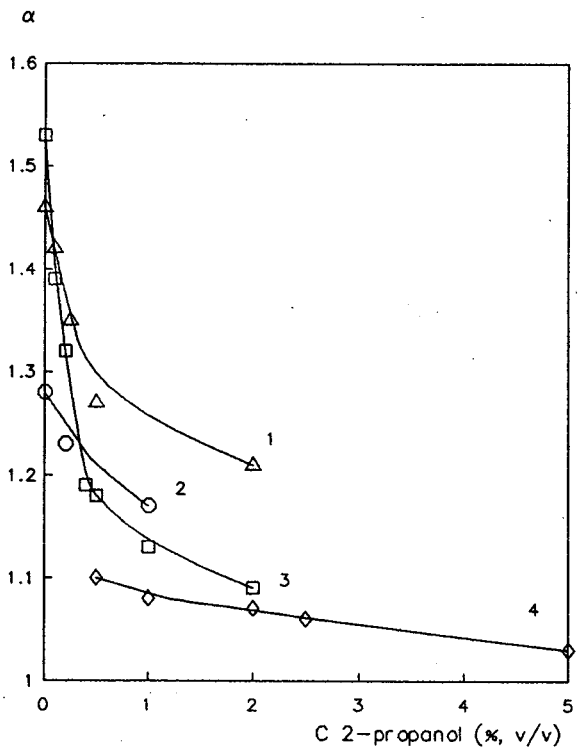

Fig. 2. Plot of the enantioselectivity α of (*R*,*S*)-TFAE *versus* the content of 2-propanol in (1) benzene, (2) toluene, (3) carbon tetrachloride and (4) hexane.

weakly retained enantiomer of TFAE are not in a good agreement with the polarity of the chosen solvents. Thus, k'_1 values of 0.41 and 11.91 were observed respectively; with dibutyl ether ($P = 1.65$) and carbon tetrachloride ($P = 1.56$), the corresponding values of α are 1.00 and 1.53, respectively. The correlation of enantioselectivity with solvent selectivity parameters was carried out to obtain a better understanding of the results obtained and optimization of the mobile phase.

Two scales are mainly used to classify solvent properties in liquid chromatography. The first and most common is the Snyder solvent triangle [21] and the other is the solvatochromic scale of Kamlet *et al.* [22]. Both of them characterize hydrogen donor–acceptor ability and dipolarity–polarizability properties of solvents. It should be noted that a good correlation has been established between the solvent triangle and solvatochromic scales of solvent strength and selectivity [21].

The solvatochromic scale of Kamlet *et al.* includes the parameters π, α, β and δ, describing the solvent dipolarity–polarizability, hydrogen bond acidity, hydrogen bond basicity and the polarizability correction factor, respectively. The

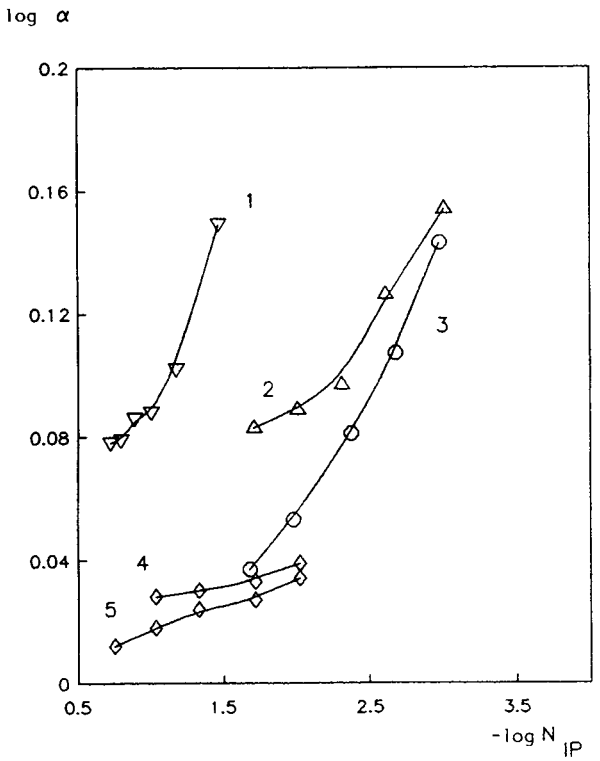

Fig. 3. Plot of log α *versus* log (content of polar solvent in the mobile phase). Stationary phases: (1) diamide-L-valine CSP and (2–5) quinine CSP. Solutes: (1) N-acetyl-D,L-leucine O-methyl ester, (2–4) (*R*,*S*)-TFAE and (5) (*R*,*S*)-β,β-binaphthol. Mobile phases: (1,4,5) hexane–2-propanol, (2) benzene–2-propanol and (3) carbon tetrachloride–2-propanol. Curve 1 was calculated from literature data [8].

values of these parameters are presented in Table 2. The polarizability correction term δ is zero for non-chlorinated alyphatic solvents, 0.5 for polychlorinated aliphatics and 1.0 for aromatic solvents. The correlations of enantioselectivity with the corresponded solvatochromic parameters are presented in Fig. 4.

Often these solvent parameters are used as linear energy parameters in an LSER (linear solvation energy relationship) [21]. Following the above reasoning and in accordance with previous results [21]:

$$\alpha = \alpha_0 + s\pi + a\alpha^* + b\beta + d\delta \quad (1)$$

The corresponding strong correlation of enantioselectivity with π, α^*, β and δ observed for TFAE is

$$\alpha = 1.54 + 0.13\pi - 0.67\alpha^* - 1.24\beta - 0.16\delta \quad (2)$$

$n = 10$, $r = 0.886$, F value = 4.57, significance = 0.063. The values of the parameters indicate that

Table 2
Solvatochromic parameters of solvents used as mobile phases

Solvent	Solvatochromic parameters[a] [22]		
	π	α^*	β
Hexane	−0.04		
Benzene	0.59	0	0.10
Toluene	0.55	0	0.11
Ethylbenzene	0.48		0.12
m-Xylene	0.47	0	0.13
p-Xylene	0.51	0	0.12
Methylene chloride	0.82	0.30	0
Chloroform	0.58	0.44	0
Ethylene dichloride	0.81	0	0
Carbon tetrachloride	0.28	0	0
Dibutyl ether	0.24	0	0.46
2-Propanol	0.48	0.76	0.95
Bromobenzene	0.79	0	0.06
Benzonitrile	0.90	0	0.41

[a] π = Dipolarity and polarizability; α^* = hydrogen bond donating acidity; β = hydrogen bond accepting basicity.

Table 3
Effect of the nature of the solvents on the enantioselectivity of the separation of (*S*)- and (*R*)-TFAE

No.	Mobile phase	*P* [21]	k'_1	k'_2	α
1	Benzene	3.19	2.80	4.09	1.46
2	Toluene	2.68	1.36	1.74	1.28
3	Ethylbenzene		1.65	1.87	1.14
4	*o*-Xylene		1.74	2.19	1.26
5	*m*-Xylene		2.00	2.70	1.35
6	*p*-Xylene	2.55	1.44	1.81	1.26
7	Dichloromethane	4.29	0.80	1.14	1.43
8	Chloroform	4.31	0.41	0.52	1.19
9	Carbon tetrachloride	1.56	15.04	23.01	1.53
10	Dichloroethane		0.26	0.40	1.50
11	Dibutyl ether	1.65	0.41	0.41	1.00
	Hexane–dichloromethane (60:40)		8.17	11.36	1.39
	Hexane–benzonitrile (80:20)		1.74	1.81	1.04

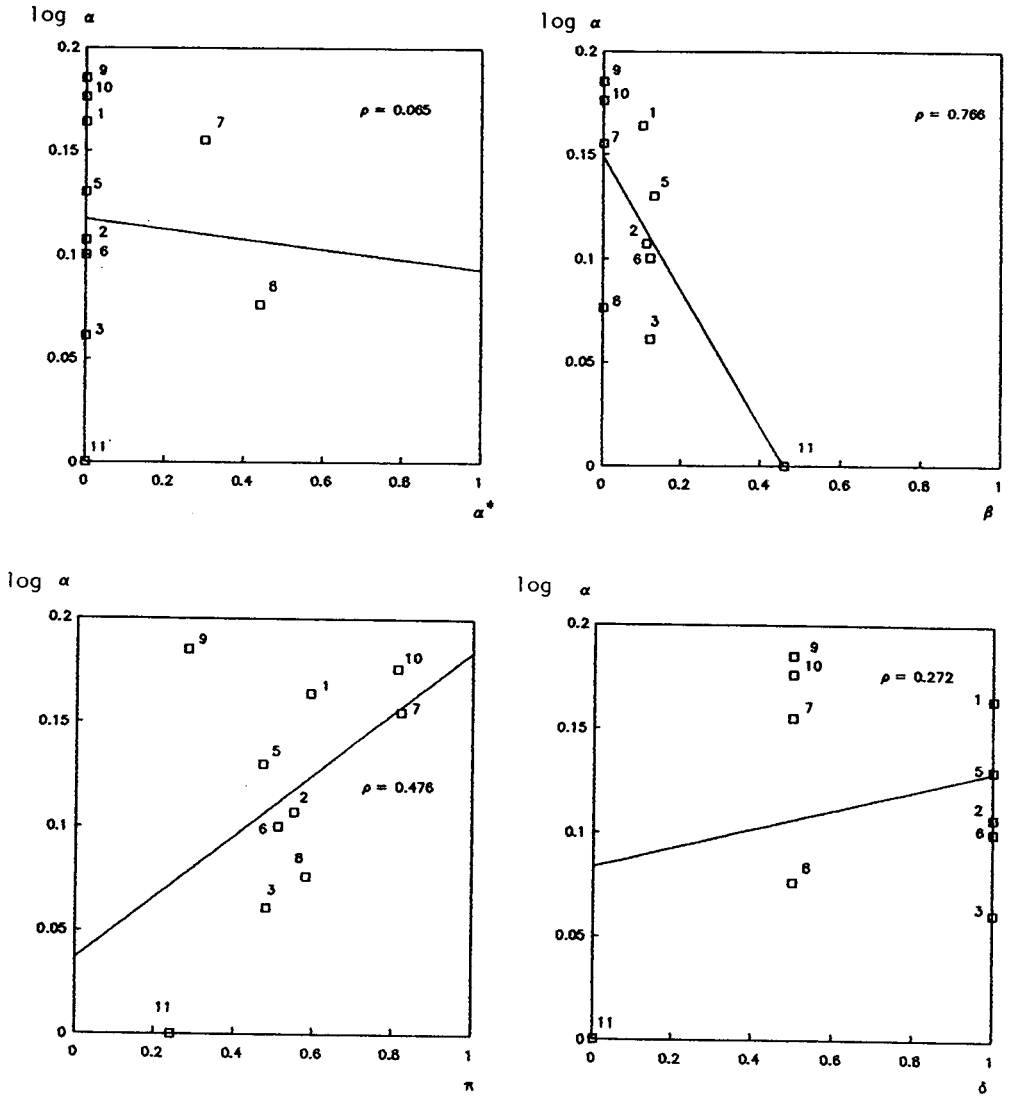

Fig. 4. Plot of enantioselectivity (α) *versus* solvatochromic parameters of organic solvents used as mobile phases. The numbering of the points for different solvents corresponds to those in Table 3.

a dipolarity–polarizability parameter was responsible for the separation of (*R*,*S*)-TFAE on the quinine CSP. Generally, it should be noted that the best enantioselectivity was achieved for solvents with weak hydrogen donor–acceptor ability (α, β) and high dipolarity–polarizability properties (π). The value of the free term 1.54 in eqn. 2 is equal to the hypothetical enantioselectivity in pure hexane.

The multiple linear regression analysis of the data obtained could be of more significance. Unfortunately, there were insufficient data for a representative analysis owing to the limited number of available organic solvents with known selectivity parameters and appropriate eluting power.

In practice, the use of non-polar and aprotic mobile phases in the absence of polar admixtures considerably increased the enantioselectivity for (*R*,*S*)-TFAE on a CSP with bonded quinine. The

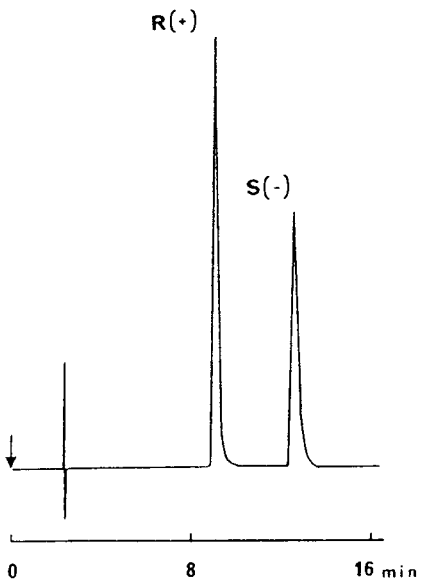

Fig. 5. Chromatographic separation of (*R*)- and (*S*)-TFAE on the quinine CSP. Mobile phase, carbon tetrachloride; flow-rate, 1 ml/min; UV detection at 365 nm.

best separation was achieved with carbon tetrachloride as mobile phase (Fig. 5).

This approach of correlating solvent characteristics could be useful for other CSPs that are thought to bind significantly via a hydrogen-bonding mechanism. A similar dependence of the enantioselectivity on the nature of solvent has already been observed in a study of asymmetric catalysis using alkaloids (quinine, ephedrine) covalently bonded to silica gel as a catalyst in the Michael reaction between conjugated cycloalkenones and aromatic thiols [23].

4. Conclusions

The solvent-induced effect on the chiral recognition of (*R*,*S*)-TFAE by a quinine CSP seems to be of great importance. The enantioselectivity is optimum with weakly polar, aprotic solvents as mobile phases. The presence of polar components in the mobile phase might change the enantioselectivity significantly. The results obtained confirmed the priority of the formation of a hydrogen bond between the chiral analyte TFAE and bonded quinine as CSP. The optimization of the mobile phase composition can be considered as an important means of improving the enantioselectivity of separation on other chiral stationary phases but with dominant hydrogen-bonding interactions for chiral recognition.

5. Acknowledgements

The authors are very grateful to W. Lindner (Karl-Franzens University, Graz, Austria) for fruitful discussions and valuable comments.

6. References

[1] M. Lienne, M. Caude, A. Tambute and R. Rosset, *Analysis*, 15 (1987) 431.
[2] V.A. Davankov *Zh. Vses. Khim. Ova.*, 34 (1989) 377.
[3] R. Dappen, V.R. Meyer and H. Arm, *J. Chromatogr.*, 361 (1986) 93.
[4] W.H. Pirkle, M.H. Hyun and B. Bark, *J. Chromatogr.*, 316 (1984) 585.
[5] Y. Saotome, T. Miyazawa and T. Endo, *Chromatographia*, 28 (1989) 513.
[6] M. Zief and L.J. Crane (Editors) *Chromatographic Chiral Separations*, Marcel Dekker, New York, 1988, Ch. 12.
[7] L. Siret, A. Tambute, M. Caude and R. Rosset, *J. Chromatogr.*, 498 (1990) 67.
[8] A. Dobashi, Y. Dobashi and S. Hara, *J. Liq. Chromatogr.*, 9 (1986) 243.
[9] W.H. Pirkle, M.H. Hyun and B. Bank, *J. Chromatogr.*, 316 (1984) 585.
[10] C.E. Dalgliesh, *J. Chem. Soc.*, (1952) 137.
[11] C. Rosini, C. Bertucci, D. Pini, P. Altemura and P. Salvadori, *Tetrahedron Lett.*, 26 (1985) 3361.
[12] H.W. Stuurman, J. Kohler and G. Shomburg, *Chromatographia*, 25 (1988) 265.
[13] C. Rosini, C. Bertucci, D. Pini, P. Altemura and P. Salvadori, *Chromatographia*, 24 (1987) 671.
[14] D. Pini, C. Rosini, C. Bertucci, P. Altemura and P. Salvadori, *Gazz. Chim. Ital.*, 116 (1986) 603.
[15] P.N. Nesterenko, V.V. Krotov and S.M. Staroverov, *Zh. Fiz. Khim.*, 65 (1991) 2671.
[16] L.R. Snyder and T.C. Shunk, *Anal. Chem.*, 54 (1982) 1764.
[17] R.P.W. Scott and P.J. Kucera, *J. Chromatogr.*, 149 (1978) 93.
[18] M.C. Hennion, C. Picard, C. Combellas, M. Caude and R. Rosset, *J. Chromatogr.*, 210 (1981) 211.

[19] P. Salvadori, C. Rosini, D. Pini, C. Bertucci, P. Altemura, G. Ucello-Baretta and A. Raffaelli, *Tetrahedron*, 43 (1987) 4969.
[20] A. Dobashi, K. Oka and S. Hara, *J. Am. Chem. Soc.*, 102 (1980) 7122.
[21] S.C. Rutah, P.W. Carr, W.J. Cheong, J.H. Pork and L.S. Snyder, *J. Chromatogr.*, 463 (1989) 21.
[22] M.J. Kamlet, J.L.M. Aboud, M.H. Abraham and R.W. Taft, *J. Org. Chem.*, 48 (1983) 2877.
[23] V.V. Krotov, S.M. Staroverov, P.N. Nesterenko and G.V. Lisichkin, *Zh. Obshch. Khim.*, 56 (1987) 2460.

ELSEVIER

Journal of Chromatography A, 667 (1994) 29–35

JOURNAL OF CHROMATOGRAPHY A

Determination of distribution coefficients for some 5-HT_3 receptor antagonists by reversed-phase high-performance liquid chromatography

Claude Kugel*, Blanche Heintzelmann, Joseph Wagner

Marion Merrell Dow Research Institute, 16 Rue d'Ankara, 67080 Strasbourg Cedex, France

(First received July 27th, 1993; revised manuscript received December 20th, 1993)

Abstract

It is of major interest to determine the physico-chemical properties, dissociation constants and lipophilicity of potential drugs owing to their implication in absorption mechanisms. The HPLC capacity factors appear to be attractive and readily accessible lipophilic parameters. An isocratic HPLC method was designed using a C_8 column to determine the relative lipophilicity for two sets of 5-HT_3 receptor antagonists, including tropine and quinolizine analogues. Dimethyloctylamine was added to the eluent to mask silanophilic interactions and lead to a predominant partitioning mechanism. The capacity factors determined by a monocratic procedure showed good correlations with the distribution coefficients obtained by the shake-flask method, showing the validity of capacity factors as lipophilicity descriptors for close analogues.

1. Introduction

The importance of lipophilic properties and electrostatic effects in drug–receptor interactions has long been recognized [1,2]. The dissociation constants (pK_a) of compounds influence directly their lipophilicity and therefore their absorption mechanism and their interaction with specific receptors. Lipophilicity, which can be represented by the logarithm of the partition coefficient (log P) of a compound between octanol and an aqueous buffer, is one of the properties often modified to improve the biological activity or the transport properties of a molecule.

The use of reversed-phase chromatography has been proposed as an alternative to the traditional shake-flask procedure for the lipophilicity determination of compounds. Highly significant correlations have been reported between the logarithm of the octanol–water partition coefficients, log P, and the logarithm of the reversed-phase capacity factors, log k' [3,4].

The use of different types of HPLC systems (octanol-like, reversed-phase, polymer-based or deactivated columns) has been reviewed [5] and illustrates the difficulties in finding a common methodology for quantitative structure–activity relationship (QSAR) studies using chromatographic parameters. As the development of pharmaceutical drugs involves the synthesis of large series of analogues, the situation is favoured because correlations are generally ob-

* Corresponding author.

0021-9673/94/$07.00
SSDI 0021-9673(93)E0066-4

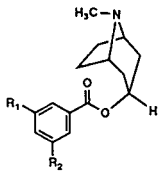

Compounds	Axial/Equat	R_1	R_2
1 (MDL 72222)	Ax	Cl	Cl
2	Eq	Cl	Cl
3	Ax	Me	Me
4	Eq	Me	Me
5	Ax	H	Me
6	Ax	F	F

Fig. 1. Structures of tropine analogues.

tained between log k' and log P for close analogues [6].

In this paper, we report the determination of the capacity factors of a series of 5-HT_3 receptor antagonists with tropine- and quinolizine-like structures [7,8], and their comparison with the corresponding shake-flask distribution coefficients. The HPLC method was first optimized to ensure the measurement of the chromatographic

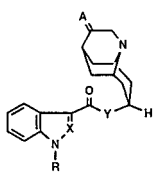

Compounds	Axial or Equat	X	Y	R	A
7 (MDL 73147)	Ax	CH	O	H	O
8	Eq	CH	O	H	O
9	Ax	CH	O	H	(H)(OH)
10	Eq	CH	O	H	(H)(OH)
11	Ax	CH	O	H	(H)(H)
12	Eq	CH	O	H	(H)(H)
13	Ax	N	NH	Me	O
14	Eq	N	NH	Me	O
15	Ax	N	NH	Me	(H)(OH)

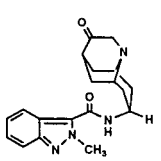

16

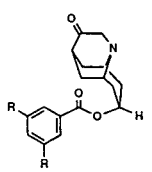

17 R = Me
18 R = Cl

Fig. 2. Structures of quinolizine analogues.

parameters with a predominant partitioning mechanism. The dissociation constants are also presented in order to highlight the importance of ionization. The structures of the compounds studied are given in Figs. 1 and 2.

2. Experimental

2.1. Reagents and materials

The 5-HT_3 receptor antagonists studied were synthesized at the Marion Merrell Dow Research Institute using the general scheme described previously [8] and were characterized by ^1H NMR spectrometry and elemental analysis (C,H,N). Their purities were checked by HPLC with UV detection. 1-Octanol and sulphuric acid were obtained from Merck (Darmstadt, Germany), dimethyloctylamine (DMOA) from ICN Pharmaceuticals (Plainview, NY, USA) and triethylamine (TEA) from Pierce (Rockford, IL, USA). The buffers were prepared with $NaH_2PO_4 \cdot H_2O$ and $Na_2HPO_4 \cdot 7H_2O$ (Merck) dissolved in water purified with a Milli-Q water system (Millipore) and the pH values were adjusted with dilute H_3PO_4 and NaOH (Merck). Acetonitrile (RS per HPLC grade) was obtained from Carlo Erba (Milan, Italy).

2.2. Determination of distribution coefficients (D) [9,10]

1-Octanol (500 ml) was washed three times with 50 ml of 2 M H_2SO_4, twice with deionized water, three times with 50 ml of 2 M NaOH and ten times with 50 ml of deionized water until the pH of the aqueous phase was neutral. Finally, the octanol was saturated with the buffer used.

The phosphate buffers were prepared by mixing the appropriate volumes of 0.1 M H_3PO_4, 0.1 M NaH_2PO_4, 0.1 M Na_2HPO_4 and 0.1 M NaOH to obtain the desired pH [11]. Volumes of 1–5 ml of approximately 10^{-3} M solutions of the compounds in the buffer or octanol were prepared and mixed with an equal volume of octanol or buffer, respectively, in 15-ml screw-capped vials. The mixtures were then shaken on

a reciprocal shaker at 24°C for 1 h. Afer centrifugation at 3900 rpm (24 600 *g*) for 10 min, the two phases were carefully separated and the concentrations of the compounds in the two phases were determined by HPLC. Usually partition experiments were run in duplicate and two HPLC analyses were carried out per sample. The distribution coefficients were calculated using the expression

$$D = \frac{\text{peak area in octanol phase}}{\text{peak area in buffer phase}}$$

2.3. Determination of capacity factors (k')

The k' values were determined on a Merck LiChroCART Superspher 60 RP-8e column (250 × 4 mm I.D.; 4 μm) with 600 ml of 0.01 *M* NaH_2PO_4, 400 ml of CH_3CN and 20 ml of DMOA (pH 7.4) at 40°C and a flow-rate of 1.2 ml/min using a Vista 5500 liquid chromatograph (Varian, Palo Alto, CA, USA) with a WISP 710 autosampler (Waters, Milford, MA, USA) and a UV 200 spectrophotometer (Varian) operated at 240 nm.

The k' value of each compound was calculated as $(t - t_0)/t_0$, where t is the retention time of the compound and t_0 the retention time of an unretained compound which was determined by injection of methanol.

2.4. Determination of protonation constants

Some of the compounds, *e.g.*, **7** (MDL 73147), were readily soluble at acidic pH in the 0.1 *M* KNO_3 medium used, but precipitated at pH values where deprotonation was more or less complete. It was therefore necessary to work with methanol–water (70:30) with no added inert salt.

For determination in water, 5×10^{-3} *M* solutions of the different compounds were obtained by dissolving a weighed amount of ligand (5–15 mg) in 5 or 10 ml of 0.1 *M* KNO_3 with an added excess of 1 *M* HCl (1.1–1.5 equiv.).

Titrations were performed using a semi-automatic Mettler DL20 Compact Titrator with a 1-ml burette (Mettler DV 401) and a combined microelectrode. Two types of electrodes were used: Metrohm EA 125 or Ross 8103 for the titration of small volumes, *i.e.*, 2 ml and Metrohm EA 120 for 5-ml volumes. The electrodes and pH meter were calibrated to read the pH values with six aqueous buffer solutions (pH 2.00, 4.00, 6.98, 9.94, 10.90 and 12.45). For the measurements in methanol–water (70:30), the glass electrode was conditioned overnight in the mixed solvent. Volumes of 2 or 5 ml of the 5×10^{-3} *M* solutions were back-titrated under nitrogen at 25°C with 0.1 *M* KOH. The Mettler titrator was linked to an IBM PC and the titration points were stored on floppy disk. Several programs were developed on the PC to calculate the equivalence points and plot the experimental titration curves. A simulation program was also written on the PC which allowed the calculation of the pK_a value by "best fit" between the experimental and simulated titration points.

3. Results and discussion

3.1. Determination of dissociation constants

It is well known that the partition coefficients (log P) and the capacity factors (log k') vary with pH in a sigmoidal manner for ionizable molecules [12–14]. Dissociation constants are key parameters if one wants to know the degree of ionization of a given compound. Tables 1 and 2 present pK_a values determined for some tropine and quinolizine analogues, respectively.

The values obtained for tropine and pseudotropine in methanol–water (70:30) mixture are 0.6–0.7 pH unit lower than in water. This decrease is in agreement with the variations observed for other amines [15].

The results for the quinolizine derivatives clearly show that the basicity of the tertiary amine of the quinolizine increases from the ketone **7** (MDL 73147) to the alcohol **9** and to the CH_2 analogues **11**; these increases are similar to those expected from the variations observed with various amines [2].

A wide range of acid dissociation constants

Table 1
Dissociation constants of the tropine analogues

Compound	pK_a [a]
Tropine	10.40[b], 9.85
Pseudotropine	10.05[b], 9.35
1 (MDL 72222)	8.70
2	8.45
3	8.90
4	8.60

[a] pK_a values obtained in methanol–water (70:30) at 25°C unless stated otherwise.
[b] pK_a values obtained in 0.1 *M* KNO_3 at 25°C.

were obtained from 6.35 for **7** to 9.2 for **11**, which leads to large differences in the ionization percentages at a given pH between 5 and 10. Therefore, it is essential to correlate log *D* and log *k'* determined at the same pH, as emphasized previously [16]. In this case the comparison of all the compounds as neutral species would require working at a pH above 10, which is not practical with silica-based reversed-phase packings. Polymer-based columns would be recommended for use at high pH but they appear to be less rugged [5] and have a poor separation efficiency owing to the low plate number. Nevertheless, the pH must not be considered as a limitation for chromatographic assessment of lipophilicity, as most of the time the pH of interest for pharmacological testing is the physiological pH 7.4, which is within the pH limitations for most reversed-phase packings.

Table 2
Dissociation constants of the quinolizine analogues

Compound	pK_a [a]
7 (MDL 73147)	6.35
9	8.10
11	9.17
13	6.35
15	8.60
18	5.95

[a] pK_a values obtained in methanol–water (70:30) at 25°C.

3.2. Effect of pH on retention times

The effect of pH on retention times is presented to demonstrate that log *k'* varies non-linearly with pH and therefore must be measured at the same pH as used for log *D* determinations.

As expected for these basic compounds, the retention times increase with increase in pH (Fig. 3). The pH variation experiments normally give sigmoidal curves. For the compounds studied the final plateau is not reached owing to the pH limitations of the column as discussed above except for **7** (MDL 73147), which has a lower pK_a of *ca.* 6.3. In addition, the pH effect appears much more important with the tropine analogues than with the quinolizine analogues: the presence of 40% of acetonitrile in the eluent gives shorter retention times for the quinolizine derivatives and hence the capacity factors are less affected by the pH changes than those of the tropine analogues, for which slight variations are easily noticeable owing to their much later elution.

3.3. Effect of amine modifier

The addition of dimethyloctylamine to the eluent decreases the retention times, as shown in

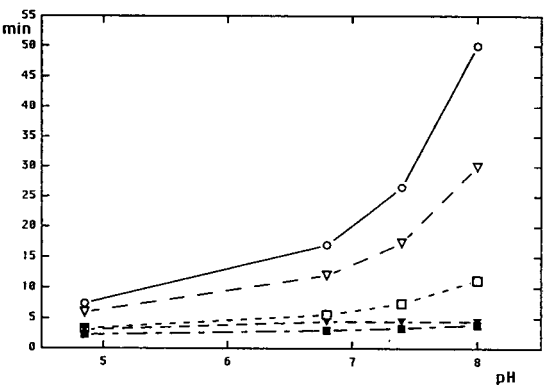

Fig. 3. Plot of retention times *versus* pH for various MDL compounds. Column, Merck 60 RP-8e; mobile phase, 0.01 *M* NaH_2PO_4–CH_3CN–DMOA (60:40:2, v/v/v) with adjusted pH; flow-rate, 1.2 ml/min; temperature, 40°C; UV detection at 240 nm. ○ = **1** (MDL 72222); ▽ = **3**; ▼ = **7** (MDL 73147); ■ = **9**; □ = **11**.

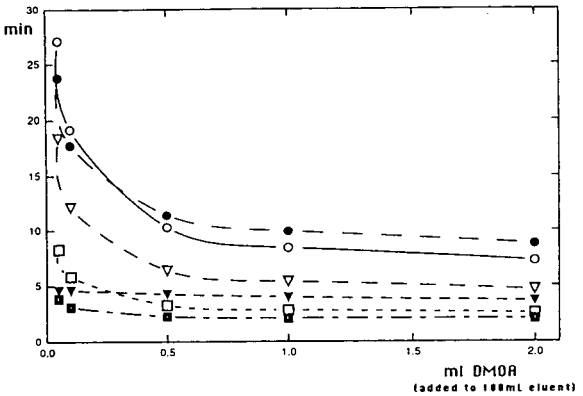

Fig. 4. Plot of retention times *versus* amount of DMOA for selected MDL compounds. Column, Merck 60 RP-8e; mobile phase, 0.01 *M* NaH_2PO_4–CH_3CN–DMOA (60:40:*x*, v/v/v) (pH 7.4); flow-rate, 1.2 ml/min; temperature, 40°C; UV detection at 240 nm. ○ = **1** (MDL 72222); ● = **2**; ▽ = **3**; ▼ = **7** (MDL 73147); ■ = **9**; □ = **11**.

Fig. 4. The effect is noticeable up to 0.5% DMOA and levels off between 0.5% and 2% DMOA. The tropine analogues appear to be more sensitive than the quinolizine analogues to the DMOA addition, except for **11**, which has a higher pK_a. Owing to their higher pK_a values, the tropine analogues show a greater percentage of protonated form at a given pH and therefore may interact more strongly with the residual silanols of the reversed-phase packing which are not fully masked by low percentages of DMOA. Similar variations were observed on adding triethylamine in the eluent. The addition of 1–2% of tertiary amine ensures the determination of the capacity factors resulting mainly from the partitioning mechanism, by minimizing the hydrogen bonding effects. The amine is dynamically coated on the stationary phase and interacts preferentially with the residual silanols, rendering them less accessible to hydrogen bonding with the eluted compounds.

Highly deactivated commercial columns may be used, as suggested by Kaliszan *et al.* [17], without a requirement for amine modifiers to obtain capacity factors as lipophilicity descriptors, but were not available at the beginning of this study. A deactivated column has subsequently been tested, but the peak shapes were not satisfactory and the addition of DMOA was still necessary [18].

3.4. Correlation between log D and log k'

The log k' values were obtained with an HPLC eluent containing 40% of acetonitrile rather than determining the log k'_w (capacity factor in a totally aqueous eluent). Although log k'_w is very attractive for constructing a lipophilicity scale [3,4,17], it is extrapolated from capacity factors measured at different percentages of organic modifier. A simplified and quicker method of lipophilicity determination in which a single measurement is made was found to be more suitable for our needs. In addition, correlations between log k' measured in aqueous organic mixtures and log P have been obtained for well defined classes of compounds [4,6].

Our approach after having optimized the chromatographic system by varying some fundamental parameters (percentage of organic modifier, buffering capacity) was to use these conditions for the measurement of capacity factors.

The capacity factors for the tropine analogues determined on a C_8 column are given in Table 3, along with the corresponding octanol–water distribution coefficients at the same pH (7.4). A significant correlation is obtained between log $D_{7.4}$ and log k'; the equation obtained by linear regression (Eq. 1) is given below and Fig. 5 shows the resulting plot.

$$\log D_{7.4} = 2.291\ (\pm 0.226) \log k' + 0.685\ (\pm 0.081) \quad (1)$$

$n = 6$; $r = 0.981$; S.D. = 0.114

The satisfactory linear correlation with a slope different from unity indicates similar physicochemical properties for the two partitioning processes, but with different intrinsic thermodynamic behaviours, which are termed homeoenergetic [19].

Similarly, a correlation was obtained for the quinolizine analogues (Eq. 2) between the capacity factors and log $D_{7.4}$ given in Table 4, as shown in Fig. 6.

Table 3
Capacity factors obtained with the C_8 column and distribution coefficients for the tropine analogues

Compound	k' [a]	Log k'	Log $D_{7.4}$ [a] (octanol–pH 7.4 buffer)
1 (MDL 72222)	3.19	0.50	1.78
2	4.21	0.62	2.03
3	1.66	0.22	1.34
4	2.01	0.30	1.51
5	0.96	−0.02	0.59
6	1.07	0.03	0.64

Chromatographic conditions for log k' determination: column, Merck LiChroCART 60 RP-8e (250 × 4 mm I.D.; 4 μm); mobile phase, 0.01 *M* NaH_2PO_4–CH_3CN–DMOA (60:40:2, v/v/v) (pH 7.4); flow-rate, 1.2 ml/min; temperature, 40°C; UV detection at 240 nm. Distribution coefficients, log $D_{7.4}$, between 1-octanol and 0.1 *M* phosphate buffer (pH 7.4); temperature, 24°C.
[a] Values are given ±0.05.

$$\log D_{7.4} = 1.616\,(\pm 0.152)\log k' + 1.719\,(\pm 0.077) \quad (2)$$
$$n = 12;\ r = 0.958;\ \text{S.D.} = 0.252$$

Again, in view of the slope value, the free energies involved in both processes are similar but not identical.

These correlations can be used to predict the partition coefficients of new compounds from their capacity factors, which are easily measured by chromatography. In both instances (tropine and quinolizine), the dynamic equilibrium descriptor of lipophilicity, log k', was found to correlate with the slow equilibrium descriptor, log D.

The poor correlation factor ($r = 0.82$) obtained on analysing both series of compounds together (Eq. 3) highlights that this approach must be used only for structurally related compounds.

Table 4
Log $D_{7.4}$ and log k' values obtained with the C_8 column for quinolizine analogues

Compound	k'	Log k'	Log $D_{7.4}$ (octanol–pH 7.4 buffer)
7 (MDL 73147)	1.39	0.143	2.33
8	1.41	0.149	2.25
9	0.27	−0.569	0.87
10	0.43	−0.371	1.36
11	0.42	−0.377	1.05
12	0.42	−0.377	1.35
13	0.97	−0.013	1.39
14	0.70	−0.157	1.53
15	0.16	−0.796	0.12
16	0.46	−0.337	0.85
17	6.01	0.779	2.85
18	8.97	0.953	3.10

Log k' and log $D_{7.4}$ determination: see comments in Table 3.

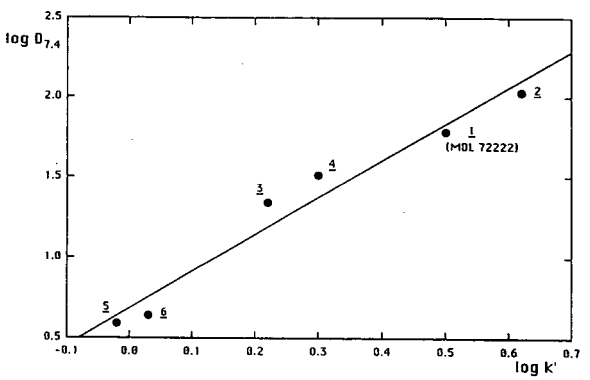

Fig. 5. Plot of octanol–buffer distribution coefficients (log $D_{7.4}$) *versus* capacity factors (log k'), obtained by reversed-phase HPLC, for six tropine analogues. Column, Merck 60 RP-8e; mobile phase, 0.01 *M* NaH_2PO_4–CH_3CN–DMOA (60:40:2, v/v/v) (pH 7.4); flow-rate, 1.2 ml/min; temperature, 40°C; UV detection at 240 nm.

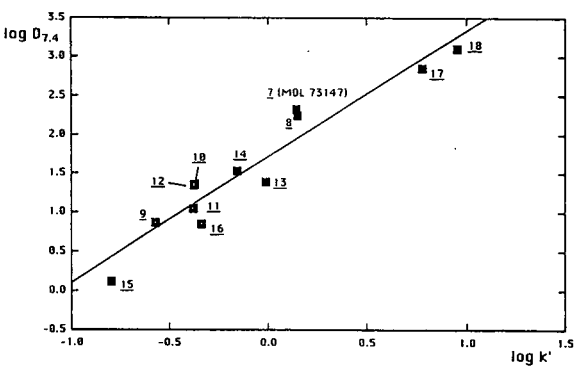

Fig. 6. Plot of octanol–buffer distribution coefficients (log $D_{7.4}$) *versus* capacity factors (log k'), obtained by reversed-phase HPLC, for twelve quinolizine analogues. Column, Merck 60 RP-8e; mobile phase, 0.01 *M* NaH_2PO_4–CH_3CN–DMOA (60:40:2, v/v/v) (pH 7.4); flow-rate, 1.2 ml/min; temperature, 40°C; UV detection at 240 nm.

$$\log D_{7.4} = 1.357\,(\pm 0.240)\log k' + 1.446\,(\pm 0.111) \quad (3)$$

$n = 18$; $r = 0.816$; S.D. = 0.455

Similar studies were conducted using the same set of quinolizine analogues with a C_{18} phase, but gave a poor correlation coefficient of 0.72 [18]. Other workers have reported better correlations with C_8 than with C_{18} stationary phases [20]. The residual silanols appear to be more easily accessible to the amine modifier (DMOA or TEA) for octyl than octadecyl phases, leading to a more efficient lowering of silanophilic interactions and therefore a partitioning system that better mimics the octanol–water system.

4. Conclusions

The measurement of HPLC retention data as lipophilicity descriptors presents many advantages over the determination of traditional shake-flask partition coefficients: it appears simple, rapid and readily automatable. In addition, it allows an estimation of hydrophobicity for highly lipophilic compounds or compounds available only in small amounts. The final interest for pharmaceutical molecules is the tentative correlation of the lipophilicity parameters with biological data, leading to QSAR studies. Obviously, the hydrophobic parameters are not the only ones that influence the biological activity, and electronic or steric parameters may play a significant role, but lipophilicity appears to be the main factor for membrane penetration and therefore bioavailability. A more detailed quantitative structure–retention relationship (QSRR) study with multivariate correlation would be necessary to determine the influence of the different parameters (hydrophobic, steric and electronic) on the retention of the tropine and quinolizine analogues in HPLC. Nevertheless, considering the range of variations generally observed with biological data and the good level of correlation between log k' and log $D_{7.4}$ for some ionizable 5-HT_3 receptor antagonists, the capacity factors obtained on a C_8 column in the presence of DMOA are considered to be good descriptors of relative lipophilicities.

5. Acknowledgement

We thank Dr. M.W. Gittos for his contribution to this work through his constant interest in the subject and the synthesis of the compounds.

6. References

[1] C. Hansch and A. Leo, *Substituent Constants for Correlation Analysis in Chemistry and Biology*, Wiley, New York, 1979.
[2] S.H. Yalkowsky, A.A. Sinkula and S.C. Valvani, *Physical Chemical Properties of Drugs*, Marcel Dekker, New York, 1980.
[3] D.J. Minick, D.A. Brent and J. Frenz, *J. Chromatogr.*, 461 (1989) 177.
[4] T. Braumann, *J. Chromatogr.*, 373 (1986) 191.
[5] R. Kaliszan, *Quant. Struct. Act. Relat.*, 9 (1990) 83.
[6] M.J.M. Wells and C.R. Clark, *J. Chromatogr.*, 284 (1984) 319.
[7] R.C. Miller, M. Galvan, M.W. Gittos, P.L.M. van Giersbergen, P.C. Moser and J.R. Frozard, *Drug Dev. Res.*, 28 (1993) 87.
[8] M.W. Gittos and M. Fatmi, *Actual. Chim. Ther.*, 16 (1989) 187.
[9] T. Fujita, J. Iwasa and C. Hansch, *J. Am. Chem. Soc.*, 86 (1964) 5175.
[10] A. Leo, C. Hansch and D. Elkins, *Chem. Rev.*, 71 (1971) 525.
[11] G. Gomori, *Methods Enzymol.*, 1 (1955) 143.
[12] C. Horváth, W. Melander and I. Molnár, *Anal. Chem.*, 49 (1977) 142.
[13] S.H. Unger and G.H. Chiang, *J. Med. Chem.*, 24 (1981) 262.
[14] K. Miyake, *Chem. Pharm. Bull.*, 33 (1985) 769.
[15] K.K. Mui, W.A.E. Mc Bryde and E. Nieboder, *Can. J. Chem.*, 52 (1974) 1821.
[16] A.P. Cheung and D. Kenney, *J. Chromatogr.*, 506 (1990) 119.
[17] R. Kaliszan, A. Kaliszan, T.A.G. Noctor, W.P. Purcell and I.W. Wainer, *J. Chromatogr.*, 609 (1992) 69.
[18] C. Kugel and J. Wagner, unpublished results.
[19] W. Melander, J. Stoveken and C. Horváth, *J. Chromatogr.*, 199 (1980) 35.
[20] D.J. Minick, J.H. Frenz, M.A. Patrick and D.A. Brent, *J. Med. Chem.*, 31 (1988) 1923.

ELSEVIER

Journal of Chromatography A, 667 (1994) 37–45

JOURNAL OF CHROMATOGRAPHY A

Hydrophobicity parameters of 2-chloro-2′-deoxyadenosine and some related analogues and retention in reversed-phase liquid chromatography

Viera Reichelová*[,a,b], Freidoun Albertioni[a], Jan Liliemark[a]

[a]*Department of Clinical Pharmacology, Karolinska Hospital, S-171 76 Stockholm, Sweden*

[b]*Cancer Research Institute, Bratislava, Slovak Republic*

(First received August 9th, 1993; revised manuscript received November 23rd, 1993)

Abstract

Hydrophobicity parameters expressed as the logarithm of the partition coefficient (log P) and ionization constants (pK_a) for 2-chloro-2′-deoxyadenosine and some related nucleoside analogues (2-fluoroarabinosyladenine, 2-chloroadenosine and 5′-chloro-5′-deoxyadenosine) are reported. The effects of methanol concentration and the pH of the mobile phase on the retention of the studied compounds in a reversed-phase system were examined. The relationship between hydrophobicity parameters and the retention in the HPLC system was investigated. A fairly good linear correlation was obtained when log k' values ($r = 0.960$) and/or log k'_w values (extrapolated from the relationship between log k' and the percentage of methanol to 100% water) ($r = 0.959$ and 0.967, respectively) were correlated with log P values.

1. Introduction

2-Chloro-2′-deoxyadeonosine (CdA; Cladribine) (Fig. 1) is a purine analogue that has shown great therapeutic efficacy in phase I and II clinical trials in lymphoid malignancies [1–3]. Although well tolerated by patients after oral administration, the bioavailability of CdA is only approximately 50% [4]. Several factors are of primary importance for oral absorption, including drug aqueous solubility, resistance to loss from the absorption site due to enzymatic or chemical degradation and the partition coefficient of the drug.

The pH partition hypothesis for gastrointestinal drug absorption assumes that only the non-ionized form of the drug passes through a biological membrane which is regarded as lipoidal in nature [5]. The more lipophilic character the drug possesses, the more easily it passes through the membranes and enters the blood circulation. Knowledge of the partition coefficient (P) of CdA is therefore important when predicting the drug absorption through the wall of gastrointestinal mucosa. Moreover, the determination of lipophilicity may provide useful information about the potential of the drug for penetration of the blood–brain barrier and thus drug delivery to the CNS.

The n-octanol–water system was chosen by Hansch and Dunn [6] as the standard for the determination of P, as several properties of n-

* Corresponding author. Address for correspondence: Department of Clinical Pharmacology, Karolinska Hospital, S-171 76 Stockholm, Sweden.

0021-9673/94/$07.00
SSDI 0021-9673(94)00027-7

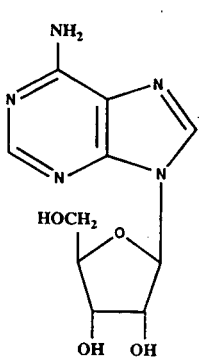

Ado

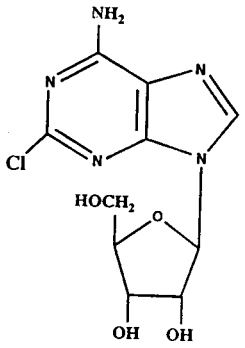

2-Cl-Ado

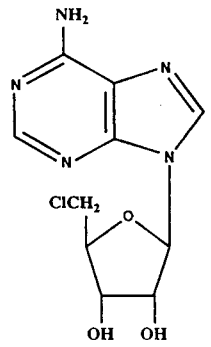

5′-Cl-5′-dAdo

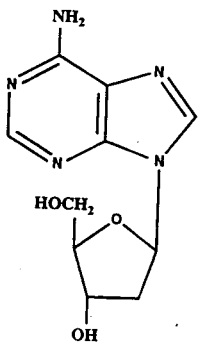

dAdo

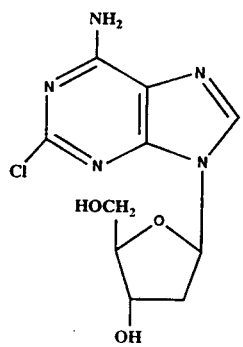

CdA

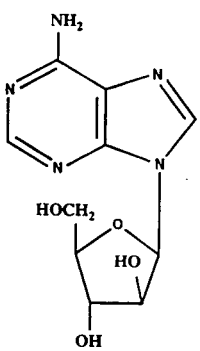

ara A

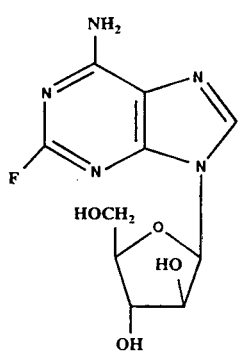

F-ara A

Fig. 1. Structural formulae of the compounds studied.

octanol allowed it to serve as a model for the hydrophobic and hydrogen-bonding effects that might be encountered in biological membranes. The shake-flask method for the determination of P is conventional, but laborious and time consuming.

The isotropic nature of octanol [7] is in contrast to the strongly anisotropic typical biomembrane (with phospholipids and cholesterol molecules forming a bilayer in which proteins and other lipids are incorporated). Therefore, there have been numerous proposals to use HPLC to determine the hydrophobicity of the drug [7–10]. A chemically bonded phase does not behave as a liquid and hence the retention in a reversed-phase LC system seems to resemble the dynamic partitioning in biological membranes more than the static liquid–liquid distribution in the *n*-octanol–water system.

The purpose of this paper is to report the apparent partition coefficients (P values determined by the shake-flask method) and ionization constants (pK_a values determined by UV spectrophotometry) of CdA and some structurally related nucleoside analogues including 2-fluoroarabinosyladenine (F-araA), 2-chloroadenosine (2 Cl-Ado) and 5′-chloro-5′-deoxyadenosine (5′-Cl-5′-dAdo) (Fig. 1) and to investigate the relationship between hydrophobicity parameters and retention in a reversed-phase LC system.

2. Experimental

2.1. Materials

The nucleosides Ado, dAdo, 2-Cl-Ado, araA and 5′-Cl-5′-dAdo and 1-octanol were obtained from Sigma (St. Louis, MO, USA). F-araA was a generous gift from Dr Ze've Shaked (Berlex, Alameda, CA, USA). CdA was synthesized by Dr. Zygmunt Kazimierczuk (Foundation for the Development of Diagnostics and Therapy, Warsaw, Poland). Methanol was of HPLC grade (J.T. Baker, Deventer, Netherlands). Analytical-reagent grade potassium dihydrogenphosphate (KH_2PO_4), sodium dihydrogenphosphate ($NaH_2PO_4 \cdot H_2O$), disodium hydrogenphosphate ($Na_2HPO_4 \cdot 2H_2O$), citric acid ($C_6H_8O_7 \cdot H_2O$), formic acid (HCOOH), acetic acid (CH_3COOH), orthophosphoric acid (H_3PO_4) and hydrochloric acid (HCl) were purchased from Merck (Darmstadt, Germany) and potassium hydroxide (KOH) from Kebo (Spånga, Sweden).

2.2. Determination of partition coefficients (P)

The shake-flask method according to Cheung and Keney [11] was utilized for the determination of P values for CdA, 2-Cl-Ado, F-araA and 5′-Cl-5′-dAdo. Individual solutions for nucleosides with concentrations in the range 10^{-6}–10^{-5} M in 0.05 M KH_2PO_4 (pH 7) presaturated with 1-octanol were used for recording the UV spectra from 300 to 200 nm with a Hitachi U-2000 spectrophotometer. The absorbances at 260 nm were plotted against their concentrations and these linear plots were used for the calculation of the molar absorptivity (ε_{max}).

Volumes of 5 ml of freshly prepared buffer solutions were transferred into individual centrifuge tubes and 5 ml of 1-octanol presaturated with the buffer were added. The mixtures were shaken 100 times followed by centrifugation at 1000 g for 1 h. The partitioning between buffer and 1-octanol was performed at 22°C. The aqueous and the organic phases were separated and the UV spectra in the aqueous phases were recorded. The apparent P value of each nucleoside was determined according to the equation

$$P = \frac{(c)_{aq,0} - (c)_{aq,1}}{(c)_{aq,1}} \quad (1)$$

where $(c)_{aq,0}$ and $(c)_{aq,1}$ are the concentrations in the aqueous phases before and after partitioning, respectively. This calculation of the P values was used because only limited amounts of the compounds studied were available and the method using the approximation of P values from the decrease in the concentrations in the aqueous phase has been reported previously [12].

2.3. Determination of capacity factors (k′)

The capacity factors (k') were determined isocratically on a high-speed C_{18} (3-μm) column

(80 × 4.6 mm I.D.) (Perkin-Elmer, Norwalk, CT, USA) at 22°C using a Shimadzu (Kyoto, Japan) LC-9A pump, a CMA-240 autosampler (Carnegie Medicine, Stockholm, Sweden) and a Milton Roy (LDC Division, Riviera Beach, FL, USA) variable-wavelength detector at 265 nm. A Macintosh Classic computer (Apple, Chicago, IL, USA) equipped with Chromac 3.1. software (Drew, London, UK) was used for collecting the HPLC data. Aqueous mobile phases of 0.01 *M* KH_2PO_4 with various percentages of methanol and pH values at a flow-rate of 1 ml/min were used. The pH was adjusted with a few drops of either KOH or H_3PO_4 before methanol was added using a PHM 62 standard pH meter (Radiometer, Copenhagen, Denmark). A 20-pmol amount of each compound was injected.

The k' values were calculated as $(t_r - t_0)/t_0$, where t_r is the retention time of an individual compound and t_0 is the retention time of an unretained compound, which was determined as the time from injection to the first distortion of the baseline.

Linear regression analyses for the relationship between log k' or log k'_w and log P were performed on an IBM AT personal computer.

2.4. Determination of ionization constants (pK_a)

The ionization constants of all the compounds studied were determined by UV spectrophotometry according to Albert and Serjeant [13]. The method depends on the direct determination of three variables: the absorbances of the molecular species (neutral molecule), the totally ionized species and the partly ionized species.

Aqueous stock solutions of the compounds with concentrations of $2 \cdot 10^{-4}$–$5 \cdot 10^{-4}$ *M* were prepared. Glass-distilled water free from carbon dioxide was used for the preparation of all solutions and buffers.

The stock solutions were diluted tenfold with appropriate non-absorbing buffers whose pH values were chosen so that the compounds to be measured were present either as molecular species (phosphate buffer, pH 7.22) or totally ionized species (0.1–2 *M* HCl). Spectra in the range 200–300 nm of both species were compared for each compound and a wavelength was chosen at which the greatest difference between the absorbances of the two species was observed. The analytical wavelength chosen was 280 nm for Ado, dAdo, araA, CdA, 2-ClAdo and 5′-Cl-5′-dAdo and 250 nm for F-araA. A_i (absorbance of the ionized species) and A_m (absorbance of the molecular species) were then measured.

To determine the absorbance of the partly ionized species, the stock solutions were diluted as before but with 0.01 *M* buffers of citrate–phosphate (pH 3–3.6), formate (pH 3.7) and acetate (pH 4.3) and with 0.1–0.5 *M* HCl. The pH of all buffers was measured at 22°C. The absorbance of these solutions, A, was determined and the pK_a value for each compound was calculated from the appropriate equation:

$$pK_a = pH + \log\left(\frac{A - A_m}{A_i - A}\right) \quad \text{when } A_i > A_m \quad (2)$$

$$pK_a = pH + \log\left(\frac{A_m - A}{A - A_i}\right) \quad \text{when } A_i < A_m \quad (3)$$

where A is the absorbance of a partly ionized substance measured in a buffer of a known pH.

3. Results and discussion

The ionization constants and the partition coefficients of CdA and related nucleoside analogues are given in Table 1.

When the pK_a values of Ado, dAdo and araA are compared with those of their analogues with a halogen atom (chlorine or fluorine) at the C-2 position of the purine ring, a tendency towards significantly lower values (by 2.5 pH units on average) is observed. In the case of CdA, substitution with a chlorine atom at the C-2 position of the purine ring decreases the basicity of the N-1 atom [14], which was confirmed by the finding of differences in protonation sites (the N-1 atom of dAdo and the N-7 atom of CdA) and differences in the pK_a values (1.4 for CdA compared with 3.8 for dAdo) [15]. This change renders the drug resistant to adenosine deaminase (ADA).

The pK_a value of CdA determined spectro-

Table 1
Partition coefficients and capacity factors of CdA and related nucleoside analogues

Compound	pK_a	$P \pm$ S.D.	Log P	k'	Log k'
Ado	3.47 (3.5)[a]	0.105 ± 0.003[a]	−0.979	25.52	1.41
araA	3.40	0.111 ± 0.004[a]	−0.955	19.01	1.28
F-araA	0.90	0.158 ± 0.015	−0.801	31.99	1.51
dAdo	3.79 (3.8)[b]	0.245 ± 0.002[a]	−0.611	35.24	1.55
2-ClAdo	0.79	0.429 ± 0.046	−0.368	87.90	1.94
5′-Cl-5′-dAdo	3.90	0.881 ± 0.051	−0.055	105.93	2.03
CdA	1.28 (1.4)[b]	1.059 ± 0.053	0.025	101.16	2.01

pK_a values were determined by UV spectrophotometry, P values by the shake-flask method (at four different concentrations of the compound), capacity factors by HPLC on a high-speed C_{18} (3 μm) column (80 × 4.6 mm I.D.) with a mobile phase of 0.01 M KH_2PO_4 with 3% MeOH (pH 7.0), flow-rate 1 ml/min and detection at 265 nm.
[a] Data from ref. 11.
[b] Data from ref. 15.

photometrically seems to be slightly lower than that in the literature (1.28 *vs.* 1.4). Although variations in pK_a values determined with different methods (such as UV spectrophotometry and potentiometry) have been reported [16], there may be other possible explanations. As the totally ionized species of the bases must be determined at not less than 2 pH units below pK_a, stronger acids, such as 1 M HCl, should be used for diluting the compounds with expected $pK_a < 2$. However, the acid-catalysed hydrolysis of the glycosidic bond of CdA [15], 2-Cl-Ado and to a lower extent also F-araA (data not shown) has been observed. In this way the accuracy of spectrophotometric determination of pK_a of such compounds may differ from that when other methods are used. Thus, the pK_a of 2-Cl-Ado and F-araA may be slightly higher than those we determined.

The position of the chlorine substituent is apparently of importance for the pK_a of the compound, as the pK_a of 5′-Cl-5′-dAdo, an adenosine analogue with a chlorine atom in the C-5 position of the sugar moiety, was found to differ from that of 2-Cl-Ado with a chlorine atom in the purine ring instead (3.90 for 5′-Cl-5′-dAdo *vs.* 0.79 for 2-Cl-Ado).

As regards the lipophilicity, these data clearly confirm that the introduction of a halogen atom into the molecule increases the lipophilic character of the compound [17,18]. The replacement of the hydrogen atom at the C-2 position of the purine ring in the molecules of Ado and dAdo with a chlorine atom increased the P values *ca.* fourfold (0.429 for 2-Cl-Ado *vs.* 0.105 for Ado, and 1.059 for CdA *vs.* 0.245 for dAdo). When the chlorine atom replaced the hydroxy group at the C-5 position of the sugar moiety, an eight-fold difference in partition coefficients of the halogenated and the parent compounds was found ($P = 0.881$ for 5′-Cl-5′-dAdo *vs.* 0.105 for Ado). In agreement with the literature [19], higher P values were observed for purine nucleosides and their halogenated analogues than their pyrimidine counterparts (Table 2).

As the traditional shake-flask method has a number of practical disadvantage [20], there has been considerable interest in the development and utilization of relationships between *n*-octanol–water partition coefficients (log P) and

Table 2
Partition coefficients of some purine and pyrimidine nucleosides and their halogenated analogues

Compound	P	Log P
Ado	0.105	−0.979
5′-Cl-5′-dAdo	0.881	−0.055
araC[a]	0.009	−2.050
5′-Cl-araC[a]	0.195	−0.710

[a] Data from ref. 25.

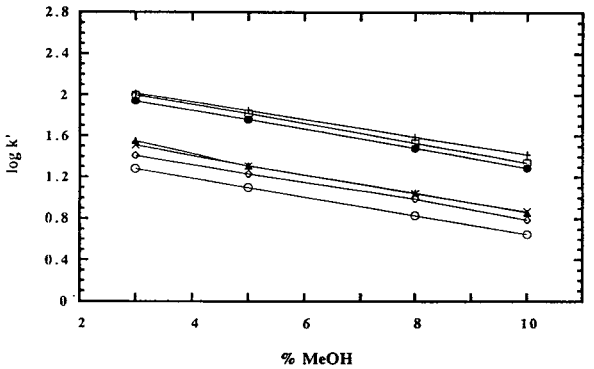

Fig. 2. Effect of the concentration of methanol in the mobile phase (pH 7) on the logarithm of the capacity factors ($\log k'$) of (○) araA, (◇) Ado, (▲) dAdo, (×) F-araA, (●) 2-ClAdo, (□) CdA and (+) 5′-Cl-5′-dAdo. Other conditions as in Experimental.

capacity factors ($\log k'$) in reversed-phase LC systems.

3.1. Retention in the reversed-phase LC system

We investigated the influence of methanol concentration and pH of the mobile phase on the retention of the compounds studied in reversed-phase LC. Good linearity between $\log k'$ for the compounds studied and the percentage of methanol in the mobile phase was observed at pH 7.0 (Fig. 2). However, the elution order of araA, dAdo and 5′-Cl-5′-dAdo did not follow the retention order predicted by P values (Table 1).

When mobile phases with various contents of methanol and pH were used, araA was always

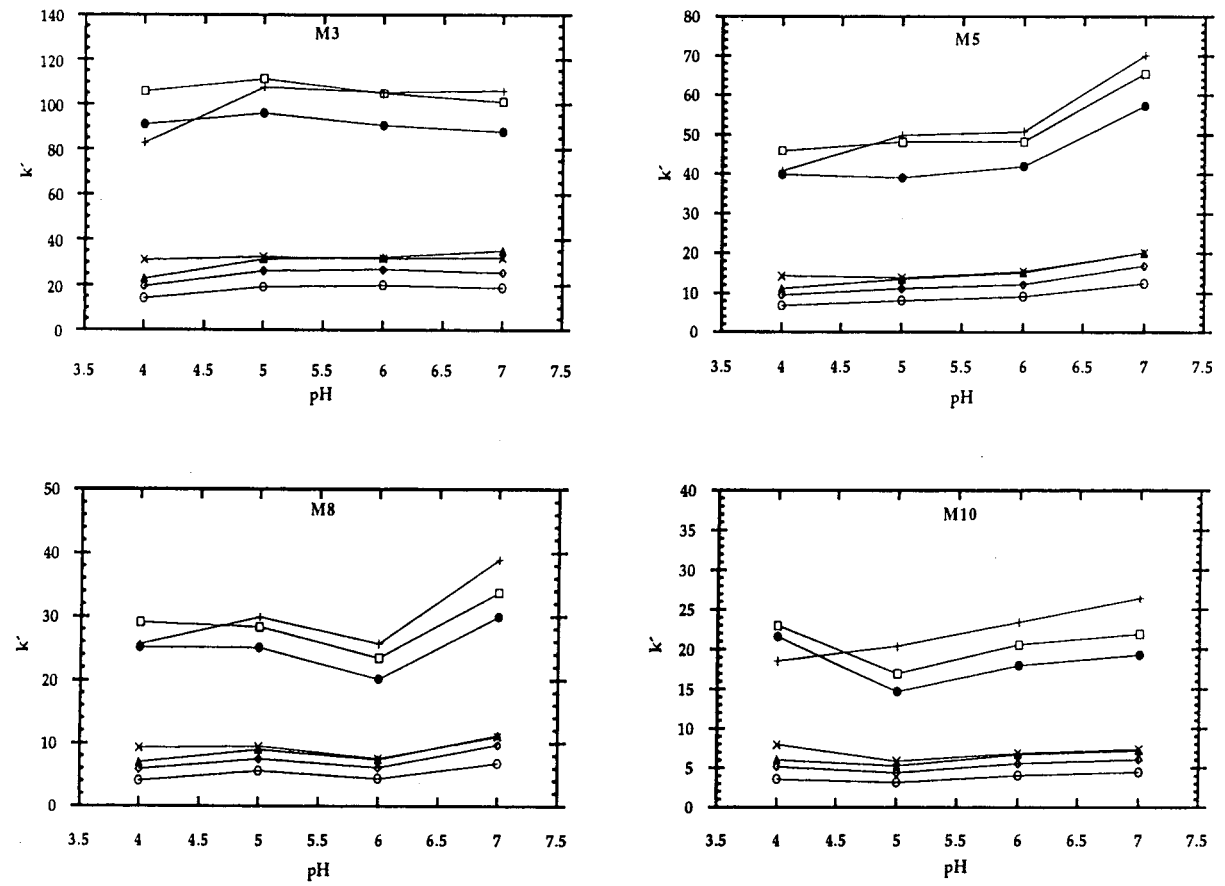

Fig. 3. Effect of pH of the mobile phase on capacity factors (k') of (○) araA, (◇) Ado, (▲) dAdo, (×) F-araA, (●) 2-ClAdo, (□) CdA and (+) 5′-Cl-5′-dAdo in the mobile phase with 3% (M3), 5% (M5), 8% (M8) and 10% (M10) of methanol.

eluted before Ado (Fig. 3). The same elution order in the reversed-phase system was observed by Cheung and Keney [11], despite the fact that the P value determined by the shake-flask method for araA was slightly higher than that of Ado (0.110 for araA *vs.* 0.105 for Ado). The calculated P value was lower (0.09) [11] but it was the same for both araA and Ado. In general, fairly large differences have been observed among partition coefficients determined by the shake-flask method by various workers [21,22]. Thus, a knowledge of the retention characteristics in a reversed-phase system is of great importance when the hydrophobicity is evaluated.

Despite its higher hydrophobicity compared with F-araA, dAdo ($P = 0.245$) was eluted before F-araA ($P = 0.158$) when the pH of the mobile phase was in the range of 4–5. This can be explained by the ionization of dAdo (pK_a = 3.8) with pH values in the range of $pK_a \pm 1$ or $pK_a \pm 2$ as dAdo was eluted after F-araA (pK_a = 0.90) when the pH of the mobile phases was 7.0.

In the mobile phases with pH > 5 and with more than 3% of methanol, 5′-Cl-5′-dAdo was retained longer than expected from its partition coefficient. Its elution order changed only when the pH of the mobile phase was changed from 4 to 5, seemingly owing to the ionization as the pK_a determined spectrophotometrically was 3.90.

Optimum separation of all compounds was accomplished with a mobile phase containing 8% of methanol at pH 7.0 (Fig. 4).

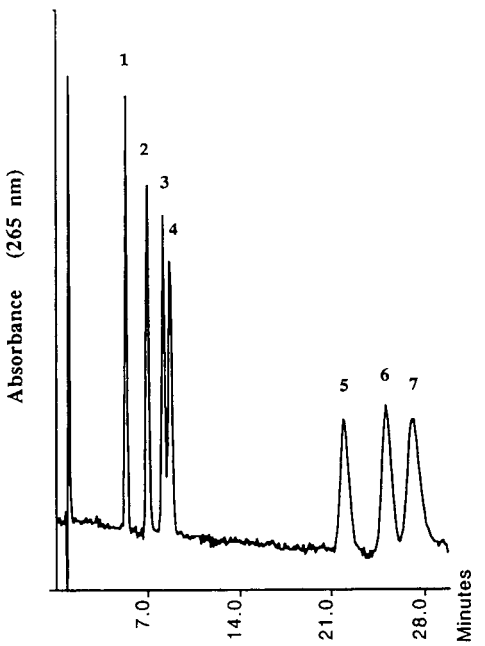

Fig. 4. Reversed-phase chromatographic separation of (1) araA, (2) Ado, (3) F-araA, (4) dAdo, (5) 2-ClAdo, (6) CdA and (7) 5′-Cl-5′-dAdo. Column, high-speed C_{18} (3 μm) (80 × 4.6 mm I.D.); mobile phase, 0.01 M KH_2PO_4 (pH 7.0) with 8% of methanol; flow-rate, 1 ml/min; detection 265 nm, 0.01 aufs; 20 pmol of each nucleoside injected.

3.2. Correlation between partition coefficients and capacity factors

In order to investigate whether the hydrophobicity of the compounds studied could be predicted by HPLC, the log k' values determined with a mobile phase containing 3% of methanol were plotted against log P values determined by the shake-flask method (Table 1, Fig. 5).

Using this monocratic approach, with a single mobile phase, a fair linear correlation was obtained as shown by the equation

$$\log k' = 2.06(\pm 0.062) + 0.72(\pm 0.094) \log P \quad (4)$$

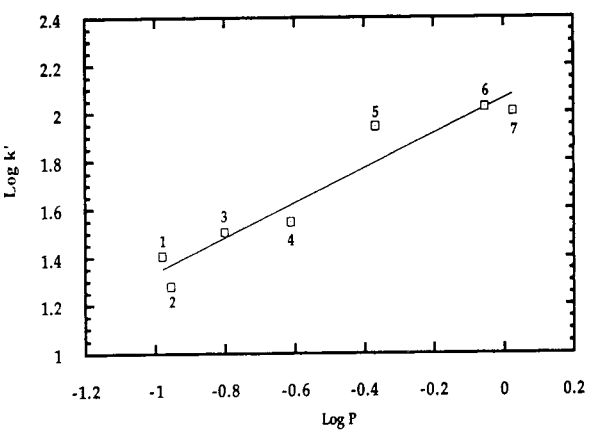

Fig. 5. Linear plot of log k' *vs.* log P of (1) Ado, (2) araA, (3) F-araA, (4) dAdo, (5) 2-ClAdo, (6) 5′-Cl-5′-dAdo and (7) CdA in a mobile phase of 0.01 M KH_2PO_4 (pH 7.0) with 3% of methanol. Other conditions as in Fig. 4.

$n = 7$, $r = 0.960$, S.D. = 0.095

where n is the number of compounds studied, r is the correlation coefficient and S.D. is the standard deviation of the equation.

However, strong evidence has been provided by several studies that extrapolated $\log k'_w$ values are more closely related to $\log P$ than the isocratic capacity factors [7,23,24], so $\log k'_w$ was proposed to describe the hydrophobicity of the solute directly.

When the polycratic approach was applied (using several mobile phases containing different percentages of methanol), both quadratic

$$\log k' = \log k'_w(\text{quadr}) + A\varphi^2 - S(\text{quadr})\varphi \quad (5)$$

and linear

$$\log k' = \log k'_w(\text{lin}) - S(\text{lin})\varphi \quad (6)$$

equations, where A and S(quadr, lin) are constants for a given solute–solvent combination and φ is the volume fraction of the organic modifier, were used to describe the relationship between solute retention and the composition of the binary mobile phase. The resulting data from regression analyses given in Table 3 clearly demonstrate a very good linear correlation with $r > 0.997$, despite the fact that the methanol content, φ, was in the range 0.03–0.10.

When $\log k'_w$ and $\log P$ were correlated, as good a linear correlation as that obtained using the monocratic approach was obtained, as represented by the equations

$$\log k'_w(\text{quadr}) = 2.35(\pm 0.057) + 0.74(\pm 0.087)\log P \quad (7)$$

$n = 7$, $r = 0.967$, S.D. = 0.088

$$\log k'_w(\text{linear}) = 2.33(\pm 0.063) + 0.73(\pm 0.095)\log P \quad (8)$$

$n = 7$, $r = 0.959$, S.D. = 0.096

Recently, several investigators have studied the relationship between lipophilicity and retention in a reversed-phase system for different classes of nucleosides and nucleoside analogues. Good linear correlations between $\log P$ values in n-octanol–water and retention times [17], $\log k'$ using the monocratic approach [11,25] or extrapolated $\log k'_w$ determined by the polycratic approach [26] were reported.

This work shows that hydrophobicity parameters of nucleoside analogues can be calculated from their $\log k'$ or $\log k'_w$ values. As many nucleoside analogues are used as drugs in the treatment of cancer and AIDS, the importance of physico-chemical properties including $\log P$ and pK_a should be emphasized, not only for retention in reversed-phase systems, but mostly for drug absorption and biological activity in general.

Based on the similarity of CdA lipophilicity

Table 3
Calculation of $\log k'_w$ values from the relationship between the percentage of methanol, φ, and $\log k'$ for nucleoside analogues

Compound	Regression[a]			
	Quadratic $\log k'_w$	r	Linear $\log k'_w$	r
Ado	1.63	0.999	1.67	0.9989
araA	1.55	1.000	1.55	1.000
F-araA	1.82	1.000	1.77	0.999
dAdo	1.89	0.998	1.82	0.997
2-ClAdo	2.22	1.000	2.23	1.000
5′-Cl-5′-dAdo	2.29	1.000	2.28	1.000
CDA	2.29	1.000	2.29	1.000

[a] Regression analyses were performed using the quadratic Eq. 5 and the linear Eq. 6 for the extrapolation of retention to $\varphi = 0$ (100% water); r = regression correlation coefficient.

(expressed as log P) with that of another clinically used drug, azidothymidine (AZT) (0.025 for CdA *vs.* 0.038 [11] or 0.05 [19] for AZT), which is known to enter the CNS, one would expect CdA to be able to penetrate the blood–brain barrier. This is indeed the case, as has recently been shown [3,27].

4. Acknowledgement

This work was supported by grants from the Swedish Cancer Society.

5. References

[1] E. Beutler, *Lancet*, 340 (1992) 952.
[2] G. Juliusson and J. Liliemark, *J. Clin. Oncol.*, 11 (1993) 679.
[3] A. Saven, H. Kawasaki and C. Carrera, *J. Clin. Oncol.*, 11 (1993) 671.
[4] J. Liliemark, F. Albertioni and M. Hassan, *J. Clin. Oncol.*, 10 (1992) 1514.
[5] R.E. Notari, *Biopharmaceutics and Clinical Pharmacokinetics*, Marcel Dekker, New York, 1980.
[6] C. Hansch and W. Dunn, *J. Pharm. Sci.*, 61 (1972) 1.
[7] T. Braumann, *J. Chromatogr.*, 373 (1986) 191.
[8] D.J. Minick, J. Sabatka and D. Brent, *J. Liq. Chromatogr.*, 10 (1987) 2565.
[9] D.J. Minick, J.H. Frenz and M.A. Patrick, *J. Med. Chem.*, 31 (1988) 1923.
[10] C. Yamagami, T. Ogura and N. Takao, *J. Chromatogr.*, 514 (1990) 123.
[11] A. Cheung and D. Keney, *J. Chromatogr.*, 506 (1990) 119.
[12] Z. Budvári-Bárány, G. Szász and K. Takács-Novák, *J. Liq. Chromatogr.*, 13 (1990) 1485.
[13] A. Albert and E.P. Serjeant, *The Determination of Ionization Constants*, Chapman and Hall, New York, 1984.
[14] L. Bennett, C. Chang and P. Allan, *Nucleosides Nucleotides*, 4 (1985) 107.
[15] Z. Kazimierczuk, J. Vilpo and F. Seela, *Helv. Chim. Acta*, 75 (1992) 2289.
[16] D. Shugar and J.J. Fox, *Biochim. Biophys. Acta*, 9 (1952) 199.
[17] J. Balzarini, M. Cools and E. De Clercq, *Biochem. Biophys. Res. Commun.*, 158 (1989) 413.
[18] B. Barbieri, F.C. Giuliani and T. Bordoni, *Cancer Res.*, 47 (1987) 4001.
[19] J.J. Barchi, V.E. Marquez and J.S. Driscoll, *J. Med. Chem.*, 34 (1991) 1647.
[20] D.A. Brent, J.J. Sabatka and D.J. Minick, *J. Med. Chem.*, 26 (1983) 1014.
[21] C. Hansch and A. Leo, *Substituent Constants for Correlation Analysis in Chemistry and Biology*, Wiley, New York, 1979.
[22] J.C. Dearden and G.M. Bresnen, *Quant. Struct.-Act. Relat.*, 7 (1988) 133.
[23] W.E. Hammers, G.J. Meurs and C.L. de Ligny, *J. Chromatogr.*, 247 (1982) 1.
[24] M. Harnisch, H.J. Möckel and G. Schulze, *J. Chromatogr.*, 282 (1983) 315.
[25] V. Reichelová and L. Novotny, *J. Chromatogr.*, 588 (1991) 147.
[26] G. Biagi, M. Guerra and A. Barbaro, *J. Liq. Chromatogr.*, 13 (1990) 913.
[27] J. Liliemark and G. Juliusson, *Blood*, 80 (1992) 471.

ELSEVIER

Journal of Chromatography A, 667 (1994) 47–57

JOURNAL OF CHROMATOGRAPHY A

Ultra-trace analysis of phenols in water using high-performance liquid chromatography with on-line reaction detection

Günther Lamprecht, Josef F.K. Huber*

Institute for Analytical Chemistry, University of Vienna, Währinger Strasse 38, A-1090 Vienna, Austria

(First received March 8th, 1993; revised manuscript received December 1st, 1993)

Abstract

An ultra-sensitive HPLC method for the determination of phenols in water based on flow-through reaction is described. The phenols are concentrated by a two-step liquid–liquid extraction with dichloromethane and after evaporation of the organic solvent the separation is carried out on an octadecyl-silica column by a gradient of water–acetonitrile. Detection is performed by an on-line twin detection system. First dinitrophenols are detected by UV-absorption measurement followed by oxidation of phenols with cerium(IV) in a tubular flow-through reactor and fluorescence measurement of cerium(III). Detection limits in the lower ppt range can be achieved. The influence of reaction time, temperature and reagent concentration on reaction yield was investigated. Identification and quantitation is improved by use of internal standards. The method was applied to samples of surface and drinking water.

1. Introduction

The determination of phenols in very low concentrations in water is a problem frequently encountered in environmental analysis [1–4]. In drinking and surface water they occur in the ppt mass fraction range. It is therefore necessary to carry out an enrichment step prior to separation and detection.

Commonly used methods for sample preconcentration are liquid–liquid and liquid–solid extraction. Liquid–liquid extraction is carried out off-line either discontinuously or continuously [5] or by use of liquid–liquid extraction columns (*e.g.* Chem Elut, Extrelut). Trace enrichment by liquid–solid extraction is achieved by adsorption [2,4,6–10] or by anion exchange [6,11,12] on solid surfaces. For non-polar phenols octadecyl-silicas, for medium polar species copolymer-based adsorbents (XAD, PRP-1, PLRP-S) were used, whereas highly polar phenols are efficiently adsorbed on porous graphitic carbon [13]. Enrichment on solid sorbents can be automated and performed on-line during analysis of the previous sample. If, however, enrichment takes longer than the following analysis steps it is best carried out not in sequence but simultaneously by offering the possibility of enrichment of several samples at the same time. For high-speed operation membrane extraction disks can also be regarded as an alternative [14].

Numerous phase systems have been applied to

* Corresponding author.

0021-9673/94/$07.00
SSDI 0021-9673(93)E0006-G

solve the separation problem by HPLC such as reversed-phase columns with isocratic elution [15–24] or gradient elution [4,18,19,25–30], ion-exchange chromatography [1,31,32] and solvent-generated ion-exchange chromatography [33].

Existing solutions for the selective detection in very low concentrations still need improvement. In acidic aqueous solution phenols show an absorption maximum in the 265–280 nm wavelength range, but measuring in this range is hardly selective and the absorption coefficients of most phenols allow mass detection limits in the higher nanogram range [17–19,27–29]. Measuring the native fluorescence of some phenols is more selective and can lead to lower mass detection limits in the higher picogram range [6,28], but most phenols show only low fluorescence or no fluorescence at all. Electrochemical detection is rather sensitive and allows determinations down to the higher picogram range, but the method suffers from a lack of long time stability due to contamination of the electrode surface and a severely drifting baseline at gradient elution [1,3,4,34–37].

Attempts have therefore been made to solve the detection problem by means of reaction detection either by pre-column or post-column reactions leading to reaction products with better detection properties for chemiluminescence [38], electrochemical detection [2,37] or UV absorption [39–44]. Pre-column reactions in which a group is attached to the phenol in order to achieve a more sensitive detection have the disadvantage that phenol derivatives are formed which are more similar than the original phenols and therefore are more difficult to separate. Post-column reactions can be carried out batchwise after collecting fractions of the eluate or in flow-through mode. Carrying out the reaction batchwise is tedious and time consuming, especially in the case of high-performance separations of many analytes, since a large number of fractions has to be analyzed in order to preserve the resolution achieved in the separation. On the other hand post-column reaction detection requires rapid reactions and reaction products with favourable detection properties in high yields. Wolkoff and Larose [45] have described the oxidation of phenols by cerium(IV) sulphate in a flow reactor and the detection of the cerium(III) produced by fluorescence measurement in an attached flow detector. This paper deals with the optimization of this principle and its application for the determination of phenols in surface and drinking water. The combination of a liquid chromatographic separation with the on-line oxidation by cerium(IV) and the selective fluorimetric detection add up to a method selective for phenols with mass detection limits down to the low-nanogram range.

2. Experimental

2.1. Chemicals

For sample preparation the analytical-grade solvents dichloromethane and methanol (E. Merck, Darmstadt, Germany) and the analytical-grade reagents hydrochloric acid, formic acid, acetic acid and sodium hydroxide (E. Merck) were used.

For HPLC analysis acetonitrile (LiChrosolv, E. Merck) and analytical-grade sodium acetate trihydrate (E. Merck) were used. The water was bidistilled in a quartz distillation apparatus.

Analytical-grade cerium(IV) sulphate tetrahydrate, sodium bismuthate (E. Merck) and sulphuric acid (Loba, Fischamend, Austria) were used for post-column reaction.

A priority pollutant phenol standard mixture (Supelco, Bellefonte, PA, USA) was applied for chromatographic calibration. A series of diluted solutions in methanol–water in the ppb to ppt range was prepared.

As internal standards analytical-grade *p*-cresol, 2-chloro-5-methylphenol (E. Merck) and 3,5-dichlorophenol (Aldrich, Steinheim, Germany) were added to the samples. All standard solutions were protected from light and stored at 4°C.

2.2. Apparatus

The chromatographic system used is shown in Fig. 1. It consists of a high-pressure liquid

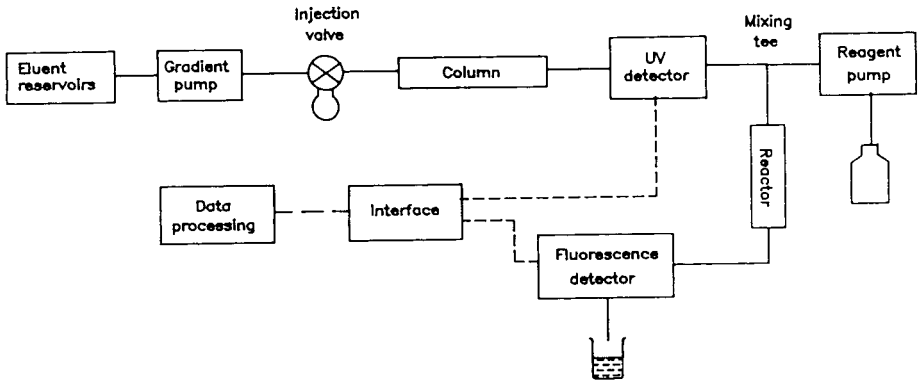

Fig. 1. Scheme of the HPLC apparatus.

chromatograph for gradient elution equipped with an UV–Vis-absorption detector and a flow-through reactor coupled on-line to a fluorimetric detector.

The high-performance liquid chromatograph uses a low-pressure binary gradient former (Model 5000; Varian, Walnut Creek, CA, USA) and an injection valve (Model 7125; Rheodyne, Berkeley, CA, USA) with a 1-ml sample loop.

Separation was performed on a 250 mm × 4 mm octadecyl-silica column (Hibar, LiChrospher RP-18, E. Merck), packed with 5-μm particles.

Absorption detection was carried out by a variable-wavelength spectrophotometer (Model UV 50, Varian) with a 7.9-μl flow cell.

For post-column reaction detection the mobile phase was mixed in a mixing tee with a cerium(IV) solution delivered by a reagent pump (Model 655A-13, E. Merck). A PTFE capillary with the dimensions 1.6 m × 0.5 mm I.D. was used as flow reactor and thermostatted by a column heater (WO Industrial Electronics, Langenzersdorf, Austria). Detection of the reaction product cerium(III) was performed by a flow-through fluorescence spectrophotometer (Model F1000, E. Merck) equipped with a 12-μl flow cell.

Both detector signals were digitized by an intelligent data acquisition module (Model 763; Nelson Analytical, Cupertino, CA, USA). Data storage and data processing were carried out on a personal computer (Model XT; IBM, Boca Raton, FL, USA) by use of chromatographic software (Nelson Analytical).

2.3. Operation

Sample pretreatment

For liquid–liquid extraction of phenols from aqueous solutions solvents offering a high solubility of phenols in the organic phase are used [19]. Dichloromethane was chosen as extraction solvent showing satisfactory large extraction coefficients for phenols in aqueous solution.

The glassware, employed for sample preparation, is cleaned with chromic sulphuric acid, water and methanol. A 200-ml volume of a water sample was filtered through a paper filter (Machery–Nagel, Düren, Germany) to remove solid particles, transferred into a separation funnel and acidified with 2 ml of 4% (v/v) hydrochloric acid, adjusting a pH value between 2 and 2.5. After addition of 200 μl internal standard solution the sample is extracted twice with 20 ml dichloromethane. The combined organic extracts are transferred into a 100-ml round-bottom flask and 0.8 ml of an aqueous solution of 8% sodium hydroxide are added. The organic layer is evaporated at room temperature in a rotating evaporator (Büchi Laboratoriums-Technik, Flawil, Switzerland) and the aqueous residue is transferred to a 25-ml pointed flask, rinsing twice with methanol. The organic solvent is evapo-

rated and the residue (volume *ca.* 0.8 ml) acidified to pH 2.5 to 3.0 with 4 to 5 drops of a solution of formic acid–hydrochloric acid–water (40:10:50, v/v/v). The total volume is used for HPLC analysis.

HPLC separation

Separation is carried out on a hydrophobic adsorbent in acidic aqueous medium suppressing the ionisation of phenols. Elution is performed at constant flow-rate with a binary gradient as given in Table 1. The polar eluent constituent consists of bidistilled water acidified to pH 3.7 with acetic acid which is favourable to achieve peak sharpening and which suppresses asymmetric peak shapes. Acetonitrile is used as organic modifier since it was observed that it causes a lower noise level in fluorescence reaction detection compared to methanol, another organic modifier commonly used for the LC separation of phenols.

Detection

UV absorption detection is performed at 260 nm setting the slit width to 8 nm.

Fluorescence reaction detection is carried out by monitoring the concentration of cerium(III), produced by reaction of cerium(IV) with phenols. The formation of cerium(III) is catalyzed by heterogeneous surfaces like glass walls or precipitants. Special attention must therefore be paid to the selection of the material for the reagent reservoir and the preparation of the reagent solution. Dark glass bottles are used since they were found to be preferable to plastic bottles with respect to the stability of the reagent solution. The reaction is carried out in a 310-μl tubular flow-through reactor. For fluorescence detection the excitation wavelength is set to 260 nm, measuring the emission wavelength at 350 nm.

3. Results and discussion

3.1. Recovery of extraction

For recovery experiments, 200 ml of bidistilled water were spiked by addition of 200 μl of internal standard mixture and variable volumes of the phenol standard mixture (60 ppt–1 ppb). These test solutions were extracted and analyzed by HPLC. Table 2 presents the recoveries found for the phenols included in the study, ranging

Table 1
Gradient programme of one analytical cycle

Time (min)	B (%)	Flow-rate (ml/min)	Comments
0	0	0.8	Analysis
3	27	0.8	
5	32	0.8	
9	35	0.8	
12	37	0.8	
19	37	0.8	
22	40	0.8	
29	47	0.8	
37	100	0.8	
41	100	0.8	End of analysis
43	100	1.5	Cleaning of the column
44	0	1.5	Reequilibration of the column
53	0	1.5	
54	0	0.8	End of the cycle

Eluents: A = water adjusted to pH 3.7 with acetic acid; B = acetonitrile.

Table 2
Recoveries of phenols for a two-fold liquid–liquid extraction from 200 ml acidified water with 20 ml of dichloromethane each time

Analytes	Extraction with dichloromethane and solvent evaporation (%)	Back extraction into alkaline solution (%)
Phenol	61	57
4-Nitrophenol	44	43
2-Chlorophenol	82	75
2-Nitrophenol	93	78
2,4-Dimethylphenol	88	14
4-Chloro-3-methylphenol	94	68
2,4-Dichlorophenol	92	72
2,4,6-Trichlorophenol	95	88
Pentachlorophenol	90	57
2,4-Dinitrophenol	96	93
4,6-Dinitro-*o*-cresol	98	96
Internal standards		
3,5-Dichlorophenol	91	88
p-Cresol	82	55
2-Chloro-5-methylphenol	85	80

Reproducibility: ± (2–4)%, except pentachlorophenol ± 10%.

from 44 up to 98%. Dichloromethane is generally a good solvent for many organic substances. Therefore a reduction of the coextracted compounds was aspired by back extraction of phenols into an alkaline aqueous solution leading to a decrease of the amounts of other substances absorbing in the UV range. Back extraction was achieved with 0.8 ml of an aqueous solution of sodium hydroxide (pH 11), followed by evaporation of the organic solvent. Table 2 shows the recoveries obtained by this procedure. For almost all phenols satisfactory recoveries ranging from 43 to 96% were found except for 2,3-dimethylphenol, for which a recovery of only 14% was observed. Even extraction with a more alkaline solution (pH 12 and above) did not improve the recovery significantly. In view of the fact that the pK_a values of phenols are within a small range, this result may be due to the low solubility of this compound in water [46].

In addition different batches of dichloromethane were tested for interferences in the chromatograms with the phenol peaks at the trace level. Only such batches showing negligible interferences with the analyte peaks were used.

3.2. Separation of priority phenols by HPLC

A chromatogram of a standard mixture of phenols is shown in Fig. 2. In the first part of the chromatogram strongly hydrophilic phenols are eluted, followed by moderate hydrophilic phenols and finally hydrophobic chlorophenols. All phenols are well resolved. Each cycle is completed by a cleaning and reequilibration step.

3.3. Optimization of detection

For selection of an appropriate reservoir vessel several bottles of dark glass were filled with a 10^{-5} *M* solution of cerium(IV) sulphate and allowed to stand for several days. The bottles were then filled with the reagent solution and those showing the lowest cerium(III) level were selected for analysis. Generally the lowest cerium(III) levels are achieved by using fresh double distilled water for the preparation of the reagent. After addition of sulphuric acid and cerium(IV) sulphate, sodium bismuthate was added to reduce the formation of cerium(III)

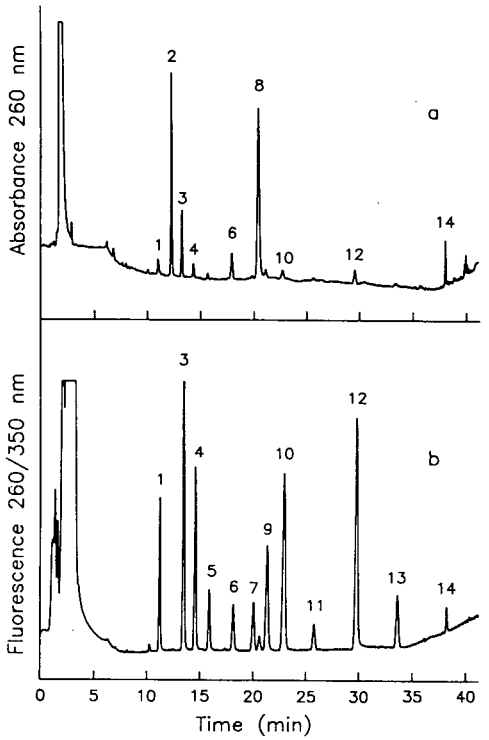

Fig. 2. Chromatograms of standard mixtures of phenols. (a) Absorption detection at 260 nm, (b) fluorescence reaction detection at 260/350 nm. Column: LiChrospher RP-18, gradient see Table 1, eluent flow-rate 0.8 ml/min. Injection volume 200 μl. Reactor: temperature 25°C, reagent 400 mg/l $Ce(SO_4)_2$, reagent flow-rate 0.5 ml/min. Sample: 1 = 50 ng phenol; 2 = 150 ng 2,4-dinitrophenol; 3 = 250 ng 4-nitrophenol; 4 = *p*-cresol (reference); 5 = 50 ng 2-chlorophenol; 6 = 50 ng 2-nitrophenol; 7 = 50 ng 2,4-dimethylphenol; 8 = 250 ng 4,6-dinitro-*o*-cresol; 9 = 2-chloro-5-methylphenol (reference); 10 = 250 ng 4-chloro-3-methylphenol; 11 = 50 ng 2,4-dichlorophenol; 12 = 3,5-dichlorophenol (reference); 13 = 150 ng 2,4,6-trichlorophenol; 14 = 150 ng pentachlorophenol.

due to aging. A solution with a concentration of 400 mg/l $Ce(SO_4)_2$, prepared and stored in the above described manner has a stable cerium(III) concentration for 8 days at a temperature beyond 25°C. Higher temperatures (above 30°C) lead to an untolerable raise of the baseline due to an accelerated formation of cerium(III) within 2 days. The addition of greater amounts of sodium bismuthate (100–200 mg/l) brings only a slight reduction of the cerium(III) concentration, but reduces significantly the yield of the oxidation of phenols.

At the conditions chosen no precipitation of cerium was observed.

The oxidation of phenols by cerium(IV) is strongly influenced by their structure. An overview of the relative reactivity at two different reagent concentrations is given in Table 3. The highest reaction yield is found for phenol itself. Electron-attracting groups like nitro and halogen substituents decrease the reaction rate. If two nitro groups or several halogen atoms are attached to the ring system, the reactivity is drastically decreased.

The reaction yield improves with increasing concentration of the reagent, especially for less reactive phenols. A tenfold increase of the cerium(IV) concentration leads to a 4.4-fold improvement of the yield for 2,4,6-trichlorophenol and to a 5.4-fold improvement for pentachlorophenol and nitrophenols. Therefore analysis was carried out at a high concentration of 400 mg/l cerium(IV) sulphate and operating the detector in the least sensitive mode. In this manner the signal response of accompanying substances with fluorescence properties is reduced.

If two nitro groups are attached to the aromatic ring, the reaction yield is lowered to such an extent that measuring the absorption signal at 260 nm is more favourable than fluorescence. Pentachlorophenol can be measured with comparable intensity by both detection systems, but more selectively with fewer disturbances from accompanying substances by reaction fluorescence detection.

The oxidation reaction is further influenced by temperature. Table 3 shows the influence of temperature on the reactivity of phenols. Increasing the reaction temperature from 30 to 60°C strongly increases the reaction yield of the less reactive compounds. 2,4-Dinitrophenol shows a 19-fold increase, 2,4,6-trichlorophenol and pentachlorophenol a 2.6-fold increase. The baseline shifts however from 10 to 41% full scale, the noise level shows a 2.2-fold increase and the signal intensity of accompanying oxidizeable substances is also increased.

The degree of conversion is further controlled by the reaction time. The reaction yields at 30°C

Table 3
Dependence of the oxidation reaction of phenols with cerium(IV) on the reagent concentration and the temperature

Analytes	(Area units × 10^{-3})/ng analyte			
	Temperature 25°C, concentration $Ce(SO_4)_2$ (mg/l)		Concentration $Ce(SO_4)_2$ 80 mg/l, temperature (°C)	
	40	400	30	60
Phenol	198	199	205	215
4-Nitrophenol	33	90	73	97
2-Chlorophenol	78	105	79	86
2-Nitrophenol	45	66	62	84
2,4-Dimethylphenol	70	102	81	110
4-Chloro-3-methylphenol	78	90	78	90
2,4-Dichlorophenol	44	59	48	69
2,4,6-Trichlorophenol	8	37	16	42
Pentachlorophenol	2	9	7	18
2,4-Dinitrophenol	<1	2	<1	2
4,6-Dinitro-*o*-cresol	<1	2	1	2

Eluent flow-rate 0.8 ml/min; reagent flow-rate 0.4 ml/min, reaction time 0.24 min; reagent concentrations: 40 mg/l $NaBiO_3$, 25 ml/l H_2SO_4; amount of analytes: 50 to 250 ng.

depending on reaction time are shown in Fig. 3. Many phenols have a maximum at 1.5 to 2.0 min. Long reaction times lead to broader peak profiles affecting the chromatographic resolution. Using capillaries with an I.D. of 0.5 mm as reactors and changing the reaction time by using capillaries of varying length from 0.5 to 1.5 min leads at a flow-rate of 0.4 ml/min to a 1.6-fold increase of the peak variance and corresponding decrease of resolution. Simultaneously a shift of the baseline and a magnification of the noise level of the baseline is observed, resulting in reduced dynamic and detection limit.

In conclusion the following conditions for reaction detection were chosen: the optimum reagent solution contains 25 ml/l sulphuric acid, 40 mg/l sodium bismuthate and 400 mg/l cerium(IV) sulphate in bidistilled water.

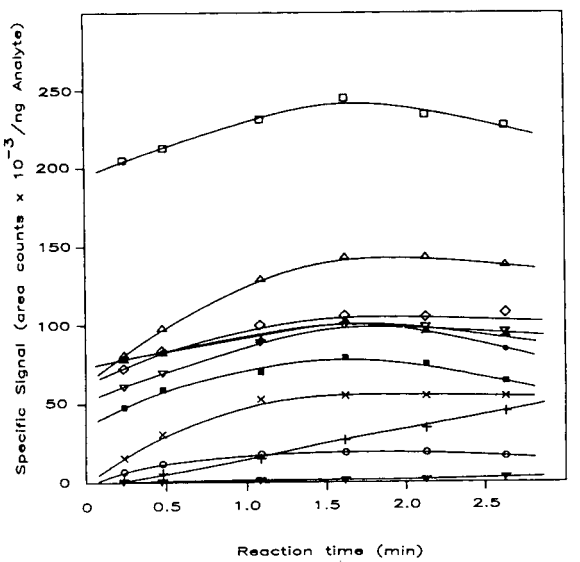

Fig. 3. Effect of reaction time on reaction yield. Column as in Fig. 2. Flow reactor: capillaries of varying length with 0.5 mm I.D., temperature 30°C, reagent flow-rate 0.4 ml/min, reagent concentrations: 80 mg/l $Ce(SO_4)_2$, 40 mg/l $NaBiO_3$, 25 ml/l H_2SO_4. Sample: □ = phenol; △ = 2,4-dimethylphenol; ■ = 2,4-dichlorophenol; ▲ = 4-chloro-3-methylphenol; ● = 2-chlorophenol; × = 2,4,6-trichlorophenol; ○ = pentachlorophenol; ▼ = 2,4-dinitrophenol; ◇ = 4-nitrophenol; + = 4,6-dinitrophenol; ▽ = 2-nitrophenol.

3.4. Method validation

The analytes are identified chromatographically by measuring their retention times (Table 4). The retention times are highly reproducible. For five injections of a standard mixture of phenols, the relative standard deviation of the retention

Table 4
Retention time in column and detector

	Analytes	Time (min)	Selectivity
1	Phenol	11.1	
2	2,4-Dinitrophenol	12.1	1.11
3	4-Nitrophenol	13.3	1.12
4	*p*-Cresol (reference)	14.4	1.10
5	2-Chlorophenol	15.7	1.11
6	2-Nitrophenol	18.0	1.17
7	2,4-Dimethylphenol	19.8	1.11
8	4,6-Dinitro-*o*-cresol	20.2	1.02
9	2-Chloro-5-methylphenol (reference)	21.1	1.05
10	4-Chloro-3-methylphenol	23.1	1.11
11	2,4-Dichlorophenol	25.5	1.12
12	3,5-Dichlorophenol (reference)	29.5	1.17
13	2,4,6-Trichlorophenol	33.3	1.14
14	Pentachlorophenol	37.8	1.15

Conditions see Experimental. Hold up time in the reaction detection system is 0.24 min.

times was found to be better than ± 0.9%. Possible retention shifts, due to the influence of accompanying substances, are corrected by the use of internal standards. Identification is performed by calculation of relative retentions with reference to the internal standards *p*-cresol, 2-chloro-5-methylphenol and 3,5-dichlorophenol.

Quantitation of the analytes is achieved by determining the peak area by integration. The chromatographic system is calibrated by repetitive injections of series of dilutions ($n = 4$) made from a standard mixture of phenols. The injection volume was 40 to 500 μl corresponding to 5 ng for the phenol with the lowest concentration and to 1375 ng for the phenol with the highest concentration. The calibration factors, C_i, of the reaction detection system for the phenols were calculated by linear regression of the experimental data according to $x_i = C_i(y_i - y_0)$, where x_i = amount (ng) of analyte i, y_i = peak area (area units), y_0 = intersection of the calibration line and C_i = slope of the calibration line = calibration factor. The values of the calibration factors for the phenols tested are given in Table 5. The calibration factor range describes the selectivity of the reaction detection system. The correlation coefficients of the calibration functions were better than 0.995 with one exception (0.991 for 4-nitrophenol). The precision of the reaction detection system was found to be in the order of 3% for 50 ng except for pentachlorophenol for which a precision of 5% was found. The mass detection limits for the tandem detection system are listed in Table 6. They were found to be in the order of 1 ng except for pentachlorophenol (14 ng). The overall detection limit of the total procedure including sample

Table 5
Calibration: linear regression data

Analytes	Calibration factor (pg/area unit)	Correlation coefficient
Fluorescence detection (260/350 nm)		
Phenol	$1.63 \cdot 10^{-2}$	0.998
4-Nitrophenol	$4.26 \cdot 10^{-2}$	0.991
2-Chlorophenol	$3.10 \cdot 10^{-2}$	0.999
2-Nitrophenol	$3.98 \cdot 10^{-2}$	0.999
4-Chloro-3-methylphenol	$3.55 \cdot 10^{-2}$	0.997
2,4-Dimethylphenol	$2.94 \cdot 10^{-2}$	0.999
2,4-Dichlorophenol	$5.22 \cdot 10^{-2}$	0.999
2,4,6-Trichlorophenol	$7.53 \cdot 10^{-2}$	0.999
Pentachlorophenol	$2.99 \cdot 10^{-1}$	0.996
Absorption detection (260 nm)		
2,4-Dinitrophenol	$6.96 \cdot 10^{-1}$	0.999
4,6-Dinitro-*o*-cresol	$6.56 \cdot 10^{-1}$	0.999

Conditions see Experimental.

Table 6
Detection limits in amounts and mass fractions for a signal-to-noise ratio of 3

Analytes	Detection limit	
	Mass (ng)[a]	Mass fraction (ppt)[b]
Fluorescence detection (260/350 nm)		
Phenol	0.7	5.7
4-Nitrophenol	1.6	16
2-Chlorophenol	1.4	8.7
2-Nitrophenol	1.5	8.5
2,4-Dimethylphenol	1.4	8.5
4-Chloro-3-methylphenol	1.6	8.8
2,4-Dichlorophenol	2.5	11
2,4,6-Trichlorophenol	4.0	17
Pentachlorophenol	14	78
Absorption detection (260 nm)		
2,4-Dinitrophenol	2	8.3
4,6-Dinitro-*o*-cresol	2	8.1

Conditions see Experimental.
[a] Mass detection limits for the detector.
[b] Mass fraction detection limits including sample preparation.

enrichment with respect to the concentration in a water sample of 200 ml can be calculated considering the yield of extraction given in Table 2 and using the data presented in Table 6. The results of this estimation are included in Table 6.

The noise of the reaction detection system was mainly caused by the low frequency of the reciprocating reagent pump. At a reagent concentration of 400 mg/l $Ce(SO_4)_2$ a mean noise level of 0.75% full scale was found. An improvement of the detection limit can be expected by using a pump with a better damping characteristic.

The internal standards were also used to control the sample preparation procedure. They are added to the sample at the beginning of the extraction step and deviations from their standard recoveries (Table 2) allows the calculation of correction factors for the analytes. If a negative deviation greater than 35% from the target value is found for the standards, the result is dismissed and the analysis is repeated. The peak of 3,5-dichlorophenol, which is not disturbed by other test components and was not found in representative surface water samples, was chosen as internal reference for quantitative calculations.

3.5. Application in water analysis

The method was tested by analysing more than 200 samples from rivers and lakes of the Austrian territory and the results were published elsewhere [47]. Samples were collected in regular intervals within one year and treated in the manner described above. Two typical chromatograms of samples of the Danube, taken from the upper and lower course in Austria, are shown in Fig. 4. The legislative stated tolerance limits for priority pollutant phenols (2 ppb) were not exceeded, whereby the relatively highest values were determined in Vienna. Generally the highest content of phenols was found in samples taken in Winter whereas the lowest levels were determined in Summer probably because of the increased biological activity causing degradation of phenols. It was also found that rivers which were known in the past to be polluted, at present have very low concentrations of phenols due to

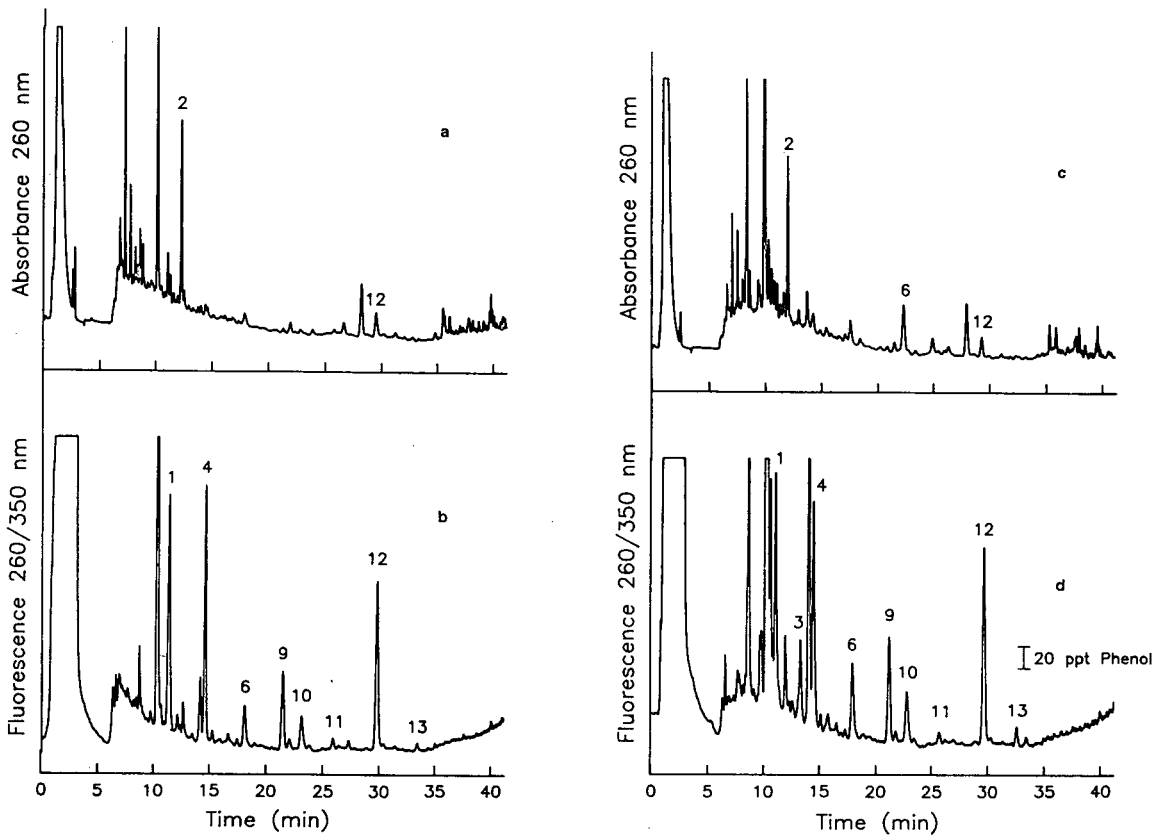

Fig. 4. Chromatograms of samples from the Danube. Working conditions as in Fig. 2 except injection volume 0.8 ml. (a, b) Sampling location at the border to Germany: (a) absorption detection at 260 nm, (b) fluorescence detection at 260/350 nm. (c, d) Sampling location at the border to the Slovak Republic: (c) absorption detection at 260 nm, (d) fluorescence detection at 260/350 nm.

preventions which were taken to improve their water quality.

4. Acknowledgements

The authors are obliged to the "Bundesanstalt für Wassergüte" for supplying the water samples and acknowledge gratefully the financial support of the "Bundesministerium für Land- und Forstwirtschaft".

5. References

[1] D.A. Baldwin and J.K. Debowski, *Chromatographia*, 16 (1988) 186.
[2] F.P. Bigley and R.L. Grob, *J. Chromatogr.*, 350 (1985) 407.
[3] D.N. Armentrout, J.D. McLean and M.W. Long, *Anal. Chem.*, 51 (1979) 1039.
[4] R.E. Shoup and G.S. Mayer, *Anal. Chem.*, 54 (1982) 1164.
[5] J. Czuczwa, C. Leuenberger, J. Tremp, W. Giger and M. Ahel, *J. Chromatogr.*, 403 (1987) 233.
[6] M.W. Nielen, J. de Jong, R.W. Frei and U.A.Th. Brinkman, *Int. J. Environ. Anal. Chem.*, 25 (1986) 37.
[7] M. Dressler, *J. Chromatogr.*, 165 (1979) 167.
[8] F.A. Maris, J.A. Stäb, G.J. de Jong and U.A. Th. Brinkman, *J. Chromatogr.* 445 (1988) 129.
[9] R.E. Majors, *LC·GC Int.*, 4 (1991) 10.
[10] Y.-B. Yang and M. Verzele, *J. Chromatogr.*, 445 (1988) 129.
[11] F. Reber Brown and W.M. Droper, *J. Chromatogr.*, 479 (1989) 441.
[12] C.D. Chiswell, R.C. Chang and J.S. Fritz, *Anal. Chem.*, 47 (1975) 1325.

[13] V. Coquart and M.C. Hennion, *J. Chromatogr.*, 600 (1992) 195.
[14] R.E. Majors, *LC·GC Int.*, 6 (1991) 208.
[15] C.P. Ong, H.K. Lee and S.F.Y. Li, *J. Chromatogr.*, 464 (1989) 405.
[16] P. Alarcon and A. Bustos, *Chromatographia*, 24 (1987) 613.
[17] N.G. Buckman, J.O. Hill R.J. Magee and M.J. McCormick, *J. Chromatogr.*, 284 (1984) 441.
[18] J.C. Hoffsommer, D.J. Glover and C.Y. Hazzard, *J. Chromatogr.*, 195 (1980) 435.
[19] P.A. Realini, *J. Chromatogr. Sci.*, 19 (1981) 124.
[20] M.K. Lee, S.F.Y. Li and Y.H. Tay, *J. Chromatogr.*, 438 (1988) 429.
[21] C.J. Dowle, A.P. Malyan and A.M. Matheson, *Analyst*, 115 (1990) 105.
[22] J. Yamaguchi and T. Hanai, *J. Chromatogr. Sci.*, 27 (1989) 710.
[23] S. Yamauchi and H. Mori, *J. Chromatogr.*, 515 (1990) 305.
[24] S. Yamauchi, *J. Chromatogr.*, 635 (1993) 61.
[25] J.F. Schabron, R.J. Hurtubise and H.F. Silver, *Anal. Chem.*, 50 (1978) 1911.
[26] H.A. McLeod and G. Laver, *J. Chromatogr.*, 244 (1982) 385.
[27] K. Ugland, E. Lundanes, T. Greibrokk and A. Björseth, *J. Chromatogr.*, 213 (1981) 83.
[28] G.K.-J. Chao and J.C. Suatoni, *J. Chromatogr. Sci.*, 20 (1982) 436.
[29] K. Ogan and E. Katz, *Anal. Chem.*, 53 (1981) 160.
[30] Y. Arai, M. Hirukawa and T. Hanai, *J. Liq. Chromatogr.*, 10 (1987) 635.
[31] P. Jandera, J. Churacek, J. Caslavsky and D. Szabo, *Chromatographia*, 14 (1981) 100.
[32] J. Malowska and W. Pietek, *J. Chromatogr.*, 201 (1980) 293.
[33] C.P. Terweij-Groen and J.C. Kraak, *J. Chromatogr.*, 138 (1977) 245.
[34] C.-Y. Li and M.W. Kemp, *J. Chromatogr.*, 455 (1988) 241.
[35] P.J. Rennie and S.F. Mitchell, *Chromatographia*, 24 (1987) 319.
[36] A. Liberti, C. Morgia and M. Mascini, *Anal. Chim. Acta*, 173 (1985) 157.
[37] C.-Y. Li and M.W. Kemp, *J. Chromatogr.*, 455 (1988) 241.
[38] P.J.M. Kwakman, J.G.J. Mol, D.A. Kamminga, R.W. Frei, U.A.Th. Brinkman and G.J. de Jong, *J. Chromatogr.*, 459 (1988) 139.
[39] C. Baiocchi, E. Campi, M.C. Gennaro, E. Mentosti and P. Mirti, *Chromatographia*, 15 (1982) 660.
[40] J. Gasparic, D. Svoboda and A. Matyaova, *J. Chromatogr.*, 88 (1974) 364.
[41] C. Baiocchi, E. Campi, M.C. Gennaro, E. Mentosti and R. Aruga, *Anal. Lett.*, 15 (1982) 1539.
[42] G. Blo, F. Dondi, A. Betti and C. Bighi, *J. Chromatogr.*, 257 (1983) 69.
[43] G. Blo, F. Dondi and C. Bighi, *J. Chromatogr.*, 295 (1985) 231.
[44] S.K. Ratanathanawangs and S.R. Crouch, *Anal. Chim. Acta*, 192 (1987) 267.
[45] A.W. Wolkoff and R.H. Larose, *J. Chromatogr.*, 99 (1974) 731.
[46] C. Columbic, M. Orchin and S. Weller, *J. Am. Chem. Soc.*, 71 (1949) 2624.
[47] J.F.K. Huber, *Wasserwirtschaftskataster*, Bundesministerium für Land- und Forstwirtschaft, Vienna, 1988, p. 171.

ELSEVIER

Journal of Chromatography A, 667 (1994) 59–66

JOURNAL OF CHROMATOGRAPHY A

High-performance liquid chromatographic determination of naturally occurring flavonoids in *Citrus* with a photodiode-array detector

Yoichi Nogata[a], Hideaki Ohta[*,a], Koh-Ichi Yoza[a], Mark Berhow[b], Shin Hasegawa[b]

[a]*Chugoku National Agricultural Experiment Station, Ministry of Agriculture, Forestry and Fisheries, Fukuyama City, Hiroshima 721, Japan*

[b]*Fruit and Vegetable Chemistry Laboratory, Agricultural Research Service, US Department of Agriculture, 263 South Chester Avenue, Pasadena, CA 91106, USA*

(First received October 29th, 1993; revised manuscript received December 22nd, 1993)

Abstract

High-performance liquid chromatography (HPLC) coupled with ultraviolet–visible spectrophotometry using a photodiode-array detector was used as a routine method for the simultaneous separation and determination of 25 naturally occurring *Citrus* flavonoids. The separation system consisted of a C_{18} reversed-phase column, a gradient system of 0.01 *M* phosphoric acid (A) and methanol (B), and a photodiode-array detector. Each of the 25 flavonoids was eluted from the column with a gradient system composed of three periods: (1) 0–55 min, 70–55% (v/v) A in B, (2) 55–95 min, 55–0% A in B, and (3) 95–100 min, isocratic, 100% B, and quantified by spectrophotometric detection at 285 nm. Identifications of specific flavonoids were made by comparing their retention times (t_R) and UV spectra with those of standards. The relative standard deviations of t_R values were 0.029–0.321%. The recoveries of pure eriocitrin, naringin, hesperidin and tangeretin added to tissues prepared from Unshiu (*Citrus unshiu* Marc.) and Hirado-buntan (*Citrus grandis* Osbeck f. Hirado) and subsequent extraction were 97.47–103.13% from the mesocarp and 96.87–104.93% from the juice with standard deviations of 2.32–5.72% and 2.18–5.96%, respectively.

1. Introduction

The flavonoid constituents of *Citrus* continue to claim attention not only for their remarkable taste properties [1–3] but also their therapeutic and pharmacological activities. For example, they have been shown to possess biological activities such as anti-carcinogenic effects [4–9], anti-inflammatory properties [10,11], and inhibitory activities against histamine release [12,13]. Further, in early chemotaxonomic studies, several flavanone glycosides unique to *Citrus* and even to specific cultivars were examined in relation to taxonomic classification [14–16]. For these kinds of studies, precise quantitative data on the occurrence of flavonoids in *Citrus* are needed.

There have been many reports on the HPLC of flavonoids [17–20]. Wulf and Nagel [21] elaborated the theory and practicality of separating a dozen flavone compounds. They used a solvent system consisting of methanol–acetic acid–water (30:5:65) on a C_{18} column. Daigle and Conker-

* Corresponding author.

0021-9673/94/$07.00
SSDI 0021-9673(93)E0080-E

ton [22] reported the HPLC of 34 selected flavonoids using a water–acetic acid (495:5)–methanol isocratic system on a μBondapak C_{18} column. Van de Casteele *et al.* [23] reported retention times (t_R) of 141 flavonoids ranging from triglycosides to aglycones using a C_{18} column and a gradient elution system of formic acid–water (5:95)–methanol. However, reports on the application of HPLC to the determination of flavonoids are limited both in number and scope. In the determination of flavonoids in *Citrus*, attention has been paid only to particular flavones such as polymethoxylated flavones [24,25] and certain major flavonoids [26,27].

The objective of this work was to develop a routine, dependable and accurate method for the determination of flavonoids in extracts prepared from various *Citrus* tissues using reversed-phase HPLC with photodiode-array detection [28].

2. Experimental

2.1. Apparatus for HPLC

The system consisted of Model L-6210 and L-6010 pumps, a Model AS-2000 autosampler, a Model L-3000 photodiode-array detector, a Model D-6100 interface (Hitachi, Tokyo, Japan), a C_{18} reversed-phase analytical HPLC column (LiChrospher 100 RP-18, 250 mm × 4.0 mm I.D., 5 μm particle size; Merck, Darmstadt, Germany), a Model 545B degassing unit (GL Sciences, Tokyo, Japan), a Model CTO-6A column oven (Shimadzu, Kyoto, Japan) and a Model 3852-2 colour printer (IBM, Armonk, NY, USA). The system was controlled by a Hitachi D-6100 Data Station HPLC Manager.

2.2. Chemicals and standards of flavonoids

Neodiosmin was isolated and characterized by NMR at the Fruit and Vegetable Chemistry Laboratory, US Department of Agriculture, Agricultural Research Service, Pasadena, CA, USA, and other HPLC-grade flavonoid standards were purchased from Extrasynthese (Genay, France). Sep-Pak C_{18} cartridges, used for sample clean-up, were obtained from Waters (Milford, MA, USA). All other chemicals were of analytical-reagent grade (Wako, Osaka, Japan).

2.3. Materials

Unshiu (*Citrus unshiu* Marc.) and Hirado-buntan (*Citrus grandis* Osbeck f. Hirado) were grown at the Okitsu Branch, National Fruit Tree Research Station, Shimizu, Japan. From the same tree, 5–20 leaves (young but well expanded) were harvested in June and 5–15 fruits were harvested in November 1992. Four different tissue samples were dissected from the detached fruits and stored at −20°C until processed for analysis: the epicarp, the mesocarp, the endocarp and the juice. Leaves were frozen directly in liquid nitrogen and stored at −20°C until processed.

2.4. Sample preparation

After lyophilization, the epicarp, mesocarp, endocarp and leaf tissue samples were ground using an Ultra Centrifugal Mill (Mitamura Riken Kogyo, Tokyo, Japan) with a 0.5-mm filter. Portions (100 mg) of these powdered tissues were extracted for 12 h with 5 ml of extraction solvent [methanol–dimethyl sulphoxide (DMSO) (1:1, v/v)] in glass-stopped vessels on a wrist-action shaker at ambient temperature. After centrifugation at 3000 *g* for 10 min, the extract of each sample was decanted and the remaining solid residue was extracted twice more with 1 ml of the same solution. To remove polar compounds, the combined extract for each sample was diluted tenfold with water and passed through a Sep-Pak cartridge that had been preconditioned with 5 ml of methanol followed by 10 ml of 10% methanol. The eluate was discarded and the cartridge was washed with 15 ml of 10% methanol. The retained flavonoids were eluted with 4.8 ml of elution solvent [methanol–DMSO (1:1, v/v)]. The final volume of the eluate for each sample was adjusted to 5 ml with the same solvent.

Juice samples were prepared by homogenizing

the sarcocarp tissue after another three fruit tissues had been removed from each sample fruit with a mixer. The juice was clarified by centrifugation at 15 000 *g* for 20 min, and 3 ml of each juice sample were passed through a Sep-Pak cartridge as described above. Solutions to be analysed by HPLC were filtered through membrane filters (0.5-μm pore size; Advantec, Tokyo, Japan) prior to injection.

2.5. HPLC conditions

The detector monitored the eluent at 285 nm and measured spectra from 200 to 360 nm. A two-solvent gradient system was used. The gradient programme consisted of three periods: (1) 0–55 min, 70–55% (v/v) A (0.01 *M* phosphoric acid) in B (methanol), (2) 55–95 min, 55–0% A in B, and (3) 95–100 min, isocratic, 100% B. The resulting chromatographic data on the absorbing peaks was integrated up to 90 min. The flow-rate was 0.6 ml/min with a column head pressure of 1000–1550 p.s.i. (1 p.s.i. = 6894.76 Pa). The column was operated at 40°C. The sample injection volume was 10 μl. Identifications of compounds were made by comparing their t_R values and UV spectra with those of standards stored in a data bank. Concentrations of the compounds were calculated from integrated peak areas of the sample and corresponding standards.

2.6. Recovery studies

The recovery efficiency was determined by adding measured amounts of pure flavonoid standards (eriocitrin, naringin, hesperigin and tangeretin) to either the extraction solvent for mesocarp tissues described above or directly to juice samples to a final concentration of 100 ppm. The samples were prepared as described above and 10 μl of the filtrate were injected on to the HPLC column. Controls were prepared from the same tissue samples. The recoveries were determined by subtracting the values obtained for the control tissue preparation from those of the samples prepared with the added standards. The recovery experiment was performed with five replicates and mean values with standard deviations are reported.

3. Results and discussion

3.1. Separation and identification

Fig. 1 illustrates the separation of 25 flavonoids on LiChrospher 100 RP-18 using the 0.01 *M* phosphoric acid–methanol gradient elution system. As a means of qualitative identification, retention data including mean values of t_R with standard deviation (S.D.) of five replicates, the relative retention value (α) and UV absorption maxima of each standard are given in Table 1. Because the S.D. values were within 0.02–0.10 min and not dependent on t_R, the relative standard deviations of t_R grew smaller with the progression of retention time, 0.284% for the early-eluting flavonoid standard eriocitrin and 0.047% for the final-eluting standard tangeretin.

The widths of the peaks of compounds eluted after 60 min were narrower than those eluted before 60 min. For compounds that eluted before 60 min, such as hesperidin and rutin, α values of more than 1.05 were needed to establish a baseline separation, whereas the separation of acacetin and tangeretin, which eluted after 60 min, was successfully achieved with even smaller α values of 1.03 or less.

The elution order of the standards in this system was the same as for corresponding com-

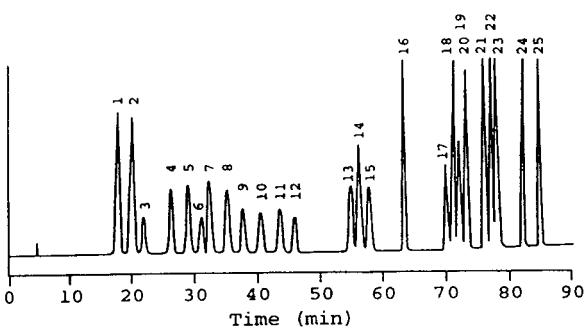

Fig. 1. Separation of flavonoid standards. For the elution system, see Experimental. For the identity of peaks, see Table 1.

Table 1
Retention times (t_R), capacity factors (k'), relative retentions (α) and UV absorbance maxima (λ_{max}) of the flavonoids investigated

No.	Common name	Systematic name	$t_R \pm$ S.D.[a] (min)	α	λ_{max}[b] (nm)
1	Eriocitrin	Eriodictyol-7-β-rutinoside	17.59 ± 0.05		285
2	Neoeriocitrin	Eriodictyol-7-β-neohesperidoside	19.85 ± 0.05	1.17	285
3	Robinetin	3,7,3′,4′,5′-Pentahydroxyflavone	21.81 ± 0.07	1.23	251, 318
4	Narirutin	Naringenin-7-β-rutinoside	25.97 ± 0.07	1.24	282
5	Naringin	Naringenin-7-β-neohesperidoside	28.81 ± 0.07	1.13	284
6	Rutin	Quercetin-3-β-rutinoside	30.81 ± 0.07	1.08	258, 360
7	Hesperidin	Hesperetin-7-β-rutinoside	32.09 ± 0.08	1.05	285
8	Neohesperidin	Hesperetin-7-β-neohesperidoside	34.95 ± 0.08	1.10	284
9	Isorhoifolin	Apigenin-7-β-rutinoside	37.33 ± 0.08	1.08	267, 336
10	Rhoifolin	Apigenin-7-β-neohesperidoside	40.27 ± 0.08	1.09	268, 336
11	Diosmin	Diosmetin-7-β-rutinoside	43.17 ± 0.07	1.08	253, 268, 345
12	Neodiosmin	Diosmetin-7-β-neohesperidoside	46.11 ± 0.06	1.08	255, 268, 345
13	Neoponcirin	Isosakuranetin-7-β-rutinoside	54.64 ± 0.06	1.20	284
14	Quercetin	3,3′,4′,5,7-Pentahydroxyflavone	56.32 ± 0.10	1.03	256
15	Poncirin	Isosakuranetin-7-β-neohesperidoside	57.65 ± 0.06	1.03	284
16	Luteolin	3′,4′,5,7-Tetrahydroxyflavone	62.93 ± 0.06	1.10	242, 256, 351
17	Kaempferol	3,4′,5,7-Tetrahydroxyflavone	70.02 ± 0.02	1.12	253, 266
18	Apigenin	4′,5,7-Trihydroxyflavone	71.55 ± 0.06	1.02	269, 335
19	Isorhamnetin	3,4′,5,7-Tetrahydroxy-3′-methoxyflavone	72.01 ± 0.08	1.01	253
20	Diosmetin	3′,5,7-Trihydroxy-4′-methoxyflavone	73.25 ± 0.04	1.02	252, 268, 347
21	Rhamnetin	3,5,3′,4′-Tetrahydroxy-7-methoxyflavone	76.51 ± 0.03	1.05	256
22	Isosakuranetin	5,7-Dihydroxy-4′-methoxyflavanone	77.28 ± 0.05	1.01	282
23	Sinensetin	3′,4′,5,6,7-Pentamethoxyflavone	77.84 ± 0.06	1.01	240, 265, 326
24	Acacetin	5,7-Dihydroxy-4′-methoxyflavone	82.19 ± 0.04	1.06	269, 301, 329
25	Tangeretin	4′,5,6,7,8-Pentamethoxyflavone	84.88 ± 0.04	1.03	271, 322

[a] Mean values and standard deviations of retention times for five replicate determinations.
[b] Measured in the eluate, the composition of which varies with t_R.

pounds reported by Daigle and Conkerton [22], except that rutin eluted immediately prior to hesperidin (Fig. 1). In the separation system developed by Van de Casteele *et al.* [23], naringin, rutin, hesperidin and neohesperidin were not separated well with t_R values of 15.71, 15.76, 16.3 and 16.62 min, respectively. These compounds were separated sufficiently for quantification in our system (Fig. 1 and Table 1).

The column was found to perform satisfactorily when the precolumn was changed periodically and the column was cleaned occasionally with methanol. However, individual columns may require slightly different conditions for optimum performance.

The UV maxima in absolute methanol for the flavonoid compounds studied in this work have been reported [29,30]. To determine the authenticity of our standards, each was dissolved in absolute methanol and their UV maxima were determined. There was excellent agreement with the reported values. The reported maxima also correlated well with those obtained by the photodiode-array detector during the experimental runs (Table 1). The values obtained differed not more than 3 nm from the reported values. Therefore, the identification of neighbouring peaks was ensured by comparing t_R values and their spectra.

3.2. Quantitative analysis

In order to check the linearity of the relationship between flavonoid concentration and peak area, solutions of 200 ppm of the each standard

were prepared and suitably diluted with methanol. Aliquots of five different concentrations (10, 25, 50, 100 and 200 ppm) of each of these standard solutions were injected on to the HPLC column and the peak areas were determined at 285 nm. The relationship between the concentration and the peak area is shown by the a, b and r values in Table 2, where a and b are the coefficients of the regression equation $y = ax + b$, x being the concentration of flavonoid (ppm) and y the peak area, and r is the correlation coefficient of the equation. All the flavonoids exhibited good linearity ($r = 0.988–1.000$) and obeyed Beer's law in the investigated concentration range of 10–200 ppm.

The detection limits, which were arbitrarily determined as the amounts exhibiting the area of the compound equivalent to that of the largest noise peak, ranged from 0.5 ppm for apigenin and acacetin to 2.5 ppm for rutin and robinetin. These results suggest that the proposed HPLC method is sufficiently sensitive for the determination of flavonoids.

3.3. Recovery of flavonoids from Citrus mesocarp and juice segment

Known amounts of four flavonoid standards were added to the extraction solvents or dissolved in juice samples. The samples were then extracted and prepared as described under Experimental. To elute the retained flavonoids from the Sep-Pak cartridge, we used methanol–DMSO (1:1) because of the insolubility of hesperidin and certain flavone compounds in methanol. Hesperidin does not dissolve completely in methanol at 200 ppm at ambient temperature and diosmin and diosmetin are almost insoluble in methanol. Methanol–DMSO (1:1) dissolved hesperidin up to 3000 ppm and diosmetin up to 400 ppm. This solvent was used for all Sep-Pak elutions in the sample preparations.

The recoveries of the added flavonoids are given in Table 3. In this study, eriocitrin is the most and tangeretin the least polar compound among the selected flavonoids. It is obvious that these two compounds are retained on the Sep-Pak cartridge and efficiently recovered; the recoveries were from 101.93–102.82% and 99.68–103.13% with S.D.s 2.18–2.52% and 2.85–3.34% for added eriocitrin and tangeretin, respectively. There were slight differences in the recoveries of these two flavonoids from mesocarp extraction and juice samples between the two *Citrus* species. Hesperidin is known to be the major flavonoid constituent in Unshiu tissues, whereas naringin is the major flavonoid constituent in Hirado-buntan tissues [15]. The S.D.s of the recovery of hesperidin from Unshiu and of naringin from Hirado-buntan vary slightly more than those of the other standards from each segment.

3.4. Application

The flavonoid content in the two *Citrus* species were determined to demonstrate the validity of this method. Table 4 gives the results of the HPLC analysis expressed as milligrams of flavonoid per gram (fresh mass). The smaller peaks, which were insufficient for the measurement of their UV spectra, were not quantified even if one had a t_R value that corresponded to that of the standard. Nishiura *et al.* [14,15] investigated the occurrence and distribution of ten flavanone glycosides in five tissues from several varieties of *Citrus* using thin-layer chromatography. The main flavonoids that they found in Unshiu tissues were narirutin and hesperidin. On the basis of their t_R values and UV spectra, these compounds are readily identified. Among the five different tissues examined, the narirutin content was lowest in the leaves, which agreed with the results reported elsewhere [15]. The less polar flavonoids occurred more commonly in the epicarp than in the other four tissues. The highest concentrations of flavonoids occurred in the mesocarp, which had concentrations about 100 times greater than those found in the juice. Leaves had considerably higher concentrations of flavones and flavon-3-ols, whereas juice and endocarp had little of these compounds.

In Hirado-buntan tissues, naringin and rhoifolin predominate among the flavonoids, as reported previously [14]. In addition to these compounds, we found that neohesperidin occurs

Table 2
Relationships between flavonoid levels and peak areas of flavonoids investigated

Flavanones					Flavones					Flavon-3-ols				
No.	Compound	$a(\times 10^6)^a$	$b(\times 10^3)^a$	r^b	No.	Compound	$a(\times 10^6)^a$	$b(\times 10^3)^a$	r^b	No.	Compound	$a(\times 10^6)^a$	$b(\times 10^3)^a$	r^b
1	Eriocitrin	2.89	2.50	0.999	9	Isorhoifolin	1.27	−0.73	0.999	3	Robinetin	0.74	−3.22	1.000
2	Neoeriocitrin	2.41	−3.56	0.999	10	Rhoifolin	1.01	−0.36	0.999	6	Rutin	0.65	−13.63	0.988
4	Narirutin	2.37	2.36	0.999	11	Diosmin	1.23	−1.82	0.997	14	Quercetin	1.11	−8.32	1.000
5	Naringin	2.20	−2.30	0.999	12	Neodiosmin	1.04	−3.69	1.000	17	Kaempferol	1.47	−1.64	1.000
7	Hesperidin	2.21	−9.31	1.000	16	Luteolin	2.00	10.82	0.999	19	Isorhamnetin	1.63	−15.79	1.000
8	Neohesperidin	2.16	1.33	0.999	18	Apigenin	3.22	0.72	1.000	21	Rhamnetin	1.41	−8.00	0.999
13	Neoponcirin	1.54	5.13	0.999	20	Diosmetin	2.23	−1.82	0.997					
15	Poncirin	1.46	5.75	0.999	23	Sinensetin	2.40	9.27	0.999					
22	Isosakuranetin	3.17	8.29	1.000	24	Acacetin	3.39	−4.63	1.000					
					25	Tangeretin	3.12	−0.73	0.999					

[a] Coefficients of the regression equation $y = ax + b$, where x is flavonoid concentration (ppm) and y is peak area, for concentrations ranging from 10 to 100 ppm.
[b] Correlation coefficients of the regression equation.

Table 3
Recoveries of eriocitrin, naringin, hesperidin and tangeretin from mesocarp and juice samples of Unshiu (*Citrus unshiu* Marc.) and Hirado-buntan (*Citrus grandis* Osbeck F. Hirado)

Compound	Mean recovery ± S.D.[a] (%)			
	Unshiu		Hirado-buntan	
	Mesocarp	Juice	Mesocarp	Juice
Eriocitrin	102.46 ± 2.38	102.82 ± 2.52	101.93 ± 2.32	102.68 ± 2.18
Naringin	97.47 ± 3.71	96.87 ± 3.77	102.58 ± 5.13	101.14 ± 5.03
Hesperidin	101.55 ± 5.72	104.93 ± 5.96	98.46 ± 4.09	98.22 ± 3.90
Tangeretin	103.13 ± 3.12	102.96 ± 3.34	99.68 ± 2.85	102.34 ± 3.05

For operating conditions, see text.
[a] Mean values and standard deviations for five replicates.

in all five tissues examined. The flavones and flavon-3-ols are also abundant in leaves as found with Unshiu. The flavonoid content in the epicarp is considerably lower than that found in the Unshiu epicarp, whereas Hirado-buntan juice contained relatively larger concentrations of flavonoids than did Unshiu juice. The occurrence and distribution of flavonoids in each tissue of

Table 4
Contents of flavonoids in epicarp, mesocarp, endocarp, juice and leaf samples of Unshiu and Hirado-buntan

No.	Compound	Content[a] (mg per g fresh mass)									
		Unshiu					Hirado-buntan				
		Epicarp	Mesocarp	Endocarp	Juice	Leaf	Epicarp	Mesocarp	Endocarp	Juice	Leaf
1	Eriocitrin	0.020	0.028	0.018	0.002	0.123	–[b]	–	–	–	–
2	Neoeriocitrin	–	–	–	–	–	–	–	–	0.020	0.130
4	Narirutin	0.745	4.938	2.896	0.154	0.084	0.026	0.015	0.014	–	0.141
5	Naringin	–	–	–	–	–	1.363	13.952	11.187	0.785	4.013
6	Rutin	0.126	tr[c]	tr	0.029	1.170	0.053	–	–	–	0.975
7	Hesperidin	9.452	21.030	4.225	0.087	9.155	–	0.011	0.013	0.017	–
8	Neohesperidin	–	–	–	–	–	0.074	0.120	0.060	0.015	0.671
9	Isorhoifolin	0.048	0.029	–	–	0.681	–	–	–	–	–
10	Rhoifolin	0.101	0.026	–	–	0.441	0.105	0.161	0.061	0.056	2.323
11	Diosmin	0.044	0.020	–	0.014	0.775	0.036	–	–	0.006	0.119
12	Neodiosmin	0.019	0.023	–	–	0.282	–	0.028	0.023	0.011	–
13	Neoponcirin	0.195	0.871	0.343	tr	tr	0.015	0.064	0.052	tr	–
15	Poncirin	–	–	–	–	–	–	–	–	–	tr
16	Luteolin	–	–	–	–	–	0.019	0.011	–	tr	0.058
17	Kaempferol	0.017	–	–	–	tr	–	–	–	–	–
18	Apigenin	0.008	–	–	–	–	–	–	–	–	–
20	Diosmetin	0.057	–	–	–	–	0.017	–	–	–	–
23	Sinensetin	0.022	–	–	–	0.031	0.021	–	0.014	tr	–
24	Acacetin	0.025	tr	tr	–	0.076	–	–	–	–	–
25	Tangeretin	0.076	0.019	–	–	0.117	0.078	–	–	–	–
	Total	10.955	26.984	7.482	0.286	12.935	1.807	14.362	11.424	0.910	8.430

[a] Mean values for four replicates.
[b] Dashes indicate not detected.
[c] tr = trace, not measurable in UV spectra.

Hirado-buntan was as characteristic as that found in Unshiu. Robinetin, quercetin, isorhamnetin, rhamnetin and isosakuranetin either were not present or were present in insufficient concentrations to be detected in these two *Citrus* species.

4. Conclusions

A routine and simultaneous HPLC method for the determination of 25 flavonoids that naturally occur in *Citrus* tissues was established. The flavonoids in epicarp, mesocarp and endocarp tissues of fruits and in leaf tissues were lyophilized, milled and extracted with methanol–DMSO (1:1). The resulting supernatant from these extractions was diluted ten-fold with water and the flavonoids were retained on a Sep-Pak C_{18} cartridge. After elution with methanol–DMSO (1:1), the extracts were filtered and injected on to an HPLC column. Clarified juice samples were examined in a similar fashion. The separated compounds were identified by comparing both their t_R values and UV spectra.

5. Acknowledgement

This work was supported in part by an integrated research programme for effective use of biological activities to create new demand (Bio Renaissance Programme) from the Ministry of Agriculture, Forestry and Fisheries (BRP-93-VII-B-3).

6. References

[1] D. Guadagni, V.P. Maier and J.G. Turnbaugh, *J. Sci. Food Agric.*, 24 (1973) 1277.
[2] D. Guadagni, V.P. Maier and J.G. Turnbaugh, *J. Food Sci.*, 41 (1976) 681.
[3] G.E. DuBois and R.A. Stephenson, *J. Agric. Food Chem.*, 30 (1982) 676.
[4] R. Kato, T. Nakadate, S. Yamamoto and T. Sugiyama, *Carcinogenesis*, 4 (1983) 1301.
[5] H. Nishino, M. Nagao, H. Fujiki and T. Sugiyama, *Cancer Lett.*, 21 (1983) 1.
[6] Jp. Armand, M. De Forni, G. Recondo, L. Cals, E. Cvitkovic and Jn. Munck, in V. Cody, E. Middleton and J.F. Harborne (Editors), *Plant Flavonoids in Biology and Medicine II: Biochemical, Cellular, and Medicinal Properties —Proceedings of a Meeting on Plant Flavonoids in Biology and Medicine, Strasbourg, France, August 31–September 3, 1987*, Alan R. Liss, New York, 1988, p. 235.
[7] A.K. Verma, J.A. Johnson, M.N. Gould and M.A. Tanner, *Cancer Res.*, 48 (1988) 5754.
[8] H. Wei, L. Tye, E. Bresnick and D.F. Birt, *Cancer Res.*, 50 (1990) 499.
[9] E.E. Deschner, J. Ruperto, G. Wong and H.L. Newmark, *Carcinogenesis*, 7 (1991) 1193.
[10] W.W. Busse, D.E. Kopp and E. Middleton, Jr., *J. Allergy Clin. Immunol.*, 73 (1984) 801.
[11] R. Landolfi, R.L. Mower and M. Steiner, *Biochem. Pharmacol.*, 33 (1984) 1525.
[12] E. Middleton, Jr., and G. Drzewiecki, *Biochem. Pharmacol.*, 21 (1984) 3333.
[13] C. Bronner and Y. Landry, *Agents Actions*, 16 (1985) 147.
[14] M. Nishiura, S. Esaki and S. Kamiya, *Agric. Biol. Chem.*, 33 (1969) 1109.
[15] M. Nishiura, S. Esaki and S. Kamiya, *Agric. Biol. Chem.*, 35 (1971) 1691.
[16] J.H. Tatum, R.E. Berry and C.J. Hearn, *Proc. Fla. State Hortic. Soc.*, 87 (1974) 75.
[17] W.A. Court, *J. Chromatogr.*, 130 (1977) 287.
[18] D. Strack and J. Krause, *J. Chromatogr.*, 156 (1978) 359.
[19] M. Vanhaelen and R. Vanhaelen-Fastre, *J. Chromatogr.*, 187 (1980) 255.
[20] D. Treutter, *J. Chromatogr.*, 436 (1988) 490.
[21] L.W. Wulf and C.W. Nagel, *J. Chromatogr.*, 116 (1976) 271.
[22] D.L. Daigle and E.J. Conkerton, *J. Chromatogr.*, 240 (1982) 202.
[23] K. Van de Casteele, H. Geiger and C.F. Van Sumere, *J. Chromatogr.*, 240 (1982) 81.
[24] S.V. Ting, R.L. Rouseff, M.H. Dougherty and J.A. Attaway, *J. Food Sci.*, 44 (1979) 69.
[25] R.L. Rouseff and S.V. Ting, *J. Chromatogr.*, 176 (1979) 75.
[26] J.F. Fisher and T.A. Wheaton, *J. Agric. Food Chem.*, 24 (1976) 898.
[27] R.L. Rouseff, S.F. Martin and C.O. Youtsey, *J. Agric. Food Chem.*, 35 (1987) 1027.
[28] K. Kanes, B. Tisserat, M. Berhow and C. Vandercook, *Phytochemistry*, 32 (1993) 967.
[29] M. Anis and Aminuddin, *Plant Biochem. J.*, 8 (1981) 56.
[30] R.M. Horowits and B. Gentili, in S. Nagy, P.E. Shaw and M.K. Veldhuis (Editors), *Citrus Science and Technology*, Vol. 1, Avi Publishing, Westport, CT, 1977, p. 397.

ELSEVIER

Journal of Chromatography A, 667 (1994) 67–73

JOURNAL OF CHROMATOGRAPHY A

Separation of lactose, lactobionic acid and lactobionolactone by high-performance liquid chromatography☆

Peter J. Simms, Kevin B. Hicks *, Rebecca M. Haines, Arland T. Hotchkiss, Jr., Stanley F. Osman

US Department of Agriculture, ARS, Eastern Regional Research Center, 600 E. Mermaid Lane, Philadelphia, PA 19118, USA

(First received October 21st, 1993; revised manuscript received December 20th, 1993)

Abstract

Complete separation of the three title compounds has been achieved for the first time on either a β-cyclodextrin- or an aminopropyl-silica gel-bonded-phase HPLC column eluted with acetonitrile–aqueous buffer mixtures. An HPLC system using either of these stationary phases and a refractive index detector directly quantified lactose, lactobionic acid and lactobionolactone at levels between 0.3 and 40 μg of analyte per injection. Simple separations of lactose and lactobionic acid were also readily accomplished on a calcium-form cation-exchange type column eluted with 1.2 m*M* $CaSO_4$ solution. These methods are useful for monitoring the chemical or enzymatic conversion of lactose into the valuable derivatives, lactobionic acid and lactobionolactone.

1. Introduction

Aldonic acids have a broad range of important biological and chemical functions. Aldonic acids such as gluconic acid, for instance, are useful metal chelators because of their ability to form stable complexes with metal ions through coordination complexes involving their carboxyl and hydroxyl groups. Lactobionic acid, 4-O-β-D-galactopyranosyl-D-gluconic acid, has recently gained importance in the pharmaceutical industry by having the ability to solubilize and stabilize drugs such as erythromycin [1] and to preserve the viability of human organs, prior to transplant [2]. Such aldonic acid disaccharides, which can be synthesized by oxidation [3–6] of neutral sugars, establish pH-dependent solution equilibria with their lactone forms.

The separation and quantitative analysis of sugar acids or lactones has been performed by various high-performance liquid chromatographic (HPLC) methods using reversed-phase [7–9], anion-exchange [10–14] and cation-exchange [3,15] columns. HPLC methods have also been developed for the separation of some monosaccharide uronic and aldonic acids from their lactones [16,17] and for separation of uronic acid oligomers [18]. Few methods currently exist, however, for the analysis of glycosyl aldonic acids such as lactobionic acid. One method has been published [3], but it does not permit the direct separation and quantification of lactose, lactobionic acid and lactobionolactone. In our laboratory, we are developing bio-catalytic methods for the oxidation of the surplus dairy by-product, lactose, to produce the valuable deriva-

* Corresponding author.

☆ Presented in part at the *203rd ACS National Meeting, San Francisco, CA, April 5–10, 1992*, paper CARB-60.

SSDI 0021-9673(93)E0064-2

tives, lactobionic acid and lactobionolactone (4-O-β-D-galactopyranosyl-D-glucono-1,5-lactone). In order to fully characterize the efficiency and selectivity of our bio-catalysts, it was necessary to rapidly quantify amounts of lactose, lactobionic acid and lactobionolactone in reaction mixtures. We now report the first HPLC methods for accomplishing this analysis.

2. Experimental[a]

2.1. Materials

Calcium lactobionate, lactobionic acid and lactose were obtained from Sigma (St. Louis, MO, USA). Lactobionolactone and potassium lactobionate were obtained from Pfanstiehl Labs. (Waukegan, IL, USA). All HPLC solvents were obtained from Baxter (Muskegon, MI, USA) and were purified through 0.45-μm nylon filters. Water used for HPLC analyses was purified using a Milli-Q filtration system obtained from Millipore (Bedford, MA, USA).

2.2. Chromatography

β-Cyclodextrin-bonded-phase columns (Cyclobond I, 250 × 4.6 mm) were purchased from Advanced Separation Technology (Whippany, NJ, USA). Reversed-phase (C_{18}) columns (Econosphere, 250 × 4.6 mm, 5 μm particle size) were purchased from Alltech (Deerfield, IL, USA). The Dynamax-NH_2 aminopropyl-silica gel (APS) columns were purchased from Rainin (Woburn, MA, USA). The HPX-87C column (300 × 7.8 mm) was obtained from Bio-Rad Labs. (Richmond, CA, USA).

The HPLC system used was a Gilson Model 303 dual-pump system equipped with a Model 811 dynamic mixer and a Rheodyne Model 7125 fixed-loop (20-μl) injector. Samples were detected with a Waters Model R-403 differential refractometer and the data were recorded on a Varian 4270 integrator. Samples were also chromatographed with a DuPont Model 8800 pump, equipped with a heated column compartment, a Rheodyne Model 7125 fixed-loop (20-μl) injector, an ERMA ERC-7520 refractive index detector and a Spectra-Physics 4270 integrator.

[a] Reference to brand or firm names does not constitute an endorsement by the US Department of Agriculture over others of a similar nature not mentioned.

3. Results and discussion

3.1. Calcium-form cation-exchange chromatography

Calcium-form cation-exchange columns have been used to separate neutral mono- and disaccharides on both the analytical and the preparative level [19,20]. Hydrogen-form cation-exchange resins have been used for similar separations of uronic and aldonic acids and related lactones [16,19]. There are no reports, however, on the use of calcium-form cation-exchange resins for separation of sugars and sugar acids. When lactose, lactobionolactone and lactobionic acid were chromatographed on the calcium-form cation-exchange column, lactose and lactobionolactone co-eluted, but lactobionic acid was nearly baseline resolved from the other two carbohydrates (Fig. 1). The separations were affected primarily by column temperature and the concentration of calcium ion in the mobile phase. As the temperature was increased from room temperature to an optimal temperature of 85°C, the retention times of all the analytes increased and the peaks became much sharper and symmetrical. The addition of calcium sulfate to the mobile phase increased the retention times of all the compounds, improved the resolution between lactose and lactobionic acid, and regenerated the stationary phase calcium ions that had been removed by complexation with lactobionate. Optimal separations were achieved with a calcium ion concentration of about 1.2 m*M*. The presence of calcium ions did have one disadvantage. Injection of samples containing phosphate and other inorganic anions led to the formation of insoluble calcium salts that precipitated in the HPLC system. Treatment of such samples to

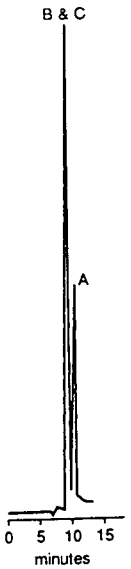

Fig. 1. Chromatogram of (A) lactobionic acid, (B) lactose and (C) lactobionolactone on a Bio-Rad HPX-87C column at 85°C, eluted at 1 ml/min with 1.2 m*M* $CaSO_4$ as the mobile phase. Refractive index detection.

remove inorganic anions, prior to injection, is required.

Since lactose and lactobionolactone co-eluted by this method, the concentration of each of these compounds could not be determined directly. It was possible, however, to saponify the lactobionolactone, using published methods [13,21], prior to HPLC analysis. A quantitative comparison of the resulting chromatogram with that of the unsaponified sample enables one to determine amounts of all three analytes. If one only wants to determine concentrations of lactose and lactobionate (ionized lactobionic acid plus saponified lactobionolactone) this method is simple, rapid, and practical.

3.2. Reversed-phase HPLC

Reversed-phase HPLC has often been used in the separation of carbohydrates [22] and small organic acids [23,24]. Separation of lactose, lactobionic acid and lactobionolactone on a C_{18}-type reversed-phase column produced the optimized separation shown in Fig. 2. Although some resolution of the three species was obtained, lactobionic acid eluted in the void volume of the column along with unretained sample contaminants which made quantification problematic. Lowering the pH of the mobile phase resulted in longer retention times for lactobionic acid, but poorer separation between lactobionic acid and lactose. Reversed-phase columns were, therefore, not considered further for these separations.

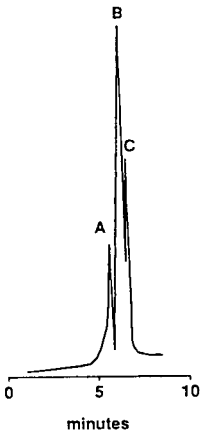

Fig. 2. Econosphere reversed-phase separation of (A) lactobionic acid, (B) lactose and (C) lactobionolactone using distilled water as the mobile phase at room temperature, eluted at 0.5 ml/min. Refractive index detection.

3.3. Aminopropyl-silica gel columns

APS columns are typically used in the normal-phase mode (acetonitrile–water mobile phases) for separation of neutral carbohydrates. Under those conditions, however, acidic carbohydrates bind tightly to the APS phase. Previous workers [25–27] have used APS columns in a weak anion-exchange mode, with buffered mobile phases for separating uronic, aldonic and aldaric acids. Under those conditions, sugar acids are eluted with reasonable analysis times. Since the present separation involved both neutral and acidic carbohydrates, it was necessary for the APS column to function as a weak ion exchanger as well as a normal-phase column. Therefore, a mobile phase of acetonitrile–aqueous buffer was used [25]. The percent of organic modifier and the buffer concentration were varied to determine

the optimized separation conditions. Lactose, lactobionic acid and lactobionolactone were baseline resolved in about 12 min using a acetonitrile–sodium phosphate buffer (50 m*M*, pH 5.0) (60:40) (Fig. 3). Reduction of acetonitrile below the 60% level resulted in poorer resolution between lactose and lactobionolactone. The retention times of the neutral sugars varied little with a change in buffer molarity, but the retention of lactobionate was greatly affected. When buffer molarity was decreased below 50 m*M*, the retention time and peak width of lactobionate increased. When pure water was used as the aqueous component (0 buffer molarity) lactobionate did not elute from the column.

It is important to note that since these three carbohydrates have low solubilities in acetonitrile, the HPLC samples in this case and in those on the β-cyclodextrin column described below were prepared as follows: the sample was first dissolved in buffer and then an equal amount of acetonitrile was added. Failure to follow this order resulted in occasional precipitation of analytes.

3.4. β-Cyclodextrin-bonded-phase column

β-Cyclodextrin-bonded-phase columns are highly selective and have recently been used to separate many types of compounds. Like APS columns, cyclodextrin-bonded phases have the ability to separate analytes by different chromatographic modalities. When a large percentage of organic modifier is used, the column functions in the normal-phase mode [28]. When a large percentage of aqueous component is used, the column functions in the reversed-phase mode [29]. Cyclodextrin-bonded-phase columns have mainly been used for separating chiral compounds [29,30]. To date, the only carbohydrates separated on this stationary phase have been various neutral mono-, di-, tri- and tetrasaccharides, deoxysugars and sugar alcohols [28], and carbohydrate anomers [31].

To achieve separation of lactose, lactobionic acid and lactobionolactone, we used the column in the normal-phase mode. Therefore, various compositions of acetonitrile–water were examined as a suitable mobile phase. Surprisingly, under these conditions, lactobionate was very tightly bound as it had been on the APS column. Hence, a buffered aqueous component was used. The optimized separation of lactose, lactobionic acid and lactobionolactone (Fig. 4) was achieved in approximately 11 min using acetonitrile–sodium phosphate buffer (50 m*M*, pH 5.0) (70:30). A similar separation was achieved in under 10 min using acetonitrile–ammonium acetate buffer (0.2 *M*, pH 5.0) (70:30); however, there was a negative peak that appeared between lactose and lactobionolactone that made quantification of

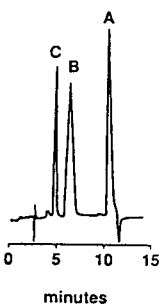

Fig. 3. The separation of (A) lactobionic acid, (B) lactose and (C) lactobionolactone on a Dynamax-NH_2 column using acetonitrile–NaH_2PO_4 buffer (50 m*M*, pH 5.0) (60:40) at 1 ml/min and at room temperature. Refractive index detection.

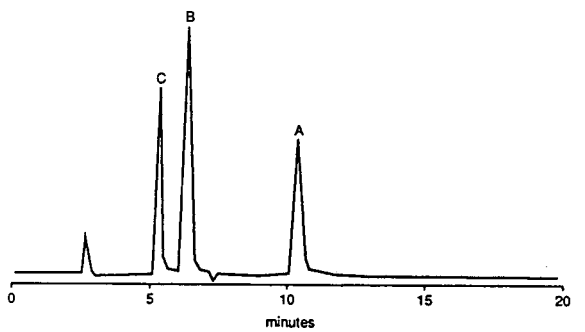

Fig. 4. The separation of (A) lactobionic acid, (B) lactose and (C) lactobionolactone on a Cyclobond I column using acetonitrile–NaH_2PO_4 buffer (50 m*M*, pH 5.0) (70:30) at 1 ml/min and at room temperature. Refractive index detection.

these two carbohydrates difficult. The effect of the molarity of buffer in the mobile phase was examined for this system. As with the APS column, increasing the molarity of buffer led to a decrease in the retention time of lactobionate and, when water was used as the aqueous part of the mobile phase, as mentioned above, lactobionate did not elute from the column. It is important to note that the cyclodextrin column was more stable than the APS column, and over more than two years of use, there was no loss in resolution or capacity. Therefore, the cyclodextrin-bonded-phase column system was most useful and practical for most laboratory applications, such as monitoring the bio-catalytic oxidation of lactose to produce lactobionolactone and lactobionic acid (Fig. 5).

The resolution and the capacity factors for all the different stationary phases used in this work are shown in Table 1. Resolution was calculated as follows: $R_s = \Delta t / t_w$, where Δt is the distance between the two peaks in question and t_w is the average width of the peaks at the baseline. The capacity factor, k', was calculated using the equation $k' = (t_R - t_0)/t_0$, where t_R is the retention time of the peak in question and t_0 is the retention time of a non-retained solute. The data confirm that the best resolution was obtained for all three compounds on the β-cyclodextrin and APS columns.

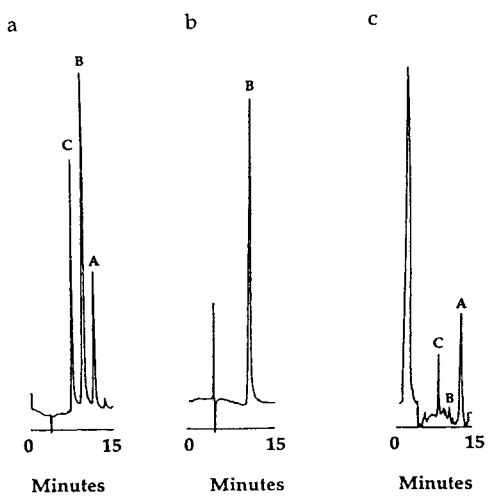

Fig. 5. Bio-catalytic oxidation of lactose monitored by HPLC. (a) Standard lactobionic acid (A), lactose (B) and lactobionolactone (C). (b) Analysis of initial reaction mixture containing lactose. (c) Analysis of reaction mixture after reaction with bio-catalyst. See Fig. 4 for chromatographic system.

Table 1
Capacity factors and resolution values for lactose, lactobionic acid and lactobionolactone obtained for the various HPLC methods

Column[a]	Carbohydrate	k'	R_s
Econosphere	Lactobionic acid	0[b]	
			1.30
	Lactose	0.22	
			0.44
	Lactobionolactone	0.36	
Dynamax-NH_2	Lactobionolactone	0.85	
			1.5
	Lactose	1.32	
			13.1
	Lactobionic acid	2.27	
Cyclobond I	Lactobionolactone	1.12	
			2.6
	Lactose	1.60	
			7.8
	Lactobionic acid	3.28	
HPX-87C	Lactose	0.31	
			0[c]
	Lactobionolactone	0.31	
			1.28
	Lactobionic acid	0.50	

[a] For mobile phases, see Figs. 1–4.
[b] Lactobionic acid eluted in the void volume on this stationary phase.
[c] Lactose and lactobionolactone co-eluted on this stationary phase.

The sensitivity and linearity of detection of lactose, lactobionic acid and lactobionolactone in these HPLC systems were determined. The calcium-form cation-exchange column, APS column and the β-cyclodextrin-bonded-phase column showed linear detector responses from 0.015 mg/ml to at least 2 mg/ml of analyte. With a 20-μl injector loop, this corresponds to a linear range of 0.3 to 40 μg of analyte per injection.

Table 2
Summary of advantages and disadvantages of HPLC methods developed for separation of lactose, lactobionic acid and lactobionolactone

Column	Advantage	Disadvantage
HPX-87C	Simple mobile phase, short analysis time	Lactose and lactobionolactone co-elute; inorganic anions may precipitate as calcium salts
Econosphere	Simple mobile phase, short analysis time	Lactobionic acid elutes in the void volume
Dynamax-NH_2	Baseline resolution of all three compounds in under 12 min	Relatively low solubility of compounds in the mobile phase; stationary phase less stable than others in table
Cyclobond I	Rapid baseline resolution of all three compounds; stable stationary phase	Relatively low solubility of compounds in the mobile phase

4. Conclusions

The relative advantages and disadvantages of each stationary phase for the separation of lactobionic acid, lactose and lactobionolactone are shown in Table 2. For the separation of lactose from lactobionic acid only, use of the HPX-87C column is recommended. This system uses a simple, aqueous mobile phase and a stable stationary phase. If samples also contain lactobionolactone, levels of all three analytes can be determined by quantitative analysis of chromatograms of the samples before and after lactone saponification. Use of the APS or β-cyclodextrin-bonded silica gels will allow the direct analysis of all three compounds. This is the first time a β-cyclodextrin-bonded stationary phase has been applied to separations of sugar acids. Because of its exceptional durability and selectivity, it is highly recommended for this application.

5. References

[1] S.K. Dutta and S.B. Basu, *Pharmaceuticals*, 90 (1979) 365.
[2] J.A. Walberg, R.A. Love, L. Landegaard, H.H. Southard and F.O. Belzer, *Transplantation*, 43 (1987) 5–9.
[3] L.A.Th. Verhaar, H.E.J. Hendriks, W.P.Th. Groenland and B.F.M. Kuster, *J. Chromatogr.*, 549 (1991) 113–125.
[4] H.E.J. Hendriks, B.F.M. Kuster and G.B. Marin, *Carbohydr. Res.*, 204 (1990) 121–129.
[5] H.E.J. Hendriks, B.F.M. Kuster and G.B. Marin, *Carbohydr. Res.*, 214 (1991) 71–85.
[6] K.K. Sen Gupta, S. Sen Gupta and A. Mahapatra, *J. Carbohydr. Chem.*, 8 (5) (1989) 713–722.
[7] A. Heyraud and C. Rochas, *J. Liq. Chromatogr.*, 5 (1982) 403–412.
[8] J.W. Finley and E. Duang, *J. Chromatogr.*, 207 (1981) 449–453.
[9] C.S. Tsao and S.L. Salimi, *J. Chromatogr.*, 245 (1982) 355–358.
[10] S.V. Prabhu and R.P. Baldwin, *J. Chromatogr.*, 503 (1990) 227–235.
[11] L.W. Doner and K.B. Hicks, *Anal. Biochem.*, 115 (1981) 225–230.
[12] P.J.M. Dijkgraaf, L.A.Th. Verhaar, W.P.T. Groenland and K. Van Der Wiele, *J. Chromatogr.*, 329 (1985) 371–378.
[13] J.D. Blake, M.L. Clarke and G.N. Richards, *J. Chromatogr.*, 312 (1984) 211–219.
[14] J.M.H. Dirkx and L.A.Th. Verhaar, *Carbohydr. Res.*, 73 (1979) 287–292.
[15] E. Rajakylä, *J. Chromatogr.*, 218 (1981) 695–701.
[16] K.B. Hicks, P.C. Lim and M.J. Haas, *J. Chromatogr.*, 319 (1985) 159–171.
[17] K.B. Hicks, *Carbohydr. Res.*, 145 (1986) 312–318.

[18] A.T. Hotchkiss, Jr. and K.B. Hicks, *Anal. Biochem.*, 184 (1990) 200–206.
[19] K.B. Hicks, S.M. Sondey and L.W. Doner, *Carbohydr. Res*, 168 (1987) 33–45.
[20] K.B. Hicks, E.V. Symanski and P.E. Pfeffer, *Carbohydr. Res.*, 112 (1983) 37–50.
[21] K.B. Hicks, *Adv. Carbohydr. Chem. Biochem.*, 46 (1988) 17–329.
[22] G.D. McGinnis, S. Prince and J. Lowrimore, *J. Carbohydr. Chem.*, 5 (1986) 83–97.
[23] C.S. Tsao and M. Young, *J. Chromatogr.*, 330 (1985) 408–411.
[24] S. Bulusu, G.A. Mills and V. Walker, *J. Liq. Chromatogr.*, 14 (1991) 1757–1777.
[25] Y.-A. Wei and J.-N. Fang, *J. Chromatogr.*, 513 (1990) 227–235.
[26] A.G.J. Voragen, H.A. Schols, J.A. de Vries and W. Pilnik, *J. Chromatogr.*, 244 (1982) 327–336.
[27] E.I. Laakso, R.A. Tokola and E.L. Hirvisalo, *J. Chromatogr.*, 278 (1983) 406–411.
[28] D.W. Armstrong and H.L. Jin, *J. Chromatogr.*, 462 (1989) 219–232.
[29] G. Vigh, G. Quintero and G. Farkas, *J. Chromatogr.*, 484 (1989) 237–250.
[30] M. Pawlowska, *J. Liq. Chromatogr.*, 14 (1991) 2273–2286.
[31] D.W. Armstrong and H.L. Jin, *Chirality*, 1 (1989) 27–37.

ELSEVIER

Journal of Chromatography A, 667 (1994) 75–83

JOURNAL OF CHROMATOGRAPHY A

Improved fractionation of sialylated glycopeptides by pellicular anion-exchange chromatography

Jeffrey S. Rohrer*

Dionex Corporation, 1228 Titan Way, Sunnyvale, CA 94086, USA

(First received September 7th, 1993; revised manuscript received December 24th, 1993)

Abstract

The glycoprotein bovine fetuin was treated with trypsin and the Asn-81 tryptic glycopeptide was purified (90% pure by Edman sequencing) by reversed-phase chromatography (RP-HPLC). The Asn-81 glycopeptide, which eluted as a single peak by RP-HPLC, was separable into five peaks on the NucleoPac PA100 column, a pellicular anion-exchange column. Each of the five Asn-81 glycopeptide peaks was shown to contain N-linked oligosaccharides by treatment of each peak with peptide N^4-(N-acetyl-β-D-glucosaminyl) asparagine amidase F (PNGase F) and subsequent oligosaccharide analysis by high-pH anion-exchange chromatography with pulsed amperometric detection. High-pH anion-exchange chromatography–pulsed amperometric detection oligosaccharide analysis revealed that each peak contained a different population of sialylated N-linked oligosaccharides. Hence each peak contained a different group of glycopeptide glycoforms. It was observed that the longer the retention time of the Asn-81 glycopeptide peak on the anion-exchange column, the greater the oligosaccharide sialylation. Two glycopeptide peaks which differed in their distribution of disialylated oligosaccharides demonstrated that the glycopeptide separation was a result of something more than gross differences in sialic acid content. The two other N-linked tryptic glycopeptides of fetuin were also separated into multiple peaks on the NucleoPac PA100 column and these separations were shown to be due to differences in oligosaccharide sialylation. The separations of the three fetuin N-linked glycopeptides demonstrate that pellicular anion-exchange chromatography offers improved separation speed and resolution for the separation of sialylated glycopeptides.

1. Introduction

Glycoproteins are microheterogenous with respect to their attached oligosaccharide structures. This heterogeneity arises because glycoproteins may differ in number of sites of oligosaccharide attachment and in the degree of occupancy of each site. Additionally, each site may possess its own set of oligosaccharides. Glycoproteins having an identical polypeptide but differing in glycosylation site occupancy, oligosaccharide structure, or location of the oligosaccharide structures, are called glycoforms. Similarly, glycopeptides having an identical peptide but differing in oligosaccharide content, are glycopeptide glycoforms. IgG has 30 glycoforms which vary reproducibly with physiological state and were shown to be a marker of rheumatoid arthritis [1]. The population of glycoforms present when glycoproteins are produced recombinantly is dependent upon cell type and cell culture conditions (for review, see ref. 2), and a

* Corresponding author.

* Address for correspondence: Dionex Corporation, 470 D Lakeside Drive, Sunnyvale, CA 94086, USA.

0021-9673/94/$07.00
SSDI 0021-9673(94)00006-U

glycoprotein's oligosaccharide structure can affect the protein's specific activity, clearance rate and immunogenicity [3].

The separation of glycoprotein and glycopeptide glycoforms is a challenging analytical problem. Recently, capillary electrophoresis has shown promise in separating glycoprotein glycoforms, but capillary electrophoresis techniques are limited because fractions can not be collected for further analysis [4–7]. Concanavalin A–crossed affinoimmunoelectrophoresis has been used to separate human transferrin into three groups of glycoforms based on the oligosaccharide branching at the protein's two N-linked (*i.e.*, asparagine-linked) glycosylation sites [8]. Rice *et al.* [9] showed that RP-HPLC at pH 7 could separate each of the three tryptic N-linked glycopeptides of bovine fetuin into groups of glycoforms based on the number of sialic acid residues on each glycopeptide.

Pellicular anion-exchange resins have been successfully used to separate oligonucleotides [10], protein isoforms due to deamidation [11] and oligosaccharide linkage isomers [12]. This paper shows that the Asn-81 glycopeptide of bovine fetuin (amino acid residues 54–84), which elutes as a single peak by RP-HPLC, can be separated into five peaks on a pellicular anion-exchange column. These peaks are glycopeptides which possess different populations of sialylated oligosaccharides. Hence each peak has a different population of sialylated glycopeptide glycoforms. Additionally, this manuscript shows that the two other N-linked tryptic glycopeptides of fetuin can be separated into multiple peaks on the pellicular anion-exchange column.

2. Experimental

2.1. Materials

Bovine fetuin was obtained from Gibco (Grand Island, NY, USA; lot No. 14P7696). Acetonitrile and 50% NaOH were obtained from Fisher Scientific (Pittsburgh, PA, USA). Trifluoroacetic acid (TFA) was obtained from J.T. Baker (Phillipsburg, NJ, USA). Polypropylene tubes (1.5 ml) for fraction collection were purchased from Sarstedt (Catalogue No. 72-692; Princeton, NJ, USA). Glycerol-free peptide N^4-(N-acetyl-β-D-glucosaminyl)asparagine amidase F (PNGase F) and *Arthrobacter ureafaciens* neuraminidase were purchased from Boehringer Mannheim (Indianapolis, IN, USA). The water for all eluents and sample preparations was deionized water which was glass-distilled by a Corning Mega-Pure system. The distilled water was collected directly into a glass container.

2.2. Purification of the fetuin glycopeptides

Fetuin was reduced, alkylated, and treated with trypsin as previously described [13]. About 600 μg of a fetuin tryptic digest were separated on a DuPont Zorbax C_{18} RP-300 column (15 × 0.93 cm, Dionex) and fractions were collected [FOXY II fraction collector (ISCO)] into 100 × 13 mm polypropylene tubes (Fisher, Catalogue No.14-956-7A). This and all other separations were on a GlycoStation (Dionex) equipped with a variable-wavelength detector (VDM-2). The first five minutes of the separation were isocratic at 5% eluent B [0.1% TFA in acetonitrile–water (90:10)] and 95% eluent A (0.1% aqueous TFA). This was followed by a linear gradient of 5 to 52% of B in the final 55 min. The flow-rate was 4.0 ml/min. Fractions were collected with the slope sensitivity set to "normal". The maximum fraction size was set to 4.0 ml. Fractions were immediately dried in a SpeedVac (Savant, Model SVC100). Two preparations of each glycopeptide, which were previously identified [13], were combined, dried and redissolved in water (600 μl). To assess the purity of each glycopeptide, an aliquot (2 μl) was rechromatographed on an analytical (15 × 0.46 cm) reversed-phase column (Zorbax C_{18} RP-300) with the same gradient used for the purification. The flow-rate was 1.0 ml/min.

The experimental strategy for analyzing the purified fetuin Asn-81 glycopeptide is shown in Fig. 1.

2.3. Peptide sequence analysis

The amino terminal sequence was determined for the fetuin Asn-81 glycopeptide to assess its

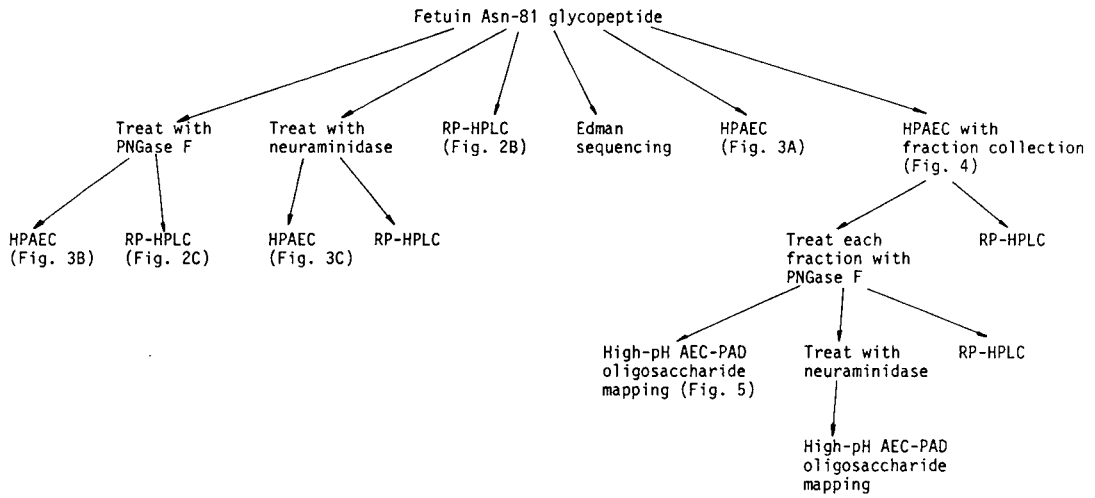

Fig. 1. Experimental scheme for the analysis of the fetuin Asn-81 glycopeptide after RP-HPLC purification. The right side of the diagram outlines the analysis of individual fractions from the anion-exchange separation (AE-HPLC) of the glycopeptide.

purity. A Porton Instruments (Tarzana, CA, USA) PI2090E integrated microsequencing system was used for the analysis. About 400 pmol (10 μl) of the glycopeptide was sequenced after deposition on a glass fiber "peptide support" (Porton). There was greater than 83% repetitive yield.

2.4. Anion-exchange separation of the fetuin glycopeptides

Each fetuin glycopeptide preparation and the neuraminidase and PNGase F digestions of these preparations were separated on a NucleoPac PA100 column (25 × 0.4 cm, Dionex). Tris–HCl (15 m*M*) pH 8.0 was installed as eluent A and 0.5 *M* NaCl, 15 m*M* Tris–HCl pH 8.0 was installed as eluent B. Both eluents were filtered through a 0.22-μm filter. The glycopeptide was separated with a gradient of 25 to 250 m*M* NaCl (5 to 50% B) in 30 min. The column was then returned to starting conditions over 2 min and held at starting conditions for 15 min prior to the next injection. The flow-rate was 1.0 ml/min and the absorbance was monitored at 215 nm. Fractions were prepared from a separation of 140 μl of the Asn-81 glycopeptide with a fraction collector slope sensitivity setting of "high" and the maximum fraction size set to 1 ml. The fractions were dried in the SpeedVac, redissolved in water (125 μl), and dialyzed against water using a microdialyzer (Pierce, System 100) with M_r 1000 cut-off dialysis tubing (Spectra, Los Angeles, CA, USA). After microdialysis, the fractions were dried.

2.5. Enzyme digestions

An aliquot (20 μl) of each fetuin glycopeptide was dried, and then dissolved in 100 μl of 50 m*M* sodium phosphate buffer pH 7.6 containing 10 m*M* EDTA and 0.5 units of PNGase F. EDTA was omitted from the buffer in the analyses of the Asn-138 and Asn-158 glycopeptides to make the chromatograms easier to interpret. These PNGase F digests were mixed and allowed to incubate for 18 h in a 37°C water bath. Fractions from the anion-exchange separation of the fetuin Asn-81 glycopeptide were redissolved in water (50 μl) and each added to a 1.5-ml polypropylene tube containing 50 μl of 50 m*M* sodium phosphate + 10 m*M* EDTA pH 7.6 and 0.5 units of PNGase F. To create a larger sample volume to work with, all PNGase F digests were diluted with 100 μl of water. An aliquot (40 μl) of each PNGase F digestion was analyzed by RP-HPLC (the same method described in section 2.2) to determine if the digestion was complete [14].

An aliquot (20 μl) of each fetuin glycopeptide

and an aliquot (50 μl) of each PNGase F digest of fractions from the anion-exchange separation of the fetuin Asn-81 glycopeptide were treated with 10 μl of a 1 mU/μl solution of *Arthrobacter ureafaciens* neuraminidase (in 0.1 *M* sodium acetate pH 5.0) and then brought to a total volume of 200 μl with 0.1 *M* sodium acetate pH 5.0. All samples were mixed and incubated at 37°C for 24 h.

2.6. Oligosaccharide analysis

PNGase F and neuraminidase digests were analyzed for oligosaccharides with a CarboPac PA100 column (25 × 0.4 cm, Dionex) and its guard column (5 × 0.4 cm). NaOH (100 m*M*) and 100 m*M* NaOH + 1.0 *M* sodium acetate were installed as eluents C and D, respectively. The NaOH eluents were prepared from appropriate dilutions of 50% NaOH. The sodium acetate eluent was filtered through a 0.22-μm filter. Oligosaccharides were separated with 100 m*M* NaOH and 20 m*M* sodium acetate (2% D) for 5 min followed by 100 m*M* NaOH and a gradient of 20 to 200 m*M* sodium acetate (2 to 20% D) over the next 65 min. The eluent was returned to starting conditions over the next 2 min and kept there for 15 min prior to the next injection. The flow-rate was 1.0 ml/min and the detector sensitivity was 100 nA.

3. Results

Fig. 2A shows the RP-HPLC separation of 7.5 μg of a bovine fetuin tryptic digest. The peak with a retention time of 41.9 min was previously identified as one of the three fetuin N-linked glycopeptides [13]. This glycopeptide has 31 amino acid residues (residues 54–84) and the carbohydrate is attached to Asn-81. Rechromatography of the purified fetuin Asn-81 glycopeptide (2 μl) is shown in Fig. 2B. Fig. 2C shows the RP-HPLC separation of the Asn-81 glycopeptide PNGase F digestion. PNGase F treatment removes the glycopeptide's oligosaccharide. The deglycosylated peptide elutes 2.1 min later than the native peptide, which suggests

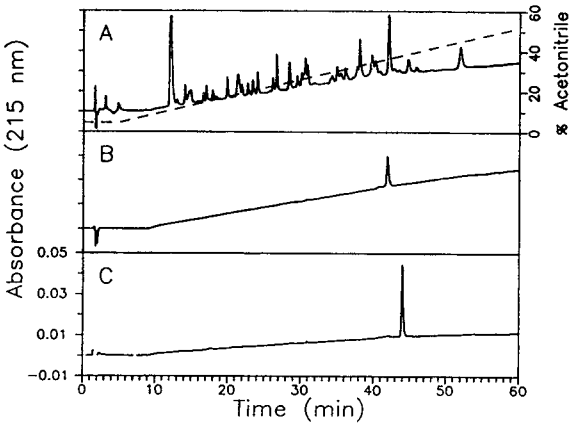

Fig. 2. RP-HPLC separations of bovine fetuin tryptic peptides (A), the purified fetuin Asn-81 glycopeptide (B), and the purified fetuin Asn-81 glycopeptide digested with PNGase F (C). The gradient is displayed with the dashed line in panel A. The separation conditions are described in section 2.2.

that the PNGase F digestion is complete [14]. RP-HPLC of glycopeptide PNGase F digestions is used in this manuscript to assess the extent of deglycosylation.

Fig. 3A shows the anion-exchange separation of the fetuin Asn-81 glycopeptide preparation. This preparation, which is one peak when separated by RP-HPLC (Fig. 2B), is separated into

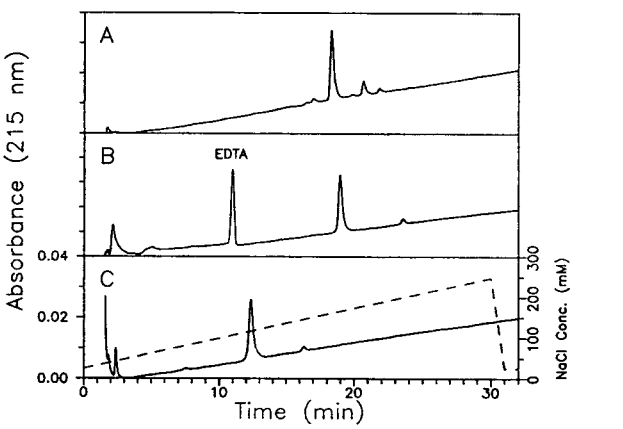

Fig. 3. Anion-exchange separations of the fetuin Asn-81 glycopeptide (A), the PNGase F digestion of the fetuin Asn-81 glycopeptide (B), and the neuraminidase digestion of the fetuin Asn-81 glycopeptide (C). The gradient is displayed with the dashed line in panel C. Each chromatogram represents 4 μl of the glycopeptide. The separation conditions are described in section 2.4.

seven peaks. Fig. 3B shows the anion-exchange separation of a PNGase F digest of the fetuin Asn-81 glycopeptide. The PNGase F treatment reduces the number of peaks. The peaks in the first 5 min of the chromatogram are also found in the blank (no substrate) digest (chromatogram not shown). The peak with a retention time of 10.5 min is EDTA, a component of the digestion buffer. The peak at 19 min is believed to be the deglycosylated fetuin Asn-81 glycopeptide. When this peak was collected and then separated by RP-HPLC, it coeluted with the deglycosylated fetuin Asn-81 glycopeptide (chromatogram not shown). The identity of the peak with a retention time of 23.5 min is unknown. Fig. 3C shows the anion-exchange separation of a neuraminidase digestion of the fetuin Asn-81 glycopeptide. This treatment also reduces the number of peaks. The peaks in the first 5 min of the chromatogram are also found in the blank digest (chromatogram not shown). The peak with a retention time of 12.5 min is believed to be the desialylated fetuin Asn-81 glycopeptide. When this peak was collected and then separated by RP-HPLC, it coeluted with the desialylated fetuin Asn-81 glycopeptide (chromatogram not shown). The identity of the peak at 16.5 min is unknown. When the Asn-81 glycopeptide preparation is incubated in either the PNGase F or the neuraminidase digest buffer and separated by anion-exchange chromatography, there is no change in the retention times of any peaks or the evolution of any new peaks (chromatograms not shown).

Fig. 4 shows the anion-exchange separation of 140 μl of the fetuin Asn-81 glycopeptide preparation. Seven peaks, numbered 1–7, were collected for further analysis. Each of the seven peaks was analyzed by RP-HPLC and only peaks 1 and 7 did not coelute with the Asn-81 glycopeptide peak. Using initial yields from Edman sequencing, the yield and purity of the fetuin Asn-81 glycopeptide was estimated to be 24 nmol and 90.8%, respectively. Edman sequencing of about 400 pmol (10 μl) of the glycopeptide preparation revealed that there were three peptide impurities. The amino-terminal sequences of the three contaminating peptides could be found in the amino acid sequence

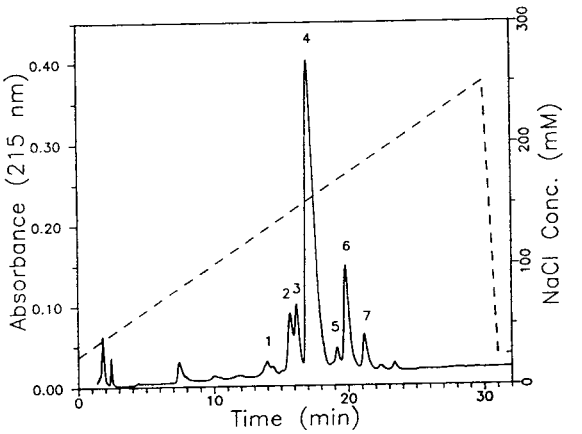

Fig. 4. Preparation of fractions from the anion-exchange separation of the fetuin Asn-81 glycopeptide. Peak numbers correspond to fractions digested with PNGase F. The dashed line shows the NaCl gradient. This is a separation of 140 μl of the glycopeptide. The separation conditions are described in section 2.4.

of bovine fetuin [15] and match the amino-terminal sequences of the following three fetuin tryptic peptides, residues 228–288, residues 103–113 and residues 295–315, which will be designated peptides A, B and C, respectively. Peptides A, B and C, which had been previously purified by RP-HPLC and sequenced [16], were analyzed on the anion-exchange column. Peptide A, which contains fetuin's three O-linked (*i.e.*, Ser/Thr-linked) glycosylation sites, coeluted with peak 1 and had the same doublet shape. Peptide A also had a small peak that coeluted with peak 3. Peptide B coeluted with peak 5 and peptide C coeluted with peak 1.

Fig. 5 shows the respective oligosaccharide profiles when the RP-HPLC purified fetuin Asn-81 glycopeptide (panel A) and individual fractions of the anion-exchange separation of the fetuin Asn-81 glycopeptide (panels B–E) are treated with PNGase F. The oligosaccharide profile in panel A shows a direct injection of 40 μl of the fetuin Asn-81 glycopeptide PNGase F digest. The peaks labeled 1 and 2 in Fig. 5A are trisialylated triantennary oligosaccharides and peaks 3 and 4 are tetrasialylated triantennary oligosaccharides. Townsend *et al.* [12] identified these structures in the high-pH anion-exchange

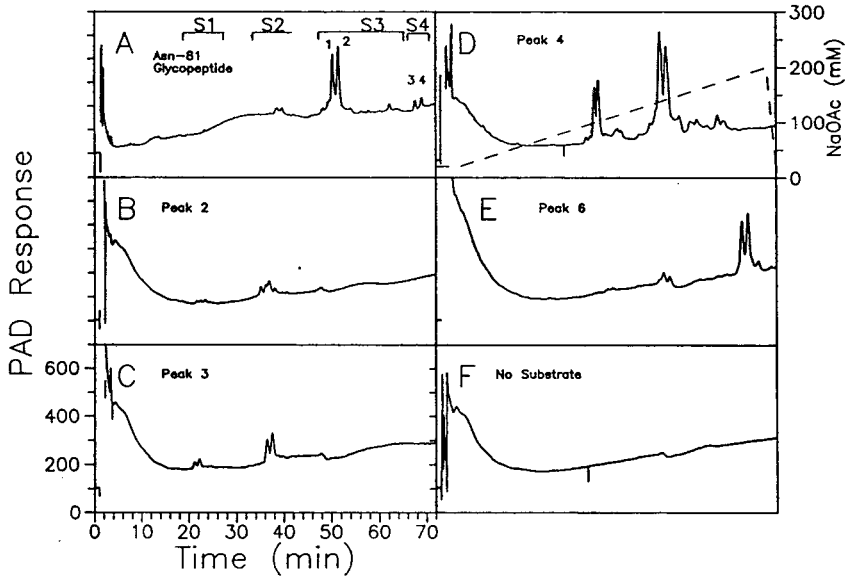

Fig. 5. High-pH AEC–PAD oligosaccharide maps of the PNGase F digestions of the fetuin Asn-81 glycopeptide and its anion-exchange fractions. (A) PNGase F digestion of the fetuin Asn-81 glycopeptide, (B–E) PNGase F digestions of fractions 2, 3, 4 and 6, respectively, (F) enzyme blank. The gradient is displayed with the dashed line in panel D. The injection volume for panel A was 20 μl and the injection volumes for panels B–F were 50 μl. The approximate retention times of mono-, di-, tri- and tetrasialylated oligosaccharides are indicated by S1, S2, S3 and S4, respectively. The separation conditions are described in section 2.6. The peak numbers are discussed in the text.

chromatography (AEC)–pulsed amperometric detection (PAD) chromatogram of fetuin N-linked oligosaccharides. The peaks at 20–24 min and 35–40 min are at the retention times where mono- and disialylated oligosaccharide standards elute, respectively. Panels B and C show the oligosaccharide profiles of peaks 2 and 3 (collected fractions, Fig. 4). Both peaks possess mainly disialylated oligosaccharides with some monosialylated oligosaccharides. The distribution of mono- and disialylated oligosaccharides differs between peaks 2 and 3. The oligosaccharide profile of peak 4, the main peak in the anion-exchange separation of the fetuin Asn-81 glycopeptide, is shown in panel D. Panel D shows that peak 4 contains di- and trisialylated oligosaccharides. Many of the peaks between 50 and 62 min have been shown to be other trisialylated triantennary oligosaccharides [12]. Peak 4 does not have any monosialylated oligosaccharides or either of the two known tetrasialylated oligosaccharides of fetuin. Panel E shows the oligosaccharide profile of peak 6. This peak contains the two tetrasialylated oligosaccharides of fetuin as well as a small amount of two trisialylated oligosaccharides. Panel F shows the blank (no substrate) digestion. No oligosaccharides were observed in the PNGase F digests of peaks 1 and 7 and a small amount of trisialylated oligosaccharides was observed in the PNGase F digest of peak 5 (chromatograms not shown). A RP-HPLC analysis of each PNGase F digest confirmed that all digestions were complete. Each PNGase F digest was treated with neuraminidase and analyzed by high-pH AEC–PAD oligosaccharide mapping (chromatograms not shown). This analysis confirmed the identification of sialylated oligosaccharides. The oligosaccharide analysis confirms that five of the seven peaks (peaks 2–6) contain the fetuin Asn-81 glycopeptide and the other two peaks (peaks 1 and 7) are impurities.

To determine if the pellicular anion-exchange column could be used to fractionate other

sialylated glycopeptides, the two other glycopeptides of fetuin (Asn-138 and Asn-158) were separated on the NucleoPac PA100 column. These glycopeptides were purified by RP-HPLC [13] and rechromatography suggested that both glycopeptides contained impurities (data not shown). It was previously shown that the Asn-138 glycopeptide elutes in two fractions by the RP-HPLC [13]. The earlier-eluting fraction was used for this study due to its greater purity (contains one peptide impurity [13]). Panels A and D of Fig. 6 show the high-performance (HP) AEC separations of the Asn-138 and Asn-158 glycopeptides, respectively. These glycopeptides are fractionated into multiple peaks by HPAEC. Treatment of the glycopeptides with PNGase F reduces the number of HPAEC peaks (panels B and E). Injection of equal volumes of the enzyme blank (no substrate, panels C and F) shows that many of the peaks in panels B and E are derived from the enzyme preparation and the digestion buffer. The peak with a retention time of 10.5 min coelutes with EDTA, a component of the enzyme preparation. Treatment of the Asn-138 and Asn-158 glycopeptides with neuraminidase abolishes all binding to the column except for one small peak with a retention time of 7 min in the Asn-158 glycopeptide sample (chromatograms not shown). The HPAEC analysis of the Asn-138 and Asn-158 glycopeptides shows that the NucleoPac PA100 column can fractionate other sialylated glycopeptides and the separation is due to oligosaccharide sialylation.

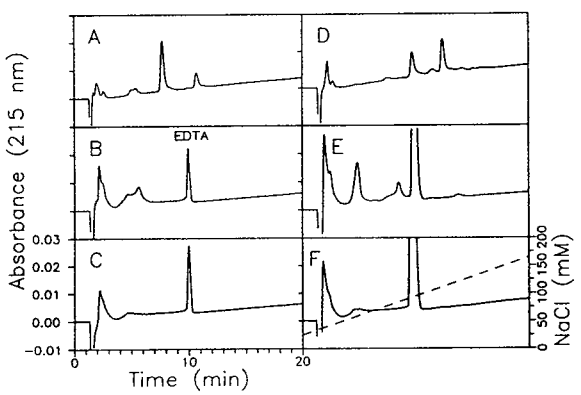

Fig. 6. Anion-exchange separations of the fetuin Asn-138 glycopeptide (A), the PNGase F digest of the Asn-138 glycopeptide (B), the PNGase F blank (C and F), the fetuin Asn-158 glycopeptide (D), and the PNGase F digest of the Asn-158 glycopeptide (E). The dashed line in panel F shows the NaCl gradient. The injection volumes for panels A–F are 4, 40, 40, 10, 100 and 100 μl, respectively. The separation conditions are described in section 2.4.

4. Discussion

The N-linked carbohydrate of bovine fetuin, a glycoprotein isolated from fetal calf serum, is microheterogeneous. Most of this microheterogeneity resides in the amount of N-acetylneuraminic acid, its location, and its linkage to galactose [17]. Additionally, fetuin's three N-linked glycosylation sites differ in their sialylated oligosaccharide content [13]. In this paper, the fetuin Asn-81 tryptic glycopeptide was purified to a single peak by RP-HPLC and then fractionated by pellicular AEC (NucleoPac PA100 column). The pellicular anion-exchange separation yielded seven peaks, five of which were identified as the Asn-81 glycopeptide. Using high-pH AEC–PAD in combination with enzyme treatments, the Asn-81 glycopeptide peaks were shown to differ in their sialylated oligosaccharide content. In the order of their elution, the first two peaks (peaks 2 and 3) have mainly mono- and disialylated oligosaccharides, the third and fourth peaks (peaks 4 and 5) have mainly trisialylated oligosaccharides, and the fifth peak (peak 6) has mainly tetrasialylated oligosaccharides. Thus, as the sialylation of the Asn-81 glycopeptide increases, its retention time on the NucleoPac PA100 column increases. Additionally, this manuscript shows that the NucleoPac PA100 column can fractionate two other sialylated glycopeptides of fetuin due to their attached oligosaccharide.

The relationship between the Asn-81 glycopeptide's sialylation and its retention on the NucleoPac PA100 column suggests that oligosaccharide sialylation is controlling the separation of this glycopeptide on the NucleoPac PA100 column. For peptides larger than 20 amino acids, secondary and tertiary structure develops as chain length increases [18]. This

three-dimensional structure makes it difficult to predict the peptide's RP-HPLC retention time from the peptide's amino acid composition [19]. It has been hypothesized that when large peptides (greater than 20 amino acids) and proteins are separated on reversed-phase or ion-exchange resins, only part of the molecule interacts with the resin [18]. This part of the molecule has been defined as the chromatographic contact area. The fetuin tryptic N-linked glycopeptides are 31 (Asn-81), 15 (Asn-138) and 28 (Asn-158) amino acids in length. Both neuraminidase and PNGase F treatments support the conclusion that the oligosaccharide of each glycopeptide is at least a portion of the glycopeptide's chromatographic contact area on the NuceloPac PA100 column. Neuraminidase treatment collapsed the five Asn-81 glycopeptide peaks into one peak with a shorter retention time. Treatment of the Asn-81 glycopeptide with PNGase F collapses the five glycopeptide peaks into one peak with a longer retention time than the largest of the five peaks. Unlike neuraminidase which only removes sialic acids, leaving the remainder of the oligosaccharide intact, PNGase F removes the whole N-linked oligosaccharide. The results of the PNGase F digestion suggest that the removal of the Asn-81 glycopeptide's carbohydrate exposes at least some of the glycopeptide's six acidic amino acids. This exposure increases the peptide's retention on the NucleoPac PA100 column.

Using RP-HPLC at pH 7, Rice *et al.* [9] have shown that individual fetuin glycopeptides can be separated into groups of glycoforms based on their degree of sialylation. Unlike the separation of the Asn-81 glycopeptide reported here, these glycoforms elute in the order of greatest to least number of sialic acid residues with a single peak for each charge group. When tryptic digests of glycoproteins are separated by RP-HPLC at pH 2, it has been observed that glycopeptide peaks are broad [20]. Examination of glycopeptide peaks with on-line mass spectrometry has shown that the heaviest glycoforms elute at the front of the glycopeptide peak [21,22]. The results of Rice *et al.* [9] at neutral pH are consistent with a heaviest to lightest glycoform elution order.

In conclusion, pellicular AEC can be used to fractionate sialylated glycopeptides. This fractionation is not only based on the number of sialic acids, but on the structure of the attached sialylated oligosaccharides. This is exhibited by peaks 2 and 3 in Fig. 4 which have different populations of disialylated oligosaccharides. The fractionated sialylated glycopeptides can be purified for further study. As noted by Rice *et al.* [9], glycopeptide glycoforms can be used as substrates for glycopeptidase studies and to study the influence of peptide sequence on oligosaccharide conformation.

5. Acknowledgements

The author thanks Gregg Cooper for performing the Edman sequencing of the fetuin Asn-81 glycopeptide and Dr. Michael Weitzhandler for his critical review of this manuscript.

6. References

[1] P.M. Rudd, R.J. Leatherbarrow, T.W. Rademacher and R.A. Dwek, *Molec. Immunol.*, 28 (1991) 1369.
[2] D.A. Cumming, *Glycobiology*, 1 (1991) 115.
[3] T.W. Rademacher, R.B. Parekh and R.A. Dwek, *Ann. Rev. Biochem.*, 57 (1988) 785.
[4] S.-L.Wu, G. Teshima, J. Cacia and W.S. Hancock, *J. Chromatogr.*, 516 (1990) 115.
[5] Y.W. Yim, *J. Chromatogr.*, 559 (1991) 401.
[6] A.D. Tran, S. Park, P.J. Lisi, O.T. Huynh, R.R. Ryall and P.A. Lane, *J. Chromatogr.*, 542 (1990) 459.
[7] E. Watson and F. Yao, *J. Chromatogr.*, 630 (1993) 442.
[8] T.J. Hahn and C.F. Goochee, *J. Biol. Chem.*, 267 (1992) 23982.
[9] K.G. Rice, N.B.N. Rao and Y.C. Lee, *Anal. Biochem.*, 184 (1990) 249.
[10] S.M. Gryaznov and R.L. Letsinger, *Nucl. Acids Res.*, 20 (1992) 1879.
[11] A. Tuong, M. Maftouh, C. Ponthus, O. Whitechurch, C. Roitsch and C. Picard, *Biochemistry*, 31 (1992) 8291.
[12] R.R. Townsend, M.R. Hardy, D.A. Cumming, J.P. Carver and B. Bendiack, *Anal. Biochem.*, 182 (1989) 1.
[13] J.S. Rohrer, G.A. Cooper and R.R. Townsend, *Anal. Biochem.*, 212 (1993) 7.
[14] J.S. Rohrer and H.B. White III, *Biochem. J.*, 285 (1992) 275.
[15] K.M. Dziegielewska, W.M. Brown, S.-J. Casey, D.L. Christie, R.C. Foreman, R.M. Hill and N.R. Saunders, *J. Biol. Chem.*, 265 (1990) 4354.

[16] J.S. Rohrer and G.A. Cooper, unpublished results.
[17] E.D. Green, G. Adelt, J.U. Baenzinger, S. Wilson and H. van Halbeek, *J. Biol. Chem.*, 263 (1988) 18253.
[18] F.E. Regnier, *LC·GC*, 5 (1987) 230.
[19] J.L. Meek, *Proc. Natl. Acad. Sci. U.S.A.*, 77 (1980) 1632.
[20] R.J. Harris, S.M. Chamow, T.J. Gregory and M.W. Spellman, *Eur. J. Biochem.*, 188 (1990) 292.
[21] V. Ling, A.W. Guzzetta, E. Canova-Davis, J.T. Stults, W.S. Hancock, T.R. Covey and B.I. Shushan, *Anal. Chem.*, 63 (1991) 2909.
[22] M.E. Hemling, G.D. Roberts, W. Johnson, S.A. Carr and T.R. Covey, *Biomed. Environ. Mass Spectrom.*, 19 (1990) 677.

ELSEVIER

Journal of Chromatography A, 667 (1994) 85–89

JOURNAL OF CHROMATOGRAPHY A

Enantiomeric purity determination by high-performance liquid chromatography with coupled polarized photometric/UV detection
Analysis of adulterative addition of synthetic malic and tartaric acids

Atushi Yamamoto*[,a], Akinobu Matsunaga[a], Eiichi Mizukami[a], Kazuichi Hayakawa[b], Motoichi Miyazaki[b]

[a]*Toyama Institute of Health, 17-1, Nakataikoyama, Kosugi-machi, Toyama 939-03, Japan*
[b]*Faculty of Pharmaceutical Sciences, Kanazawa University, 13-1, Takara-machi, Kanazawa 920, Japan*

(First received October 26th, 1993; revised manuscript received November 17th, 1993)

Abstract

A high-performance liquid chromatographic method for determining the enantiomeric purity of malic and tartaric acids with the combined use of UV and polarized photometric detectors in series has been established, in which no physical separation of enantiomers is required. Complexation with molybdate significantly increases the specific rotation of these acids. Thus, coupling polarized photometric detection with anion-exchange chromatography using a molybdate solution as the eluent makes possible the highly sensitive detection of optically active analytes with the conventional system. The proposed method can detect synthetic racemic acids in adulterated fruit juices at the 5% level.

1. Introduction

There are many optically active compounds in foodstuffs. In Japan, several synthetic racemates are approved for use as food additives. In particular, synthetic hydroxy carboxylic acids such as malic and tartaric acids are frequently used as acidulants to reduce production costs. Since each enantiomer might have different effects in biological systems and the safety of an unnatural form is open to question, it is important to determine the enantiomeric purity of the commercial products. Conventional enantiomeric resolution techniques involving liquid chromatography utilize interactions between an analyte and chiral solid and/or mobile phases resulting in diastereoisomeric products, and a racemate separates into two peaks [1–3]. The problem then arises as to how to resolve the racemates and avoid interference from other ingredients in the sample. So far, studies on the simultaneous chiral separation of these hydroxy acids for practical use have apparently not been published. It has been reported that the use of a detector based on measuring the rotation of polarized light combined with another type of

* Corresponding author.

0021-9673/94/$07.00
SSDI 0021-9673(93)E0018-P

detection such as UV or refractive index (RI) in series is ideal for the determination of the enantiomeric ratio without the separation of each enantiomer [4,5]. However, to determine the enantiomeric composition of low optically active acids using this method, derivatization is required to increase their optical rotations [6]. In general, besides introducing the chromophore into the chiral centre of the analyte, the formation of a metal complex significantly changes its optical rotation (Pfeiffer effect) [7]. It is known that the optical rotations of sugars [8] and hydroxy acids [9,10] are significantly increased by the formation of molybdate complexes.

Recently, we developed a novel detection method, polarized photometric detection (PPD), for detecting non-chromophoric, optically active analytes photometrically. In this system two polarizers are placed on either side of the UV–visible absorbance detector flow cell [11–13]. PPD can measure the optical rotation as the change in light intensity transmitted through the analyte placed between the polarizers. PPD has a sensitivity similar to a conventional polarimetric detector based on the Faraday effect. It is fortunate that a conventional and popular photometric detector is easily used as the PPD system. We report here the determination of synthetic acidulants based on the UV and PPD responses with the molybdate eluent system.

2. Experimental

All reagents were of guaranteed grade. D-Malic acid was purchased from Aldrich (Milwaukee, WI, USA), L-tartaric acid from Tokyo Kasei (Tokyo, Japan), ammonium molybdate, L-malic and D-tartaric acids from Wako (Osaka, Japan). Ammonium molybdate solution at 0.1 *M* concentration was prepared as a stock solution and serially diluted to obtain the desired concentration. All eluents were filtered through a 0.45-μm membrane filter.

Four readily available grape juices were used for the experiment. The only pretreatment of the sample was ultrafiltration through a Tosoh Ultracent-10 disposable cartridge, except that the highly coloured sample was decoloured by activated charcoal (recovery of malate and tartrate >90%) (Wako Darco G-60) prior to ultrafiltration.

The chromatographic separation was performed on a 250 × 4.6 mm I.D. anion-exchange column (TSK gel QAE-2SW, Tosoh, Tokyo, Japan) maintained at 45°C by a Tosoh CO-8011 column oven. An eluent containing 70 m*M* molybdate (adjusted to pH 5.9 with sodium hydroxide solution) was delivered by a Tosoh CCPD pump at a flow-rate of 0.7 ml/min. Injections were made through a Rheodyne Cotati, CA, USA) Model 7125 injector with a 100-μl loop.

A Shimadzu (Kyoto, Japan) SPD-10AV UV–visible detector for PPD was equipped with two Polaroid (Norwood, MA, USA) type HN32 polarizers on either side of the flow cell, where the inclination of the transmitting axis of the polarizer on the transmitting light side relative to that on the incident light side is set at an angle of 1 radian to the left as one faces the light source. The PPD sensitivity of this detector was improved by maximizing the intensity of the tungsten lamp and by setting the time constant at the slowest value (10 s). Thus the sensitive detection of optically active analytes becomes possible. Ultraviolet detection at 333 nm (Shimadzu SPD-6AV) was used in series with PPD at 520 nm. Quantitative determinations and linearity plots were obtained by measuring the peak heights.

3. Results and discussion

Because PPD detects optical rotation as a change in absorbance, it is unsuitable for light-absorbing analytes. Molybdate provides colourless complexes with hydroxy acids in acidic solutions, whose ratios of metal to ligand are 1:1 and 1:2 [14,15]. Fig. 1 shows the relationship between the specific rotations of the complexes at 589 nm, determined by a flow-injection analysis of the PPD system [13], and the ratios of molybdate to hydroxy acid ligands at a 70 m*M* concentration of molybdate at a pH around 5.3. The specific rotations of both acids of L-form

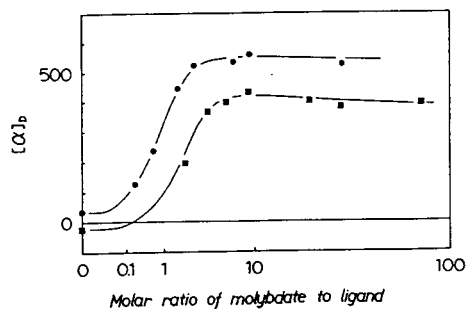

Fig. 1. Dependence of the specific rotation on the molar ratio variation of molybdate to L-tartrate (●) and L-malate (■).

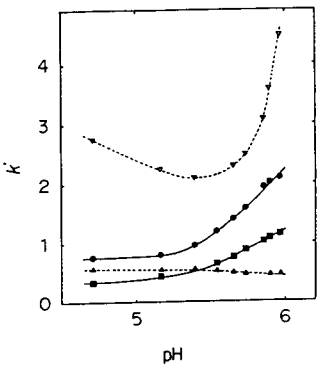

Fig. 2. Capacity factors of analytes and system peaks as a function of 70 m*M* molybdate eluent pH. Symbols are the same as in Fig. 1 except for the system peaks indicated by the open triangles.

showed positive (dextrorotatory) shifts as the molar ratio of molybdate to the acids increased, and their values plateaued in the presence of excess molybdate solution. Their specific rotations under conditions in which the molybdate existed sufficiently in excess increased as the measuring wavelength became shorter. Thus, highly sensitive PPD of the optically active hydroxy acids can be obtained using molybdate.

Recently, it has been reported that these complexes are retained in an anion-exchange column [16]. Investigations of the elution behaviour of these acids in the molybdate eluent system using various columns revealed that an increase in the exchange capacity of the column improved their separation and peak shapes. The choice of Tosoh QAE-2SW as an analytical column, whose ion-exchange capacity is 3.7 mequiv./g or more, made possible the sensitive determination of these acids polarized photometrically with the simplest apparatus without derivatization. In this system, an improvement in analyte peak shape was achieved by increases in both the column temperature and the eluent concentration. Increased molybdate concentration is desirable for the quantitative complexation with analyte acids, but excess addition exerts a negative influence on the stainless-steel tubing in HPLC or lowers the UV sensitivity as a result of increasing the baseline absorbance. Thus a molybdate concentration of 70 m*M* was chosen and a column temperature of 45°C, which is the upper limit for this column.

The influence of the eluent pH on the retention of the acids under the conditions stated above is shown in Fig. 2. They became strongly retained as the pH was increased. It seems that the negative charges of their complexes increase with an increase in the eluent pH, as suggested by Maruo *et al.* [16]. In this system, there are two extraneous peaks, called system peaks, arising from the component in the molybdate eluent. When the pH of the eluent was 5.9, both acids eluted within the capacity ratio of 2 and satisfactory separated from the system peaks.

The detection wavelength was set at 520 nm for PPD, where the signal-to-noise (S/N) ratio is best, and the flow-rate was decreased to 0.7 ml/min to prevent the peak width from being broadened at the largest time constant of this detector. Typical chromatograms of authentic malic and tartaric acids solutions obtained under the above-described conditions are shown in Fig. 3, in which the top figure is the trace from the UV detector and the bottom that from the PPD. In sequence are injections of L-isomers (A) followed by the racemic mixture (B) and D-isomers (C) at 20-min intervals. In the UV trace, the peak around 7 min is malic acid, the one around 11 min is tartaric acid and the negative ones both in the front and in the rear are the system peaks. Although UV detection always gave positive peaks for each acid, PPD gave a positive one for each L-isomer, a negative one

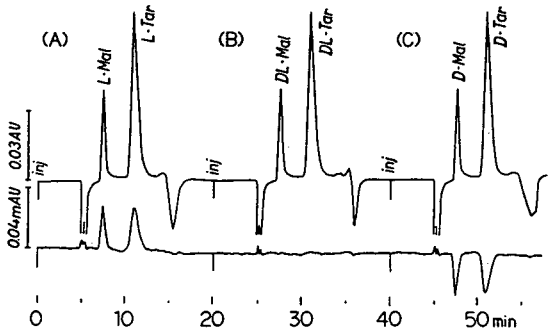

Fig. 3. Comparison of the chromatograms obtained by UV at 333 nm and PPD at 520 nm of mixtures of malic and tartaric acids on a QAE-2SW column. Sample amounts injected were 20 μg of malate and 12 μg of tartrate of each.

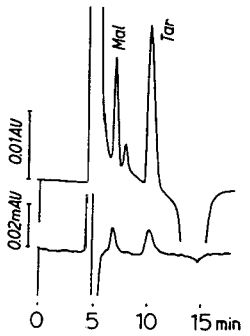

Fig. 5. UV and PPD chromatograms of a commercially available grape juice.

for the D-isomer and none for the racemate. Plots of peak-height units for PPD *versus* amounts of optically active samples showed good linearities up to 60 μg for malic acid and up to 30 μg for tartaric acid, and their detection limits are about 2 μg and 1 μg, respectively, at the $S/N =$ 3 level. Various enantiomer ratios were injected, with the total amounts of both acids kept constant at 20 μg for malic acid and at 12 μg for tartaric acid. The results are plotted in Fig. 4 as the peak-height ratio of PPD and UV detection *versus* the enantiomeric ratio in the sample. Both acids showed good linear relationships with a standard deviation (σ) of less than 1%. This means that the enantiomeric purities of both acids can be determined with an accuracy of $\pm 2.5\%$ at 3σ, *i.e.*, a food to which the addition of synthetic acids over the 5% level can be classified as adulterated at 20 μg of malate and/or 12 μg of tartrate injection level.

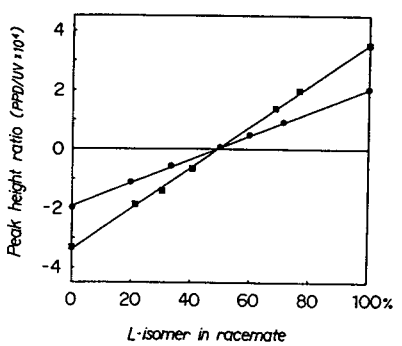

Fig. 4. Peak-height ratios *versus* composition of enantiomers for tartrate (●) and malate (□).

As an application of the proposed method, synthetic malic and tartaric acids in commercially available grape juices were determined. In this system, peaks are only obtained with the species complexed with molybdate. Other chelating compounds, such as citric or glutamic acid, eluted immediately after the dead volume of the column and did not interfere with the measurement of synthetic acidulants. However, PPD is subject to interference from the colouring matter. Although Fig. 5 illustrates actual chromatograms of highly coloured Concord grape juice, after pretreatment with activated charcoal prior to ultrafiltration no interference was observed in the PPD (bottom trace). Addition of synthetic racemates was not observed in all of the samples analysed by the proposed method.

In conclusion, we have successfully coupled a molybdate eluent HPLC system with PPD for the detection of synthetic malic and tartaric acids. The coupled PPD/UV detection system does not require the physical separation of L- and D-isomers. The primary advantage of PPD is the diversion of a conventional photometric detector to this purpose. The proposed method is suitable for the routine examination of grape juice adulteration.

4. References

[1] S. Weinstein, M.H. Engel and P.E. Hare, *Anal. Biochem.*, 121 (1982) 370.

[2] T.A. Eisele and J.R. Heuser, *J. Food Sci.*, 55 (1990) 1614.

[3] A. Yamamoto, A. Matsunaga, E. Mizukami, K. Hayakawa and M. Miyazaki, *J. Chromatogr.*, 585 (1991) 315.

[4] W. Boehme, G. Wagner, U. Oehme and U. Priesnitz, *Anal. Chem.*, 54 (1982) 709.

[5] A. Mannschreck, D. Andert, A. Eigelsperger, E. Gmahl and H. Buchner, *Chromatographia*, 25 (1988) 182.

[6] B.S. Reitsma and E.S. Yeung, *Anal. Chem.*, 59 (1987) 1059.

[7] P. Pfeiffer and W. Christeleit, *Z. Physiol. Chem.*, 247 (1937) 262.

[8] M. Hamon, C. Morin and R. Bourdon, *Anal. Chim. Acta*, 46 (1969) 255.

[9] H.A. Krebs and L.V. Eggleston, *Biochem. J.*, 37 (1943) 334.

[10] L.V. Eggleston and H.A. Krebs, *Biochem. J.*, 45 (1949) 578.

[11] A. Yamamoto, A. Matsunaga, K. Hayakawa, E. Mizukami and M. Miyazaki, *Anal. Sci.*, 7 (1991) 719.

[12] A. Yamamoto, A. Matsunaga and E. Mizukami, *Shokuhin Eiseigaku Zasshi*, 33 (1992) 301.

[13] K. Hayakawa, A. Yamamoto, A. Matsunaga, E. Mizukami, N. Nishimura and M. Miyazaki, *Biomed. Chromatogr.*, in press.

[14] A. Beltran-Porter, A. Cervilla, F. Caturla and M.J. Vila, *Transition Met. Chem.*, 8 (1983) 324.

[15] A. Cavaleiro, V.M.S. Gil, J.D. Pedrosa de Jesus, R.D. Gillard and P.A. Williams, *Transition Met. Chem.*, 9 (1984) 62.

[16] M. Maruo, N. Hirayama, A. Shirota and T. Kuwamoto, *Anal. Sci.*, 8 (1992) 511.

ELSEVIER

Journal of Chromatography A, 667 (1994) 91–98

JOURNAL OF CHROMATOGRAPHY A

Monitoring carboxylic acid formation in engine oils by liquid chromatography with fluorescence detection

Simon W. Lewis[a], Paul J. Worsfold *,[a], Euan H. McKerrell[b]

[a] *Department of Environmental Sciences, University of Plymouth, Plymouth PL4 8AA, UK*
[b] *Shell Research Ltd., Thornton Research Centre, P.O. Box 1, Chester CH1 3SH, UK*

(First received October 12th, 1993; revised manuscript received December 24th, 1993)

Abstract

Straight chain aliphatic carboxylic acids (C_6–C_{22}) were selectively derivatized in oxidised engine oils with the fluorescent label 9-anthracenemethanol after dialysis of the oils to remove polymeric additives, organometallic oxidation products and solid debris. The ester derivatives were separated by reversed-phase liquid chromatography and quantified using fluorescence detection ($\lambda_{ex} = 251$ nm; $\lambda_{em} = 412$ nm). Calibrations over the range 1–4 mg ml^{-1} were linear ($0.9987 \leq r^2 \leq 1.0000$). The limit of detection ($S/N = 3$) for octadecanoic acid was 85 μg ml^{-1} in *n*-heptane (4.3 ng on-column). Results showed that carboxylic acids are formed during the oxidation of oils in car engines and that their concentrations are directly related to the degree of oil degradation.

1. Introduction

Oxidation of an engine oil occurs when the hydrocarbon constituents in the oil react with dissolved oxygen under the extreme conditions of heating and agitation within the engine. This process is promoted by the affects of contact with the metal construction of the engine and the presence of contaminants in the oil [1,2]. The performance of the oil is degraded by the formation of suspended solids and sludges which block filters, oil lines and lubrication grooves.

Formation of these sludges is a complex process which is not fully understood [3]. It is known that oxidation involves a radical chain mechanism with primary products that include alcohols, aldehydes, ketones, carboxylic acids and water. Condensation polymerisation and further oxidation leads to an increase in the average molecular size of the products and the formation of sludges [4]. It is therefore desirable to monitor the intermediates and products of oxidation *e.g.* aldehydes, ketones and carboxylic acids, to aid the elucidation of the oxidation pathways.

Techniques such as thin-layer chromatography (TLC) and Fourier transform infrared spectroscopy (FT-IR) have been used to quantify total oxidised species and to identify functional groups respectively. This information has been correlated with results from traditional methods such as titrimetry [5,6] and viscosity determinations.

The present emphasis in used oil analysis, however, is the identification and quantification of individual species at the mg ml^{-1} level. Carboxylic acids are major primary products of

* Corresponding author.

0021-9673/94/$07.00
SSDI 0021-9673(94)00005-T

oil oxidation in engines and their presence can be used to monitor the degree of degradation. Gas chromatography (GC) has been used to determine carboxylic acids in a variety of matrices including crude oils [7], petroleum [8] and edible oils [9]. Analysis of used engine oils by GC however is aggravated by the presence of additives in the oil which lead to complex chromatograms. In addition, due to the nature of the sample matrix, extensive cleanup is required. Liquid chromatography (LC) with pre-column derivatization is one possible approach to achieve the required selectivity for the determination of carboxylic acids.

A wide range of labelling reagents for ultraviolet (UV) [10,11], fluorescence [12–21] and chemiluminescence (CL) detection [22–26] have been reported for the determination of carboxylic acids. Most of these derivatization reactions have been developed for clinical applications and are not suitable for the analysis of used oils because they are incompatible with the matrix.

One possible candidate as a fluorescence label for non-aqueous media is 9-anthracenemethanol [27], which has been used in conjunction with CL detection for the analysis of carboxylic acids in used engine oils [28]. The derivatives were separated by isocratic reversed-phase LC and detected using a post-column peroxyoxalate CL reaction. This method separated acid derivatives (C_8–C_{16}) in 45 min but this is a longer runtime than would be desirable for routine analysis. The separation of these acids could be achieved in a shorter time using gradient elution but the peroxyoxalate CL reaction is sensitive to changes in mobile phase composition [28,29].

This communication describes a procedure for the determination of individual carboxylic acids (C_6–C_{22}) in oxidised engine oils by pre-column derivatization with 9-anthracenemethanol followed by gradient elution LC with fluorescence detection. Polymeric additives, organometallic oxidation products and solid debris were removed from samples by dialysis prior to derivatization. The method was applied to the analysis of a series of oxidised oils sampled from a test engine after different periods of operation.

2. Experimental

2.1. Reagents

High-quality deionized water from a Milli-Q system (Millipore) and analytical-grade reagents were used unless otherwise stated. Acetonitrile (ACN), dichloromethane (DCM), *n*-heptane, petroleum spirit (b.p. 60–80°C) and tetrahydrofuran (THF) were of HPLC grade (Rathburn).

Solutions of 9-anthracenemethanol (Fluka) and 4-pyrrolidinopyridine (Aldrich) were prepared daily in DCM. Dicyclohexylcarbodiimide (DCC; Fluka) was used as the solid. Solutions of hexanoic (C_6), heptanoic (C_7), octanoic (C_8), nonanoic (C_9), decanoic (C_{10}), dodecanoic (C_{12}), hexadecanoic (C_{16}), octadecanoic (C_{18}), eicosanoic (C_{20}) and docosanoic (C_{22}) acids (all Aldrich) were prepared in *n*-heptane. All carboxylic acids were reagent grade.

2.2. Sample pretreatment

The oil samples were initially fractionated using a continuous dialysis system as shown in Fig. 1. Solutions of oil in light petroleum (b.p. 60–80°C) were contained within a semipermeable membrane around which warm petroleum spirit (b.p. 60–80°C) was continually circulated. The membrane was a dry, hypo-allergenic incontinence sheath rubber membrane (London Rubber Co.; product No. Q100-251, C10103900).

The dialysis proceeded for 24 h to allow low-molecular-mass material to diffuse through the membrane (the nominal molecular mass cutoff was 1000). Solvent was removed from the dialysate by rotary evaporation.

2.3. Precolumn derivatisation

Carboxylic acid standard solutions and oil dialysate samples, both unspiked and spiked with mixtures of acids (250 μl) were separately added to a mixture of dicyclohexylcarbodiimide (0.25 g), 9-anthracenemethanol in DCM (1 ml, $2.1 \cdot 10^{-2}$ *M*), 4-pyrrolidinopyridine in DCM (1 ml,

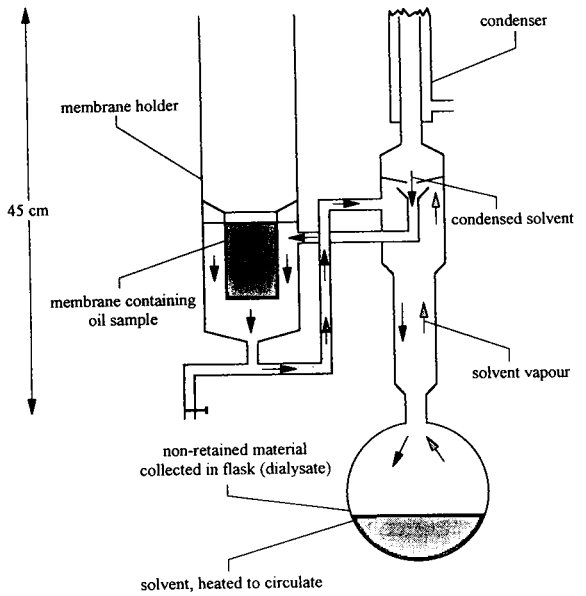

Fig. 1. Schematic diagram of continuous dialysis system. The dialysis solvent was petroleum spirit (b.p. 60–80°C) and the membrane was a dry, hypo-allergenic incontinence sheath rubber membrane (London Rubber Co.; product No. Q100-251, C10103900).

$1.0 \cdot 10^{-2}$ *M*) and *n*-heptane (15 ml) which was heated under reflux for 15 min. The reaction mixture was allowed to cool for 5 min before the solvent was removed by rotary evaporation. The residue was dissolved in ACN–THF (40:60, v/v) (25 ml).

2.4. Liquid chromatography

LC was carried out using a liquid chromatograph (Hewlett-Packard HP1090M) with a dual grating fluorescence detector (Hewlett-Packard HP1046A). To measure the excitation and emission spectra of the label and the derivatives, species were isolated in the fluorescence detector flow cell by a manual switching valve (Rheodyne). The optimum wavelengths for excitation and emission were 251 and 412 nm, respectively.

The instrument, containing an integral ternary solvent pump with helium sparging, an automated injector and a column oven (40°C) was controlled by a Hewlett-Packard Chemstation. The Chemstation was also used to control the detector and acquire and manipulate the data generated.

Separation of the carboxylic acid derivatives was achieved with two separate columns (stainless steel, 150 × 4.6 mm I.D.; Hichrom) packed with (1) Spherisorb S5 C_8 and (2) Hichrom RPB, a reversed-phase base-deactivated material. The solvent gradient was as follows; 0.0 min, water–ACN–THF (40:50:10, v/v/v); 5.0 min, water–ACN–THF (40:50:10); 15.0 min, ACN–THF (60:40); 20.0 min, ACN–THF (60:40); 21.0 min water–ACN–THF (40:50:10); 25.0 min water–ACN–THF (40:50:10). The injection volume was 5 μl and the flow-rate was 1.0 ml min^{-1}.

3. Results and discussion

All concentrations quoted relate to the original sample.

3.1. Dialysis

A lubricating oil comprises of a base oil plus additives and dialysis is used for the bulk fractionation of such into a dialysis residue (high-molecular-mass species, usually $M_r > 1000$) and a dialysate (base oil plus low-molecular-mass species).

The procedure is commonly used as a de-oiling process, but in this case it is used to remove higher-molecular-mass compounds and debris that could interfere with the pre-column derivatisation of the carboxylic acids.

3.2. Liquid chromatography

Carboxylic acids lack a chromophore or a fluorophore and so require derivatization prior to LC to achieve enhanced selectivity and sensitivity. Fluorescence labelling reagents based on 7-methoxycoumarin, especially 4-bromomethyl-7-methoxycoumarin (BrMMC) [12], aryldiazoalkanes [15] and halogenobenzofurazans [19] have

all been used for the analysis of carboxylic acids. Coumarin derivatives [24,25], 3-aminoperylene [22] and N-(bromoacetyl)-N′-[5-(dimethylamino)-naphthalene-1-sulphonyl]piperazine [26] have also been used as selective labels for carboxylic acids in conjunction with peroxyoxalate CL detection. These procedures are unsuitable for the analysis of carboxylic acids in used oils as the derivatization reactions and the separations either used polar solvents that are incompatible with the used oil matrix, or, as in the case of 3-aminoperylene, used a solvent (benzene) that is undesirable for health reasons.

9-Anthracenemethanol can be directly coupled with carboxylic acids in non-polar media using DCC as a coupling agent. Separation of the 9-anthracenemethanol esters on a Spherisorb S5 ODS2 column using a water–ACN–THF mobile phase has been achieved, under both isocratic [28] and gradient conditions [30], with CL detection. However, the isocratic method was unable to provide sufficient resolution for oxidised oil samples and the gradient method was not used for quantification due to the effect of varying mobile phase composition on the response factors.

The same label has been used with fluorescence detection for the determination of carboxylic acids [27]. It has been shown that the sensitivities of fluorescence and CL detection for these derivatives are of the same order of magnitude [31] although these figures are clearly instrument dependent. However, the attraction of using this label with fluorescence detection (as opposed to CL detection) is its greater tolerance to changes in mobile phase composition. To determine the optimum excitation and emission wavelengths for the ester derivatives, a mixture of three acids [hexanoic (C_6), decanoic (C_{10}) and octadecanoic (C_{18}) acids] were derivatised and separated using the gradient profile given above. As the excess label peak and each acid derivative was eluted in turn, it was isolated in the fluorimeter flow cell and the emission and excitation wavelengths scanned. On the basis of these profiles the excitation wavelength was set at 251 nm and the emission wavelength was set at 412 nm for all subsequent work.

Separation of 9-anthracenemethanol derivatives has been carried out on columns packed with Spherisorb S5 ODS2 [28,30]. Spherisorb S5 C_8 columns are less retentive of these derivatives due to the shorter C_8 alkyl chains of the stationary phase [32]. Several different water–ACN–THF gradients were investigated and the conditions which gave the shortest runtime with baseline resolution of the acid derivatives (C_6–C_{22} straight-chain acids) are presented in Table 1. Preliminary results showed that the Hichrom RPB column could also be used for this application and gave lower capacity factors (*e.g.* 9.7 *vs.* 13.0 for octadecanoic acid) and narrower baseline peak widths (*e.g.* 0.09 *vs.* 0.15 min for octadecanoic acid) than the S5 C_8 column.

3.3. Oil analysis

Two oil formulations, oil 1 and oil 2, differing only in the presence of an anti-oxidant additive in oil 2, were tested in a car engine. The oil in the sump of the engine was sampled after 0, 16, 40 and 64 h continuous running of the engine. At 64 h, oil 1 had thickened and degraded to beyond the point of use while oil 2 still held its lubricating properties.

When analysed by TLC–flame ionisation detection, the concentration of polar oxidation products in the dialysates of both oils was shown to increase with time from a negligible amount at 24 h to a high proportion (30%, m/m) at 64 h. FT-IR spectra of the 64-h dialysates indicated the presence of acid carbonyl groups.

Calibration data

The fresh (0 h) oil dialysate of oil 1 was spiked at varying concentration levels (0–4 mg ml^{-1}) with a mixture of straight-chain carboxylic acids (C_6–C_{22}) in *n*-heptane prior to derivatization. Separation of the derivatives was achieved on the Spherisorb S5 C_8 column within 20 min, with negligible interference from the oil dialysate matrix (except on the hexanoic acid derivative). Three components with retention times between 10.5 and 12 min interfere with the hexanoic acid derivative. These peaks are not present in the reagent blank (derivatization mixture without a

Table 1
Retention data for carboxylic acid-9-anthracenemethanol derivatives in *n*-heptane and fresh oil 1 dialysate matrices, identification of carboxylic acids in 64-h used oil dialysates of oil 1 and oil 2

Acid derivative	Carbon number	Capacity factor (k')[a]			
		Solvent matrix	Fresh oil dialysate matrix	Oil 1, 64-h dialysate	Oil 2, 64-h dialysate
Hexanoic acid	6	8.0	8.0	Not found	Not found
Heptanoic acid	7	8.9	8.9	Not found	Not found
Octanoic acid	8	9.6	9.6	9.6	Not found
Nonanoic acid	9	10.2	10.2	Not found	Not found
Decanoic acid	10	10.7	10.7	10.7	10.7
Dodecanoic acid	12	11.5	11.5	11.5	11.5
Hexadecanoic acid	16	12.6	12.6	12.6	12.6
Octadecanoic acid	18	13.0	13.0	13.0	13.0
Eicosanoic acid	20	13.3	13.3	13.3	13.3
Docosanoic acid	22	13.6	13.6	13.6	13.6

[a] $t_0 = 1.24$ min.

spike of oil dialysate or acid standard) and so are probably due to acidic additives in the oil, *e.g.* salicylic acid-based detergents. The reagent blank is compared with the fresh oil dialysates in Fig. 2 whilst the fresh oil 1 dialysate and the fresh oil 1 dialysate spiked with the complete mixture of acids at the 2 mg ml^{-1} level are compared in Fig. 3. Retention data for the acid derivatives in the fresh oil dialysate and in pure solvent are presented in Table 1. As can be seen by comparison of the capacity factors (k') the oil dialysate matrix does not affect the retention times of the derivatives.

Calibration graphs for all of the acids over the range of interest (1–4 mg ml^{-1}) were linear (Table 2), with correlation coefficients (r^2) over the range 0.9987–1.0000. The limit of detection ($S/N = 3$) for octadecanoic acid (determined using standards covering the range 0–0.15 mg ml^{-1}) was 85 μg ml^{-1} in *n*-heptane (4.3 ng on-column) which is more than adequate for this application. Recoveries for the derivatisation

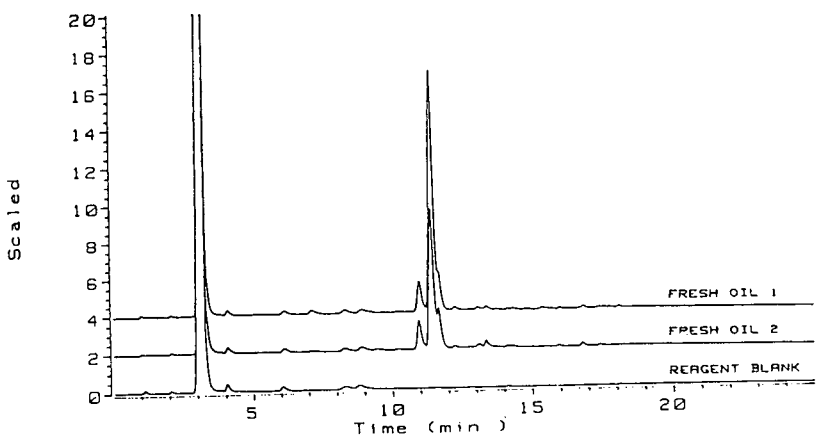

Fig. 2. Chromatograms of a reagent blank (derivatization mixture without spike of oil dialysate or acid standard) compared with chromatograms of fresh oil dialysates of oil 1 and oil 2.

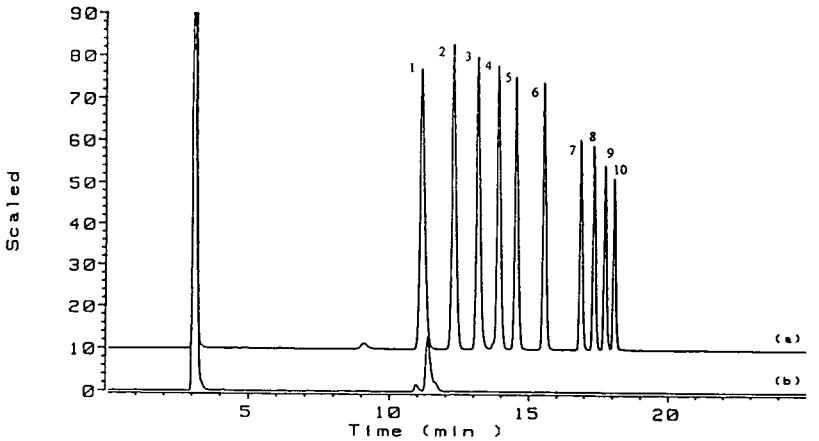

Fig. 3. Comparison of chromatograms of (b) fresh oil dialysate of oil 1 and (a) of the same dialysate spiked with a mixture of carboxylic acids at the level of 2 mg ml^{-1}. Peak assignment; 9-anthracenemethanol, (1) hexanoate (C_6), (2) heptanoate (C_7), (3) octanoate (C_8), (4) nonanoate (C_9), (5) decanoate (C_{10}), (6) dodecanoate (C_{12}), (7) hexadecanoate (C_{16}), (8) octadecanoate (C_{18}), (9) eicosanoate (C_{20}) and (10) docosanoate (C_{22}).

reaction were in the range 100–103% (Table 2) for the fresh oil dialysate (oil 1) spiked with the mixture of acids (C_6–C_{22}) at the 3 mg ml^{-1} level.

To determine whether the derivatives have a similar detector response, the calibration data were recalculated with the concentrations of the acids converted from mg ml^{-1} to *M*. The slopes of the lines of best fit for ten acids covering the range C_6–C_{22} are very similar (in the range 35 495–37 367, mean 36 640), with a relative standard deviation of 1.8%. It can be inferred from this that the detector response of the 9-anthracenemethanol esters of straight-chain aliphatic carboxylic acids is independent of chain length and the solvent gradient.

Comparison of engine test oils

The two series of dialysates for oil 1 and oil 2 over the time course of the engine test were derivatised and analysed and gave very similar results; the chromatograms for the entire series

Table 2
Linear fit and recovery data for carboxylic acids in fresh oil 1 dialysate matrix

Acid	Slope [concentration (mg ml^{-1})]	Intercept	Concentration found in fresh oil dialysate spiked with mixture of acids (mg ml^{-1})	Concentration of acid standard spike (mg ml^{-1})	Recovery (%)
Hexanoic acid	318.5	−185.5	3.0	2.9	103
Heptanoic acid	277.6	−168.5	3.2	3.2	100
Octanoic acid	257.6	−148.0	3.1	3.0	103
Nonanoic acid	232.9	−141.0	3.2	3.1	103
Decanoic acid	216.6	−125.7	3.0	3.0	100
Dodecanoic acid	185.2	−108.1	3.2	3.1	103
Hexadecanoic acid	143.2	−81.9	3.0	2.9	103
Octadecanoic acid	128.5	−76.2	3.1	3.1	100
Eicosanoic acid	116.6	−67.8	3.0	3.0	100
Docosanoic acid	105.7	−62.2	3.0	3.0	100

for oil 1 and the two 64-h samples are presented in Fig. 4. The peaks tentatively identified as additives disappear from the oil dialysates between 0 and 24 h of the test, as would be expected, as they are used up in the course of carrying out their functions. No measurable carboxylic acids appear until 64 h, at which time an homologous series of acids starting at C_8 and going beyond C_{22} can be clearly seen superimposed on a "hump" of unresolved components. The carboxylic acids identified by capacity factors (and confirmed by spiking) in the two 64-h samples are shown in Table 1.

The difference between the two 64-h samples was calculated by summing the areas of the peaks with retention times between 15.07 and 18.31 min and dividing by the mass of oil dialysate taken. This time window was selected because it contained the bulk of the carboxylic acids and was free of interference from the label and oil additives. It gives an indication of total carboxylic acid content and allows direct comparison of different oils. The area/mg is greater in oil 1 (2.8 area units mg^{-1}) than oil 2 (2.3 area units mg^{-1}), indicating that the hydrocarbon fraction of oil 1 has been oxidised to a greater extent than that of oil 2. This is in agreement with the physical characteristics of the two oils. The most important physical characteristic is thickening (change in viscosity) and the cut-off point is a 270% increase in viscosity compared to that of the fresh oil at the start of the engine test.

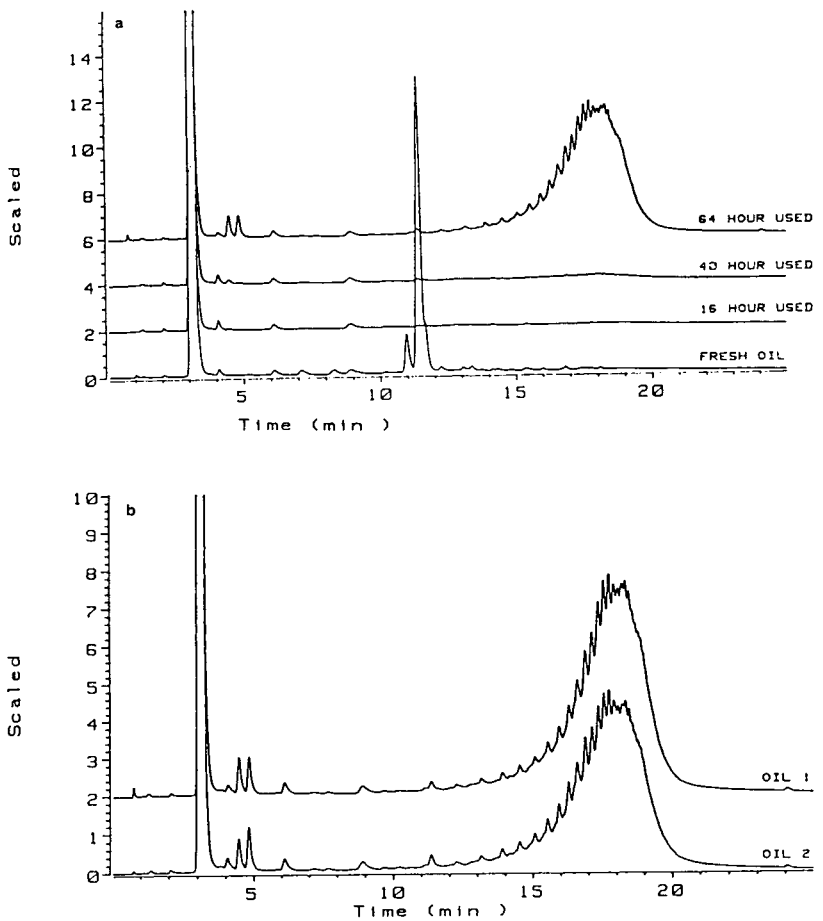

Fig 4. Chromatograms of derivatised engine oil dialysates (a) oil 1 engine test (b) 64-h used engine oils.

In the case of oil 1 there was a 950% increase in viscosity after 64 h as compared with a 215% increase for oil 2.

4. Conclusions

This procedure allows for the rapid and simple determination of aliphatic carboxylic acids (C_6–C_{22}) in used oil matrices by selective derivatization with 9-anthracenemethanol and gradient reversed-phase LC with fluorescence detection. Calibrations over the range 1–4 mg ml^{-1} were linear ($0.9987 \leq r^2 \leq 1.0000$). The limit of detection ($S/N = 3$) for octadecanoic acid was 85 μg ml^{-1} in *n*-heptane (4.3 ng on-column). It was shown by analysis of two series of oils from engine tests that carboxylic acids are formed during the oxidation of engine oils and that their concentrations are directly related to the degree of degradation. Work in this laboratory is now aimed at developing procedures for the determination of species intermediate in the oxidation mechanism, *e.g.* aldehydes.

5. Acknowledgement

One of us (S.W.L.) would like to thank Shell Research Ltd. for financial support.

6. References

[1] M.J. Nunney, *Automobile Lubrication*, Butterworth, London, 1985, p. 13.
[2] M. Billett, *Industrial Lubrication*, Pergamon Press, Oxford, 1979, p. 6.
[3] P.G. Harrison, D.A. Creaser and C.C. Perry, *Lub. Eng.*, 48 (1992) 752.
[4] D. Klamen, *Lubricants and Related Products*, Verlag Chemie, Basle, 1984, p. 44.
[5] *Standards for Petroleum and its Products*, Institute of Petroleum, London, 1992, IP Standard 177.
[6] *Standards for Petroleum and its Products*, Institute of Petroleum, London, 1992, IP Standard 139.
[7] M. Gough and S.J. Rowland, *Energy Fuels*, 5 (1991) 869.
[8] J.M. Schmitter, P. Arpino and G. Guiochon, *J. Chromatogr.*, 167 (1978) 149.
[9] H. Konishi, W.E. Neff and T.L Mounts, *J. Chromatogr.*, 629 (1993) 237.
[10] E. Grushka, H.D. Durst and E.J. Kitka, *J. Chromatogr.*, 112 (1975) 673.
[11] M. Marce, M. Calull, J.C. Olucha, F. Borrull and F.X. Rius, *Anal. Chim. Acta*, 242 (1991) 25.
[12] S. Lam and E. Grushka, *J. Chromatogr.*, 158 (1978) 207.
[13] J.B.F. Lloyd, *J. Chromatogr.*, 178 (1979) 249.
[14] J.B.F. Lloyd, *J. Chromatogr.*, 189 (1980) 359.
[15] N. Nimura, T. Kinoshita, T. Yoshida, A. Uetake and C. Nakai, *Anal. Chem.*, 60 (1980) 2067.
[16] C.M.B. van den Beld, H. Lingemann, G.J. van Ringen, U.R. Tjaden and J. van der Greef, *Anal. Chim. Acta*, 205 (1988) 15.
[17] F.A.L. van der Horst, M.H. Post, J.J.M. Holthuis and U.A.Th. Brinkman, *Chromatographia*, 28 (1989) 267.
[18] M. Yamaguchi, T. Iwata, K. Inoue, S. Hara and M. Nakamara, *Analyst*, 115 (1990) 1363.
[19] T. Toyo'oka, M. Ishibashi, Y. Takeda, K. Nakashima, S. Akiyama, S. Uzu and K. Imai, *J. Chromatogr.*, 588 (1991) 61.
[20] R. Gatti, V. Cavrini and P. Roveri, *Chromatographia*, 33 (1992) 13.
[21] A. Nakanishi, H. Naganuma, J. Kondo, K. Watanabe, K. Hirano, T. Kawasaki and Y. Kawahara, *J. Chromatogr.*, 591 (1992) 159.
[22] K. Honda, K. Miyaguchi and K. Imai, *Anal. Chim. Acta*, 177 (1985) 111.
[23] T. Kawasaki, M. Maeda and A. Tsuji, *J. Chromatogr.*, 328 (1985) 121.
[24] M.L. Grayeski and J.K. DeVasto, *Anal. Chem.*, 59 (1987) 1203.
[25] M. Tod, M. Prevot, J. Chalom, R. Farinotti and G. Mahuzier, *J. Chromatogr.*, 542 (1991) 295.
[26] P.J.M. Kwakman, H.P.van Schaik, U.A.Th. Brinkman and G.J. de Jong, *Analyst*, 116 (1991) 1385.
[27] H. Lingemann, A. Hulshoff, W.J.M. Underberg and F.B.J.M. Offermann, *J. Chromatogr.*, 290 (1984) 215.
[28] S.W. Lewis, P.J. Worsfold, A. Lynes and E.H. McKerrell, *Anal. Chim. Acta*, 266 (1992) 277.
[29] J.W. Birks, *Chemiluminescence and Photochemical Reaction Detection in Chromatography*, VCH, New York, 1989, p. 114.
[30] B. Yan, S.W. Lewis, P.J. Worsfold, J.S. Lancaster and A. Gachanja, *Anal. Chim. Acta*, 250 (1991) 145.
[31] A. Gachanja and P.J. Worsfold, *Anal. Chim. Acta*, 290 (1994) in press.
[32] S. Ahuja, *Selectivity and Detectability Optimizations in HPLC*, Wiley, New York, 1989, p. 171.

ELSEVIER

Journal of Chromatography A, 667 (1994) 99–104

JOURNAL OF CHROMATOGRAPHY A

Luminol chemiluminescent determination of hydrogen peroxide at picomole levels using high-performance liquid chromatography with a cation-exchange resin gel column

Teruo Miyazawa*, Sittiwat Lertsiri, Kenshiro Fujimoto, Michiko Oka

Department of Applied Biological Chemistry, Tohoku University, Tsutsumidori Amamiyamachi 1-1, Sendai 981, Japan

(First received August 31st, 1993; revised manuscript received December 28th, 1993)

Abstract

The optimum conditions of high-performance liquid chromatography combined with luminol chemiluminescence detection were established for the determination of hydrogen peroxide at picomole levels using a cation-exchange gel column. The gel column with distilled water as the mobile phase allowed a good separation of H_2O_2 without causing any irreversible binding of H_2O_2 to the column surface. The detection limit and the quantification limit of H_2O_2 were 4 and 6–600 pmol, respectively. The suitability of the present method was verified by the determination of H_2O_2 present in coffee drinks.

1. Introduction

Hydrogen peroxide (H_2O_2) is an oxidizing agent and has been used in sterilization and bleaching of food products. Previous studies have reported the formation of H_2O_2 in the oxidation of oily foods [1], in the oxidation of ascorbic acid in beverages [2] and in several food systems, and this has still not been well explained [3]. H_2O_2 has been found to cause duodenal cancer in mice following oral intake [4].

H_2O_2 is generally determined by means of electrochemical [5,6], spectrophotometric [7,8], fluorimetric [9,10] and chemiluminescence [11–16] techniques. Among these methods, luminol chemiluminescence assay is the most popular because of its excellent sensitivity. In both food and biological systems, it is known that ascorbic acid, tocopherols and lipid peroxides interfere with the chemiluminescent reaction in H_2O_2 determination [17]. Therefore, separation of H_2O_2 from these compounds is needed.

We have previously reported the presence of phospholipid hydroperoxides in human blood plasma, rat liver and brain using high-performance liquid chromatography with chemiluminescence detection (HPLC–CL) with a mixture of luminol and cytochrome *c* as a postcolumn chemiluminescent reagent with a silica-based aminopropyl column [17,18]. In the determination of lipid hydroperoxides, cytochrome *c* is favoured as a catalyst because of its higher hydrophobicity than that of microperoxidase, a haem peptide prepared from cytochrome *c* [19].

In this work, the optimum conditions of HPLC–CL, consisting of a cation-exchange resin gel column and a mixture of luminol and mi-

* Corresponding author.

0021-9673/94/$07.00
SSDI 0021-9673(93)E0089-D

croperoxidase as chemiluminescent reagent, were studied in order to determine H_2O_2 present in aqueous systems. The method was based on separation of H_2O_2 with the gel column and postcolumn detection of H_2O_2-dependent chemiluminescence catalysed by microperoxidase under alkaline conditions. Under the recommended conditions, the determination of 6–600 pmol of H_2O_2 was quantitative without irreversible binding of H_2O_2 to the column surface. The detection limit of the total system was 4 pmol. The suitability was verified by the determination of H_2O_2 present in coffee drinks.

2. Experimental

2.1. Reagents

Distilled water (HPLC grade) and hydrogen peroxide (30% aqueous solution) were obtained from Kanto Chemical (Tokyo, Japan) and Santoku Chemical (Tokyo, Japan), respectively. The hydrogen peroxide concentration was standardized by iodimetry [20]. Luminol (3-aminophthaloylhydrazine) was purchased from Wako (Osaka, Japan). Peroxidase (from *Arthromyces ramosus*, EC 1.11.1.7) was a gift from Suntory (Osaka, Japan) [21]. Cytochrome *c* (Type IV from equine heart), microperoxidase (MP-11 from equine heart cytochrome *c*) and catalase (C-10 from bovine liver, EC 1.11.1.6) were obtained from Sigma (St. Louis, MO, USA). Other chemicals were of analytical-reagent grade.

2.2. HPLC–CL

A schematic diagram of the HPLC–CL system for H_2O_2 determination is shown in Fig. 1. The system consisted of an HPLC column packed with a cation-exchange resin gel of sulphonated styrene–divinylbenzene copolymer (Shodex Ionpak KS-801, 300 mm × 8 mm I.D.; Showa Denko, Tokyo, Japan) placed in a column oven (Jasco 860CO; Japan Spectroscopic, Tokyo, Japan) at 24°C, two HPLC pumps (Jasco 880PU) with a Rheodyne Model 7125 sample loop injection (20 μl), a UV detector (Jasco 875UV) and chemiluminescence detector (Jasco 825CL) equipped with a spiral flow cell (200 μl).

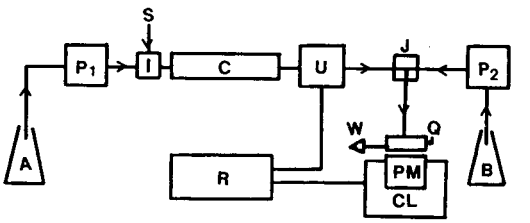

Fig. 1. Schematic diagram of HPLC–CL system for the assay of hydrogen peroxide. A = mobile phase (distilled water); P_1 and P_2 = pumps (Jasco 880PU), flow-rate 1 ml/min; I = sample injection valve (Rheodyne Model 7125, 20 μl); S = sample (20 μl); C = HPLC column (Ionpak KS-801, 300 mm × 8 mm I.D., in a Jasco 860CO column oven at 24°C); U = UV detector (Jasco 875UV); J = mixing joint (Kyowa Seimitsu Y type); B = chemiluminescent reagent consisting of 1.0 μg/ml luminol and 1.0 μg/ml microperoxidase in borate buffer (200 m*M* $H_3BO_3 \cdot KCl$–Na_2CO_3, pH 10.4); Q = flow cell; PM = photomultiplier; CL = chemiluminescence detector (Jasco 825CL); R = multiple recorder and integrator; W = waste.

The chemiluminescent reagent was prepared by dissolving luminol (1.0 μg/ml) and microperoxidase (1.0 μg/ml) in 200 m*M* $H_3BO_3 \cdot KCl$–Na_2CO_3 buffer at pH 10.4. The mixture was filtered through a cellulose nitrate filter (pore size 0.45 μm; Advantec Toyo, Tokyo, Japan) before use. The pH of the chemiluminescent reagent was stable at least for 48 h after preparation. The flow-rate of distilled water used as the mobile phase and that of the chemiluminescent reagent were 1 ml/min.

The chromatograms with chemiluminescence and UV detection (at 210 nm) were simultaneously recorded with a multiple pen recorder (SS-250F; Sekonic, Tokyo, Japan). The chemiluminescence peak area of H_2O_2 was calculated with a Chromatocorder 12 (System Instruments, Tokyo, Japan). The assays were performed in a temperature-controlled room at 24°C. The concentration of H_2O_2 present in a sample solution was determined from a calibration graph prepared with standard H_2O_2 solutions.

3. Results and discussion

3.1. Optimum conditions of HPLC–CL for H_2O_2 determination

We employed Ionpak KS-801, an HPLC column packed with a cation-exchange resin gel, in order to avoid the irreversible binding of H_2O_2 to the column surface. Nahum *et al.* [22] reported that silica-based columns are not suitable for H_2O_2 detection owing to the binding of H_2O_2 to the column surface.

First, a standard solution of H_2O_2 (18 nmol) was assayed by HPLC–CL using a chemiluminescent reagent consisting of luminol and cytochrome *c* [18] that has been employed in the determination of lipid hydroperoxides. A sharp chemiluminescence peak ascribed to H_2O_2 appeared at 11.0 min (Fig. 2). H_2O_2 at nanomole levels was also detectable by UV spectrophotometry (210 nm).

To increase the sensitivity, peroxidases other than cytochrome *c* were examined as catalysts,

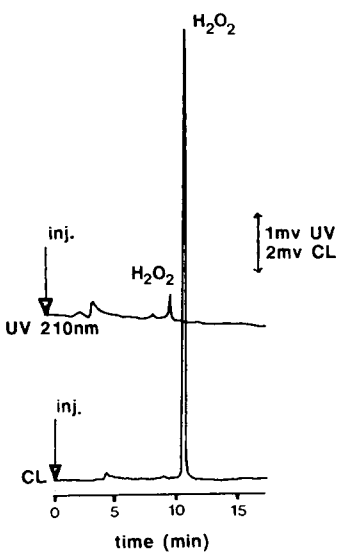

Fig. 2. Typical chromatogram of hydrogen peroxide (18 nmol) recorded by HPLC–CL with an Ionpak KS-801 column. Chemiluminescent reagent, mixture of 1.0 μg/ml luminol and 10.0 μg/ml cytochrome *c* in 50 m*M* borate buffer (pH 10.4) [19]. Other analytical conditions as in Fig. 1.

i.e., microperoxidase, *A. ramosus* peroxidase and horseradish peroxidase (HRP). Each peroxidase (1.0 μg/ml of microperoxidase, 1.0 μg/ml of *A. ramosus* peroxidase and 10.0 μg/ml of HRP) was added to a 200 m*M* $H_3BO_3 \cdot KCl$–Na_2CO_3 buffer that contained luminol (1.0 μg/ml). The chemiluminescent reagent consisting of microperoxidase and luminol was adjusted to pH 10.4 [18], that of *A. ramosus* peroxidase and luminol to pH 9.0 [21] and that of HRP and luminol to pH 10.4 [18]; 6, 20 and 60 pmol of H_2O_2, respectively, were introduced into the HPLC–CL system. Microperoxidase yielded H_2O_2-dependent chemiluminescence, *i.e.*, $7.4 \cdot 10^5$ counts at 6 pmol, $2.2 \cdot 10^6$ counts at 20 pmol and $7.2 \cdot 10^6$ counts at 60 pmol of H_2O_2. *A. ramosus* peroxidase yielded slightly higher chemiluminescence than that of microperoxidase. Both peroxidases gave linear relationships between integrated chemiluminescence counts and amount of H_2O_2 ($r = 0.99$; data not shown). In the absence of the catalyst, the integrated chemiluminescence count for 600 pmol of H_2O_2 was only 7200, indicating the importance of peroxidase as the catalyst in producing H_2O_2-dependent chemiluminescence. The signal-to-noise ratios for microperoxidase and *A. ramosus* peroxidase were 100 times higher than those for cytochrome *c* and HRP. This might be due to the difference in the hydrophilicity of the two peroxidases compared with cytochrome *c* and HRP. The high hydrophilicity of microperoxidase and *A. ramosus* peroxidase would result in dissolution of the chemiluminescent reagent by the column mobile phase (distilled water). This may relate to the high chemiluminescence production and baseline low noise (high signal-to-noise ratio) when using these peroxidases. As a result, both microperoxidase and *A. ramosus* peroxidase were suitable for H_2O_2 detection with this HPLC–CL system. Fig. 3 shows the HPLC–CL trace of H_2O_2 (60 pmol per 20-μl injection) for the total system, employing microperoxidase as a catalyst. Considering the commercial availability of the catalysts, we selected microperoxidase as the catalytic constituent of the luminol-containing chemiluminescent reagent.

The optimum concentrations of luminol and

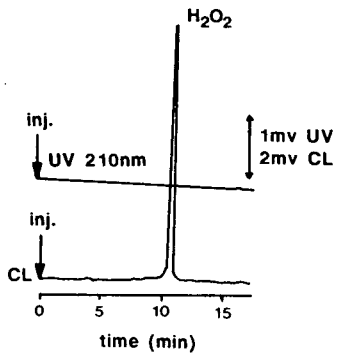

Fig. 3. Chromatogram of hydrogen peroxide (60 pmol) for the total system. Microperoxidase (1.0 μg/ml) was employed as a catalyst instead of cytochrome *c*. Other analytical conditions as in Fig. 1.

microperoxidase in the chemiluminescent reagent were examined. When the luminol concentration was fixed at 1.0 μg/ml in the chemiluminescent reagent, the chemiluminescence yield increased with increase in microperoxidase concentration from 0.1 to 5.0 μg/ml (Fig. 4a). The best signal-to-noise ratios at H_2O_2 amounts of 60 pmol (24) and 600 pmol (235) were observed with 1.0 μg/ml of microperoxidase. Much higher concentrations of microperoxidase (*i.e.*, over 2.0 μg/ml) caused significant increases in the noise levels and resulted in instability of the chemiluminescence baseline. This might result from the impurities in the microperoxidase. In the same way, 1.0 μg/ml of luminol was sufficient to yield the maximum H_2O_2-dependent chemiluminescence in HPLC–CL (Fig. 4b).

Considering the HPLC conditions, the column temperature and the mixing joint temperature were set at 24°C, taking into account the column pressure and retention time of H_2O_2. Above 24°C, the baseline (background counts) in chemiluminescence detection became unstable.

From these results, the optimum HPLC–CL conditions for the determination of H_2O_2 as given in Fig. 1 were confirmed. With the optimized HPLC–CL conditions, the calibration line from 6 to 600 pmol (6, 20, 60, 200 and 600 pmol) of H_2O_2 showed good linearity (correlation coefficient $r = 0.9992$). In four determinations of each H_2O_2 concentration, the standard errors

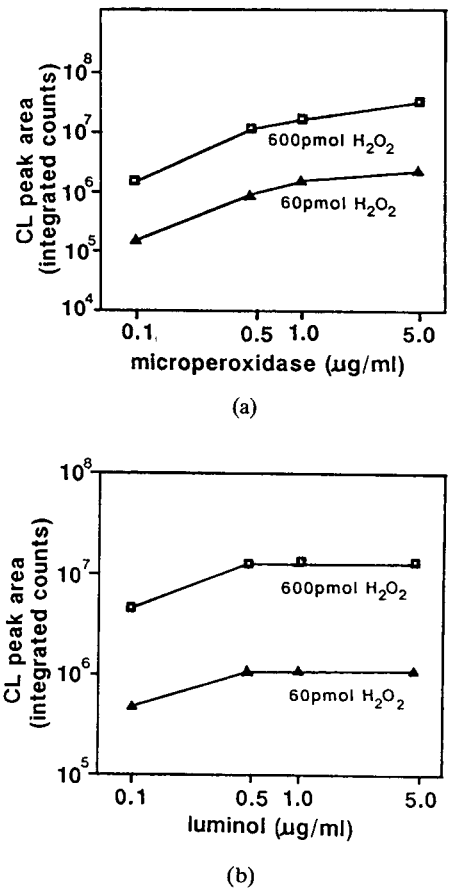

Fig. 4. Effect of microperoxidase and luminol concentrations on H_2O_2-dependent chemiluminescence. (a) In the chemiluminescent reagent, graded amounts (0.1, 0.5, 1.0, 5.0 μg/ml) of microperoxidase were included, in which the luminol concentration was fixed at 1.0 μg/ml in 200 m*M* borate buffer (pH 10.4). (b) In the chemiluminescent reagent, graded amounts (0.1, 0.5, 1.0, 5.0 μg/ml) of luminol were included, in which the microperoxidase concentration was fixed at 1.0 μg/ml in 200 m*M* borate buffer (pH 10.4). Other analytical conditions in Fig. 1; 60 and 600 pmol of H_2O_2 were determined.

were within 5% of the mean values. The detection limit of the total system was 4 pmol of H_2O_2 (signal to noise ratio = 3).

3.2. Interferences

Under the established optimum HPLC–CL conditions, ascorbic acid was found to give a

quenching peak (negative chemiluminescence peak) with a retention time of 5.5 min and was clearly separated from H_2O_2 (data not shown). In order to prevent the deterioration of the column, particles and proteins in the sample solution should be eliminated prior to the HPLC–CL analysis.

3.3. Application

Three types of powdered instant coffees (normal, caffeine-free and espresso types) and coffee beans for making drip coffee were purchased commercially. Coffee drinks were prepared by dissolving 2.0 g of powdered coffee in 140 ml of boiling water. The drip coffee was prepared by pouring 150 ml of boiling water on to 15.0 g of freshly milled roast coffee beans on a filter-paper. To each coffee drink (9.9 ml) 0.1 ml of 20% (w/v) sulphosalicylic acid solution was added to precipitate proteins. An aliquot of this sample suspension was then diluted 100-fold with distilled water. Prior to application to the HPLC–CL system, the diluted sample was filtered through a cellulose nitrate filter disc (pore size 0.45 μm) to remove proteins precipitated and particles. A typical chromatogram of H_2O_2 found in the drip coffee is shown in Fig. 5. The H_2O_2 content in coffee drinks was 67.1–165.0 μM (Table 1). The value determined here was identical with that in a previous report [3] in which an electrochemical method was used for the determination. The negative (quenching) peak in Fig. 5 might be ascribed to antioxidants, such as chlorogenic acid and ascorbic acid, present in the coffee drink. The chemiluminescence peak of H_2O_2 disappeared completely after treating the sample solution with catalase before the filtration procedure, indicating that H_2O_2 detected in the coffee drinks was not an artifact.

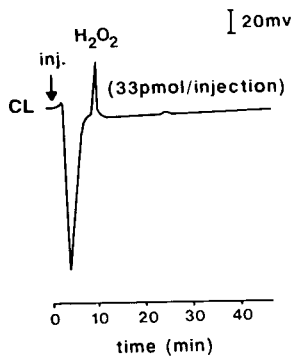

Fig. 5. Chromatogram of H_2O_2 in coffee drinks. Analytical conditions as in Fig. 1.

Table 1
Determination of hydrogen peroxide found in coffee drinks by HPLC–CL.

Coffee drink	H_2O_2 found (μM)
Normal	67.1 ± 3.8
Caffeine-free	64.7 ± 2.1
Espresso	99.7 ± 9.7
Drip	165.0 ± 5.3

Analytical conditions as in Fig. 1. Data are means ± standard errors ($n = 4$). Normal, caffeine-free and espresso coffee drinks were prepared by dissolving 2.0 g of powdered instant coffee in 140 ml of boiling water. Drip coffee was prepared by pouring 150 ml of boiling water on to 15.0 g of freshly milled coffee beans on a filter-paper.

4. Conclusions

The proposed HPLC–CL method is suitable for the determination of H_2O_2 with good selectivity, sensitivity and reproducibility. A cation-exchange resin gel column (Ionpak KS-801) is used that does not cause irreversible binding of H_2O_2 to the column surface. The sensitivity was equivalent to that of the most sensitive fluorimetric method. The small sample volume required as compared with those in other methods with the same sensitivity is another advantage of this HPLC–CL method. The applicability was verified by the determination of H_2O_2 present in coffee drinks. An environmental advantage is that no organic solvent is used in the column mobile phase.

Measurement of the oxygen metabolite H_2O_2 in biological fluids is of interest because it might indicate participation of toxic oxygen species in tissue injury [23–27]. The present HPLC–CL method should be useful also for application to biological systems.

5. References

[1] D.T. Coxon, N.M. Rigby, W.S. Chan, B.M. Lund and S.M. George, *J. Sci. Food Agric.*, 40 (1978) 367.
[2] T. Hamano, Y. Mitsuhashi and S. Yamamoto, *J. Chromatogr.*, 411 (1987) 423.
[3] Y. Fujita, K. Wakabayashi, M. Nagao and T. Sugimura, *Mutat. Res.*, 144 (1985) 227.
[4] A. Ito, M. Naito, Y. Naito and H. Watanabe, *Gann*, 73 (1982) 315.
[5] M. Cosgrove, G.J. Moody and J.D.R. Thomas, *Analyst*, 113 (1988) 1811.
[6] M. Toyoda, Y. Ito, M. Iwaida and M. Fujii, *J. Agric. Food Chem.*, 30 (1982) 346.
[7] Y. Saito, M. Mifune, S. Nakashita, J. Odo, Y. Tanaka, M. Chikuma and H. Tanaka, *Anal. Sci.*, 3 (1987) 171.
[8] R.E. Childs and W.G. Bardsley, *Biochem. J.*, 145 (1975) 93.
[9] K. Zaitzu and Y. Ohkura, *Anal. Biochem.*, 109 (1980) 109.
[10] G.G. Guilbault, D.N. Kramer and E. Hackly, *Anal. Chem.*, 39 (1967) 271.
[11] K. Hool and T.A. Nieman, *Anal. Chem.*, 60 (1988) 834.
[12] S. Sakura and H. Imai, *Anal. Sci.*, 4 (1988) 9.
[13] H. Watanabe, N. Mitsuhida, M. Andoh, M. Takeda, M. Maeda and A. Tsuji, *Anal. Sci.*, 2 (1986) 461.
[14] C.L. Malehorn, T.E. Riel and W.L. Hinze, *Analyst*, 111 (1986) 941.
[15] B. Olsson, *Anal. Chim. Acta*, 136 (1982) 113.
[16] T.M. Freeman and W.R. Seitz, *Anal. Chem.*, 50 (1978) 1242.
[17] T. Miyazawa, K. Yasuda, K. Fujimoto and T. Kaneda, *J. Biochem.*, 103 (1988) 744.
[18] T. Miyazawa, T. Suzuki, K. Fujimoto and K. Yasuda, *J. Lipid Res.*, 33 (1992) 1051.
[19] T. Miyazawa, K. Yasuda and K. Fujimoto, *Anal. Lett.*, 20 (1987) 915.
[20] A. Senzel, H. Reynolds and D.L. Park, in W. Horwitz (Editor), *Official Methods of Analysis of the Association of Official Analytical Chemists*, Association of Official Analytic Chemists, Washington, DC, 12th ed., 1975, Ch. 32, p. 605.
[21] Y. Shimmen, S. Asami, S. Shimizu and H. Yamada, *Agric. Biol. Chem.*, 50 (1986) 247.
[22] A. Nahum, L.D.H. Wood and I. Sznajder, *Free Rad. Biol. Med.*, 6 (1989) 479.
[23] T. Miyazawa, *Free Rad. Biol. Med.*, 7 (1989) 209.
[24] K.C. Bhunyan and D.K. Bhunyan, *Biochim. Biophys. Acta*, 497 (1970) 641.
[25] K.M. Toth, D.P. Clifford, E.M. Berger, C.W. White and J.E. Repine, *J. Clin. Invest.*, 74 (1984) 292.
[26] K.R. Maddipati, C. Gasparski and L.J. Marnett, *Arch. Biochem. Biophys.*, 254 (1987) 9.
[27] T.S. Test and S.J. Weiss, *J. Biol. Chem.*, 259 (1984) 399.

ELSEVIER

Journal of Chromatography A, 667 (1994) 105–111

JOURNAL OF CHROMATOGRAPHY A

Determination of protein amino acids as butylthiocarbamyl derivatives by reversed-phase high-performance liquid chromatography with precolumn derivatization and UV detection

Kang-Lyung Woo*, Su-Hag Lee

Department of Food Engineering, Kyungnam University, 449 Wolyoung-dong, Masan 631-701, South Korea

(First received August 16th, 1993; revised manuscript received October 26th, 1993)

Abstract

Twenty-two protein amino acids were derivatized to butylthiocarbamyl derivatives by precolumn reaction at 40°C for 30 min with butyl isothiocyanate. All of the derivatives were quantitatively resolved in 27 min by RP-HPLC on a Nova-Pak C_{18} column and detected at 250 nm with a UV detector. Asparagine and serine were resolved in a single peak. The relative standard deviations of the relative molar responses with respect to the methionine peak were less than 5% for all of the derivatives except cysteine. The calibration graphs showed good linearity in the range 0.5–2.5 nmol. Correlation coefficients for all of the calibration graphs were highly significant ($p < 0.001$). The stability of the derivatives at room temperature was about 8 h.

1. Introduction

The determination of amino acids by high-performance liquid chromatography (HPLC) has developed substantially in recent years owing to its sensitivity and speed of analysis compared with specialized amino acid analysers. Especially analysis with a reversed-phase (RP) column and UV detection following precolumn derivatization is popular owing to the greater versatility of the instrument.

The formation of *o*-phthalaldehyde (OPA) [1,2], dansyl [3,4], dabsyl [5,6], phenylthiocarbamyl (PTC) [7–9] and phenylthiohydantoin (PTH) derivatives of amino acids has been widely adapted used in RP-HPLC. However, these derivatives have several disadvantages. With the OPA derivatives, secondary amino acids, proline and hydroxyproline, were not detected because OPA does not react with secondary amines in the absence of oxidizing agents. Moreover, as OPA derivatives are unstable, complete automation of the precolumn reaction with accurate control of the reaction time is essential for acceptable reproducibility [10]. For higher sensitivity, fluorescence instead of UV detection is essential.

Dansyl derivatives are formed under optimum conditions at pH 9–9.5 and room temperature within 30–35 min in the dark. Dansylamino acids are unstable towards prolonged reaction times, solvents and exposure to light and interfering peaks arise due to the by-products during the derivatization process [4].

* Corresponding author.

0021-9673/94/$07.00
SSDI 0021-9673(93)E0004-E

It was reported that the sulphonamide bond of dabsyl derivatives was very stable [6]. The limitation of the dabsyl derivative method is that the presence of an excess amount of urea, salt, phosphate or ammonium hydrogencarbonate will change the pH of the reaction buffer and interfere with derivatization [5,6]. The standard of dabsyl amino acids must be prepared by hydrolysis of an amino acid standard mixture and derivatized in parallel with unknown samples under the same conditions [10].

Derivatization of amino acids with phenylisothiocyanate (PITC), which has been used for several decades in the Edman degradation, is an excellent precolumn derivatization method especially for secondary amino acids, proline and hydroxyproline [8,9,11,12]. Excess reagent and by-products produced during derivatization of PTC-amino acids must be completely removed with a high vacuum system in order to avoid interfering peaks.

Identification of PTH-amino acids is almost exclusively used in the elucidation of the structures of protein and this derivatization is unsuitable in a general method for the determination of amino acids.

There is a need for a simple, sensitive and stable precolumn derivatization reagent for RP-HPLC with UV detection. In this work, we chose butyl isothiocyanate for this purpose and applied it to the determination of 22 standard protein amino acids.

2. Experimental

2.1. Materials

Butyl isothiocyanate (BITC) was obtained from Aldrich (Milwaukee, WI, USA), standard amino acids from Sigma (St. Louis, MO, USA) and HPLC-grade acetonitrile from Merck (Darmstadt, Germany). All other reagents and solvents were of analytical-reagent grade.

2.2. Derivatization

A mixture of standard amino acids (60 μl of solution containing 1.25 μmol/ml of 0.01 *M* HCl) was placed in a 1-ml conical vial and the solvent was completely evaporated with dry nitrogen at 50°C. About 50 μl of acetonitrile were added and the mixture was evaporated with dry nitrogen. The residue was dissolved in 50 μl of coupling buffer [acetonitrile–methanol–triethylamine (10:5:2)] with ultrasonic treatment for 1 min and 3 μl of BITC were added. After tightly capping the vial with an open-hole screw-cap with a septum, the contents were derivatized using various temperatures and times as indicated later. After derivatization, two stainless-steel injection needles were pierced through the septum into the vial. One needle was connected with a nitrogen supply and the other with a vacuum pump. Nitrogen was infused into the vial and simultaneously evacuated with the vacuum pump until the contents were completely dried (*ca.* 15 min), and then 100 μl of acetonitrile were injected into the vial with a microinjection syringe and the contents were continuously dried with nitrogen. After completely drying, residue was dissolved in 500 μl of 0.2 *M* ammonium acetate solution and filtered through a 0.20-μm membrane filter. A 10-μl volume of the filtrate was injected into the HPLC system.

2.3. Chromatography

The HPLC system consisted of a Spectra-Physics 8800 ternary solvent-delivery system and a Spectra 200 programmable wavelength UV detector. The column temperature was maintained at 40°C with an Eppendorf CH-30 column heater. The column was Nova-Pak C_{18} (300 × 3.9 mm I.D.; 4-μm dimethyloctadecylsilyl-bonded amorphous silica) (Waters). The solvents for separation were kept under a blanket of helium with a solvent stabilization system (Spectra-Physics). The solvent system consisted of three eluents: (A) 0.05 *M* ammonium acetate (pH 6.7, adjusted with phosphoric acid); (B) solvent A–acetonitrile (50:50); and (C) acetonitrile–water (70:30). The flow-rate was 1.0 ml/min. The gradient was as follows: 0 min, 100% A; 8.0 min, 85% A–15% B; 14.0 min, 70% A–20% B–10% C; 20 min, 60% A–20% B–20% C; 25 min, 20% A–80% C; 30 min, 100% C.

After this a washing step was programmed with 100% C for 5 min.

3. Results and discussion

3.1. UV spectrum of BTC amino acid derivative

We assumed that the derivatization reaction between amino acids and BITC proceeds as follows:

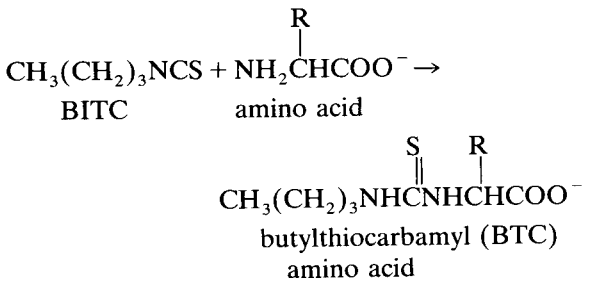

The UV spectra of the BTC-amino acid mixture and BITC, the coupling reagent, are shown in Fig. 1. The λ_{max} of BTC-amino acids was about 234 nm, but the most efficient wavelength was 250 nm, which avoided the absorption spectra of the impurities and the electrolyte (ammonium acetate) in the solvent.

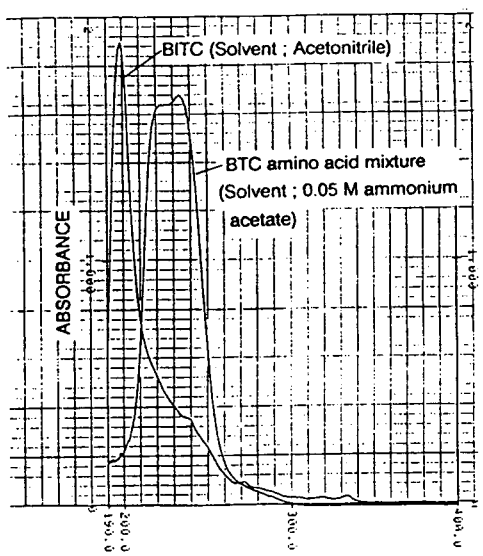

Fig. 1. UV spectra (*x*-axis in nm) of BTC-amino acid mixture and the coupling reagent BITC. Absorbance of solvents at 250 nm = 0.

3.2. Chromatography

The chromatographic elution of BTC-amino acids derivatized by reaction at 40°C for 30 min is shown in Fig. 2. All 22 protein amino acids were resolved in 27 min. Especially secondary amino acids, hydroxyproline and proline, were completely detected with high peak responses as PTC-amino acids [7–9]. Glutamine and asparagine were also separated from their acids, but asparagine and serine could not be resolved.

Incompletely resolved derivatives were threonine, alanine and arginine. The separation of tyrosine and valine is not as good as for the standard PTC derivatives [8]. All of the BTC derivatives were resolved into single peaks. However, glutamine stored in 0.01 *M* HCl for a long period showed three peaks. This phenomenon seems to be due to the partial conversion of glutamine into ammonia and glutamic acid on prolonged storage of the standard in acidic solution (Fig. 3). It has been reported that glutamine is converted into pyroglutamic acid on prolonged storage at low pH [13–15]. However, no pyroglutamic acid peak appeared on the chromatogram and also we could not derivatize standard L-pyroglutamic acid to the BTC derivative although we consider that this acid is produced in the standard solution on prolonged storage. The ammonia peak in Fig. 3 seemed to be produced by derivatization of non-volatile ammonium chloride formed between the amino group deaminated from glutamine and HCl on prolonged storage, because it was not observed with an aqueous ammonia solution (Fig. 3) but it

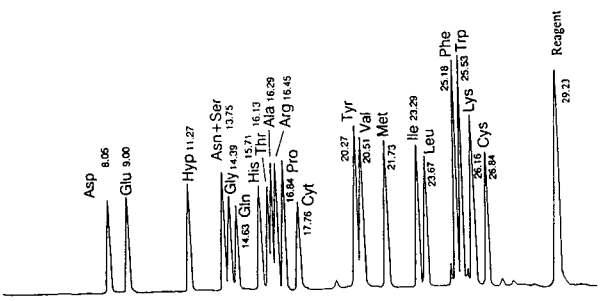

Fig. 2. Chromatogram of BTC-amino acids resolved on a Nova-Pak C_{18} column (300 × 3.9 mm I.D.). Amount injected, 1.5 nmol. Numbers at peaks indicate retention times in min.

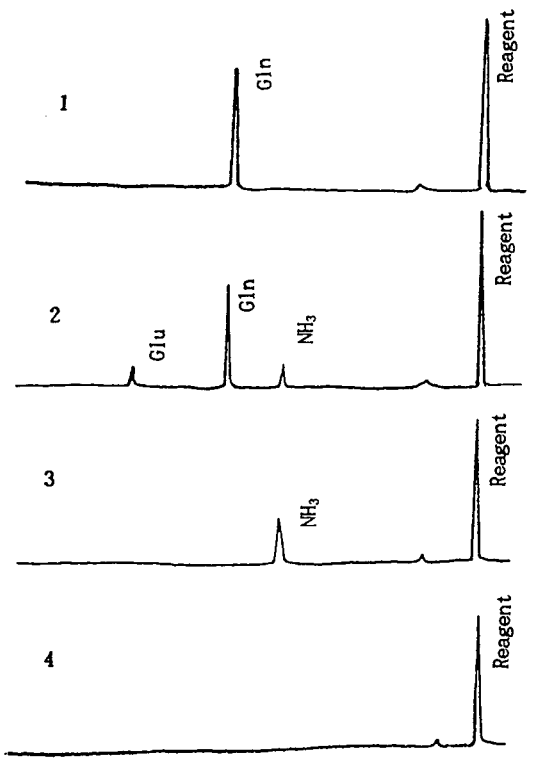

Fig. 3. Chromatogram of BTC-glutamine. (1) Chromatogram of glutamine derivatized immediately after preparation of standard solution with 0.01 *M* HCl; (2) chromatogram of glutamine derivatized after prolonged storage of standard solution; (3) chromatogram of NH_3 with derivatization with NH_3–0.01 *M* HCl solution; (4) chromatogram of NH_3 with derivatization with NH_3 solution.

was observed with an aqueous solution of ammonium chloride.

The order of resolution of BTC-amino acids in this study was similar to that of PTC-amino acids on a Pico-Tag column except for cystine (Cyt), cysteine (Cys) and arginine [11,16].

Although it is a methodological problem, there is a report that when the guard column is regularly changed after 120 analyses to avoid the damage of the column that can arise as a result of incomplete removal of the excess reagent, the separation remains satisfactory for at least 700 analyses with OPA, 800 analyses with fluorenylmethyl chloroformate, 150 analyses with PITC and 500 analyses with dansyl chloride [17]. With the BTC derivatives in this study, the resolution and peak response remained satisfactory for more than 700 samples without the need for a guard column.

The reagent peak appeared at 29 min after all of the amino acid derivatives had been resolved, so there is no risk of interfering peaks due to incomplete removing of excess reagent. The boiling point of BITC (70–71°C/35 mmHg; 1 mmHg = 133.322 Pa) is much lower than that of PITC (117.1°C/33 mmHg), so the excess BITC reagent will be more easily removed than PITC.

3.3. Relative molar response (RMR), peak response and calibration graphs

The RMRs with respect to the methionine derivative for reaction times of 10, 20, 30, 60, 120 and 180 min at 40°C and for reaction temperatures of 25, 40, 50, 60 and 70°C for 30 min were determined. The highest precision was obtained with reaction at 40°C for 30 min, although the RMRs and the peak area responses were higher for the reaction at 40°C for 120 min (Table 1, Fig. 5).

The amount of each amino acid injected was 1.5 nmol. The derivative that showed the highest relative standard deviation (R.S.D.) on reaction for 30 min at 40°C was cysteine (5.24%); all other R.S.D.s were less than 5%.

The peak-area responses on using various reaction temperatures for 30 min and various reaction times at 40°C are shown in Figs. 4 and 5. The peak-area responses on various reaction temperatures were the highest at 40°C for 30 min for almost all derivatives. The highest peak-area responses appeared at a reaction of 120 min at 40°C, but the R.S.D.s were higher than those for reaction for 30 min, although they were not so high to prevent these conditions being used for quantitative purposes (Table 1). With the PTC derivatives the derivatization reaction was completed in 10–20 min at room temperature [12], but with the BTC derivatives 120 min were required at 40°C. The peak response of cystine derivatives on reaction for 120 min compared with that for reaction for 30 min showed the greatest difference of 4.2-fold and the second was arginine with 1.6-fold. The differences for

Table 1
Relative molar responses of BTC-amino acids with reaction at 40°C for 30 and 120 min

Amino acid[a]	30 min			120 min		
	RMR[b]	S.D.[c]	R.S.D. (%)[c]	RMR[b]	S.D.[c]	R.S.D. (%)[c]
Asp	0.50	0.007	1.40	0.54	0.014	2.59
Glu	0.48	0.006	1.25	0.57	0.011	1.93
Hyp	0.67	0.011	1.64	0.63	0.027	4.29
Asn + Ser	0.66	0.003	0.45	0.66	0.026	3.94
Gly	0.52	0.005	0.96	0.58	0.014	2.41
Gln	0.71	0.009	1.27	0.75	0.025	3.33
His	0.62	0.007	1.13	0.65	0.011	1.69
Thr	0.29	0.005	1.72	0.33	0.013	3.94
Ala	0.75	0.019	2.53	0.74	0.028	3.78
Arg	0.44	0.003	0.68	0.69	0.012	1.74
Pro	0.71	0.011	1.55	0.67	0.017	2.54
Cyt	0.49	0.021	4.29	1.69	0.068	4.02
Tyr	0.83	0.011	1.33	0.92	0.010	1.09
Val	0.88	0.034	3.86	1.03	0.035	3.40
Ile	0.84	0.007	0.83	0.80	0.039	4.88
Leu	0.86	0.019	2.21	0.73	0.044	6.03
Phe	1.01	0.026	2.57	0.91	0.039	4.29
Trp	0.93	0.036	3.87	0.99	0.043	4.34
Lys	1.10	0.036	3.27	1.25	0.032	2.56
Cys	0.63	0.033	5.24	0.47	0.030	6.38

[a] Cyt = Cystine; Cys = cysteine.
[b] Values relative to methionine = 1.
[c] $n = 3$.

the other amino acid derivatives were *ca.* 1.2-fold. If we consider only the precision and economy of analytical time rather than higher sensitivity, however, the optimum conditions for determination are 30 min at 40°C.

Calibration graphs for all of the amino acid derivatives with reaction 40°C for 30 min showed good linearity in the range 0.5–2.5 nmol. The correlation coefficients (r) of the calibration graphs for all the derivatives were highly signifi-

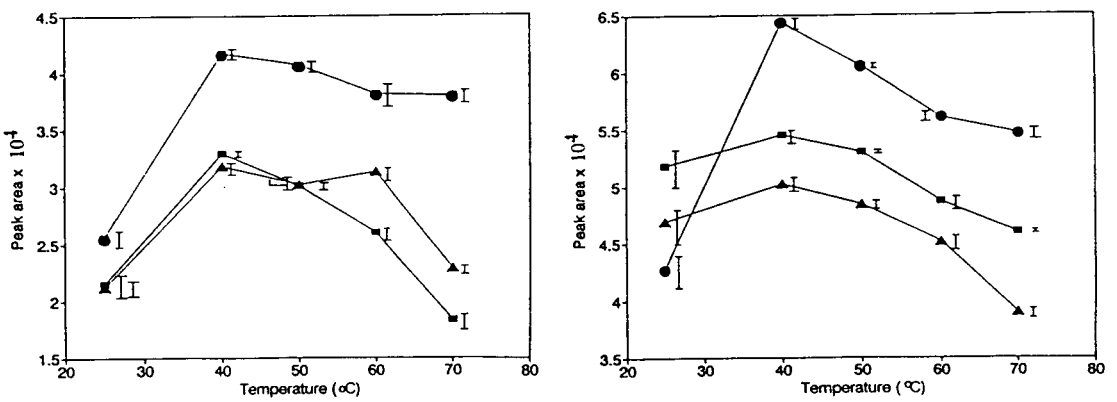

Fig. 4. Effect of reaction temperature on the formation of BTC-amino acids. Reaction time, 30 min. Left: ■ = Asp; ● = Hyp; ▲ = Glu. Right: ■ = Ile; ● = Phe; ▲ = Leu.

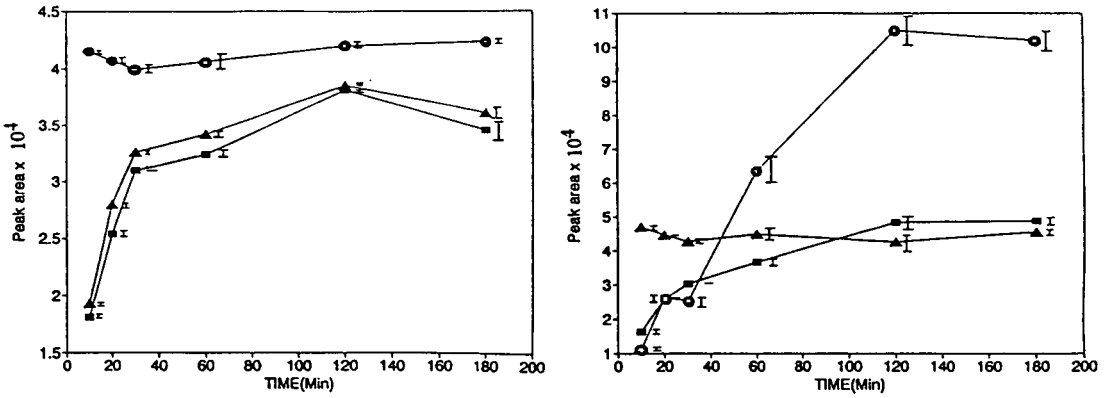

Fig. 5. Effect of reaction time on the formation of BTC-amino acids. Reaction temperature, 40°C. Left: □ = Asp; ○ = Hyp; ▲ = Glu. Right: □ = Arg; ○ = Cyt; ▲ = Pro.

cant ($p < 0.001$) and the lowest value was $r = 0.926$ for the cystine derivative. It has been reported that the linearity of the calibration graph for PTC-cystine was the poorest compared with those of other derivatives, but the correlation coefficient exceeded 0.999 [8]. However, there is a report that the linearity for PTC-cystine was so poor that it could not be used for quantitative purposes [17]. In this study, BTC-cystine showed good linearity for quantitative analysis. We also carried out PTC-cystine derivatization with the method used in this study. The linearity for PTC-cystine ($r = 0.997$) was as good as that for BTC-cystine.

3.4. Stability of BTC derivatives

The variation in the peak-area responses of BTC derivatives (with reaction at 40°C for 30 min) with storage time at room temperature is shown in Fig. 6. Up to 2 h of storage the peak-area responses increased for most of the derivatives, which indicated that the derivatization reaction was continuing at room temperature. After 8 h of storage the derivative that showed the greatest decrease was cysteine (17.3%); the loss of the other derivatives after 8 h was in the range 0–6.9%. The derivatives that decreased to less than 5% after 14 h were glutamic acid, asparagine + serine, glutamine, threonine, tyrosine, proline, lysine and tryptophan. With the PTC derivatives, the optimum pH of the solvent used to dissolve the derivatives was 7.5 and in solution, at this optimum pH, the loss of derivatives was in the range 0–10% after 10 h at room temperature [12]. We assumed that the stability of BTC-amino acids was similar to that of the PTC derivatives.

4. Conclusions

The derivatizing agent BITC reacts quantitatively with all of the protein amino acids at 40°C for 30 min to yield BTC-amino acids. All 22

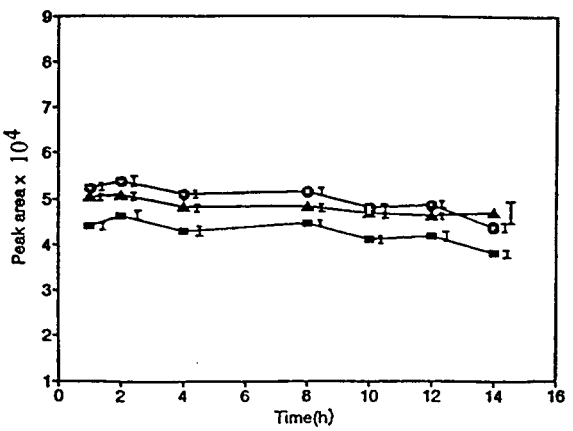

Fig. 6. Stability of BTC-amino acids at room temperature. □ = Glu; ○ = Ile; ▲ = Leu.

BTC-amino acids were separated on the Nova-Pak C_{18} column (300 × 3.9 mm I.D.; 4 μm), except asparagine and serine, which were resolved as a single peak. The calibration graphs showed good linearity and the R.S.D.s of the relative molar response were less than 5% except for cysteine (5.24%). The stability at room temperature was estimated to be *ca.* 8 h. This method could be useful for the determination of protein amino acids.

5. References

[1] M. Roth, *Anal. Chem.*, 43 (1971) 880.
[2] K. Yaegaki, J. Tonzetich and A.S.K. Ng, *J. Chromatogr.*, 356 (1986) 163.
[3] Y. Tapuhi, D.E. Schmidt, W. Lindner and B.L. Karger, *Anal. Biochem.*, 115 (1981) 123.
[4] C. De Jong, G.J. Hughes, E. Van Wieringen and K.J. Wilson, *J. Chromatogr.*, 241 (1982) 345.
[5] J.K. Lin and J.Y. Chang, *Anal. Chem.*, 47 (1975) 1634.
[6] R. Knecht and J.Y. Chang, *Anal. Chem.*, 58 (1986) 2375.
[7] D.R. Koop, E.T. Morgan, G.E. Tarr and M.J. Coon, *J. Biol. Chem.*, 257 (1982) 8472.
[8] B.A. Bidlingmeyer, S.A. Cohen and T.L. Tarvin, *J. Chromatogr.*, 336 (1984) 93.
[9] R.L. Heinrikson and S.C. Meredith, *Anal. Biochem.*, 136 (1984) 65.
[10] J.A. White and R.J. Hart, in L.M.L. Nollet (Editor), *Food Analysis by HPLC*, Marcel Dekker, New York, 1992, p. 53.
[11] J.A. White, R.J. Hart and J.C. Fry, *J. Autom. Chem.*, 8 (1986) 170.
[12] S.A. Cohen and D.J. Sytrydom, *Anal. Biochem.*, 174 (1988) 1.
[13] H. Wilson and R.K. Cannan, *J. Biol. Chem.*, 119 (1937) 309.
[14] J.P. Greenstein and M. Winitz, *Chemistry of Amino acids*, Vol. 3, Wiley, New York, 1961, p. 1934.
[15] G. Fortier, D. Tenaschuk and S.L. MacKenzie, *J. Chromatogr.*, 361 (1986) 253.
[16] R.F. Ebert, *Anal. Biochem.*, 154 (1986) 431.
[17] P. Fürst, L. Pollack, T.A. Graser, H. Godel and P. Stehle, *J. Chromatogr.*, 499 (1990) 557.

ELSEVIER

Journal of Chromatography A, 667 (1994) 113–118

JOURNAL OF CHROMATOGRAPHY A

Liquid chromatographic determination of carnitine by precolumn derivatization with pyrene-1-carbonyl cyanide

Kunihiro Kamata*, Misako Takahashi, Kiyosi Terasima, Motohiro Nishijima

Tokyo Metropolitan Research Laboratory of Public Health, 24-1 Hyakunincho, 3-chome, Shinjuku-ku, Tokyo 169, Japan

(First received August 2nd, 1993; revised manuscript received December 24th, 1993)

Abstract

A method is described for the determination of carnitine chloride in pharmaceutical preparations by precolumn derivatization and high-performance liquid chromatography (HPLC). Carnitine chloride is derivatized by reaction with pyrene-1-carbonyl cyanide (PCC) in dimethyl sulphoxide. The PCC derivative of carnitine is then used for quantitative HPLC analysis on a cation-exchange column with fluorescence detection. The calibration graph was linear over a sample concentration range from 2.0 to 20 μg/ml; the limit of detection was 0.5 μg/ml under the conditions studied. The proposed method was applied satisfactorily to the determination of carnitine chloride in pharmaceutical preparations.

1. Introduction

Carnitine [β-hydroxy-γ-trimethylaminobutyric acid] is one the most active biological substances known, being a mitochondrial fatty acid acyltransferase cofactor. Enzymatic and radioenzymatic methods are generally, used to determine carnitine in biological samples [1–6]. Carnitine has also been determined by various spectrophotometric methods based on the binding of its quaternary ammonium functionality and anionic chromophores such as periodide [7] and bromophenol blue [8,9].

It has recently been demonstrated that high-performance liquid chromatography (HPLC) is suitable for the determination of carnitine, and numerous applications of this technique to pharmaceutical preparations have been reported [10–12]. Carnitine is difficult to determine by conventional HPLC techniques because it does not have an adequate UV chromophore and must be measured with refractive index or low-wavelength UV detection. Neither of these detection methods is very sensitive or selective. Another method is based on the formation of UV-absorbing or fluorescent esters of carnitine and their determination by direct UV spectrophotometry or spectrofluorimetry, respectively [11,13–15]. The most appropriate method of determining carnitine is fluorimetry owing to its selectivity and sensitivity. Precolumn labelling with a fluorophore usually involves the carboxyl group of carnitine. Yoshida *et al.* [11] described a method using 9-anthryldiazomethane for the determination of carnitine by HPLC with fluorimetric detection. This procedure, however, has problems with the stability of the reagent.

In this paper, we report the precolumn re-

* Corresponding author.

0021-9673/94/$07.00
SSDI 0021-9673(93)E0078-9

action and fluorimetric detection of carnitine with pyrene-1-carbonyl cyanide and separation from the sample constituents by ion-exchange HPLC. The proposed method was applied to a profile analysis of carnitine in pharmaceutical preparations.

2. Experimental

2.1. Reagents and standards

DL-Carnitine chloride was obtained from Sigma (St. Louis, MO, USA). A stock standard solution was prepared by dissolving carnitine in 2% ammonia solution to give a concentration of 100 μg/ml. Working standard solutions were prepared by diluting the stock standard solution with 2% ammonia solution.

Pyrene-1-carbonyl cyanide (PCC) (used as a reagent for fluorescence labelling) was purchased from Wako (Osaka, Japan) and triamterene (used as an internal standard) from Sigma. The fluorescent reagent was prepared by dissolving PCC in dimethyl sulphoxide (DMSO) at a concentration of 0.2 mg/ml. PCC is stable in DMSO, but the solution was prepared freshly approximately every 3 weeks.

A stock standard solution of the internal standard was prepared by dissolving triamterene in DMSO to give a concentration of 5 mg/ml. A working standard solution was prepared by diluting the stock standard solution in acetonitrile to give a concentration of 50 μg/ml.

Amberlite CG-120 (100–200 mesh, Na^+ form) cation-exchange resin was purchased from Fluka (Buchs, Switzerland). Acetonitrile, $(NH_4)_2HPO_4$, DMSO, ammonia solution and phosphoric acid were obtained from Nacalai Tesque (Kyoto, Japan). All reagents and solvents were of analytical-reagent grade. Water was purified with a Milli-Q II water purification unit (Nihon Millipore, Tokyo, Japan).

2.2. Derivatization

A 0.5-ml volume of carnitine solution (2.0–20 μg/ml) and 0.5 ml of internal standard solution were placed in a 5-ml reaction vial and the solvent was evaporated to dryness at 50°C under reduced pressure in a rotary evaporator. To the residue, 1 ml of a DMSO solution of PCC (200 μg/ml) was added and the reaction vial was loosely stoppered and heated for 30 min at 80°C. The reaction solution was then analysed by HPLC under the described conditions.

A calibration graph for carnitine of peak-height ratio of carnitine to the internal standard *versus* concentration was established over a sample concentration range of 2.0–20 μg/ml. All standard solutions were analysed in duplicate to construct the calibration graph.

2.3. Chromatography

The HPLC apparatus consisted of a JASCO Model BIP-1 pump (Japan Spectroscopic, Tokyo, Japan), a Rheodyne (Berkeley, CA, USA) Model 7125 injector equipped with a 1-μl loop, a JASCO Model 860-CO column oven, a JASCO Model 821-FP fluorescence detector set at excitation and emission wavelengths of 355 and 420 nm, respectively, and a Chromatopac CR-3A digital integrator (Shimadzu, Kyoto, Japan). The HPLC column used was a TSKgel SP-2SW (Tosoh, Tokyo, Japan) (250 × 4.6 mm I.D.; 5 μm). The mobile phase was acetonitrile–0.01 *M* $(NH_4)_2HPO_4$ (adjusted to pH 7.5 with phosphoric acid) (25:75, v/v). Before use it was filtered through a Millipore (Bedford, MA, USA) membrane filter (0.45 μm) followed by degassing using sonication under vacuum. The eluent was pumped at a flow-rate of 1.0 ml/min at a column oven temperature at 40°C.

2.4. Sample preparation

A suitable amount of the carnitine preparation was placed in a 50-ml volumetric flask and about 40 ml of water were added. If the dosage form was tablet composites, a representative number of tablets (usually 20) were accurately weighed and finely powdered. After sonication for 20 min, the flask was cooled and the solution was made up to volume. The mixture was then centrifuged at 2000 rpm (1300 *g*) for 10 min. The

final carnitine concentration was 25–250 μg/ml. Exactly 2.0 ml of the sample solution was transferred into a 15 × 1 cm I.D. column of cation-exchange resin (2 g) and the column was washed with 25 ml of water, discarding the washings. The receiver was changed to a 25-ml volumetric flask, carnitine was eluted with 20 ml of 2% ammonia solution and the eluate was made up to volume with water. A 0.5-ml volume of this solution was subjected to derivatization and HPLC as described above.

3. Results and discussion

Goto *et al.* [16] applied 1-anthroyl nitrile as a fluorescence labelling reagent, which is effective for secondary hydroxyl groups on bile acids. Kudoh *et al.* [17] also used 1-anthroyl nitrile as a fluorescence labelling reagent for lauryl alcohol ethoxylate and nonylphenol ethoxylates. We found that carnitine was also derivatized quantitatively into fluorescent compounds by 1-anthroyl nitrile. Three fluorescence labelling regent having a carbonyl nitrile group (9-anthronyl cyanide, 1-anthroyl nitrile and PCC) were tested for the determination of carnitine. The extent of each reaction product using these labelling regents was calculated from the fluorescence intensity. The following relative fluorescence intensities (%) were obtained: PCC, 100; 9-anthronyl cyanide, 10; 1-anthroyl nitrile, 18. Hence the best sensitivity was obtained with PCC. The reaction is probably as shown in Fig. 1.

The optimum conditions for the fluorescent derivatization of carnitine with PCC were determined. First, seven organic solvents (acetone, acetonitrile, DMSO, chloroform, hexane, tetrahydrofuran and N,N-dimethylformamide) were tried in order to determine the differences in the

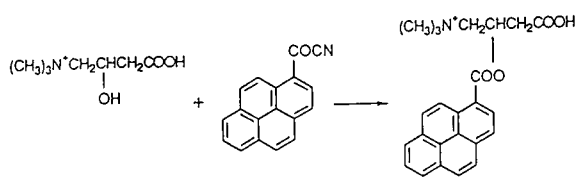

Fig. 1. Fluorescence derivatization of carnitine with PCC.

reaction system with each solvent. An aprotic solvent, DMSO, was selected as the solvent for the samples because it gave the highest fluorescence intensity.

The effect of the PCC concentration was studied in the range 10–500 μg per 10 μg of carnitine. Constant peak heights were obtained above 100 μg of PCC. The amount of PCC chosen was 200 μg.

Fig. 2 shows the effects of reaction temperature and reaction time on the derivatization of carnitine with PCC. The peak heights of the PCC derivative of carnitine obtained increase in proportion to the increase in reaction temperature and time. As shown in Fig. 2, the optimum reaction temperature and time were adopted 80°C and 30 min, respectively.

Fig. 3 shows the yield of carnitine ester as a function of the water content in the reaction mixture. The yield of carnitine ester obtained decreased in proportion to the increase in water content. Therefore, the sample solution was evaporated to dryness before reaction.

The separation of carnitine has usually been performed by reversed-phase HPLC. The separation of the carnitine ester was therefore first examined using reversed-phase (C_{18}) HPLC. However, the retention time of carnitine ester was very close to that of impurities in the PCC

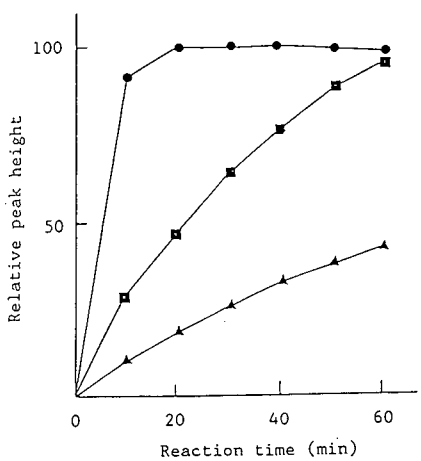

Fig. 2. Effect of reaction time and reaction temperature on the reaction yield of carnitine–PCC ester. ○ = 80°C; □ = 60°C; ▲ = 40°C.

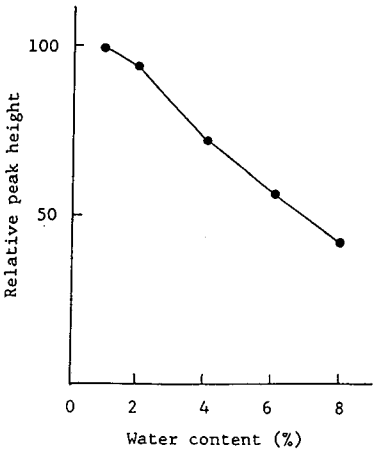

Fig. 3. Effect of water content in the reaction mixture on the reaction yield of carnitine–PCC ester.

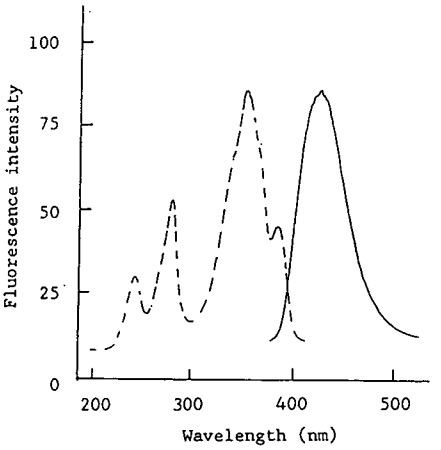

Fig. 4. Fluorescence excitation (solid line) and emission (dashed line) spectra of carnitine–PCC ester.

derivatives. In this study, the carnitine ester was separated by cation-exchange HPLC with a mobile phase consisting of acetonitrile and $(NH_4)_2HPO_4$ solution, because its structure containing quaternary ammonium ion. The composition of the mobile phase (percentage of water, salt concentration and pH) had a strong influence on the separation of the carnitine ester. The optimum mobile phase composition was chosen for each condition to give the best separation of the carnitine ester from impurities in the PCC derivatives. The influence of acetonitrile concentration, $(NH_4)_2HPO_4$ concentration and mobile phase pH on the chromatographic characteristics of carnitine ester was systematically examined. The retention time increased with decreasing concentration of acetonitrile and with increasing pH and was not sensitive to the concentration of $(NH_4)_2HPO_4$. The optimum concentration of $(NH_4)_2HPO_4$ for separating carnitine ester was 0.01 *M*. From the results, the solvent system finally chosen was acetonitrile–0.01 *M* $(NH_4)_2HPO_4$ (adjusted to pH 7.5 with phosphoric acid) (25:75, v/v).

When carnitine ester was eluted in the flow-through cell of the detector, the flow-rate of the mobile phase was stopped and both the excitation and emission wavelengths were measured (Fig. 4). The maximum excitation and emission wavelengths were found to be at 355 and 420 nm, respectively.

Fig. 5 shows chromatograms of (A) a derivatized standard solution and (B) the reagent blank. The carnitine ester peak was clearly separated from the impurities in the PCC derivatives.

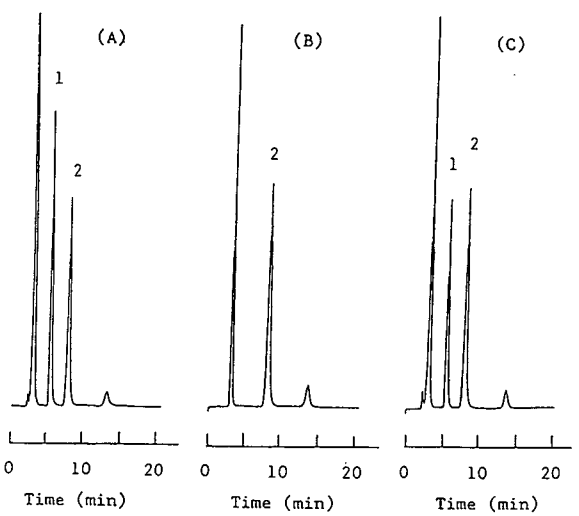

Fig. 5. Chromatograms of (A) a derivatized standard solution, (B) a reagent blank and (C) a derivatized commercial tablet sample. Peaks: 1 = carnitine–PCC ester; 2 = triamterene (internal standard).

The calibration graph of carnitine chloride to triamterene peak-height ratio *versus* sample concentration was found to be linear over the sample concentration range 2.0–20 μg/ml. The linear regression coefficient was 0.999, the slope was 0.199 and the intercept on the ordinate was −0.015. The reproducibility of this procedure was also adequate; the relative standard deviation (R.S.D.) for 10 μg/ml of carnitine chloride was 1.12% ($n = 5$). The detection limit of carnitine chloride under the conditions adopted was about 0.5 μg/ml with a 1-μl injection (signal-to-noise ratio = 3).

The determination of carnitine chloride in pharmaceutical dosage forms is markedly influenced by the clean-up procedure employed. For this purpose Amberlite CG-120 resin was chosen, based on previous work [12]. Several sources of interferences in the reaction of PCC such as water-soluble vitamins, crude extract and sugar were eliminated by the column clean-up procedure. The results obtained with the clean-up of pharmaceutical dosage forms were satisfactory with respect to reproducibility and recovery.

The proposed procedure was applied to the determination of carnitine chloride in pharmaceutical preparations. Table 1 reports the results obtained in the analysis of commercial samples of carnitine chloride and Fig. 5C shows a chromatogram of the PCC derivative of carnitine from a commercial tablet sample. Neither the derivatization nor the chromatographic separation was influenced by other compounds; for example, the major components contained in these samples are water-soluble vitamins (vitamins B_1, B_2 and B_6, nicotinamide and pantothenol), caffine, ethanol, inositol, sucrose, glucuronolactone and crude extract (gentian, ginseng, glycyrrhiza, cinnamom bark and coptis rhizome). The results indicate that, in each instance, the values are within acceptable limits, with a minimum recovery of 93.4%. The R.S.D. % is within 3.54% ($n = 5$). The chromatograms of all the other samples also showed a sharp peak for carnitine ester with no interference from other substances. The results indicate that this method is suitable for the determination of carnitine chloride in pharmaceutical preparations.

Table 1
Determination of carnitine chloride in commercial preparations

Sample	Declared	Found (%)[a]	R.S.D. (%)
A (tablet)	40 mg per 3 tablets	98.7 ± 2.0	2.02
B (capsule)	50 mg per capsule	93.4 ± 2.1	2.20
C (syrup)	100 mg/ml	101.4 ± 3.6	3.54
D (drink)	100 mg/ml	96.9 ± 3.3	3.36
E (drink)	80 mg/30 ml	95.1 ± 2.9	3.04

[a] Each value is the mean ±S.D. of five measurements.

This work has shown that PCC is a very promising fluorescent reagent for determining carnitine chloride in commercial drugs and should be applicable for the analysis of other biological samples with low concentrations of carnitine chloride. Studies are in progress on the determination of carnitine chloride in human urine.

4. References

[1] N.R. Marquis and I.B. Fritz, *J. Lipid Res.*, 5 (1964) 184.
[2] J.D. McGarry and D.W. Foster, *J. Lipid Res.*, 17 (1976) 277.
[3] E.P. Brass and C.L. Hoppel, *J. Biol. Chem.*, 253 (1978) 2688.
[4] A. Daveluy, R. Parvin and S.V. Pande, *Anal. Biochem.*, 119 (1982) 286.
[5] N. Takeyama, D. Takagi, K. Adachi and T. Tanaka, *Anal. Biochem.*, 158 (1986) 346.
[6] R.E. Dugan, M.J. Schmidt, G.E. Hoganson, J. Steele, B.A. Gilles and A.L. Shug, *Anal. Biochem.*, 160 (1987) 275.
[7] J.S. Wall, D.D. Christianson, R.J. Dimler and F.R. Senti, *Anal. Chem.*, 32 (1960) 870.
[8] S. Friedman, *Arch. Biochem. Biophys.*, 75 (1958) 24.
[9] M.A. Mehhlman and G. Wolf, *Arch. Biochem. Biophys.*, 98 (1962) 146.
[10] A. Fujita and R. Yamamoto, *Katei Kenkyuu*, 7 (1988) 40.
[11] T. Yoshida, A. Aetake and H. Yamaguchi, *J. Chromatogr.*, 445 (1988) 175.
[12] M. Takahashi, K. Nakayama, S. Uehahara, K. Kamata, T. Hagiwara and K. Akiyama, *Annu. Rep. Tokyo Metrop. Res. Lab. Public Health*, 41 (1990) 51.

[13] P.E. Minkler, S.T. Ingalls, S. Kormos, D.E. Weir and C.L. Hoppel, *J. Chromatogr.*, 336 (1984) 271.
[14] J. Gorham, *J. Chromatogr.*, 361 (1986) 301.
[15] P.E. Minkler, S.T. Ingalls and C.L. Hoppel, *J. Chromatogr.*, 420 (1987) 385.
[16] J. Goto, M. Saito, T. Chikai, N. Goto and N. Nambara, *J. Chromatogr.*, 276 (1983) 289.
[17] M. Kudoh, H. Ozawa, S. Fudano and K. Tsuji, *J. Chromatogr.*, 287 (1984) 337.

ELSEVIER

Journal of Chromatography A, 667 (1994) 119–124

JOURNAL OF CHROMATOGRAPHY A

Effect of mobile phase composition on the separation of thyrotropin-releasing hormone and some metabolites by reversed-phase ion-pair chromatography

Sandra Contreras Martinez[a], Luz Elena Vera-Avila[b,*]

[a]*Instituto de Biotecnología de la UNAM, 62100 Cuernavaca Mor., Mexico*

[b]*Departamento de Química Analítica, Facultad de Química, Universidad Nacional Autónoma de México, 04510 México, D.F., Mexico*

(Received November 26th, 1993)

Abstract

Sodium dodecyl sulphate was used for the separation of thyrotropin-releasing hormone (TRH) and the related compounds deamido-TRH (TRHOH), histidylprolinediketopiperazine, proline and prolineamide by reversed-phase ion-pair chromatography. The effects of mobile phase composition on retention and selectivity were determined. The parameters studied included acetonitrile, pairing ion and salt concentrations, salt type and pH. The results show that the separation of TRH and its analogue TRHOH can be easily adjusted by small modifications of the pH in the vicinity of pH 2. A remarkable improvement of peak width and peak shape was observed for some analytes when a potassium salt was added to the mobile phase.

1. Introduction

Reversed-phase ion-pair chromatography (RP-IPC) has become a popular technique for the separation of peptides. Hydrophilic and hydrophobic pairing ions have been used and their effects on peptide retention, selectivity and peak shape have been widely described [1–6]. Small polar peptides, such as thyrotropin-releasing hormone (TRH) and other di- and tripeptides, have been separated by the addition of hydrophobic alkyl sulphonates or alkyl sulphates, from C_5 to C_{12}, to the mobile phase [4–6]. The separation and elution time were improved by varying the percentage of organic modifier in the eluent and the chain length of the pairing ion.

In previous studies [7,8] we have shown that other parameters, such as pairing ion concentration, salt concentration, salt type and pH, can also be used to manipulate retention times and selectivity in RP-IPC with hydrophobic pairing ions. However, the multiple possibilities provided by this technique have not been sufficiently exploited in the case of peptides.

One purpose of this paper is to show the effect of each mobile phase component on the retention of small peptides and amino acids in RP-IPC. The other is the application of these effects to improve the separation of the important tripeptide TRH and some metabolites.

* Corresponding author.

0021-9673/94/$07.00
SSDI 0021-9673(93)E1305-J

2. Experimental

2.1. Apparatus and materials

Chromatographic experiments were carried out on a Waters (Milford, MA, USA) HPLC system consisting of two piston pumps, Models 45 and 590, an RCM-100 radial compression module, a Model 481 UV spectrophotometer and a U6K valve injector. Radial compression cartridges, Resolve C_{18} from Waters (10 cm × 8 mm I.D., particle size 10 μm, containing 4 g of packing), were used throughout. Fixed conditions for all experiments were isocratic elution, flow-rate 1.3 ml/min, ambient temperature and detection wavelength 215 nm.

HPLC-grade acetonitrile (density 0.78 kg/l) from Merck (Darmstadt, Germany) and purified water obtained from a Milli-Q system (Millipore, Bedford, MA, USA) were used to prepare sample solutions and mobile phases. Sodium dodecyl sulphate (SDS) from Bio-Rad Labs. (Richmond, CA, USA) was used as the pairing ion. Salts added to the mobile phase, lithium, sodium and potassium dihydrogenphosphate, were obtained from J.T. Baker (Phillipsburg, NJ, USA). The pH of the eluent was adjusted with orthophosphoric acid (J.T. Baker). Sample solutes, pyroglutamylhistidylprolineamide (TRH), proline (PRO) and prolineamide ($PRONH_2$), were purchased from Sigma (St. Louis, MO, USA), and pyroglutamylhistidylproline (TRHOH) and histidylproline-diketopiperazine (DKP) from Peninsula Labs. (San Carlos, CA, USA).

2.2. Methods

For each experiment, the pH of an aqueous solution containing the required amounts of SDS and one of the inorganic salts was adjusted with 10% orthophosphoric acid solution. Mobile phases were prepared in 500-ml volumetric flasks, adding the above solution, a weighed amount of acetonitrile and the necessary volume of water.

The volume of mobile phase needed to equilibrate the column was evaluated for each experiment. The following equation, relating adsorption of alkyl sulphates on reversed phases to mobile phase composition, was used [7]:

$$\log[C]_{st} = -0.25 - 0.66\varphi_{org} + 0.06N_c + \log[C]_m[0.72 + 1.68\varphi_{org} - 0.05N_c] \quad (1)$$

where $[C]_{st}$ is the concentration of pairing ion in the stationary phase at equilibrium (mmol/g), $[C]_m$ is the concentration of this species in the eluent (mmol/ml), φ_{org} is the volume fraction of acetonitrile in the mobile phase (w/v fraction/density) and N_c is the number of carbon atoms in the alkyl sulphate molecule.

The volume of eluent that must pass through the column to reach equilibrium (V_{eq}) was calculated from $[C]_{st}$ using the relationship

$$V_{eq} = \frac{[C]_{st}M_{st}}{[C]_m} + V_m \quad (2)$$

where M_{st} is the mass of stationary phase in the column and V_m is the void volume.

For dodecyl sulphate and the different mobile phase compositions used in this work, the calculated volume of eluent to equilibrate the Resolve C_{18} cartridge varied from 37 to 78 ml. Eq. 1 was deduced for a different reversed-phase packing (LiChrosorb RP-8 from Merck), and therefore equilibrium was always tested by repetitive injections of a solute before injection of the sample.

Hold-up times were determined by injection of $NaNO_3$ solution. Measurements were made for each mobile phase composition, but without a pairing ion present.

After each experiment, the column was washed with 30 ml of acetonitrile–water (1:1, v/v) to remove all SDS from the stationary phase.

All peptides and amino acids were taken up in 0.01% acetic acid and, prior to injection, made up in the mobile phase. The amount of each compound in 5 μl of injected sample varied from 0.25 to 3 μg. Fig. 1 shows the structures of the analytes used in this work.

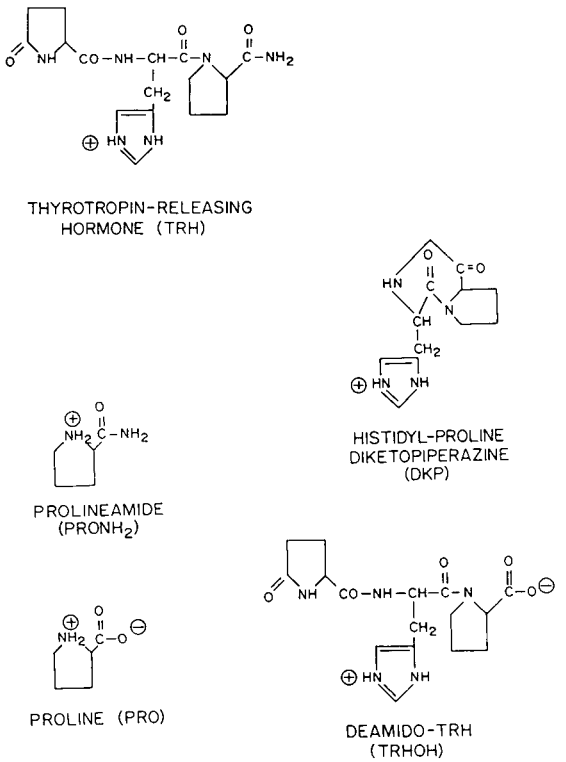

Fig. 1. Structures of TRH and some metabolites.

3. Results and discussion

The percentage of acetonitrile and the concentration of SDS in the mobile phase have a strong effect on solute retention, as illustrated in Figs. 2 and 3. For all solutes, the capacity factor, k', decreases almost exponentially when the concentration of acetonitrile in the eluent increases. On the other hand, k' increases with increasing pairing ion concentration but tends to a constant value at high concentrations. Both effects are characteristic of RP-IPC with hydrophobic pairing ions and have been observed with many different solutes [7–10].

Figs. 2 and 3 also show that the selectivity slightly increases with increase in retention, but TRH and its analogue TRHOH cannot be baseline separated, even at the highest k'. However, the separation of these compounds can be dramatically improved by a small change in the pH of the mobile phase, from 2.15 to 2.5 (Fig. 4). This is possible because TRHOH has an ionizable carboxylic acid group (Fig. 1) with a pK_a value of *ca.* 2. Small pH changes near this value induce large variations in the solute net

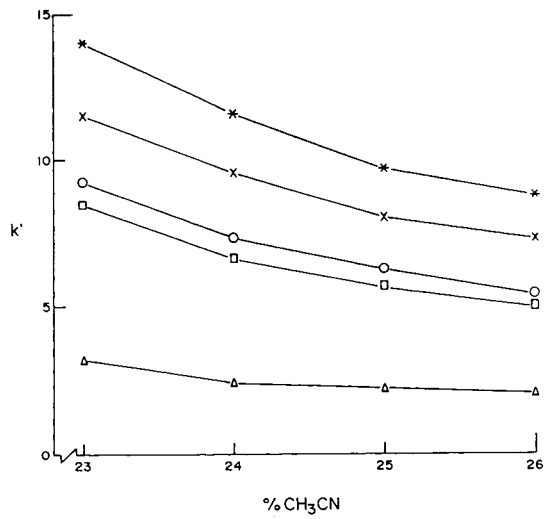

Fig. 2. Effect of acetonitrile concentration (in %, w/v) on the retention of small peptides and amino acids. Mobile phase, acetonitrile–water containing 5.19 m*M* SDS and 15 m*M* LiH_2PO_4 (pH 2.15). △ = PRO; □ = TRHOH; ○ = TRH; × = $PRONH_2$; * = DKP.

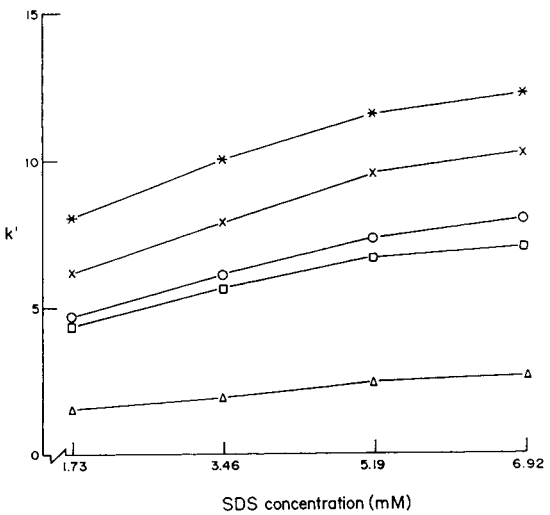

Fig. 3. Effect of pairing ion concentration on the retention of TRH and metabolites. Mobile phase, acetonitrile (24%, w/v)–water containing SDS and 15 m*M* LiH_2PO_4 (pH 2.15). Symbols as in Fig. 2.

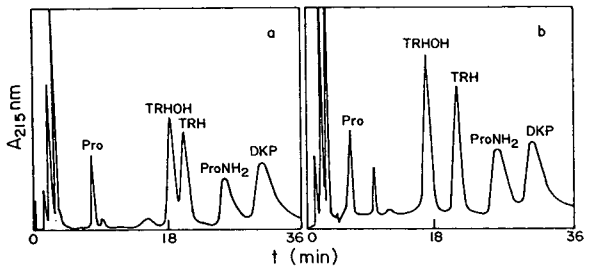

Fig. 4. Influence of pH on the separation of TRH and TRHOH. Mobile phase, acetonitrile (24%, w/v)–water containing 5.19 m*M* SDS and 15 m*M* LiH_2PO_4. (a) pH 2.15; (b) pH 2.5.

charge. As the pH and ionization of the carboxylic group increase, the interaction of TRHOH with the negatively charged dodecyl sulphate becomes weaker and retention progressively decreases. The same effect is observed for the amino acid proline.

In previous work [7,8], we demonstrated that an ion-exchange mechanism is, in great part, responsible for solute retention in RP-IPC with hydrophobic pairing ions. Therefore, another parameter that can be used to control the separation and analysis time is the salt concentration in the eluent and, in particular, the concentration of ions of the same charge as the solute (co-ions). Fig. 5 shows the effect of Li^+ concentration on retention and selectivity. It can be seen that retention decreases in a hyperbolic manner with increase in Li^+ concentration and, because this effect is stronger for the most retained solutes, selectivity is also affected. Complete separation of TRH and TRHOH can be achieved, even at pH 2.15, by using low salt concentrations, but at the expense of longer analysis times and more asymmetric peaks for $PRONH_2$ and DKP (Fig. 6).

Co-ions compete with solutes for association with the adsorbed pairing ion. Different co-ions have different affinities for the ionic stationary phase. Therefore, the solute retention also depends on the type of co-ion present in the mobile phase. Fig. 7 shows the separation of the five solutes using an eluent of pH 2.85 with a Li^+, Na^+ or K^+ salt. The retentions of TRH, $PRONH_2$ and DKP decrease in the order $Li^+ <$

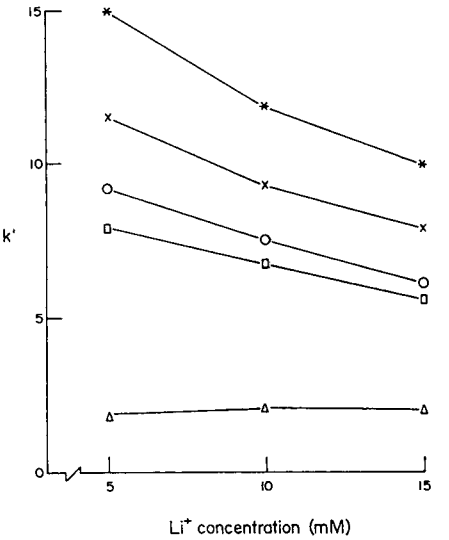

Fig. 5. Effect of salt concentration on the retention of TRH and its metabolites. Mobile phase, acetonitrile (24%, w/v)–water containing 5.19 m*M* SDS and LiH_2PO_4 (pH 2.15). Symbols as in Fig. 2.

$Na^+ < K^+$, meaning that this is the affinity order of the three cations in the RP-IPC system. In fact, the same affinity order is found in ion-exchange chromatography.

There are two interesting observations in Fig. 7. First, PRO is almost unretained and TRHOH behaves ambiguously, probably because at pH 2.85 their net charge approaches zero and the effects of pairing ion and co-ion are negligible. Second, the wide peaks of $PRONH_2$ and DKP become narrower and more symmetrical when K^+ is present in the mobile phase. To our knowledge, this effect of co-ion type has not been reported before in RP-IPC.

4. Conclusions

RP-IPC with hydrophobic pairing ions is a powerful technique for the separation of small peptides. The retention can be adjusted by variation of at least four parameters of the mobile phase: acetonitrile, pairing ion and salt concentrations and salt type. Changes in the proportion of organic solvent in the eluent have the strongest effect on solute retention. There-

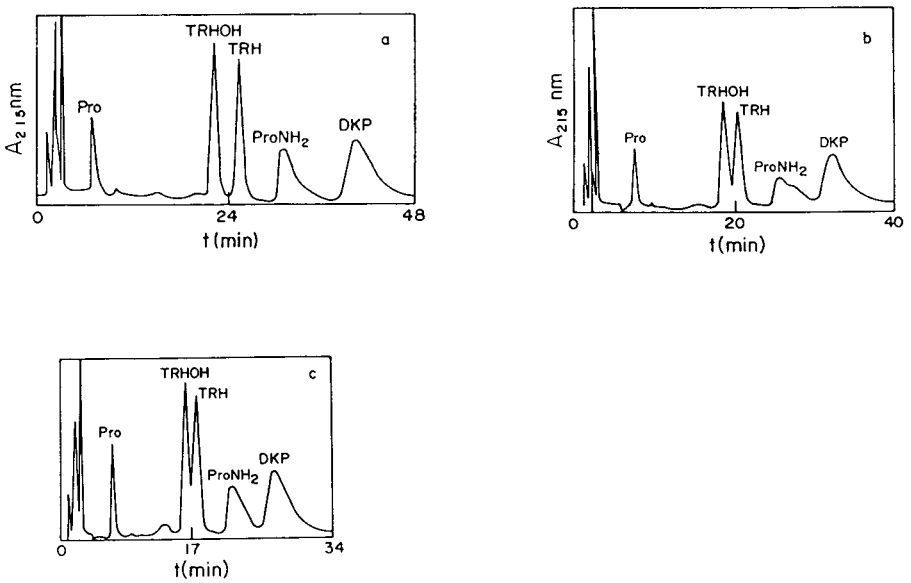

Fig. 6. Separation of TRH and some metabolites at various concentrations of LiH_2PO_4: (a) 5; (b) 10; (c) 15 m*M*. Other conditions as in Fig. 5.

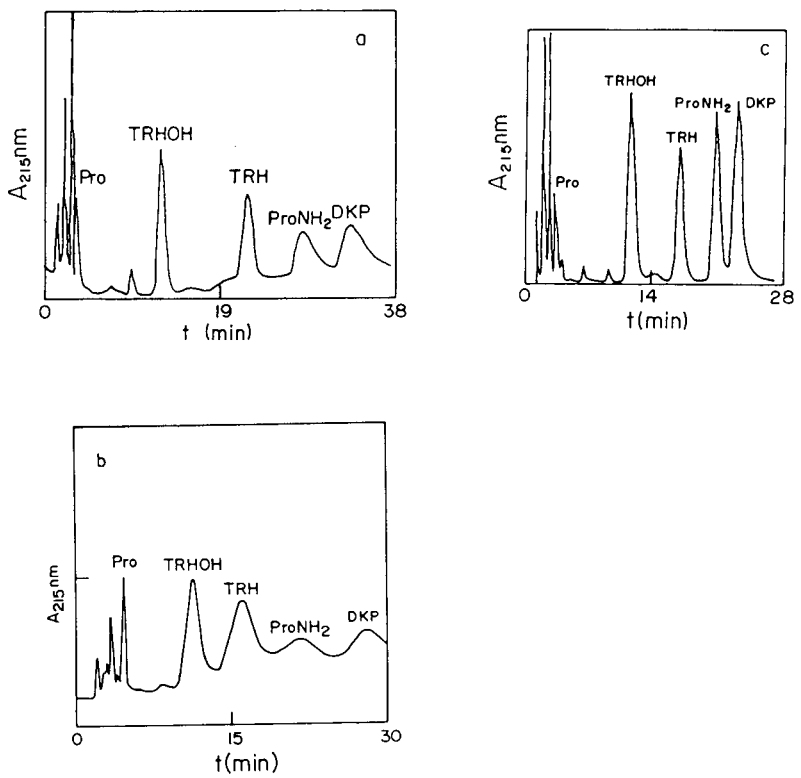

Fig. 7. Influence of salt type on the separation of TRH and some metabolites. Mobile phase, acetonitrile (24%, w/v)–water containing 5.19 m*M* SDS and 15 m*M* phosphate salt (pH 2.85). (a) LiH_2PO_4; (b) NaH_2PO_4; (c) KH_2PO_4.

fore, to obtain reproducible results, this parameter must be carefully controlled. On the other hand, the parameter of choice for improving selectivity is pH, but only if the analytes have functional acid–base groups with different pK_a values. Finally, the results of this work indicate that the peak width and peak shape of some solutes can be dramatically modified by a change of co-ion, even if the new ion is a member of the same chemical family. This interesting effect is being studied.

5. Acknowledgements

The authors are indebted to Dr. Jean Louis Charlie (Biotechnological Institute, National University of Mexico) for providing the peptides, amino acids and solvents used in this work and to Leopoldo Güereca and Salvador Antonio Pérez for technical assistance.

6. References

[1] J.L. Meek and Z.L. Rossetti, *J. Chromatogr.*, 211 (1981) 15.
[2] W.S. Hancock, C.A. Bishop, R.L. Prestidge, D.R.K. Harding and M.T.W. Hearn, *J. Chromatogr.*, 153 (1978) 391.
[3] D. Guo, C.T. Mant and R.S. Hodges, *J. Chromatogr.*, 386 (1987) 205.
[4] E. Spindel and R.S. Wurtman, *J. Chromatogr.*, 175 (1979) 198.
[5] E. Spindel, D. Pettibone, L. Fisher, J. Fernstrom and R. Wurtman, *J. Chromatogr.*, 222 (1981) 381.
[6] W.S. Hancock, C.A. Bishop, L.J. Meyer, D.R.K. Harding and M.T.W. Hearn, *J. Chromatogr.*, 161 (1978) 291.
[7] L.E. Vera-Avila, M. Caude and R. Rosset, *Analusis*, 10 (1982) 36.
[8] M.E. Del Rey and L.E. Vera-Avila, *J. Liq. Chromatogr.*, 11 (1988) 2885.
[9] B.A. Bidlingmeyer, S.N. Deming, W.P. Price, Jr., B. Sachok and M. Petrusek, *J. Chromatogr.*, 186 (1979) 419.
[10] J.H. Knox and R.A. Hartwick, *J. Chromatogr.*, 204 (1981) 3.

ELSEVIER

Journal of Chromatography A, 667 (1994) 125–130

JOURNAL OF CHROMATOGRAPHY A

Rapid purification method for human recombinant tumor necrosis factor alpha

Alain Paquet, Ann Lévesque, Michel Pagé*

Department of Biochemistry, Faculty of Medicine, Université Laval, Sainte-Foy, Québec, G1K 7P4, Canada

(First received June 25th, 1993; revised manuscript received December 31st, 1993)

Abstract

Human recombinant tumor necrosis factor alpha was purified in a single step to about 95% purity from *Escherichia coli* lysate by chromatography on hydroxyapatite. The last traces of contaminants were removed by fast protein liquid chromatography on a Mono Q column. The final product was found to be pure by gel electrophoresis with silver staining. A molecular mass of approximately 17 000 and a specific activity of $4.3 \cdot 10^6$ U/mg after a single purification step were found.

1. Introduction

Tumor necrosis factor (TNF) is a monokine produced by activated macrophages [1,2] and it is believed to be present mainly in two forms, as a monomer of M_r 17 000 and as a trimer [3,4].

This cytokine has an action both as a messenger on the immune system and also in the necrosis of tumor cells [5]. Although the precise role of TNF has not yet been elucidated, it is one of the most important monokines of the immune reaction. This product has been cloned most of the time in *Escherichia coli* [6–8] and it is usually purified by many steps including gel chromatography, ion exchange and absorption chromatography [9–11]. The total yields reported are about 20% [12]. We report here the purification of recombinant human TNF from *E. coli* lysate in a single purification step on hydroxyapatite followed by a rapid Mono Q chromatography to remove the last traces of impurities.

2. Experimental

2.1. Human recombinant TNF alpha and E. coli

E. coli cells carrying the expression vector for TNF alpha were grown at 37°C in LB medium containing 50 μg/ml of ampicillin. When the absorbance at 600 nm reached about 1.0, the culture was stopped and cells were collected by centrifugation. After washing the suspension, cells were lysed with buffer containing lysozyme at 1 mg/ml in 20 m*M* Tris–HCl (pH 7.4)–25%

* Corresponding author.

0021-9673/94/$07.00
SSDI 0021-9673(94)00010-7

sucrose–10 m*M* EDTA containing 1 m*M* (0.001%) phenylmethylsulfonyl fluoride (PMSF) to block proteolysis. The insoluble fraction was removed by centrifugation at 3000 *g* for 15 min.

2.2. Residual TNF

The insoluble fraction was solubilized by boiling for 5 min in a minimum volume of 10 m*M* Tris–HCl (pH 8.0)–1 m*M* EDTA containing 2.5% sodium dodecyl sulfate (SDS) and 5% β-mercaptoethanol. This fraction was analysed by SDS–polyacrylamide gel electrophoresis (PAGE) as described below.

2.3. Hydroxyapatite chromatography

The supernatant was dialyzed against 0.05 *M* phosphate buffer (pH 7.0) and applied on a 50 × 1.6 cm I.D. column filled with HTP hydroxyapatite (Bio-Rad Labs., Mississauga, Ontario, Canada) equilibrated with the same buffer. This sample was applied at 1 ml/min and, after washing with one column volume of starting buffer, a linear phosphate buffer gradient (from 0.05 to 0.30 *M*, pH 7.0) was applied. Proteins were eluted at 2 ml/min and monitored at 280 nm on a fast protein liquid chromatographic (FPLC) system (Pharmacia Canada, Montreal, Canada) using two P-500 pumps connected to a GP-250 gradient programmer and a Pharmacia LK-UV-M2 monitor connected to a Pharmacia–LKB Model 102 recorder.

2.4. Mono Q chromatography

Positive fractions were pooled and dialyzed against 20 m*M* Tris–HCl buffer (pH 8.0). The pool was applied to a Mono Q column (Pharmacia Canada) equilibrated with the starting buffer. TNF was eluted from the column with a linear NaCl gradient from 40 to 75 m*M* in starting buffer at 1 ml/min [12]. Positive fractions were screened as described before and analyzed by SDS-PAGE [13].

2.5. Assay for TNF activity

The activity of TNF was monitored by a previously described cell lysis assay [12]. Briefly, mouse L-929 fibroblasts obtained from the American Type Culture Collection were grown in a 96-well flat-bottomed plate (Falcon Plastics 3040) at 50 000 cells per well in 0.1 ml of culture medium in the presence of 1 μg/ml of actinomycin D and incubated with a serially diluted test sample of TNF in a humidified atmosphere at 37°C with 5% CO_2. After 18 h, the test sample was removed, the plates were washed and cell lysis was detected by staining the plates with a 0.5% solution of crystal violet in methanol–water (1:4, v/v). The end-point on the microtitration plates was determined with a Thermomax ELISA reader (Molecular Devices, CA, USA) set for absorption at 540 nm. One unit of TNF is defined as the amount required for 50% cell lysis [12].

2.6. Protein determination

Protein concentration was determined at 280 nm using a factor of 1.62 for the molar absorptivity of a 0.1% TNF solution as described previously [7].

2.7. Gel electrophoresis

SDS-PAGE was performed on the various fractions and on the purified material using an 8–25% polyacrylamide gel gradient on a Phast system (Pharmacia Canada). After electrophoresis, the gels were stained with silver using a silver-staining kit (Pharmacia Canada). Proteins were also stained with 2% Coomassie Brilliant Blue R-250 (Bio-Rad Labs.) in 10% (v/v) acetic acid. Gels were destained in the Phast system using methanol–acetic acid–H_2O (3:1:6). Molecular mass standards (Bio-Rad Labs.) were also run on the same gel.

2.8. Amino acid analysis

About 3 mg of the purified TNF were extensively dialysed against HPLC-grade water and

2.5 μg were placed in Corning culture tubes (Cat. No. 9820, 50 × 6 mm I.D.) which were previously heated in a muffle furnace at 450°C overnight. The tubes were placed in Waters reaction vials and samples were dried in a Waters Pico-Tag workstation (Waters, Division of Millipore, Mississauga, Ontario, Canada). Constant-boiling HCl (200 μl) containing 1% of phenol was added to the vial and alternately purged (with dried nitrogen) and evacuated. After three purges, the vial was heated at 150°C for 1, 2, 3 and 4 h under vacuum. The values for ten amino acids stable to acid hydrolysis were not corrected. Values for Ser, Thr and Tyr were extrapolated to zero time and those for Ile and Val were extrapolated to infinity. Tryptophan was determined by alkaline hydrolysis [14] and cysteine was determined as cysteic acid after performic acid oxidation [15]. The analysis was performed on a Beckman System 6300 high-performance analyzer according to the general procedures of Spackman *et al.* [16].

2.9. Capillary electrophoresis

Capillary electrophoresis was performed at 20°C using a BioFocus 3000 (Bio-Rad Labs.). The coated capillary (24 cm × 25 μm I.D.; No. 148-3031, Bio-Rad Labs.) was washed for 1 min with distilled water, followed by a 2-min wash with 0.3 *M* borate buffer (pH 8.5). Electrophoresis was run at 10 kV with a constant current of 50 μA and monitored at 280 nm.

3. Results

3.1. Purification on hydroxyapatite

HTP hydroxyapatite was used in the first step in process chromatography as it eliminates most of the contaminating material and yields about 95% pure TNF at the end of the gradient. Fig. 1 shows the elution pattern in which we observed a large peak of contaminating proteins which is eluted with the void volume whereas TNF under the conditions applied is retained on the hydroxyapatite. The linear gradient used allows the separation of TNF from some of the major constituents of the cell lysate. This material still contains some minor impurities which may be observed by silver staining but not with Coomassie Blue, as shown in Fig. 2.

3.2. Purification on Mono Q

The last traces of impurities could be removed easily in a single step on a Mono Q anion-exchange column, as shown in Fig. 3. We obtained two peaks in this chromatographic step and both contain pure TNF without any difference in specific lytic activity.

As shown in Table 1, this purification pro-

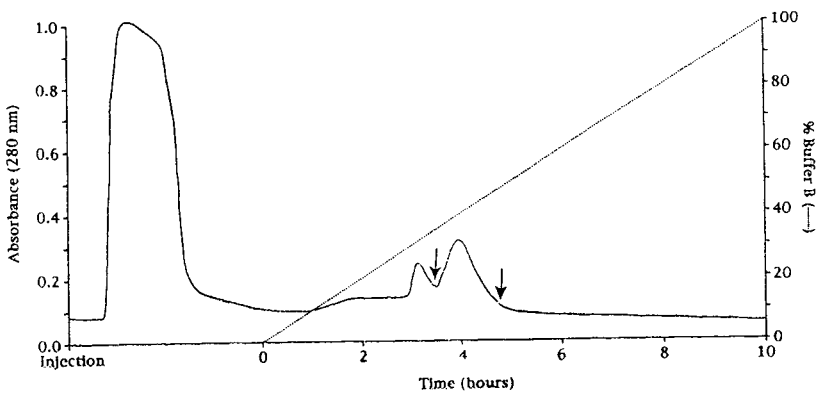

Fig. 1. Elution pattern of TNF on the HTP hydroxyapatite column eluted with a linear gradient. Buffer A = $NaHPO_4$–Na_2PO_4 (0.05 *M*); buffer B = $NaHPO_4$–Na_2PO_4 (0.30 *M*). The arrows indicate the TNF-containing peak.

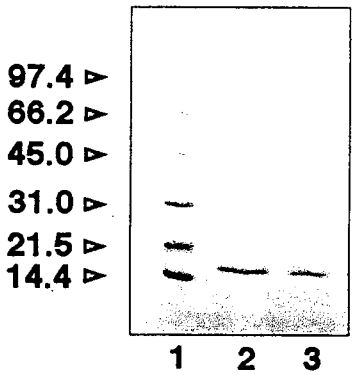

Fig. 2. SDS-PAGE of TNF with a polyacrylamide gel gradient (8–25%, w/v) using 10 m*M* Tris–HCl (pH 8.0)–1 m*M* EDTA–5% β-mercaptoethanol–2.5% SDS. The proteins were detected in the gel by staining with Coomassie Brilliant Blue R-250. Lanes: 1 = molecular mass standards (M_r values $\times 10^{-3}$ on the left); 2 = purified TNF; 3 = purified TNF diluted twice.

cedure gives a 3580-fold increase in specific activity while conserving most of the TNF content of the cell lysate. As the number of steps

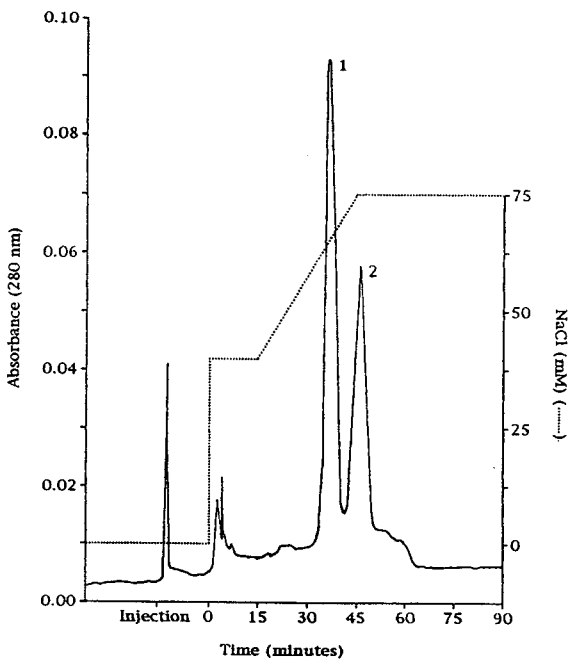

Fig. 3. Elution pattern of TNF using the Mono Q column. Peaks 1 and 2 represent two forms of TNF, as found by identical amino acid content.

was decreased by developing conditions that would eliminate most of the contaminants while TNF was retained on the column, the purification yield was greatly improved. We also found that by using Bio-Gel HTP hydroxyapatite, one could scale up almost linearly the purification procedure from a small Econo HTP column (V_t = 5 ml) to a semi-preparative scale (V_t = 100 ml) without changing the conditions.

3.3. Residual TNF

Integration of three different scans of the electrophoresis of the solubilized residual fraction showed that 15.8% of the total TNF was left in this fraction. This was considered to be negligible compared with the degree of purification obtained with the method described. The specific activity of TNF could not be determined owing to the presence of various proteases and toxic material in the insoluble fraction.

3.4. Analysis of the final product

The final product was found to be pure by SDS-PAGE and silver staining. A single band corresponding to a molecular mass of about 17 000 had the same electrophoretic mobility as reference TNF obtained from Dr. V. Korobko (Shemyakin Institute, Moscow, Russian Federation) (Fig. 4). The results of amino acid analysis of the final product agreed very closely with the theoretical amino acid content reported [11] (Table 2). Capillary electrophoresis gave the expected three peaks corresponding to the monomer, dimer and trimer isoforms of human TNF without any trace of impurities (Fig. 5).

4. Discussion

The method described here for the purification of tumor necrosis factor from *E. coli* is highly reproducible and may be scaled up from an analytical column of Bio-Gel HTP hydroxyapatite to a semi-preparative column that was used for this separation. We found an almost

Table 1
Purification of human TNF from *E. coli*

Step	Total protein (mg)	Specific activity[a] (U/mg)	Total activity (U/mg)	Total protein (%)	Increase in specific activity
E. coli homogenate	217.0	$1.2 \cdot 10^4$	$2.60 \cdot 10^6$	100	–
Hydroxyapatite	13.6	$4.3 \cdot 10^6$	$5.85 \cdot 10^7$	6.26	3580×
Mono Q	8.21	$1.44 \cdot 10^7$	$11.8 \cdot 10^7$	3.78	12 000×

Yields are calculated for 2 l of culture medium.
[a] Specific activity of TNF was calculated as described in under Experimental; this value is an approximation for the *E. coli* homogenate, which contains various toxic factors and possible inhibitors of TNF activity.

linear correlation between the elution volume and the column size under the conditions adopted. Most of the published methods for the purification of recombinant human TNF alpha consist of 5–6 purification steps with yields varying from 5% to 30%. The above procedure using a single step with hydroxyapatite yields 95% pure TNF while a second step with Mono Q anion-exchange chromatography allows the elimination of the last traces of contaminants while conserving the lytic activity. It is believed that this efficient purification method may be used for the large-scale purification of TNF in industrial settings.

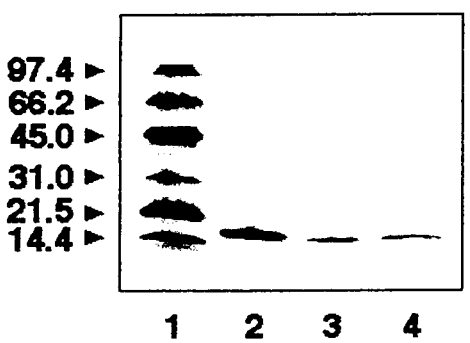

Fig. 4. SDS-PAGE of TNF with a polyacrylamide gel gradient (8–25%, w/v) using 10 m*M* Tris–HCl (pH 8.0)–1 m*M* EDTA–5% β-mercaptoethanol–2.5% SDS. Proteins were detected by silver staining. Lanes: 1 = molecular mass standards (M_r values $\times 10^{-3}$ on the left); 2 = reference TNF; 3 = Mono Q-purified TNF (peak at 60 m*M* NaCl); 4 = Mono-Q purified TNF (peak at 75 m*M* NaCl).

5. Acknowledgements

We are grateful to Dr. V. Korobko of the Shemyakin Institute, Moscow, for supplying us

Table 2
Amino acid composition of TNF

Amino acid	Theoretical number of residues	Number of residues found
Ala	13	12.73
Arg	9	8.80
Asx[a]	12	12.00
Cys[b]	2	1.86
Glx	20	20.39
Gly	11	11.07
His	3	3.01
Ile	8	8.02
Leu	18	18.00
Lys	6	6.04
Phe	4	4.01
Pro	10	10.30
Ser	13	12.07
Thr[c]	6	6.10
Trp[d]	2	1.78
Tyr[c]	7	6.89
Val	13	12.22

Proteins were gas-phase hydrolysed in 6 *M* HCl containing 0.1% phenol for 1, 2, 3 and 4 h at 150°C.
[a] As Asx is stable to acid hydrolysis, it was taken as the reference residue.
[b] Determined as cysteic acid by performic acid oxidation prior to acid hydrolysis [15].
[c] Determined by extrapolation to zero time.
[d] Determined by alkaline hydrolysis with 12 *M* NaOH at 110°C for 16 h [14].

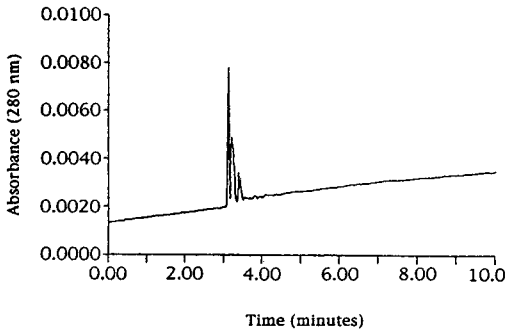

Fig. 5. Capillary electrophoresis of TNF.

with the TNF plasmid and to Dr. B. Gibbs of the Institute of Biotechnology, Montreal, for the amino acid analyses.

6. References

[1] A.E. Carswell, L.J. Old, S. Green, N. Fiore and B. Williamson, *Proc. Natl. Acad. Sci. U.S.A.*, 72 (1975) 3666.
[2] D. Pennica, G.E. Nedwin, J.S. Hayflick, P.H. Seeburg, R. Derynck, M.A. Palladino, W.J. Kohr, B.B. Aggarwal and D.V. Goeddel, *Nature*, 312 (1984) 724.
[3] P. Wingfield, R.H. Pain and S. Craig, *FEBS Lett.*, 211 (1987) 179.
[4] A. Lewit-Bentley, R. Fourme, R. Kahn, T. Prangé, P. Vachette, J. Tavernier, G. Hauquier and W. Fiers, *J. Mol. Biol.*, 199 (1988) 389.
[5] G. Camussi, E. Albano, C. Tetta and F. Bussolino, *Eur. J. Biochem.*, 202 (1991) 3.
[6] Y. Tanobe, K. Noguchi, A. Morikawa, D.-I. Mizuno and G.-I. Soma, *Biochem. Biophys. Res. Commun.*, 179 (1991) 683.
[7] J.M. Davis, M.A. Nurachi, N.K. Alton and T. Arakawa, *Biochemistry*, 26 (1987) 1326.
[8] T. Arakawa and D.A. Yphantis, *J. Biol. Chem.*, 262 (1987) 7484.
[9] K. Sreekrishra, L. Nellis and R. Potenz, *Biochemistry*, 28 (1989) 4117.
[10] T. Tamatani, S. Kimuca, T. Hashimoto and K. Orosaki, *J. Biochem.*, 105 (1989) 55.
[11] B.B. Aggarwal, W.J. Kohn, P.E. Hass, B. Moffat, S.A. Spencer, W.J. Henzel, T.S. Bringman, G.E. Nedwin, D.V. Goeddel and R.N. Harkins, *J. Biol. Chem.*, 260 (1985) 2345.
[12] B.B. Aggarwal and W.J. Kohn, *Methods Enzymol.*, 116 (1985) 443.
[13] U.K. Laemmli, *Nature*, 227 (1970) 680.
[14] T.E. Hugli and S. Moore, *J. Biol. Chem.*, 247 (1972) 2828.
[15] A.N. Glazer, R.J. De Lange and D.S. Sigman, *Chemical Modification of Proteins*, Elsevier, New York, 1975, p. 23.
[16] D.H. Spackman, W.H. Stein and S. Moore, *Anal. Chem.*, 30 (1958) 2764.

ELSEVIER

Journal of Chromatography A, 667 (1994) 131–139

JOURNAL OF CHROMATOGRAPHY A

Hydrophobic interaction chromatography for the purification of cytolytic bacterial toxins

Bernd Schoel*, Manuela Welzel, Stefan H.E. Kaufmann

Department of Immunology, University of Ulm, Albert-Einstein-Allee 11, D-89081 Ulm, Germany

(Received November 30th, 1993)

Abstract

The usefulness of hydrophobic interaction chromatography for the simple purification of cytolytic bacterial toxins was studied. Conditions are described for different hydrophobic interaction chromatographic media for purifying with high yields two different kinds of such haemolysins, the thiol-activated toxin listeriolysin O from *Listeria monocytogenes* and alpha-toxin from *Staphylococcus aureus*. For listeriolysin O, purification on butyl-Sepharose was followed by gel filtration chromatography. From butyl-Sepharose the recovery was 84%. The final product had a specific activity of 620 000 U/mg with an overall recovery of 22%. Alpha-toxin was obtained by a single purification step from alkyl-Superose with 80% recovery and a specific activity of 29 000 U/mg. On sodium dodecyl sulphate polyacrylamide gel electrophoresis purified listeriolysin O and alpha-toxin showed a single band. Another thiol-activated toxin, streptolysin O from group A streptococci, showed a recovery of 38% from butyl-Sepharose. The results suggest the feasibility of using hydrophobic interaction chromatography, particularly with columns of weak hydrophobicity, for the purification of bacterial haemolysins in high yield.

1. Introduction

Several pathogenic bacteria produce extracellular haemolysins as important virulence factors. Listeriolysin O, secreted by the intracellular bacterium *Listeria monocytogenes*, is a well characterized haemolysin contributing to its intracellular lifestyle [1]. After adherence of the bacterium to target cells and its phagocytosis, listeriolysin O promotes bacterial evasion from the endosome into the cytosol of the host cell [2–5]. Listeriolysin O is a member of the family of sulphydryl (SH)-activated bacterial toxins that are produced by various Gram-positive species with streptolysin O from group A streptococci as prototype. These toxins have a similar molecular mass of *ca.* 60 000 and their haemolytic activity is destroyed by exposure to oxygen and restored by addition of reducing agents such as cysteine. These toxins bind to cholesterol-containing membranes where they oligomerize to form arc- and ring-shaped multimeric structures containing up to 100 toxin monomers. They span the membrane and promote transition of large molecules through the membrane [6]. The alpha-toxin from *Staphylococcus aureus* represents a different type of haemolysin. This toxin is independent of sulphydryl and has a molecular mass of 34 000. It forms hexamers, causing small transmembrane pores in the target membrane. These pores of defined size allow the translocation only

* Corresponding author.

0021-9673/94/$07.00
SSDI 0021-9673(94)00043-9

of small molecules such as amino acids, whereas larger entities such as proteins are retained by the membrane [7,8].

Haemolysins are also of great interest for numerous cell-biological studies. Because listeriolysin O is most active under weakly acidic conditions of about pH 6, its function can be modulated by pH changes [9]. This toxin is useful for studies concerned with protein translocation from acidified endosomal compartments to the cytosol, *e.g.*, studies of antigen presentation. The alpha-toxin is used for permeabilizing cell preparations, allowing studies on the influence of small molecules on cellular processes [10]. Because of the wide application of haemolysins in functional studies, their rapid purification is of increasing interest. So far sulphydryl-activated haemolysins have been purified by covalent chromatography on thiol-activated columns as a major purification step [11]. For the purification of alpha-toxin, the use of cation-exchange chromatography [12] and porous glass beads [13] has been described.

We were interested in purified listeriolysin O, for which covalent chromatography gives a low recovery [9]. In an attempt to obtain a high recovery of listeriolysin O and other cytolysins, we were looking for a simple alternative purification method: as haemolysins interact with hydrophobic membranes it appeared reasonable to exploit this feature for their purification by hydrophobic interaction chromatography (HIC). HIC columns bind proteins via hydrophobic patches on their surface. Parameters that influence this chromatographic process are HIC columns with ligands of different hydrophobic strength on the one hand, and variation of the hydrophobic character of the protein on the other. The method most widely used for increasing the hydrophobicity of a protein is the addition of antichaotropic agents such as ammonium sulphate [14]. Screening the literature for procedures based on HIC to purify cytolytical bacterial toxins, we found reports for the thiol-activated toxins pneumolysin from *Streptococcus pneumoniae* [15] and tetanolysin from *Clostridium tetani* [16], for extracellular cytolysins from halophilic bacteria [17,18] and for a cytolytic enterotoxin from *Bacteroides fragilis* [19]. Employing HIC for listeriolysin and alpha-toxin, we were successful in purifying haemolysins of scientific and technological interest in high yield by a one- or two-step procedure. Hence HIC may prove a simple and powerful method for purifying membrane-attacking bacterial toxins in general.

2. Experimental

2.1. Production of haemolysins

Listeriolysin O

From an overnight preculture of *Listeria monocytogenes* WTD [20] a 1% inoculum was grown overnight in 350 ml of medium (Bacto tryptic soy broth from Difco Labs., Detroit, MI, USA) in 1-l erlenmeyer flasks on a rotary shaker (120 rpm at 37°C). Bacteria were removed by centrifugation (20 min at 10 000 rpm, 17 000 *g*, and 10°C) and the supernatants were filtered through 0.2-μm membrane filters. This sterile supernatant was either used directly for chromatography or alternatively precipitated at 4°C with ammonium sulphate (80% saturation), and the collected precipitate was dissolved in 20 m*M* sodium phosphate (pH 6.5). Crude haemolysin stocks were stored frozen at −20°C until used.

Alpha-toxin

This toxin from *Staphylococcus aureus* (strain Wood 46, ATCC 10832, DSM 20491) was prepared according to Lind *et al.* [12]. Briefly, a 1% inoculum of an exponentially growing preculture was cultured overnight in 350 ml of medium (Bacto tryptic soy broth) in a 1-l indended erlenmeyer flask on a rotary shaker (150 rpm at 37°C). After 18 h, the bacteria were removed as described above and ammonium sulphate was added at 4°C to the supernatant (75% saturation). The haemolysin was solubilized from the precipitate with 10 m*M* sodium acetate–20 m*M* sodium chloride (pH 5.0) and stored frozen at −20°C in aliquots.

Streptolysin O

Streptolysin O was purchased from Diagnostics Pasteur (Marnes-la-Coquette, France). The material of one 25-ml vial was dissolved in 2.5 ml of 10 m*M* sodium phosphate (pH 7.0).

2.2. Chromatography

Alkyl-Superose HR5/5, butyl-Sepharose, phenyl-Sepharose Cl-4B, octyl-Sepharose Cl-4B, the Pharmacia HIC test kit, Mono S HR5/5, Mono Q HR5/5 and Superose 12 HR10/30 were obtained from Pharmacia Biosystems (Freiburg, Germany) and Econo-Pac methyl-HIC cartridges from Bio-Rad Labs. (Munich, Germany).

Listeriolysin O

Chromatography was carried out on a fast protein liquid chromatographic (FPLC) system (Pharmacia Biosystems) at room temperature. For HIC on butyl-Sepharose (5-ml column, 1-cm diameter) the material was adjusted to 27% saturation of ammonium sulphate. Either the culture supernatant was directly adjusted by adding ammonium sulphate or, alternatively, the fraction obtained after 80% ammonium sulphate precipitation was dissolved and dialysed in 20 m*M* sodium phosphate (pH 6.5) and then ammonium sulphate was added to 27% saturation. After loading on to the column equilibrated with 25% ammonium sulphate in 20 m*M* sodium phosphate (pH 6.5), washing was carried out with 25% ammonium sulphate in the same buffer because with 27% ammonium sulphate proteins occasionally precipitated on the column. Elution was performed with a decreasing linear gradient of ammonium sulphate from 25% to 0% in the same buffer. The flow-rate was 1 ml/min. Gel filtration was carried out with Superose 12 HR10/30 in phosphate-buffered saline (PBS) (50 m*M* sodium phosphate buffer containing 150 m*M* sodium chloride) of pH 6.0.

Alpha-toxin

All chromatographic steps were carried out at 4°C because at room temperature the recoveries dropped by about 40%. The toxin fraction after 75% ammonium sulphate precipitation in 20 m*M* sodium phosphate buffer (pH 7.0) was adjusted to 45% of ammonium sulphate and loaded on to an alkyl-Superose HR5/5 (1 ml) equilibrated with 45% ammonium sulphate in the same buffer. Elution was done with a decreasing linear gradient of ammonium sulphate in 20 m*M* sodium phosphate (pH 7.0). The flow-rate was 0.5 ml/min.

Streptolysin O

The conditions were identical with those described for alpha-toxin purification except that 35% instead of 45% ammonium sulphate was used as the initial salt concentration.

2.3. Sodium dodecyl sulphate polyacrylamide gel electrophoresis (SDS-PAGE) and western blotting

Electrophoresis was carried out under reducing conditions in a discontinuous 12.5% polyacrylamide gel according to standard procedures in a mini-PROTEAN II electrophoresis system (Bio-Rad Labs.) and the gels were silver stained [21]. For immunological detection of specific bands, proteins were transferred to reinforced nitrocellulose (Schleicher and Schüll, Dassel, Germany) in a semi-dry blotting system. After blocking the membrane with 3% skim-milk powder (Fluka, Neu-Ulm, Germany) in 50 m*M* Tris–hydrochloric acid (pH 7.5), the mAb B8B20-3-2 [22] against listeriolysin O was used as first antibody (1 μg/ml). Further incubation steps were done with alkaline phosphatase conjugated goat anti-mouse IgG (Jackson Immuno Research Labs., West Grove, PA, USA). The blots were then developed with 0.8 μg/ml 5-bromo-4-chloro-3-indolylphosphate *p*-toluidine salt and 1.6 μg/ml 4-nitrotetrazolium blue chloride (both from Fluka) in 1 *M* diethanolamine–hydrochloric acid, 0.5 m*M* magnesium chloride (pH 9.8).

2.4. Determination of haemolysins

Listeriolysin O

The sample was serially diluted in PBS (pH 6.0) containing 0.1% bovine serum albumin and then activated by adding cysteine (20 m*M* final

concentration). Diluted samples (100 μl) were incubated at 37°C for 45 min with 50 μl of sheep erythrocytes ($6 \cdot 10^8$ cells/ml in PBS, pH 6.0 [23]) in U-bottomed 96-well plates. After centrifugation (1200 rpm, 5 min, 300 *g*) 50 μl of the supernatant were transferred into a flat-bottomed 96-well plate containing 50 μl of PBS per well. The concentration of haemolysin was determined spectrophotometrically at 405 nm in an enzyme-linked immunosorbent assay (ELISA) reader. For total haemolysis a concentrated sample of haemolysin was used. The dilution of haemolysin lysing 50% of erythrocytes was determined and the reciprocal value was used to calculate the haemolytic units (*U*) per millilitre of the undiluted sample.

Alpha-toxin

A 10-μl volume of serially diluted sample in PBS (pH 7.0) was incubated with 100 μl of rabbit erythrocytes ($2.5 \cdot 10^8$ cells/ml) at 37°C for 45 min in U-bottomed 96-well plates [12]. The subsequent procedure was as described above for listeriolysin O.

Streptolysin O

The assay was carried out as described for listeriolysin O but at pH 7.5 instead of pH 6.0.

2.5. Protein assay

The BCA test from Pierce (Oud Beijerland, Netherlands) was used with bicinchoninic acid as the test reagent [24]. Contaminating substances were removed by precipitating the proteins with trichloroacetic acid. The sample was mixed with at least 10% (v/v) of 3 *M* trichloroacetic acid, incubated for 5 min, centrifuged (15 min, 12 000 *g*) and the sediment was washed once with 200 μl of 1 *M* hydrochloric acid. The sample was centrifuged once more and the sediment was air dried after the supernatant had been discarded. The sediment was dissolved in 200 μl of BCA test reagent and, after incubation for 30 min at room temperature, 150 μl were transferred into a flat-bottomed 96-well plate. Absorbance at 570 nm was measured in an ELISA reader. For calibration, bovine serum albumin was used in a range from 2 to 100 μg in the assay.

3. Results

3.1. General conditions for HIC of haemolysins

We attempted to purify three bacterial haemolysins by hydrophobic interaction chromatography. HIC demands binding of proteins at high salt concentrations (usually ammonium sulphate) to increase the hydrophobic character of the protein. First, the ammonium sulphate concentration at which the haemolysins begin to precipitate was determined. Aliquots of crude culture supernatants containing $2.1 \cdot 10^3$ U/ml of listeriolysin O (60 μg/ml of protein), $1.3 \cdot 10^3$ U/ml of alpha-toxin (140 μg/ml of protein) or 55 U/ml of streptolysin O were subjected to concentrations of ammonium sulphate ranging from 20% to 50% saturation in 5% steps in PBS. After incubation for 1 h on ice, the samples were centrifuged and their haemolytic activities in the supernatants were assayed. Listeriolysin O, alpha-toxin and streptolysin O were precipitated at 30%, 50% and 40% saturation of ammonium sulphate, respectively.

In order to identify suitable HIC material for each of the haemolysins, binding experiments were performed in a batch assay using three HIC resins with increasing hydrophobicity from butyl- to phenyl- to octyl-Sepharose. Listeriolysin O ($2.4 \cdot 10^4$ U/ml, 830 μg/ml of protein) or alpha-toxin ($9.5 \cdot 10^3$ U/ml, 1.14 mg/ml of protein) after ammonium sulphate precipitation and the dissolved streptolysin O (55 U/ml) were adjusted to 27%, 45% or 35% ammonium sulphate saturation in PBS, respectively, the highest concentrations of ammonium sulphate at which no precipitation occurred. To 200 μl of packed and equilibrated HIC resins, 200 μl of haemolysin were mixed in microcentrifuge tubes. After incubation on ice for 30 min and centrifugation, the residual haemolytic activities in supernatants were determined. Each haemolysin was treated similarly with HIC resins without ammonium sulphate in order to determine whether the toxins were bound already at low ionic strength. Octyl- and phenyl-Sepharose bound all three haemolysins in the absence of ammonium sulphate (Table 1); therefore, these media were too hydrophobic to be used in purification. In con-

Table 1
Purification of the haemolysins on HIC columns

Haemolysin[a]	HIC medium	Binding condition (% ammonium sulphate)[b]	Elution from HIC column (% ammonium sulphate)[c]	Recovery (%)[d]	Specific activity (U/mg protein)
Listeriolysin O	Octyl-Sepharose CL-4B	0	NA[e]		
	Phenyl-Sepharose CL-4B	0	NA		
	Phenyl-Sepharose low binding	27	0		
	Butyl-Sepharose	27	13–0	75–85	440 000
	Alkyl-Superose	27	10–3	12	ND[f]
	Methyl-HIC cartridge	27	10–0	6	ND
Alpha-toxin	Octyl-Sepharose CL-4B	0	NA		
	Phenyl-Sepharose CL-4B	0	NA		
	Phenyl-Sepharose low binding	45	0		
	Butyl-Sepharose	45	22–5	20	17 000
	Alkyl-Superose	45	34–30	70–90	29 000
	Methyl-HIC-cartridge	45	25–17	45–50	28 000
Streptolysin O	Octyl-Sepharose CL-4B	0	NA		
	Phenyl-Sepharose CL-4B	0	NA		
	Butyl-Sepharose	35	8–0	38	ND
	Alkyl-Superose	35	11–0	5	ND
	Methyl-HIC cartridge	35	23–12	32	ND

[a] Starting material contained $2.4 \cdot 10^4$ U/ml of listeriolysin O ($2.9 \cdot 10^4$ U/mg of protein), $9.5 \cdot 10^3$ U/ml of alpha-toxin ($8.3 \cdot 10^3$ U/mg of protein) and 55 U/ml of streptolysin O.
[b] Binding at the indicated concentration (% saturation) of ammonium sulphate. Further conditions are described in the text.
[c] The range of concentration (% saturation of ammonium sulphate) of those fractions within a decreasing linear gradient of ammonium sulphate with haemolytic activity is given.
[d] Total haemolytic activity recovered related to the activity loaded on to the column.
[e] NA = not applicable.
[f] ND = not determined.

trast, butyl-Sepharose did not bind any of the toxins at low ionic strength, but completely bound listeriolysin O, alpha-toxin and streptolysin O at 27%, 45% or 35% ammonium sulphate saturation, respectively. Conversely, all three haemolysins could be eluted with decreasing concentration of ammonium sulphate (Table 1).

3.2. Separation of the three haemolysins on weak HIC columns

Butyl-Sepharose, alkyl-Superose and Econo-Pac methyl-HIC cartridges exhibit weak hydrophobicity. The three haemolysins were loaded on to each of these columns and eluted with a decreasing linear gradient of ammonium sulphate (Table 1, Fig. 1). All fractions were subjected to the haemolytic assay, positive fractions were pooled and recoveries were determined quantitatively by serial dilutions of the materials loaded on to the columns and also of the pooled fractions (Table 1). In terms of recovery, listeriolysin O was best purified on butyl-Sepharose (recovery 75–85%, purification factor 15); alpha-toxin was best purified on alkyl-Superose (recovery 70–90%, purification factor 3.5) and acceptably well on Econo-Pac methyl-HIC cartridges (recovery 45–50%, purification factor 3.4). For streptolysin O, butyl-Sepharose proved to be a suitable HIC column, with a recovery of 38%; owing to the small amounts of protein in the purchased material, the specific activity and the purification factor could not be determined reliably. Analysis of pooled haemolytic fractions by SDS-PAGE indicated

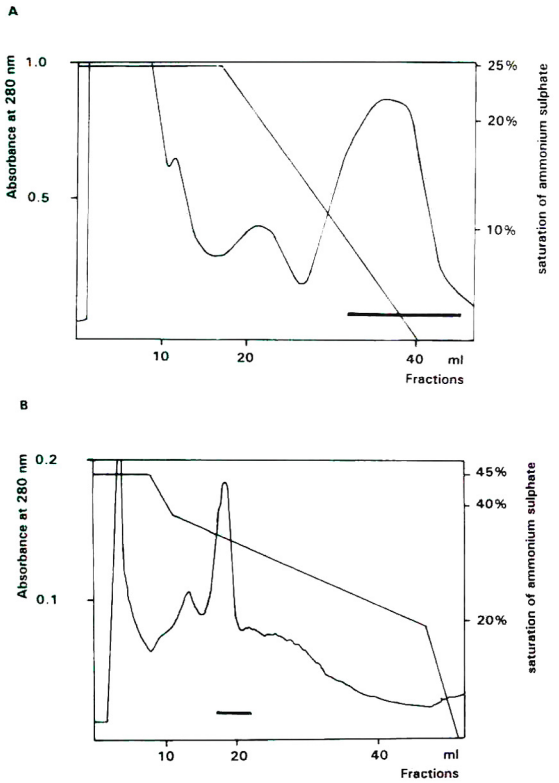

Fig. 1. Chromatography of (A) listeriolysin O on butyl-Sepharose and (B) alpha-toxin on alkyl-Superose. The decreasing gradient indicates decreasing saturation of ammonium sulphate from 25% [(A) listeriolysin O] or 45% [(B) alpha-toxin] to 0%. Haemolytic fractions are indicated with bars. A 10-ml volume (20 mg of protein) of crude listeriolysin O after precipitation with ammonium sulphate were loaded on to a 5-ml column of butyl-Sepharose and 1 ml (1.1 mg of protein) of crude alpha-toxin after precipitation with ammonium sulphate was loaded on to an alkyl-Superose HR5/5 column.

that alpha-toxin was purified to a single band (Fig. 2, lane 7). The major contaminants from the culture supernatants containing listeriolysin O had been removed by this single purification step (Fig. 2, lane 3). The identity of listeriolysin O was confirmed immunologically by western blotting with the listeriolysin O-specific mAb B8B20-3-2 [22] (Fig. 2, lane 5).

In order to evaluate the capacity of butyl-Sepharose for listeriolysin O, alkyl-Superose and Econo-Pac methyl-HIC cartridge for alpha-toxin, bacterial culture supernatants adjusted to the

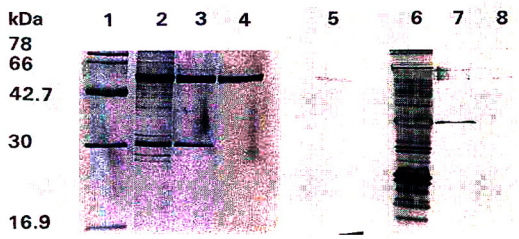

Fig. 2. SDS-PAGE of the cytolsin fractions in 12.5% polyacrylamide gels revealed by silver staining (except lane 5). Molecular mass markers are on lane 1. Listeriolysin O fractions are on lanes 2–5: 2 = culture supernatant after precipitation with ammonium sulphate (4.8 μg); 3 = after HIC (2.8 μg); 4 = after gel filtration (2.3 μg); 5 = after HIC immunologically detected with antilisteriolysin O mAb B8B20-3-2 after western blotting. Alpha-toxin fractions are on lanes 6 and 7: 6 = culture supernatant after precipitation with ammonium sulphate (18 μg); 7 = after HIC (1.6 μg). A control with sample buffer only is on lane 8. kDa = kilodalton.

appropriate ammonium sulphate concentration were pumped on to 1-ml columns (butyl-Sepharose from the HIC test kit and alkyl-Superose HR5/5) and 5-ml columns (Econo-Pac methyl-HIC cartridge) until haemolytic activities appeared in the effluent. The capacity of butyl-Sepharose for listeriolysin O was $4.6 \cdot 10^5$ U (or 1.8 mg of protein) per milliliter of resin material; this amount was contained in 200 ml of culture supernatant with $2.8 \cdot 10^3$ U/ml and 85 μg/ml of protein. The capacity of alkyl-Superose for alpha-toxin was $6.9 \cdot 10^4$ U per millilitre of resin, corresponding to 2.6 mg of toxin; this amount of toxin was contained in 110 ml of culture supernatant with 900 U/ml and 110 μg/ml of protein. A 5-ml volume of Econo-Pac methyl-HIC medium bound $5.4 \cdot 10^4$ U (or 2.4 mg of protein) from 125 ml of culture supernatant.

3.3. *Further purification of listeriolysin O*

For further purification of listeriolysin O we intended to use anion-exchange chromatography, in analogy with a published method [25] which used DEAE-Sephacel with 25 m*M* Tris–hydrochloric acid buffer (pH 8.0). When applied to the Mono Q HR5/5 anion-exchange column, listeriolysin O eluted between 0.25 and 0.27 *M* sodium chloride in this buffer. We obtained only

Table 2
Purification of listeriolysin O

Purification step	Total activity (10^5 U)	Total protein (mg)	Specific activity (U/mg protein)	Recovery (%)
Culture supernatant[a]	7.2	21	34 000	–
Ammonium sulphate precipitation	5.8	20	29 000	81
Butyl-Sepharose HIC	4.9	1.1	440 000	68
Superose 12 HR10/30 gel filtration	1.6	0.26	620 000	22

[a] Starting material was 350 ml of culture supernatant containing 2100 U/ml of listeriolysin O and 60 μg/ml of protein.

a 5% recovery but we cannot compare this result because the recovery was not reported by the previous authors. Listeriolysin O bound to the Mono S HR5/5 cation-exchange column and eluted between 0.1 and 0.11 *M* sodium chloride in 50 m*M* sodium malonate buffer (pH 6.0 or pH 7.5), each with a recovery of around 15%. However, gel filtration in PBS (pH 6.0) on a Superose 12 HR 10/30 column resulted in pure toxin and a higher recovery (32%). On SDS-PAGE, a single band was visible (Fig. 2, lane 4). In combination with the previous HIC, listeriolysin O could be purified in a two-step process to a specific activity of $6.2 \cdot 10^5$ U/mg and a total recovery of 22% (Table 2).

4. Discussion

We have described an efficient method for the purification of representative bacterial haemolysins by HIC, which is probably also applicable for other cytolysins. Both HIC resins and ion exchangers allow purification and concentration in a single step and both are appealing first-step methods for the purification and concentration of proteins from culture supernatants. Ion exchangers are particularly useful owing to (i) the low cost of further additives and the technical possibilities of floating systems where bacterial suspensions can be pumped directly through specially designed columns such as Streamline (Pharmacia), thereby avoiding the separation of culture supernatants from bacteria by centrifugation. Difficulties in using ion exchangers can arise from osmolarity of the culture medium hindering binding of the proteins of interest. HIC resins can be used especially in media of high osmolarity, but require further additives such as ammonium sulphate. In this instance the lowest possible concentration has to be tested if cost becomes a factor of consideration. HIC, however, can be very efficient for the separation of proteins of interest from contaminants. Weak HIC resins proved particularly useful purification media for crude material if the proteins of interest were bound. They allow efficient purification because only a few proteins bind to weak HIC media. In previous work we purified recombinant heat shock protein of the M_r 60 000 family from *Mycobacterium bovis* BCG from crude lysates of the host *Escherichia coli* on alkyl-Superose with high efficiency [26]. This recombinant protein could be purified in a single step from almost all contaminating proteins that did not bind to the weak HIC column. At the same time, among all the separation methods tested, only alkyl-Superose enabled us to separate this protein from a truncated heat shock protein of which the M_r was 3000 lower. Cytolysins, in contrast to most other cellular proteins, interact with membranes, *i.e.*, with hydrophobic areas. Therefore, it is reasonable to consider HIC with columns of weak hydrophobicity for the separation of cytolysins from most proteins.

According to the principles controlling HIC [14], experiments to evaluate the potential of HIC for the purification of proteins should

address the following questions: (i) at which concentration of ammonium sulphate does the protein start to become salted out; (ii) which HIC columns contain too strong hydrophobic ligands, thus binding the proteins already in the absence of antichaotropic agents; (iii) which HIC columns contain too weak hydrophobic ligands, preventing binding of the protein at the highest possible concentrations of ammonium sulphate; (iv) what are the conditions for optimum chromatography in terms of recovery and purity on those HIC columns which allow binding of the protein at high concentrations of ammonium sulphate and desorption with decreasing concentrations of ammonium sulphate?

Concentrations of ammonium sulphate at which listeriolysin O, streptolysin O and alpha-toxin still remained in solution allowed their binding to HIC media with ligands of weak hydrophobicity such as butyl-Sepharose and alkyl-Superose. HIC media of medium hydrophobicity such as phenyl-Sepharose possessed too strong binding properties for these haemolysins. Because we obtained different yields using different chromatographic resins of weak hydrophobicity, the optimum HIC resin had to be identified for each cytolysin individually. Oligomerization of varying degrees on different HIC media could provide an explanation for these different recoveries.

Comparing HIC with other separation methods, for listeriolysin O HIC was more efficient in terms of recovery than chromatography with thiol-activated Sepharose, the recoveries being 80% and 11% [9], respectively. Together with gel filtration, a specific activity of $6.2 \cdot 10^5$ U/mg was obtained, comparable to published specific activities of $10 \cdot 10^5$ U/mg, and our method resulted in a higher total recovery. For alpha-toxin, the recovery from alkyl-Superose was high (>80%) and the specific activity of $2.9 \cdot 10^4$ U/mg was comparable to published specific activities of the purified toxin, *e.g.*, $3.1 \cdot 10^4$ U/mg [12] and $2 \cdot 10^4$–$5 \cdot 10^4$ U/mg [27]. The high separation power of the HIC columns used can be perceived visually from SDS-PAGE (Fig. 2). In crude culture supernatants the haemolysins are the major protein. By comparing the protein pattern on SDS-PAGE before and after HIC, it is obvious that the haemolysins are separated from a large pool of different proteins not bound by the HIC columns. The binding capacity of the HIC columns used allowed the purification of 1 l of culture supernatant of listeriolysin O with a 5-ml column of butyl-Sepharose and of alpha-toxin with a 10-ml column of alkyl-Superose or a 40-ml methyl-HIC cartridge.

Comparing our results using HIC for listeriolysin O, streptolysin O and alpha-toxin with those of other investigators who applied HIC successfully for the purification of bacterial haemolysins [15–19], we conclude that in general high recoveries and purities can be obtained with weakly hydrophobic HIC columns. In addition to covalent chromatography on thiolated matrices as a general method for the separation of thiol-activated toxins, HIC could provide another approach of high potential for the purification of cytolytic proteins.

5. Acknowledgements

This work was supported by the Deutsche Forschungsgemeinschaft, Sonderforschungsbereich 322. We thank W. Goebel (Institute of Genetics and Microbiology, University of Würzburg, Germany) for providing us with *L. monocytogenes* WTD, G. Fuchs (Institute of Microbiology, University of Ulm, Germany) for *S. aureas* strain Wood 46 and P. Cossart (Institut Pasteur, Paris) for mAb B8B20-3-2. We are also very much obliged to Professor G. Fuchs for critically reading the manuscript. We thank K. Schilling (Pharmacia, Freiburg) for technical information on FPLC and A. Gritzan for typing the manuscript.

6. References

[1] S.H.E. Kaufmann, *Annu. Rev. Immunol.*, 11 (1993) 129.

[2] P. Berche, J.-L. Gaillard and S. Richard, *Infection*, 16 (1988) 145.

[3] P. Cossart and J. Mengaud, *Mol. Biol. Med.*, 6 (1989) 463.
[4] P. Cossart, M.F. Vicente, J. Mengaud, F. Baquero, J.C. Perez-Diaz and P. Berche, *Infect. Immun.*, 57 (1989) 3629.
[5] D.A. Portnoy, T. Chakraborty, W. Goebel and P. Cossart, *Infect. Immun.*, 60 (1992) 63.
[6] C.J. Smyth and J.L. Duncan, in J. Jeljaszewicz and T. Wadström (Editors), *Bacterial Toxins and Cell Membranes*, Academic Press, New York, 1978, p. 129.
[7] S. Bhakdi, G. Menestrina, F. Hugo, W. Seeger and J. Tranum Jensen, in F.J. Fehrenbach, J.E. Alouf, P. Falmagne, W. Goebel, J. Jeljaszewicz, D. Jürgens and R. Rappuoli (Editors), *Bacterial Protein Toxins (Zentralblatt für Bakteriologie*, Suppl. 17), Gustav Fischer, New York, 1988, p. 71.
[8] M. Thelestam and L. Blomqvist, *Toxicon*, 26 (1988) 51.
[9] C. Geoffroy, J.-L. Gaillard, J.E. Alouf and P. Berche, *Infect. Immun.*, 55 (1987) 1641.
[10] M.-F. Bader, D. Thiersé, D. Aunis, G. Ahnert-Hilger and M. Gratzl, *J. Biol. Chem.*, 261 (1986) 5777.
[11] J.E. Alouf and C. Geoffroy, *Methods Enzymol.*, 165 (1988) 52.
[12] I. Lind, G. Ahnert-Hilger, G. Fuchs and M. Gratzl, *Anal. Biochem.*, 164 (1987) 84.
[13] S. Harshman, N. Sugg and P. Cassidy, *Methods Enzymol.*, 165 (1988) 3.
[14] K.-O. Eriksson, in J.-C. Janson and Rydén (Editors), *Protein Purification*, VCH, New York, 1989, p. 207.
[15] T.J. Mitchell, J.A. Walker, F.K. Saunders, P.W. Andrew and G.J. Boulnois, *Biochim. Biophys. Acta*, 1007 (1989) 67.
[16] U. Weller, K. Bäsler, G. Ahnert-Hilger, M. Messner and S. Bhakdi, *Med. Microbiol. Immunol.*, 182 (1993) 167.
[17] M.H. Kothary and A.S. Kreger, *Infect. Immun.*, 49 (1985) 25.
[18] L.D. Gray and A.S. Kreger, *Infect. Immun.*, 48 (1985) 62.
[19] R. van Tassell, D.M. Lyerly and T.D. Wilkins, *Infect. Immun.*, 60 (1992) 1343.
[20] S. Kathariou, P. Metz, H. Hof and W. Goebel, *J. Bacteriol.*, 169 (1987) 1291.
[21] J.H. Morrissey, *Anal. Biochem.*, 117 (1981) 307.
[22] F. Nato, K. Reich, S. Lhoptial, S. Rouyre, C. Geoffroy, J.C. Mazie and P. Cossart, *Infect. Immun.*, 59 (1991) 4641.
[23] C. Geoffroy, J.-L. Gaillard, J.E. Alouf and P. Berche, *J. Gen. Microbiol.*, 135 (1989) 481.
[24] P.K. Smith, R.I. Krohn, G.T. Hermanson, A.K. Mallia, F.H. Gartner, M.D. Provenzano, E.K. Fujimoto, N.M. Goeke, B.J. Olson and D.C. Klenk, *Anal. Biochem.*, 150 (1985) 76.
[25] H. Tsukada, I. Kawamura, T. Fujimura, K.-I. Igarashi, M. Arakawa and M. Mitsuyama, *Cell. Immunol.*, 140 (1992) 21.
[26] B. Schoel and S.H.E. Kaufmann, *J. Chromatogr.*, 587 (1991) 19.
[27] J.H. Freer and J.P. Arbuthnott, in F. Dorner and J. Drews (Editors), *Pharmacology of Bacterial Toxins (International Encyclopedia of Pharmacology and Therapeutics Section*, Vol. 119), Pergamon Press, Oxford, 1986, p. 581.

ELSEVIER

Journal of Chromatography A, 667 (1994) 141–153

JOURNAL OF CHROMATOGRAPHY A

New approaches for separating and purifying apple polyphenol oxidase isoenzymes: hydrophobic, metal chelate and affinity chromatography

F. Richard-Forget*,[a], P. Goupy[a], J. Nicolas[b]

[a]*Institut National de la Recherche Agronomique, Station de Technologie des Produits Végétaux, Domaine Saint Paul BP 91, F-84143 Montfavet Cedex, France*

[b]*Conservatoire National des Arts et Metiers, Chaire de Biochimie Industrielle et Agroalimentaire, 292 Rue Saint-Martin, F-75141 Paris Cedex 03, France*

(First received September 28th, 1993; revised manuscript received December 16th, 1993)

Abstract

Apple polyphenol oxidase (PPO) was subjected to hydrophobic, metal chelate and affinity chromatography. Among numerous hydrophobic supports, Phenyl-Sepharose CL4B appeared to be the most appropriate matrix for the purification of highly hydrophobic proteins such as PPO. With immobilized copper affinity chromatography, four fractions were obtained. Using electrophoresis experiments, it was shown that these fractions differed from the isoenzymes separated by ion exchange on DEAE-Sepharose CL6B. Apple PPO was also adsorbed on synthetized affinity resins with competitive inhibitors (*p*-coumaric and *p*-hydroxybenzoic acid) coupled via an azo linkage to hexamethylenediamineagarose. These affinity matrices were also used to evaluate the inhibition constants of the ligands. Lastly, apple PPO was successively chromatographed on hydrophobic, metal chelate and affinity columns. This protocol led to a 280-fold purified fraction representing 25% of the crude extract activity.

1. Introduction

Browning reactions which occur during the handling, storage, processing and cooking of fruits or vegetables are mainly initiated by the enzyme polyphenol oxidase (*o*-diphenol: O_2 reductase, EC 1.10.3.1; PPO). Because of the deleterious effect of the enzymatic browning on food products, numerous studies have been devoted to PPO, and more precisely to its purification. Nevertheless, only a few PPOs have been purified to apparent homogeneity. These included PPOs from peach, grape, spinach, tomato and potatoes and several fungal PPOs [1].

The first step in the purification that has been commonly applied was the removal of inactive proteins by fractionation with ammonium sulphate. Further purification frequently involved conventional chromatographic methods of separation such as adsorption, gel filtration and ion-exchange chromatography. Several papers reported also the use of hydrophobic chromatography as a rapid, reproducible and effective

* Corresponding author.

0021-9673/94/$07.00
SSDI 0021-9673(93)E0060-8

purification step. This last method, introduced in 1978 by Jen and Flurkey [2] for peach PPO purification, was successfully applied to PPOs from different sources, *e.g.*, PPO from grape [3], pear [4] and broad bean [5]. Moreover, systematic studies on alkyl- and aminoalkylagarose efficiency have been carried out by Iborra *et al.* [6], Flurkey and Jen [7] and Ingebrigtsen and Flurkey [8].

Affinity chromatography was described as early as 1953 by Lerman [9] for mushroom PPO purification. However, subsequent studies on the affinity chromatography of PPO were mainly applied to fungal enzymes and only a small part to PPOs from fruits and vegetables. The ligands employed included substrates [10], competitive inhibitors [6,11,12] and antibodies [8,13]. Another affinity method, referred to as metal chelate or immobilized metal affinity chromatography (IMAC), introduced in 1975 by Porath *et al.* [14], has been successfully applied to the purification of PPO from Jerusalem artichoke [15] and carrot [16]. Nevertheless, although this technique has frequently been used to purify metalloenzymes such as superoxide dismutase [17,18] and carboxypeptidase [19], there has been no application to PPOs from other origins.

Concerning apple PPO, Harel *et al.* [20] and Walker and Hulme [21] partially purified the enzyme extracted from the peel using DEAE-cellulose chromatography, whereas Stelzig *et al.* [22] used calcium phosphate gel adsorption. Janovitz-Klapp *et al.* [23] reported the use of hydrophobic chromatography for purifying the cortex enzyme. Fractionation by ammonium sulphate precipitation followed by filtration on Phenyl-Sepharose CL4B gel resulted in 120-fold purified PPO from Red Delicious cortex, with a total yield close to 40%. However, no systematic study on the efficiency of different hydrophobic supports has been carried out by previous workers. It is not evident that Phenyl-Sepharose CL4B was the most appropriate gel for purifying apple PPO. Moreover, to our knowledge, affinity chromatographic methods have not been used to obtain highly purified apple PPO preparations. Hence, the purpose of this work was, on the one hand, to analyse the hydrophobic behaviour of apple PPO with different chromatographic supports as influenced by experimental parameters (temperature, pH and ionic strength of the elution buffer) in order to establish the optimum conditions for the enzyme purification. In addition, we applied for the purification of apple PPO the two affinity chromatographic methods, *i.e.*, IMAC and affinity chromatography using a competitive inhibitor as the ligand on agarose. Ion-exchange chromatography is also required in order to compare the heterogeneity of the apple PPO system in terms of copper affinity and isoelectric point value. This should also clarify the discrepancies that exist among the number of isoforms, which varied between one [24,25], two [21,26] and three [20,23] for apple PPO.

2. Experimental

2.1. Materials

The apples, variety Red Delicious, were picked at their commercial maturity and used as an enzyme source. DEAE-Sepharose CL6B, chelating Sepharose CL6B, Phenyl-Sepharose CL4B and Octyl-Sepharose CL4B were obtained from Pharmacia (Uppsala, Sweden). Phenylagarose, phenylaminoagarose and the two kits of alkyl- and aminoalkylagaroses, were purchased from Sigma (St. Louis, MO, USA). HMD-Ultrogel was supplied by IBF (Clichy, France). All other chemicals were of analytical-reagent grade from Sigma.

2.2. Initial purification step

The PPO was extracted with McIlvaine's buffer at pH 7.2, containing 0.5% Triton X-100 and 15 m*M* ascorbic acid, according to the method described by Janovitz-Klapp *et al.* [23]. Inactive proteins were partially removed by ammonium sulphate precipitation (30% saturation), the resulting supernatant being labelled "S_{30} extract".

2.3. PPO and protein assays

PPO activity was assayed polarographically according to the method of Janovitz-Klapp *et al.* [23]. Activity was expressed as nanomoles of oxygen consumed per second (nanokatals) under the assay conditions.

The protein content was determined according to Bradford [27] with bovine serum albumin as a standard.

2.4. Hydrophobic chromatography

On micro-columns

Chromatography was carried out at 4 and 25°C. Each hydrophobic support, *ca.* 1 ml, was packed into a small column (0.75 cm^2 section) and equilibrated with 50 m*M* sodium phosphate buffer (pH 6.5) containing 2 *M* ammonium sulphate. A 1-ml volume of "S_{30} extract" was dialysed overnight against the equilibration buffer and then applied to each column. Unbound proteins were thoroughly washed from the columns with equilibration buffer (5 × 1 ml). The adsorbed enzyme was eluted stepwise with 50 m*M* phosphate buffers (pH 6.5) containing ammonium sulphate with gradually decreasing concentration from 1.8 to 0.2 *M* in 0.1 *M* steps (5 × 1 ml). The columns were washed with water (5 × 1 ml) and 50% ethylene glycol (5 × 1 ml) to remove tightly bound enzyme. The PPO activity was determined in each 1-ml fraction.

On an analytical column

A 90-ml volume of the "S30 extract" dialysed overnight against 50 m*M* phosphate buffer (pH 6.5) containing KCl and $(NH_4)_2SO_4$ (both 0.5 *M*) was loaded on to a Phenyl-Sepharose CL4B column (8 × 2.5 cm I.D., 40-ml bed) equilibrated with the former buffer at a flow-rate of 100 ml h^{-1}. After elution of unbound proteins with the equilibration buffer, the PPO was eluted using the same buffer containing KCl and $(NH_4)_2SO_4$ (both 0.1 *M*). Proteins still bound to the gel were removed by washing with water and 50% ethylene glycol. The absorbance at 280 nm and the PPO activity were determined in each 7-ml fraction. The active fractions were combined and labelled as "first purified PPO extract".

2.5. Affinity chromatography

Preparation of the p-coumaric and p-hydroxybenzoic acid HMD-Ultrogel (p-COU-HMD and p-HBZ-HMD)

p-Coumaric and *p*-hydroxybenzoic acid were coupled to hexamethylenediamineagarose (HMD-Ultrogel) via an azo linkage, with a protocol adapted from Cuatrecasas [28], Cuatrecasas and Anfinsen [29] and Cohen [30]. This protocol included three steps, as follows.

Preparation of p-aminobenzamidohexylagarose. A 20-ml volume of hexamethylenediamineagarose was suspended in two volumes of 0.2 *M* sodium borate (pH 9.3) and cooled to 4°C. A solution of *p*-nitrobenzoyl azide (0.1 *M* in 50% dimethylformamide) was added gradually to the gel suspension with continuous stirring. The reaction mixture was then stirred at 4°C for 1 h and at 25°C for an additional 3–4 h. Completion of the acylation reaction can be checked by the loss of colour reaction with trinitrobenzenesulphonic acid [28]. The gel was then washed thoroughly with five volume of 50% dimethylformamide and ten volumes of distilled water.

The resulting *p*-nitrobenzamidohexylagarose was suspended in a solution of 0.2 *M* dithionite in 0.5 *M* sodium hydrogencarbonate (pH 8.5) and the mixture was kept at 40°C for 1 h with continuous stirring. Decoloration has to be total. The product obtained was washed with ten volumes of distilled water and in this form was stored at low temperature for later use.

Diazotation of the p-aminobenzamidohexylagarose support. The previous derivative was suspended in an equal volume of ice-cold 0.5 *M* hydrochloric acid. A solution of sodium nitrite (0.1 *M*) was added and the mixture was stirred for 7 min in an ice-bath. The gel was then

washed thoroughly with ten volumes of cold distilled water.

Coupling of phenolic ligand. The diazotized support was resuspended in an equal volume of cold 0.2 *M* acetate buffer (pH 5.5). A solution of *p*-coumaric or *p*-hydroxybenzoic acid (20 m*M*) dissolved in a similar volume of acetate buffer was added in one portion to the suspension of diazonium agarose and stirred in an ice-bath. Formation of the red azo gel began immediately and coupling was achieved in 30 min. The *p*-COU-HMD and *p*-HBZ-HMD gels were filtered, washed thoroughly with five volumes of 50% dimethylformamide followed by ten of distilled water and stored at 4°C as a suspension in distilled water supplemented with thymol (1%).

The concentrations of bound phenolic ligand were evaluated spectrophotometrically at 287 nm (*p*-coumaric acid) or 250 nm (*p*-hydroxybenzoic acid) by measuring the difference in absorbance between the initial solution at 20 m*M* and the filtered solution.

Column chromatography

A 5-ml volume of *p*-COU-HMD or *p*-HBZ-HMD was packed into a small column (1 cm^2 section) and equilibrated with 25 ml of McIlvaine's buffer (pH 4.5) at a flow-rate of 80 ml h^{-1}. A 6-ml volume of the "first purified PPO extract", dialysed overnight against the equilibration buffer, was loaded on to the column. After elution of unbound proteins by the equilibration buffer, the PPO was eluted with 0.1 *M* phosphate buffer (pH 7.5). The absorbance at 280 nm and PPO activity were determined in each 1-ml fraction.

N.B.: In order to determine non-specific or ion-exchange adsorption, the previous protocol was carried out with control columns, packed with activated but no ligand-coupled matrix.

Evaluation of inhibition constants

Protocol adapted from Graves and Wu [31]. The experiment was carried out at 4°C. A 1.6-ml volume of affinity support was equilibrated with McIlvaine's buffer (pH 4.5) in a total volume of 6 ml. A 200-μl volume (50 nkatal) of the "first purified extract" dialysed overnight against the former buffer were added after each 40 min. After each addition followed by a homogenisation step and when equilibrium was assumed to have been achieved, 2×100 μl were taken from the supernatant in order to assay in duplicate unbound PPO activity. The ratio between the two enzymatic fractions, free and trapped in the gel, was calculated and reported graphically for each enzyme addition number. Once the experiment was completed, 5 ml of McIlvaine's buffer (pH 7.5) were added to the filtered matrix in order to evaluate the total amount of bound enzyme.

Protocol adapted from Dunn and Chaiken [32]. Volumes of 4 ml of affinity supports were packed into a small column (0.75 cm^2 section) and equilibrated with 20 ml of McIlvaine's buffer (pH 4). A 1-ml volume of apple PPO "first purified extract" dialysed overnight against the former buffer was loaded on to the column. Enzyme elution was immediately achieved with McIlvaine's buffer (pH 7.5). The same experiment was repeated with nine different pH values of the elution buffer, *i.e.*, 7.5, 7.0, 6.6, 6.15, 5.9, 5.8, 5.7, 5.5 and 5.1. The pH value and PPO activity were determined in each 0.5-ml fraction. Decreasing pH values were employed to obtain different concentrations of effective bound inhibitor. As inhibition is mainly due to the protonated form of carboxylic acid [33], the concentration of effective inhibitor varied with the pH and followed the equation $[I_e] = [I_t]/(1 + 10^{pH-pK})$, where I_e and I_t represent the effective (protonated form) and total inhibitor (protonated and ionized form). For each chromatographic step, the elution volume of PPO activity was plotted against the concentration of effective inhibitor.

2.6. Ion-exchange chromatography

A 50-ml volume of the "first purified extract" was dialysed overnight against 10 m*M* sodium

phosphate buffer (pH 6.5) and applied to a DEAE-Sepharose CL6B column (10 × 2 cm I.D.) pre-equilibrated with the same buffer. The column was eluted with the equilibration buffer and the eluted protein was monitored by measuring the absorbance at 280 nm. After the absorbance had returned to the baseline, further elution was carried out with a linear salt gradient from 0 to 0.16 *M* $(NH_4)_2SO_4$ in 10 m*M* phosphate sodium buffer (pH 6.5). Proteins that were still bound to the gel were removed with 40 ml of the equilibration buffer successively supplemented with 0.16 and 0.66 *M* $(NH_4)_2SO_4$. The flow-rate was fixed at 80 ml h^{-1} and the absorbance at 280 nm and PPO activity were determined in each 5-ml fraction.

2.7. Immobilized copper affinity chromatography (IMAC)

IMAC was carried out using a method adapted from those described by Miyata-Asano *et al.* [34] and Zawistowsky *et al.* [15]. Chelating Sepharose CL6B was packed in a working column (20 × 1 cm I.D.) and in a guard column (6 × 1 cm I.D.). The working column was loaded with an aqueous solution of $CuSO_4 \cdot 5H_2O$ (6 mg ml^{-1}) until metal was observed in the eluate. The excess of copper was washed from the column with 50 m*M* phosphate buffer (pH 6.5) containing 0.1 *M* KCl at a flow-rate of 120 ml h^{-1}. Both columns coupled in sequence were equilibrated with the previous buffer. An 18-ml volume of the "first purified PPO extract" was applied to the working column. After removal of the unbound protein with 50 ml of the equilibration buffer, the PPO activity was eluted stepwise by using three eluent solutions (75 ml each) which corresponded to the equilibration buffer successively supplemented with 30 and 125 m*M* glycine and 10 m*M* histidine. The guard column was used to adsorb any copper ion that leaked from the working column during the enzyme elution. Columns were regenerated with 75 ml of the equilibration buffer containing 50 m*M* EDTA. The absorbance at 280 nm and PPO activity were determined in each 3.5-ml fraction.

2.8. Electrophoretic experiments

Isoelectrofocusing and electrophoresis in polyacrylamide gels were performed with a Phast system (Pharmacia) using Phastgels IEF 4–6.5 or Phastgels gradient 8–25. The migration conditions were those specified by Pharmacia. Gels stained for PPO activity were immersed in the substrate solution supplemented with *p*-phenylenediamine (0.05%). The specific detection of some isoforms required the addition of SDS (0.55%) to the staining solution.

3. Results and discussion

3.1. Purification of apple PPO by hydrophobic chromatography

Different factors involved in hydrophobic chromatography were analysed, *i.e.*, matrix hydrophobicity (type of spacer arm, length of alkyl or aminoalkyl head chain), temperature and pH. Applying the protocol described under Experimental to each type of gel, we measured, for each $(NH_4)_2SO_4$ concentration of the elution buffers, the ratio of cumulated eluted activity to the loaded activity. Typical graphs are shown in Fig. 1 for Sepharose CL4B, the Phenyl-Sepharose CL4B and Octyl-Sepharose CL4B at 4 and 25°C. To characterize the different packing materials, a hydrophobicity parameter termed "C50" was introduced; this represents the ammonium sulphate concentration required to elute 50% of the loaded activity, thus a low C50 value corresponded to a strong hydrophobic matrix.

Fig. 1 illustrates considerable adsorption of apple PPO on unsubstituted Sepharose CL4B. Moreover, the C50 value of 1.76 attributed to this matrix was not affected by the temperature. Because of the high salt concentrations of the equilibration buffer, this absorption, already reported by Ingebrigtsen and Flurkey [8], could not be explained by ionic interactions but was presumably due to hydrophobic interactions with methyl groups inside the matrix and the 3–6 methylene diether bridges present in every sec-

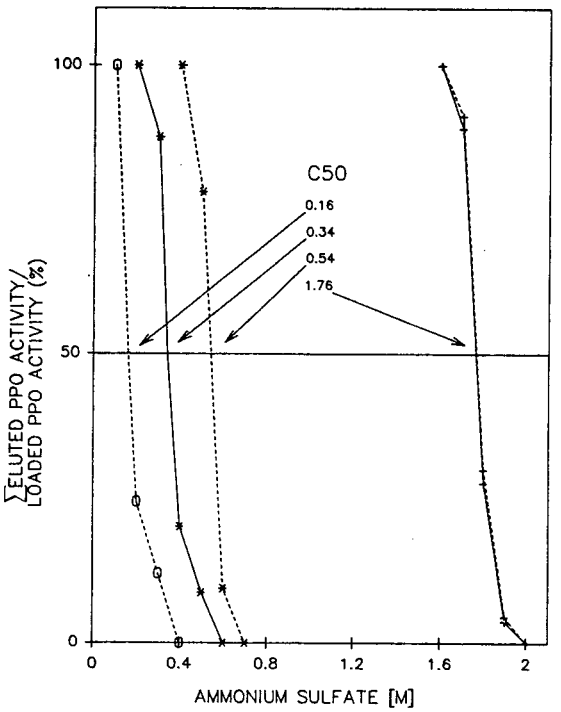

Fig. 1. C50 values determined for CL4B (+) Sepharose, (*) Phenyl-Sepharose and (○) Octyl-Sepharose at 4°C (dashed lines) and 25°C (full lines). For Octyl-Sepharose at 25°C, ethylene glycol was required to elute PPO activity.

ond galactose residue in polysaccharide chains [35,36].

Apple PPO was strongly retained on Octyl-Sepharose CL4B (Fig. 1) as ethylene glycol was required to partially elute enzyme activity at 25°C. At 4°C, full elution was achieved with very low ammonium sulphate concentrations. Under these conditions, a C50 value of 0.16 was associated with Octyl-Sepharose. Such results explain the choice of Octyl-Sepharose for the separation of proteins with low hydrophobicity. It has been successfully used for the purification of wheat gliadins [37]. Phenyl-Sepharose, for which higher C50 values (0.34 at 4°C and 0.54 at 25°C) were determined, is to be preferred for more hydrophobic proteins such as PPO [23,38,39], peroxidase [40,41] or lipoxygenase [42]. When the temperature was increased from 4 to 25°C, an increase in PPO adsorption was observed with Octyl- and Phenyl-Sepharose CL4B. Thus, the C50 value decreased by 0.2 *M* when the temperature was increased from 4 to 25°C.

Nature of the spacer arm

Three gels differing in the nature of their spacer arm were tested with apple PPO, namely an ether group (Phenyl-Sepharose purchased from Pharmacia), an amino group (phenyl-aminoagarose from Sigma) and a butyl propyl ether group (phenyl agarose ether from Sigma). The structures and C50 values associated with the three gels are given in Table 1. The highest hydrophobicity was observed for Phenyl-Sepharose. The introduction of an amino group led to considerably weaker hydrophobic interactions, in agreement with the works of Flurkey and Jen [7], who suggested the probable existence of additional electrostatic interactions in these matrices. However, under the high salt conditions employed in this investigation, the electrostatic effects should have been minimized. The lowest hydrophobicity was observed for phenyl agarose ether (C50 = 1.67 at 4°C and 1.48 at 25°C) and could be explained by intrinsic hydrophobic interactions occurring in these long chains [43].

Table 1
Structures and C50 values associated with Phenyl-Sepharose, phenylaminoagarose and phenyl agarose ether

Material	Structure[a]	C50	
		4°C	25°C
Phenyl-Sepharose (Pharmacia)	Aga–O–CH_2–CHOH–CH_2–O–C_6H_5	0.54	0.34
Phenyl-aminoagarose (Sigma)	Aga–O–CH_2–CHOH–NH–C_6H_5	1.12	1
Phenyl agarose ether (Sigma)	Aga–O–$(CH_2)_3$–O–$(CH_2)_4$–O–CH_2–CHOH–CH_2–O–C_6H_5	1.67	1.48

[a] Structures are those given by the manufacturers.

Length of the alkyl or amino alkyl head chains

The effect of chain length was investigated by the use of two hydrophobic series, alkyl- and aminoalkylagarose kits, purchased from Sigma. Because of the lack of a corresponding unsubstituted matrix, Sepharose 4B was selected as a reference. The C50 values associated with each chromatographic support are reported in Fig. 2. Within each series, an increasing chain length resulted in higher hydrophobicity. Concerning alkylagarose, a linear relationship was observed up to ten carbon atoms (the C50 value decreased from 1.88 to 1). With longer chains, a lower temperature or the use of ethylene glycol was required to elute the adsorbed PPO activity. Moreover, in this series, the influence of temperature appeared only after six carbon atoms. Similar results were reported by Shalthiel [44], Iborra *et al.* [6], Flurkey and Jen [7] and Ingebrigtsen and Flurkey [8]. Flurkey and Jen [7] reported that peach PPO was slightly retained on hexyl and fully retained on octyl columns. Iborra *et al.* [6] and Ingebrigtsen and Flurkey [8] observed that larger amounts of Dopa oxidase or mushroom tyrosinase were adsorbed as the alkyl chain length increased. Concerning the aminoalkyl kit at 25°C, a small increase in hydrophobicity was observed from no to six carbon atoms and then a larger increase for gels from six to twelve carbons, whereas at 4°C the increase in hydrophobicity was only apparent between six and twelve carbons (Fig. 2B). Concerning peach PPO, a less hydrophobic protein than apple PPO, a slight retention was observed by Flurkey and Jen [7] only after eight carbon atoms. The negative effect of introducing a charged group was revealed again by the previous studies. Despite the numerous reports in the literature on hydrophobic chromatography, no real explanation for this effect has been proposed.

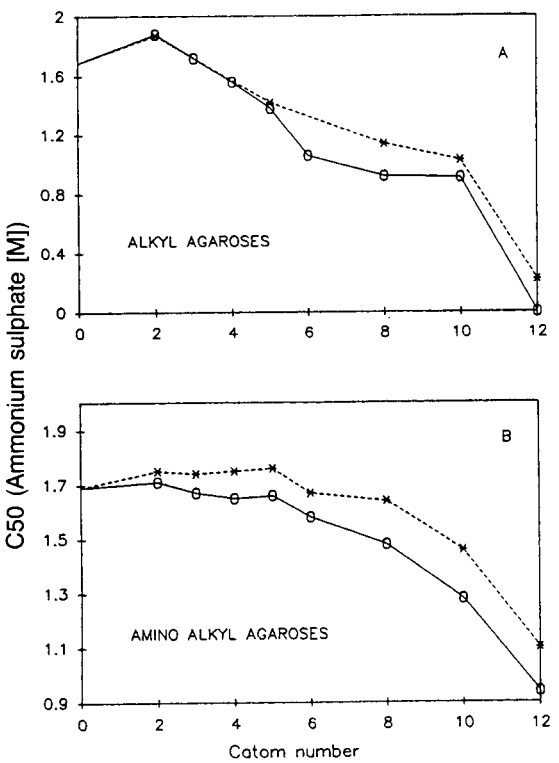

Fig. 2. Effect of head chain length on (A) alkyl- and (B) aminoalkylagarose hydrophobicity at 4°C (dashed lines) and 25°C (full lines).

pH of the elution buffer

The influence of elution pH was analysed between 4.5 and 8 for the alkyl- and aminoalkylagarose series. Concerning the alkylagarose kit, a typical result is illustrated in Fig. 3 with Phenyl-Sepharose CL4B. A negative effect of increasing pH on the gel hydrophobicity was observed. However, the modification of protein charge by changing the pH conditions has also to be taken in account. On the other hand, with aminoalkylagarose, no clear relationship was

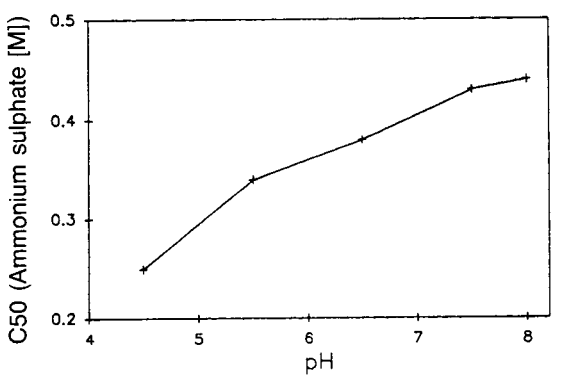

Fig. 3. Effect of pH on Phenyl-Sepharose hydrophobicity at 25°C.

obtained between pH and C50 values. Although Schmück *et al.* [45] observed maximum hydrophobic binding at a pH value equal to the isoelectric point of ovalbumin, the C50 value was not minimum for pH values close to 5, which corresponded to the isoelectric point region of apple PPO isoenzymes [23].

In conclusion to this study, for the correct application of hydrophobic chromatography to the purification of enzymatic proteins such as PPO, two main factors should be considered: first, the nature and hydrophobicity of both the adsorbent and the protein, and second, the elution conditions, including pH and temperature.

Moreover, it appears that for the purification of strong hydrophobic proteins such as apple PPO at normal temperature (25°C), Phenyl-Sepharose was the best support. Nevertheless, Octyl-Sepharose, used at 4°C, could also represent a convenient adsorbent. These conclusions were in agreement with earlier reports dealing with the suitability of Phenyl-Sepharose for grape [3], apple [23] and peach [38] PPO purification.

3.2. DEAE-Sepharose CL6B ion-exchange chromatography

A typical elution pattern of the "first purified extract" from a DEAE-Sepharose CL6B column is illustrated in Fig. 4. The eluted activity representing 90% of the loaded activity was recovered in three fractions, two major peaks labelled B and C (35 and 60%) and one minor peak labelled A (5%). These results suggested the presence of three isoenzymes characterized by different isoelectric points, lower than 6.5. The elution of inactive proteins, before and after the gradient step, reflected the further purification resulting from this procedure. The purification factor was about 3- and 7.5-fold for B and C, respectively (Table 2). These results, attesting to the purification efficiency of this chromatographic step, have been exploited in different PPO purification protocols [46–50]. Electrophoretic patterns of the "first purified extract" and of fractions A, B and C are shown in Fig. 5A

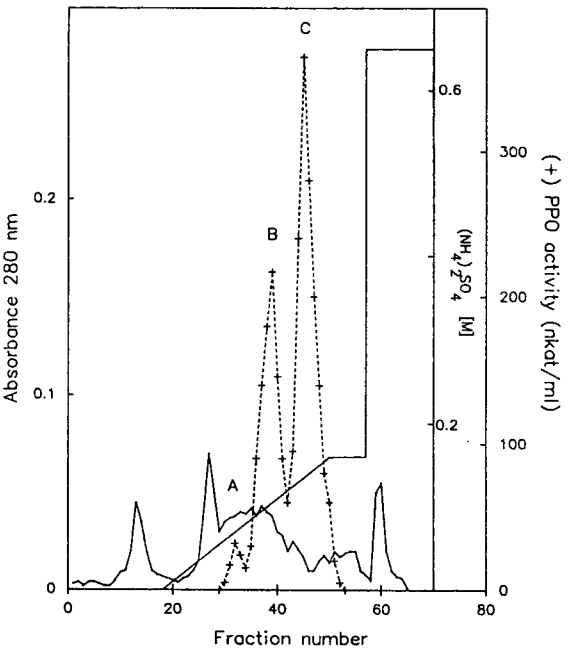

Fig. 4. Ion-exchange chromatography on DEAE-Sepharose CL6B of apple PPO.

(isoelectrofocusing pH 4–6.5) and B (normal electrophoresis). By isoelectrofocusing, the initial extract revealed two major bands in the pH 4.5–5 region and one minor, faint band whose isoelectric point was near neutral, in agreement with the results of Janovitz-Klapp *et al.* [23]. Fraction B contained one isoenzyme characterized by an isoelectric point of 5 and fraction C contained the other isoenzyme corresponding to an isoelectric point of 4.8. Concerning fraction A, the addition of SDS (0.55%) was required in order to reveal the presence of the band with an isoelectric point close to 6.5. SDS led to an increase in PPO activity, as has already been pointed out [51].

3.3. Immobilized copper affinity chromatography (IMAC)

A typical elution profile of an apple PPO "first purified extract" obtained with IMAC is shown in Fig. 6. When the column was eluted with the equilibration buffer, a small part (less than 5%) of unbound PPO activity was obtained. This

Table 2
Purification of apple PPO using DEAE-Sepharose CL6B ion-exchange chromatography, IMAC and affinity chromatography with competitive inhibitors as ligands

Method	Extract or fraction	Proteins (mg ml^{-1})	Activity (nkat ml^{-1})	Specific activity (μkat mg^{-1})	Purification factor (-fold)
	Crude extract	0.830	250	0.30	1
	First purified extract	0.058	285	4.91	16.4
DEAE-Sepharose CL6B ion-exchange chromatography	*Most actives fractions*:				
	A	0.006	30	5.33	17.8
	B	0.017	210	14.47	48
	C	0.009	360	36.4	120
IMAC	*Most actives fractions*				
	F1, 30 m*M* glycine	0.010	80	7.78	25.9
	F2, 125 m*M* glycine	0.020	425	20.1	67
	F3, 10 m*M* histidine	0.015	30	1.85	6.2
Affinity chromatography	*Most actives fractions*				
	p-COU-HMD	0.020	320	16	79
	p-HBZ-HMD	0.022	210	9.4	49

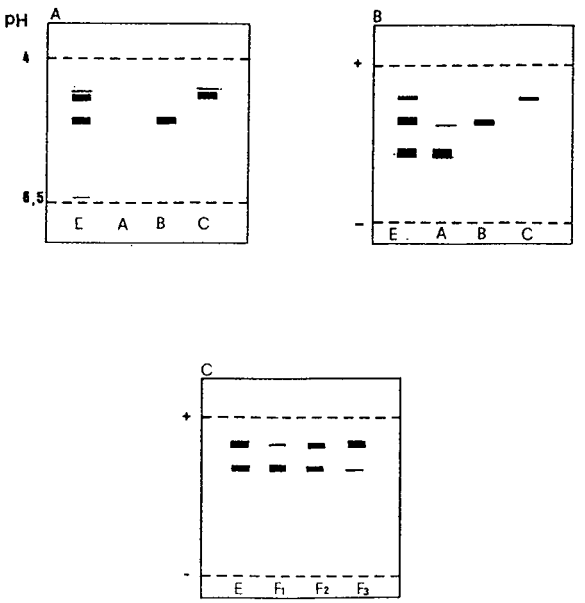

Fig. 5. Electrophoresis profiles of the "first purified extract" (E), fractions A, B and C separated by ion exchange and fractions F_1, F_2 and F_3 separated by IMAC. All gels were revealed by specific staining (PPO activity). (a) IEF (pH 4–6.5) applied to E, A, B and C; (b) electrophoresis (Phastgel 8–25, 0.55% SDS in the staining solution) applied to E, A, B and C; (c) electrophoresis (Phastgel 8–25) applied to E, F_1, F_2 and F_3.

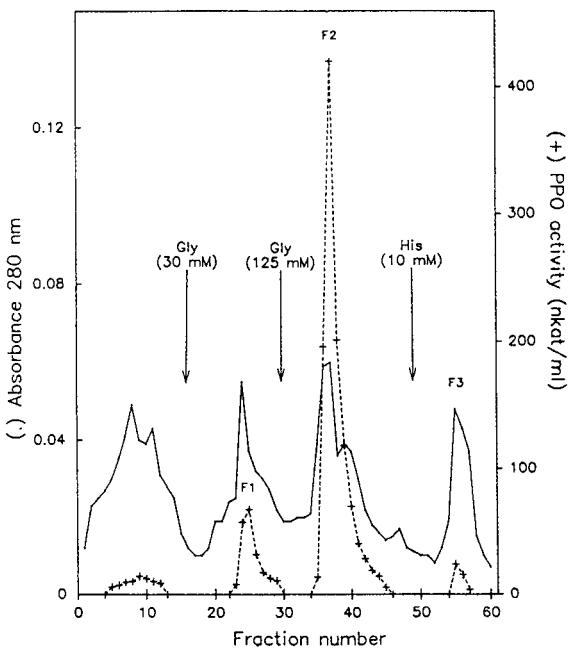

Fig. 6. IMAC of apple PPO on chelating Sepharose CL6B.

activity was not the result of overloading as the unbound percentage remained constant when the loaded activity was varied. Stepwise elution with glycine (30 and 125 m*M*) and then with 10 m*M*

histidine resulted in three additional fractions (F_1, F_2 and F_3). The bulk of the activity was recovered in fraction F_2, which contained 75% of the recovered activity, while fractions F_1 and F_3 represented 15 and 7%, respectively. Moreover, a high yield close to 100% compared with the loaded activity was obtained. Concerning the purification efficiency of this procedure (Table 2), the most active fraction (F_2) showed a purification rate of 67, F_1 was 1.6-fold purified compared with the initial extract while the purification factor of F_3 was decreased.

The difference in copper affinity among the three eluted fractions did not reflect differences in isoelectric points. Each electrophoretic pattern (Fig. 5C) revealed two bands (corresponding to the two isoenzymes characterized by isoelectric points of 4.8 and 5), the proportion of which varied with the fraction considered. According to this result, it appeared that the DEAE-Sepharose CL6B ion exchanger resolved the three isoenzymes more selectively than IMAC. The isoenzyme with an isoelectric point of 5 was predominant in F_1. An opposite result was observed for F_3. Thus, the former isoenzyme is also characterized by a weak copper affinity compared with that associated with an isoelectric point of 4.8. This difference in copper affinity presumably resulted from different numbers of copper chelating amino acid groups exposed on the surface of the enzyme molecule, in accordance with the work of Sulkowsky [52].

3.4. Affinity chromatography on p-COUM- and p-HBZ-HMD

p-Coumaric and *p*-hydroxybenzoic acid are known to be competitive inhibitors of PPO [33,53,55]. These acids were coupled to HMD-Ultrogel using the protocol described previously. The *p*-coumaric and *p*-hydroxybenzoic acid content of the synthetized affinity resins were determined spectrophotometrically to be close to 9 μmol ml^{-1} of packed gel. Considering the concentration of free NH_2 residues in the HMD-Ultrogel (between 7 and 10 μmol ml^{-1}) as stated by the manufacturer, these results corresponded to good binding yields.

Preliminary studies on activated but non-ligand-coupled matrices have shown that no adsorption due to non-specific or ion-exchange interactions occurred with apple PPO.

Column chromatography

Adsorption PPO on the derivatives was achieved at pH 4.5. At this pH, close to the p*K* value of the two carboxylic acids, the inhibition constants of *p*-coumaric and *p*-hydroxybenzoic acid were determined by Janovitz-Klapp *et al.* [33] to be 0.04 and 0.57 m*M*, respectively. According to these workers, the competitive inhibition of PPO was mainly due to the protonated form of carboxylic aromatic acids. This led us to elute enzyme activity at pH 7.5, at which *p*-coumaric and *p*-hydroxybenzoic acid were in the carboxylate form. Under these conditions, typical elution patterns obtained for apple PPO "first purified extract" on the two affinity supports are illustrated in Fig. 7. When the columns were eluted with equilibration buffer, a major

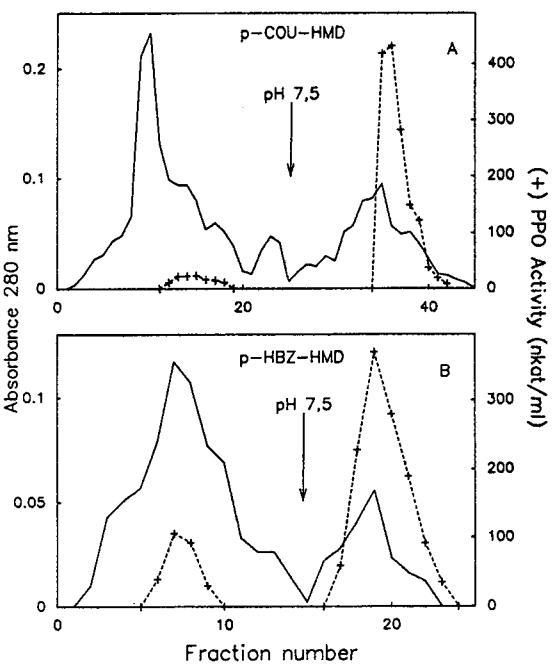

Fig. 7. Affinity chromatography of apple PPO on Ultrogel coupled with (a) *p*-coumaric acid or (b) *p*-hydroxybenzoic acid.

protein peak was eluted concomitantly with a small part of unbound PPO activity. This small percentage remained constant whatever the loaded activity was, equal to 5% and 25% with *p*-COU-HMD and *p*-HBZ-HMD, respectively. Such a difference was explained as a direct result of the value of the inhibition constants. Nevertheless, the bulk of the activity was eluted in a sharp peak when the elution buffer pH was increased to 7.5; excellent yields of recovered activity, close to 100% were obtained with the two types of resin. A fivefold purification was achieved with the chromatographic step on *p*-COU-HMD, while the purification factor was only *ca.* 3 with *p*-hydroxybenzoic acid as ligand (Table 2). This probably resulted from the higher percentage of unbound PPO activity with this affinity resin.

During the course of this study, we encountered two problems similar to those reported by O'Neill *et al.* [54] and Ingebrigtsen and Flurkey [8] concerning affinity chromatography, *i.e.*, the purified fraction was unstable after its elution and the synthetized affinity supports were found to deteriorate. The gel changed from brilliant red to brown after 2 months at 4°C. We demonstrated (data not shown) that the instability of the purified fraction can be partially ascribed to the pH variation (4.5–7.5) required for enzyme elution. Consequently in the following investigation, freshly synthesized supports were used and PPO activity was assayed immediately after its elution.

Evaluation of inhibition constants

We first applied the equilibrium model of adsorption described by Graves and Wu [31] to the two types of affinity matrices. With this model, these workers answered the simple question of how an enzyme is distributed between a solution phase (volume V) and a solid ligand-containing phase (volume v) for a fixed value of the equilibrium constant (K_i). They developed an equation that related the ratio of free to trapped enzyme with the inhibition constant of the ligand:

$$\alpha = E_0V/([L_0]v) + (K_i/L_0)[(V + v)/v] \quad (1)$$

where L_0 = concentration of bound ligand, E_0 = enzyme concentration in the solution phase and α = ratio between the two enzymatic fractions, free and trapped.

Following the protocol described under Experimental, the α values were plotted against each enzyme addition and a straight line was obtained (Fig. 8). Considering Eq. 1, K_i values of the bound carboxylic acids were estimated from the intercept with the ordinate. The values obtained (0.3 and 11 m*M* for *p*-coumaric and *p*-hydroxybenzoic acid, respectively) were higher than those obtained for the corresponding free acids by kinetic studies but close to those calculated for ferulic and vanillic acid (0.29 and 10 m*M*, respectively) [33]. This could be due to the *ortho* substitution (as regards the hydroxyl function of the aromatic ring) which occurred during the binding of the *p*-coumaric and *p*-hydroxybenzoic acid to the gel, leading to a similarity in the substitution patterns and therefore in the inhibition constants observed for the free ferulic and vanillic acid.

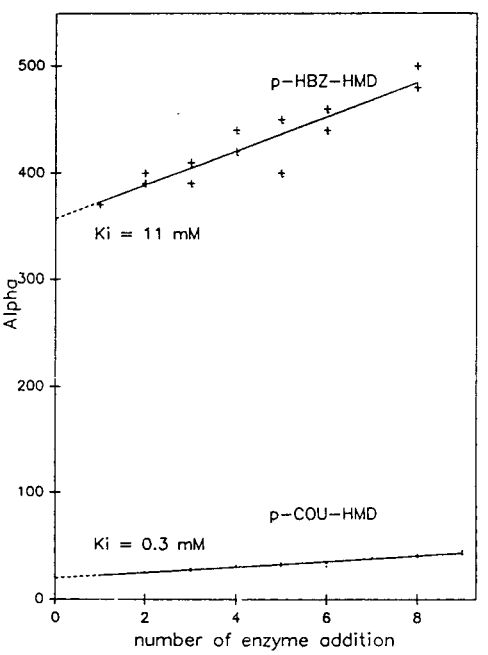

Fig. 8. Values of α *vs.* number of enzyme additions on *p*-COU-HMD and *p*-HBZ-HMD. Assay of activity was duplicated for each enzyme addition.

The second procedure aimed at determining the inhibition constant of bound *p*-coumaric acid was adapted from the work of Dunn and Chaiken [32], who considered, in their model, a variable bound ligand concentration. According to this model, the elution volume (v) of a given protein was directly linked to the bound ligand concentration ($[I_b]$):

$$v = V_0 + (V_0 - V_m)[I_b]/K_{i_b} \quad (2)$$

where V_0 = elution volume of an unretarded protein, V_m = dead volume and K_{i_b} = inhibition constant of the bound ligand.

In our experimental protocol (see Experimental), different bound ligand concentrations were obtained by varying the pH of elution buffer. Fig. 9 shows the elution profile obtained for each pH condition. An increase in PPO elution volume was observed with decreasing pH. Excellent yields higher than 80% were obtained for each chromatographic step when the pH was higher than 5.5. When elution volumes (maximum of the peak) were plotted against the corresponding bound ligand concentration, a straight line was observed. In accordance with Eq. 2, the K_i value was determined from the slope. The value obtained for *p*-coumaric acid was 0.6 m*M*, again close to that of vanillic acid. The difference observed between the two K_i values for *p*-coumaric acid obtained by the two previous protocols could result from an incorrect determination of the amount of protonated *p*-coumaric acid. For this determination, we assumed that the p*K* values of the free and bound *p*-coumaric acid were similar.

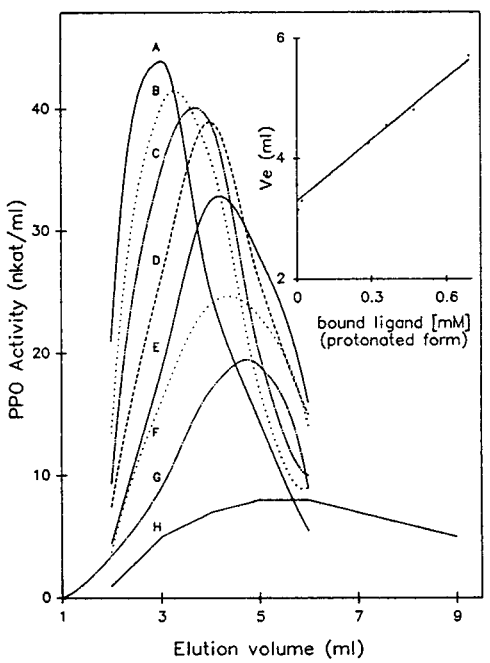

Fig. 9. Effect of buffer pH on elution volume of apple PPO on *p*-COU-HMD. Inset: elution volume *vs.* effective bound inhibitor concentration (protonated form). The pH values and inhibitor concentrations in the various experiments were as follows: experiment A, pH 7.67, 0.005 m*M*; B, pH 7.11, 0.02 m*M*; C, pH 6.61, 0.06 m*M*; D, pH 6.13, 0.18 m*M*; E, pH 5.93, 0.29 m*M*; F, pH 5.83, 0.36 m*M*; G, pH 5.71, 0.47 m*M*; and H, pH 5.53, 0.69 m*M*.

In conclusion, we have developed an easy method for the preparation of affinity gels. These gels can be used either for the purification of PPO (mainly *p*-COU-HMD) or for the determination of the inhibition constant of the ligand.

4. Conclusions

During the course of these studies, different chromatographic steps were applied to apple PPO purification and different isoforms were separated. To obtain the best result, we recommend combining the procedures in the order hydrophobic chromatography, IMAC and affinity chromatography. Applying this scheme, we obtained a fraction representing 25% of the crude extract and characterized by a 240-fold purification factor (283-fold for the most active fraction).

5. Acknowledgements

We greatly appreciate the skilful assistance of F. Gauillard and S. Gevaudan. Thanks are due to V. Mathieu (CTIFL) for supplying Red Delicious apples and to W. Oleszek for language assistance.

6. References

[1] J. Zawistowski, C.G. Biliaderis and N.A.M. Eskin, in D.S. Robinson and N.AM. Eskin (Editors), *Oxidative Enzymes in Foods*, Elsevier Applied Science, London, 1991, pp. 217–273.
[2] J.J. Jen and W.H. Flurkey, *J. Food Sci.*, 43 (1978) 1826.
[3] K.W. Wisseman and C.Y. Lee, *J. Chromatogr.*, 192 (1980) 232.
[4] K.W. Wisseman and M. Montgomery, *Plant Physiol.*, 78 (1985) 256.
[5] R.S. King and W.H. Flurkey, *J. Sci. Food Agric.*, 41 (1987) 231.
[6] J.L. Iborra, E. Cortes, A. Manjon, J. Ferragut and F. Llorca, *J. Solid-Phase Biochem.*, 1 (1976) 91.
[7] W.H. Flurkey and J.J. Jen, *J. Food. Sci.*, 45 (1980) 1622.
[8] J. Ingebrigtsen and W.H. Flurkey, *Phytochemistry*, 27 (1988) 1593.
[9] L.S. Lerman, *Proc. Natl. Acad. Sci. U.S.A.*, 39 (1953) 232.
[10] B.K. Simpson, M.R. Marshall and W.S. Otwell, *Agric. Food Chem.*, 35 (1987) 918.
[11] S. Guterridge and D.A. Robb, *Biochem. Soc. Trans.*, 1 (1973) 519.
[12] L.A. Menon and H.F. Haberman, *Acta Dermatol.*, 55 (1975) 343.
[13] A. Golan-Goldhirsh, V. Kahn and J.R. Whitaker, *Isr. J. Bot.*, 35 (1986) 203.
[14] J. Porath, J. Carlsson, I. Olsson and G. Belfrage, *Nature*, 959 (1975) 550.
[15] J. Zawistowski, R.J. Weselake, G. Blank and E.D. Murray, *Phytochemistry*, 26 (1987) 2905.
[16] I. Söderhäll and K. Söderhäll, *Phytochemistry*, 28 (1989) 1805.
[17] A. Gärtner, H.J. Hartmann and U. Weser, *Biochem. J.*, 221 (1984) 549.
[18] R.J. Weselake, S.L. Chesney, A. Petkau and A.D. Friesen, *Anal. Biochem.*, 155 (1986) 193.
[19] G.L. Hortin and B.L. Gibson, *Prep. Biochem.*, 19 (1989) 49.
[20] E. Harel, A.M. Mayer and Y. Shain, *Phytochemistry*, 4 (1965) 783.
[21] J.R.L. Walker and A.G. Hulme, *Phytochemistry*, 5 (1966) 259.
[22] D.A. Stelzig, S. Akthar and S. Ribiero, *Phytochemistry*, 11 (1972) 535.
[23] A. Janovitz-Klapp, F. Richard and J. Nicolas, *Phytochemistry*, 28 (1989) 2903.
[24] P.W. Goodenough, S. Kessel, A.G.H. Lea and T. Loeffler, *Phytochemistry*, 22 (1983) 359.
[25] M. Murata, C. Kurokami and S. Homma, *Biosci. Biotechnol. Biochem.*, 56 (1992) 1705.
[26] C. Satjawatcharaphong, K.S. Rymal, Jr., W.A. Dozier and R.G. Smith, *J. Food Sci.*, 48 (1983) 1879.
[27] M. Bradford, *Anal. Biochem.*, 72 (1976) 248.
[28] P. Cuatrecasas, *J. Biol. Chem.*, 245 (1970) 3059.
[29] P. Cuatrecasas and C.B. Anfinsen, *Methods Enzymol.*, 21 (1971) 345.
[30] L. Cohen, *Methods Enzymol.*, 34 (1974) 102.
[31] J.D. Graves and Y.T. Wu, *Methods Enzymol.*, 34 (1974) 140.
[32] B.M. Dunn and I.M. Chaiken, *Biochemistry*, 14 (1975) 2343.
[33] A. Janovitz-Klapp, F. Richard, P. Goupy and J. Nicolas, *J. Agric. Food Chem.*, 38 (1990) 926.
[34] M. Miyata-Asano, K. Ito, H. Ikeda, S. Sekiguchi, K. Arai and N. Taniguchi, *J. Chromatogr.*, 370 (1986) 501.
[35] J.L. Ochoa, *Biochemistry*, 60 (1978) 1.
[36] W.J. Gelsema, P.M. Brandts, C.L. de Ligny and A.G.M. Roozen, *J. Chromatogr.*, 295 (1984) 13.
[37] K.A. Caldwell, *J. Sci. Food Agric.*, 30 (1979) 185.
[38] J.J. Jen and W.H. Flurkey, *Hortscience*, 14 (1979) 516.
[39] P. Wesche-Ebeling and M.W. Montgomery, *J. Food Sci.*, 5 (1990) 1315.
[40] J.J. Jen, A. Seo and W.H. Flurkey, *J. Food Sci.*, 45 (1980) 60.
[41] F. Richard and J. Nicolas, *Sci. Aliment.*, 9 (1989) 335.
[42] W.H. Flurkey, L.W. Young and J.J. Jen, *J. Agric. Food Chem.*, 26 (1978) 1474.
[43] P. Shanbhag and G.C. Axelsson, *Eur. J. Biochem.*, 60 (1975) 17.
[44] S. Shalthiel, *Methods Enzymol.*, 34 (1974) 126.
[45] M.N. Schmück, M.P. Nowlan and K.M. Gooding, *J. Chromatogr.*, 371 (1986) 55.
[46] M.H. Roudsari, A. Signoret and J. Crouzet, *Food Chem.*, 7 (1981) 227.
[47] Y.L. Lam and K.K. Ho, *Plant Physiol. Biochem.*, 28 (1988) 209.
[48] Y. Oda, H. Kato, Y. Isoda, N. Takahashi, T. Yamamoto, Y. Takada and S. Kudo, *Agric. Biol. Chem.*, 53 (1989) 2053.
[49] E.J. Lourenco, J.D.S. Leao and V.A. Neves, *J. Food Sci. Agric.*, 52 (1990) 249.
[50] W. Takeuchi, H. Takahashi and M. Kojima, *Biosci. Biotechnol. Biochem.*, 56 (1992) 1134.
[51] E.L. Angleton and W.H. Flurkey, *Phytochemistry*, 23 (1984) 2723.
[52] E. Sulkowski, *Trends Biotechnol.*, 3 (1985) 1.
[53] Y.Z. Gunata, J.C. Sapis and M. Moutounet, *Phytochemistry*, 26 (1987) 1573.
[54] S.P. O'Neill, D.J. Graves and J.J. Fergusson, *J. Macromol. Sci.*, A7 (1973) 1159.
[55] J. Nicolas, F. Richard-Forget, P. Goupy, M.J. Amiot and S. Aubert, *Crit. Rev. Food Sci. Nutri.*, 34 (1994) 109.

ELSEVIER

Journal of Chromatography A, 667 (1994) 155–166

JOURNAL OF CHROMATOGRAPHY A

Determination of N-methylcarbamate pesticides in environmental water samples using automated on-line trace enrichment with exchangeable cartridges and high-performance liquid chromatography

M. Hiemstra, A. de Kok*

Food Inspection Service, Department of Pesticide Analysis, Burgpoelwaard 6, 1824 DW Alkmaar, Netherlands

(First received November 17th, 1993; revised manuscript received January 6th, 1994)

Abstract

A fully automated high-performance liquid chromatographic (HPLC) method was developed for the determination of N-methylcarbamate pesticides and their polar metabolites in various types of water. Two different, commercially available, automated trace enrichment devices (OSP-2 and Prospekt) were investigated as to their performance. Low-carbon C_{18}-bonded silica (C_{18}/OH, 40 μm particle size) was used, as a selective sorbent for solid-phase extraction and preconcentration of N-methylcarbamate pesticides from environmental water samples. PLRP-S (15–25 μm), a styrene–divinylbenzene polymeric phase, was also evaluated as an alternative to extract N-methylcarbamates.

After preconcentrating the N-methylcarbamates on an exchangeable cartridge, the analytes were eluted with the mobile phase gradient and transferred to the reversed-phase HPLC system. Detection was performed via post-column hydrolysis on a solid-phase catalyst (anion exchanger), derivatization of the methylamine formed with *o*-phthalaldehyde reagent, and fluorescence detection of the isoindole derivative.

Both trace enrichment systems showed good quantitative results for the determination of N-methylcarbamates and their metabolites at the 0.1 μg/l level. The repeatability was excellent with relative standard deviations in the range 2–10%. The method detection limits for surface water were between 30 and 50 ng/l. Sample throughput is about 30 samples per 24 h, unattended. The method proved to be suitable for monitoring N-methylcarbamate pesticides in environmental water samples.

1. Introduction

The ubiquitous presence of pesticides and organic pollutants in environmental water samples has arisen from extensive agricultural application and industrial emission in surface waterways. Therefore, monitoring the trace levels of pesticides and organic pollutants is crucial for human health protection and environmental control. The EEC has set a maximum admissible concentration of 0.1 μg/l for individual pesticides and their related compounds in drinking water [1]. As a consequence, regulatory agencies and drinking water laboratories have shown increased interest in monitoring pesticides in environmental water samples. Multiresidue methods have been established for screening these compounds in drinking, surface and waste

* Corresponding author.

0021-9673/94/$07.00
SSDI 0021-9673(94)00028-8

water, using both gas chromatography (GC) and liquid chromatography (LC).

The popularity of LC has grown rapidly in recent years owing to its suitability for the determination of relatively polar pesticides and it is widely accepted as a rapid and efficient technique. Screening of polar pesticides in water samples is mainly performed by employing HPLC in combination with diode array detection or UV detection [2–5]. In water analysis, emphasis is generally laid on the determination of herbicides (triazines, phenoxycarboxylic acids, phenylureas). This is reflected in the development of various methods for these typical pesticide/matrix combinations. Only a small proportion of analytical work on monitoring residues in water samples concerns the N-methylcarbamate pesticides. McGarvey [6] reviewed the literature concerning all aspects of determination of N-methylcarbamate residues in water, plants, and air by HPLC, including extraction, clean-up, chromatographic separation and detection.

To enhance sensitivity in water analysis, a preconcentration step, prior to LC analysis, is required. Compared with laborious and solvent-consuming liquid–liquid extraction methods, solid-phase extraction has gained in popularity. The most popular sorbents for isolating pesticides from water samples are octadecyl-bonded silica (C_{18}) [4], styrene–divinylbenzene copolymers (PLRP-S, PRP-1) [2,3,5,7] and graphitized carbon [8].

Preconcentration of the N-methylcarbamates from water samples [6] is mainly performed using conventional liquid–liquid extraction or solid-phase extraction. Very recently [9], we developed a multiresidue HPLC method for the determination of 20 N-methylcarbamate pesticides and 12 of their polar metabolites in surface water via solid-phase extraction at low ng/l levels. A new low-carbon C_{18}-bonded silica (C_{18}/OH), specially designed for polar metabolites of pharmaceuticals, was studied. Although off-line solid-phase extraction appeared to be satisfactory, some drawbacks still remain: possible losses of the analyte in the evaporation/redissolution step, loss of sensitivity due to dilution of the eluate and cost effectiveness.

More recently, both direct large-volume aqueous injections [10] and on-line trace enrichment [11–15] of N-methylcarbamates have been demonstrated by several research groups. She *et al.* [11] reported a LC method for the determination of carbaryl by using on-line preconcentration. Another LC method, reported by Chaput [12], determined aldicarb and its metabolites in water, using on-line trace enrichment. Marvin and coworkers applied their on-line preconcentration method to propoxur, carbofuran, carbaryl [13,14] and to aldicarb and its metabolites [15]. In spite of the improvements, several shortcomings still exist. Due to differences in polarity of the N-methylcarbamates and their metabolites, recovery and sensitivity were not always satisfactory for each single compound. The most studied water types were ground, well, pond and drinking waters. Surface water samples have infrequently been investigated. Most studies were done for only a limited number of N-methylcarbamates.

Chiron *et al.* [16] reported a promising trace enrichment method based on the on-line coupling of C_{18}-bonded silica Empore membrane extraction disks (4.6 mm I.D.; particle size 8 μm), stacked in a fixed membrane-disk holder and LC in combination with post-column reaction detection. Samples of 10 ml of surface water could be concentrated for the determination of 15 selected N-methylcarbamates in river water. The determination limits that could be obtained for the carbamates were 0.01 μg/l. The method was less suitable for routine monitoring water samples, because the membrane extraction disks had to be manually replaced after two runs.

With the introduction of commercially available systems for automated on-line trace enrichment (OSP-2 from Merck, Darmstadt, Germany and Prospekt from Spark Holland, Emmen, Netherlands), shortcomings of off-line solid-phase extraction can be avoided and sample volumes can be further reduced. On-line trace enrichment techniques use a precolumn containing an appropriate sorbent, which selectively retains the compounds of interest. A water sample is enriched on an exchangeable cartridge

and subsequently the preconcentrated analytes are desorbed and transferred to the analytical column using the mobile phase gradient.

The aim of this study was to automate the solid-phase extraction of N-methylcarbamate pesticides from water samples to make the method more suitable for monitoring purposes. Special attention has been paid to include the important polar sulphoxide and sulphone metabolites of butocarboxim, aldicarb, ethiofencarb, thiofanox and methiocarb. This paper describes the conversion of the off-line method into an automated on-line trace enrichment method by means of commercially available apparatus (OSP-2 and Prospekt).

2. Experimental

2.1. Chemicals

HPLC-grade acetonitrile and methanol were purchased from Rathburn (Walkerburn, UK) and water was purified using an ElgaStat UHQ water-purification system (Elga, High Wycombe, UK). Glacial acetic acid, sodium acetate, sodium thiosulphate, *o*-phthalaldehyde (OPA), 2-mercaptoethanol and disodium tetraborate were obtained from Merck.

OPA reagent was prepared by dissolving 1.0 g of disodium tetraborate in approximately 200 ml of purified water in a 250-ml volumetric flask. A solution of 50 mg of OPA in *ca.* 2 ml of acetonitrile and 0.1 ml of 2-mercaptoethanol were added. The solution was diluted to 250 ml with water.

All carbamate pesticide and metabolite standards were supplied by Promochem (Wesel, Germany), the Environmental Protection Agency Repository (Research Triangle Park, NC, USA) or the pesticide manufacturers.

2.2. Apparatus

Trace enrichment was executed by means of an OSP-2 on-line sample preparator from Merck, combined with a L-6200 intelligent pump and an AS-4000 autosampler, installed with a 5-ml loop or a Prospekt on-line sample preparation system from Spark Holland, consisting of the Prospekt apparatus, a solvent delivery unit (SDU) and a Marathon autosampler, equipped with a peristaltic pump and a 3-ml loop.

The HPLC analyses were performed with a Hewlett-Packard (Waldbronn, Germany) HP 1050 pumping system, equipped with a Rheodyne (Berkeley, CA, USA) Model 7125 six-port injection valve and 100-μl injection loop, an analytical column oven (35°C), a Kratos (Ramsey, NJ, USA) PCRS 520 post-column reaction system, equipped with a low-dead-volume T-piece, a Hewlett-Packard HP 1050 isocratic pump for OPA reagent delivery and a Hewlett-Packard HP 1046A double monochromator fluorescence detector. Data acquisition and processing were performed on a HP Vectra 486 computer using Hewlett-Packard ChemStation software.

Analytical separations were performed on a Merck LiChroCART 250 × 4.0 mm I.D. cartridge column packed with Supersphere RP-8 (4 μm) from Merck. A Merck LiChroCART 10 × 4.0 mm I.D. guard column packed with Supersphere RP-8 (4 μm) was installed in front of the analytical column.

The post-column reactor consisted of a 50 × 4.0 mm I.D. stainless-steel column packed with Aminex A-27 (15 μm) from Bio-Rad Labs. (Richmond, CA, USA) and was kept at a reaction temperature of 120–140°C. After the catalytic hydrolysis reactor, OPA reagent was added to the eluent at a flow-rate of 0.1 ml/min via a low-dead-volume T-piece. The reaction of methylamine with OPA reagent, to form the isoindole derivative, took place in a 20 cm × 0.12 mm I.D. PTFE connection capillary to the fluorescence detector. The excitation and emission wavelengths were set at 340 and 445 nm, respectively.

2.3. Procedures

Stock solutions (1.0 mg/ml) were prepared by weighing *ca.* 10–15 mg of the standard pesticide and dissolving this amount in an equivalent volume (in ml) of dichloromethane. The stock

solutions were stored at −18°C in a freezer. A standard mixture (1 μg/ml) was prepared by allowing 100 μl stock solution of each carbamate to evaporate in the air, followed by dissolution in 100 ml of acetonitrile. The standard mixture was stored in the dark, in a refrigerator at 4°C. Preparation of the internal standard solution (trimethacarb) was performed in the same way as the preparation of the standard mixture. Every day a fresh working standard solution (5 ng/ml) for direct standard injections was prepared by diluting 50 μl standard mixture to a volume of 10 ml. For fortification studies, a volume of 100 μl of standard mixture and 100 μl of internal standard solution were diluted with 1 l of blank surface or drinking water. All the aqueous standard solutions and water samples contained 0.1% glacial acetic acid to prevent hydrolysis of the carbamates. When analyzing hypochlorite-containing drinking water, hypochlorite was reduced by adding 0.5 g/l of sodium thiosulphate to avoid oxidation of the carbamates.

Chromatographic runs were performed using a ternary gradient profile. The mobile phase solvents were (A) acetonitrile–water (20:80), (B) methanol–water (20:80) and (C) acetonitrile–water (60:40). To prevent tailing of the methylamine formed during hydrolysis in the catalytic reactor, 2.5 m*M* of sodium acetate was added to each of the mobile phase solvents. Prior to use, all mobile phase solvents were filtered through a 0.45-μm filter applying a vacuum. The following linear gradient program, at a flow-rate of 0.75 ml/min, was run: 75% A and 25% B was kept for 5 min, then linearly to 100% C in 20 min and held for 5 min. Before the next injection, the initial mobile phase composition was held for 15 min.

Three types of precolumns were evaluated in this study: (1) precolumns (10 × 4.0 mm I.D.) for the OSP-2, manually dry-packed in our laboratory with 40-μm C_{18}/OH Bondesil (Varian/Analytichem, Harbour City, CA, USA), containing 55 mg of packing material; (2) precolumns (10 × 3.0 mm I.D.) for the Prospekt, dry-packed with 40-μm C_{18}/OH Bondesil by Spark Holland, containing 30 mg of packing material; (3) commercially available precolumns (10 × 3.0 mm I.D.) for the Prospekt, slurry-packed with 15–25 μm PLRP-S (Polymer Labs.) by Spark Holland.

All precolumns, packed with C_{18}/OH, were desorbed applying a forward-flush. Precolumns for the Prospekt, packed with PLRP-S, were desorbed applying a back-flush.

All cartridges were activated with 1 ml methanol followed by 1 ml of purified water at a flow-rate of 1 ml/min using either the L-6200 pump or the SDU. During the activation of the precolumn, the injection loop of the autosampler was loaded with the water sample. With the injection valve of the autosampler (Marathon or AS-4000) in the inject position, an appropriate volume (3–5 ml) of water sample was passed through the precolumn at a flow-rate of 1 ml/min. An additional volume of 0.5 ml of distilled water was allowed to pass through the precolumn in order to remove some matrix interferences. The whole trace enrichment procedure was executed within the equilibration time of the analytical column. The preconcentrated carbamates were then desorbed by switching the solid-phase extraction cartridge on-line with the HPLC system and starting the mobile phase gradient profile. Subsequently, all connection capillaries of the trace enrichment system were flushed with methanol. For further technical details of the valve switching schemes of both the OSP-2 and Prospekt, see Fig. 1.

3. Results and discussion

3.1. Chromatography and automation

In Table 1, the retention times of twenty N-methylcarbamates and twelve metabolites in the reversed-phase HPLC system Supersphere RP-8 (4 μm) with an acetonitrile–methanol–water gradient are presented. A detailed discussion of the optimized reversed-phase HPLC separation, using the linear gradient and the post-column derivatization system, using the catalytic solid-phase column, is given in ref. 9.

A review of the literature [6] shows, that UV

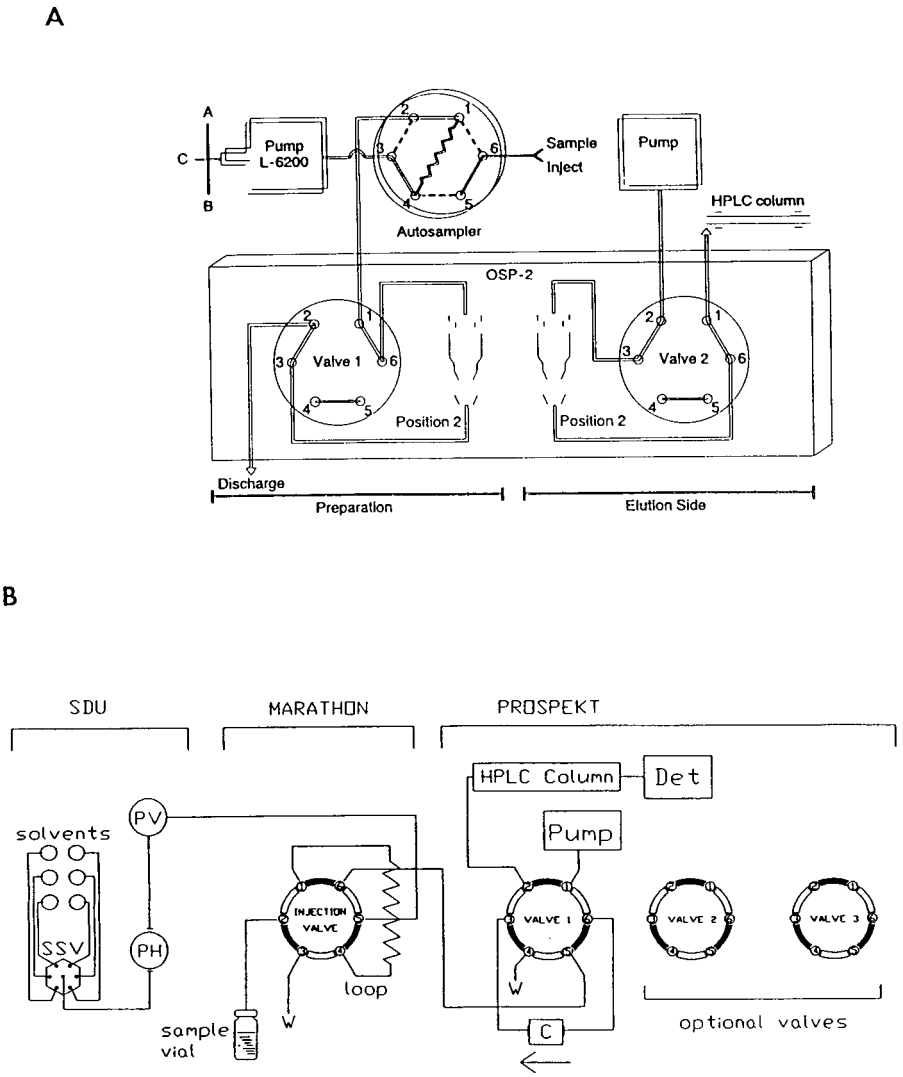

Fig. 1. Details of the valve switching systems of both the (A) OSP-2 system and (B) Prospekt system. SSV = Solenoid valve; PH = purge pump; PV = pulse damper; C = cartridge; DET = detection system; W = waste.

absorbance is the most commonly applied detection method for the determination of N-methylcarbamates in water. However, matrix interferences limit its usefulness due to lack of selectivity. Besides, sensitivity has not always been sufficient. In order to overcome these limitations, we have employed selective post-column derivatization of the N-methylcarbamates followed by sensitive fluorescence detection. A uniform response for all carbamates and metabolites is an additional advantage. Although this technique is very sensitive and selective, trace enrichment is still required, in order to meet with EEC limit concentrations. Preconcentration procedures prior to HPLC are usually performed manually applying liquid–liquid extractions or solid-phase extractions. The present availability of automated on-line trace enrich-

Table 1
Retention times of twenty N-methylcarbamate pesticides and twelve metabolites in the reversed-phase HPLC system Supersphere RP-8 with an acetonitrile–ethanol–water gradient

Carbamate/metabolite	Retention time (min)
Butocarboxim sulphoxide	5.53
Aldicarb sulphoxide	5.95
Butocarboxim sulphone	8.11
Aldicarb sulphone	8.80
Oxamyl	9.44
Methomyl	11.70
Ethiofencarb sulphoxide	12.97
Thiofanox sulphoxide	13.35
Ethiofencarb sulphone	14.99
3-Hydroxycarbofuran	15.00
Methiocarb sulphoxide	15.11
Tranid	15.15
Dioxacarb	16.45
Thiofanox sulphone	16.65
Methiocarb sulphone	18.76
Butocarboxim	19.30
3-Ketocarbofuran	20.05
Aldicarb	20.21
Cloethocarb	22.95
Propoxur	23.09
Carbofuran	23.36
Bendiocarb	23.36
Carbaryl	24.53
Thiofanox	25.00
Ethiofencarb	25.06
Isoprocarb	26.09
Trimethacarb	26.12
Carbanolate	26.75
Methiocarb	28.48
Fenobucarb	28.69
Promecarb	29.60
Bufencarb	33.52

ment systems (OSP-2, Prospekt) on the market makes the method more suitable for monitoring purposes. Both systems can perform trace enrichment of compounds from water utilizing exchangeable cartridges, unattended. Before the injection of a water sample the systems automatically insert a new solid-phase extraction cartridge, select solvents and then start the sample introduction and preparation. The systems complete the sample preparation within the analysis time of the previous sample, saving time normally used for sample preparation.

3.2. Stability studies

It has been reported [17] that carbamate and carbamoyl oxime pesticides can be degraded by acid- and base-catalyzed hydrolysis in water. Chlorinated water shortened the half-lives of all the carbamates. The effect of chlorination on half life was greater at pH 8 than pH 7. In our laboratory, carbamate stability studies were performed on untreated surface water and drinking water. Within one week, losses for all N-methylcarbamates and metabolites were observed. Especially in chlorinated water samples, the degradation of butocarboxim, aldicarb, ethiofencarb, thiofanox and methiocarb and their corresponding metabolites begins within hours. These results indicate that water contaminated with carbamates/metabolites and treated by chlorination will contain lower concentrations of these pesticides. Therefore, the analysis of N-methylcarbamates in surface water and chlorinated drinking water, requires an addition of acid/preservative directly at the sampling site, in order to prevent hydrolysis/oxidation of the carbamates. Addition of 0.1% glacial acetic acid and 0.5 g/l sodium thiosulphate to the water samples did not affect the performance of the system.

3.3. Solid-phase materials

In our previous study [9], an off-line solid-phase extraction procedure was developed, based on preconcentration of the N-methylcarbamates on C_{18}/OH cartridges. Most research groups use C_{18}-bonded silica cartridges to enrich the compounds of interest. Chaput [12] and Lesage [18] have demonstrated that C_8 material is preferred over C_{18} material for preconcentrating polar carbamates from water samples, due to its good solute retention capacity. We have shown that C_{18}/OH material has even a much better selectivity for the most polar carbamates and metabolites. This can possibly be ascribed to the number and/or accessibility of the free silanol groups on the surface of the sorbent. In on-line trace enrichment, precolumns packed with 3–10 μm particles are often used. Blockage

of the these precolumns can often occur owing to restrictions imposed by the high column back pressure at high sampling flow-rates or prolonged time of sampling. With the use of larger particles (40 μm) blockage of the precolumns is less likely to occur.

Apart from C_{18}/OH, PLRP-S, a styrene–divinylbenzene copolymer, was also studied, because PLRP-S is widely employed for the on-line trace enrichment of pesticides from water [2,7].

3.4. Recovery studies

For recovery studies, we selected those carbamates/metabolites which were most likely to occur in surface water samples and drinking water samples, because they are produced in significant quantities at industrial sites and applied intensively in agriculture.

Using 10 × 4.0 mm I.D. C_{18}/OH precolumns for the OSP-2, breakthrough volumes of a surface water sample spiked with N-methylcarbamates at 0.1 μg/l were assessed. It appeared that a sample volume of 6 ml could be preconcentrated before breakthrough of the polar carbamates or metabolites occurred. This was consistent with breakthrough volumes obtained with our off-line method. For recovery studies, a 5-ml water sample fortified with 18 selected N-methylcarbamates at the 0.1 μg/l level, was passed through the precolumns. The recoveries of the N-methylcarbamates from drinking and surface water samples were measured by comparing the peak heights of a 100-μl loop injection with the peak heights after enrichment and desorption from the precolumns. The results obtained are given in Table 2. The recoveries for the C_{18}/OH precolumn, using the OSP-2 apparatus, were in the range of 82.3–111.0% (R.S.D. 2.6–9.4%) and 79.9–102.9 (R.S.D. 2.0–8.1%) for drinking water and surface water,

Table 2
Average percent recoveries and relative standard deviations (%, in parentheses; $n = 7$) of N-methylcarbamates and metabolites from drinking and surface water, fortified at 0.1 μg/l level, after on-line trace enrichment

Carbamate/metabolite	Prospekt On-line trace enrichment of 3 ml of drinking water			OSP-2 On-line trace enrichment of 5 ml of	
	PLRP-S 10 × 2.0 mm	PLRP-S 10 × 3.0 mm	C_{18}/OH 10 × 3.0 mm	Drinking water C_{18}/OH 10 × 4.0 mm	Surface water C_{18}/OH 10 × 4.0 mm
Butocarboxim sulphoxide	73.4 (8.6)	96.1 (7.5)	95.0 (7.1)	97.9 (8.6)	98.0 (6.3)
Aldicarb sulphoxide	75.7 (8.8)	95.5 (7.7)	96.4 (7.5)	97.3 (8.6)	99.3 (6.0)
Butocarboxim sulphone	93.2 (8.2)	91.3 (9.2)	90.9 (7.3)	82.3 (8.2)	79.9 (5.7)
Aldicarb sulphone	92.3 (7.3)	93.2 (5.4)	87.3 (6.4)	92.3 (7.3)	84.1 (5.6)
Oxamyl	101.0 (7.5)	91.5 (8.0)	97.0 (7.5)	111.0 (7.5)	97.4 (6.8)
Methomyl	91.9 (6.9)	99.8 (6.1)	91.6 (5.4)	96.3 (6.9)	85.6 (4.5)
Ethiofencarb sulphoxide	94.9 (7.9)	94.7 (5.9)	102.0 (6.7)	98.9 (7.9)	99.9 (3.7)
Thiofanox sulphoxide	n.d.	n.d.	n.d.	89.6 (7.5)	97.6 (7.6)
Methiocarb sulphoxide	91.7 (3.6)	108.4 (4.3)	102.0 (5.7)	101.9 (3.6)	99.1 (3.3)
Thiofanox sulphone	n.d.	n.d.	n.d.	103.7 (3.6)	97.1 (3.2)
Methiocarb sulphone	98.5 (4.7)	104.5 (5.9)	97.3 (6.3)	107.3 (3.7)	96.4 (4.9)
Butocarboxim	96.9 (6.4)	96.4 (5.8)	80.1 (9.6)	110.1 (9.4)	101.6 (8.1)
Aldicarb	99.4 (5.1)	97.4 (5.2)	98.3 (4.8)	101.7 (5.1)	95.6 (2.0)
Propoxur	96.4 (2.6)	101.5 (4.0)	103.1 (4.2)	97.1 (2.6)	100.6 (4.0)
Carbofuran	98.6 (3.1)	104.2 (5.3)	101.9 (5.0)	98.9 (3.1)	98.9 (5.3)
Carbaryl	97.3 (2.9)	96.6 (4.2)	102.1 (3.6)	98.6 (2.9)	98.6 (5.2)
Ethiofencarb	54.0 (9.4)	60.0 (7.9)	100.1 (2.5)	99.7 (3.4)	102.9 (2.8)
Methiocarb	86.9 (5.0)	82.9 (4.8)	89.1 (3.8)	89.3 (5.0)	92.4 (5.1)

n.d. = Not determined.

respectively. Fig. 2 shows a typical chromatogram of a surface water sample fortified with the standard mixture of 18 N-methylcarbamates at 0.1 μg/l after extracting 5 ml of sample, using the OSP-2 apparatus. In spite of the use of a precolumn packed with 40 μm particles, no extra band broadening was observed for the early-eluting polar carbamates. During desorption of the carbamates, the polar carbamates were reconcentrated at the head of the analytical column and began to elute only when the proportion of organic solvent in the gradient mobile phase increased, thereby preventing any loss of separation efficiency.

From the breakthrough volumes assessed for our off-line procedure and for the 10 × 4.0 mm I.D. precolumns used with the OSP-2, we could derive that it should be possible to preconcentrate a sample volume of 3 to 4 ml on a 10 × 3.0 mm I.D. precolumn, packed with C_{18}/OH, using the Prospekt. The retention capacity of PLRP-S was compared with C_{18}/OH, both packed in 10 × 3.0 mm I.D. precolumns. For recovery studies, a 3-ml drinking water sample, fortified with the standard mixture of 16 N-methylcarbamates at a level of 0.1 μg/l, was loaded on both precolumns. The results obtained are given in Table 2. Recoveries for the C_{18}/OH and PLRP-S precolumns, using the Prospekt apparatus, ranged from 80.1–103.1% (R.S.D. 2.5–9.6%) and 60.0–108.4% (R.S.D. 4.0–9.2%), respectively. Surprisingly, ethiofencarb was not com-

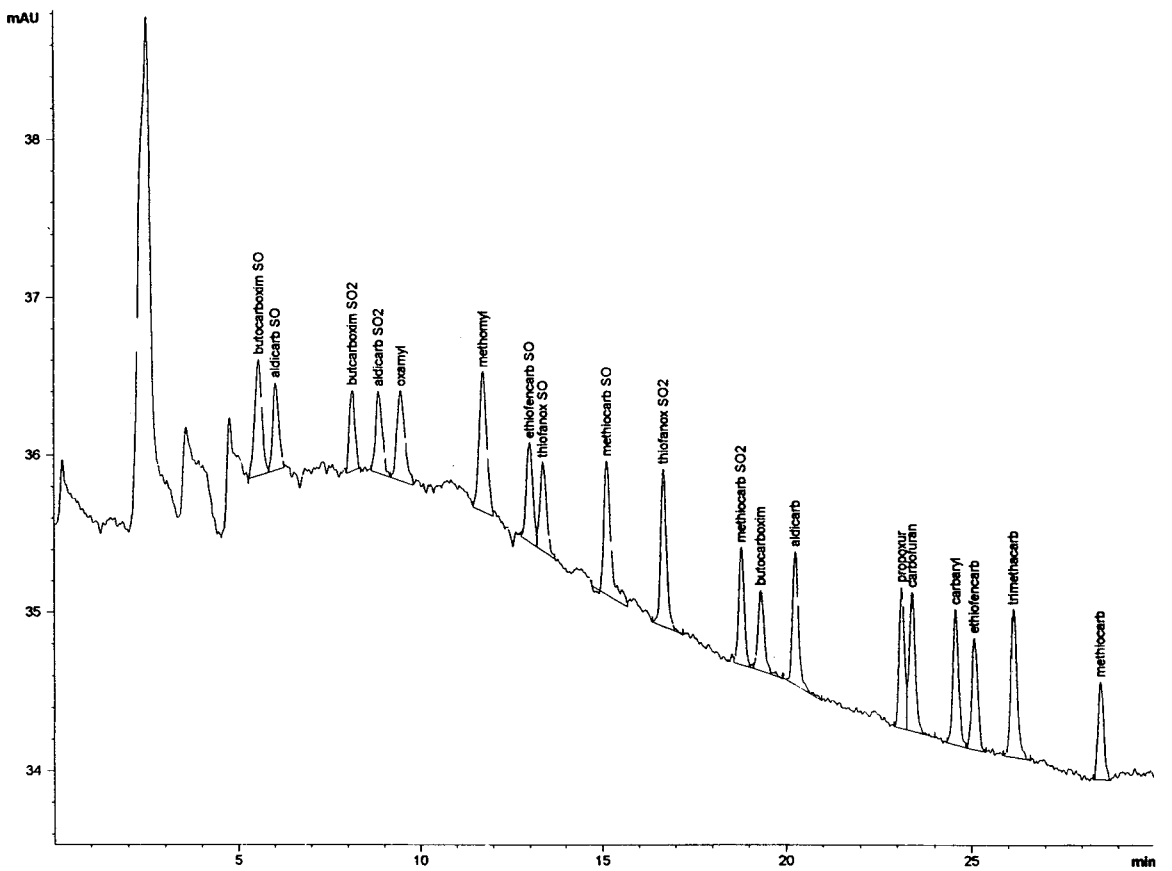

Fig. 2. HPLC chromatogram of a 5-ml surface water sample, fortified with 18 N-methylcarbamates and metabolites at the 0.1 μg/l level, after on-line trace enrichment on a 10 × 4.0 mm I.D. C_{18}/OH precolumn, using the OSP-2 system. Trimethacarb was used as an internal standard.

pletely recovered on the PLRP-S sorbent. No explanation can be given for this deviating behaviour.

A closer look at Table 2 shows that the recoveries and the repeatability obtained with the C_{18}/OH precolumns, using both automated systems, are in good agreement with one another. In comparison with the results of our previously developed off-line method [9], the relative standard deviations of the on-line method are somewhat higher, but still well below 10%. The major advantages of the automated on-line method with exchangeable solid-phase extraction cartridges are the reduced sample size required (typically 3–5 ml), a high sample throughput (30 samples per 24 h) and the absence of cross-contamination from one sample to the next one. For all N-methylcarbamates and their metabolites, the linear dynamic range of the trace enrichment procedure, using the OSP-2, was checked by using fortified surface water (0.05–1 μg/l). The average coefficient of correlation was 0.995. Method detection limits (based on a signal-to-noise ratio 3:1) were in the range 0.03–0.05 μg/l for both automated systems tested. In recent measurements with newer types of fluorescence detectors, these limits could even be lowered by a factor of three.

3.5. Comparison of C_{18}/OH and PLRP-S

A comparison of the retention capacity of the 40-μm C_{18}/OH sorbent and the 15–25-μm PLRP-S sorbent revealed no significant differences in the retention capacity for the polar carbamates. To maintain separation efficiency, the sorbent of the precolumn should have a hydrophobicity similar to that of the analytical column. In comparison with the chromatogram obtained with a direct loop injection, PLRP-S precolumns, using forward-flush, caused substantial band broadening for the later-eluting carbamates, resulting in loss of separation efficiency. This indicates that the non-polar carbamates are retained more by the PLRP-S sorbent than by the stationary phase of the analytical column. It is therefore clear that the elution efficiency of the C_{18}/OH sorbent is better than the PLRP-S sorbent. When applying a back-flush, band broadening of the non-polar carbamates does not occur. However, a major drawback of this procedure is that matrix interferences are also eluted onto the guard column, causing build up of strongly retained compounds on the guard column during analysis. Fig. 3 depicts the chromatograms of a standard mixture of 16 N-methylcarbamates extracted from 3 ml of drinking water fortified with the carbamates at the 0.1 μg/l level on both phases, using the Prospekt apparatus. Desorption of the PLRP-S precolumn was performed by applying a back-flush.

We have also studied the use of precolumns, packed with PLRP-S, with a smaller diameter (2.0 mm), in order to increase the elution efficiency and therefore minimize the loss of separation efficiency. In contrast to the results with 10×3 mm I.D. PLRP-S precolumns, with 10×2.0 mm I.D. PLRP-S precolumns the resolution between the non-polar carbamates was completely maintained, using forward-flush desorption. The recovery and precision results obtained are also given in Table 2. Despite the incomplete recoveries of the polar metabolites butocarboxim sulphoxide and aldicarb sulphoxide due to breakthrough, the repeatability was still good. Hence, precolumns, packed with PLRP-S, proved to efficiently extract N-methylcarbamates from water samples and therefore can serve as a good alternative to C_{18}/OH precolumns. However, the cost of the larger C_{18}/OH particles (40 μm) is somewhat lower than for the polymeric PLRP-S particles (15–25 μm).

3.6. Applications

During a monitoring period of six months, river Rhine water samples were analyzed for N-methylcarbamates and their metabolites, using the on-line trace enrichment method. Fig. 4 depicts the chromatograms obtained using the OSP-2 system. No detectable residues of N-methylcarbamate pesticides or their metabolites were observed. However, during the last months, unknown peaks appeared in the chromatograms. No effort was made yet to trace their identity. Elucidation of the identity of these

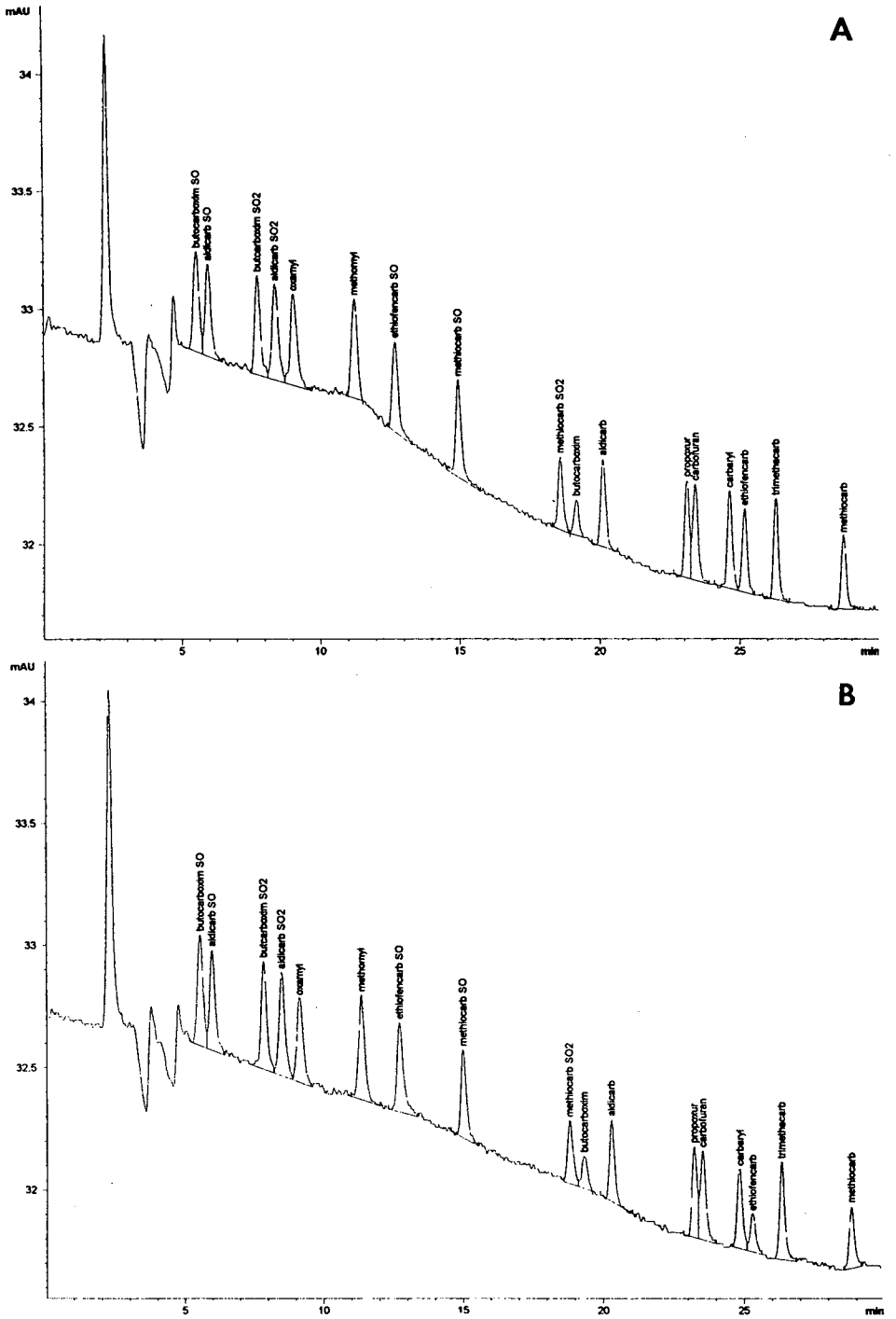

Fig. 3. HPLC chromatograms of a 3-ml drinking water sample, fortified with 16 N-methylcarbamates and metabolites at the 0.1 μg/l level, after on-line trace enrichment on (A) a 10 × 3.0 mm I.D. C_{18}/OH precolumn and (B) a 10 × 3.0 mm I.D. PLRP-S precolumn, using the Prospekt system. Desorption of the PLRP-S precolumn was performed by applying a back-flush. Trimethacarb was used as an internal standard.

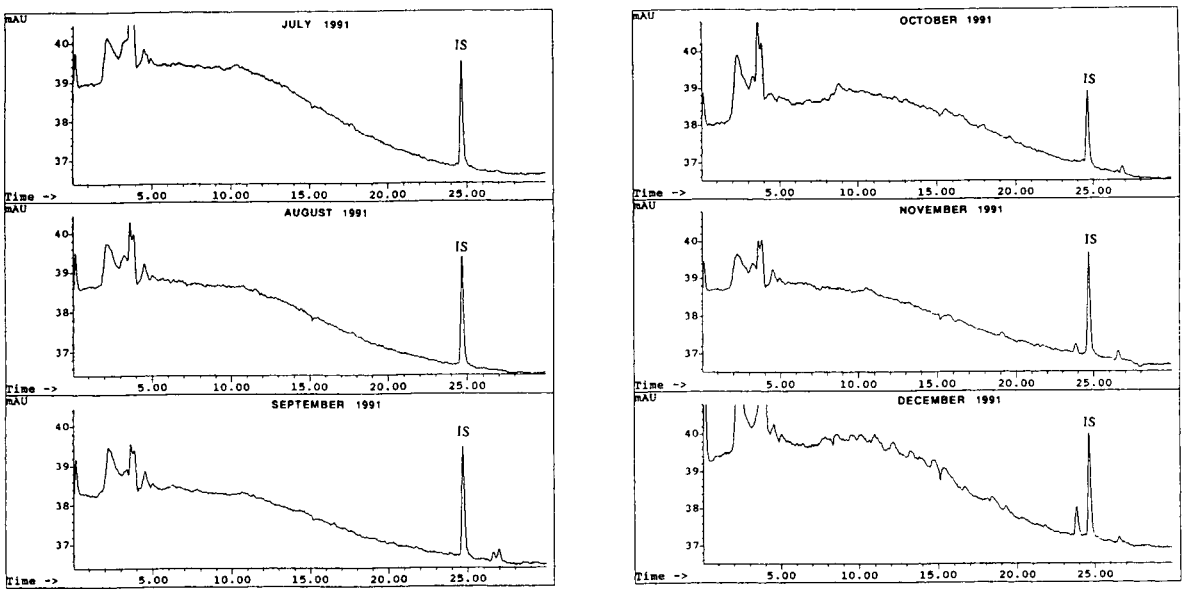

Fig. 4. HPLC chromatograms resulting from the analysis of river Rhine water samples, during a monitoring period of 6 months. The samples were analyzed using the OSP-2 system. Trimethacarb was used as an internal standard (IS). None of the peaks correspond to N-methylcarbamate standards available to us. Time in min.

unknown compounds would require the use of LC in combination with mass spectrometry [16] or diode array detection [4].

4. Conclusions

A fully automated solid-phase extraction–HPLC method has been developed for the determination of N-methylcarbamates and their metabolites in environmental water samples at low ng/l levels. Automated on-line trace enrichment apparatus (OSP-2 and Prospekt) can be effectively applied for extracting and preconcentrating trace levels of N-methylcarbamates from various types of water. Recoveries are high (80–111%), the repeatability is quite good (R.S.D. 2–10%) and a high sample throughput can be achieved (30 samples per 24 h). Method detection limits for all tested N-methylcarbamates were in the range of 0.03–0.05 μg/l.

As was already shown in the off-line method, C_{18}/OH (40 μm) offers distinct advantages over C_{18}-, C_8-bonded silica as to retention efficiency. PLRP-S appears to be a good alternative for the preconcentration of N-methylcarbamates from water samples. The C_{18}/OH phase has a superior selectivity for the more polar carbamates/metabolites and could have a much broader applicability in polar pesticide analysis in the future.

5. Acknowledgements

We are grateful to Hewlett-Packard (Waldbronn, Germany), Merck (Amsterdam, Netherlands) and SPARK Holland (Emmen, Netherlands) for the loan of the HPLC equipment, OSP-2 sample preparator and Prospekt system, respectively.

6. References

[1] *EEC Drinking Water Guideline, 80/779/EEC, EEC No. L229/11-29*, EEC, Brussels, 1980.

[2] J. Slobodnik, E.R. Brouwer, R.B. Geerdink, W.H. Mulder, H. Lingeman and U.A.Th. Brinkman, *Anal. Chim. Acta*, 268 (1992) 55–65.

[3] J. Slobodnik, M.G.M. Groenewegen, E.R. Brouwer, H. Lingeman and U.A.Th. Brinkman, *J. Chromatogr.*, 642 (1993) 359–370.
[4] R. Reupert, I. Zube and E. Plöger, *LC·GC Int.*, 5 (1992) 43–51.
[5] E.R. Brouwer, I. Liska, R.B. Geerdink, P.C.M. Frintrop, W.H. Mulder, H. Lingeman and U.A.Th. Brinkman, *Chromatographia*, 32 (1991) 445–452.
[6] B. McGarvey, *J. Chromatogr.*, 642 (1993) 89–105.
[7] R.B. Geerdink, A.M.B.C. Graumans and J. Viveen, *J. Chromatogr.*, 547 (1991) 478–483.
[8] A. Di Corcia, R. Samperi, A. Marcomini and S. Stelluto, *Anal. Chem.*, 65 (1993) 907–912.
[9] A. de Kok, M. Hiemstra and U.A.Th. Brinkman, *J. Chromatogr.*, 623 (1992) 265–276.
[10] P.D. McDonald, W.P. Leveille, A.E. Sims, W.J. Wildman, V.R. Zener and A.D. Scarchilli, *Advances in Water Analysis and Treatment, Water Quality Technology Conference Proceedings, Philadelphia, PA, 1989*, AWWA, Denver, CO, 1990, pp. 631–649.
[11] L.K. She, U.A.Th. Brinkman and R.W. Frei, *Anal. Lett.*, 17 (1984) 915.
[12] D. Chaput, *J. Assoc. Off. Anal. Chem.*, 69 (1986) 985–989.
[13] C.H. Marvin, I.D. Brindle, C.D. Hall and M. Chiba, *J. Chromatogr.*, 503 (1990) 167–176.
[14] C.H. Marvin, I.D. Brindle, R.P. Singh, C.D. Hall and M. Chiba, *J. Chromatogr.*, 518 (1990) 242–249.
[15] C.H. Marvin, I.D. Brindle, C.D. Hall and M. Chiba, *J. Chromatogr.*, 555 (1990) 147–154.
[16] S. Chiron, A.F. Alba and D. Barceló, *Environ. Sci. Technol.*, 27 (1993) 2352–2359.
[17] C.J. Miles, M.L. Trehy and R.A. Yost, *Bull. Environ. Contam. Toxicol.*, 41 (1988) 838–843.
[18] S. Lesage, *LC·GC*, 7 (1989) 268–271.

ELSEVIER

Journal of Chromatography A, 667 (1994) 167–174

JOURNAL OF CHROMATOGRAPHY A

Separation of acetylated polypropylene glycol di- and triamines by gradient reversed-phase high-performance liquid chromatography and evaporative light scattering detection

Klaus Rissler

Polymers Division, Ciba-Geigy Ltd., CH-4002 Basle, Switzerland

(First received December 27th, 1993; revised manuscript received January 11th, 1994)

Abstract

Polypropylene glycol di- and triamines, the so-called Jeffamines, were reacted with a mixture of equal volumes of acetic anhydride and pyridine to give the corresponding acetamides prior to chromatographic separation by reversed-phase high-performance liquid chromatography using a linear binary solvent gradient and evaporative light scattering detection (ELSD). The procedure was applied to decrease silanophilic interactions of the solutes with the column matrix in order either to improve the peak resolution R_s or to decrease peak tailing. Removal of excess of derivatizing agent prior to sample injection is not required owing to the volatility of pyridine, which does not yield any ELSD response. Therefore, the signals of oligomers with lower retention that are hidden by the broad and strongly tailing pyridine peak when measured by UV detection, are now clearly detectable. Separation was performed on C_{18}, C_8, C_6, C_4 and C_1 stationary phases with either acetonitrile or methanol as organic modifiers. With acetonitrile either complete elution or excellent separation of the low-molecular-mass samples ($M_r \approx 400$) is achieved on the C_{18}, C_8, C_6 and C_4 matrices. However, R_s decreases with increasing M_r but the recoveries of high-M_r samples ($M_r \approx 2000$–5000) increase markedly with decreasing hydrophobicity of the stationary phase in the order $C_{18} < C_8 < C_6 < C_4$. Complete elution of the whole family of investigated polyether amines was accomplished with either acetonitrile on a C_1 column or methanol on all sorbents used in the study. The optimum peak resolution was obtained on a C_4 column with either acetonitrile or methanol. Complete elution of all samples in particular on matrices with either high or intermediate hydrophobicity with methanol compared with acetonitrile is presumably attributable to a better solvation of the polypropylene glycol backbone by hydrogen bonding between the ether oxygens and the hydroxyl group of the protic solvent.

1. Introduction

Polypropylene glycol di- and triamines (PPG amines) are synthesized starting with propylene oxide and 1,2-propylene glycol, yielding the linear PPG amines (Fig. 1a), and/or with glycerol–trimethylolpropane, yielding the branched PPG amines (Figs. 1b and c). They play an increasing role in the synthesis of polyamides, polyurethanes, polyureas and isocyanate prepolymers and as epoxy curing agents and flexibilizers [1]. Although they are commercially available under the trade name Jeffamine [1], precise information concerning their behaviour in liquid chromatography is still lacking. This may presumably be attributable to either the poor UV absorption as the native compounds in the usual wavelength range or to their strongly

0021-9673/94/$07.00
SSDI 0021-9673(94)00036-9

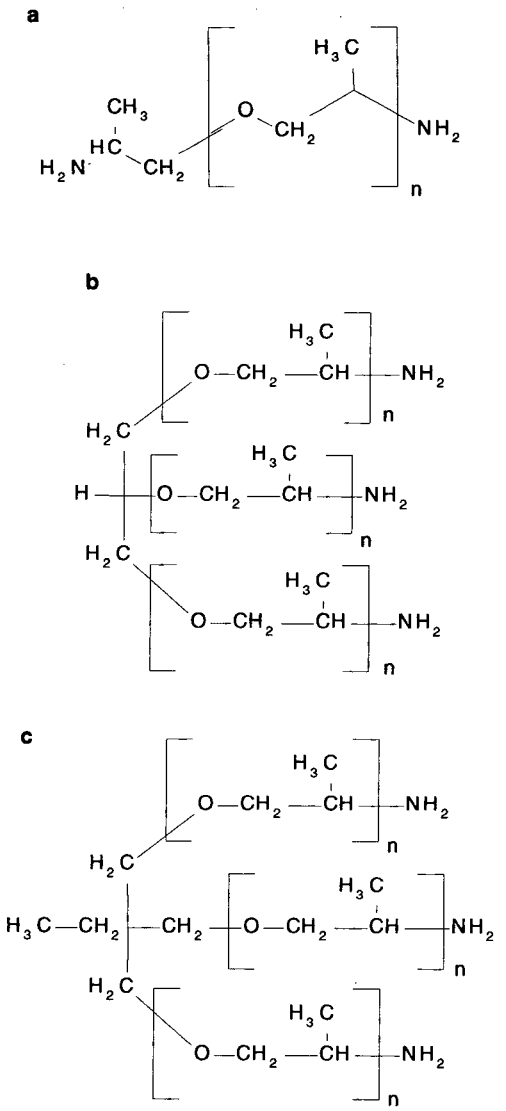

Fig. 1. Structural formulae of (a) the linear PPG amines (Jeffamine D 230, D 400 and D 2000) started with propylene-1,2-glycol and propylene oxide, (b) the branched PPG amines started with glycerol and propylene oxide (Jeffamine T 403) and (c) the branched PPG amines started with trimethylol propane and propylene oxide (Jeffamine T 3000 and T 5000).

basic properties, making them less amenable to a satisfactory chromatographic separation owing to interactions with residual silanols [2–8]. To compensate for the latter effect we converted the PPG amines into the corresponding acetyl derivatives by reacting them with an excess of acetic anhydride and pyridine as the catalyst.

We have investigated the separation of both linear (Jeffamine D 230, D 400 and D 2000) and branched (Jeffamine T 403, T 3000 and T 5000) samples over a wide molecular mass range by gradient RP-HPLC with different organic modifiers on several stationary phases differing widely in hydrophobicity and measurement of the column effluent by means of evaporative light-scattering detection (ELSD).

2. Experimental

2.1. Separation media, reagents and solvents

The PPG amine samples Jeffamine D 230[a], D 400 and D 2000 (linear) and Jeffamine T 403, T 3000 and T 5000 (branched) were purchased from Texaco Chemical (Bellaire, TX, USA). As the stationary phases Nucleosil $5C_{18}$, $5C_8$ and $5C_4$ (each column 125 × 4.6 mm I.D., 5 μm particle size, 100 Å pore diameter) from Macherey–Nagel (Oensingen, Switzerland) and Ultremex $5C_6$ and $5C_1$ (each column 150 × 4.6 mm I.D., 5 μm particle size, 80 Å pore diameter) from Phenomenex (Torrance, CA, USA) were used. Pyridine, acetic anhydride (both pro analysi), trifluoroacetic acid (purum), acetonitrile and methanol (both HPLC grade) were obtained from Fluka (Buchs, Switzerland). Water for use in HPLC was purified with a Milli-Q reagent water system from Millipore–Waters (Milford, MA, USA).

2.2. Derivatization reaction

An amount of *ca.* 25 mg of the PPG amine was dissolved in 100 μl of pyridine–acetic anhydride (1:1, v/v) and heated at 60°C for 30 min. Excess of reagent was reacted to give the methyl ester by addition of 1.5 ml of methanol and heating at 60°C for 10 min. The solution

[a] The numbers represent the average molecular mass, M_r, of the samples as specified by the manufacturer.

Table 1
Gradient programme for the elution of PPG amides with acetonitrile and methanol as organic modifiers

Time (min)	Organic solvent (%)	Water (%)
0	0	100
40	100	0
50	100	0
51	0	100
65	0	100

prepared in this manner was used for HPLC without further purification.

2.3. Analytical equipment

The HPLC apparatus consisted of an SP 8800 ternary HPLC pump, an SP 8880 autosampler equipped with a 10-μl sample loop and a PC 1000 data acquisition unit, all obtained from Spectra-Physics (San Jose, CA, USA). For ELSD a Sedex 45 apparatus from SEDERE (Vitry-sur-Seine, France) equipped with a 20-W iodine lamp was applied.

2.4. Chromatographic separation

The gradient system depicted in Table 1 was used for the separation with either acetonitrile or methanol as organic modifier. Separation was performed on the columns indicated above at ambient temperature (*ca.* 22°C) and a flow-rate of 1.5 ml/min. Aliquots of 10 μl of the solutions prepared as described were injected. For detection by means of ELSD the nebulization chamber was heated to 40°C and the nitrogen flow-rate was adjusted to 4.5 l/min, corresponding to an inlet pressure of 200 kPa.

3. Results and discussion

Detection of the polypropylene glycol di- and triamides (PPG amides) can be performed either by UV absorption at 210–220 nm owing to the amide chromophore or by ELSD. In the former instance complete removal of excess of pyridine is required (*i.e.*, an additional sample prepurification step) because the broad and strongly tailing peak of the catalyst overlaps with those of early-eluting low-M_r PPG amide oligomers. This drawback can, however, be successfully overcome by using ELSD owing to the high volatility of pyridine, which does not invoke any detector response. The ELSD method has a wide application range for non-volatile components, which easily form solid particles after loss of the surrounding solvent shell by nebulization and subsequent heating of the resulting droplets in the drift tube [9–20]. Further, a stable baseline is obtained, which is either independent of the type of organic modifier or the gradient shape [10–12, 19]. Optimization of the detection conditions for signal monitoring of polyethers was described recently [21] and was used in this study.

Owing to the large differences in M_r and the concomitant large differences in the retention of the samples, gradient RP-HPLC proved to be superior to the isocratic technique and was therefore applied. With acetonitrile as organic modifier, only the low-M_r oligomers Jeffamine D 230, D 400 and T 403 eluted quantitatively from the C_{18}, C_8, C_6 (results not shown) and C_4 stationary phases, but a marked improvement in the elution efficiency of the high-M_r samples Jeffamine D 2000, T 3000 and T 5000 was achieved in the range $C_{18} < C_8 < C_6 < C_4$. Whereas the peak resolution R_s {$R_s = 2[(t_2 - t_1)/(w_1 + w_2)]$, where t_1 and t_2 are the retention times of two adjacent peaks and w_1 and w_2 their base widths} of the low-M_r samples was excellent on these four matrices, the R_s of the high-M_r oligomers was markedly lower but increased substantially in the order $C_{18} < C_8 < C_6 \approx C_4$. Optimum results were obtained on the C_4 column (Fig. 2a–f) and, in contrast to the C_6 matrix (results not shown), nearly complete elution of Jeffamine D 2000 and T 3000 was achieved (Fig. 2d and e). Nevertheless, the recovery of Jeffamine T 5000 still remained low (Fig. 2e). The C_1 matrix permits quantitative elution of the whole family of high-M_r PPG amides (results not shown) but a marked leveling effect of analyte retention does not make the method suitable for investigations of sample mixtures, which more or less differ in M_r. Further, the peak resolution of

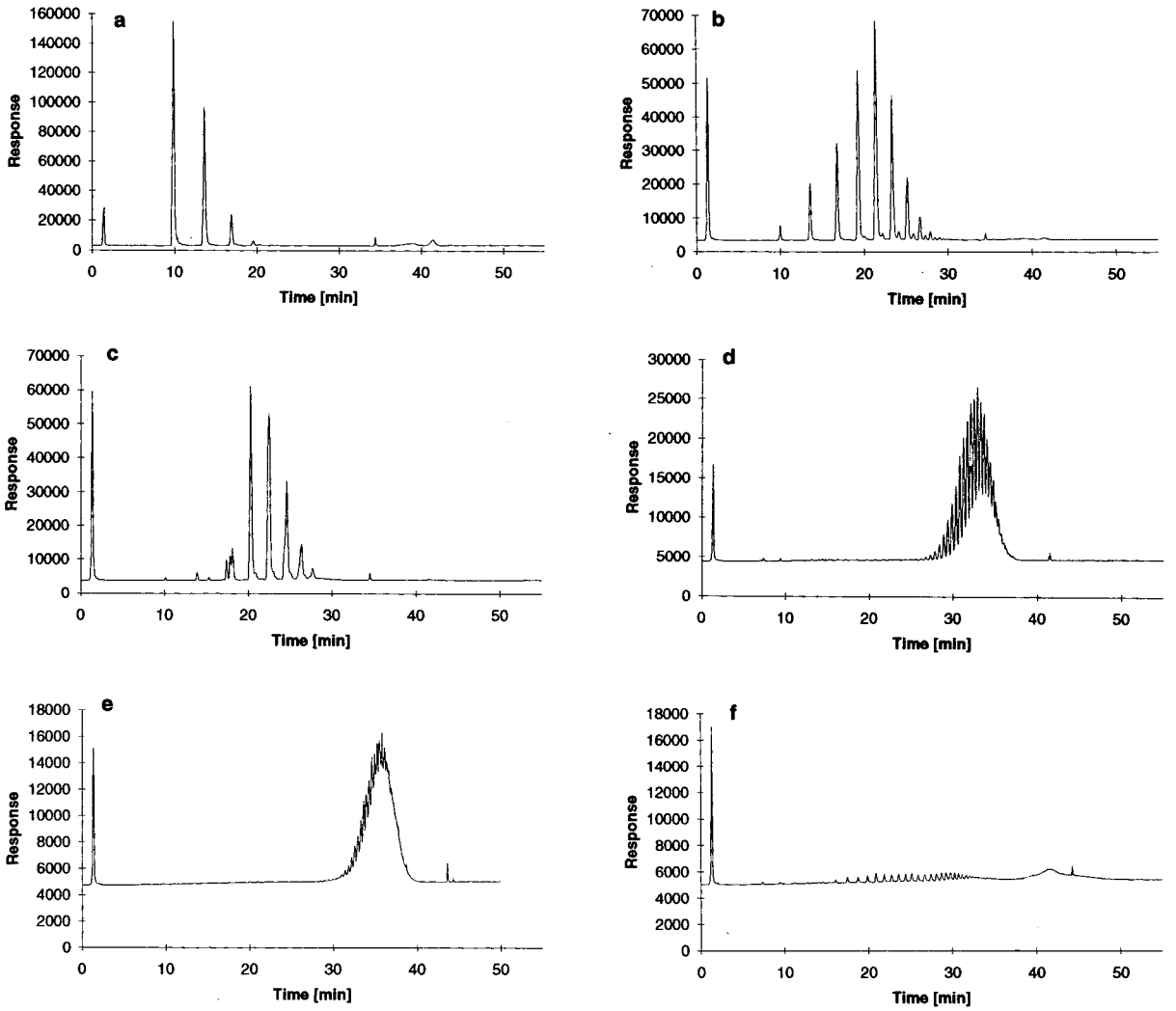

Fig. 2. Chromatograms of (a) Jeffamine D 230, (b) Jeffamine D 400, (c) Jeffamine T 403, (d) Jeffamine D 2000, (e) Jeffamine T 3000 and (f) Jeffamine T 5000 on a C_4 column with acetonitrile as organic modifier.

low-M_r oligomers is unsatisfactory and thus contrasts markedly with the separation profile of the other stationary phases. When methanol was used as the organic modifier, quantitative elution of all the investigated PPG amide samples was achieved on the C_{18}, C_8, C_6, C_1 (results not shown) and C_4 matrices (Fig. 3a–f). As already observed with acetonitrile, the C_4 stationary phase also exhibited either the best R_s of oligomers or selectivity with respect to an individual assignment of samples within mixtures.

Addition of 0.05% of trifluoroacetic acid (TFA) to the mobile phase and thus conversion of the native samples into the corresponding trifluoroacetates provides another means for measurement by ELSD without prior derivatization owing to the high volatility of excessive TFA. However, the peak broadening is markedly higher and, as a consequence, the R_s much lower compared with the corresponding amides (results not shown). Further, a "levelling effect" of retention occurs for the higher M_r samples

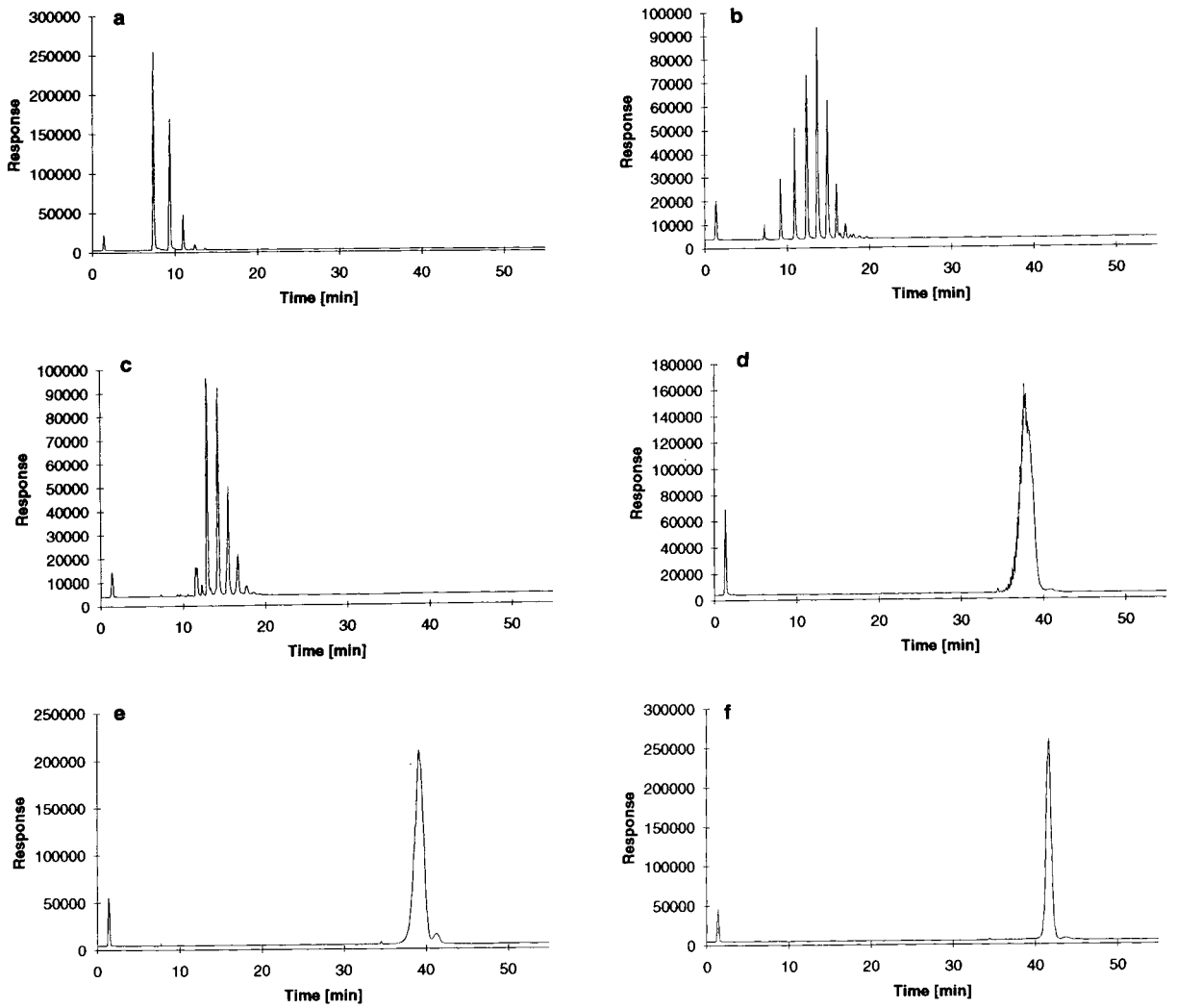

Fig. 3. Chromatograms of (a) Jeffamine D 230, (b) Jeffamine D 400, (c) Jeffamine T 403, (d) Jeffamine D 2000, (e) Jeffamine T 3000 and (f) Jeffamine T 5000 on a C_4 column with methanol as organic modifier.

(*e.g.*, Jeffamine D 2000, T 3000 and T 5000), thus making an assignment to individual PPG amine species nearly impossible. Additionally it is well known that TFA accelerates the dissociation of octadecylsilyl residues from the column matrix by increasing the concentration of free silanol groups, which in turn are responsible for a relatively rapid deterioration of chromatographic performance [22] due to marked silanophilic interactions [2–8]. In contrast, the underivatized PPG amines cannot be eluted on either reversed-phase materials (C_{18}, C_8, C_6, C_4, C_{phenyl}, C_1) or on so-called bonded-phase sorbents such as cyanopropyl (CN), aminopropyl (NH_2) and 2,3-propanediol (diol) stationary phases under "neutral" conditions, *i.e.*, no mobile phase additives such as acids, buffers and ion-pairing agents were used to suppress or at least to modulate the silanophilic solute–matrix interactions. This conclusion can be drawn from the observation that no responses were obtained from either ELSD or liquid chromatographic–

mass spectrometric (LC–MS) investigations. In the latter instance no nitrogen-containing ions of homologues differing from each other by 58 u and thus attributable to the propoxy monomeric structural unit were observed, although ionization of the polar solutes should not give rise to any problems (results not shown). However, trace amounts of polyproypylene glycol oligomers lacking nitrogen were found, which obviously have not quantitatively reacted to the corresponding PPG diamines, and their extremely low concentrations prevented detection by means of ELSD.

It is important to note that addition of buffers and other mobile phase additives will not be compatible with ELSD. This is due to the huge background invoked by the continuous generation of solid particles from the mobile phase in the heating zone of the detector after loss of the solvent shell, which completely suppresses signal monitoring of the analyte. For this reason, all solvents, even if they are supplied as "HPLC-grade" materials, have to be tested prior to use because in our experience not all of these solvents are suitable for ELSD and wide batch-to-batch and manufacturer-to-manufacturer variances exist. On the other hand, buffers will not be convenient additives for gradient elution (even if they show only negligible absorbance when UV detection is applied) owing to their generally decreasing solubility with increasing percentage of organic solvent. Therefore, derivatization of the primary amine groups of the PPG amines with an appropriate reagent offers an attractive alternative way to achieve both optimum separation efficiency and detection sensitivity. Although the 3,5-dinitrobenzoyl derivatives [21,23,24] allow signal monitoring at 254 nm, at least for low-M_r samples, partial overlapping of peaks from the (less volatile) excess of reagent and polyether have to be taken into account. For this reason, we applied the more suitable method of acetylation using equal volumes of acetic anhydride and pyridine, which yields mostly volatile components after post-derivatization methanolysis of the excess of reagent. Only the signal presumably attributable to pyridine acetate is observed, which however elutes near the column void volume and therefore does not interfere with chromatographic separation.

Whereas complete retention of underivatized PPG amines on chemically modified silica gel stationary phases can be ascribed to marked silanophilic interactions [2–8], the poor refractive index responses of the samples obtained by gel permeation chromatography (results not shown) are surprising because extensive signals should have been expected owing to the presumed negligible solute–matrix interactions between the polar PPG amines and the strongly hydrophobic divinylbenzene cross-linked polystyrene (DVB–PS) matrix used for gel permeation chromatography (GPC) A similar effect was observed by Mukoyama *et al.* [25] when they subjected polyamic acid (obtained by polycondensation of 4,4′-diaminodiphenyl ether and pyromellitic dianhydride) to GPC. Complete retention of the extremely polar solute takes place on the non-polar DVB–PS matrix in dimethylformamide as the solvent, whereas addition of phosphoric acid to the mobile phase effected its elution. At present we cannot give a reasonable answer, but "aggregation" via hydrogen bonding yielding poorly soluble "complexes" may be at least one hypothesis for an explanation. Indeed, the corresponding PPG amides exhibit a large increase in detector response, which may be explained by marked disruption of hydrogen bonding after amide formation. Perhaps a phenomenon such as this may partially also be operating in the RP-HPLC of underivatized samples and thus superimposes silanophilic interactions. The preferred retention of high-M_r PPG amides on C_{18}, C_8, C_6 and C_4 columns with acetonitrile and their quantitative release with methanol is in accordance with our recent observations reported elsewhere [21]. In these instances an increase in solubility of polyethers in methanol owing to the formation of hydrogen bonds between ether oxygens and the hydroxyl group of the protic compared with the aprotic solvent was postulated. This effect elicits a higher concentration of polyether in the methanolic solvent layer compared with its concentration in the adjacent region of hydrophobic

octadecylsilyl chains of the column matrix and thus markedly affects analyte retention. In contrast, a decrease in retention of the high-M_r PPG amides with increasing polarity of the stationary phase can be explained by smaller hydrophobic interactions of the relatively non-polar polypropylene glycol backbone with the column matrix, which decrease in the order $C_{18} > C_8 > C_6 > C_4 > C_1$ [21].

Although the samples with higher M_r show increasingly lower peak resolution, their retention depends markedly on the M_r ($R_s \sim 1/M_r$, but $t_R \sim M_r$). Thus PPG amides with a broad M_r range can be well separated in one run and a selective assignment within sample mixtures is achieved. Further, a dependence of peak resolution on the type of polyether is observed and, at least on reversed-phase matrices, R_s decreases markedly in the order polybutylene glycol > polypropylene glycol > polyethylene glycol for a given M_r [21]. PPG amides behave chromatographically similarly to polypropylene glycols, implying that retention is preponderably governed by the polyoxypropylene backbone.

4. Conclusions

Prior derivatization of PPG amines to the corresponding acetamides yields strong suppression of interactions with residual silanol groups of the column matrix, which normally invoke irreversible adsorption of the strongly basic solute. This procedure makes them amenable to separation by RP-HPLC with purely aqueous organic solvents. For this reason ELSD can be applied for signal monitoring and responses are measured with high sensitivity. The alternative method of using the native PPG amines and small amounts of TFA in the mobile phase proves to be inferior owing to marked peak broadening, lower R_s and a decreased column lifetime. PPG amides of different M_r are separated according to increasing M_r, which allows an individual assignment of samples within mixtures. Linear solvent strength gradient RP-HPLC with either acetonitrile or methanol as modifiers and a C_4 stationary phase provides an optimum chromatographic system.

5. Acknowledgements

The LC–MS investigations of selected native and derivatized samples carried out by Dr. C. Guenat and B. Inverardi (Department of Spectroscopy, Ciba-Geigy, Basle, Switzerland) are gratefully acknowledged.

6. References

[1] *Technical Data Sheet, Jeffamine™ Poly(oxypropylene) amines*, Jefferson Chemical, Houston, TX.
[2] K.E. Bij, Cs. Horvath, W.R. Melander and A. Nahum, *J. Chromatogr.*, 203 (1981) 65.
[3] H. Engelhardt, B. Dreyer and H. Schmidt, *Chromatographia*, 16 (1982) 11.
[4] P.C. Sadek and P.W. Carr, *J. Chromatogr. Sci.*, 21 (1983) 314.
[5] E.L. Weiser, A.W. Salotto, S.M. Flach and L.R. Snyder, *J. Chromatogr.*, 303 (1984) 1.
[6] W.A. Moats and L. Leskinen, *J. Chromatogr.*, 386 (1987) 79.
[7] L.C. Sander, *J. Chromatogr. Sci.*, 26 (1988) 380.
[8] G.C. Fernandez Otero and C.N. Carducci, *J. Liq. Chromatogr.*, 14 (1991) 1561.
[9] J.M. Charlesworth, *Anal. Chem.*, 50 (1978) 1414.
[10] R. Macrae and J. Dick, *J. Chromatogr.*, 210 (1981) 138.
[11] A. Stolyhwo, H. Colin and G. Guiochon, *J. Chromatogr.*, 265 (1983) 1.
[12] A. Stolyhwo, H. Colin, M. Martin and G. Guiochon, *J. Chromatogr.*, 288 (1984) 253.
[13] T.H. Mourey and L.E. Oppenheimer, *Anal. Chem.*, 56 (1984) 2427.
[14] L.E. Oppenheimer and T.H. Mourey, *J. Chromatogr.*, 298 (1984) 217.
[15] L.E. Oppenheimer and T.H. Mourey, *J. Chromatogr.*, 323 (1985) 297.
[16] T.H. Mourey, *J. Chromatogr.*, 357 (1986) 101.
[17] R. Schultz and H. Engelhardt, *Chromatographia*, 29 (1990) 517.
[18] D.E. Schaufelberger, T.G. McCloud and J.A. Beutler, *J. Chromatogr.*, 538 (1991) 87.
[19] P. Van der Meeren, J. Vanderdeelen and L. Baert, *Anal. Chem.*, 64 (1992) 1056.
[20] A.I. Hopia and V.-M. Ollilainen, *J. Liq. Chromatogr.*, 16 (1993) 2469.
[21] K. Rissler, H.-P. Künzi and H.-J. Grether, *J. Chromatogr.*, 635 (1993) 89.

[22] S. Linde and B.S. Welinder, *J. Chromatogr.*, 536 (1991) 43.
[23] A. Nozawa and T. Ohnuma, *J. Chromatogr.*, 187 (1980) 261.
[24] P.L. Desbène, B. Desmazières, J.J. Basselier and A. Desbène-Monvernay, *J. Chromatogr.*, 461 (1989) 305.
[25] Y. Mukoyama, H. Sugitani and S. Mori, *J. Appl. Polym. Sci. Appl. Polym. Symp.*, 52 (1993) 183.

ELSEVIER

Journal of Chromatography A, 667 (1994) 175–181

JOURNAL OF CHROMATOGRAPHY A

Stability-indicating method for the determination of levodopa, levodopa–carbidopa and related impurities

Johan B. Kafil*, Bhim S. Dhingra

Pharmaceutical Analysis Research and Development, Hoffmann–La Roche Inc., Nutley, NJ 07110, USA

(First received February 16th, 1993; revised manuscript received November 19th, 1993)

Abstract

A simple and sensitive high-performance liquid chromatography method was developed for the determination of levodopa and levodopa–carbidopa formulations. In the combined formulation, the method separates these drugs from their potential impurities. A C_{18} column with a 0.05 *M* acetate buffer as mobile phase was utilized for this separation. The components in the column effluent were monitored with a coulometric detector. The method is simple, precise, stability indicating and represents an improvement over the currently available methods of analysis. The method was utilized to investigate the stability of the analyte solution. Upon standing at room temperature, the analyte solution developed several peaks which correspond primarily to the degradation of 6-hydroxydopa.

1. Introduction

Levodopa is indicated in the treatment of the prominent symptoms of Parkinson's disease. Levodopa is formulated with carbidopa to prevent its decarboxylation in the extracerebral tissues [1]. The *United State Pharmacopeia National Formulary* (USP XXII) specifies two impurities in each of the two separate bulk substances (Fig. 1). Levodopa impurities, 6-hydroxydopa and 3-methoxytyrosine are quantitated by a TLC method [2]. This method is known to suffer from lengthy analysis time which results in degradation of levodopa on the TLC plate. Furthermore, 6-hydroxydopa is extremely unstable and is not easily visualized. For levodopa–carbidopa formulations the USP XXII requires that the major components be assayed by HPLC. The USP HPLC method is not developed for concurrent testing of impurities.

The chromatographic separation and amperometric detection of the combination dosage form was first reported by Rihbany and Delaney [3]. While the sensitivity and selectivity of the detector is ideal, chromatography is not optimized. Ting [4] has reported an HPLC method with UV detection. The analysis time is shorter and has a better separation. Ting's method requires an internal standard and the detector sensitivity must be changed when going from the levodopa peak to the carbidopa peak. In this paper, we report an HPLC procedure with coulometric detection. A simple mobile phase that permits the simultaneous isocratic separa-

* Corresponding author.

0021-9673/94/$07.00
SSDI 0021-9673(93)E1236-S

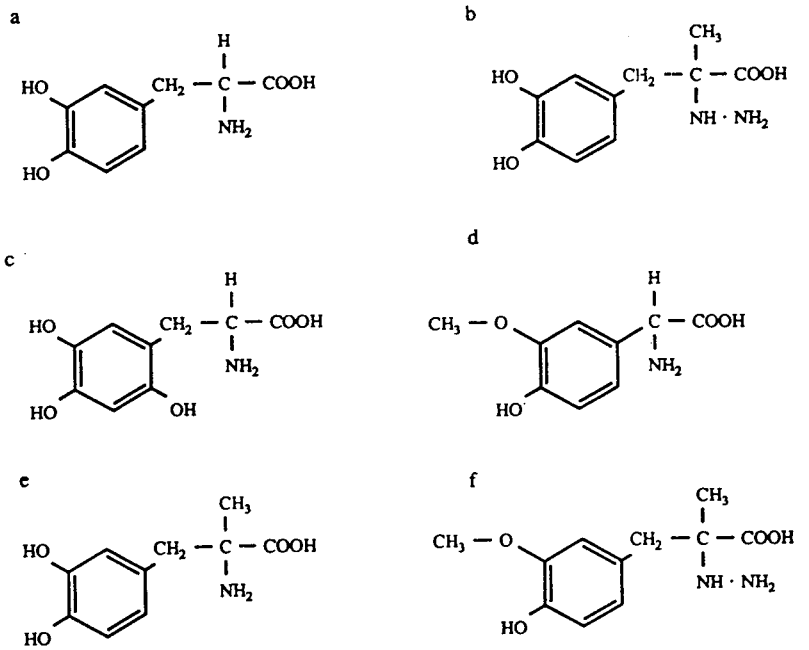

Fig. 1. Molecular structures of (a) levodopa, (b) carbidopa, (c) 6-hydroxydopa, (d) methoxytyrosine, (e) methyldopa and (f) 3-O-methylcarbidopa.

tion of carbidopa, levodopa and their potential impurities is used.

2. Experimental

2.1. HPLC apparatus

Chromatography was carried out with a Model 510 pump (Waters, Division of Millipore, Milford, MA, USA). Sample was injected via a WISP Model 710B automatic injector (Waters). Separation was achieved on a 250 × 4.6 mm I.D. μBondapak C_{18} reversed-phase column (10-μm porous support particles, Waters). The column effluent was monitored simultaneously with two detectors in series. The first detector was an ultraviolet absorption detector set at 280 nm (Model 783; Applied Biosystems, CA, USA). The second detector was a dual-electrode coulimetric detector (Model 5100A Coulochem; Environmental Sciences Assoc., Bedford, MA, USA). The detector was protected with a guard cartridge containing a 0.2-μm filter. The applied cell potential of the screen electrode was set at +0.3 V and the sample electrode +0.6 V. Technical details of this detector were first reported by Matson [5].

2.2. Chemical and reagents

Carbidopa, levodopa, methyldopa and 3-O-methylcarbidopa were USP reference standards (US Pharmacopeial Convention, Rockville, MD, USA). All other reagents were analytical-reagent grade and were purchased from Sigma (St. Louis, MO, USA).

2.3. Mobile phase preparation

The HPLC mobile phase used in the present study was 0.05 *M* ammonium acetate with 0 to 2% methanol in which the pH of acetate buffer was adjusted to 4.1 with 0.6 *M* acetic acid. A proper pH of the acetate buffer was essential to the peak resolution. The mobile phase was filtered and degassed before use.

2.4. Sample preparation

Standard and sample solutions were prepared by dissolving the appropriate amount of each compound in the mobile phase. Samples were filtered before injection into the chromatograph.

3. Results and discussion

3.1. Optimization of mobile phase

The general controlling factors for the separation of catecholamines by HPLC are well understood [6–10]. An optimum mobile phase containing sodium acetate, citric acid, sodium octyl sulfate, tetrasodium EDTA, sodium chloride and methanol was reported for the simultaneous determination of 24 neurochemicals [6]. Several mobile phases including the one proposed by Ting [4] were investigated for the present study. The mobile phase we selected for the analysis is a 0.05 *M* ammonium acetate containing up to 2% of methanol [11]. Increasing the amount of methanol in the mobile phase resulted in an overall decrease in the retention times of levodopa, carbidopa and their potential impurities. At 1 ml/min flow-rate, a composition of 1% methanol gave baseline separation for all components. For shorter analysis times, the amount of methanol in the mobile phase can be adjusted. The pH of the mobile phase was found to have a profound effect on both of the peaks. In general, the lower the pH the longer the retention time, and thus the lower the response. However, when the pH of the acetate buffer in the mobile phase was higher than 4.1 a shoulder peak next to levodopa would appear; and in addition, the 6-hydroxydopa would not be resolved from the levodopa peak. To maximize the performance of the column, therefore, a pH of 4.1 of the buffer was adopted in this study.

3.2. Optimization of the detector

The electrochemical detector used in the present study is a coulochem detector with dual electrodes in series which can be set in screen mode of operation. In this mode, the first electrode was at a potential lower than the second electrode. The coulometric efficiency of the detector thus decreased background currents and eliminated undesirable components at the first electrode while quantitating at the second electrode. In the assay development, the optimal cell potential was first explored using the pure components dissolved in mobile phase. A standard solution of the six compendial substances was chromatographed repetitively. The detector was operated in an identical manner for all injections. A series of 0.05-V step potentials was applied and the response was recorded at each potential. For each potential setting, the peak area for each component in the chromatogram was obtained. While at potential over 0.3 V all six components showed response; optimum potential was about 0.6 V. Based on these results, 0.3 and 0.6 V were then chosen for the first and second electrode, respectively.

Fig. 2 illustrates the high sensitivity of the present HPLC method. Chromatographic parameters for this separation are listed in Table 1. The peak shapes for most of the individual components of the mixture appear to be symmetrical. In spite of the use of filter element installed before the detector cell, there is no significant peak broadening.

The coulochem response for both levodopa and carbidopa was linear from 0.1 to 250 nmol. The relative standard deviation (three determinations) at the 10-nmol level for levodopa and carbidopa were 0.6 and 1.3%, respectively. For the 0.1–1 nmol range, levodopa gave a slope of 0.11 μA/nmol, and intercept of 0.05 μA and a standard error of estimate of 0.002 μA. Over the same range carbidopa exhibits a slope of 0.06 μA/nmol, an intercept of 0.02 μA and a standard error of estimate of 0.003 μA. For comparison Table 2 shows the minimum amount of each compound detected as compared to other reported methods. The current USP limits for these impurities are also listed. Fig. 3 shows a chromatogram corresponding to the determination of the six compendial compounds near the detection limit.

Excellent reproducibility was obtained for the

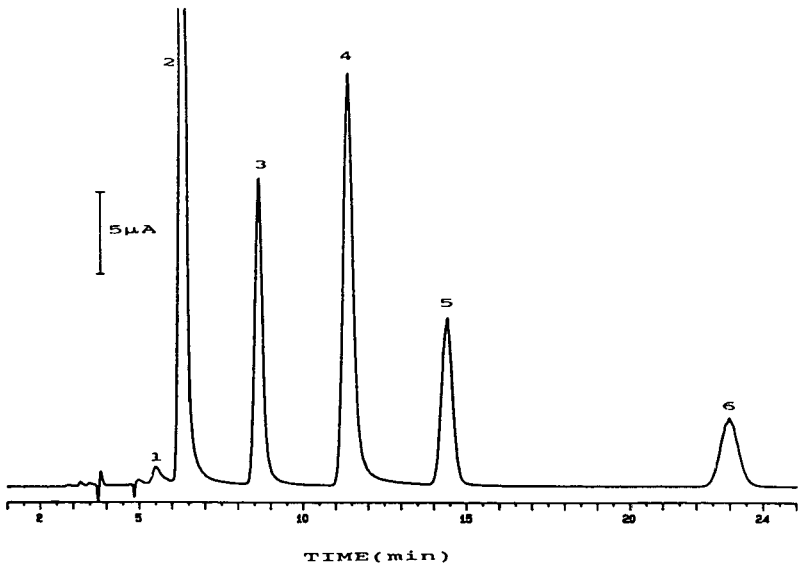

Fig. 2. Chromatogram of a mixture of 0.02 mg/ml of (1) 6-hydroxydopa, (2) levodopa, (3) methyldopa, (4) carbidopa, (5) methoxytyrosine and (6) 3-O-methylcarbidopa. Conditions: flow-rate 0.9 ml/min; applied potential, first electrode 0.3 V, second electrode 0.6 V.

Table 1
Chromatographic parameters for levodopa, carbidopa and their potential impurities

Component	Retention time (min)	Capacity factor	Tailing factor	Resolution factor
6-Hydroxydopa	5.49	0.37	1.36	2.24
Levodopa	6.35	0.59	1	5.4
Methyldopa	8.59	1.15	1.52	4.74
Carbidopa	11.41	1.85	1.22	4.25
3-Methoxytyrosine	14.31	2.58	1.02	10.42
3-O-Methylcarbidopa	22.68	4.67	0.50	

For conditions, see text. As defined in the USP XXII, under system suitability tests.

Table 2
HPLC detection limit comparison

Component	UV (280 nm) (μg/ml) (3[a])	Amperometric (ng/ml) (1[a])	Coulometric (ng/ml)	USP limit (μg/ml)
6-Hydroxydopa	1.8	20	2	2
Levodopa	1.0	–	20	–
Methyldopa	1.4	80	20	1
Carbidopa	0.2	–	2	–
3-Methoxytyrosine	100	40	40	10
3-O-Methylcarbidopa	10	60	50	1

[a] USP XXII acceptability limits for carbidopa and levodopa bulk.

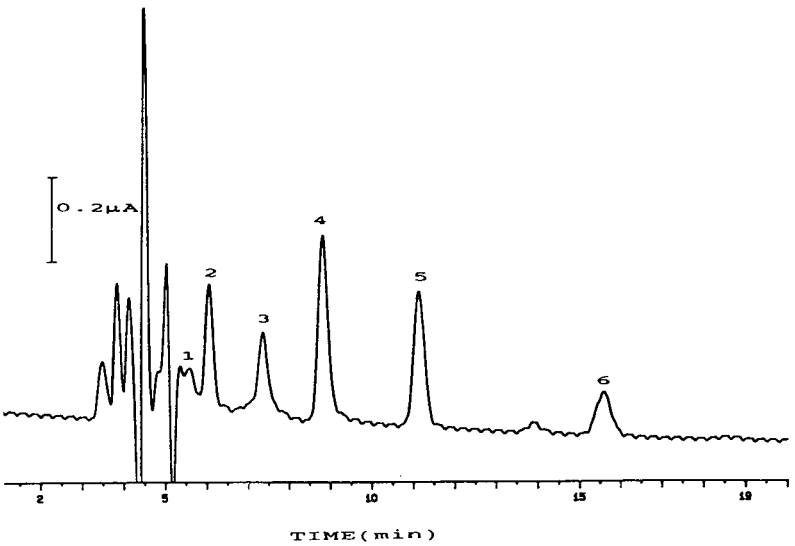

Fig. 3. Chromatogram representing the determination of the six compendial compounds near the detection limit. Peaks: 1 = 6-hydroxydopa (0.2 ng); 2 = levodopa (2.0 ng); 3 = methyldopa (2.0 ng); 4 = carbidopa (0.2 ng); 5 = methoxytyrosine (5.0 ng); 6 = 3-O-methylcarbidopa (5.0 ng). Conditions: flow-rate 1.1 ml/min; applied potential; first electrode 0.3 V, second electrode 0.6 V.

present HPLC method; relative standard deviation (R.S.D.) for six injections of carbidopa/levodopa (0.02 mg/ml) mixture was normally less than 1.0%. The intra-day precision was usually between 1.5 and 2.0%. Six replicate analyses on three different days gave inter-day precision of 2.0% for levodopa and 1.6% for carbidopa.

3.3. Stability of the analyte solution

Fig. 4 shows chromatograms a–f for a standard solution of the five compendial compounds (methyldopa was not included in this solution). Upon standing at room temperature, two major impurity peaks appeared. Peak eluting after levodopa had a retention time identical to that of methyldopa. The other peak, eluting later had a retention time different from those tested; its identity is presently under investigation. Solutions containing each individual compounds were prepared. Upon standing, 6-hydroxydopa solution developed an impurity peak corresponding to peak 4 in the standard mixture. The peak area for levodopa had fallen slightly ($<0.01\%$) after 8 h; however, no significant impurity was found. For carbidopa and levodopa, the R.S.D. for six injections with 1 h time interval were 0.8 and 1.2%, respectively.

The coulometric detector performed without particular incident for the duration of the study; however, the background noise was noticeable after about two months of continuous operation. When the manufacturer-suggested procedure was followed for cleaning the detector, signal-to-noise ratio was returned to its original level.

A 0.1 mg/ml USP primary standard solution corresponding to the analysis of a 100 mg levodopa and 25 mg carbidopa was monitored simultaneously with a UV and coulometric detector. With UV detection, change in sensitivity of the detector is required when going from the levodopa peak to the carbidopa peak because of the large difference in their respective concentrations. With coulometric detector the relative response for carbidopa is almost twice the response for levodopa. Fig. 5 shows the chromatographic separation of a Sinemet tablet containing 100 mg levodopa and 25 mg carbidopa. With coulometric detector, both actives are on scale and sensitivity change is not required.

In summary, a simple and sensitive HPLC

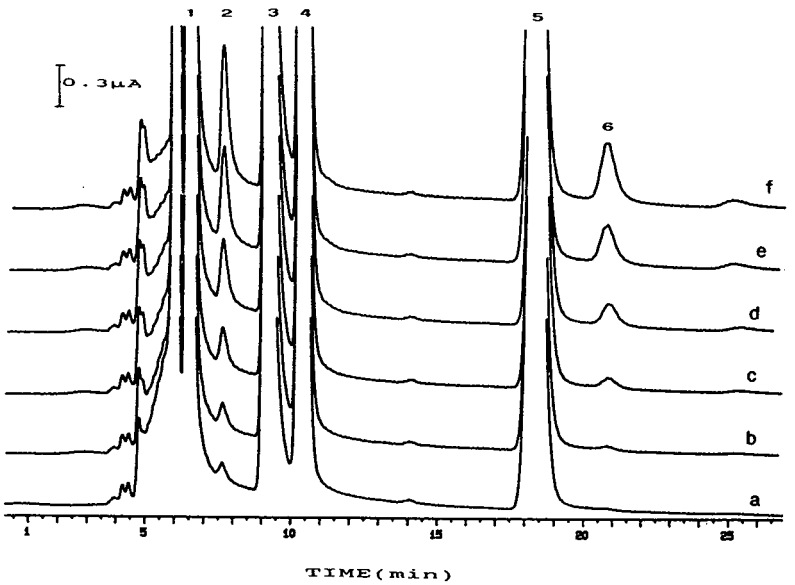

Fig. 4. Chromatograms representing the stability of the analyte solution at room temperature: Chromatograms a–f are from the same solution injected at 4 h time interval. Peaks: 1 = levodopa; 3 = carbidopa; 4 = methoxytyrosine; 5 = 3-O-methylcarbidopa. Peaks 2 and 6 were not present in the fresh standard mixture. Conditions: flow-rate 1.2 ml/min; applied potential, first electrode 0.3 V, second electrode 0.6 V.

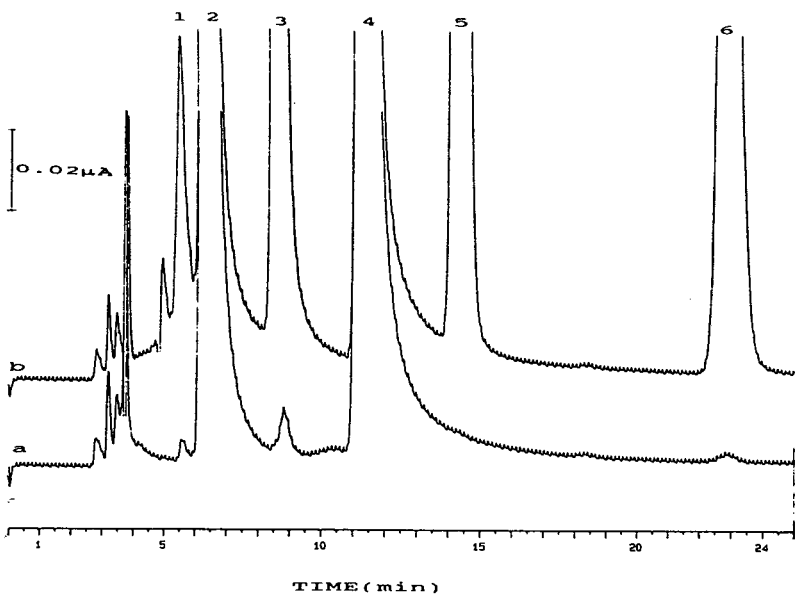

Fig. 5. Chromatograms for (a) levodopa–carbidopa tablet and (b) standard solution of (1) 6-hydroxydopa, (2) levodopa, (3) methyldopa, (4) carbidopa, (5) methoxytyrosine and (6) 3-O-methylcarbidopa. Conditions: flow-rate 0.9 ml/min; applied potential, first electrode 0.3 V, second electrode 0.6 V.

method was developed for the determination of levodopa and levodopa–carbidopa formulations. In the combined formulation, the method separates these drugs from their potential impurities and their excipients. The proposed method is stability indicating.

4. References

[1] *J. Am. Med. Assoc.*, 246 (1981) 11.
[2] R. Gomez, R.B. Hagel and E.A. Macmullan, *Analytical Profile of Drug Substance*, Vol. 5, Academic Press, New York, 1976, p. 190.
[3] L.A. Rihbany and M.F. Delaney, *J. Chromatogr.*, 248 (1982) 125.
[4] S. Ting, *J. Assoc. Anal. Chem.*, 69 (1986) 169.
[5] W.R. Matson, *US Pat.*, 4 404 065 (Sept. 13, 1983).
[6] P.V. Leung and C.S. Tsao, *J. Chromatogr.*, 576 (1992) 245.
[7] *The United State Pharmacopeia*, Mack Printing Co., Easton, PA, 22nd revision, 1990.
[8] G.W. Schieffer, *J. Pharm. Sci.*, 68 (1979) 1296.
[9] J. Lepore, N. Lalli, J. Leal, K. Moll, C. Ruperto and A. Sanchez, *Internal Report 37542*, Hoffmann–La Roche, Nutley, NJ, 1984.
[10] S.T. Hamid and J. Walker, *Anal. Chim. Acta*, 105 (1979) 403.
[11] J.B. Kafil and T.A. Last, *J. Chromatogr.*, 348 (1985) 397.

ELSEVIER

Journal of Chromatography A, 667 (1994) 183–189

JOURNAL OF CHROMATOGRAPHY A

Direct optical resolution of vesamicol and a series of benzovesamicol analogues by high-performance liquid chromatography

David L. Gildersleeve *, Yong-Woon Jung, Donald M. Wieland

Division of Nuclear Medicine, Department of Internal Medicine, University of Michigan Medical School, Ann Arbor, MI 48109-0552, USA

(First received September 14th, 1993; revised manuscript received December 6th, 1993)

Abstract

The direct optical resolution of the vesicular acetylcholine uptake inhibitors vesamicol and benzovesamicol and nine benzovesamicol analogues were performed by HPLC on a commercially available cellulose tris(3,5-dimethylphenyl carbamate) chiral stationary phase. Separation of each enantiomeric pair was optimized with respect to solvent strength and flow-rate, using mobile phase mixtures of hexane–2-propanol–diethylamine. The method has been successfully applied to the analysis of the optical purity of benzovesamicol intermediates and products, including (−)-5-[^{123}I]iodobenzovesamicol which is currently undergoing clinical evaluation as a tracer for mapping central cholinergic neurons, and the purification of both antipodes of (±)-7-[^{125}I]iodobenzovesamicol.

1. Introduction

The availability of radiolabeled tracers to visualize cholinergic function *in vivo* could add significantly to our knowledge of parasympathetic neuronal dysfunction and the relationship between cholinergic neuronal degeneration and the onset of Alzheimer's disease. It could also potentially provide a means to monitor the efficacy of future neuron-sparing drugs in the treatment or prevention of this disease.

Vesamicol (AH 5183), (−)-*trans*-2-(4-phenylpiperidino)cyclohexanol (Fig. 1), is a potent, non-competitive inhibitor of acetylcholine uptake into the vesicles of cholinergic neurons [1–4]. Structural variants of vesamicol, especially those based on benzovesamicol [*trans*-2-hydroxy-3-(4-phenylpiperidino)tetralin], exhibit even higher affinity and selectivity for the vesicular binding site [4]. We have previously reported that 5-iodobenzovesamicol (5-IBVM), labeled with iodine-125, is a highly specific *in vivo*, presynaptic marker for cholinergic neurons in the brain [5]. It exhibits an avid and prolonged uptake into cholinergic-rich regions in mouse brain that is highly stereospecific for the (−)-

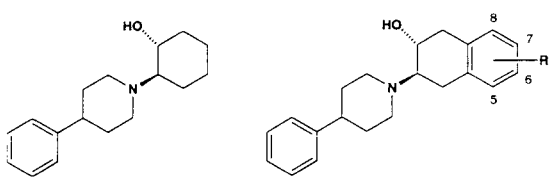

Vesamicol Benzovesamicols

Fig. 1. Structures of vesamicol and benzovesamicol analogues. R = H, I, NH_2, NH-Boc, $NHCH_3$, OH, OCH_3.

* Corresponding author.

0021-9673/94/$07.00
SSDI 0021-9673(93)E0013-K

isomer. Labeled with iodine-123, (−)-5-IBVM has been successfully used to obtain *in vivo* tomographic maps of the cholinergic nerve pattern in human brain [6,7]. Two additional tracers, (−)-5-[^{11}C]methylaminobenzovesamicol ([^{11}C]MABV) and (−)-5-[^{18}F]fluoroethoxybenzovesamicol ([^{18}F]FEOBV), are undergoing preclinical trials in our laboratories for use in positron emission tomography (PET). The [^{11}C]MABV tracer is synthesized from either (−)-5-aminobenzovesamicol [8] or (−)-5-N-Boc-aminobenzovesamicol [9]; [^{18}F]FEOBV is synthesized from (−)-5-hydroxybenzovesamicol [10].

The presence of the radiolabeled (+)-enantiomers would complicate the tomographic images and pharmacokinetic results obtained with these tracers. This could obscure differences between normal and diseased tissues. Therefore, it is essential that methods be developed both to resolve the synthetic precursors for the tracers of interest and to ensure that the final radiolabeled product is enantiomerically pure.

We previously described the use of the Chiracel OD column for the resolution of (±)-5-IBVM [5]. In support of our efforts to develop additional medical tracers for the non-invasive mapping of cholinergic nerves, this method has been extended to the resolution of additional benzovesamicol analogues. This paper describes the direct resolution, by normal-phase chiral HPLC, of the stereoisomers of (±)-benzovesamicol (BVM), (±)-5-aminobenzovesamicol (5-ABVM), (±)-5-N-methylaminobenzovesamicol (MABVM), (±)-5-N-Boc-aminobenzovesamicol (5-N-Boc-ABVM), (±)-5-iodobenzovesamicol (5-IBVM), (±)-6-iodobenzovesamicol (6-IBVM), (±)-7-iodobenzovesamicol (7-IBVM), (±)-8-iodobenzovesamicol (8-IBVM), (±)-5-hydroxybenzovesamicol (5-HOBVM) and (±)-5-methoxybenzovesamicol (5-MOBVM), as well as (±)-vesamicol (VM) itself. It also describes the application of the methods to the analysis of (−)-5-[^{123}I]-IBVM and the purification of the (−) and (+) antipodes of 7-[^{125}I]IBVM, whose (+) antipode has been found to be a highly selective marker for sigma binding sites in the brain [11].

2. Experimental

2.1. Reagents and chemicals

(±)-VM, (±)-BVM and (±)-5-ABVM were synthesized by the method of Rogers *et al.* [4]. The following compounds were synthesized by methods which we have described elsewhere: (±)-5-IBVM [5,12], (±)-6-IBVM [12] (±)-7-IBVM [12], (±)-8-IBVM [12], (±)-5-N-MABVM [8], (±)-5-N-Boc-ABVM [8], (±)-5-HOBVM [9] and (±)-5-MOBVM [13]. The enantiomers of 5-IBVM, 7-IBVM, 5-HOBVM and 5-ABVM were resolved by either preparative TLC or flash chromatography of their diastereomeric (*S*)-(−)-α-trifluoromethylphenylacetyl (MTPA) derivatives, followed by cleavage of the MTPA group [5,9,10,14]. (−)-BVM was synthesized from (−)-5-IBVM by reductive cleavage of the carbon–iodine bond with 10% palladium on activated carbon and hydrogen at atmospheric pressure. (−)-VM was obtained from Research Biochemicals (Natick, MA, USA). The racemic, positional isomers of IBVM were radiolabeled with iodine-125 by the solid-phase exchange method, which we have previously described [12,15,16].

Chromatographic solvents of HPLC grade were obtained from either EM Science (Gibbstown, NJ, USA) or Mallinckrodt Specialty Chemicals (Paris, KY, USA). Diethylamine of analytical-reagent grade was obtained from Fisher Scientific (Fair Lawn, NJ, USA) and was used without further purification. 1,3,5-Tri-*tert.*-butylbenzene was purchased from Aldrich (Milwaukee, WI, USA).

2.2. Apparatus and HPLC conditions

A Perkin-Elmer Model 241 automatic polarimeter was used to determine the identity of the optical isomers in ethanol solvent. The HPLC system consisted of a Waters Model 510 HPLC pump with U6K injection valve, and Model 486 UV–Vis detector (Millipore, Milford, MA, USA) Data were recorded on either a Spectra-Physics Model SP4400 ChromJet dual-channel integrator (San Jose, CA, USA) or

Table 1
Chromatographic conditions for analytical resolution of vesamicol and benzovesamicol analogues

Compound	*n*-Hexane–2-propanol (v/v)	Flow-rate (ml/min)
VM	99:1	1.0
BVM	95:5	1.0
5-IBVM	95:5	1.0
6-IBVM	95:5	1.0
7-IBVM	95:5	1.0
8-IBVM	95:5	1.0
5-HOBVM	85:15	1.5
5-MOBVM	99:1	1.5
5-ABVM	50:50	1.0
5-N-Boc-ABVM	95:5	1.0
5-MABVM	90:10	1.0

Millenium 2010 Chromatography Manager (Millipore). Where required, a radioactivity flow detector, consisting of a Bicron (Newbury, OH, USA) Frisk-Tech rate-meter/ monitor, fitted with a G1LE probe and a 3-μl PTFE flow-cell, was attached to the outlet of the UV–Vis detector to monitor for radioactivity eluting from the column. The column was a Chiracel OD (Daicel; 10 μm particle size, 250 × 4.6 mm I.D.) from J.T. Baker (Phillipsburg, NJ, USA). The mobile phase consisted of a mixture of *n*-hexane, 2-propanol and diethylamine as described in Table 1. Flow-rates are also listed in Table 1. Column effluent was monitored at 254 nm. The column void volume (t_0) was determined for each mobile phase mixture and flow-rate combination by injecting 10 μg of 1,3,5-tri-*tert.*-butylbenzene in 10 μl of *n*-hexane–2-propanol (98:2, v/v). Resolutions (R_s), separation factors (α) and capacity factors (k') were calculated as previously described [17].

3. Results and discussion

With the current large selection of commercially available chiral stationary phases (CSPs), choosing the proper CSP can be difficult. No one CSP is capable of resolving all classes of compounds. Fortunately, vesamicol and the benzovesamicols possess a hydroxyl group at the chiral center, much like the β-adrenergic blockers atenolol, propanolol, pindolol and metoprolol. Very efficient direct resolution of these β-blockers has been obtained on a tris(3,5-dimethylphenylcarbamate) cellulose coated silica column (Chiracel OD) [18–20]. Therefore, the Chiracel OD column was selected for this work.

As recommended by the column manufacturer, the mobile phase was limited to mixtures of *n*-hexane and 2-propanol. The mobile phase composition was optimized for each racemic pair by varying the concentration of 2-propanol until the desired capacity factors were obtained (Table 1); a small amount of diethylamine (0.1%, v/v) was added to reduce potential solute tailing, especially for 5-ABVM and its derivatives. The flow-rates were then varied to optimize column efficiency but no attempt was made to optimize the temperature, despite the observation that the efficiency of this type of chiral column can be increased by operating at an elevated temperature (40°C) [21].

The Chiracel OD column resolved all eleven racemic compounds that were tested; the results are summarized in Table 2. Resolution of the lead compounds in this series, VM and BVM, is illustrated in Fig. 2. The enantiomers of both compounds were well resolved with a resolution of 1.5 or larger. In Fig. 3, the resolution of the enantiomers of the four positional isomers of IBVM is shown. For the purposes of comparison, the experimental conditions (Table 1) were optimized for the resolution of the antipodes of (±)-8-IBVM and were then applied to the other three isomers. These compounds exhibited the most efficient resolution on this column, and the enantiomers of 5-IBVM and 7-IBVM were the most readily resolved of all the compounds tested. The resolution of the enantiomers of 8-IBVM was larger than 1.0 while that of the other three isomers was larger than 1.5. The electron-withdrawing effect of the large halogen group may be responsible for the greater resolution exhibited by this series of compounds. This hypothesis will be tested on future BVM derivatives bearing a variety of large, electron-withdrawing groups.

The enantiomers of compounds that bear an

Table 2
Capacity factors (k'_1 and k'_2), separation factors (α), resolution factors (R_s) and retention times (t_{R1} and t_{R2}) in the chiral resolution of vesamicol and benzovesamicol analogues

Compound	k'_1	k'_2	α	R_s	t_{R1} (min)[a]	t_{R2} (min)[a]
VM	2.13	2.40	1.13	1.49	9.41 (−)	10.23 (+)
BVM	2.30	2.67	1.16	1.64	9.93 (−)	11.03 (+)
5-IBVM	1.79	2.82	1.58	2.56	8.22 (−)	11.29 (+)
6-IBVM	3.33	4.45	1.34	1.70	12.72	16.02
7-IBVM	4.59	7.12	1.55	2.46	16.44 (−)	23.86 (+)
8-IBVM	3.28	4.01	1.22	1.12	12.58	14.72
5-HOBVM	2.55	3.11	1.22	0.78	6.94 (−)	8.04 (+)
5-MOBVM	2.19	2.59	1.18	0.97	9.27 (−)	10.44 (+)
5-ABVM	1.83	2.24	1.22	1.38	8.25 (+)	9.44 (−)
5-N-Boc-ABVM	4.39	5.64	1.28	1.43	15.69 (−)	19.33 (+)
5-MABVM	3.47	3.98	1.15	1.02	13.00 (−)	14.50 (+)

Column: 250 × 4.6 mm I.D. Chiracel OD; eluent mixture and flow-rate as described in Table 1.
[a] When known, the identity of the drug enantiomer is given.

electron-donating group, the amino and hydroxyl group in particular, were also resolved by the Chiracel OD column. Fig. 4 illustrates the separation the enantiomers of (±)-5-ABVM, as well as the enantiomers of its N-methyl (5-MABVM) and N-Boc (5-N-Boc-ABVM) derivatives. The enantiomers of all three compounds exhibited resolutions larger than 1.0. The separation of the enantiomers of the 5-hydroxyl derivative of BVM (5-HOBVM) and its methoxy derivative (5-MOBVM) are shown in Fig. 5. The 5-MOBVM enantiomers were separated with a resolution of almost 1.0. While being the least resolved of all of the eleven vesamicols tested, the separation of the enantiomers of 5-HOBVM, with a resolution of 0.78, was sufficient for monitoring the purification of the (−)-enantiomer as its MTPA derivative as described above. Since (−)-5-HOBVM is only an intermediate in the synthesis of (−)-5-MOBVM, additional proof of enantiomeric purity is provided by analysis of its O-methylated product (−)-5-MOBVM. It is apparent that the enantiomers of compounds that possess either electron-withdrawing or electron-donating groups can be resolved on this column.

The elution order of the enantiomers was

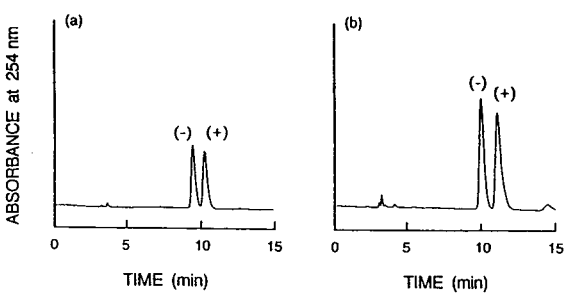

Fig. 2. Resolution of (a) vesamicol and (b) benzovesamicol enantiomers. Chromatographic conditions as described in Table 1.

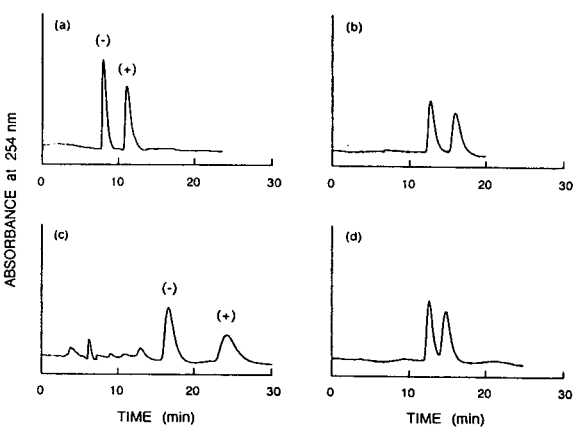

Fig. 3. Resolution of the enantiomers of positional isomers of IBVM: (a) 5-IBVM, (b) 6-IBVM, (c) 7-IBVM and (d) 8-IBVM. Chromatographic conditions as described in Table 1.

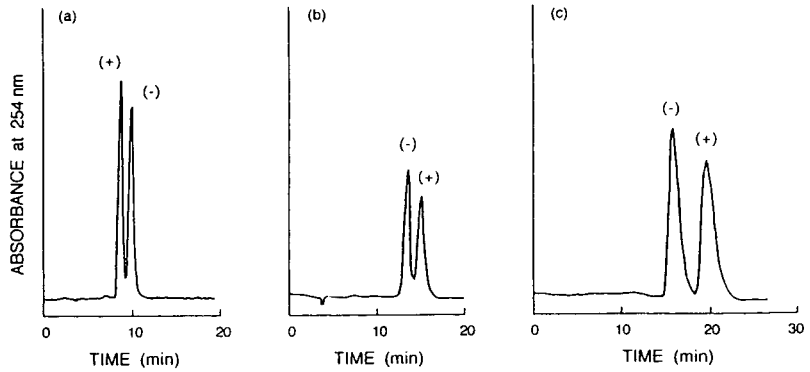

Fig. 4. Resolution of the enantiomers of (a) 5-ABVM, (b) 5-MABVM and (c) 5-N-Boc-ABVM. Chromatographic conditions as described in Table 1.

determined for nine of the eleven racemic pairs. In all cases but one, the (−)-enantiomer, which may be assigned the *R,R* configuration, eluted first. The single exception was (±)-5-ABVM, whose (+)-(*S,S*)-enantiomer eluted first. However, after derivatization of the aniline group with either a methyl group (5-MABVM) or Boc group (5-N-Boc-ABVM), the elution order reverts to the (−)-enantiomer eluting first. The mechanism responsible for this phenomenon has yet to be determined, but appears not to be due to the presence of an electron-donating group since the elution order for the antipodes of 5-HOBVM were not inverted.

This method was applied both to the direct analysis of enantiomeric purity and to the chiral purification of radiolabeled derivatives of benzovesamicol. Fig. 6 illustrates the application of this method to the analysis of optical purity of iodine-123 labeled (−)-5-IBVM, which had been synthesized via iododestannylation of the respective tributyltin precursor [22]. The 5-tributyltin-BVM precursor was itself synthesized from (−)-5-IBVM that was >98% optically pure. The radiolabeled product was identified as the (−)-enantiomer and determined to also be >98% optically pure, thus preserving the optical integrity and purity of the synthetic precursors. Fig. 7 illustrates the application of this method to

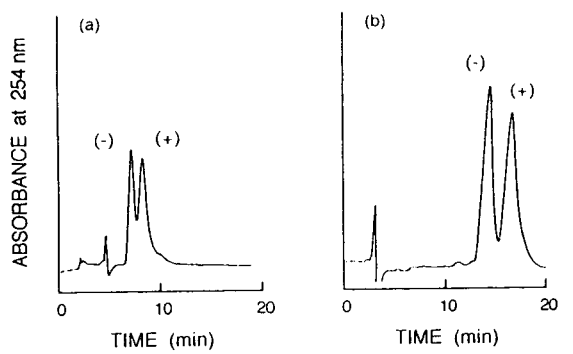

Fig. 5. Resolution of the enantiomers of (a) 5-HOBVM and (b) 5-MOBVM. Chromatographic conditions as described in Table 1.

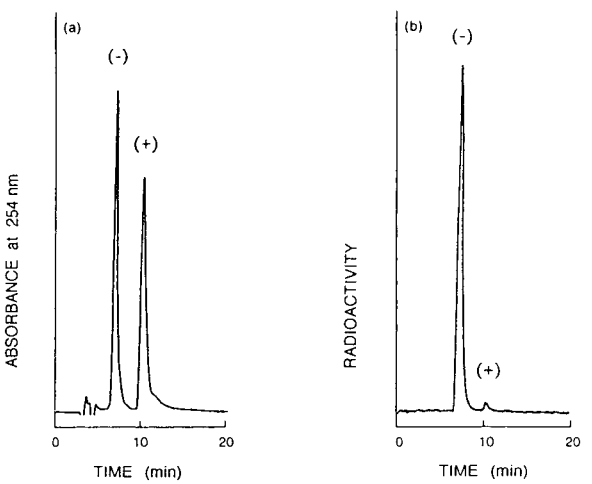

Fig. 6. Test of the optical purity of (−)-5-[^{123}I]iodobenzovesamicol spiked with carrier (±)-5-IBVM: (a) UV trace of racemic 5-IBVM carrier and (b) radioactive trace of the iodine-123 labeled product which preserves the optical purity of the precursor tin compound (optical purity >98%). Chromatographic conditions as described in Table 1.

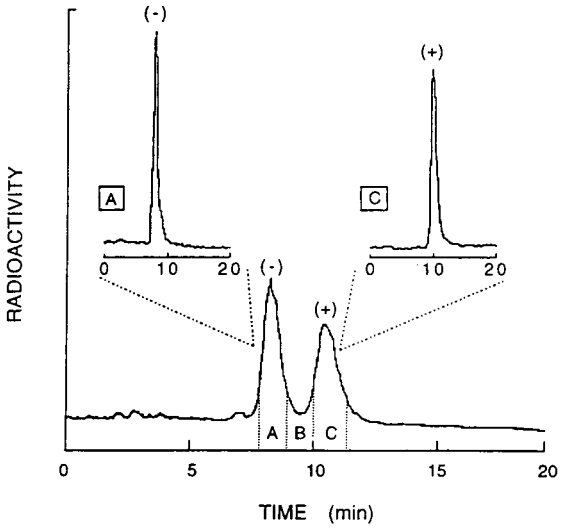

Fig. 7. Chiral purification of the (−) and (+) enantiomers of racemic 7-[^{125}I]iodobenzovesamicol. Insets: Test of enantiomeric purity of the purified antipodes. Mobile phase: *n*-hexane–2-propanol (90:10, v/v); flow-rate, 1.5 ml/min.

the purification of the (−) and (+) antipodes of iodine-125 labeled (±)-7-IBVM (specific activity >140 Ci/mmol) and the analysis of the optical purity of the isolated enantiomers, which is shown in the two insets. To improve recovery of the later eluting peak, the chromatographic conditions, described under the figure, were modified from those described in Table 1. Three fraction cuts, heart fractions of each enantiomer with an intermediate fraction containing a mixture of both, were made on the basis of the response levels of the radioactivity detector and are indicated in the figure. Reinjection of an aliquot of each of the isolated peaks onto the same column showed that both enantiomers were >99% optically pure (see insets).

In summary, the chiral HPLC technique described makes possible the rapid, direct optical resolution of all eleven vesamicols tested. This approach is especially effective in resolving (−)-5-IBVM and (+)-7-IBVM, which in radioiodinated form are selective *in vivo* markers for the vesamicol and sigma binding sites, respectively. The methodology is not only applicable to the routine determination of the chiral purity of these two radiotracers, but because of the associated low mass levels, it can also be used to purify multi-mCi amounts of chirally pure tracer from racemic mixtures for research purposes.

4. Acknowledgements

This work was supported by the National Institutes of Health Grant No. NS-25656. We thank Linder Markham for assistance in preparing the manuscript and the Phoenix Memorial Laboratory of the University of Michigan for the use of their facilities.

5. References

[1] I.G. Marshall and S.M. Parsons, *Trends Neurosci.*, 10 (1987) 174–177.
[2] M.R. Marien, S.M. Parsons and C.A. Altar, *Proc. Natl. Acad. Sci. U.S.A.*, 84 (1987) 876–880.
[3] C.A. Altar and M.R. Marien, *Synapse*, 2 (1988) 486–493.
[4] G.A. Rodgers, S.M. Parsons, D.C. Anderson, L.M. Nilsson, B.A. Bahr, W.D. Kaufman, R.S. Jacobs and B. Kirtman, *J. Med. Chem.*, 32 (1989) 1217–1230.
[5] Y.-W. Jung, M.E. Van Dort, D.L. Gildersleeve and D.M. Wieland, *J. Med. Chem.*, 33 (1990) 2065–2068.
[6] D.E. Kuhl, R.A. Koeppe, J.A. Fessler, S. Minoshima, R.J. Ackermann, J.E. Carey, K.A. Frey and D.M. Wieland, *J. Nucl. Med.*, 34 (1993) 25P.
[7] D.E. Kuhl, R.A. Koeppe, J.A. Fessler, S. Minoshima, R.J. Ackermann, J.E. Carey, D.L. Gildersleeve, K.A. Frey and D.M. Wieland, *J. Nucl. Med.*, (1994) in press.
[8] M.R. Kilbourn, Y.-W. Jung, M.S. Haka, D.L. Gildersleeve, D.E. Kuhl and D.M. Wieland, *Life Sci.*, 47 (1990) 1955–1963.
[9] G.K. Mulholland and Y.-W. Jung, *J. Lab. Compd. Radiopharm.*, 31 (1992) 253–259.
[10] G.K. Mulholland, Y.-W. Jung, D.M. Wieland, M.R. Kilbourn and D.E. Kuhl, *J. Lab. Compd. Radiopharm.*, 33 (1993) 583–591.
[11] Y.-W. Jung, D.L. Gildersleeve, M.E. Van Dort, D.E. Kuhl and D.M. Wieland, presented at the *10th International Symposium on Radiopharmaceutical Chemistry, Kyoto, 1993,* abstract, pp. 202–204.
[12] Y.-W. Jung, P.S. Sherman, M.E. Van Dort, G.K. Mulholland, A. Chen, R. del Rosario, K.A. Frey, D.E. Kuhl and D.M. Wieland, *J. Med. Chem.*, in preparation.
[13] Y.-W. Jung, G.K. Mulholland, P.S. Sherman, T.L. Pisani, M.R. Kilbourn, G.D. Hutchins and D.M. Wieland, *J. Nucl. Med.*, 32 (1991) 974.
[14] J.A. Dale, D.L. Dull and H.S. Mosher, *J. Org. Chem.*, 34 (1969) 2543–2549.

[15] T.J. Mangner, J.L. Wu and D.M. Wieland, *J. Org. Chem.*, 47 (1982) 1484–1488.
[16] M.E. Van Dort, M.R. Kilbourn, P.K. Chakraborty, E.K. Richfield, D.L. Gildersleeve and D.M. Wieland, *Appl. Radiat. Isotop.*, 43 (1992) 671–680.
[17] L.R. Snyder and J.J. Kirkland, *Introduction to Modern Liquid Chromatography*, Wiley, New York, 2nd ed., 1979, Ch. 2, pp. 22–37.
[18] Y. Okamoto, M. Kawashima, R. Aburanti, K. Hatada, T. Nishiyama and M. Masuda, *Chem. Lett.*, (1986) 1237–1240.
[19] A.M. Krstulovic, M.H. Fouchet, J.T. Burke, G. Gillet and A. Durand, *J. Chromatogr.*, 452 (1988) 477–483.
[20] M.S. Ching, M.S. Lennard, A. Gregory and G.T. Tucker, *J. Chromatogr.*, 497 (1989) 313–318.
[21] A. Katti, P. Erlandsson and R. Dappen, *J. Chromatogr.*, 590 (1992) 127–132.
[22] M.E. Van Dort, Y.-W. Jung, D.L. Gildersleeve, C.A. Hagen, D.E. Kuhl and D.M. Wieland, *Nuc. Med. Biol.*, 20 (1993) 929–937.

ELSEVIER

Journal of Chromatography A, 667 (1994) 191–203

JOURNAL OF CHROMATOGRAPHY A

Constancy of spectral response ratios in the flame photometric detector

Xun-Yun Sun ☆, Walter A. Aue *

Department of Chemistry, Dalhousie University, Halifax, Nova Scotia B3H 4J3, Canada

(First received October 19th, 1993; revised manuscript received January 20th, 1994)

Abstract

The response ratio of a chromatographic peak in two optically different channels of the flame photometric detector depends little if at all on the size of the peak (analyte concentration), as long as the latter remains within the linear range of both calibration curves. However, if *wide* wavelength ranges are monitored for analytes with *multiple* emitters of a *different* kinetic order (non-linear calibration curves), response ratios may become subject to variation. Such variation may also occur if multiple-emitter luminescence is variably quenched and/or if the linear range of the analyte is exceeded. These effects are demonstrated with compounds of Cr, Fe, Mn, P, Sn and, particularly, S. In contrast, if *narrow* ranges of properly selected wavelengths can be monitored —so that a *single* emitter predominates— the constancy of response ratios will be maintained even if heavy levels of a quencher and/or multiple emitters of different kinetic orders are present in the flame. For instance, the response ratios of sulfur remain constant under these circumstances both in the conventional quadratic and the novel linear response mode.

1. Introduction

Recent developments have significantly broadened the role of the flame photometric detector (FPD). Once limited to sulfur and phosphorus [1,2], it is now known to respond to some twenty elements [3]; once restricted to gaseous inputs, it is now used with such techniques as micro-HPLC [4] and supercritical fluid chromatography [5]. For the well responding elements, it performs superior to other types of instrumentation [6]. In its two-channel configuration it can produce chromatograms that are nominally specific (*i.e.*, of apparent infinite selectivity) for *any* luminescing element [7].

Such chromatograms are based on the response ratio (RR) of the selected element in the two FPD channels. This, however, is not the only role RRs can play. They can also serve in elemental recognition and confirmation, as well as in the subtraction of carbon matrix components [8,9] and of other types of interfering peaks. Differently expressed, RRs provide an additional, chemical dimension for chromatograms [10]. This dimension is not restricted to the FPD: any detector with two or more channels that produce synchronous peaks (or peaks of equal or at least adjustable dispersion) could be

* Corresponding author.

☆ Part of *Ph.D. Thesis*. Present address: Department of Chemistry, University of Missouri–Rolla, Rolla, MO, USA.

0021-9673/94/$07.00
SSDI 0021-9673(94)00062-E

used (*cf.* ref. 11). The obvious condition for *profitable* use of additional dimensions is their "orthogonality", *i.e.* the ability of different channels to extract significantly and sufficiently different chemical (or physical) information from the analyte.

If RR values are to play these important roles consistently and reliably in the analytical laboratory, they have to be invariant in analyte as well as quencher concentrations. (A quencher, in the narrow sense of the FPD, is a substance that reduces the luminescence of the analyte peak; a process that occurs, for instance, in the well known depression of sulfur response by co-eluting hydrocarbons [2,12–21]. In the wider context of spectroscopic flames, or of detection in general, other species or processes may perform roles similar to that of the typical FPD quencher). It is not possible to ensure the complete absence of quenchers in the FPD: column bleed, hydrocarbonaceous fragments from the analyte molecules themselves, and residual contamination from irreversibly absorbed and/or decomposed compounds are almost always present.

Although RR values in the FPD have proven to be fairly constant, exceptions have emerged [10]. Yet, no study has so far followed RR behavior over the full range of analyte and quencher concentrations. This neglect may have been justified for elements with only one emitter. For elements with multiple emitters, however —in particular when contained in multi-element samples and monitored over spectral ranges wide enough to allow optical access to *all* luminescing species— the constancy of RR values has to be ascertained before the various methods that depend on it [7–10] can be used in full confidence.

Why would the presence of more than one emitter —in other words of multiple spectra— change the constancy of RR values? The most obvious case occurs when the emitters follow different kinetic orders. The classic example here is again that of sulfur, which produces both second-order [1,12] and first-order [22] emitters. When these are simultaneously observed (*e.g.* when there is inadequate or no wavelength discrimination between the two emitters) the spectrum of the former dominates at high, that of the latter at low analyte concentrations. The spectral mix, hence the RR value, thus *changes* with concentration.

Most FPD-active elements produce solely first-order (linear) emitters. If all emitters of a particular element are linear, its spectral mix —and, in consequence, its RR value— should remain constant over the whole linear response range of analyte concentration. However, the calibration curves for the different emitters may not all start to deviate from linearity at the same concentration. Or the different emitters may be influenced by a quencher in a different way or to a different extent. *Beyond* linear range, then, and/or in the presence of variable concentrations of a quencher, RR values could loose their constancy (and with it their analytical *raison d'être*).

Other factors exist as well that could alter the spectral mix of multiple emitters: temperature (column bleed), detector memory (system contamination), long-term repeatability of flow settings, etc. However, these factors are neither consistently reproducible nor meaningfully reportable, and they do not lend themselves to the same kind of systematic investigation as the straightforward variations of analyte and quencher levels. This study will therefore be restricted to the latter.

One further variable needs to be considered here: the optical ranges in which the luminescence is to be monitored. If both FPD channels are limited to one and the same emitter, the presence of others should not matter. However, such restrictive conditions are sometimes unattainable, sometimes undesirable. Extensive band systems or continua may overlap the primary emission of interest; or a survey-type analysis may call for a spectrally wide-open range in order to register *all* FPD-active elements. Also, sensitivity considerations may demand broader optical windows.

Clearly, there exist two extreme sets of conditions for dual-channel FPD measurements: broad ("polychromatic") and narrow ("monochromatic") spectral windows. Either case (or a combination of the two) may be chosen for good analytical reasons. (Given the 10-nm bandpass typical of a narrow-band interference filter, the

term "*mono*chromatic" is used here rather loosely.)

Typical optical combinations of the polychromatic variety could comprise an open (filterless) channel plus one equipped with a shortpass (SP) or longpass (LP) filter, or two channels fitted with overlapping SP and LP filters. Both channels would carry wide-range (UV-sensitive, red extended) photomultiplier tubes. In contrast, the typical case of the monochromatic (really: bichromatic) variety would rely on two channels both fitted with narrow-band interference filters (and appropriate photomultiplier tubes).

In general, the polychromatic mode is more sensitive and offers simultaneous detection/determination for most or all FPD-active analytes; the bichromatic mode is better suited to monitoring one element only. Although the latter mode is more likely to display the desired constancy of the two-channel response ratios, the former is in even greater need of investigation because it represents —in our opinion, at least— a scenario that is analytically the more important, spectroscopically the more interesting, and technically the more demanding of the two. If RRs are wont to vary, they are more likely to do so when probed at a multitude (rather than at just a pair) of wavelengths.

Checking for the constancy of RR values could, however, become an endless task. For instance: what detector conditions should be chosen? Individually optimized conditions for each element? If so, should they be optimized for sensitivity, or selectivity, or RR constancy? And, if optimized for selectivity: selectivity against which element? Or, in contrast, should one common condition be selected that could fit all elements equally well (or badly)? Or a common condition that would be close to optimal for one (important) element while still allowing others to respond? Good analytical reasons could be found for pursuing each one of these alternatives. Each on its own would, however, require considerable experimental effort.

Since sulfur is the most important analyte in the FPD, and since we have recently described in detail a new linear mode for its detection/determination [22], it seems reasonable for us to use its conditions for all elements. Also, only the most important and/or representative of the twenty-some elements that respond in the FPD will be scrutinized: the main-group elements [7] sulfur, phosphorus and tin; and the transition metals [6] chromium, manganese and iron. We shall start with the broadest optical windows possible, but narrow them down severely as soon as the RR values start to show signs of diversion.

2. Experimental

All experiments were carried out on a 1974 Model Shimadzu GC-4BMPF gas chromatograph with dual-channel FPD. The conditions, unless otherwise indicated, were those of the linear sulfur mode described earlier [22], *i.e.* 500 ml hydrogen and 40 ml air per minute, with the quartz chimney removed. The FPD was situated under an efficient exhaust duct for safety reasons. The nitrogen flow through the 1-m 5% OV-101 packed column was usually between 20 and 26 ml/min. The column temperature was chosen such that analytes would elute at a retention time of about 2 min, with σ values of approximately 5 s. Both FPD channels carried Hamamatsu R-374 phototubes (nominal range 180 to 850 nm, maximum response at 420 nm). Optical filters were used as needed; they are described in the captions to the figures. Methane, serving as quencher, was usually added through an in-line bubble flow meter to the hydrogen supply (which mixes with the column effluent before emerging around the central air jet). In one case (Fig. 4), methane was added to the hydrogen supply line via an exponential dilution flask. (Both methods yield essentially the same result; however, the exponential dilution flask does so with greater speed, the bubble flow meter with greater accuracy.)

3. Results and discussion

Fig. 1 shows the dependence of response ratios on analyte concentration through very wide spectral windows, one completely open, the

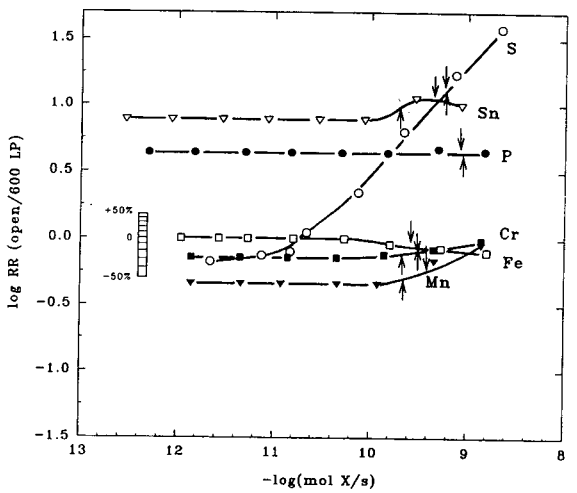

Fig. 1. Dependence of response ratios on analyte concentration for six test elements through and beyond their linear response range in the absence of a quencher. First channel: filterless; second channel: 600-nm longpass (600 LP) filter. Flow conditions are those of the linear sulfur mode. Downward and upward pointing arrows indicate the end of the linear calibration range in the first and second channel, respectively. ○ = Thianaphthene (X = S); □ = ferrocene (Fe); ▽ = tetra-*n*-butyltin (Sn); ● = diphenylmethylphosphine (P); ■ = chromium hexacarbonyl (Cr); ▼ = MMT (Mn).

other open to wavelengths above *ca.* 600 nm. The measurement starts at some convenient concentration at which the baseline noise no longer influences the measurement —inconstancy occurs at high, not low analyte levels!— and stretches deliberately beyond the analytical range of the six test elements. The conventional calibration curves themselves are not shown here, but the upper ends of their linear ranges (defined by a 10% deviation from linearity) are indicated in Fig. 1 by arrows: pointing down for the open (filterless) channel, pointing up for the 600 nm longpass-filter channel. (In the case of sulfur, the down arrow marks the end of the *quadratic* range.) A percent deviation scale is put in place for the iron curve; it can, of course, be shifted up or down to serve *any* element.

With the exception of sulfur —whose behavior will be discussed later— the RR values are *constant* over the *linear* concentration range. Their deviations in that region do not normally exceed the random error of measuring peak heights on a recorder chart. Only when the calibration curves approach or exceed the upper ends of their linear ranges do the RR values begin to diverge from their former constancy. Thus, as a rule of thumb, *spectral response ratios are independent of analyte concentration within linear range.*

For the apparently constant RR ranges —*i.e.* for the first four to six points of all curves except that of sulfur in Fig. 1— the relative standard deviation was measured as approximately 2%; it never exceeded 4%. (The same is true for Fig. 2.) This deviation is typical of the manual peak height measurements used in this study. If a worst-case 4% R.S.D. is assumed, and the condition is further imposed that each curve must be at least 6 standard deviations away from the next (*i.e.* a 99.7% correct assignment in the case of a normal error distribution), the + 1.5 to − 1.5 log RR range shown in Fig. 1 could accommodate 30 curves. (Log RR values higher than + 1.5 or lower than − 1.5 can obviously be measured, but such measurements are subject to increasingly wide error bands if carried out at trace levels of analyte.) It is, of course, statistically highly improbable that 30 curves could thus be stacked into the given space merely by the judicious choice of two wavelength regions. It is, however, equally obvious that a few more elements could be safely added to Fig. 1 (that is, under an —in this context— *incidental* spectral regime).

Thus, if the response ratios of other FPD-active elements should turn out to be as independent of analyte concentration as those of Fig. 1 (a reasonable assumption for linear emitters), most if not all of them could fit into a convenient range of RR values without overlapping —*i.e.* they could be safely used for recognition and confirmation of elemental composition [10], as well as for generation of element-specific [3,7] or otherwise computer-adjudicated [9] chromatograms. *One* chromatographic run could therefore identify, at least in theory, *all* FPD-active elements.

What, however, happens to RRs under *quenching* conditions? To answer that question, the standard quencher methane was introduced at arbitrary but constant levels; levels that re-

duced the analyte peaks to between 60 and 30% of their original height. Calibration curves were measured in the presence of methane in open and >600 nm channels. Table 1 lists for illustration and later reference the experimental flows of methane and the percent quenching they caused in the two channels; Fig. 2 shows the variation of response ratios as plots of log RR *vs.* molar analyte flow. These results are very similar to those displayed in Fig. 1 in that the *response ratios can be considered constant under constant quenching conditions over the linear range of the calibration curve.* This occurs even though the percentage of quenching often differs significantly between the two channels.

The only and obvious exception to the claimed constancy of RR values in Figs. 1 and 2 is provided by the case of sulfur. This should come as no surprise: under the flow conditions of the linear sulfur mode, but with the optical channel wide open, the linear (HSO) sulfur emission dominates at low, the quadratic (S_2) sulfur emission at medium and high concentrations. The former is situated mainly in the red [22], the latter in the near ultraviolet and violet (with considerable extensions to the blue, the green, and beyond). The "open/600 LP" RR values for the two (pure) emissions are hence very different. Since one follows first-order but the other (roughly) second-order kinetics, the composite luminescence strays over much of Figs. 1 and 2. If *constant* RR values are required, optical

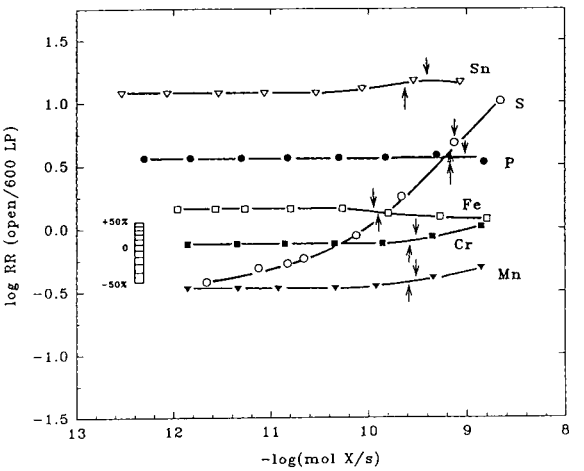

Fig. 2. Dependence of response ratios on analyte concentration in the presence of a quencher (methane). Conditions are similar to those in Fig. 1. The added constant flows of methane range from 2.0 to 8.0 ml/min, the quenching from about 30 to about 60% (see Table 1). Symbols as in Fig. 1.

conditions will have to be chosen such that *one* spectrum predominates over the entire analyte concentration range. We shall return to this problem later.

While Figs. 1 and 2 agree that RRs (that of sulfur excepted) are constant, they disagree on some (not all) of their *absolute* values. An overlay of the two figures points to particularly obvious discrepancies in the cases of tin and manganese. Given the absence of severe inter-experimental changes in flow settings, detector

Table 1
Experimental methane flows *vs.* resulting quenching for various elements in two detector channels

Analyte	Methane (ml/min)	Quenching (%)	
		Open	600 nm longpass filter
Thianaphthene	8.0	28	31
Diphenylmethylphosphine	4.3	39	50
Ferrocene	6.2	44	30
Chromiumhexacarbonyl	2.0	50	52
Tetra-*n*-butyltin	3.3	58	36
Methylcyclopentadienyl manganese tricarbonyl	4.0	32	45

contamination, etc., what basic explanation could be advanced for this behavior?

The most probable explanation is that both of these elements respond via more than one emitter. Although their spectra have not yet been measured at the flow conditions of the linear sulfur mode, their emissions at individually optimized settings have: tin produces the SnOH and SnH bands as well as a blue surface luminescence on quartz [23]; manganese yields two strong atomic lines, a sizable continuum [8], and perhaps some molecular bands. These features should be present here as well. Although the quenching mechanisms are unknown for these (as well as for all other) emitters, their relative quenching efficiencies could be expected to differ. But any such difference could cause significant differences in spectral distribution between the (partially) quenched and the unquenched luminescence, and hence lead to a significant change in RR value.

The comparison of Figs. 1 and 2, while pointing to a problem, fails to define its full extent. In Fig. 2 the quencher is present at an (arbitrarily chosen) constant level. What about varying levels of the quencher? What about varying levels of the analyte? The intuitive expectation about the quencher is, of course, that higher levels should lead to larger RR discrepancies; while the empirical expectation about the analyte is that higher levels (with the quencher concentration remaining constant) should make little or no difference. (The latter presumes that the analyte remains within the linear range of both calibration curves and, more importantly, that percent quenching is inherently independent of analyte concentration. That view is shared by most but by no means all researchers in the field [2,5,12–17], owing perhaps to the many different FPD conditions under which quenching phenomena can and have been observed.)

Fig. 3 shows the response ratios of various elements challenged by increasing levels of quencher, all at the same detector conditions. The response ratios remain constant (within 10%) until the open-mode peak is quenched by more than approximately 20% for Sn, S and Mn; 30% for Cr; 70% for P; and 90% for Fe. (Due to the

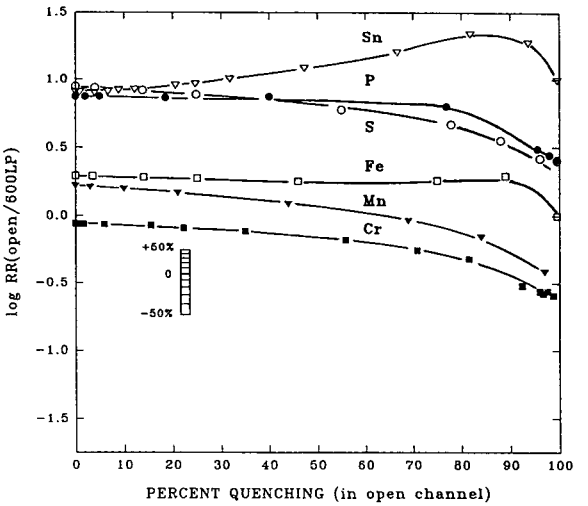

Fig. 3. Dependence of response ratios on percent quenching. Quenching percentages on the x axis are those of the filterless ("open") channel. The optical conditions are the same as in Figs. 1 and 2. However, flow conditions may have slightly changed due to time (and resetting of flows) between the two experimental series, and different test compounds were used for Mn and Cr. ○ = Thianaphthene; □ = ferrocene; ▽ = tetra-*n*-butyltin; ● = diphenylmethylphosphine; ■ = benzenechromium tricarbonyl; ▼ = cyclopentadienylmanganesetricarbonyl.

poor measurement conditions at quenching efficiencies higher than 90%, data points in that region are less reliable, though analytically also less interesting.)

The quenching of FPD peaks can be traced not only to the co-elution of hydrocarbonaceous components [12–21] of the sample —including the solvent tail— but also to column bleed [17] and other types of contaminants. Usually the latter are persistent in nature but also relatively low in concentration and small in effect. Often that effect is already included in the calibration curves and hence would not be separately recognized by the analyst.

Note that the data points describe the response ratio in two different optical channels of the *same* eluting peak, hence refer to the self-same quencher concentration. However, the extent of quenching as measured in the two channels may strongly differ. A choice has therefore to be made which channel to use for the —analytically important— "percent quenching"

efficiency shown on the abscissa. The open (= filterless) channel is chosen because it represents the most general and the most widely applicable of optical conditions.

It may be asked how the same quencher concentration can lead to apparently different percentages of quenching (compare Table 1) on two different optical channels. A variety of circumstances can cause such an effect.

First, and by far most likely, the analyte may produce two or more different emitters that are (directly or indirectly) quenched to different extents. Second, a single emitter may be excited by two or more processes of energy transfer (as an example only: 4.5 eV from H + H and 5.2 eV from H + OH) in which (a) the same emitter reaches different upper vibrational (in the case of atoms: electronic) levels and (b) the relative concentration of the radicals responsible (in this example: H and OH) is influenced by the concentration of the quencher. Third, different excited states of even the same emitter may be quenched to different degrees. Fourth, emissions may be present that originate from species other than the analyte, and are subject to quenching by a different mechanism and to a different extent. The always present OH or the usually present CH provide cases in point. Fifth, the ubiquitous —and often slowly changing— FPD background (baseline luminescence) may also be quenched differently at different wavelengths. For instance, the analyte itself could be draining the excitation energy of ambient emissions. Several more scenarios, or combinations thereof, appear possible. In general, such effects are likely to be exacerbated if FPD conditions change (by temperature programming, premature sample decomposition, etc.) and/or if different emitters follow different kinetic orders.

An example of the degree to which two emitters of a different kinetic order can influence the response ratio is shown in Fig. 4. It is presented here not only to illustrate a particular problem —which will later be explored and rectified— but also to address, at least in passing, the most prominent mode of the most prominent FPD analyte. The analyte is (of course) sulfur, but the detector flow conditions

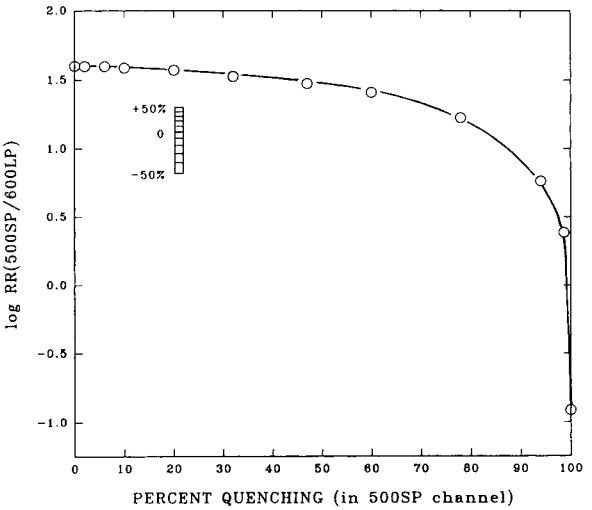

Fig. 4. Dependence of sulfur response on percent quenching at conditions of the quadratic mode. Analyte: 8 ng bis(*tert.*-butyl)disulfide. Flows in ml/min: hydrogen (total) 50, air 40, nitrogen (column) 26. This measurement series uses the commercial quartz chimney and introduces methane (the quencher) into the hydrogen flow via an exponential dilution flask. 500SP = 500-nm shortpass filter.

chosen here are not those of the new linear mode [22] as used for Figs. 1–3, but those of the conventional quadratic mode [2,12]. The 500-nm shortpass filter admits almost all of the quadratic S_2 emission while the 600-nm longpass filter accepts mainly the linear sulfur emitter (though the latter under less than ideal circumstances). The two emitters are influenced to different degrees by the presence of the quencher, resulting in a dramatic effect: the response ratio displayed in Fig. 4 varies by more than two orders of magnitude! A similarly dramatic variation of the response ratio occurs when the concentration of the analyte —rather than that of the quencher— is changed. In fact, it was a comparable experiment that provided the first clue to the presence of a linear sulfur emitter in the FPD [10].

Clearly, it should be demanding as well as rewarding to change the optical conditions such that —in the ideal case— only two transitions off the same excited state are sampled and that, therefore, the response ratios do remain constant *regardless* of quencher and analyte concentra-

tions. Only then could the analyst who is exclusively interested in, say, sulfur, draw conclusions about the presence or absence of that element in chromatographic peaks without having to be mindful of sample composition, peak height correlation and detector contamination. (At the same time, the analyst interested in a broad range of elements may well prefer the widest optical conditions for an all-inclusive though conceivably precarious and possibly preliminary look at the elemental composition of peaks contained in a complex sample.)

If previous thoughts about multiple spectra and/or excitation modes are any guide, the best chance for obtaining constant response ratios for sulfur in the quadratic mode seems to lie in monitoring, through narrow-band interference filters, two strong bands of the dominant S_2 system —preferably two bands that originate from the same upper vibrational level ($v' = 0$ is, of course, the most likely candidate). We happened to have available two 11-nm bandpass interference filters of wavelengths 394 and 405 nm, which fitted well to the S_2 transitions at 393.89 nm (0,9) and 404.56 nm (0,10) [24]. While these filters do not represent the *ideal* choice and do not exclude *all* interference from CH, they are still suited to the task.

Fig. 5 shows the outcome of the experimental variation of quencher and analyte concentrations. To set the conditions as demanding as possible, the experimental variation of analyte was carried out in the presence of a constant level of methane, and was driven beyond the quadratic range of the analyte. (Here, as in some later figures, the solid line is drawn deliberately at slope zero. The degree to which individual data points deviate from this ideal RR constancy can thus be judged. In contrast, linear or non-linear regression lines would show a slight slope for the whole group, thereby minimizing individual deviations.) The 394/405 nm response ratio for sulfur in the quadratic mode is now practically non-variant, despite the fact that the percentage of peak quenching, and the amount of analyte injected, vary over extremely wide ranges.

This strongly suggests that the same emitter is

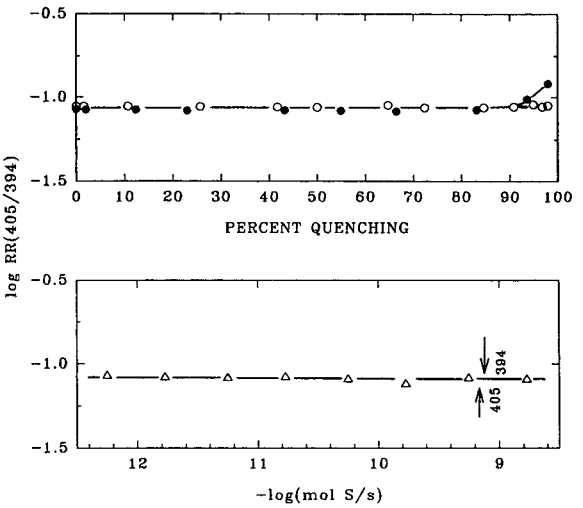

Fig. 5. Constancy of response ratios for quadratic sulfur (S_2) at different quenching intensities and analyte levels. Interference filters: 394 and 405 nm, both of 11 nm bandpass. Commercial quartz chimney around flame. Analyte: 20 ng (open circles) and 300 ng (full circles) of thianaphthene. Gas flows in ml/min: hydrogen 50, air 40, nitrogen (column) 20; methane variable (upper plot), or equivalent to a 60% reduction in peak height on both channels (lower plot).

being monitored —predominantly if not exclusively— in the two channels. A further indication to that effect arises from a comparison of the quenching percentages for analyte peaks appearing simultaneously in the two channels. The percentages are not just directly proportional (which would be sufficient to ensure the constancy of response ratios) but they are practically identical. Identical quenching percentages for quadratic sulfur concur with the findings of Sugiyama *et al.* [13], who characterized the decrease in S_2 emission as "independent of wavelength and almost uniform over the whole wavelength range".

(It may be parenthetically noted that the use of response ratios —which are highly sensitive to small changes in relative emission intensities— and of huge experimental variations in quencher and analyte concentrations could offer a second, more discerning look at sulfur luminescence. Our first attempt of establishing response ratio constancy for the S_2 system used an available 340/394 nm interference filter combination, and

resulted in RR values that were by far not as constant as those shown in Fig. 5 [25]. Whether this was related to the different S_2 upper vibrational levels in the 340 nm region [24], or to the presence and/or reactions of other emitters, has not been determined.)

As with varying quencher concentrations, the 394/405 nm S_2 response ratio remains constant in the face of a strongly varying *analyte* concentration as well. It does so over the whole quadratic range of the calibration curves (whose upper ends are marked in Fig. 5 by two arrows) and, reassuringly, even beyond.

Yet, to modify the behavior of *quadratic* sulfur was not the main objective of this study. More important to us was the behavior of sulfur's response ratio under the flow conditions of the *linear* mode [22]. As Figs. 1, 2 and 3 demonstrate, response ratios can become grossly unstable under latitudinarian monitoring. The main emissions of the linear mode appear to be the 0,0 and 1,1 bands at 696 and 711 nm, and the 0,1 band at 749 nm, of the $^2A'-^2A''$ transition of HSO [26]. Therefore, the available combination of a 700-nm wideband filter (of 70 nm bandpass) and a 750-nm wideband filter (of 40 nm bandpass) was chosen. When observed only through these spectral windows, linear sulfur turned out to be well behaved indeed. This is demonstrated in Fig. 6 by a response ratio that remains constant in the face of large variations in quencher and analyte.

The quencher-variation data of Fig. 6 were obtained with two, relatively high levels of analyte (where the challenge from S_2 emissions is the most acute). Still, the RR values remain constant even under severe quenching conditions, quite unlike those of the otherwise comparable sulfur curve of Fig. 3.

The analyte-variation data of Fig. 6 were obtained at a constant methane level (equivalent to 47% quenching). Again, the constancy of the RR value —quite unlike that of the otherwise comparable sulfur curve in Fig. 2— is maintained over a wide range of analyte concentrations. Furthermore, the RR values of the two plots are identical, thereby lending further credence to their overall constancy, and hence to the supposition that the *same single* emitter is being monitored on the two channels.

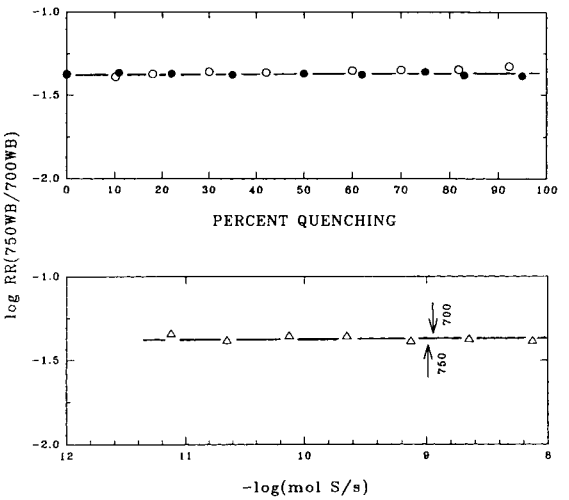

Fig. 6. Constancy of response ratios for linear sulfur (HSO) at different quenching intensities and analyte levels. Interference filters: 700 nm wideband (bandpass 70 nm) (700WB), 750 nm wideband (bandpass 40 nm) (750WB). Analyte: 100 ng (open circles) and 1000 ng (full circles) of thianaphthene. Conditions are those of the linear sulfur mode as defined in the Experimental section. Methane flow: variable in upper plot; equivalent to a 47% peak height reduction in both channels in lower plot. Arrows indicate the upper ends (−10%) of the linear calibration curves.

Sulfur, the most prominent FPD element to determine (and the most difficult one to determine well) thus produces constant RR values in both the conventional quadratic and the novel linear mode. Under carefully selected optical conditions, then, either mode is capable of providing constant, hence diagnostic response ratios. This means that various computer-manipulated chromatographies [7–10] can detect sulfur reliably, even in the case of ill-defined hydrocarbonaceous sample matrices.

This successfully concludes the study of sulfur. However, the FPD responds not only to sulfur but (so far) to some twenty other elements as well. Sulfur, while outstanding in its prominence as FPD analyte, does differ from all other elements of this study in its kinetic behavior. Thus it may be worthwhile to consider, by way of example and however briefly, a couple of selected elements that (a) show particularly

strong RR deviations in Fig. 3, (b) differ considerably in their (constant-range) RR values between Figs. 1 and 2, (c) are known to produce multiple emitters, and (d) hold proven or potential significance as analytes in the FPD. The elements selected by these criteria are tin and manganese.

Organotins have been the target of many environmental analyses [27], quite a few of which made use of the FPD (*e.g.* ref. 28). Authentic FPD spectra are available [23]. In contrast, organomanganese compounds have only recently been suggested as FPD analytes [8]. Yet, future use of the FPD seems likely for determining manganese in industrial and environmental samples. Also, a suitable spectrum, from the common gasoline additive methylcyclopentadienylmanganese tricarbonyl (MMT), has been measured in the FPD [8].

So far, the same detector conditions —*i.e.* conditions optimized for linear sulfur detection— have been used for all elements. This appears reasonable for multi-element analysis with sulfur as the prime target, but makes little sense for single-element determinations of tin or manganese. Clearly, compounds of these two metals are best observed at their own, individually optimized conditions.

This forces a choice in the case of tin: Although tin's blue surface luminescence on quartz is far more sensitive than either the broad SnOH continuum or the sharp SnH bands [27,28], the latter are still favored by many environmental laboratories. Also, they appear more amenable to accepting the intended spectral probe. The main heads of the (0,0) SnH band's $^4\Sigma$–$^2\Pi_{1/2}$ and $^4\Sigma$–$^2\Pi_{3/2}$ components are located at 609.5 and 689.2 nm [24].

The spectral characteristics of manganese are quite different. The predominant FPD emission, at 403 nm, contains most likely one or more of the (usually very strong) atomic lines at 403.076, 403.307 and 403.449 nm. The other prominent emission, at 540 nm, may represent one or both of the (usually very weak) lines at 539.467 and 543.255 nm. All of these lines represent transitions to the ground state, *i.e.* they occur from *different* excited states. Furthermore, both of these sharp emissions rest on a continuum, of minor intensity at 403 nm, but of major intensity at 540 nm [8]. The present task of achieving constancy for RR values would perhaps be served best by sampling the continuum, or by exploring further manganese emissions in the red and near infrared. However, since the 403-nm lines are the obvious choice for the practical FPD determination of Mn, the decision was made to pair them with the 540-nm emission, despite the latter's uncertain nature and underlying continuum.

Fig. 7 demonstrates the constancy of the tin (SnH) response ratio *vis-a-vis* large variations in quencher and analyte concentrations. The slight slope of the quenching curve for 5 ng of tetra-*n*-butyltin may be due to interference from the strong surface luminescence continuum, which saturates at about the 30-ng level [23]; however, this assumption has not been further investigated. Note that the absolute RR values are essentially identical in the two plots; and that, in stark contrast to the polychromatic tin curves

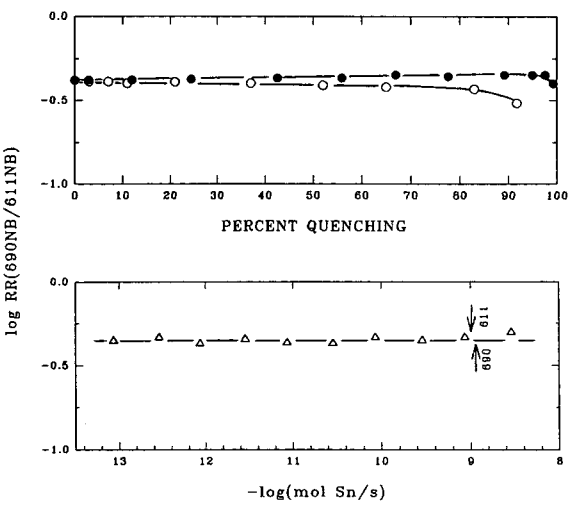

Fig. 7. Constancy of response ratios for tin (SnH) at different quenching intensities and analyte levels. Interference filters: 690 (690NB) and 611 nm (611NB), both of 12 nm bandpass. Analyte: 5 ng (empty circles) and 100 ng (full circles) tetra-*n*-butyltin. Flows in ml/min: hydrogen 300, air 150, carrier nitrogen 20; methane variable in upper plot, or equivalent to a 40% peak height reduction in both channels in lower plot. Arrows indicate the linear-range end of the calibration curves.

shown in Figs. 2 and 3, they are close to invariant. The difference between the two types of behavior may be reasonably attributed to monitoring one *vs.* more than one emitter.

A somewhat different picture emerges from the bichromatic assessment of manganese shown in Fig. 8. Its response ratios, at 10 and 300 ng levels of the injected analyte MMT, stay constant in the analytically more important first half of peak height reduction, but grow then progressively worse. Large and small amounts of manganese are affected to the *same* extent (as is typical of FPD quenching behavior, the above case of tin notwithstanding). The shape of the curve appears consistent with a mechanism in which the continuum that underlies (mainly) the 540-nm emission is quenched significantly less than the two (sets of) atomic lines. However, other spectrochemical rationalizations cannot be excluded at this point. Manganese response through the full range of quenching is, as expected, significantly better under bichromatic than under polychromatic (Fig. 3) conditions.

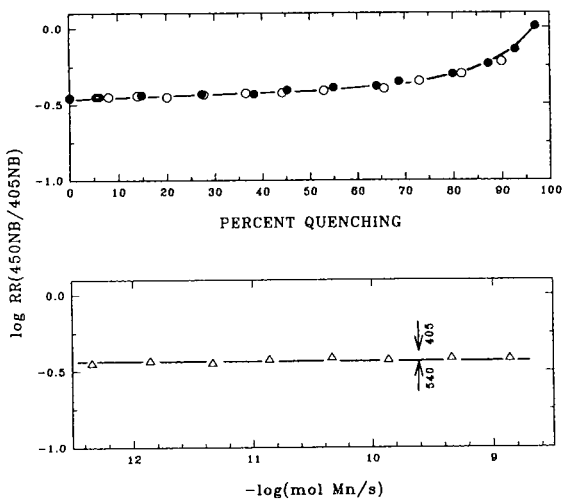

Fig. 8. Response ratios for manganese (Mn) (two emitters?) at different quenching intensities and analyte levels. Interference filters: 450 nm (9 nm bandpass) (450NB) and 405 nm (11 nm bandpass) (405NB). Analyte: 10 ng (empty circles) and 300 ng (full circles) of methylcyclopentadienylmanganese tricarbonyl (MMT). Flows in ml/min: hydrogen 300, air 55, carrier nitrogen 20; methane variable in upper plot, or equivalent to a 47% reduction in peak height on both channels in lower plot.

Furthermore, the response ratio of manganese is perfectly non-variant over four orders of analyte variation (compare Fig. 2). Here as elsewhere, the full variation of the analyte appears to mount less of a challenge to the constancy of response ratios than the full variation of the quencher.

It should be recognized in this context, though, that a plot of dual-channel response ratios represents an exquisitely sensitive probe of quenching behavior. This becomes obvious by looking at Fig. 9, where raw data from Figs. 6–8 are displayed in the form of conventional quenching curves [29].

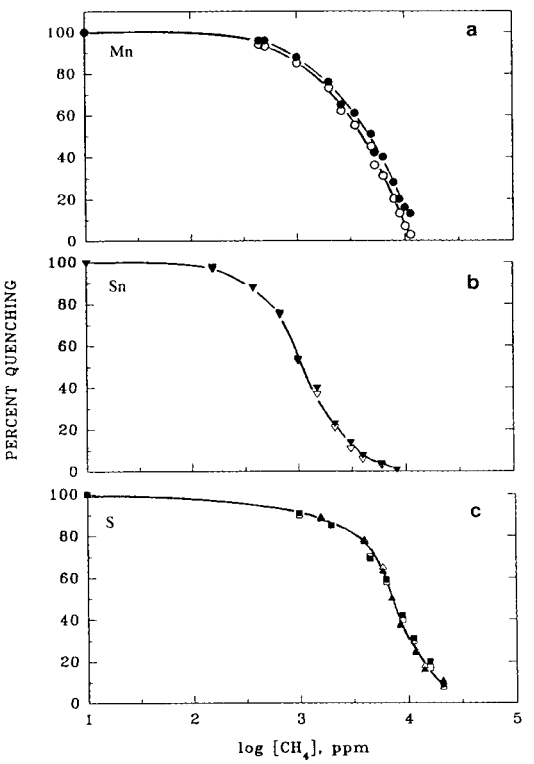

Fig. 9. Percent quenching of manganese, tin and linear sulfur luminescences at individually optimized conditions *vs.* quencher concentration. The abscissa refers to the molar (*i.e.* volume) concentration of methane in the *unburnt* flame gases. Conditions for 300 ng MMT (Mn) are those of Fig. 8; for 100 ng tetra-*n*-butyltin (SnH) those of Fig. 7; and for 100 and 1000 ng thianaphthene (HSO) those of Fig. 6. (a) MMT: 300 ng, ○ = 405 nm, ● = 450 nm. (b) Tetra-*n*-butyltin: 100 ng, ▽ = 611 nm, ▼ = 690 nm. (c) Thianaphthene: □ = 0.1 μg, 700 nm wideband; △ = 0.1 μg, 750 nm wideband; ■ = 1 μg, 700 nm wideband; ▲ = 1 μg, 750 nm wideband.

For manganese (MMT), these typically sigmoid curves portray the fractional quenching of the larger of the two analyte amounts. In contrast to Fig. 8, the small difference in behavior at the two wavelengths is hardly noticeable. (The smaller amount of MMT produces like results.) Similarly, only the larger amount of tin (as tetra-*n*-butyltin) is shown. For tin, no difference is expected from Fig. 7 and none is found. To complete this round of comparisons, the full data set for linear sulfur (the same set as used for Fig. 6) is redrawn in this "kinetic" representation. The latter demonstrates well (a) that the percentage of quenching is independent of analyte concentration, and (b) that the two channels register essentially identical behavior —hence, most likely, the same emitter.

Graphic contrast aside, the main reason for showing the quenching curves of these three key elements at three different sets of conditions is that they exemplify and quantify the typical dependence of "percent quenching" —the particular measure used in this study— on the spectrochemically important molar concentration of the quencher methane in the (unburnt) flame gases.

4. Conclusions

Response ratios from dual-channel detectors offer additional chemical information and can therefore aid the identification or confirmation of chromatographic peaks on the qualitative side, and the suppression of interferences or background features on the quantitative side. The obvious requisite is, however, that they remain non-variant *vis-a-vis* large changes in analyte and/or quencher concentrations.

In the case of the FPD, the most obvious and most effective means for achieving unlimited response ratio constancy is based on the selection of the two monitored wavelength regions. Yet, that selection also determines whether the analysis will scan a wider array of elements or focus on one element only. Polychromatic conditions (wide wavelength ranges) yield constant ratios if the analyte produces a single emitter. If it produces more than one emitter —a common occurrence— the response ratios will remain constant if all emitters are linear (*i.e.* if their luminescence is first order in analyte) *and* if they remain within their respective linear calibration ranges. Although such a linear multi-emitter FPD system will tolerate a constant or weakly variable influx of quencher, it will not normally tolerate a strongly variable one.

In contrast, bichromatic conditions (in the ideal case: two transitions off the same excited state, with no other emissions around) may have to be chosen if multiple emitters of different reaction orders are present, if the analyte exceeds linear range, and/or if the concentration of the quencher (usually a co-eluting matrix component) fluctuates excessively among samples.

Possible sets of such bichromatic conditions have been successfully defined for both the quadratic and the linear response mode of the most important FPD element, sulfur. Under these conditions, sulfur response ratios remain constant at any concentration of quencher and analyte. Additional exploratory experiments with tin and manganese suggest that the constancy of response ratios can be achieved not only for sulfur, but also for most if not all elements that are known (or will still be found) to luminesce in the FPD.

5. Acknowledgement

This study has been supported financially by NSERC research grant A-9604.

6. References

[1] S.S. Brody and J.E. Chaney, *J. Gas Chromatogr.*, 4 (1966) 42.
[2] M. Dressler, *Selective Gas Chromatographic Detectors* (*Journal of Chromatography Library*, Vol. 36), Elsevier, Amsterdam, 1986, pp. 133–160.
[3] W.A. Aue, B. Millier and X.-Y. Sun, *Anal. Chem.*, 63 (1991) 2951.
[4] V.L. McGuffin and M. Novotny, *Anal. Chem.*, 53 (1981) 946.

[5] S.V. Olesik, P.A. Pekay and E.A. Paliwoda, *Anal. Chem.*, 61 (1989) 58.
[6] X.-Y. Sun, B. Millier and W.A. Aue, *Can. J. Chem.*, 70 (1992) 1129.
[7] W.A. Aue, X.-Y. Sun and B. Millier, *J. Chromatogr.*, 606 (1992) 73.
[8] W.A. Aue, B. Millier and X.-Y. Sun, *Anal. Chem.*, 62 (1990) 2453.
[9] W.A. Aue, B. Millier and X.-Y. Sun, *Can J. Chem.*, 70 (1992) 1143.
[10] B. Millier, X.-Y. Sun and W.A. Aue, presented at the *75th Canadian Institute of Chemistry Conference, Edmonton, June 1992.*
[11] I. Berglund and P.K. Dasgupta, *Anal. Chem.*, 63 (1991) 2175 and 64 (1992) 3007.
[12] S.O. Farwell and C.J. Barinaga, *J. Chromatogr. Sci.*, 24 (1986) 483.
[13] T. Sugiyama, Y. Suzuki and T. Takeuchi, *J. Chromatogr.*, 80 (1973) 61.
[14] M. Maruyama and M. Kakemoto, *J. Chromatogr. Sci.*, 16 (1978) 1.
[15] W.E. Rupprecht and T.R. Phillips, *Anal. Chim. Acta*, 47 (1969) 439.
[16] S.-A. Fredriksson and A. Cedergren, *Anal. Chem.*, 53 (1981) 614.
[17] M. Dressler, *J. Chromatogr.*, 270 (1983) 145.
[18] P.L. Patterson, *Anal. Chem.*, 50 (1978) 345.
[19] T.L. Chester, *Anal. Chem.*, 52 (1980) 638.
[20] B.J. Ehrlich, R.C. Hall, R.J. Anderson and H.G. Cox, *J. Chromatogr. Sci.*, 19 (1981) 245.
[21] G.H. Liu and P.R. Fu, *Chromatographia*, 27 (1989) 159.
[22] W.A. Aue and X.-Y. Sun, *J. Chromatogr.*, 633 (1993) 151.
[23] C.G. Flinn and W.A. Aue, *Can.J. Spectr.*, 25 (1980) 141.
[24] R.W.B. Pearse and A.G. Gaydon, *The Identification of Molecular Spectra*, Chapman & Hall, London, 4th ed., 1976.
[25] J.A. Gebhardt, Dalhousie University, Halifax, 1992–1993, unpublished thesis work.
[26] U. Schurath, M. Weber and K.H. Becker, *J. Chem. Phys.*, 67 (1977) 110.
[27] R.J. Maguire, *Water Poll. Res. J. Canada*, 26 (1991) 243.
[28] G.B. Jiang, P.S. Maxwell, K.W.M. Siu, V.T. Luong and S.S. Berman, *Anal. Chem.*, 63 (1991) 1506.
[29] W.A. Aue and X.-Y. Sun, *J. Chromatogr.*, 641 (1993) 291.

ELSEVIER

Journal of Chromatography A, 667 (1994) 205–211

JOURNAL OF CHROMATOGRAPHY A

Comparison of universal chromatographic detectors for trace gas analysis

R.T. Talasek*, M.P. Schoenke

Texas Instruments, Inc., PO Box 655012 M/S 301, Dallas, TX 75265, USA

(First received September 1st, 1993; revised manuscript received December 29th, 1993)

Abstract

Various performance parameters of three detector systems used in trace level gas analysis, helium ionization detection (HID), discharge ionization detection (DID), and gas chromatography–mass spectrometry (GC–MS), have been compared. The detectors were compared for sensitivity, sample matrix effects, and stability. While detection limits were roughly comparable for all three detectors, both GC–MS and DID out-performed HID in various matrix effects and stability tests. Furthermore, HID demonstrated non-linear behavior over a relatively small concentration range.

1. Introduction

The analysis of sub-ppm level impurities in high purity gases has gained great interest in the last several years, especially in the semiconductor industry. Much of this analysis is done chromatographically, and almost every conceivable chromatographic detector is used for these analyses. The most active area for this application involves detectors that respond universally to impurities other than the carrier. While the thermal conductivity detector and the ultrasonic detector both fall into this category, their detection capabilities are generally limited to the low ppm level, and they will not be considered further. The helium ionization detection (HID) system has gained wide acceptance in this application because of its excellent sensitivity [1,2]. HID uses a tritium source of beta emission for ionization, the ions are accelerated by an electrical potential, and detected by a standard electrometer configuration [3–5]. Although much work has been done on the ionization process [6,7], the exact mechanism is not well understood. A common misconception is that ionization occurs through a "simple" Penning ionization. However, this fails to explain a number of unusual behaviors of this detection system. When carrier gas of sufficient purity is used, both positive and negative peaks result. The contribution of various impurities in the carrier may cause all positive peaks, enhance sensitivity, or suppress detection entirely [8–12]. A complex associative ionization mechanism has been proposed which more closely matches these observed behaviors [13]. Still, HID is a useful and widely accepted analytical tool for gas analysis.

Two other detection systems, discharge ionization detection (DID) and mass spectrometry (GC–MS), are beginning to be used more exten-

* Corresponding author.

0021-9673/94/$07.00
SSDI 0021-9673(94)00008-W

sively in these applications. DID employs a DC helium corona discharge, supported by a separate gas flow from the carrier, as its ionization source. The detector is configured in a two-cell arrangement, with the discharge cell connected to the detection cell by a windowless aperture. The carrier flows into the detection cell, where it is ionized by the discharge and detected by a standard electrometer configuration [14–16]. Although photoionization has been claimed as the ionization mechanism, other pathways such as electron impact probably contribute to ionization.

The standard mass spectrometer has often been used as a detector for the chromatographic analysis of molecular impurities in many gases [17–21]. The advent of porous layer open tubular (PLOT) columns with many standard stationary phases used in gas analysis have made direct interfacing of the column to the mass spectrometer possible, allowing analysis of lower molecular weight impurities such as oxygen and nitrogen without the sensitivity losses associated with these analytes using other interface types (*e.g.*, jet and membrane separators) [22–35]. This development has placed GC–MS in the group of methods available for trace level gas analysis.

A comparison of various performance criteria is in order for these detectors. While sensitivity is an important consideration, it is not the only aspect of detector performance that must be considered. Response linearity is consideration when accurate quantitation is important. The effects of a sample matrix on the detector are significant. Finally, detector stability over time is important with respect to baseline drift and response. This consideration is especially important when the analysis is conducted continuously in an on-line application. A comparison of these parameters for these detectors is presented here.

2. Experimental

A Valco (Houston, TX, USA) 3000 gas chromatograph with dual helium ionization detectors was used for the HID part of the comparison. This instrument contains all components (columns, valves, fittings, and detectors) inside a helium-purged housing held at slightly positive pressure. This instrument, because of this configuration, is limited to packed columns. The plumbing configuration is such that heart-cutting and backflushing can be done, although only direct injection with a 1 ml sample loop is used here. Two ten-foot (1 ft. = 30.48 cm) Hayesep A columns were used for all determinations presented here, except the response and baseline recovery studies, and detection limit evaluations where additional chromatographic resolution was needed. Here, a 10-foot molecular sieve was substituted for the second Hayesep A column.

A Tracor (Austin, TX, USA) 540 GC system fitted with a discharge ionization detector was used for DID performance testing, fitted with dual six-port Valco valves, one for sample injection with a 1 ml sample loop, and one for switching a Molsieve 5A PLOT column in and out of series with a PoraPLOT Q column (Chrompack, Rariton, NJ, USA). All determinations were done with the PoraPLOT column only, except the response and baseline recovery studies, and detection limit determinations where additional chromatographic resolution was required. Packed columns were also used in matrix effect portion of the comparison to provide a bridge between the HID and GC–MS data. No helium purging was used for any components in this system.

GC–MS evaluations were conducted on a Hewlett-Packard (Avondale, CA, USA) 5988A quadrupole mass spectrometer equipped with a 5890 gas chromatograph. The mass spectrometer uses a differentially-pumped electron impact (EI) source, which enables it to maintain sufficient source vacuum at relatively high carrier flow (approximately 15 ml/min). This mass spectrometer is only capable of mass determinations down to $m/z = 4$. Therefore no determinations of hydrogen concentration were possible. All valves and fittings are housed in a helium-purged housing. The GC–MS system uses a plumbing configuration similar to that described for the DID system, including the use of PLOT columns. The interface between columns and the

source vacuum consisted of a 5 m × 0.2 μm linear restrictor of deactivated fused silica. Because of the reduced capacity of this restrictor, a 0.2 ml sample loop is used with this instrument. All evaluations discussed here were performed with the PoraPLOT Q column only, except response and baseline recovery studies, and detection limit evaluations where additional chromatographic resolution was required.

Linearity and detection limit evaluations required the preparation of mixtures with ppb level impurities. Due to the uncertainties in stabilities of low ppm mixtures, it was decided that they should be prepared by dynamic blending of mixtures containing higher levels of impurities. A two-stage dynamic blender (Fig. 1) was constructed using mass flow controllers (Omega Engineering, Stamford, CT, USA) to allow dilution over a range of 1:100 to $1:10^6$. This blender used all VCR (Cajon Co., Macedonia, OH, USA) type connections to guarantee a leak-tight system. Dilution gas (helium) was purified with a zirconium-based metal getter manufactured by SAES Getters (Colorado Springs, CO, USA), which reduced each impurity concentration to below detectable levels. Flow from each output port was controlled by venting through an excess flow valve, thereby minimizing active components in the flow path of interest. This blender was used to verify concentrations of individual components in the high-level mixture, using pure gases at the blender input. The high-level mixture was introduced into the blender through a deep-purge regulator, purged with purified helium. It was dynamically blended to appropriate levels for linearity and detection limit evaluations.

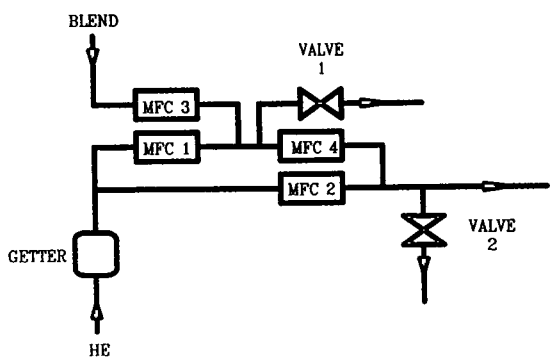

Fig. 1. Schematic diagram of dynamic blender used for preparation of low-level blends. Pure gases or ppm level blends with confirmed compositions are introduced at point marked BLEND. Helium is introduced at point marked HE. MFC 2 and 4 are 1 l/min full-scale electronic mass flow controllers. MFC 1 and 3 are 10 ml/min full-scale mass flow controllers. Valves 1 and 2 are manually adjusted excess flow needle valves. Single stage blender output is from OUTPUT 1 (upper horizontal arrow) and dual stage from OUTPUT 2 (lower horizontal arrow).

3. Useful detection limits and linearity

Detection limits at ppb levels have been reported for all these detectors previously. Often these determinations involved operating conditions that cannot be easily maintained in daily operation because of their contribution to instrument instability. Because of this, an extremely conservative definition for useful detection limits has been chosen. A signal-to-noise level of 5:1 was chosen. DID and HID parameters (*e.g.*, HID polarization voltage, DID discharge current, etc.) were chosen such that the baseline drift over the course of analysis was less than one full scale of electrometer output. GC–MS parameters were chosen such that background signal changed by less than ± 100%. Low level blends were prepared within a factor of two of this value using the dynamic blender described above, and the reported detection limit was extrapolated from this point. Except for the determination of carbon monoxide, chromatographic parameters (*e.g.*, carrier flow, column temperature) were chosen to maximize detection performance while allowing chromatographic resolution of all components determined. All blends were prepared with a helium balance gas, so matrix effects should often be expected to degrade this performance.

Table 1 summarizes the detection limits (in ppbv) as defined above for six common impurities. In all cases except hydrogen, which could not be determined with the instrument used in this study, the GC–MS system showed equivalent or superior detection limits compared

Table 1
Detection limits in ppbv for six common analytes

Analyte	HID	GC–MS	DID
H_2	5	N/A [a]	50
O_2	50	1	10
N_2	10	1	10
CO	25	10	5
CH_4	5	10	5
CO_2	5	0.1	15

[a] N/A = Not analyzed.

to the other two instruments. In fact, GC–MS has sensitivity of 1 ppbv or below in 3 out of 5 analytes evaluated. While HID showed superior performance when hydrogen was the analyte, DID was superior to HID for oxygen determination.

Linearity was evaluated over the range of 10 ppbv to 10 ppmv for several impurities for each detector utilizing dynamic blending. Analytes for each detector were chosen from those for which the individual detector had sufficient sensitivity. Fig. 2a–c summarizes the results achieved for each detector. While both DID and GC–MS demonstrated linear behavior over this range, HID showed significant curvature. The exact concentration–response relationship has not been explored further because it seems likely that several types of expressions could approximate the curvature over such a narrow data range. Because of the relatively small dynamic range of this detector, extending the range of this evaluation is not possible.

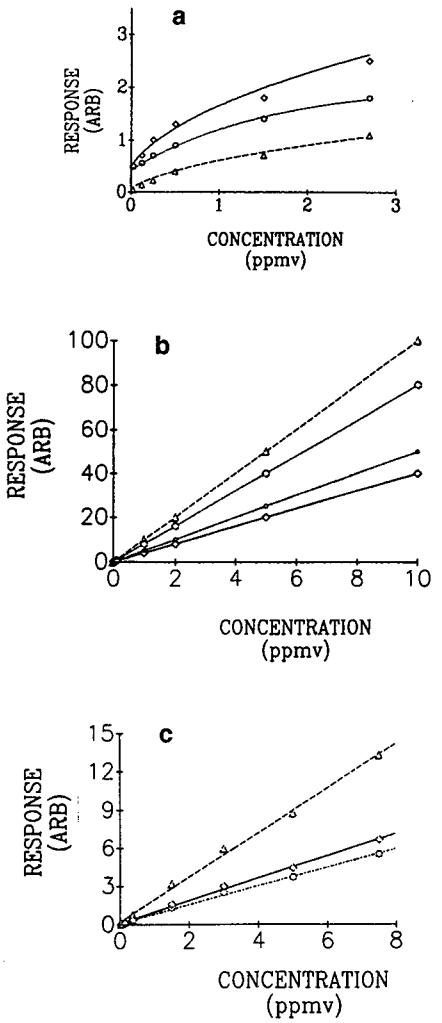

Fig. 2. Plots of concentration in ppbv *vs.* detector response in arbitrary units for the three detectors. Response units are not comparable for the three plots. (a) HID response for hydrogen (△), argon (○), and nitrogen (◇). (b) GC–MS response for oxygen (△), nitrogen (○), methane (◇), and carbon dioxide (●). (c) DID response for nitrogen (◇), carbon monoxide (○), and methane (△).

4. Sample matrix effects

While the above performance parameters are significant, helium is only one of many potential sample matrices of interest to the semiconductor industry. Often it is impossible or impractical to use heart-cutting or backflushing techniques to reduce or eliminate the sample matrix. Therefore it is important to consider the effect of sample matrix on each detector's performance.

The first consideration is compatibility with materials of construction of the detector. While this is extremely important, this information is readily available in the literature, and will not be considered further. Other influences of balance gas include the tendency of certain gases (*e.g.*, oxygen) to quench the discharge of the DID

system, making it unusable with these gases. Also to be considered are baseline recovery after introduction of the major sample component, and recovery of detector response during and after the baseline recovery period.

To evaluate baseline recovery, a stable baseline was achieved with each detector with the appropriate parameters adjusted to achieve approximately 0.1 ppmv sensitivity for nitrogen. A sample of high purity argon was injected into each system, and the detector's ability to return to initial baseline was monitored. Fig. 3 illustrates each detector's ability to recover, expressed as a percentage of electrometer output for the HID and DID systems, and as a percentage of background signal at $m/z = 28$ for the GC–MS system. While both the DID and the GC–MS systems recovered within the time to make one analysis (with GC–MS it was almost immediate), over two hours were required for the HID system to recover. Since dead volume within packed columns was a suspected issue, the DID part of the experiment was run with both packed and PLOT columns, and similar results were achieved in both cases.

To evaluate response recovery, detector response to approximately 2 ppmv of nitrogen in helium was measured utilizing the same detector settings as in the baseline recovery study. Then, a sample of high purity argon was injected into each system. Finally, the helium mixture was repeatedly reanalyzed until detector response reached initial response levels. The results in Fig. 4 are plotted as a percentage of initial response. Again, both the GC–MS and DID

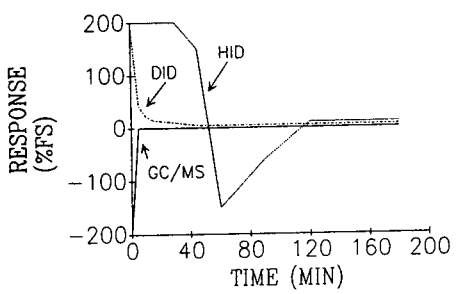

Fig. 3. Detector signal *vs.* time after injection of sample matrix of argon.

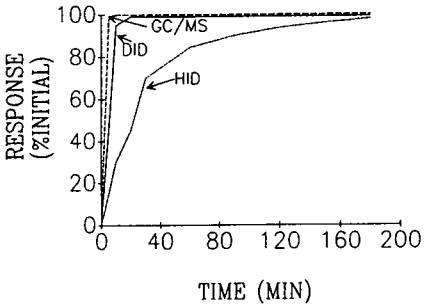

Fig. 4. Detector response *vs.* time to 2 ppmv nitrogen in helium after injection of a sample matrix of argon.

systems recovered within the time required for a single analysis, while the HID system experienced response suppression for a significant period after baseline recovery was achieved.

5. Detector stability

Gas chromatographs are often used as on-line analyzers. They are also used in laboratories where a high sample throughput is important. In both applications, detector stability is an important consideration. Both baseline drift and detector response can be considered as a function of stability. Both were monitored over a five-day period, using the same criteria and detector parameters as were used in the matrix effect evaluation. Fig. 5 illustrates baseline drift of the three detectors over this period. Both the DID and the HID systems show excursions of over 10% during this period, with the HID system showing more extreme excursions both positive and negative directions. Background

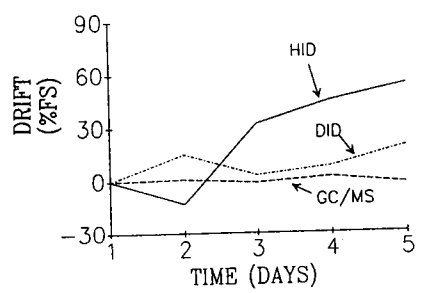

Fig. 5. Baseline drift over five days.

Table 2
Comparison of the detection systems evaluated

System	Advantages	Disadvantages
HID	- Best sensitivity for H_2 - Some identification of impurities	- Poor O_2 sensitivity - Balance gas effects - Stability
DID	- Excellent stability - Excellent sensitivity	- Poor H_2 sensitivity - O_2 balance gas effect
GC–MS	- Most sensitive - Most stable - Least affected by matrix - Positive impurity identification - Limited chromatography necessary	- Cost - $m/z > 10$

signal for the GC–MS system changed little over the five-day period.

Fig. 6 shows the change in detector response to 2 ppmv nitrogen over the same period. The poor response stability of the HID system requires frequent recalibration for on-line use, while both the DID and GC–MS systems demonstrate calibration drift of less than 10% over this period, lending themselves to less frequent calibration. This makes these instruments more amenable to on-line applications.

6. Summary

Table 2 presents a summary of the evaluation discussed here, with pertinent miscellaneous facts. Generally, the DID or GC–MS system should be considered the optimum choice where detector stability is important. Sensitivity of the DID and HID systems is roughly comparable, with each having distinct advantages for specific analytes. While GC–MS provides superior performance for most parameters considered here, the cost of a research-grade instrument as a routine analyzer may be prohibitive in many cases. No one single detector can be shown to be ideal in all situations, however the facts presented here should provide the basic information necessary to choose the right detector for most common gas analysis applications.

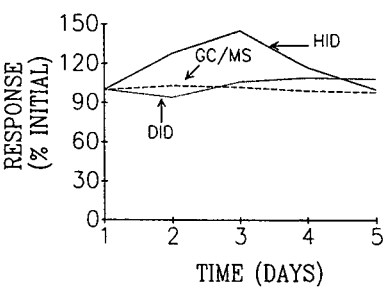

Fig. 6. Detector response to 2 ppmv nitrogen over five days.

7. References

[1] F.F. Andrawes and S. Greenhouse, *J. Chromatogr. Sci*, 26 (1988) 53–159.
[2] R.A. Carpio and E. Lindt, *Semicond. Int.*, May 1989, 164–167.
[3] J.E. Lovelock, *J. Chromatogr.*, 1 (1958) 35–46.
[4] F.F. Andrawes and R. Ramsey, *J. Chromatogr. Sci.*, 24 (1986) 513–518.
[5] J. Sevcik, *Detectors in Chromatography*, Elsevier, New York, 1976, p. 131.
[6] E. Bros and J. Lasa, *J. Chromatogr.*, 94 (1974) 13–24.
[7] S. Lukac and J. Sevcik, *Chromatographia*, 5 (1972) 311–316.
[8] F.F. Andrawes and E.K. Gibson, Jr., *Anal. Chem.*, 50 (1978) 1146–1151.
[9] F.F. Andrawes and E.K. Gibson, Jr., *Anal. Chem.*, 52 (1980) 846–851.
[10] F.F. Andrawes, T.B. Byers and E.K. Gibson, Jr., *Anal Chem.*, 53 (1981) 1544–1545.
[11] E. Bros and J. Lasa, *Chromatographia*, 13 (1980) 567–572.

[12] F.F. Andrawes, E.R. Gibson and D.A. Bafus, *Anal. Chem.*, 52 (1980) 846–849.
[13] R.T. Talasek, *Abstracts of the Pittsburgh Conference on Analytical Chemistry and Spectroscopy, New York City, March 5–9, 1990*, No. 63.
[14] D.M. Williams, *Abstracts of the Pittsburgh Conference on Analytical Chemistry and Spectroscopy, New Orleans, LA, February 22–26, 1988*, No. 679.
[15] D. Clay and D.M. Williams, *Abstracts of the Rocky Mountain Conference, Denver, CO, July 31–August 4, 1988*, No. 233.
[16] Cook, Robert D. *U.S. Pat.*, 4 789 783, 1988.
[17] R.T. Talasek, *Abstracts of the Pittsburgh Conference on Analytical Chemistry and Spectroscopy, Atlanta, GA, March 6–10, 1989*, No. 63.
[18] R.T. Talasek, *Abstracts of the Eastern Analytical Symposium, New York City, September 24–29, 1989*, No. 45.
[19] R.T. Talasek and R.E. Daugherty, *J. Chromatogr. Sci.*, 30 (1992) 131–135.
[20] R.T. Talasek and K.E. Daugherty, *J. Chromatogr.*, 635 (1993) 265–270.
[21] R.T. Talasek and R.E. Daugherty, *J. Chromatogr.*, 639 (1993) 221–226.
[22] R.F. Arrendale, R.F. Severson and D.T. Chortyk, *Anal. Chem.*, 56 (1984) 1533–1537.
[23] M. Blumer, *Anal. Chem.*, 40 (1968) 1590–1592.
[24] E.J. Bonelli, M.S. Story and J.B. Knight, *Dynamic Mass Spec.*, 2 (1971) 177–180.
[25] C. Brunee, H.J. Bultemann and G. Rappus, *Abstracts of the 17th Annual Conference on Mass Spectroscopy and Allied Topics*, No. 46, Dallas, TX, 1969.
[26] J. Copet and J. Evans, *Org. Mass. Spectr.*, 3 (1970) 1457–1461.
[27] M.A. Grayson and R.L. Levey, *J. Chromatogr. Sci.*, 9 (1971) 687–689.
[28] M.A. Grayson and J.J. Bellina, *Anal. Chem.*, 45 (1973) 487–491.
[29] M.A. Grayson and C.J. Wolf, *Anal. Chem.*, 42 (1970) 426–430.
[30] D. Henneberg, U. Henrichs, H. Husmann and G. Schomburg, *J. Chromatogr.*, 167 (1978) 139–147.
[31] P.M. Krueger and J.A. McCloskey, *Anal. Chem.*, 41 (1969) 1930–1935.
[32] P.M. Llewellyn and D.P. Littlejohn, *Pittsburg Conf. Anal. Chem. Spectr.*, 1966.
[33] W.H. McFadden, *J. Chromatogr. Sci.*, 17 (1979) 2–16.
[34] R. Rhyage, *Anal. Chem.*, 36 (1964) 759–764.
[35] J.J. Stern and B. Abraham, *Anal. Chem.*, 50 (1978) 2161–2164.

ELSEVIER

Journal of Chromatography A, 667 (1994) 213–218

JOURNAL OF CHROMATOGRAPHY A

Design and construction of a simple supercritical fluid extraction system with semi-preparative and preparative capabilities for application to natural products

Silvia R. Sargenti, Fernando M. Lanças*

Universidade de São Paulo, Instituto de Física e Química de São Carlos, C. Postal 369, 13560-970 São Carlos, SP, Brazil

(First received July 20th, 1993; revised manuscript received December 20th, 1993)

Abstract

The construction of a simple and versatile preparative-scale supercritical fluid extraction (SFE) system is described. The system has several options for the extraction cell and avoids the need for a special pump for fluid pressurization, one of the most expensive parts of a typical SFE system. The extracts obtained using this system are similar to those obtained by steam distillation under less favourable experimental conditions.

1. Introduction

Soxhlet extraction is the most widely used method for the extraction of vegetable material with solvents of different polarities, for both the usual extraction and selective extraction. However, this technique is time consuming and does not always produces the desired results. Comparative studies of these techniques and supercritical fluid extraction (SFE) have shown that SFE gives better yields, requires less solvent, has a shorter extraction time and is able to extract labile compounds sensitive to thermal decomposition [1–3].

Carbon dioxide is the most popular supercritical solvent for SFE because of its favourable characteristics, including mild critical conditions [$T_c = 31°C$ and $P_c = 72.9$ atm (1 atm = 101 325 Pa)], high volatility and diffusibility, low viscosity, non-toxicity, non-reactivity, non-flammability, easy and ready availability and relative cheapness. These characteristics make it the ideal solvent for supercritical extraction, mainly of thermally unstable materials [4–6].

Although there are extensive experimental data on the solubility and extractivity of natural products, including steroids, alkaloids, antitumor compounds, essential oils and caffeine, in both pure and modified supercritical CO_2, there are few publications describing the construction and adaptation of preparative-scale SFE systems optimized for phytochemical work that allow the direct extraction of vegetable material [7–10].

Most of the published work involved complex and expensive SFE systems. In this paper we describe an SFE system for preparative- and semi-preparative-scale use with natural products that is simple and inexpensive in construction

* Corresponding author.

0021-9673/94/$07.00
SSDI 0021-9673(93)E0058-3

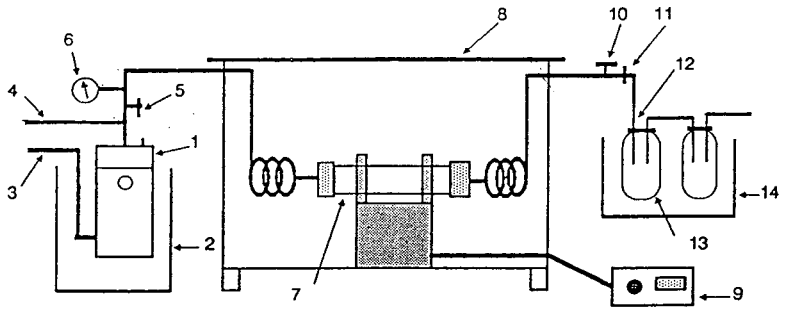

Fig. 1. Supercritical fluid extraction system with both analytical and semi-preparative capabilities. 1 = Vessel; 2,14 = cryogenics; 3 = CO_2; 4 = nitrogen; 5 = valve 1; 6 = gauge; 7 = cell; 8 = oven; 9 = heater; 10 = valve 2; 11 = filter; 12 = restrictor; 13 = collectors.

and versatile to use. The application of this system to the extraction of vegetable material, *Cymbopogon citratus*, in both dynamic and sequential extraction modes, using modified supercritical CO_2, is also described.

2. Experimental

2.1. Construction of the preparative SFE system

The complete system, as illustrated in Fig. 1, was constructed of stainless steel. It consists of a pressurization vessel (1) with two inlets, one for carbon dioxide (3) and the other for nitrogen (4), which is used to pressurize the system. Valve 1 (5) installed before the gauge (6) allows the use of a static mode when closed along with valve 2 (10). The temperature of the extraction cell (7), installed in an oven (8), is controlled through an electrical heater (9). The second valve (10) controls the exit of the extract to a filter (11) and to a tapered stainless-steel (0.03 mm) restrictor (12). The extract is collected in the sample collector vessel (13) with cryogenic capabilities when desired (14). The dimensions of the major components of the designed SFE system are listed in Table 1.

2.2. Chromatographic conditions

Chromatograms were obtained with a Hewlett-Packard (HP) Model 5890 Series II system, employing a 0.33-μm HP-1 fused-silica capillary column (12 m × 0.2 mm I.D.) with hydrogen as the carrier gas and the following temperature programme: 100°C for 2 min, increased at 3°C/min to 150°C and then at 6°C/min to 280°C, held

Table 1
Dimensions of the major components of the SFE system

Parameter	Pressurization vessel (mm)		Extraction cell (mm)				Oven (mm)
	1	2	1	2	3	4	
External diameter	100	137	0.4	0.9	45	49	
Internal diameter	65	102	0.2	0.7	30	34	
External length	175	150	222	217	439	345	700
Internal length	153	140	210	205	424	330	
Thickness	18	17	0.1	0.1	8	8	1.5
Width							300
Height							300
Total volume (ml)	507.44	1143.39	0.7	7.9	299.5	299.5	63 000

for 20 min. Volumes of 1.5 μl of a dichloromethane solution (8 mg/ml) were injected using the split mode (1:28). Flame ionization detection (FID) was applied.

2.3. Plant material

Leaves of *Cymbopogon citratus* were collected in the UNAERP (Universidade de Ribeirão Preto) vegetable biotechnology facilities. The plant was dried, ground and stored before use.

2.4. Calibration and supercritical fluid extraction

Calibration of the SFE system was done by measuring the extraction time [the total time that all the supercritical fluid contained in the pressurization vessel (500 ml) took in traversing the system]. The temperature and the loading of the extraction cell were fixed (75°C and 80 g of plant material, respectively). Three different pressures (80, 100 and 120 atm) were used for supercritical CO_2 and for CO_2 modified with 10% of hexane, ethyl acetate or methanol.

The SFE of *C. citratus* was performed in the SFE system shown in Fig. 1. The extraction was done with CO_2 modified with 10% of hexane, followed by sequential extraction of the same sample with CO_2 modified by 10% of acetone. Amounts of 45 g of plant material were used for these extractions. The SFE conditions were temperature 75°C, pressure 80 atm and volume of supercritical fluid for each extraction 1000 ml. Each extraction was completed in 90 min. A conventional extraction of the essential oils was done by steam distillation in a conventional distillation system with 45 g of plant material and 1000 ml of distillate water at its boiling point over 4 h. After a clean-up, these extracts were chromatographed by high-resolution GC using the described conditions.

3. Results and discussion

The extraction system developed in this work (Fig. 1 and Table 1) is versatile as it allows the use of different extraction cells and a wide variety of solvents and modifiers for CO_2. In addition, it allows the use of several extraction techniques, including static extraction, when both valves 1 and 2 are closed after loading the extraction cell, or dynamic extraction when both valves 1 and 2 are open. Having the same matrix in a dynamic extraction and changing the supercritical fluid, a sequential extraction, such as that presented in this paper, is carried out.

This system has the additional advantage of being less expensive than most commercially available systems and can be constructed very simply in an ordinary workshop. Its limited operational conditions of pressure (nitrogen) and temperature (about 100°C) are suitable for the extraction of most natural products, where there are many thermally unstable products of great interest. This limitation is compensated for by the possibility of using different modifiers and the ease of operation.

The use of a variety of modifiers during the system calibration (Fig. 2 and Table 2) showed that the extraction time is directly proportional to the modifier density, *i.e.*, the higher the density the longer is the extraction time. This is well exemplified by ethyl acetate, which is denser than any of the other modifiers studied. This suggests that the extraction capability and the selectivity depend on the fluid density and can be changed with the type of the modifier. For pure fluids (exemplified by CO_2 in the dense gas state) an increase in temperature will produce an increase in viscosity. As a consequence, an increase in the extraction time will be observed.

The yields obtained by steam distillation, SFE with CO_2–10% hexane and SFE with CO_2–10% acetone extraction are 0.2066, 0.0217 and 0.0074 g (0.46, 0.05 and 0.02%), respectively.

The chromatographic profiles obtained by high-resolution GC (Fig. 3) were analysed and show that, in region I, the extracts obtained using CO_2 modified with 10% of hexane and steam distillation contain the same compounds, although with a visible intensification of some peaks, such as 4, 14 and 15. A further supercritical fluid extraction, with CO_2 modified with 10% of acetone, on the same matrix extracted differ-

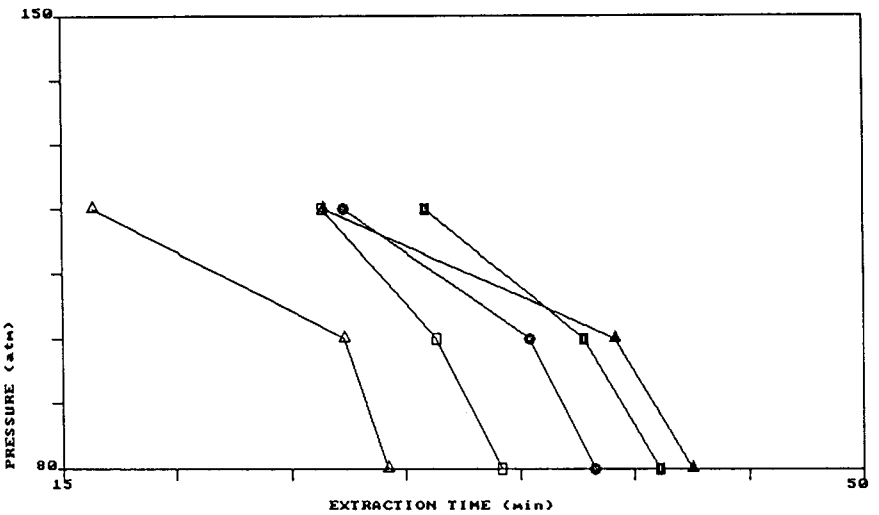

Fig. 2. Calibration graph for the designed system showing pressure *vs.* extraction time for several fluids. △ = CO_2 (75°C); ▲ = CO_2 (95°C); □ = CO_2–10% hexane (75°C); ● = CO_2–10% methanol (75°C); ■ = CO_2–10% ethyl acetate (75°C).

ent compounds, such as 9, 12 and 13, not present in the other extracts. In region II, several compounds can be observed that are not present in the steam distillation extract (Fig. 3a) and were extracted only by modified CO_2. In region III, the CO_2–acetone extract shows enhancement of several compounds while compounds 20, 21 and 22 were not extracted with the other solvents.

4. Conclusions

The system described shows sufficient versatility to be used in several extraction modes, allows the use of several modifiers, either gas or liquid, is inexpensive in construction and easy to operate and maintain. It also presents both analytical and semi-preparative capabilities.

The results for natural products obtained with this system indicate that SFE using modified CO_2 can be selectively tuned by choosing the type and percentage of the modifier utilized. Sequential extraction can be extremely useful when there is a need to extract selected compounds, to enhance the extraction yields or to remove compounds that will interfere in subsequent analysis.

This contribution may open up new perspectives in the study of CO_2 modifiers, mainly in studies with plants and their volatile compounds.

Table 2
Extraction time obtained in the SFE system calibration

Pressure (atm)	Extraction[a] time (min)				
	1	2	3	4	5
80	42.5	29.2	34.2	41.1	38.3
100	39.2	27.3	31.3	37.8	35.4
120	26.4	16.4	26.4	30.9	27.3

[a] 1 = CO_2 (95°C); 2 = CO_2 (75°C); 3 = CO_2–10% hexane (75°C); 4 = CO_2–10% ethyl acetate (75°C); 5 = CO_2–10% methanol (75°C).

5. Acknowledgements

The authors thank the Coordenação de Aperfeiçoamento de Pessoal de Nível Superior (CAPES) for financial support. They also thank the mechanical shop team of the DQFM, USP, São Carlos, for the manufacture of the components of the SFE system. Dr. Suzelei de Castro França and Ana Maria Soares Pereira, Departamento de Biotecnologia, UNAERP, Ribeirão Preto, SP, Brazil, are thanked for donating the plant material.

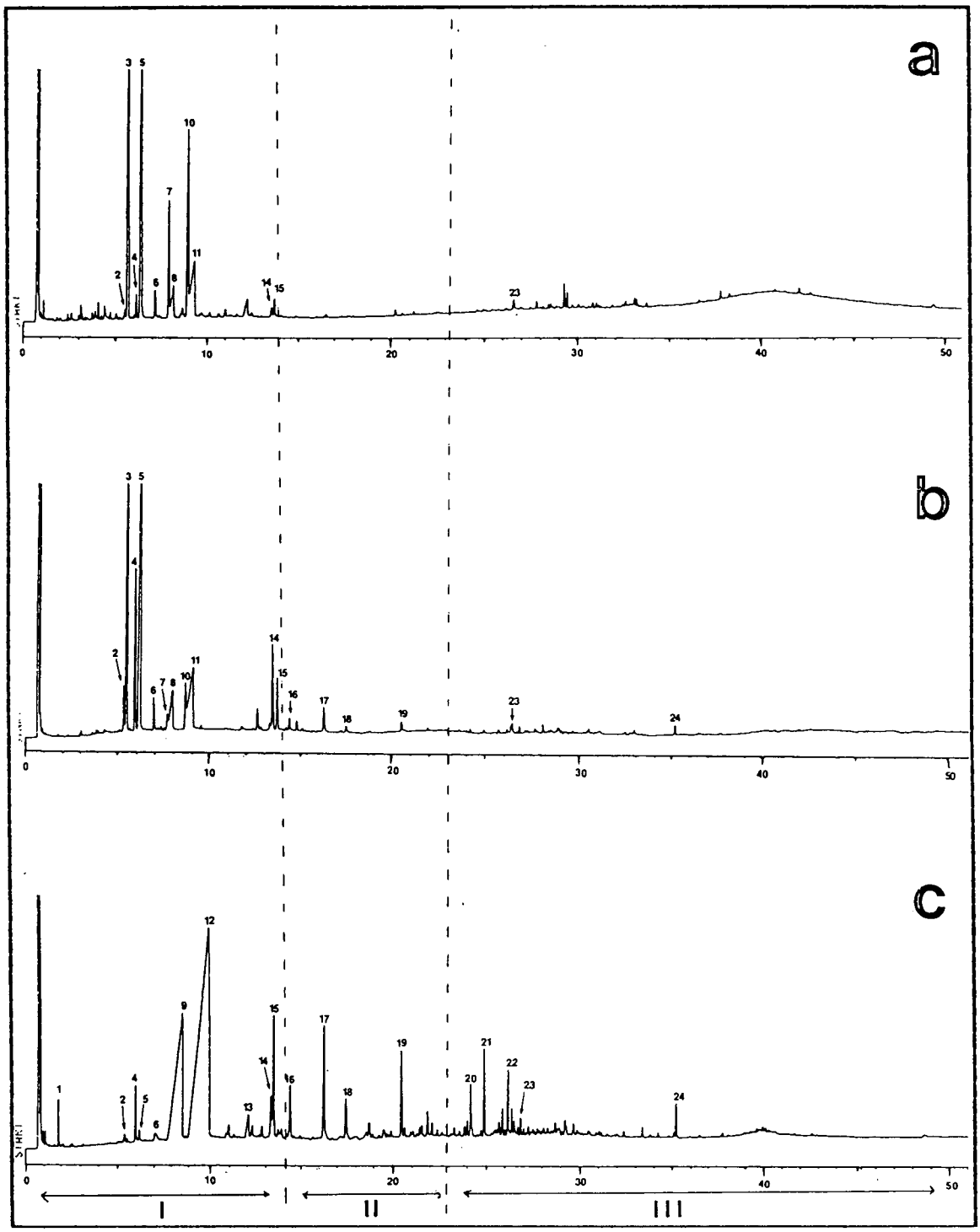

Fig. 3. Chromatograms obtained by high-resolution GC–FID of extracts from *C. citratus* obtained by (a) steam distillation, (b) SFE with CO_2–10% hexane and (c) SFE with CO_2–10% acetone. Time scale in min.

6. References

[1] F.M. Lanças, B.S. DeMartinis and M.A.A. da Matta, *J. High Resolut. Chromatogr.*, 12 (1990) 838.
[2] S.B. Hawthorne and D.J. Miller, *J. Chromatogr. Sci.*, 24 (1986) 258.
[3] S.B. Hawthorne and D.J. Miller, *Anal. Chem.*, 59 (1986) 1705.
[4] S.S.H. Rizvi, A.L. Benado, J.A. Zollweg and J.A. Daniels, *Food Technol.*, 40, No. 6 (1986) 55–64.
[5] H. Brogel, *Chem. Ind. (London)*, 12 (1982) 385–390.
[6] T.R. Bott, *Chem. Ind. (London)*, 12 (1982) 394–396.
[7] M. McHug and V. Krukonis, *Supercritical Fluid Extraction, Principles and Practice*, Butterworths, Boston, MA, 1986.
[8] E. Stahl, *Rev. Latinoam. Quim.*, 11, No. 1 (1980) 1–7.
[9] J.A. Hyatt, *J. Org. Chem.*, 49 (1984) 50–97.
[10] D.K. Dandge, J.P. Heller and V. Wilson, *Ind. Eng. Chem., Prod. Res. Dev.*, 24 (1985) 162–166.

ELSEVIER

Journal of Chromatography A, 667 (1994) 219–223

JOURNAL OF CHROMATOGRAPHY A

Determination of sulphonic compounds as their thiotrifluoroacetate derivatives by gas chromatography with ion trap detection

Xiao-dong Li*, Zi-sen Lin

Research Centre of Analysis and Measurement, Fudan University, Shanghai 200433, China

(First received September 6th, 1993; revised manuscript received November 23rd, 1993)

Abstract

A reductive method for the derivatization of sulphonates is described that is rapid (completed in a few minutes at room temperature) and uses mild conditions. Aromatic and aliphatic sulphonates were converted into the corresponding thiotrifluoroacetate derivatives using the reductive system sodium iodide–dimethylformamide–trifluoroacetic anhydride. 2-Amino-5-naphthol-7-sulphonic acid (J acid) was also derivatized successfully under the same conditions. All the derivatives were stable and could be separated easily by GC. The abundances of the molecular ion peaks were high on the ion trap detector and were convenient for identification.

1. Introduction

Sulphonic compounds are highly polar, non-volatile compounds that are applied extensively in the chemical and pharmaceutical industries. Methods such as IR, NMR and mass spectrometry and GC and HPLC are commonly used for the determination of sulphonates [1–3].

GC determinations are normally performed after converting sulphonates into volatile derivatives. The derivatization methods include sulphonyl esterification [4,5], trimethylsilylation [6], chlorination [7] or fluorination [8], desulphonation with acids [9,10] and alkali fusion [11]. However, the usefulness of these methods may be limited by the time-consuming derivatization process and the poor volatility of some derivatives.

Based on the high volatility of thiols, we attempted to establish a method of reducing sulphonates to their thiol derivatives. There were few reports on direct reduction methods for sulphonates before the 1980s owing to the inert chemical properties of the sulphonic group. The common method was to convert the sulphonates into sulphonyl chloride [12,13] and then to use reductive reagents such as Zn–HCl or $LiAlH_4$ [14] to form the thiol. In 1980, Numats *et al.* [15] reported a reductive system composed of $(CF_3CO)_2O$–Bu_4Ni–CH_2Cl_2 and the direct reduction of sulphonates to thiols. Direct reduction methods were subsequently extended with the use of triphenylphosphine [16,17], polyphosphoric acid [18] and boron halides [19].

After investigating many compounds and making various improvements, we have adopted a reductive system consisting of sodium iodide–dimethylformamide–trifluoroacetic anhydride

* Corresponding author.

0021-9673/94/$07.00
SSDI 0021-9673(93)E1259-3

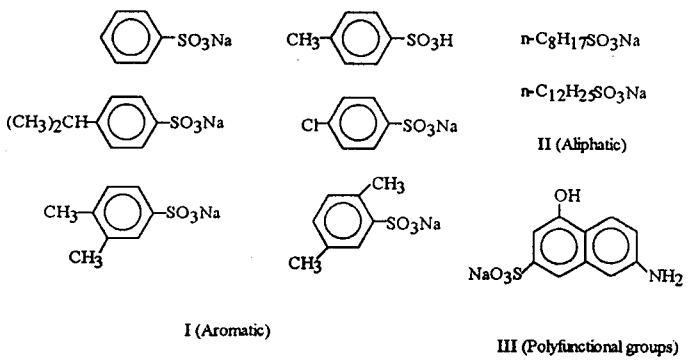

[NaI–DMF–$(CF_3CO)_2O$]. Many kinds of sulphonates have been reduced with the system and the derivatives have been characterized successfully by GC with ion trap detection (ITD).

2. Experimental

2.1. Reagents

p-Toluenesulphonic acid as the free acid and benzene-, 2,5-dimethylbenzene-, 3,4-dimethylbenzene-, dodecyl- and 2-amino-5-naphthol-7-sulphonate as sodium salts were purchased from Shanghai No. 1 Chemical Reagents Factory (Shanghai, China). Sodium octanesulphonate was purchased from Nacalai Tesque (Kyoto, Japan). *p*-Chlorobenzene and *p*-isopropylbenzene as sodium salts were synthesized in the laboratory [20] and confirmed by their IR spectra (Nicolet 5BX Fourier transform IR spectrometer). Sodium iodide and N,N-dimethylformamide were purchased from Shanghai No. 1 Chemical Reagents Factory. Trifluoroacetic anhydride was purchased from Merck.

2.2. Gas chromatography with ion trap detection

A Model 8810 gas chromatograph–Finnigan Mat Model 800 ion trap detector with a DB-5 capillary column (30 m × 0.25 mm I.D.) was employed under following conditions: carrier gas (helium) flow-rate, 25 ml/min; injection port temperature, 250°C; column temperature, 90°C isothermal for 3 min, then increased at 10°C/min to 250°C and maintained at 250°C for 10 min; transfer line temperature, 200°C; ion trap temperature, 200°C; amplifier voltage, 1350 V; mass range scanned, 45–650 u; 1.000 s per scan. Version 4.1 of the ITDS software (Finnigan Mat) was used with the instruments.

2.3. Derivatization procedure

A 10–30-mg amount (about 0.1 mmol) of sulphonate was dissolved in DMF (2 ml) containing 5–12 equiv. of $(CF_3CO)_2O$ and NaI. The solution was allowed to stand at room temperature for several minutes and the resulting solution became coloured dark red with free iodine. A 0.1-μl volume of the solution was injected in the GC–ITD system.

3. Results and discussion

3.1. Derivatization reaction

Sulphonates were converted into the corresponding thiols after reduction with NaI–DMF–$(CF_3CO)_2O$ and the excess of $(CF_3CO)_2O$ reacted with thiols to form thiotrifluoroacetates eventually:

$$RSO_3Na + (CF_3CO)_2O + NaI \xrightarrow[DMF]{\text{room temperature}} RSCOCF_3 + I_2 + CF_3CO_2Na$$

The reaction was rapid, being completed in a

few minutes at room temperature, and the thiotrifluoroacetate was the sole product. The optimum conditions were 8 equiv. of NaI and 10 equiv. of $(CF_3CO)_2$ with respect to the sulphonates. The yields ranged from 75% to 85% measured by the internal standard method (naphthalene as standard).

Many reports [16–18] have considered the mechanism of the reduction. The reaction rates were accelerated if the polar aprotic solvent DMF was used, which might be due to the following reasons [21,22]: the nucleophilicity of I^- was strengthened in DMF because of the creation of "naked anions", making I^- more reactive; and the charges on the sulphonate molecule and its intermediate were dispersed in DMF, the weakened solvation causing the molecule to be attacked more readily.

The advantage of this approach is that no by-products are present in the solution after derivatization and therefore interferences from by-products are avoided in the chromatographic separation. Further, the retentions of iodine, trifluoroacetic anhydride and the solvent DMF were very short on the capillary column and therefore they do not affect the separation and identification of the derivatives. The residual sulphonates and inorganic salts such as $NaCO_2CF_3$ and NaI are non-volatile and are incapable of generating chromatographic peaks, hence the reaction solution can be injected directly into the GC system without treatment.

3.2. Derivatives

The structures of all the derivatives were confirmed by GC–ITD. The experiments showed that not only do the thiotrifluoroacetates have good chromatographic properties but also the high abundance of the molecular ion in the ITD system made structure identification easy.

The mass spectrum of *p*-toluic thiotrifluoroacetate is shown in Fig. 1. The molecular ion peak (M^+) with the postulated *m/z* 220 and the prominent fragment ion peaks at *m/z* 151 ($M^+ - CF_3$), 123 ($M^+ - COCF_3$) and 91 ($M^+ - SCOCF_3$) were observed and were useful for structure elucidation.

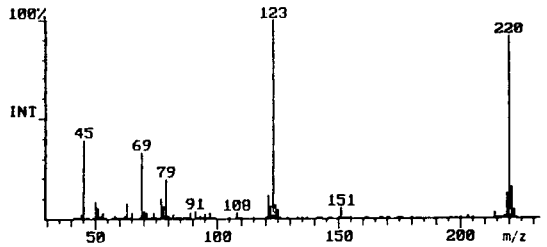

Fig. 1. Mass spectrum of *p*-toluic thiotrifluoroacetate.

In addition to the derivatization of aromatic sulphonates, the reductive system could also be employed as a derivatization reagent for aliphatic sulphonates.

A solution of dodecylsulphonate derivatized under the same procedure as above was prepared and 0.1 μl of the sample was injected into the GC system. The chromatographic peak of derivatives of aliphatic sulphonates were stable and underwent no thermal decomposition during GC–ITD. The mass spectrum of dodecyl thiotrifluoroacetate is shown in Fig. 2.

The formation of the $(M + 1)^+$ ion is attributed to the self-chemical ionization and space charging in the ion trap [23]. The principal fragmentation pathway of dodecyl thiotrifluoroacetate is shown in Fig. 3.

2-Amino-5-naphthol-7-sulphonic acid (J acid):

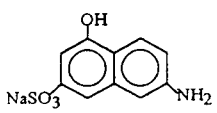

is a dye synthetic intermediate with hydroxyl, amino and sulphonic groups in the molecule. Because of this variety of groups, J acid is

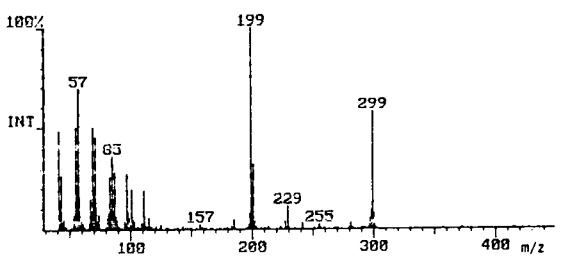

Fig. 2. Mass spectrum of dodecyl thiotrifluoroacetate.

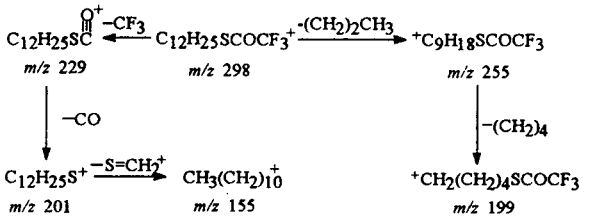

Fig. 3. Principal fragmentation pathway of dodecyl thiotrifluoroacetate.

difficult to separate and identify. The acylation of NH_2, OH and SH groups with trifluoroacetic anhydride is one of the most commonly used derivatization methods and proceeds under mild conditions [24]. The reduction products of J acid were acylated by the excess of trifluoroacetic anhydride in the reductive system. We considered that the OH and NH_2 groups could be acylated while the sulphonate was being reduced, which could improve the volatility of the compounds.

The results indicated that the sulphonic group of J acid was reduced to the thiol and the three polar functional groups (OH, NH_2 and SH) were trifluoroacetylated. The material representing the chromatographic peak of the J acid derivative was separated in a DB-5 capillary column at 250°C. Because of the conjugated bonds in the structure of the derivatives, the molecular ion peak was the base peak and few fragments were produced. The mass spectrum of the J acid derivative is shown in Fig. 4.

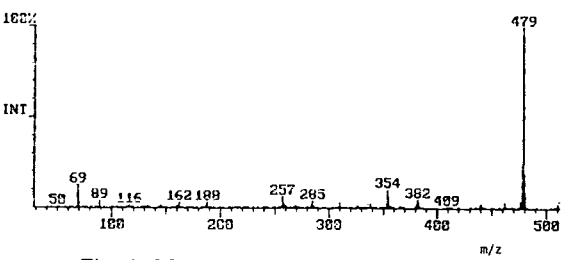

Fig. 4. Mass spectrum of J acid derivative.

The molecular ion at m/z 479 has the structure

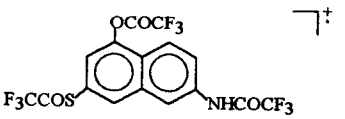

To examine a sulphonate mixture, eight sodium sulphonates were mixed and derivatized as described above, and 0.1 μl of the solution was injected into the GC–ITD system. Fig. 5 shows the total ion current chromatogram obtained. Each chromatographic peak represented different amounts of derivatives, ranging from 20 to 400 ng.

It could be concluded that all sulphonates were derivatized to thiotrifluoroacetates by the reductive system and were separated well by GC.

The derivatives of 2,5-dimethylbenzene sulphonate and 3,4-dimethylbenzene sulphonate were separated in the column, indicating that compounds with very similar structures could be separated by GC after derivatization. Different fragmentation pathways of the two isomers could be inferred from their mass spectra. For exam-

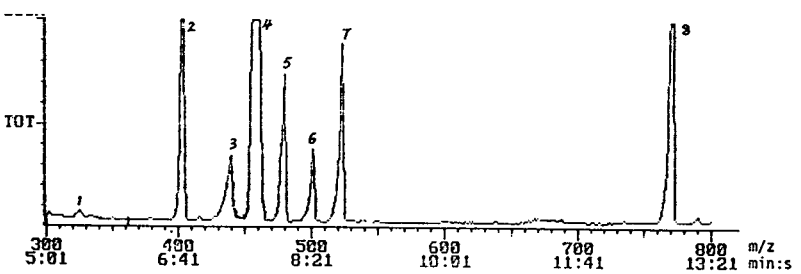

Fig. 5. Total ion current chromatogram of sulphonates as the thiotrifluoroacetate derivatives. Peaks: 1 = phenyl; 2 = toluic; 3 = *p*-chlorophenyl; 4 = *n*-octyl; 5 = 2,5-dimethylphenyl; 6 = 3,4-dimethylphenyl; 7 = *p*-isopropylphenyl; 8 = dodecyl thiotrifluoroacetate.

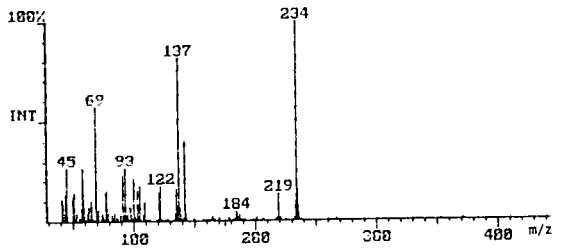

Fig. 6. Mass spectrum of 2,5-dimethyl thiotrifluoroacetate.

ple, the fragments ion at m/z 219 of the 2,5-dimethyl compound was deduced to be the fragment $(M^+ - CH_3)$ and the steric exclusion between the *o*-methyl and trifluoroacetyl groups of the 2,5-dimethyl compound led to high abundances of the fragment ions at m/z 137 and 69 which differed from the abundances for the 3,4-dimethyl compound. Figs. 6 and 7 show the mass spectra of the two isomers.

4. Conclusions

Aromatic and aliphatic sulphonates and sulphonates with polyfunctional groups could be derivatized in a few minutes at the room temperature by a simple reduction method. The resolution of two isomeric derivatives of dimethylbenzene sulphonates revealed that the derivatives showed excellent GC behaviour and the derivatization of J acid showed that this method has potential application to the GC analysis of complicated sulphonates.

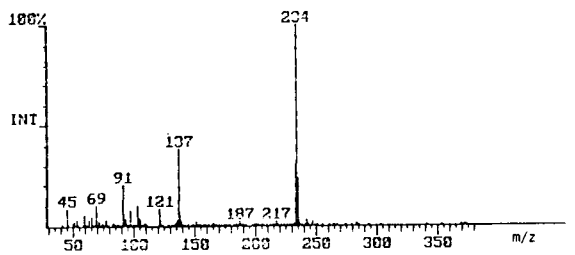

Fig. 7. Mass spectrum of 3,4-dimethyl thiotrifluoroacetate.

5. References

[1] A. Nakae, K. Tsuji and M. Yamanaka, *Anal. Chem.*, 53 (1981) 1812.
[2] P. Agozzino, L. Coranlo, M. Ferrngia, E. Caponetti, F. Intravaia and R. Triolo, *J. Colloid Interface Sci.*, 114 (1986) 26.
[3] A. Heywood, A. Mathias and A.E. Williams, *Anal. Chem.*, 42 (1970) 1272.
[4] A.E. Homsi, B. Gilot and J.P. Canselier, *J. Chromatogr.*, 151 (1978) 413.
[5] J.J. Kirkland, *Anal. Chem.*, 32 (1960) 1388.
[6] J. Eagles, *Anal. Chem.*, 43 (1971) 1697.
[7] J.S. Parson, *J. Chromatogr. Sci.*, 11 (1973) 659.
[8] J.S. Parson, *J. Gas Chromatogr.*, 5 (1967) 254.
[9] J.D. Knight and R. Honse, *J. Am. Oil Chem. Soc.*, 36 (1959) 195.
[10] E.A. Setzkorm and A.B. Carel, *J. Am. Oil Chem. Soc.*, 40 (1963) 57.
[11] T. Nakagawa, K. Miyajima and T. Uno, *J. Gas Chromatogr.*, 6 (1968) 292.
[12] H. Alper, *Angew. Chem.*, 81 (1969) 706.
[13] D. Cipris and P. Douli, *Synth. Commun.*, 9 (1979) 207.
[14] O. Hisashi and K. Tsugio, *Bunseki Kagaku*, 28 (1979) 410.
[15] T. Numats, H. Awano and S. Oae, *Tetrahedron Lett.*, 21 (1980) 1235.
[16] K. Fujimori, H. Togo and S. Oae, *Tetrahron Lett.*, 21 (1980) 4921.
[17] S. Oae and H. Togo, *Synthesis*, (1981) 371.
[18] S. Oae and H. Togo, *Synthesis*, (1982) 152.
[19] G.A. Olah, S.C. Narang, L.D. Field and R. Karpeles, *J. Org. Chem.*, 461 (1981) 2408.
[20] C.M. Suter and A.W. Weston, *Org. React.*, 3 (1950) 141.
[21] T.F. Magners, G. Caldwell, J. Sunner, S. Ikata and P. Kebarle, *J. Am. Chem. Soc.*, 106 (1984) 6140.
[22] A.J. Parker, *Pure Appl. Chem.*, 53 (1981) 1437.
[23] L.K. Pannell, Q.L. Pu, H.M. Fales, R.T. Mason and J.L. Stephenson, *Anal. Chem.*, 61 (1989) 2500.
[24] M. Donike, *J. Chromatogr.*, 78 (1973) 273.

ELSEVIER

Journal of Chromatography A, 667 (1994) 225–233

JOURNAL OF CHROMATOGRAPHY A

Determination of neutral lipids from subcutaneous fat of cured ham by capillary gas chromatography and liquid chromatography

J.A. García Regueiro*, J. Gibert, I. Díaz

IRTA, Unitat de Tecnologia Analítica, Centre de Tecnologia de la Carn, Granja Camps i Armet, 17121 Monells (Girona), Spain

(First received May 5th, 1993; revised manuscript received December 6th, 1993)

Abstract

The determination of neutral lipids in fat of cured ham is reported. Fat samples were extracted with chloroform–methanol (2:1) and neutral lipids and free fatty acids were separated on an aminopropyl minicolumn, the first fraction with chloroform–2-propanol (neutral lipids) and the second fraction with 2% acetic acid in diethyl ether (free fatty acids). Neutral lipids were fractionated with minicolumns, with aminopropyl and silica stationary phases. Two fractions were obtained with the first column: (A) triglyceride and cholesteryl esters and (B) cholesterol and mono- and diglycerides. Fraction A was applied to the silica column to obtain two new fractions: (C) cholesteryl esters and (D) triglycerides. Fractions B and C were analysed by capillary gas chromatography (cGC) and fraction D by cGC and HPLC. The R.S.D.s obtained were below 5% except for the monoglycerides (8%). Cholesteryl esters were determined by cGC in 5 min with R.S.D. 5%. The main triglycerides identified were PPO, POS, POO, POL and OOO (P = palmitic acid, O = oleic acid, L = linoleic acid; S = stearic). Monoglyceride and diglycerides having 18, 34 and 36 carbon atoms were the most abundant. The determination of triglycerides by HPLC was more difficult than by cGC because the linearity with HPLC was concentration dependent. The procedure allowed the determination of neutral lipid classes without derivatization of mono- and diglycerides.

1. Introduction

Neutral lipids are the main components of fat tissues. Triglycerides are the most abundant class of neutral lipids (90% or more), but minor constituents such as cholesterol, cholesteryl esters and mono- and diglycerides must be considered when characterizing a fat and studying lipolysis during the production of fatty foods. Fatty acids have been used to establish the fat composition and to evaluate lipid degradation in some kinds of food products, and in particular in cured ham and sausages fatty acids have been determined in order to study changes produced by lipid oxidation and hydrolysis [1–3]. However, fatty acid profiles do not reveal specific changes in a neutral lipid class as they are an indirect measure of the true molecular species. Biochemical changes during the production of meat products (cured ham, sausages) can be better characterized on the basis of the depletion

* Corresponding author.

0021-9673/94/$07.00
SSDI 0021-9673(93)E0011-I

of some triglycerides and the subsequent increase in mono- and diglyceride production [4]. The determination of neutral lipid classes is generally carried out only to measure the total percentage of each lipid class by TLC or HPLC without separating them into individual components [5–8], although there are methods for determining the molecular species of diglycerides or monoglycerides by HPLC or GC [9–11]. However, with meat products a suitable method for determining neutral lipid classes has not been reported. An important aspect of lipid analysis is the prior fractionation to separate neutral lipids from polar and complex lipids, and different materials (silica, silicic acid, Florisil) have been used for this purpose [12–14].

The development of thermally stable stationary phases has allowed the analysis of neutral lipids by capillary GC (cGC) on the basis of carbon number (CN) and the number of double bonds (NDB) in the same CN [15–17]. HPLC analysis with light-scattering detection is an alternative technique for determining neutral lipids as gradient elution can be used to increase the peak resolution [18–20]. The separation of triglycerides by HPLC is carried out on the basis of the equivalent carbon number (ECN) defined as $ECN = CN - 2NDB$ or $ECN = CN\text{-}a NDB$, where a is calculated by linear regression [21]. The peak assignment is easier in cGC as the elution pattern with medium-polarity stationary phases is related to the NDB; the higher the NDB, the greater is the retention time in the same CN. Quantification is more complicated in HPLC because the linearity changes with the concentration range [18,22].

This paper describes a method for determining neutral lipids in ham fat by cGC and HPLC using prior separation of neutral lipids into three fractions: triglyceride, cholesteryl esters and cholesterol and mono- and diglycerides.

2. Experimental

The following abbreviations are used: MG = monoglycerides; DG = diglycerides; CP = cholesteryl palmitate; CS = cholesteryl stearate; fatty acids: P = palmitic (C16:0); S = stearic (C18:0); O = oleic (C18:1); L = linoleic (C18:2) and araquidonic (C20:4); triglycerides: POS = palmitoyloleoylstearoyl. This nomeclature does not indicate the position of the fatty acid in triglyceride molecules.

2.1. Samples and extraction

Subcutaneous fat from cured ham, at 5 months of ageing, was taken for analysis. Lipids were extracted from subcutaneous fat (1 g) with 50 ml of chloroform–methanol 2:1 [23]. The extract was evaporated to dryness and the residue was dissolved in a 10 ml of chloroform.

2.2. Lipid fractionation

The method used is a combination of previous methods [13,14,24] to achieve a complete separation of cholesteryl esters from triglycerides. An alliquot (10 mg of extractable fat) of the dissolved extract was applied to an aminopropylsilica minicolumn (100 mg; Analytichem). A prior fractionation was applied to obtain free fatty acids, first with 2 ml of chloroform–2-propanol (neutral lipids) and second with 3 ml of 2% acetic acid in diethyl ether (free fatty acids). The first fraction was applied to a second aminopropylsilica minicolumn (500 mg; Analytichem) and neutral lipid classes were collected under the following conditions: (A) 5 ml of 1% diethyl ether and 10% dichloromethane in hexane (triglycerides and cholesteryl esters) and (B) 5 ml of chloroform–methanol (2:1) (mono- and diglycerides and cholesterol). Fraction A was evaporated to dryness and the residue was dissolved in 1 ml of isooctane, then the solution was applied to a silica minicolumn (500 mg; Millipore) to separate triglycerides from cholesteryl esters by the following procedure: (C) 4 ml of hexane–diethyl ether (98:2) (cholesteryl esters) and (D) 5 ml of hexane–diethyl ether (90:10) (triglycerides).

2.3. Chromatographic analysis

Fraction D was analysed by HPLC and cGC. The HPLC conditions were as follows: LiChrospher RP-18 column (250 × 4 mm I.D.) (Merck)

at ambient temperature (<20°C); mobile phase: gradient from 30 to 60% dichloromethane in acetonitrile in 50 min at a flow-rate of 1.00 ml/min; detection, light-scattering detector (ACS) at 70°C; and injection volume 10 μl via a Rheodyne valve. The pump system was an LKB 2152 HPLC pump controller and an LKB 2150 HPLC controller (Pharmacia). For cGC analysis, two fused-silica open tubular (FSOT) columns, 10 m × 0.2 mm I.D. (0.1 μm film thickness) coated with methylsilicone (MS) and 25 m × 0.2 mm I.D. (0.15 μm film thickness) coated with 50% phenyl–methylsilicone (PMS) (Rescom, Belgium), were used, connected to a deactivated retention gap (1 m × 320 μm I.D.) (Supelco, Bellefonte, PA, USA). The MS column was used for cholesterol and mono- and diglyceride analysis and the PMS column for triglyceride analysis. The carrier gas was helium at 50 cm/s (MS) and 60 cm/s (PMS), with temperature programming from 150 to 310°C at 5°C/min for the MS and from 330 to 360°C at 1.5°C/min for the PMS column. A flame ionization detector at 380°C and on-column injection with high-temperature secondary cooling were used. The gas chromatograph used was a Carlo Erba HRGC 5300HT Mega series.

The analysis of free fatty acids as methyl esters (FAMEs) was carried out by cGC. A 1-ml volume of 14% BF_3 in methanol was used to obtain methyl esters (20 min at 50°C), which were recovered in 2 ml of hexane. A FSOT column (25 m × 0.25 mm I.D.) coated with 60% cyaonopropylsilica (SH-90) (Rescom) (0.20 μm) was used to separate FAMEs under the following conditions: temperature, programmed from 140 to 180°C at 3°C/min, held at 180°C for 5 min; detector and injector temperatures, 250°C; carrier gas helium at 1.00 ml/min at constant flow; split injection mode (splitting ratio 1:40); and gas chromatograph, Hewlett-Packard 5890 Series II with electronic pressure control.

2.4. Standard solutions

Three standard solutions of monolein (MG18), distearin (SS), cholesterol (40 ng/μg), cholesteryl palmitate and stearate (CP, CS) (20 ng/μl) and triglycerides (PPO, POS, POO, OSO and SOS), PPO (1,2-dipalmitoyl-3-oleoyl-*rac*-glycerol), POS (1-palmitoyl-2-oleoyl-3-stearoyl-*rac*-glycerol), POO (1,2-dioleoyl-3-palmitoyl-*rac*-glycerol) OSO (1,3-dioleoyl-2-stearoyl-*rac*-glycerol) and SOS (1,3-distearoyl-2-palmitoyl-*rac*-glycerol) (20 and 500 ng/μl) were prepared in isooctane. Standard solutions of pentadecanoic and heptadecanoic acids (50 ng/μl) were used for the determination of free fatty acids. All the compounds were obtained from Sigma (St. Louis, MO, USA).

2.5. Repeatibility and linearity

Standard and sample fraction (A, B, C and D) solutions were injected seven times and subjected to the different chromatographic techniques described. Linearity, using four points, was established with standard solutions.

2.6. Fraction repeatibility

A fat sample was fractionated five times and each fraction was analysed by the procedure described. Peak areas obtained for the selected compounds (Table 1) were used to determine the fraction repeatibility.

3. Results and discussion

3.1. Sample preparation

The complete determination of neutral lipids in the same run is possible, but with fat samples the high concentration of triglycerides (>90%) limited this possibility because it was necessary to concentrate the extract to allow the analysis of minor neutral lipid classes which caused the simultaneous concentration of triglycerides, resulting in large amounts being introduced into the gas chromatograph (*e.g.*, 500 ng/μl). To avoid this problem, it was necessary to preseparate triglycerides from the other neutral lipid classes. In the first instance the use of the aminopropyl column to obtain three fractions, (1) cholesteryl esters, (2) triglycerides and (3) cholesterol and mono- and diglycerides, was evaluated, but it was not possible to separate triglycerides from cholesteryl esters owing to the

Table 1
Selected compounds evaluated for determination of fraction repeatibility

Fraction	Compound
B	Monolein, cholesterol, diolein
C	Cholesteryl palmitate and stearate[a]
D	Triglycerides (PPO, POS, POO, POL, OOO)
Free fatty acids	C16:0, C18:0, C18:1, C18:2, C20:4

[a] Spiked sample.

high content of triglycerides. The silica column allowed the separation of cholesteryl esters from triglycerides. The fraction repeatibilities showed R.S.D.s below 10% for fractions B, C and D obtained from fat samples and considering the selected compounds used to evaluate them (Table 1), but in fraction B the R.S.D. obtained for monoglyceride was 15%. The more difficult analysis of underivatizated monoglyceride could contribute to this poorer repeatibility. On the other hand, cross-contamination of fractions was not observed. When standards of each neutral lipid class were added to samples the recovery was >90%. Free fatty acids showed a high repeatibility (R.S.D. < 10%).

3.2. Triglycerides

Triglycerides were analysed by HPLC and cGC. The repeatibility of both techniques was good, showing R.S.D.s below 5% (Tables 2 and 3). cGC allowed easier peak assignment and the calibration graph was not concentration dependent as in HPLC with light scattering detection. However, the peaks of POO and PSL were not completely separated. It was possible to identify eight peaks by this technique (Fig. 1) on the basis of NDB in a same CN. Linearity for plots of certain selected triglyceride peak areas *versus* concentration showed the following correlation coefficients (r): 0.999 (POP), 0.998 (POS), 0.999 (POO), 0.999 (SOS) and 0.999 (OSO). Retention gaps of 530 μm showed greater peak broadening than 320 μm. HPLC analysis was easier from the point of view of temperature analysis but the calibration graphs were concentration dependent, the slope obtained in the range 50–20 μg being 2649 (SOS) and that in the range 20–5 μg being 749 (SOS); the r values obtained in the range 50–20 μg were 0.989 (POP), 0.991 (POS), 0.999 (POO), 0.989 (SOS) and 0.976 (OSO). The analysis time was longer using HPLC than cGC and the peak assignment was more complicated. A tentative identification

Table 2
Repeatibilities of retention times[a] and concentrations[b] of triglycerides[c] in capillary GC

Compound	x^a	s^a	(%) R.S.D.[a]	x^b	s^b	(%) R.S.D.[b]
PPO	7.49	0.03	0.40	32.20	0.98	3.04
POS	9.03	0.04	0.44	108.10	5.75	5.32
POO	9.19	0.03	0.32	230.00	12.80	5.57
POL	9.44	0.04	0.42	62.10	1.99	3.20
SOO	11.06	0.03	0.27	39.10	1.97	5.04
OOO	11.23	0.03	0.27	46.00	1.94	4.21

[a] Minutes.
[b] Concentrations in mg/g extractable fat.
[c] Ham fat sample.

Table 3
Repeatibilities of retention times[a] and concentrations[b] of triglyceride[c] analysis of HPLC

Triglyceride	x^a	s^a	(%) R.S.D.[a]	x^b	s^b	(%) R.S.D.[b]
POL	19.43	0.07	0.36	66.10	2.87	4.34
OOO	21.56	0.12	0.56	61.70	2.00	3.25
POO	22.64	0.13	0.57	220.40	5.00	2.26
PPO	24.02	0.16	0.67	33.10	1.53	4.60
SOO	25.73	0.16	0.62	30.80	1.27	4.13
POS	27.06	0.17	0.63	105.80	3.42	3.24

[a] Minutes.
[b] Concentrations in mg/g extractable fat.
[c] Ham fat sample.

was made with known standards and by the ECN; thus, ten peaks were identified based on the ECN and by comparison with the results reported by other workers [25] (Fig. 2). HPLC with UV detection could be also used to identify low percentages of polyunsaturated triglycerides (peaks, 1, 2, 3 and 4 in Fig. 2) because of their high relative responses in this detector. Good agreement was observed for concentrations determined by HPLC and cGC expected for OOO, which showed a higher value in HPLC, reflecting the more critical separation of OOO by cGC (Fig. 1).

3.3. Cholesteryl esters

The analysis time for separating cholesteryl esters of 16 and 18 CN by cGC was 5 min (Fig. 3). The R.S.D.s of the retention times and absolute peak areas were <5% (Table 4) for

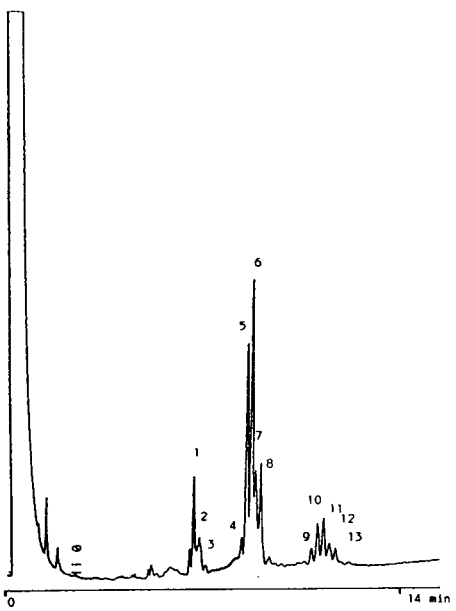

Fig. 1. cGC analysis of triglycerides from ham fat. Peaks identified: 1 = PPO; 5 = POS; 6 = POO; 7 = PLS; 8 = POL; 9 = SOS; 10 = SOO; 11 = OOO; 12 = SOL. For conditions, see text.

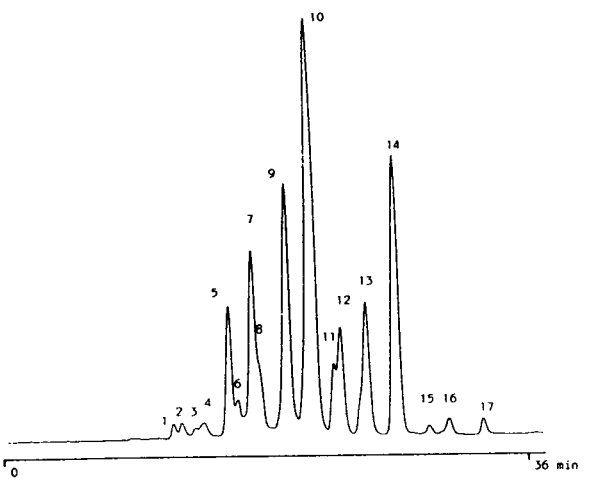

Fig. 2. HPLC analysis of triglycerides from ham fat. Peaks identified: 5 = OOL; 7 = POL; 9 = OOO; 10 = POO; 11 = PSL; 12 = PPO; 13 = SOO; 14 = POS; 16 = SSO; 17 = PSS. For conditions see text.

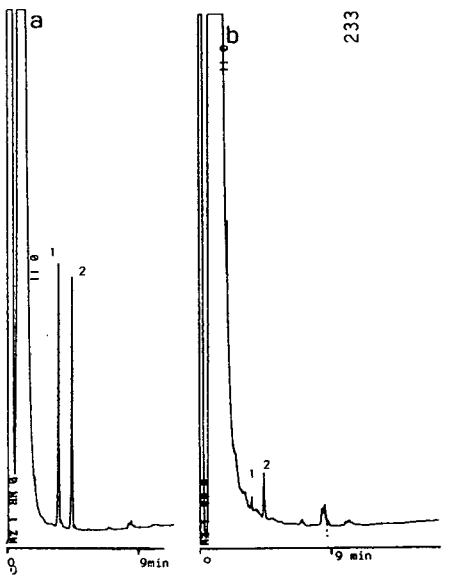

Fig. 3. cGC analysis of fraction B. (a) Ham fat spiked with cholesteryl esters. Peaks: 1 = cholesteryl palmitate (CP); 2 = cholesteryl stearate (CS). (b) Unspiked sample. Peaks: cholesteryl esters of (1) CN 16 and (2) CN 18. For conditions, see text.

standard solutions, but higher values were obtained for fat samples. Cholesteryl ester concentrations are low in fats, and to facilitate the evaluation of the repeatibility the samples were spiked with CP and CS to increase the peak heights. In this instances the R.S.D.s obtained were lower (Table 4) and similar to those obtained with standard solutions. Cholesteryl esters detected in fat samples were associated with 16 and 18 CN, only single peaks were detected and the esterified fatty acid was not assigned. However, the retention time observed for the main compound (CN 18) was shorter than that of CS standard, suggesting the possibility of cholesteryl oleate (OC). Linear plots of concentration in ng/μl (y) *versus* peak area (x) *were* obtained for CP and CS standards: $y = -0.84 + 6.49 \cdot 10^{-5}x$ ($r = 0.999$) and $y = -0.67 + 6.53 \cdot 10^{-5}x$ ($r = 0.998$), respectively.

3.4. Cholesterol and mono- and diglycerides

This fraction was determined without derivatization (Fig. 4). Underivatizated monoglycerides were difficult to analyse and the peak symmetry was poorer than for cholesterol and diglycerides. These difficulties were reflected by the higher R.S.D. (8%) obtained for the repeatibility of the absolute peak area of monoolein. The other compounds showed R.S.D.s below 5% for absolute peak area and retention time repeatibilities (Table 5). Monoglyceride analysis could be improved by derivatization to obtain trimethylsilyl derivatives. The peak identification was based on the retention times of standards and the NDB. Monoolein was the main monoglyceride and diglycerides with 34 and

Table 4
Repeatibilities of retention times[a] and concentrations[b] of cholesteryl esters

Compound	x^a	s^a	(%) R.S.D.[a]	x^b	s^b	(%) R.S.D.[b]
CP[c]	3.51	0.02	0.62	356 140[c]	11800	3.31
CS[c]	4.42	0.03	0.61	342 667[c]	10896	3.18
CE16[d]	3.57	0.01	0.35	94.80	4.93	5.20
CE18[d]	4.37	0.02	0.44	437.30	25.37	5.80
CP[e]	3.51	0.03	0.89	2350.90	81.57	3.47
CS[e]	4.41	0.04	0.89	246.17	55.14	2.24

[a] Minutes.
[b] Concentrations in μg/g extractable fat.
[c] Absolute peak areas corresponding to a concentration of 20 ng.
[d] Sample CE 16 and CE 18 are cholesteryl esters of CN 16 and CN 18, respectively, in fat samples.
[e] Spiked sample.

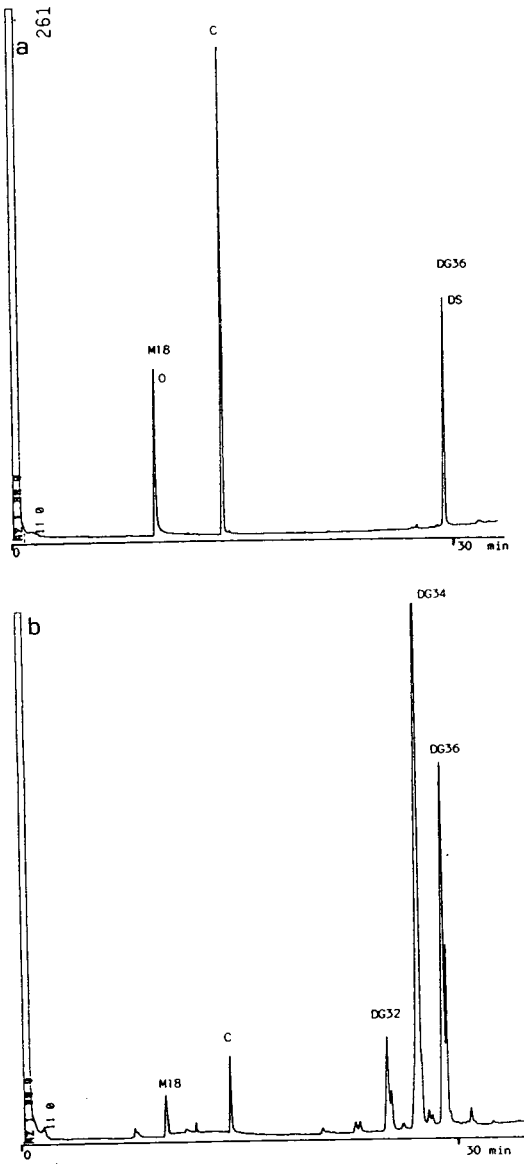

Fig. 4. cGC analysis of fraction B. (a) Standard solution. Peaks: M18 = monoleine; C = cholesterol; DS = distearin. (b) Ham fat. Peaks: M18 = monoglyceride; DG32, DG34 and DG36 = diglycerides of CN 32, 34 and 36, respectively. For conditions, see text.

36 CN were the most abundant. Tentative identifications considering the NDB were made (Fig. 4) and PO, OO and SO were considered the most probable. Linear regression for concentration in ng/μl (y) *versus* peak area were $y = 9.97 + 1.16 \cdot 10^{-4}x$ ($r = 0.990$) for monoolein, $y = 1.99 + 6.36 \cdot 10^{-5}x$ ($r = 0.997$) for cholesterol and $y = 7.29 + 1.14 \cdot 10^{-4}x$ ($r = 0.990$) for distearin.

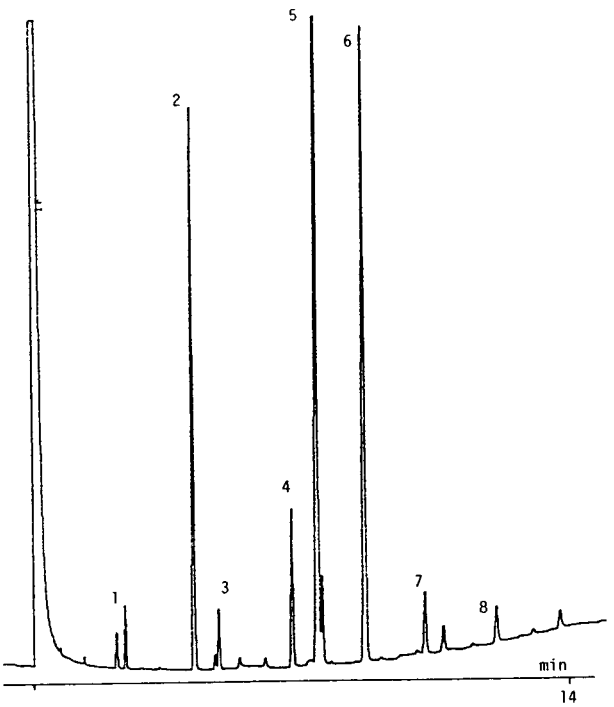

Fig. 5. cGC of free fatty acid fraction. Peaks: 1 = myristic; 2 = palmitic; 3 = palmitoleic; 4 = stearic; 5 = oleic; 6 = linoleic; 7 = linolenic; 8 = arachidonic acid. For conditions, see text.

3.5. Free fatty acid fraction

The separation of fatty acids as FAMEs by GC has been intensively investigated and they were included in this work because they are an important fraction related to lipid changes in food products. The origin of free fatty acids in cured ham is not only associated with neutral lipids; phospholipid breakdown produces free fatty acids but in fat samples this contribution is smaller because of the low percentage of phospholipids. The use of bonded and stabilized polar stationary phases allows the effective separation of FAMEs on the basis of the NDB in the same CN (Fig. 5). The R.S.D.s obtained for

Table 5
Repeatibilities of retention times[a] and concentrations[b] of cholesterol and mono- and diglycerides

Compound	x^a	s^a	(%) R.S.D.[a]	x^b	s^b	(%) R.S.D.[b]
MG18	9.49	0.04	0.44	2286.50	176.97	7.74
Cholesterol	13.73	0.01	0.09	768.35	30.58	3.98
DG32	24.05	0.02	0.07	1975.07	66.17	3.35
DG32	24.26	0.01	0.04	1844.47	76.91	4.16
DG34	26.06	0.01	0.06	26 655.05	927.59	3.48
DG36	27.68	0.01	0.03	20 243.85	734.85	3.63

MG18 = monolein; for diglycerides DG32, DG32, DG34 and DG36, see Fig. 4.
[a] Minutes.
[b] Concentrations in μg/g extractable fat.

Table 6
Repeatibilities of retention times[a] and concentrations[b] of free fatty acids[c] in capillary GC

Fatty acid	x^a	s^a	(%) R.S.D.[a]	x^b	s^b	(%) R.S.D.[b]
C14:0	2.81	0.01	0.35	1.15	0.02	2.13
C16:0	4.38	0.01	0.23	18.11	0.07	0.40
C16:1	4.88	0.01	0.20	2.13	0.07	3.28
C18:0	6.50	0.01	0.15	6.25	0.04	0.62
C18:1	7.05	0.01	0.14	34.81	0.16	0.47
C18:2	8.08	0.01	0.12	27.21	0.19	0.73
C18:3	9.31	0.01	0.10	2.80	0.03	0.94
C20:4	12.37	0.01	0.08	1.89	0.12	6.17

[a] Minutes.
[b] Concentrations in mg/g extractable fat.
[c] Ham fat sample.

both absolute peak areas and for concentrations were below 5% (Table 6). The concentration of free fatty acids can vary as a function of lipolysis intensity and of ageing time.

4. Acknowledgement

This work was supported by the CICYT (Project No. ALI88-0677-C02-01).

5. References

[1] C. Cantoni, M.A. Bianchi, S. D'Aubert, P. Renon and F. Cerutti, *Arch. Vet. Ital.*, 21 (1970) 213.
[2] J. Flores, P. Nieto, S. Bermell and J. Arberola, *Rev. Agroquim. Tecnol. Aliment.*, 27 (1987) 599.
[3] J. Flores, P. Nieto, S. Bermell and J. Arberola, *Rev. Agroquim. Tecnol. Aliment.*, 28 (1988) 90.
[4] J.A. García Regueiro, I. Díaz, F. David and P. Sandra, in *Proceedings of the 35th Congress of Meat Science and Technology*, Vol. III, Danish Meat Research Institute, Copenhagen, 1989, p. 719.
[5] J.E. Storry and B. Tuckley, *Lipids*, 2 (1967) 501.
[6] V.P. Pchelkin and G. Vereshchagin, *J. Chromatogr.*, 209 (1981) 49.
[7] W.W. Christie, *J. Lipid Res.*, 26 (1985) 507.
[8] O.S. Privett, K.A. Douherty, W.L. Erdahl and A. Stolyhwo, *J. Am. Oil Chem. Soc.*, 50 (1973) 516.
[9] J.J. Myher and A. Kuksis, *Can. J. Biochem.*, 60 (1982) 638.
[10] L. Motta, M. Brianza, F. Stanga and G. Amelotti, *Riv. Ital. Sostanze Grasse*, 60 (1983) 625.
[11] H. Takamura, H. Narita, R. Urade and M. Kito, *Lipids*, 21 (1986) 356.

[12] K.K. Carroll, J.H. Cutts and G.D. Murray, *Can. J. Biochem.*, 46 (1968) 899.
[13] K.K. Carroll, in G.V. Marinetti (Editor), *Lipid Chromatographic Analysis*, Vol. 1, Marcel Dekker, New York, 2nd ed., 1976, pp. 173–214.
[14] G. Rouser, G. Kritchevsky and A. Yamamoto, in G.V. Marinetti (Editor), *Lipid Chromatographic Analysis*, Vol. 3, Marcel Dekker, New York, 2nd ed., 1976, pp. 713–776.
[15] E. Geeraert and D. De Schepper, *J. High Resolut. Chromatogr. Chromatogr. Commun.*, 5 (1982) 80.
[16] E. Geeraert and D. De Schepper, *J. High Resolut. Chromatogr. Chromatogr. Commun.*, 6 (1983) 123.
[17] E. Geeraert and P. Sandra, *J. High Resolut. Chromatogr. Chromatogr. Commun.*, 8 (1985) 415.
[18] A. Stolywho, H. Colin and G. Guiochon, *Anal. Chem.*, 57 (1985) 1342.
[19] B. Herslof and G. Kindmark, *Lipids*, 20 (1985) 783.
[20] O. Podlaha and B. Töregrad, *J. High Resolut. Chromatogr. Chromatogr. Commun.*, 5 (1982) 553.
[21] B. Herslöf, O. Podlaha and B. Töregard, *J. Am. Oil Chem. Soc.*, 56 (1979) 864.
[22] A. Stolywho, H. Colin, M. Martin and G. Guiochon, *J. Chromatogr.*, 288 (1984) 253.
[23] J. Folch, M. Lees and O.H.S. Stanley, *J. Biol. Chem.*, 266 (1957) 497.
[24] M.A. Kaluzny, L.A. Duncan, M.V. Merritt and D.E. Epps, *J. Lipid Res.*, 26 (1985) 135.
[25] J.-L. Perrin and A. Prévot, *Etud. Rech.*, 33 (1986) 437.

ELSEVIER

Journal of Chromatography A, 667 (1994) 235–240

JOURNAL OF CHROMATOGRAPHY A

Residual solvent analysis by headspace gas chromatography

Narendra Kumar*, John G. Gow

Department of Analytical and Physical Chemistry, Rhône-Poulenc Rorer Central Research, 500 Arcola Road, P.O. Box 1200, Collegeville, PA 19426-0107, USA

(First received September 1st, 1993; revised manuscript received December 13th, 1993)

Abstract

An automated headspace GC method was developed and validated for the analyses of eight common process solvents and the five solvents whose quantification is required by the US Pharmacopeia. The sample is dissolved in dimethylformamide solvent and the equilibrium headspace gas formed at 60°C is analyzed using a megabore capillary column. Quantification is performed by the standard addition technique to eliminate any possibility of matrix effects. This method is sensitive, precise, accurate and linear in the range of interest.

1. Introduction

The quality and stability of a pharmaceutical drug substance, product and excipient could be affected by the presence of volatile impurities. Volatile impurities are often residual solvents used in the synthesis and crystallization which escape drying. Solvents can be bound to the drug substance with varying strengths depending on the mechanism. Solvates contain the solvent molecules as a part of the crystal lattice. This type of solvent cannot be analyzed without first releasing it in a homogeneous solution. Solvents are best analyzed by gas chromatography [1–4]. Direct injection, purge-and-trap and headspace injections are common ways of introducing the sample in GC. Direct injection of a solution of a non-volatile drug substance could be detrimental to the performance of the injection system of the gas chromatograph and also to high-performance capillary columns. Further, interaction between the solvents and the sample in the injection port could lead to recovery problems [5]. For reliable results, it is important that the chromatographic flow path is clean and free from residues and contaminants at all times. Built-up charred material in the injector from multiple injection of a non-volatile sample requires frequent and time-consuming cleaning procedures.

We describe here a general GC method that employs equilibrium headspace injection to eliminate the above problems associated with direct injection. The method utilizes a megabore capillary column for the separation of thirteen process solvents including benzene, methylene chloride, chloroform, 1,4-dioxane and trichloroethylene whose testing is required by the US Pharmacopeia (USP). The USP method IV describes the analysis of these solvents by headspace chromatography using manual injection [6]. This method is fully automated, sensitive, precise, accurate and linear over the range 30–300% of the target concentration of 30 ppm for all of the solvents. Quantification was performed

* Corresponding author.

0021-9673/94/$07.00
SSDI 0021-9673(93)E0050-5

by the method of standard additions to eliminate any possible drug matrix effect.

2. Experimental

2.1. Reagents and materials

Drug samples were obtained from the Chemical Process Research Department of Rhône-Poulenc Rorer Central Research. Solvents used were of ≥99% purity and were purchased from the following sources: acetone, acetonitrile, ethyl acetate, methanol, methylene chloride, 2-propanol, ethanol, chloroform, benzene, trichloroethylene, toluene, 1-propanol, 1,4-dioxane and methane from Fischer Scientific (Malvern, PA, USA), tetrahydrofuran from Fluka (Buchs, Switzerland) and dimethylformamide (DMF) of Omni-Solv grade, used as the solvent to dissolve the sample and to prepare a standard of the above thirteen solvents, from VWR Scientific (Bridgeport, NJ, USA). DMF was purged with helium for 2 h to free it from trace-level volatiles prior to use.

2.2. Chromatographic system

Experiments were performed on a Hewlett-Packard Model 5890 Series II gas chromatograph equipped with a Model 19395A automated headspace unit. Flame ionization detection was used. Chromatographic data were collected and handled via the in-house Waters ExpertEase chromatographic data management system.

2.3. Chromatographic method

A Supelco Nukol, acid-modified, bonded polyethylene glycol capillary column (60 mm × 0.53 mm I.D.) with a 0.50-μm film thickness was utilized for chromatographic separation of the solvents. The carrier gas was helium at a total flow-rate of 4.2 ml/min. A minimum helium flow-rate of 0.2 ml/min from the GC injector was used to avoid any sample backup in the latter during injection from the headspace autosampler. The remainder of the gas flow was obtained from the headspace autosampler. Injections were made in the splitless mode through a packed-column injector adapted for megabore operation. The injector was maintained at 150°C and the detector temperature was 250°C. Helium, at a flow-rate of 20 ml/min, was used as make-up gas. The temperature program involved an initial oven temperature of 35°C for 10 min, increased at 2°C/min to 50°C and then at 3°C/min to 80°C. In order to remove the solvent DMF, the ramp rate was then increased to 20°C/min up to 190°C and held there for 5 min. Headspace autosampler conditions were as follows: servo air pressure, 3.0 bar; auxiliary pressure, 1.2 bar; bath temperature, 60°C; injection loop temperature, 100°C; sample thermal equilibration time, 15 min; sample vial pressurization for 10 s; headspace vent opened for 15 s; and inject time, 18 s. These headspace events were all separated from each other by a 3-s delay time.

2.4. Sample and standard preparation, quantification and calculations

A standard containing 1000 μg/ml of each of the thirteen solvents was prepared by first partially filling a 50-ml volumetric flask with the solvent DMF, weighing it with the stopper, injecting 0.050 g of each solvent into the flask and weighing it again after replacing the stopper. This solution was then diluted to volume with DMF and stored in a refrigerator after use.

Sample solution was prepared by weighing accurately 100 mg of the drug substance in a 10-ml volumetric flask and dissolving it in the same batch of DMF followed by dilution to volume. Four 1.0-ml aliquots of this solution were placed in four separate 10-ml capacity headspace vials. Standard additions were made in three of these vials by introducing 10, 20 and 30 μl of the standard solution. All four of the vials were sealed properly with a crimper before placing them in the headspace.

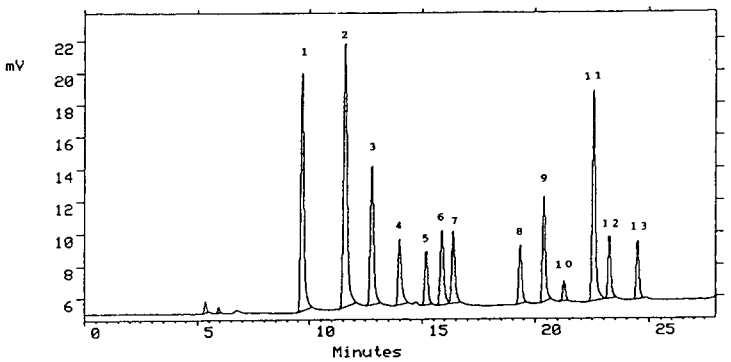

Fig. 1. Headspace GC of a 10 ppm standard solution containing thirteen solvents. Peaks: 1 = acetone; 2 = tetrahydrofuran; 3 = ethyl acetate; 4 = methanol; 5 = methylene chloride; 6 = benzene or 2-propanol; 7 = ethanol; 8 = trichloroethylene; 9 = acetonitrile; 10 = chloroform; 11 = toluene; 12 = 1-propanol; 13 = 1,4-dioxane.

3. Results and discussion

In a sealed vial, an equilibrium is reached between a liquid and its vapor. The composition of the vapor phase is the same as that of the liquid at a given temperature and pressure. By analyzing the vapor phase, the content of the solvents in the solution can be determined.

The use of wide-bore capillary columns in GC determinations has specific advantages owing to the capacity and the efficiency characteristics of these columns. Columns of 0.53 mm I.D. have become popular for headspace analysis because they can be operated in a range of carrier gas flow-rates which is suitably high to reduce peak broadening due to the dead volumes in headspace autosampler components [7]. We employed a 60 m × 0.53 mm I.D. Nukol column, which provided the selectivity required for the separation of the thirteen solvents contained in the standard solution described above. The choice of DMF as the solvent was based on its solvent strength and retention on the Nukol column, which allows its elimination from the system after the peaks of interest but within a reasonable analysis time of 35 min. Fig. 1 shows a chromatogram resulting from a headspace injection of the standard solution. Under these chromatographic conditions, 2-propanol co-elutes with benzene. These two solvents can be analyzed by this method if they are not present together.

The concentration of a solvent in the headspace is dependent on the temperature of the solution. We selected 60°C as the lowest temperature that was required to obtain a sufficient signal from an injection made under the given headspace conditions from a 10.0-ml capacity headspace vial containing 1 ml of a 10 ppm standard solution. Higher temperatures provide better sensitivity but the possibility of thermal degradation will also increase.

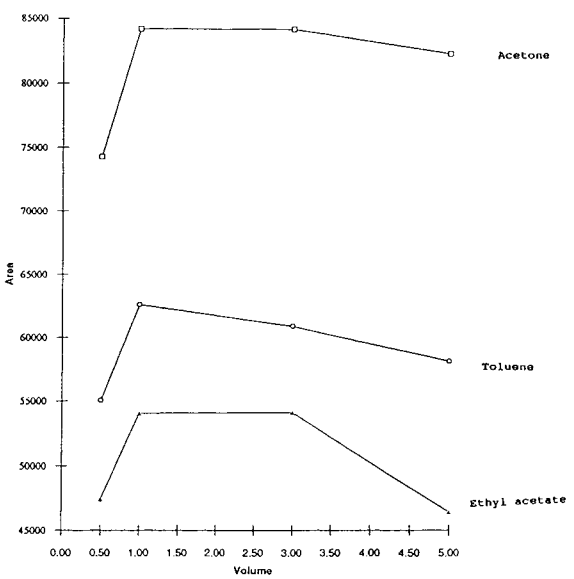

Fig. 2. Effect of sample solution volume on the peak areas of three solvents for an equilibration time of 15 min.

The choice of a 1-ml volume of the sample solution (10 mg/ml) in a 10-ml capacity vial was based on choosing a ratio of solution-phase and gas-phase volumes which provides the best sensitivity. We studied the effect of varying the ratios of liquid- to gas-phase volumes on the sensitivity of three different solvents. Fig. 2 shows that the best sensitivity is achieved with a sample volume of 1 ml contained in a 10-ml vial for a 15-min equilibration time.

For solubility reasons, the minimum concentration to achieve the desired sensitivity will be desirable. Lower concentrations are also preferable to minimize any possible matrix effects. Solute–solvent interaction in the sample solution can influence the activity of an analyte solvent [8]. In the presence of such a matrix effect, quantification by an external standard method may provide misleading results. We therefore decided to employ the standard additions method for quantification. In this standard additions method, a sample is analyzed alone and after addition of three incremental levels of a standard solution. The detector response from the four vials is plotted on the ordinate against the amount (ppm) of standard added. A standard plot is thus obtained for each sample. The x-intercept can be determined by dividing the y-

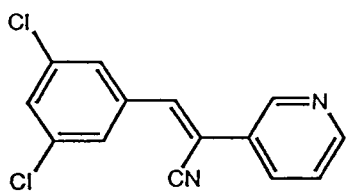

(1)
Basic

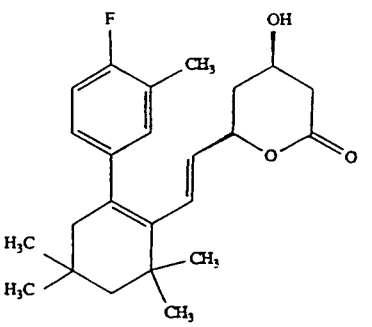

(2)
Neutral

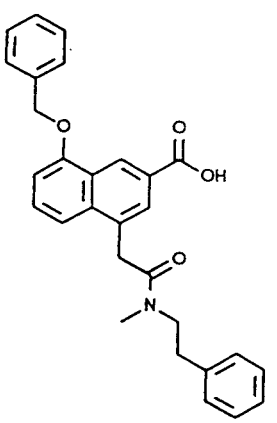

(3)
Acidic

Fig. 3. Structures of the three compounds used to demonstrate recovery and linearity from acidic, basic and neutral matrices.

intercept of the fitted line by the slope. The amount of solvent (ppm, w/w) in the sample was calculated as follows:

$$\text{solvent (ppm)} = \frac{x}{y} \cdot 1000$$

where x is the x-axis intercept (ppm) and y is the mass of the sample in nanograms.

Linearity and recovery experiments were performed using three types of analytes including a basic, an acidic and a neutral drug substance (Fig. 3). The results of linearity experiments for the fourteen solvents using compound **2** (Fig. 3) as the sample matrix are given in Table 1. Comparable results were obtained for compounds **1** and **3**.

Recovery experiments were performed using compounds **1**, **2** and **3** at eight levels from 1 to 50 ppm. Table 2 gives typical recovery results for 10, 30 and 50 ppm levels obtained for compound **2**. The recovery results for compounds **1** and **3** were comparable.

An analysis time of 3 h is required for the standard additions method described here. This time is acceptable for bulk drug lot analysis as the method is fully automated. For higher throughput work, this method can easily be converted into one-point standard addition or external standard methods [2].

4. Conclusions

An automated headspace GC method was developed to analyze eight common process and five USP solvents. This method employs a high-

Table 1
Linearity data using compound **2** as the sample matrix
Linearity of detector response of all fourteen residual solvents

Solvent	Intercept (ppm)	Slope	r^2
Acetone	0.78	12288.12	0.9999
Tetrahydrofuran	0.47	15173.33	0.9999
Ethyl acetate	0.93	7207.32	0.9999
Methanol	1.74	3377.45	0.9998
Methylene chloride	0.55	2726.40	0.9999
2-Propanol	0.66	570.87	0.9998
(Benzene)	0.19	17342.11	0.9999
Ethanol	2.14	3688.07	0.9997
Trichloroethylene	0.75	2523.98	0.9999
Acetonitrile	2.00	4880.66	0.9994
Chloroform	2.78	770.10	0.9991
Toluene	0.99	8556.96	0.9995
1-Propanol	2.08	2253.50	0.9992
1,4-Dioxane	0.88	2362.54	0.9998

Typical residuals table depicting the solvent ethyl acetate

Concentration (ppm)	y Observed	y Predicted	Residual
9.52	$6.43 \cdot 10^4$	$6.18 \cdot 10^4$	2498.40
19.04	$1.29 \cdot 10^4$	$1.30 \cdot 10^4$	−1405.80
38.08	$2.68 \cdot 10^4$	$2.68 \cdot 10^4$	1118.78
47.60	$3.32 \cdot 10^4$	$3.36 \cdot 10^4$	−4012.92
76.16	$5.43 \cdot 10^4$	$5.42 \cdot 10^4$	1416.48
95.20	$6.78 \cdot 10^4$	$6.79 \cdot 10^4$	475.08

Table 2
Recoveries of the thirteen solvents spiked at 0.001%, 0.003% and 0.005% levels

Solvent	0.0001% spike (10 ppm)		0.003% spike (30 ppm)		0.005% spike (50 ppm)	
	Recovery (%)	r^2	Recovery (%)	r^2	Recovery (%)	r^2
Acetone	94.09	0.9997	98.27	0.9994	102.62	0.9994
Tetrahydrofuran	96.13	0.9998	95.71	0.9968	102.83	0.9994
Ethyl acetate	93.49	0.9998	97.84	0.9992	98.32	0.9991
Methanol	101.20	0.9999	99.17	0.9975	98.95	0.9991
Methylene chloride	95.98	0.9996	94.71	0.9945	100.38	0.9991
2-Propanol	92.80	0.9988	102.70	0.9973	95.48	0.9994
Ethanol	98.04	0.9984	93.53	0.9995	96.42	0.9998
Chloroform	94.25	0.9994	980.8	0.9999	101.38	0.9994
Acetonitrile	95.45	0.9999	99.32	0.9979	98.81	0.9994
Trichloroethylene	94.57	0.9999	99.44	0.9979	101.57	0.9997
Toluene	90.85	0.9997	99.00	0.9997	94.95	0.9982
1-Propanol	96.82	0.9992	99.79	0.9978	94.04	0.9946
1,4-Dioxane	94.99	0.9996	103.59	0.9988	98.94	0.9996

Percentage calculated on 10 mg of drug substance mass basis as described in Section 2.4.

performance megabore capillary column and standard additions for quantification. The method has been shown to be general, sensitive, precise, accurate and linear in the range of concentrations of interest.

5. References

[1] F. Matsui, E.G. Lovering, J.R. Watson, D.B. Black and R.W. Sears, *J. Pharm. Sci.*, 73 (1984) 1664–1666.
[2] J.E. Haky and T.M. Stickney, *J. Chromatogr.*, 321 (1985) 137–144.
[3] J.P. Guimbard, M. Person and J.P. Vergnaud, *J. Chromatogr.*, 403 (1987) 109–121.
[4] C. B'Hymer, *J. Chromatogr.*, 438 (1988) 103–107.
[5] B.S. Kersten, *J. Chromatogr. Sci.*, 30 (1992) 115–119, and references cited therein.
[6] *US Pharmacopeia XXII, National Formulary XVII, Supplement IV*, US Pharmacopeial Convention, Rockville, MD, 1991, Method IV, p. 2510.
[7] D.W. Foust and M.S. Bergen, *J. Chromatogr.*, 469 (1989) 161–173.
[8] J.P. Guimbard, M. Person and J.P. Vergnaud, *J. Chromatogr.*, 403 (1987) 109–121.

ELSEVIER

Journal of Chromatography A, 667 (1994) 241–248

JOURNAL OF CHROMATOGRAPHY A

Determination of organophosphorus and triazine pesticides in ground- and drinking water by solid-phase extraction and gas chromatography with nitrogen–phosphorus or mass spectrometric detection

Maria Psathaki, Efi Manoussaridou, Euripides G. Stephanou*

Division of Environmental Chemistry, Department of Chemistry, University of Crete, 71409 Heraclion, Greece

(First received July 12th, 1993; revised manuscript received October 12th, 1993)

Abstract

Trace enrichement and determination of ethoprophos, fenamiphos, fenthion, isophenphos, mevinphos, monocrotophos, atrazine and simazine were performed by solid-phase extraction on XAD-2 columns and Sep-Pak C_{18} cartridges, subsequent elution with an organic solvent and determination by GC with nitrogen–phosphorus detection (NPD) and mass spectrometry in the selected-ion monitoring mode (MS-SIM). Ground- and drinking water volumes of 1–2.5 l at concentrations levels of 0.1–5 μg/l were used for application of the method. Both adsorbents provided recoveries of 75–95%. The limits of detection were 0.08–0.60 μg/l with NPD and 0.03–0.13 μg/l with MS-SIM.

1. Introduction

Natural waters are contaminated with various pesticides because of their widespread use. Herbicides and nematicides are potential contaminants of natural waters because they are directly applied to soil and are transported into groundwater or leached to surface water [1,2]. A large proportion of foliar sprays that do not reach their target also contribute greatly to soil residues. Another source of pesticides in soil is the residues of these chemicals (such as various insecticides) in the atmosphere, either in dust or rain water, which are washed out by precipitation and fall on to the soil. Therefore, insecticides are transported into groundwater [1]. During the last decade at least 46 pesticides have been reported to be leached into ground waters of the USA [2].

Screening methods for various pesticide groups, in various water matrices, generally consist of an appropriate extraction and isolation technique by which compound enrichement is achieved, followed by clean-up and chromatographic determination. Enrichement methods have been developed using liquid–liquid extraction (LLE) [3] and solid-phase extraction (SPE) with short Amberlite XAD-2 and XAD-4 resin columns [4,5], C_{18} cartridges [6–11] or membrane extraction discs [12].

LLE is an effective method of extracting organic compounds from water samples. Al-

* Corresponding author.

0021-9673/94/$07.00
SSDI 0021-9673(93)E1304-I

though LLE, because of its simplicity and because it is a fully developed technique, is used in most official methods for pesticide analysis [3], it has some disadvantages, such as evaporation of large solvent volumes [8], emulsification, contact of laboratory personnel with hazardous organic solvents [12], time consuming, laborious and expensive [13]. Comparisons between LLE and SPE have been well documented [14]. Because of these disadvantages the use of solid-phase preconcentration techniques has expanded substantially. Among them the extraction of analytes on bonded-phase silica is preferred to preconcentration on XAD, because the latter has the disadvantage of requiring extensive clean-up, On the other hand, XAD resins can generally be reused several times, making them an economical choice, especially if one takes into consideration the cost of bonded-phase cartridges and membranes.

We present here a comparative study in which triazine and organophosphorus pesticides were simultaneously determined in ground and drinking water, by using a preconcentration step on an XAD-2 column or a C_{18} bonded-phase cartridge, and determination by capillary gas chromatography with nitrogen–phosphorus detector (NPD) or mass spectrometric detection in the selected-ion monitoring mode (MS-SIM) Emphasis is given to the use of MS–SIM. The compounds studied were chosen on the basis of the following criteria: (a) their use as pesticides locally, (b) their water solubility (>20 mg/l), (c) their hydrolysis half-life (>20 weeks) and (d) their toxicity (oral acute $LD_{50} < 50$ mg/kg). With the exception of triazines the other compounds satisfy these criteria [15].

2. Experimental

2.1. Materials

All solvents of Pestanal grade were purchased from Mallinckrodt (St. Louis, MO, USA). Standard organophosphorus pesticides were purchased form Ehrenstorfer (Augsburg, Germany) and triazines were provided by the US Environmental Protection Agency (EPA). Amberlite XAD-2 (20–50 mesh, surface area 330 m^2/g) was purchased from Fluka (Buchs, Switzerland) and Sep-Pak C_{18} cartridges (0.3 g) from Waters (Milford, MA, USA). All materials used (glass and cotton-wool, paper filters, anhydrous sodium sulphate, etc.) were Soxhlet extracted, overnight and kept dry until use.

Groundwater samples were collected at three locations in the Heraclion area (Crete, Greece). The ground- and well water samples had pH values of 7.50–8.09, conductivities of 325–435 μS/cm and anion concentrations of Cl^- 25.0–28.0, NO_3^- 0 and SO_4^{2-} 11.0–30.0 mg/l. Tap water was obtained from the laboratory.

2.2. Solid-phase extraction

The standard compounds, dissolved in acetone, were added to 1 l of Nanopure-grade water and to 1 l of pre-analysed groundwater or tap water. The compounds were added at levels of 0.1, 0.5 and 5 μg in order to obtain concentrations of 0.1, 0.5 and 5 μg/l.

XAD-2 resin was sonicated three times (30 min each) with acetonitrile. The cleaned resin was kept in methanol. The purified XAD resin as a methanol slurry was placed in a 20×1 cm I.D. column until a resin bed 6 cm high was obtained. The methanol was drained and then the resin was washed with three 20-ml portions of Nanopure water. A 1-l reservoir, capped with a nitrogen pressure source, was attached to the top of the column. The nitrogen pressure was regulated in order to obtain a flow-rate 8–10 ml/min at the bottom of the column. When the sample had passed through the column, the nitrogen pressure was continued for 5–10 min. The pesticides were eluted from the XAD-2 column with 100 ml of acetone at a flow-rate of 1–2 ml/min. The acetone was evaporated to 1–2 ml with a Kuderna–Danish apparatus. The internal standard was added and the solvent was further evaporated to 50–100 μl with a gentle stream of nitrogen.

The C_{18} cartridges were connected at the bottom of the previously described apparatus. Prior to use, the cartridges were flushed with two

5-ml portions of dichloromethane, one 5-ml portion of methanol and one 3-ml portion of Nanopure water. The nitrogen pressure was regulated in order to obtain a 8–10 ml/min flow-rate of the water sample. After the cartridges had been purged with nitrogen for 30 min, the analytes were desorbed with 5 ml of dichloromethane on to a sodium sulphate microcolumn. The column was further washed with 2.5 ml of dichloromethane. After addition of internal standard the solution was concentrated to 100–200 μl for GC–MS analysis. The dichloromethane was evaporated using a gentle stream of nitrogen and replaced with 100–200 μl of hexane for GC–NPD.

2.3. GC–MS-SIM and GC–NPD

GC–MS analyses were carried out using a Hewlett-Packard mass-selective detector with the appropriate data system. A Hewlett-Packard Model 5890 gas chromatograph, equipped with a Grob-type split–splitless injector, was directly coupled with the fused-silica capillary column (SE-54, 25 m × 0.25 mm I.D.) to the ion source. Helium was used as the carrier gas with a back-pressure of 0.8 atm (1 atm = 101 325 Pa). The electron impact ionization conditions were as follows: ion energy, 70 eV; ion source temperature, 195°C; mass range, 45–450 m/z full scan; in the SIM mode for quantitative determinations the masses scanned were m/z 192, 224 and 162 (20–30 min), m/z 127, 158, 201, 215 and 223 (30–39 min) and m/z 213, 278, 303, 125, 109 and 154 (39–60 min); and electron multiplier voltage, 1680–1850 V. In Table 1 are shown the ions, with their tentative structures, selected for each compound.

GC–NPD analyses were performed on a Hewlett-Packard Model 5890 gas chromatograph with a Hewlett-Packard Chemstation data system, equipped with an SP 2100 (30 m × 0.25 mm I.D.) fused-silica capillary column (Supelco). Helium was used as the carrier gas with a back-pressure of 0.8 atm.

The chromatographic conditions for both techniques were as follows: injector temperature, 290°C; detector temperature (NPD), 290°C; temperature programme, 50°C (1 min), increased from 60 to 290°C at 4°C/min, held at 290°C for 10 min. Aliquots of 1–2 μl were injected in the splitless mode (split closed for 45 s) and the hot needle technique was applied.

The internal standard for GC–NPD was parathion ethyl [relative response factors (RRF) for triazines 2.5–3.1 and for organophosphorus pesticides 0.4–1.5] and for GC–MS-SIM it was hexamethylbenzene (m/z 162 in the SIM mode; for RRF see Table 1).

3. Results and discussion

Fig. 1A shows the GC–NPD trace obtained for a sample of groundwater containing 5 μg/l of each pesticide and extracted on the XAD-2, column and Fig. 1B shows the corresponding GC–NPD trace with extraction on the C_{18} cartridge. Fig. 1C shows the GC–MS-SIM trace for a drinking water sample containing 0.25–0.30 μg/l of each compound and extracted with a Sep-Pak C_{18} cartridge. Fig. 2 shows (A) the GC–NPD trace for a groundwater sample extracted with a C_{18} cartridge and (B) a coinjection trace for the same sample with reference compounds. Table 1 gives details of the ions selected for each compound for GC–MS analysis. Table 2 gives the mean recoveries for different spiking levels. Table 3 gives the limits of detection (LOD) for several analytes following extraction with C_{18} cartridges and determination by GC–NPD and GC–MS-SIM.

3.1. Blanks

The XAD-2 resin cleaned by sonification only did not give disturbing blank peaks in the region of interest when NPD was used for detection (Fig. 2A). Several workers have found resin artefacts, such as alkylbenzenes, biphenyl, hydrocarbons and phthalate esters. Higher concentrations of artefacts have been associated with XAD-4 than with XAD-2 resin [5,16]. Specific detection methods such as NPD are insensitive to most of the artefacts reported. This advantage becomes obvious when the chromatographic trace in Fig. 1A is examined.

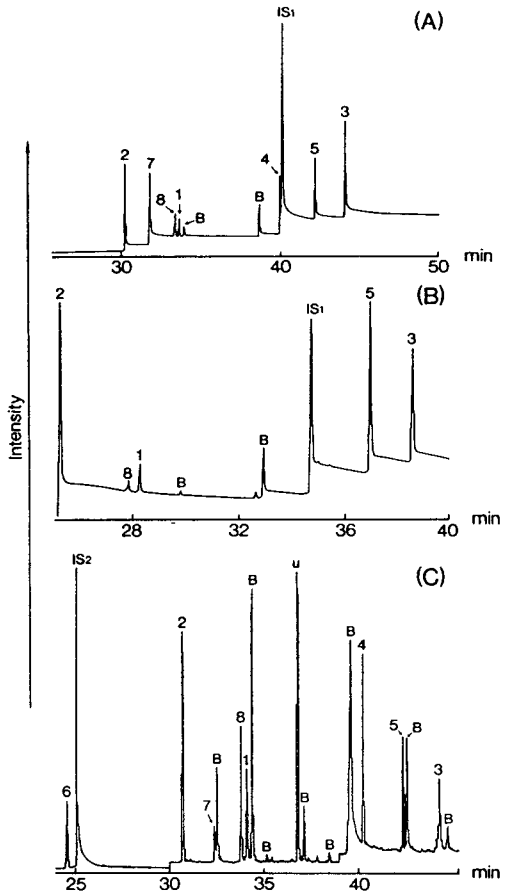

Fig. 1. (A) GC–NPD trace obtained for a groundwater sample spiked with 5 μg/l of each pesticide and extracted on XAD-2 resin. (B) GC–NPD trace for a groundwater sample spiked with the same concentration of pesticides and extracted on a Sep-Pak C_{18} cartridge. (C) GC–MS-SIM trace for a groundwater sample spiked with 0.25–0.3 μg/l of each compound and extracted with a Sep-Pak C_{18} cartridge. B = peaks corresponding to blanks; u = unidentified compounds; IS_1 = parathion ethyl; IS_2 = hexamethylbenzene. For compound numbers, see Table 1.

With respect to the blank peaks corresponding to the C_{18} cartridges (Fig. 2B), we did not observe a significant difference in favour of the Sep-Pak cartridges when NPD was used. Blanks occurring when Sep-Pak cartridges are used could be more disturbing when the MS detection is applied. Nevertheless, even with MS-SIM the cartridges also produced relatively clean chromatograms in the region of interest (Fig. 1C).

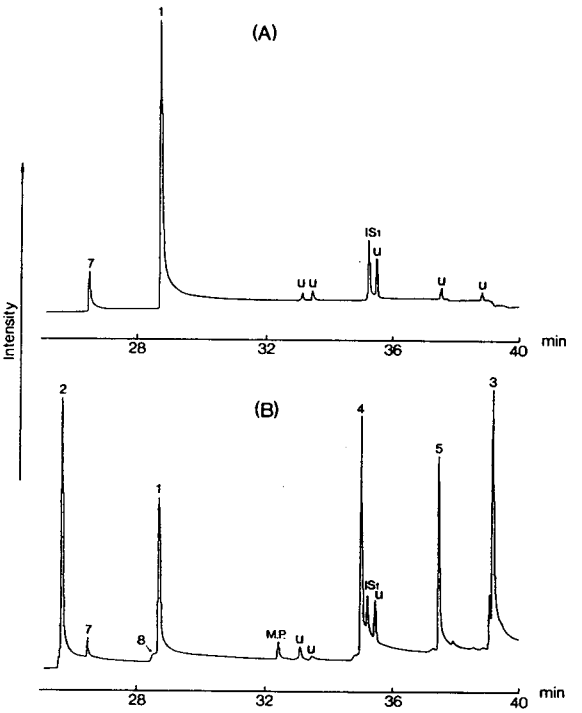

Fig. 2. (A) NPD trace for a groundwater sample. (B) Coinjection of the same sample with a solution containing standard compounds. IS_1 = Parathion ethyl; M.P. = Parathion methyl; u = unidentified compounds. For compound numbers, see Table 1.

3.2. SPE capacity

Table 2 shows the different pesticide recoveries obtained at different spiking levels for 1 l of ground water. Preliminary recovery experiments performed with Nanopure and tap water, with the same spiking levels, did not show significant differences (<2–5%) compared with the recoveries obtained when groundwater samples were used.

Reuse of XAD-2 resin (three times) showed the same recovery efficiency, and at the same time the amount of artefacts released decreased. Groundwaters with different conductivities (*e.g.*, 325 and 435 μS/cm) did not affect the recovery of the compounds studied, probably because they are not ionizable. Also in the range of pH values (7.50–8.09) measured in the ground waters used, no difference was noticed concerning

Table 1
Main ions, relative abundances and relative response factors (RRF, selected ion for internal standard m/z 162) of organophosphorus and triazine pesticides used for the GC–MS-SIM

Molecular mass	No.	Compound and ions (m/z and tentative identification)	Relative abundance (%)	RRF
215	1	Atrazine		1.9
		215 $[M]^+$	58	
242	2	Ethoprophos		0.7
		158 $[CH_3CH_2OPO(SH)_2]^+$	100	
303	3	Fenamiphos		1.4
		303 $[M]^+$	69	
		154 $[m\text{-}CH_3,\ p\text{-}CH_3SC_6H_3OH]^+$	100	
278	4	Fenthion		0.4
		278 $[M]^+$	100	
		125 $[SP(OCH_3)_2]^+$	78	
345	5	Isophenphos		1.2
		213 $[M-(CH_3)_2COCH_3CH_2O]^+$	88	
224	6	Mevinphos		1.3
		224 $[M]^+$	4	
		192 $[M-CH_3OH]^+$	23	
223	7	Monocrotophos		0.4
		223 $[M]^+$	3	
		127 $[(CH_3O)_2P(OH)_2]^+$	100	
201	8	Simazine		1.4
		201 $[M]^+$	100	

Table 2
Mean recoveries (%) and standard deviation (%) (in parentheses) of the pesticides used ($n = 3$–5 for each compound) in spiked groundwater samples using XAD-2 resin and Sep-Pak C_{18} cartridges

Pesticide	XAD-2			Sep-Pak C_{18}		
	5 μg/l	0.5 μg/l	0.1 μg/l	5 μg/l	0.5 μg/l	0.1 μg/l
Atrazine	83 (11)	82 (12)	85 (9)	81 (10)	80 (9)	78 (3)
Ethoprophos	79 (8)	76 (8)	68 (9)	95 (12)	104 (18)	103 (5)
Fenamiphos	82 (3)	78 (6)	71 (50)	90 (8)	89 (9)	92 (8)
Fenthion	81 (4)	70 (8)	63 (9)	91 (14)	88 (9)	89 (10)
Isophenphos	78 (5)	80 (5)	69 (8)	101 (10)	103 (15)	98 (13)
Mevinphos	88 (6)	89 (7)	72 (5)	96 (8)	101 (8)	95 (11)
Monocrotophos	85 (8)	82 (5)	68 (7)	89 (16)	93 (8)	90 (7)
Simazine	79 (10)	83 (15)	80 (9)	78 (7)	75 (6)	74 (5)

Water volume, 1 l. Determinations of analytes were performed by GC–NPD.

Table 3
Limits of detection (LOD) for pesticides following extraction with C_{18} cartridges and determination by GC–NPD or GC–MS-SIM

Pesticide	LOD (μg/l)	
	NPD	MS-SIM
Atrazine	0.30	0.05
Ethoprophos	0.20	0.03
Fenamiphos	0.10	0.13
Fenthion	0.08	0.04
Isophenphos	0.20	0.05
Mevinphos	0.30	0.04
Monocrotophos	0.10	0.08
Simazine	0.60	0.06

Spiking levels, 1–0.1 μg/l; water volume, 2.5 l; peak measured when signal-to-noise ratio was 5.

the recoveries. Lower recoveries were observed when we passed from a high spiking level (5 ppb) to a lower spiking level (0.1 ppb), and especially for the most lipophilic compounds such as fenamiphos, fenthion and isophenphos. The concentration of the analytes in the water did not affect the extraction recoveries of atrazine and simazine. The recovery of the adsorbed organophosphorus pesticides from the XAD-2 resin was affected by the presence of water on the resin during the elution procedure. Flushing with nitrogen, after the sample had passed through the XAD-2 column, for less than 10 min resulted in lower recoveries for ethoprophos, fenamiphos and isophenphos. The recoveries obtained in this study are comparable to those obtained in other studies with other organophosphorus pesticides [17].

The recoveries obtained when Sep-Pak solid-phase extraction was used are given in Table 2. The recoveries, especially for the organophosphorus compounds, are higher than those obtained with the XAD-2 columns. The environmental factors measured (pH, conductivity, etc.) do not vary extensively (see Experimental) so as to affect the extraction recoveries of both the triazine and organophosphorus pesticides. A study [7] concerning the effect of pH on the recovery showed that pH values between 5 and 8 gave the best recoveries (77–98%) for other organophosphorus pesticides. As the natural groundwater pH was within this range, we also obtained the optimum recoveries without adjustment of the working pH. The higher affinity of the different organophosphorus pesticides, ethoprophos, fenamiphos, fenthion and isophenphos, compared with those of atrazine and simazine can be seen in Table 2. This was also confirmed by the retention times observed when these compounds were determined using reversed-phase HPLC [18]. Triazines showed shorter retention times than the organophosphorus compounds. The use of dichloromethane as the eluent was satisfactory especially for the more lipophilic organophosphorus compounds.

Comparable extraction recoveries have been reported for other organophosphorus pesticides when the analytes were eluted from C_{18} cartridges with a mixture of ethyl acetate, *n*-hexane and light petroleum [7]. In contrast to XAD-2 extraction, with the C_{18} material cartridges we did not find significant differences in recoveries between high (5 μg/l) and low (0.1 μg/l) spiking levels (Table 3).

Comparing the two SPE materials, the use of C_{18} cartridges for preconcentration of pesticides has an important advantage concerning collection efficiency for the simultaneous determination of triazine and organophosphorus compounds in ground- and drinking water samples.

3.3. Detection systems

GC–NPD gave satisfactory results for the determination of both triazine and organophosphorus compounds. The greater sensitivity of NPD for organophosphorus compounds than for triazines makes it suitable for the determination of low concentration levels of organophosphorus pesticides in a mixture. This is evident when we compare the limits of detection (LOD) for the organophosphorus compounds with those of triazines (Table 3). The relative response factors obtained for both compound classes also indicate that NPD is inherently more sensitive to organophosphorus than to triazine compounds. This fact has been stressed by other workers [3,9].

In the SIM technique, ions for determination

were chosen on the basis of the structural characteristics of each compound and also with respect to high abundance, maximum selectivity and low susceptibility to interference from other compounds. Monocrotophos and mevinphos both have as the most abundant ion that at m/z 127. Therefore, for mevinphos another characteristic ion, with respect to its structure, was chosen (Table 1). A comparison of the results obtained by the combination of Sep-Pak C_{18} cartridges with GC–MS-SIM for atrazine, simazine and fenamiphos with those obtained with Empore C_{18} extraction discs and liquid chromatography–thermospray mass spectrometry in the positive- and negative-ion modes [12] revealed lower limits of detection when the former technique was used (Table 3 and Fig. 1C). For compounds amenable to GC conditions, the use of MS-SIM with differentially programmed mass scanning has important advantages over NPD, especially if specific ions (for each compound structure, Table 1) are selected, *i.e.*, high sensitivity and specific compound identification. GC–MS-SIM can be used for the reliable determination of pesticides, and not only for the purpose of confirmation [19].

Although liquid chromatographic systems have some advantages over GC for the determination of polar and thermally labile pesticides, these are limitations (UV adsorbability) when UV detection is used. The use of NPD (or MS) does not necessitate the inclusion of UV absorbability as a criterion, as is the case when HPLC is used [8,10]. We could determine, with sufficient sensitivity, ethoprophos using GC–NPD (Fig. 1A and Table 3) or GC–MSD-SIM (Fig. 1C and Table 3). This compound was not detectable using HPLC–UV detection [18].

We applied the combination of C_{18} cartridge extraction with both GC–NPD and GC–MS-SIM techniques to the determination of pesticides in ground- and well water samples collected in Crete. The GC–NPD analysis of a groundwater samples and also the coinjection of these sample extracts with standard compounds indicated the presence of atrazine, isophenphos and monocrotophos (Fig. 2B). GC–MS-SIM confirmed only the presence of atrazine in some of the samples, at concentrations of 0.07–0.42 μg/l. This means that any GC–NPD method which makes use of only one GC column for the identification of a large number of pesticides has a high probability of producing false-positive results. Therefore, NPD, in combination with other detection systems, is a usefull screening technique for organophosphorus and triazine pesticides. If a thermionic detector is the only available detector, confirmation through a second analysis on a capillary column of different polarity is certainly needed.

4. Conclusions

The results presented here show that capillary GC–NPD and GC–MS-SIM combined with solid-phase extraction using XAD-2 resin or Sep-Pak C_{18} cartridges have some important advantages over HPLC–UV detection for the determination of semi-polar or non-polar organophosphorus and triazine pesticides. The use of NPD and MS-SIM techniques allows the sensitive determination of the above compound classes without specific blank problems and without the inclusion of UV compound absorbability as an analysis criterion, when lability is not a limiting factor. The use of a second capillary GC column for identification purposes is considered necessary if NPD is the only available detection method.

The GC–MS-SIM technique was more suitable for the identification and determination of all the compounds examined, with very low detection limits.

5. Acknowledgement

This study was financed by the Mediterranean Integrated Programme of the European Community.

6. References

[1] S.U. Khan, *Pesticides in the Soil Environment*, Elsevier, Amsterdam, 1980, p. 5.

[2] *Pesticides in Ground Water Data Base: 1988 Interim Report*, Office of Pesticide Programs, Environmental Protection Agency, Washington, DC, 1988.
[3] C.D. Watts, L. Clark, S. Hennings, K. Moore and C. Parker, in B. Crathorne and G. Angeletti (Editors), *Pesticides: Analytical Requirements for Compliance With EC Directives, Water Pollution Research Report 11*, Commission of the European Communities, Brussels, 1989, pp. 1–67.
[4] G.A. Junk and J.J.J. Richard, *J. Res. Natl. Bur. Stand.*, 93 (1988) 274.
[5] S.A. Daignault, D.K. Noot, D.T. Williams and P.M. Huck, *Water Res.*, 22 (1988) 803.
[6] D.A. Hinkley and T.F. Bidleman, *Environ. Sci. Technol.*, 23 (1989) 995.
[7] J. Manez Vinuesa, J.C. Molto Cortez, C. Igualda Canas and G. Font Perez, *J. Chromatogr.*, 472 (1989) 365.
[8] M.W. Brooks, J. Jenkins, M. Jimenez, T. Quinn and J. Marshall Clark, *Analyst*, 114 (1989) 405.
[9] M.W. Brooks, D. Tessier, D. Soderstrom, J. Jenkins and J. Marshall Clark, *J. Chromatogr. Sci.*, 28 (1990) 487.
[10] A. Di Corcia and M. Marchetti, *Environ. Sci. Technol.*, 26 (1992) 66.
[11] R. Bagnati, E. Benfenati, E. Davoli and R. Fanelli, *Chemosphere*, 17 (1988) 59.
[12] D. Barceló, G. Durand, V. Bouvot and M. Nielen, *Environ. Sci. Technol.*, 27 (1993) 271.
[13] D. Barceló, *Analyst*, 116 (1991) 681.
[14] T.A. Bellar and W.L. Budde, *Anal. Chem.*, 60 (1988) 2076.
[15] W. Perkow, *Wirksubstanzen der Pflanzenschutz- und Schädlingsbekämpfungsmittel*, 2nd ed., Paul Parey, Berlin, Hamburg, 1985.
[16] M.W. Tabor and J.C. Loper, *Int. J. Environ. Anal. Chem.*, 19 (1985) 281.
[17] G.L. LeBel, D.T. Williams and F.M. Benoit, *J. Assoc. Off. Anal. Chem.*, 62 (1981) 241.
[18] E. Stephanou, S. Kornilios and N. Stratigakis, unpublished results, 1993.
[19] H.J. Stan, *J. Chromatogr.*, 467 (1989) 85.

ELSEVIER

Journal of Chromatography A, 667 (1994) 249–255

JOURNAL OF CHROMATOGRAPHY A

Effect of temperature and density on the performance of micropacked columns in supercritical fluid chromatography

E. Ibáñez, J. Tabera, M. Herraiz*, G. Reglero

Instituto de Fermentaciones Industriales, CSIC, c/Juan de la Cierva 3, 28006 Madrid, Spain

(First received August 20th, 1993; revised manuscript received October 19th, 1993)

Abstract

The effects on the efficiency of micropacked columns in supercritical fluid chromatography (SFC) of density at fixed temperature and of temperature at fixed density were investigated. The variation of the retention and resolution achievable for a given pair of solutes with the mobile phase density under different isothermal conditions was also studied. The linear velocity was varied using several flow restrictors of different lengths and inner diameters. The column type investigated was characterized by an inside diameter of <1 mm and the use of large particles (by HPLC standards), resulting in a particle-to-column diameter ratio of 0.1–0.3. Owing to the better permeability derived from both the large particle diameters and the high value of the interparticle porosity, the use of these columns may be an interesting approach in SFC.

1. Introduction

Supercritical fluid chromatography (SFC) is becoming increasingly important for the analysis of thermally labile and non-volatile compounds. Capillary, packed and one type of micropacked columns having particle-to-column inner diameter ratios far lower than 0.1 have been used for SFC and several papers have reported the advantages and disadvantages of these classes of columns [1–14]. In recent years, capillary SFC has been widely used because of its high efficiency, its relatively low degree of activity and its high permeability. However, the low sample capacity of capillary columns may be an inconvenience for the analysis of trace compounds. Further, capillary SFC demands linear flow-rates higher than the optimum in order to achieve a reasonable speed of analysis.

The use of packed columns is favoured when higher sample volumes are demanded (*i.e.*, for the analysis of compounds occurring at low concentrations). Also, packed columns are superior to open-tubular columns in terms of analysis time.

However, some of the packed columns currently used in SFC may occasionally exhibit a high degree of activity, mainly due to disturbing silanol–sample interactions [5]. Working with packed columns may also have an important disadvantage related to the high values obtained for the optimum linear velocity of the mobile phase, and the cost of the eluent, the volume flow capability of the SFC pumping system and the upper flow limit of the detector being used must be carefully considered.

A large difference between capillary and

* Corresponding author.

0021-9673/94/$07.00
SSDI 0021-9673(93)E0088-C

packed columns exists in the permeability and hence in the pressure drop required over the column. The pressure drop across packed columns can be great, causing significant differences in fluid densities in different parts of the column. In this respect, most studies conclude that at pressure drops greater than 20 bar, considerable eluting power can be lost across the column, resulting in lower chromatographic efficiency [4,5,15–18]. A few reports, however, contradict this observation [19–22], but it is generally admitted that the study of the consequences of a high column pressure drop in terms of resolution and selectivity demands further investigation in SFC.

In previous papers [23,24] we studied the possibilities in SFC of micropacked columns loaded with liquid stationary phases typically used in GC, immobilized on large particles (by HPLC standards). This type of micropacked column exhibits a particle-to-column inner diameter ratio (d_p/d_c) of 0.1–0.3 whereas a second type of micropacked column used by others in SFC [11–14] is packed with very fine-grained materials resulting in d_p/d_c values far lower than 0.1. Undoubtedly, a high number of theoretical plates can be achieved at the price of a significant pressure drop even for smaller column lengths. The latter type of column is often called packed capillary, although some workers suggest restricting this name to columns with particle-to-column inner diameter ratios of 0.2–0.5 and inner diameters of less than 0.5 mm. The same workers proposed an excellent classification of chromatographic columns which should be considered for distinguishing unambiguously different classes of columns used in SFC [25,26].

With regard to the first-mentioned type of micropacked columns ($0.1 < d_p/d_c < 0.3$), the large particle diameter and the high value of the interparticle porosity allow better permeabilities to be obtained.

A theoretical study of several parameters affecting the permeability of a micropacked column, and its efficiency in gas chromatography, has been reported previously [27] and several applications of this type of column have already appeared [28–31]. Concerning its use in SFC, the initial results obtained in our laboratory [23,24] were highly encouraging, as they showed that micropacked columns are capable of producing acceptable specific efficiencies (*i.e.*, efficiencies per metre of column length), resolution and analysis times, the pressure drop across the column being similar to that of capillary columns and lower than that of typical packed columns having 5- or 10-μm diameter packings. In fact, the low pressure drop observed over micropacked columns could be an essential factor concerning the use of this type of column in SFC.

Also, micropacked columns could be more advantageous than open-tubular columns for specific applications demanding the analysis of fairly complex samples for compounds present at low concentrations. Additional advantages of micropacked columns are that interfacing with ionization detectors or MS detectors is made easier owing to the low flow-rates required for micropacked columns. On the other hand, it should be emphasized that an interesting advantage of the use of micropacked columns is that different supports impregnated with different percentages of any stationary phase may be considered in order to optimize a specific separation [25,27].

In view of the above, the use of micropacked columns should be considered as a useful approach in SFC in addition to the packed and capillary columns currently in use. To date, however, the evaluation of column performance in SFC has mainly involved capillary and packed columns [21,32–34].

The aim of this work was to investigate the effect of various experimental parameters on the chromatographic efficiency, resolution and retention achieved for a given pair of solutes with an SFC micropacked column.

2. Experimental

Chromatographic measurements were made with a Carlo Erba (Milan, Italy) Model SFC 3000 supercritical fluid chromatograph equipped with a flame ionization detector.

Carbon dioxide of supercritical grade was pumped by using an SFC 300 pump (Carlo Erba). Samples were injected on to the micropacked column through a time-controlled rotating valve (Vici) having a 1-μl internal loop. The sampled volume was 1 μl and a flow split ratio of 1:50 was established for each injection.

A test mixture of n-C_{20}, n-C_{22} and n-C_{24} alkanes containing 5 μg/μl of each component in pentane and a 0.5 m × 0.53 mm I.D. micropacked column containing 3% of SE-54 in Volaspher A-2 (desilanized) were used. Volaspher A-2 is a siliceous synthetic support from Merck which has a narrow size distribution and an average particle size between 100 and 125 μm. It is a stable, spherical support with a uniform porous structure. The chromatographic column was made from a deactivated stainless-steel tube following a procedure described previously [27]. The stationary phase was cross-linked by adding dicumyl peroxide (0.5 mg per 100 mg) and increasing the column temperature at 5°C/min, under a nitrogen flow, from 100 to 160°C. The final temperature was maintained for 3 h.

The linear velocity of the mobile phase was varied by using different linear restrictors of 8 μm I.D. (length 7.5, 10 and 13 cm) and 10 μm I.D. (length 30, 40 and 50 cm), which were made from fused-silica tubing.

Each experiment was performed under isopycnic and isothermal conditions. The density of the mobile phase was varied (at a constant temperature of 100°C) from 0.25 to 0.45 g/ml. Further experimentation was carried out at densities of the mobile phase of (a) 0.25, (b) 0.35 and (c) 0.45 g/ml by considering in each instance different temperatures (from 60 to 160°C). The injection port and the detector were maintained throughout at 40 and 375°C, respectively. In all instances, at least two replicates of each injection were made.

3. Results and discussion

The value of the specific permeability coefficient (B^0) for the micropacked column used was determined experimentally to be $8.6 \cdot 10^6$ cm^{-2}, and a value close to 0.03 bar was established for the pressure drop per metre of column length.

Experimental data obtained for H (height equivalent to a theoretical plate) and u (mobile phase linear velocity) were fitted to the Van Deemter equation (Eq. 1) by using the BMDP statistical package [35] (BMDP-1R program, linear regression).

$$H = A + \frac{B}{u} + Cu \quad (1)$$

This equation can be expanded to

$$H = 2\lambda d_p + \frac{2\gamma D_M}{u} + \left[\frac{8kd_f^2}{\pi^2(1+k)^2 D_L} + \frac{1+6k+11k^2}{96(1+k)^2} \cdot \frac{d_p^2}{D_M}\right]u \quad (2)$$

where λ is the eddy diffusion coefficient, γ (assumed to be 1) is the tortuosity factor, d_p is the average particle size of the column packing, D_M is the diffusion coefficient of the solute in the gas phase, D_L is the diffusion coefficient of the solute in the liquid phase, d_f is the average thickness of the film of stationary liquid phase on the support and k is the capacity factor.

Different curves were obtained (Table 1) by fitting to Eq. 1 experimental data collected either at fixed temperature under various isopycnic conditions or at fixed density under different isothermal conditions. For each curve, a minimum of fifteen data points were considered and acceptable values of the standard errors of estimation (s) and the coefficients of determination (R^2) were achieved in all instances.

Experimentally, values of A not significantly different from zero were found, in agreement with data previously reported by several workers for packed columns [36,37]. This is why only B and C terms were finally considered [23].

Fig. 1 includes several plots showing the variation of H with u for the micropacked column described under Experimental. These curves were obtained at four densities ranging from 0.25 to 0.45 g/ml. In all instances the column temperature was maintained at 100°C. The statistical analysis performed on the data by using the BMDP-1R program showed that all curves de-

Table 1
Values of B and C parameters of Van Deemter equation obtained by fitting experimental data at different densities and temperatures

Density (g/ml)	Temperature (°C)	$B(\times 10^{-4})$	C	$R^{2\,a}$	s^b
0.25	100	10.46	0.177	0.977	0.0073
0.25	120	8.00	0.174	0.986	0.0058
0.25	140	7.92	0.158	0.988	0.0051
0.25	160	7.56	0.146	0.991	0.0038
0.35	80	5.90	0.231	0.981	0.0067
0.35	100	5.74	0.178	0.967	0.0074
0.35	120	5.55	0.178	0.983	0.0059
0.35	140	4.40	0.181	0.983	0.0053
0.40	100	4.32	0.205	0.996	0.0030
0.45	60	5.33	0.252	0.981	0.0062
0.45	80	3.89	0.247	0.998	0.0017
0.45	100	3.21	0.257	0.986	0.0043

Column, 0.5 m × 0.53 mm I.D.; 3% SE-54 in Volaspher A-2 (desilanized), 100–125 μm.
[a] Coefficient of determination.
[b] Standard error of the estimation.

picted in Fig. 1 are significantly different (confidence level 95%).

As can be seen, the decrease in column efficiency observed under isopycnic conditions when the linear velocity is increased is more evident at the highest densities. Accordingly, an appreciable decrease in the micropacked column efficiency occurs when the density is increased from 0.25 to 0.45 g/ml and the mobile phase velocities are higher than the optimum. However, values of H corresponding to the optimum velocity of the mobile phase (*i.e.*, $H_{u\,opt}$) decrease when the density is increased, as shown in Table 2, which also includes the confidence limits for $H_{u\,opt}$ corresponding to a confidence level of 95%.

The above-mentioned trend may be explained by considering the effect of the density on the longitudinal diffusion and the resistance to mass transfer (B and C terms, respectively, on the Van Deemter equation). Under isothermal conditions, an increase in mobile phase density leads to higher viscosity values, and thereby a decrease in the solute diffusivity in the mobile phase (D_M)

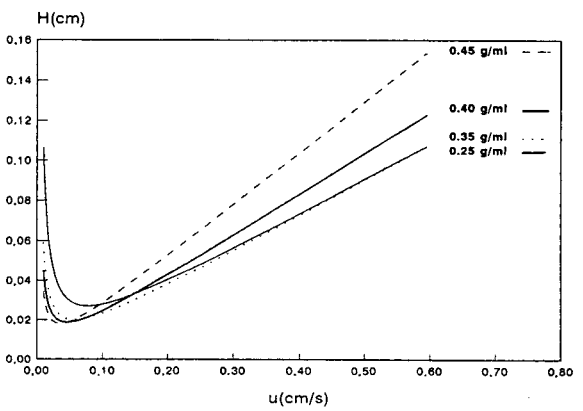

Fig. 1. Effect of the mobile phase density on efficiency: Van Deemter plots, obtained by fitting experimental data, at 100°C and different densities of the mobile phase for a micropacked column. Solute: n-C_{20}.

Table 2
Efficiency of a micropacked column in SFC at constant temperature (100°C) and different mobile phase densities

Density (g/ml)	u_{opt} (cm/s)	$H_{u\,opt}$ (cm)[a]	Intervals[b]
0.25	0.077	0.027	0.024–0.031
0.35	0.057	0.020	0.017–0.023
0.40	0.046	0.019	0.017–0.021
0.45	0.035	0.018	0.014–0.021

[a] Values of H at the optimum velocity of the mobile phase.
[b] Confidence limits for the average value of $H_{u\,opt}$ (confidence level 95%) [38].

should result. Taking into account that the longitudinal diffusion term is proportional to D_M whereas it appears in the denominator of the C term, it is clear that a decrease in D_M may imply an increase in efficiency if the effect of B on H dominates over that of C on efficiency. Nevertheless, experimentation is commonly performed at linear velocities higher than the optimum, thus causing the B/u term to decrease to such an extent that the effect of the C term on efficiency may become clearly dominant. Consequently, lower column efficiencies should be observed at the highest densities (Fig. 1).

Fig. 2 shows the effect of temperature on the micropacked column efficiency at three different densities of the mobile phase, namely 0.25, 0.35 and 0.45 g/ml.

It is clear that the influence of temperature is greater the lower is the mobile phase density. Fig. 2a shows that increasing the temperature at a fixed density results in a higher column efficiency. This happens because the C term of the Van Deemter equation is lowered. Nevertheless, when working at this fixed lower density (0.25 g/ml), significant differences in H values are only found between those analyses performed at higher temperatures (140–160°C) and those carried out at lower temperatures (100–120°C).

If operation is accomplished at a density of 0.35 g/ml (Fig. 2b) and the temperature is varied from 100 to 140°C, no significant differences are observed between the variation of H with u corresponding to each curve. At 80°C, however, the curve obtained is significantly different from those resulting at higher temperatures. Curves obtained at the highest density (0.45 g/ml) at different temperatures are not significantly different (Fig. 2c). In all instances the statistical study was performed by considering a confidence level of 95%.

Fig. 3 illustrates the effect of variations in both density and temperature on retention in a micropacked column. It is clear that increasing the density at a fixed temperature results in faster elution of the solute from the column, whereas the opposite effect (*i.e.*, a retention increase) is observed when working at a fixed density if the temperature is decreased.

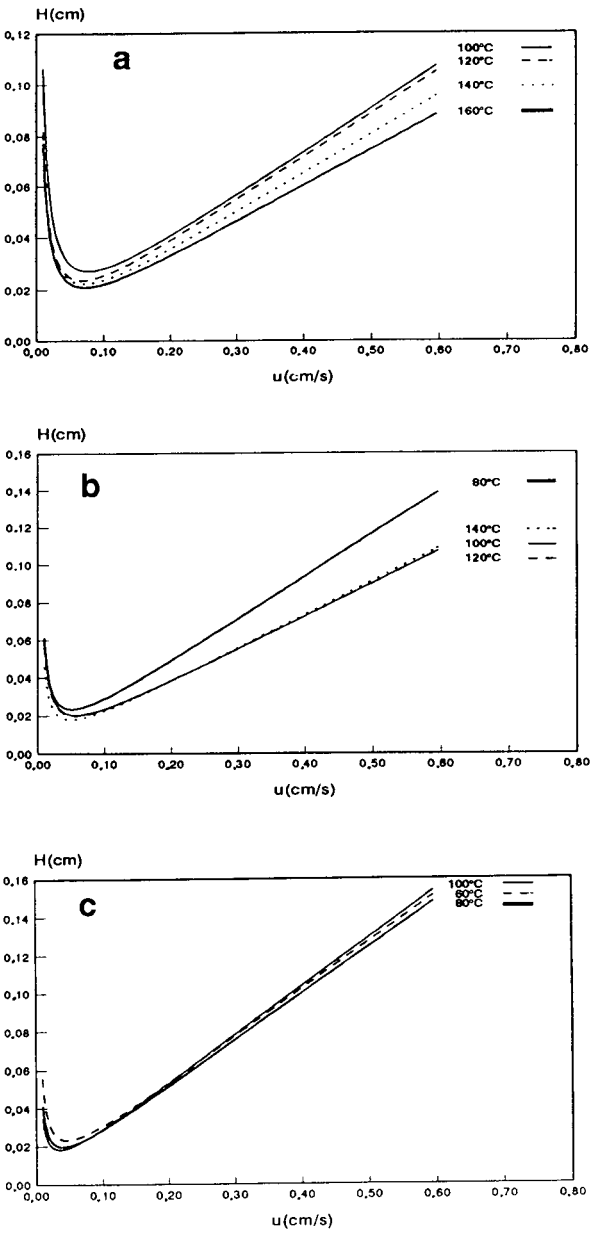

Fig. 2. Effect of temperature on efficiency: Van Deemter plots, obtained by fitting experimental data, at different temperatures, at densities of (a) 0.25, (b) 0.35 and (c) 0.45 g/ml for a micropacked column. Solute: n-C_{20}.

With respect to the resolution achieved for a given pair of solutes in a micropacked column, Fig. 4 shows its variation with density and temperature. To understand the observed vari-

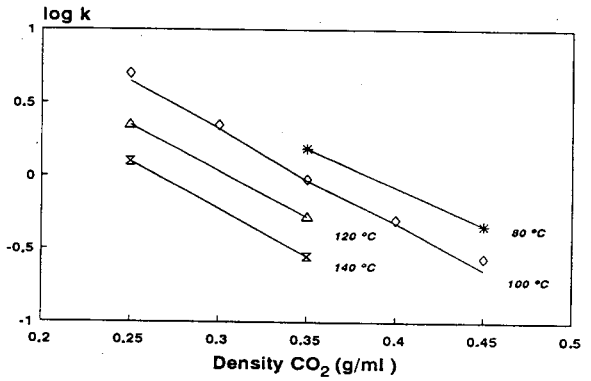

Fig. 3. Variation of the logarithm of the capacity factor (k) with the mobile phase density at different temperatures for a micropacked column. Solute: n-C_{20}.

ation of the resolution, the combined influence of three factors, namely column efficiency (N), relative retention (α) and column capacity factor (k), described by the Purnell resolution equation, should be considered.

Working under isothermal conditions, it is evident that decreasing the density gives higher k values but also, according to Fig. 1, lower H values may be achieved. Thus higher resolutions are finally observed.

If operation is performed at a fixed density, it is also clear that variation of the temperature causes an important variation of the partition coefficient (K_D). Specifically, increasing the temperature (under isopycnic conditions) brings about a diminution of both K_D and k. Conversely, changes in column efficiency at fixed density (Fig. 2) may contribute to obtaining better resolution if the temperature is increased. The influence of k on the resolution achievable must dominate over that of N, as a diminution of the resolution is ultimately observed.

The data obtained reveal that the effect of variations in both density and temperature on the retention and resolution achievable in a micropacked column is similar to the effect reported previously by several workers for capillary and packed columns in SFC [32,39–41].

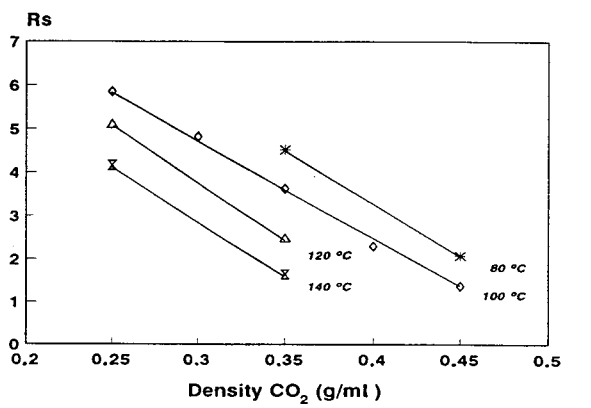

Fig. 4. Dependence of the resolution (R_s) on the mobile phase density at different temperatures for a micropacked column. Solutes: n-C_{20}/n-C_{22}.

4. Acknowledgements

Financial support for this work by the Dirección General de Investigación Científica y Técnica (Project PB 88-0034) is gratefully acknowledged. E. Ibáñez also thanks the Ministerio de Educación y Ciencia for a grant.

5. References

[1] M. Novotny, S.R. Springston, P.A. Peaden, J.C. Fjeldsted and M.L. Lee, *Anal. Chem.*, 53 (1981) 407A.
[2] M. Novotny and S.R. Springston, *J. Chromatogr.*, 279 (1983) 417.
[3] H.E. Schwartz, P.J. Barthel, S.E. Moring and H.H. Lauer, *LC·GC*, 5 (1987) 490.
[4] P.J. Schoenmakers, in R.M. Smith (Editor), *Supercritical Fluid Chromatography*, Royal Society of Chemistry, London, 1988, Ch. 4.
[5] F. Pacholec, D.S. Boyer, R.K. Houck and A.C. Roselli, in C.M. White (Editor), *Modern Supercritical Fluid Chromatography*, Hüthig, Heidelberg, 1988, Ch. 2.
[6] M.L. Lee and K.E. Markides (Editors), *Analytical Supercritical Fluid Chromatography and Extraction*, Chromatography Conferences, Provo, UT, 1990, Ch. 2.
[7] M. Petersen, *J. Chromatogr.*, 505 (1990) 3.
[8] H.G. Janssen and C.A. Cramers, *J. Chromatogr.*, 505 (1990) 19.
[9] L.T. Taylor and H.-C. Karen Chang, *J. Chromatogr. Sci.*, 28 (1990) 357.
[10] H.G. Janssen, H.M.J. Snijders, J.A. Rijks, C.A. Cramers and P.J. Schoenmakers, *J. High Resolut. Chromatogr.*, 14 (1991) 438.
[11] Y. Hirata, F. Nakata, *J. Chromatogr.*, 295 (1984) 315.
[12] Y. Hirata, F. Nakata and M. Kawasaki, *J. High Resolut. Chromatogr. Chromatogr. Commun.*, 9 (1986) 633.

[13] K.M. Payne, B.J. Tarbet, J.S. Bradshaw, K.E. Markides and M.L. Lee, *Anal. Chem.*, 62 (1990) 1379.
[14] D. Steenackers and P. Sandra, *J. High Resolut. Chromatogr.*, 14 (1991) 842.
[15] P.J. Schoenmakers and F.C.C.J.G. Verhoeven, *J. Chromatogr.*, 352 (1986) 315.
[16] C.M. White and R.K. Houck, *J. High Resolut. Chromatogr. Chromatogr. Commun.*, 9 (1986) 4.
[17] J.A. Graham and L.B. Rogers, *J. Chromatogr. Sci.*, 18 (1980) 75.
[18] P.J. Schoenmakers and L.G.M. Uunk, *Chromatographia*, 24 (1987) 51.
[19] T.A. Berger and J.F. Deye, *Chromatographia*, 30 (1990) 57.
[20] D.R. Gere, R. Board and D. McManigill, *Anal. Chem.*, 54 (1982) 736.
[21] T.A. Berger and J.F. Deye, *Chromatographia*, 31 (1991) 529.
[22] T.A. Berger and W.H. Wilson, *Anal. Chem.*, 65 (1993) 1451.
[23] E. Ibáñez, P.J. Martin-Alvarez, G. Reglero and M. Herraiz, *J. Microcol. Sep.*, 5 (1993) 371.
[24] E. Ibáñez, M. Herraiz and G. Reglero, *J. High Resolut. Chromatogr.*, 16 (1993) 615.
[25] C.A. Cramers and J.A. Rijks, *Adv. Chromatogr.*, 17 (1979) 101.
[26] I. Halász and E. Heine, *Adv. Chromatogr.*, 4 (1967) 207.
[27] G. Reglero, M. Herraiz, M.D. Cabezudo, E. Fernández Sánchez and J.A. García Domínguez, *J. Chromatogr.*, 348 (1985) 327.
[28] T. Herraiz, G. Reglero, M. Herraiz, R. Alonso and M.D. Cabezudo, *J. Chromatogr.*, 388 (1987) 325.
[29] G. Reglero, T. Herraiz, M. Herraiz and M.D. Cabezudo, *Chromatographia*, 22 (1986) 358.
[30] A. Olano, M.M. Calvo and G. Reglero, *Chromatographia*, 22 (1986) 538.
[31] T. Herraiz, G. Reglero and M. Herraiz, *Food Chem.*, 29 (1988) 177.
[32] S. Shah and L.T. Taylor, *Chromatographia*, 29 (1990) 453.
[33] M. Novotny, W. Bertsch and A. Zlatkis, *J. Chromatogr.*, 61 (1971) 17.
[34] T.A. Berger, *J. Chromatogr.*, 478 (1989) 311.
[35] W.J. Dixon (Editor), *BMDP. Statistical Software Manual*, University of California Press, Los Angeles, 1990.
[36] J.C. Giddings and R.A. Robinson, *Anal. Chem.*, 34 (1962) 885.
[37] W.L. Jones, *Anal. Chem.*, 33 (1961) 829.
[38] *Statgraphics Version 5, Statistical Graphics Corporation Reference Manual*, STSC, Rockville, MD, 1991.
[39] F.P. Schmitz and E. Klesper, *J. High Resolut. Chromatogr. Chromatogr. Commun.*, 10 (1987) 519.
[40] T.L. Chester and D.P. Innis, *J. High Resolut. Chromatogr. Chromatogr. Commun.*, 8 (1985) 561.
[41] V. Van Wasen and G.M. Schneider, *Chromatographia*, 8 (1975) 274.

ELSEVIER

Journal of Chromatography A, 667 (1994) 257–270

JOURNAL OF CHROMATOGRAPHY A

Computer simulation for capillary zone electrophoresis A quantitative approach

Sergey V. Ermakov[☆], Pier Giorgio Righetti*

Faculty of Pharmacy and Department of Biological Sciences and Technologies, University of Milan, Via Celoria 2, Milan 20133, Italy

(Received November 15th, 1993)

Abstract

The simulation results for peak quantification and for describing a peak shape and transit time in capillary zone electrophoresis (CZE) are described. For peak quantification, two approaches are described and compared: a differential and an integral method. An attempt is made at describing by computer simulation the *temporal dependence* of a detector signal, as typical of output data in experimental runs, instead of as a *space distribution*, as offered by earlier computer modelling. The peak shape and transit times are evaluated as a function of the concentration of sample within a single peak and the presence of several analytes in the injected sample mixture. The phenomena of peak fronting and tailing due to conductivity differences and anomalies of migration time due to the effect of absolute sample molarities on the degree of ionization in mixtures of weak and strong electrolytes can be correctly assessed and predicted by the present computer program. Unlike previous computer modelling performed by different workers, good *quantitative* coincidence of simulated and experimental results for real operating parameters used in everyday practice was demonstrated. This is the first time that an approach to "dry chemistry", prior to actual "wet" runs, has been performed under real experimental conditions in CZE, as is typically done in high-performance liquid chromatography.

1. Introduction

The evolution of chemical species in free fluid solution under the effect of an electric field, known as electrophoresis, has been the subject of computer modelling for more than 10 years [1]. During these years a unified mathematical model for electrophoresis was developed; with it four basic migration modes: zone electrophoresis, isotachophoresis, isoelectric focusing and moving boundary electrophoresis were simulated. The modelling started from the relatively simple problem of studying the evolution of a boundary between two weak monovalent electrolytes [2,3]; later it was extended to multicomponent systems and proteins [4–7]. These results were summarized by Mosher *et al.* [8]; an extensive review of work on computer simulation in electrophoresis has also been published [9].

However, in the field of electrophoresis, there is still some mistrust of computer modelling. Probably this can be explained first by the absence of a correct quantitative comparison between experimental and simulated data, as all of the work mentioned above gave only quali-

* Corresponding author.

☆ Permanent address: Keldysh Institute of Applied Mathematics, Russian Academy of Sciences, Miusskaya Sq. 4, 125047, Russian Federation.

0021-9673/94/$07.00
SSDI 0021-9673(94)00035-8

tative information. Direct quantitative comparison assumes that simulations should be performed for parameters corresponding to the real experimental conditions and also both experimental and calculated electropherograms should be presented on the same plot with the same coordinate system. There is no doubt that previous simulations helped to reveal and explain a lot of details in separation patterns, while providing the necessary background for future research. However, in recent years, electrophoretic methods have been developed to such an extent that the reproducibility of experimental results with only 2–3% errors became the normal practice. In this situation a pure qualitative description could not be considered satisfactory. At the same time, new achievements in experimental science created the basis for an accurate verification of the mathematical model [8] used in simulations. This circumstance became the main stimulating motive for starting work on quantitative comparisons of experiment and computer simulation. Among other factors that impinged on this work were the progress in high-performance capillary electrophoresis (HPCE), offering excellent reproducibility with short analysis times and computer data processing, and the development of efficient, high-resolution numerical algorithms [10], allowing for simulation of real experimental conditions.

There were several problems that made impossible the direct comparison of experimental and computer modelling results earlier. One of them is the simulation of experiments with input parameters that do not correspond to the actual conditions used in practice. We mean here not the inevitable restrictions implied by the mathematical model such as isothermal conditions, one-dimensional consideration, constant pK and mobility values. Simply in most of the work the simulations were performed for input parameters that were known in advance to be far from real [6]. Some of the reasons for this discrepancy were that computer simulations did not have as a goal the comparison of experimental and simulated results, and that available numerical algorithms did not allow solutions to be obtained at reasonable computational expense. Attempts to use the simplified models allowing for the analytical solutions usually gave predictions that might be considered only as a first approximation to reality [11,12].

The other cause of difficulties in comparison is connected with different ways of data presentation in experiment and in computer simulations. In the experimental runs the output data are given in the form of a *temporal dependence* for the detector signal whereas computer simulation results are usually presented as a *space distribution* along the electrophoretic column axis. The comparison of spatial distribution and temporal signal is not so obvious as it may seem at first. For example, in temporal electropherograms, the peak width for sample species depends on the migration velocity of each component [13]. Another aspect complicating the data comparison is that in experiments a UV absorbance signal is obtained, whereas simulations are performed in terms of concentrations. Two standard procedures are mostly used for quantifying the electropherograms: according to the peak height and according to the peak area [14]. Although there are no substantial difficulties in recalculating the absorbance electropherograms into concentration profiles and then plotting them on the same axis system, usually this is not done.

It is worth mentioning that the sampling techniques are also of importance for quantitative analysis. Electropherogram quantification by means of peak areas needs accurate information on analyte mass; in addition, for simulation purposes, one should know precisely the amount of sample injected. The problem of quantitative injection and the advantages and drawbacks of electrokinetic and hydrodynamic modes have been considered previously [14,15].

In this work dealing with the comparison of experimental and simulated results we tried to overcome the above problems. The main aim of this study was to perform computer simulation of electrophoretic runs for parameters as close as possible to those of the real experiment. The shape of the concentration profiles for sample species and their migration time characteristics were considered as the subject for comparison. Weak monovalent acids and bases with good UV absorbance were the sample constituents. We took these substances as their mathematical

description is the simplest compared with others. They are completely characterized by only two constants, the pK value and the ionic mobility, which are usually well known. For experimental runs we used an HPCE unit run in the capillary zone electrophoresis (CZE) mode. HPCE provides a unique opportunity for comparison, because it gives highly reproducible results ready for computer handling within a few minutes. Another unique feature of this technique is the use of thin capillaries, for which it is relatively easy to maintain isothermal conditions in a buffer. The thermal problem in this instance is reduced to temperature corrections for substance ionic mobilities. The influence of hydrodynamics on separation patterns is caused by the effect of electroosmotic flow. Since it has a uniform "flat" velocity profile, it does not cause an additional zone distortion. It can be accounted for by adding the electroosmotic velocity to the electrophoretic migration. All these circumstances significantly simplified the mathematical description compared with column or free flow electrophoresis.

We displayed the results, both experimental and computed, as a detector signal, *i.e.*, temporal dependence of concentration, scaled to the same axis system. For this purpose the two quantification methods mentioned above were tested. The use of buffer systems with different pH values allowed the study of the evolution of samples with full and partial dissociation comprising one or more chemical species. Experimental and computer simulation results were compared with analytical solutions [11].

2. Theory

For computer simulations we used a mathematical model based on mass and charge conservation laws, the assumption of local electroneutrality and chemical equilibria equations described previously in detail [16]. The only modification of this model was the explicit introduction of electroosmotic velocity to the convective terms in mass transport equations, describing the evolution of electrolyte constituents. A high-resolution finite-difference scheme [10] for solving the non-linear partial differential equations underlaid the numerical algorithm used in simulations. It exhibited excellent results when it was compared with the other algorithms used in electrophoresis simulations [17].

The model mentioned above assumes isothermal conditions during the experiment, so it is necessary to take the following run parameters, for which this approximation holds true. Thermal problems connected with capillary electrophoresis have been extensively examined in recent years [18–21]. The temperature distribution in solution is determined by the amount of Joule heat, G, generated per unit capillary length [18]. As has been shown [19], under normal operational conditions the radial temperature profile could be considered to be parabolic with good accuracy, so the radial temperature difference, δT, between the capillary axis and its wall can be estimated as [18]

$$\delta T = \frac{GR_1^2}{4k_1} \tag{1}$$

where R_1 is the internal capillary radius and k_1 is the thermal conductivity of buffer solution (water). As Joule heat generation is given by

$$G = \frac{VI}{\pi R_1^2 L} = \frac{EI}{\pi R_1^2} \tag{2}$$

Eq. 1 can be rewritten in the form

$$\delta T = \frac{EI}{4\pi k_1} \tag{3}$$

where V is applied voltage, I is current, L is the total length of the capillary and E is the field strength. For estimates let us suppose that the field strength and current do not exceed $3 \cdot 10^4$ V/m and 15 μA, respectively, and the thermal conductivity of the buffer solution is equal to that of water, $k_1 = 0.609$ (at $T = 27°C$) [20]. Then the radial difference $\delta T \approx 0.06$, so we can neglect it and consider the temperature over the capillary cross-section to be uniform.

It is difficult to measure the temperature directly in solution within a capillary so only the temperature of the medium surrounding the

capillary is usually known. The problem of how to determine precisely the temperature within the capillary for the HPCE units has been described [21]. For calculating the excess of temperature in the buffer, ΔT, compared with the temperature of the coolant (air) we use the simple equation [21]

$$\Delta T = \frac{VI}{2\pi Bi_{OA} k_1 L} = \frac{EI}{2\pi Bi_{OA} k_1} \quad (4)$$

where Bi_{OA} is the overall Biot number, which specifies the outer heat transfer from the capillary. For the Waters Quanta 4000 HPCE unit, which we used in our experiments, this parameter was determined as $Bi_{OA} \approx 0.055$ [21]. Taking this Biot number and the same parameters as chosen previously, one can easily calculate $\Delta T \approx 2.1$. For such small deviations it is possible to consider ionic mobility to be linearly dependent on temperature and to use simple corrections assuming an increase of 2% for every 1°C increase.

In order to compare the simulated results and the experimental electropherograms in terms of concentration, one should establish somehow a correspondence between absorbance as a function of time $f(t)$ and concentration $c(t)$. One of the ways is to construct a calibration function relating absorbance and sample concentration. For this purpose let us consider a function $k(c)$ which equals the sample concentration c divided by absorbance f, *i.e.*, $k(c) = c/f$. Measuring $k(c)$ for several c values over the range of concentrations expected in experiments, we then approximate these data by one of the best fit curves $\bar{k}(c)$ (linear, polynomial, exponential, etc.). When $\bar{k}(c)$ has been calculated, the following equation is obtained:

$$\bar{k}(c) = c(t)/f(t) \quad (5)$$

with c as an unknown and t as an argument. When $\bar{k}(c)$ is a linear function of concentration, $\bar{k}(c) = \alpha c + \beta$ (α, β = constants are the best fit parameters), the equation has a solution

$$c(t) = \frac{\beta f(t)}{1 - \alpha f(t)} \quad (6)$$

Determining α and β from best fitting and using Eq. (6), one can easily transform the absorbance curve into a concentration profile. For $\alpha = 0$ the simplest relationship between c and f is derived as $c(t) = \beta f(t)$, which resembles the Lambert–Beer law. For more complex functions $\bar{k}(c)$, Eq. 5 can be solved numerically.

The crucial point in such a technique is a calibration procedure from f to c. It can be performed by injecting a sample plug of known concentration and observing its UV response. At the moment of detection, in addition to absorbance, which is monitored by a detector, an experimenter needs to know the precise value of the sample concentration at this point. Usually the concentration profile for a short sample pulse has a rectangular form (or close to it) with a plateau of known concentration only for a limited period of time just after injection. Travelling along the capillary and being distorted by a number of dispersive mechanisms [22], by the moment of detection the sample zone has a symmetrical gaussian or skewed shape. The concentration at the peak apex is unknown and there is a probability that it can be different from the initial value. In order to avoid the uncertainty in concentration at the detection point we offer the following procedure. It is necessary to inject the sample continuously until it reaches the detector. The absorbance profile $f(t)$ would then have the shape of a step (Fig. 1), with the lower level f_l corresponding to zero concentration and the upper level f_u corresponding to the concentration of the sample. There is a relatively small transition region due to the action of diffusion where the absorbance changes from f_l to f_u. The difference $f_u - f_l$ gives the relative absorbance value corresponding to the sample concentration. It is clear that the sample should be injected hydrodynamically, as during the electrokinetic injection the electromigration dispersion due to the variances in conductivity may significantly spread the transition region.

Another way to quantify the UV absorbance electropherogram in terms of concentration is to take the total mass of the sample m as a reference point. At the detection point it is calculated as

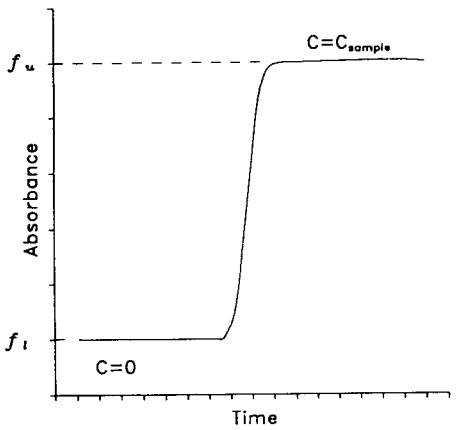

Fig. 1. Absorbance profile with continuous sample loading for calibration procedure. Absorbance level f_l corresponds to pure buffer and f_u corresponds to absorbance by a substance with concentration $c = c_{sample}$.

$$m = \pi R_1^2 \int_0^{+\infty} v(t)c(t)\,dt = \pi R_1^2 \bar{v} \int_0^{+\infty} c(t)\,dt$$

$$= C_0 \int_0^{+\infty} c(t)\,dt \quad (7)$$

or

$$m/C_0 = \int_0^{+\infty} c(t)\,dt \quad (8)$$

where $v(t)$ is an instantaneous velocity of sample zone at the detection point at moment t and $\bar{v}$ is its average velocity. The zeroth moment of the electropherogram also gives the value corresponding to the mass of the sample:

$$F_0 = \int_0^{+\infty} f(t)\,dt \quad (9)$$

Comparing Eqs. 8 and 9 and assuming the linear dependence $c(t) = kf(t)$ with k = constant, one can easily derive that

$$\int_0^{+\infty} c(t)\,dt = \frac{m}{F_0 C_0} \int_0^{+\infty} f(t)\,dt$$

or

$$c(t) = \frac{m}{F_0 C_0} f(t) \quad (10)$$

The value of m/C_0 is calculated from the simulated profile $c(t)$ and F_0 from the experimental electropherogram.

As in the first method the absorbance profile is recalculated into a concentration profile using a number of calibration points and in the second method the only integral characteristic (area under the curve) is used, from here, for the sake of brevity, we shall refer to the first method of quantification as a differential and to the second method as an integral method.

3. Experimental

All chemicals used were of analytical-reagent or research grade. Most of them were purchased from Merck (Darmstadt, Germany), picric acid from Carlo Erba (Milan, Italy) and acrylamide from Bio-Rad Labs. (Richmond, CA, USA). Fused-silica capillaries of length 37.7 cm with nominal I.D. 75 μm were obtained from Polymicro Technologies (Phoenix, AZ, USA). The detection path for this capillary was 30.0 cm. We performed experiments on a Waters Quanta 4000 capillary electrophoresis system (Millipore, Milford, MA, USA) equipped with a personal computer running under Baseline 810 software (Dynamic Solutions, Division of Millipore). The unit was equipped with a UV absorbance detector (mercury lamp, 254-nm filter) and it worked in a voltage-stabilized regime of 10 kV. The air temperature within the capillary unit and the magnitude of the electric current were also monitored during the experiments. Typical values for temperature lay within the range 26–28°C. For injection, a sample hydrostatic loading method was used, as the amount of a sample loaded did not depend on the velocity of electroosmotic flow and the electrophoretic mobility of the sample. During injection, lasting 10 s, the sample volume loaded was *ca.* 20.6 nl, which corresponded to a sample plug length of 0.466 cm within the capillary. The total amount of sample depended on the particular concentra-

tion. Between successive runs the capillary was rinsed only with buffer for 5 min. In each series of experiments we performed one control run in order to measure the velocity of electroosmotic flow. For this purpose a small pulse of 5 m*M* acrylamide as a neutral marker was injected. According to its migration time the velocity of electroosmosis was calculated.

Computer simulations were performed on an AT 486 personal computer running at 33 MHz. The computer code was written in Fortran algorithmic language using the Microsoft Fortran (Version 5.1) Development System, as used earlier for simulation of capillary electrophoresis [16]. For this work we changed the method of data presentation, giving the concentration profiles as a temporal signal at a given point of the capillary. During simulations a finite-difference grid covered only that part of capillary where sample species were located at a given time moment. This helped to reduce the computational expenses. Initial conditions specified the distribution of all sample and buffer components, their ionic mobilities, p*K* values, capillary geometry, applied voltage and temperature. For handling the experimental electropherograms a special computer program was written, which allowed us to cut the desired part of the electropherogram, to calculate the baseline level, subtract it, if necessary, calculate the moments and finally recalculate the electropherogram in terms of concentration.

4. Results

The weak monovalent picric and salicylic acids were chosen as sample species. We took negatively charged substances in order to minimize the probability of sample adsorption on the capillary wall, because as a rule it is negatively charged owing to ionization of silanol groups. Buffer solutions were 20 m*M* formic acid titrated with NaOH to pH 3.0 or 20 m*M* acetic acid titrated with NaOH to pH 5.0. The concentration of the sample species was within the range 0.02–10 m*M*. The input data for the substances used in the simulation are summarized in Table 1. It is worth noting that there are some discrepancies in data given by different sources. For example, the ionic mobility of salicylic acid at 25°C according to ref. 23 is $3.73 \cdot 10^{-8}$ m^2 V^{-1} s^{-1}, but in ref. 24 the value $3.53 \cdot 10^{-8}$ m^2 V^{-1} s^{-1} is given. The difference is more than 5%, which cannot be considered as negligible, especially for quantitative analysis.

Table 1
Input data for computer simulations

Substance	pK_a	μ (10^{-8} m^2 V^{-1} s^{-1})
Acetic acid	4.75	4.24
Formic acid	3.75	5.66
Salicylic acid	2.937[a]	3.73
Picric acid	0.38	3.15
Na^+	–	5.19
H^+	–	36.2
OH^-	–	20.5

All values at 25°C from ref. 23 except where indicated otherwise.
[a] Data from ref. 24.

The first series of experiments was performed with picric acid as a sample in acetate buffer. We started with the calibration procedure described under Theory, which was necessary for differential quantification method. Samples with concentrations of 0.02, 0.1, 0.5, 1, 5 and 10 m*M* were used. The results of the calibration are presented in Fig. 2 where the measured points and best fit line $\bar{k}(c)$ are plotted. The best fit line was approximated by a linear dependence $\bar{k}(c) = 2.11c + 22.53$. This calibration graph was used in the quantification of experimental electropherograms.

The experimental electropherograms (solid lines) together with computer simulation results (dashed line) are plotted for six different sample concentrations, $c_0 = 0.02$, 0.1, 0.5, 1, 5 and 10 m*M*, in Fig. 3A, B, C, D, E and F, respectively. The two different experimental electropherograms in each panel represent different quantification methods: The solid lines without symbols are the results obtained by the differential method and those with solid circles are the data for the integral quantification method. The experimental and calculated electropherograms

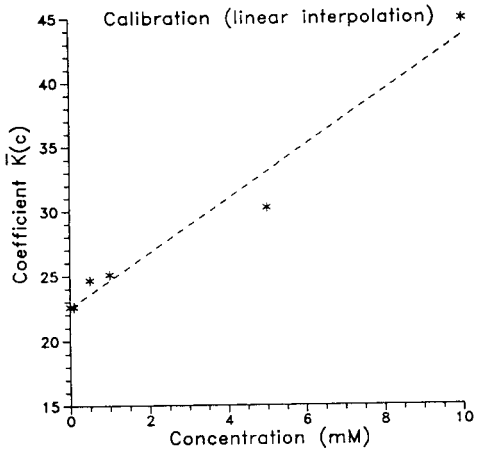

Fig. 2. Calibration graph for picric acid: dependence of parameter $k(c) = f/c$ on sample concentration. * = Experimental points; dashed line = best fit line.

demonstrate good qualitative and quantitative agreement when the shapes of the concentration profiles, migration times or maximum concentration values are compared. The simulated profiles have small false spikes near the sharp concentration boundaries. They should not be taken into account because of their purely computational origin.

It can be clearly seen that for sample concentrations $c_0 = 0.02$ and 0.1 mM (Fig. 3A and 3B), which are low compared with that of the background electrolyte (20 mM), the sample zone is subjected mainly to diffusion dispersion. Its concentration profile is close to gaussian. The slight skew in the experimental profiles can probably be explained by the interaction with the wall. Starting from $c_0 = 0.5$ mM (Fig. 3C), electromigration dispersion due to conductivity differences between the sample zone and background electrolyte plays the major role. It changes the zone shape to a typical triangular form. This transition in sample evolution from a diffusion-controlled regime to a state with a predominant influence of electromigration dispersion was confirmed by computer simulations. Another phenomenon observed in the experiments and proved by simulations is the decrease in migration time with increase in sample concentration. The migration time measured according to the front boundary position decreased from *ca.* 6.1 min ($c_0 = 0.02$ mM, Fig. 3A) to 5.4 min ($c_0 = 10$ mM, Fig. 3F) in experiments compared with 5.8 and 5.2 min, respectively, in simulations. The differences are 0.7 min and 0.6 min, respectively. This phenomenon is explained by the fact that the velocity of sample particles is higher in the regions with higher concentration [25]. In this case the sample "triangle" has sharp leading edge and tailing rear boundary, as observed in the figures.

Careful analysis of the data reveals some differences between simulation and experiment. Among them there are features observed in all figures. First, it should be noted that the differential quantification method gives a better coincidence with simulated results for the sample peak height, but it exaggerates the total area under the curve. The difference in peak concentration was of the order of 8%, whereas the difference in peak area reached 30%. Second, the sample zones in experiments are always wider than those predicted in simulations. Third, the migration time given by simulations is less than experimentally observed. Its value was calculated as a migration time for the sample centre of mass using moment analysis [26].

For migration times the deviation of experimental and simulation data did not exceed 5% and the discrepancy can be explained by a number of factors. As we have already noted, the input data for ionic mobilities and pK values taken from the literature are known to have some errors. Usually their determination within a deviation of ±3% may be considered to be reasonable. The next factor affecting the sample migration time is electroosmosis. The velocity of electroosmotic flow was about 20% of that of the sample. However, this value might vary from run to run and, probably, the actual velocity in each experiment was slightly different from that used in simulations. A further cause of the discrepancy is the error in temperature data measured within the HPCE unit. It may also make some contribution to the total error.

It is more difficult to find reasonable explanations for the first two discrepancy features. The excessive width of the sample zone and its

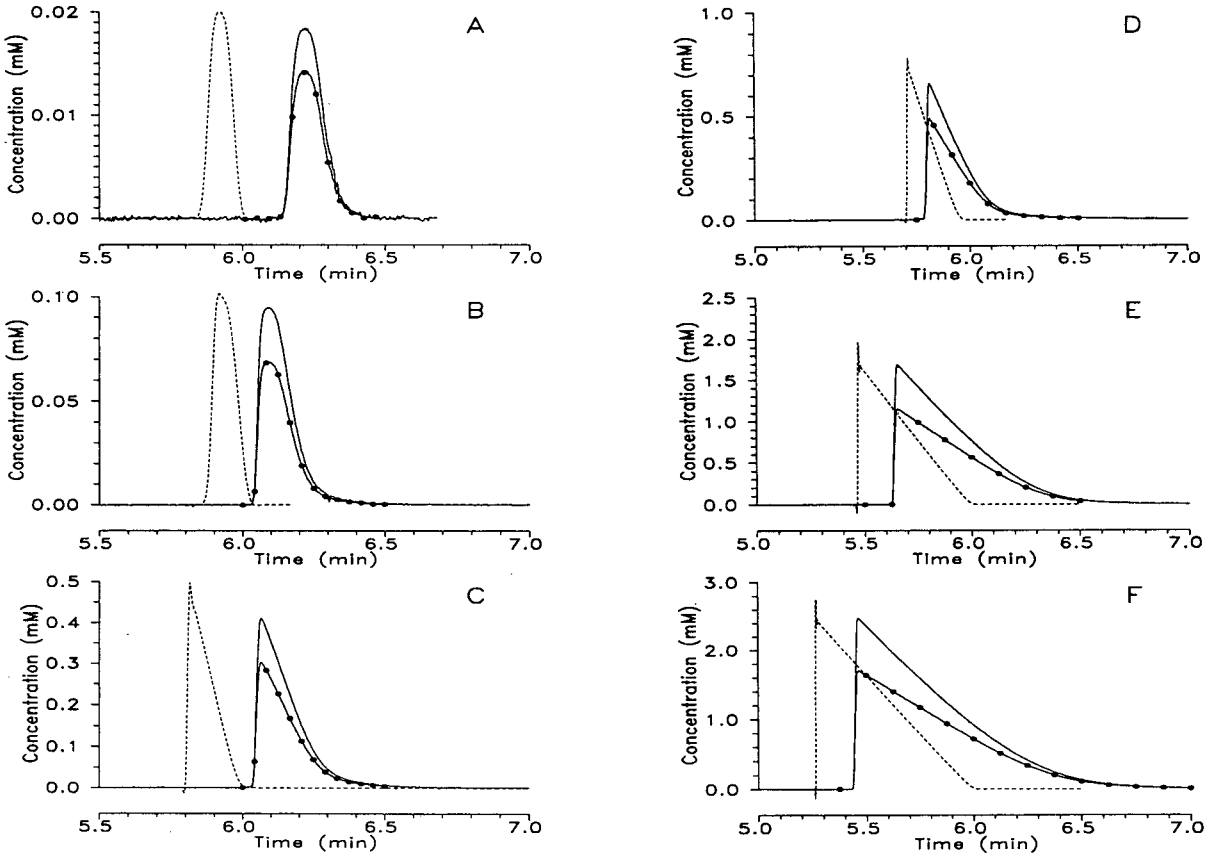

Fig. 3. Comparison of computer simulation and experimental electropherograms. Buffer, 20 m*M* acetic acid–NaOH (pH 5.0); sample, picric acid of concentration (A) 0.02, (B) 0.1, (C) 0.5, (D) 1.0, (E) 5.0 and (F) 10.0 m*M*. Here and also in Figs. 3–6 the solid line with symbols represents experimental data obtained by the differential method and the solid line without symbols represents experimental data obtained by integral method. The dashed line is the computer simulation.

excessive mass might mean that the actual injected mass was larger than that used as input data in calculations. However, this suggestion was not confirmed in the subsequent series of experiments with this and the other substances. There is an alternative reason explaining the additional sample zone dispersion observed in all experiments. We assume that despite the negative charge of sample species there was still some adsorption on the capillary walls. This might lead to additional sample spreading and to its lower effective mobility, as part of the time it rested on the wall surface. This provides one more possible cause for the increased migration time. Adsorption on the wall was possible because the wall surface charge was small, as shown by a weak electroosmotic flow, the velocity of which is directly proportional to the surface charge.

The next series of experiments and computer simulations was performed with picric acid as a sample, but using 20 m*M* formate buffer (pH 3). The experimental and calculated sample concentration profiles are plotted in Fig. 4A, B and C for initial sample concentrations of 1, 5 and 10 m*M*, respectively. The concentration profiles have a typical triangular shape, but unlike the previous instance the front boundary is dispersive whereas the rear boundary is sharp. This shape helps to reveal the additional dispersion mechanism, affecting the sample zone. It appeared in some experimental electropherograms as a tail adjacent to the rear boundary of the

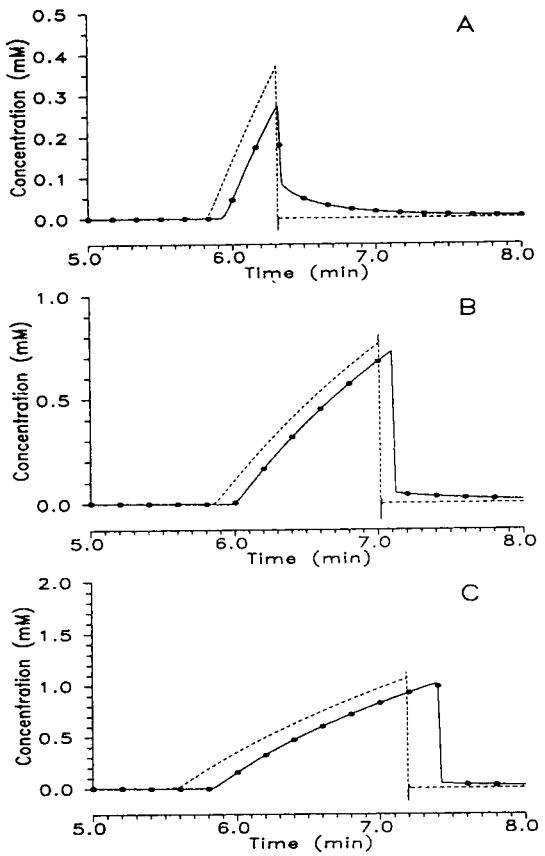

Fig. 4. Comparison of computer simulation and experimental electropherograms. Buffer, 20 m*M* formic acid–NaOH (pH 3.0); sample, picric acid of concentration (A) 1.0, (B) 5.0 and (C) 10.0 m*M*. For explanation see also Fig. 3.

sample zone. The concentration profile has an unusual bend at the point where the almost vertical part of the profile is followed by a smooth curve with concentration decreasing to zero. The last part of the profile is absent in simulated profiles, as the mathematical model does not account for this phenomenon. We assume that this additional dispersion is caused by sample adsorption. On the previous electropherograms this tailing phenomenon was obscured by tailing due to electromigration dispersion. We suspect it only from the excessive width of the sample zone. The relative effect of adsorption on the total sample transport depends on its concentration. For small concentrations (Fig. 4A) this tail contains a considerable part of the sample mass, which results in a decrease in the concentration maximum at the profile apex. For higher concentrations (Fig. 4B and C) the relative influence of adsorption is less and the shape of the experimental electropherograms approaches the simulated plot. In this series, the experimental electropherograms obtained with the use of differential and integral quantification methods virtually coincide. As in the preceding runs, the migration time observed in experiments is slightly longer than that predicted by computer simulations.

The above experiments involved a sample substance that was almost fully ionized, because for picric acid $pK = 0.38$ while the buffers used had pH 5 and 3. It was interesting to investigate the evolution of a sample with a pK value close to the pH of the buffer electrolyte, when the degree of its dissociation may change significantly within the sample zone. Salicylic acid dissolved in 20 m*M* formic acid buffer (pH 3.0) was a good candidate for this purpose. The results of experiments and computer simulations for sample concentrations of 1, 5 and 10 m*M* are plotted in Fig. 5A, B and C, respectively. The shapes of experimental and calculated concentration profiles are quite similar especially for larger concentrations. The effect of adsorption is noticeable only for the 1 m*M* sample, which gave a small tail behind the rear zone boundary (Fig. 5A). The difference in the absolute values of the migration time between experiment and simulations is greater than for the previous series. However, this error divided by the total migration time is approximately the same, as the effective mobility for salicylic acid was lower.

In order to evaluate the quality of predictions made by means of computer modelling they were compared with theoretical results obtained using the analytical solution [11]. Fig. 6A and B present the concentration profiles of picric acid as obtained by experiment, computer simulation and analytical solution. Fig. 6A shows the electropherograms for the sample in formate buffer and Fig. 6B for that in acetate buffer. The initial sample concentration was 10 m*M*. Experimental and simulated data were taken from Figs. 4C and 3F, respectively, the concentration profile de-

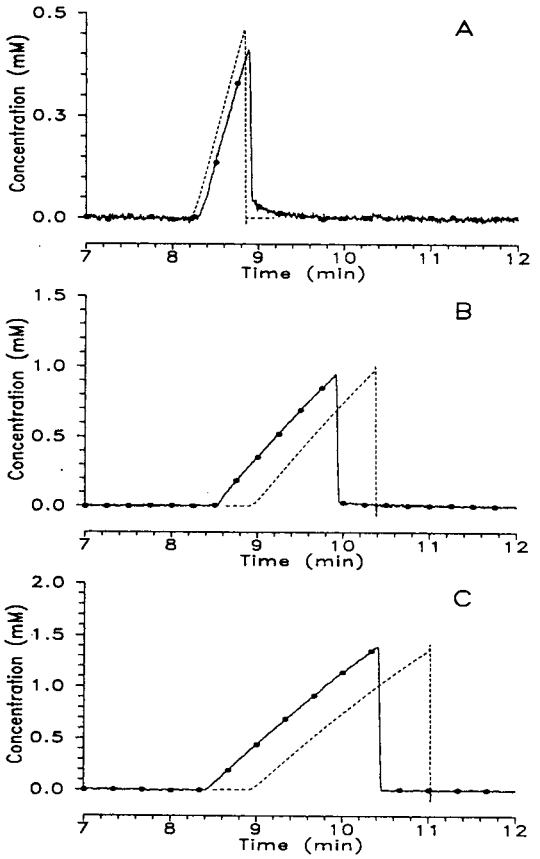

Fig. 5. Comparison of computer simulation and experimental electropherograms. Buffer, 20 m*M* formic acid–NaOH (pH 3.0); sample, salicylic acid of concentration (A) 1.0, (B) 5.0 and (C) 10.0 m*M*. For explanation see also Fig. 3.

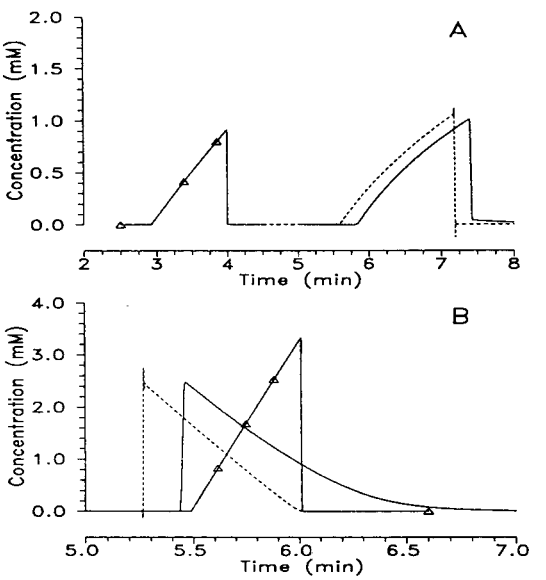

Fig. 6. Comparison of experimental and computer simulation and results with analytical solution [11]. (A) Corresponds to experimental results presented in Fig. 4C; (B) corresponds to experimental results presented in Fig. 3F. △ = Electropherogram calculated using ref. 11. For explanation see also Fig. 3.

rived from ref. 11 are marked with triangles. For the sake of clarity only one experimental electropherogram representing the differential quantification method is presented. As can be seen, the analytical results from ref. 11 are far from the experimental and computer-simulated data with formate buffer (Fig. 6A) the shape of electropherogram predicted by analytical solution is similar to that observed experimentally, but the sample migration time is halved. Such a large difference is explained by simplifications assumed in the mathematical model for which the analytical solution was obtained. It neglects the contribution of H^+ ions to the specific conductivity despite the fact that for this particular buffer solution it reaches 46%. Owing to the increase in sample velocity its zone passes through the detector in a shorter time, so the zone width is less than that given by computer simulation (Fig. 6A).

With acetate buffer the sample migration time predicted by analytical solution [11] agrees well with the experimentally observed data (Fig. 6B). For 20 m*M* buffer (pH 5) the contribution of hydrogen and hydroxyl ions to the specific conductivity is negligible, so they may be excluded from consideration. At the same time, the shape of the concentration profile given by analytical solution [11] is wrong. The "direction" of sample zone asymmetry is opposite to that of the experimental and calculated electropherograms. In ref. 11 the "direction" of peak asymmetry depends on the sign of the difference between the sample effective mobility $\bar{u}_S$ and that of background electrolyte co-ion $\bar{u}_A$. When $\bar{u}_S > \bar{u}_A$ the

zone front boundary is dispersive whereas the rear boundary is sharp (as in Fig. 6A), and for $\bar{u}_S < \bar{u}_A$ the situation is the opposite. For this particular case when pH = 5, $\bar{u}_S = 3.15 \cdot 10^{-8}$ m^2 V^{-1} s^{-1} and $\bar{u}_A = 2.71 \cdot 10^{-8}$ m^2 V^{-1} s^{-1}, *i.e.*, $\bar{u}_S > \bar{u}_A$, which corresponds to the shape of the concentration profile. However, more correct predictions are based on the consideration of specific conductivity variations. If it is higher in the sample zone compared with that of the background electrolyte, the concentration profile would have a "direction" of asymmetry analogous to that in Fig. 6A. It would have the opposite "direction" in another case. The latter is realized in the experiment shown in Fig. 6B. Thus, in this particular run the analytical results obtained in ref. 11 have features different from the experimental data on both quantitative (compare the maximum sample concentrations at the peak apex) and qualitative levels (the shape of the concentration profile).

We also performed experiments with samples consisting of two different substances. It was interesting to study how the computer simulation can predict the evolution not only of a solitary zone but also the interaction of sample components when there are several of them. This interaction is significant if the concentration of the sample species is comparable to that of the buffer.

Experimental and calculated electropherograms for 2.5 m*M* picric acid + 5 m*M* salicylic acid sample in 20 m*M* formate buffer (pH 3.0) are plotted in Fig. 7. Parts of the curves representing salicylic acid are marked with circles. For both substances the simulated and experimental data agreed fairly well. Note that the migration time for salicylic acid is slightly longer than that observed in Fig. 5B for the same concentration when the sample consisted solely of this substance. Its front boundary reached the detector at $t_b \approx 9.3$ min, whereas for the pure substance $t_b \approx 8.5$ min. Simultaneously for picric acid the migration time hardly changed. At the beginning of the separation the presence of stronger picric acid in the sample decreases the dissociation of salicylic acid. Hence when the sample substances are still not spatially separated, the salicylic acid has a lower effective mobility than for the pure substance. This effect is confirmed by computer simulation results.

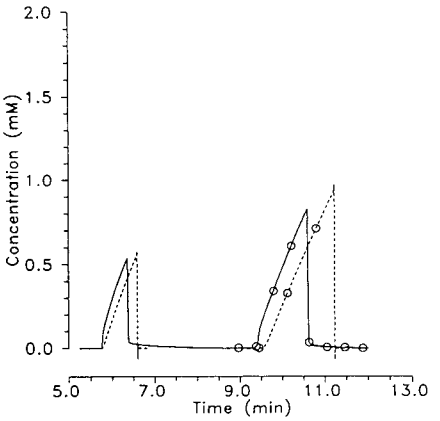

Fig. 7. Comparison of computer simulation and experimental electropherograms. Buffer, 20 m*M* formic acid–NaOH (pH 3.0); sample, 5 m*M* salicylic acid–2.5 m*M* picric acid. Solid lines represent experimental data and dashed lines simulated data. Lines without symbols are for picric acid; ○ = salicylic acid.

5. Discussion

From the present computer modelling and experimental results, it is clear that there are several factors influencing both the peak shape and its transit time in CZE. Among them are the reproducibility of electroosmotic flow (due to the degree of ionization of silanols on the inner surface), the potential interaction of analytes with the silica wall, the conductivity difference between the analyte and the surrounding background electrolyte and the presence of several analytes in the injected sample mixture. It has been impossible here to account for all of these aspects, which will need more extensive studies and more complex algorithms even for an approach to a solution. For example, there is still a hot debate on the reproducibility of the electroosmotic flow. As reported by Lambert and Middleton [27], among other factors, it seems that μ_{eos} also depends strongly on the precondi-

tioning of the fused-silica column. The μ_{eos} values obtained from a column previously exposed to acidic conditions are consistently lower than those using columns previously exposed to alkaline conditions. This hysteresis phenomenon is consistent with a slow equilibration of the surface, and it might take as long as a few weeks for the process to reach a plateau. This study suggests that there are still some phenomena responsible for μ_{eos} that are not yet fully understood.

We also have not investigated here the potential interaction of analytes with the capillary wall (be it by ionic or silanophilic or even hydrophobic interactions); this is a complex problem requiring the simultaneous solution of electrophoretic mass transport equations combined with equations describing different types of chromatographic interaction with the wall. What we have addressed here is how the peak shape and transit times are affected by the last two factors: (a) the concentration of a sample within a single peak and, as a consequence, the conductivity difference between the analyte and surrounding background electrolyte; and (b) the presence of several analytes in the injected sample mixture. Phenomenon (a) was recognized long ago by Everaert's group in their pioneering work on CZE [25]. Qualitatively, this mechanism of band broadening can be described as follows: if the conductivity in the sample zone (A) is lower than that in the background electrolyte (B), there will be a higher voltage gradient in A, resulting in dispersion of the rear boundary and sharpening of the front boundary; this phenomenon is called "tailing" (*e.g.*, see Fig. 3 D–F). Conversely, if the conductivity in A is greater than in B, the voltage gradient in A will be lower than in B, and molecules of analytes retarded in the front part of the sample zone will be accumulated on the rear boundary. This will result in sharpening of the rear boundary and dispersion of the front boundary (a phenomenon called "fronting", *e.g.*, Figs. 4 and 5A–C). Hjertén [22] derived a simple approximate expression describing this conductivity-induced band broadening quantitatively. Note in addition that our model correctly predicts the shape of the peaks and can describe with a very good approximation both fronting and tailing; conversely, the model proposed by Šustáček *et al.* [11] fails in some instances (see Fig. 6B).

Phenomenon (b) (how different analytes in a single zone influence each other's migration) is more subtle and deserves further comments. A case in point is represented by the mixture of picric acid (a stronger acid, $pK = 0.38$) and salicylic acid (a weaker acid, $pK = 2.94$). When present in the same zone, the stronger acid suppresses the ionization of the weaker acid, which results in a retardation of salicylic acid migration (see Fig. 7). This phenomenon, often overlooked, might be an important cause of irreproducibility of peak transit times, often blamed on fluctuations of electroosmotic flow. As a final remark, an important cause of peak irreproducibility is the molarity of the sample injected. As seen in the series of experiments in Fig. 3A–F, at progressively higher molarities of injected sample (0.02–10 m*M* picric acid), the migration time, as measured from the position of the front boundary, decreases substantially from 6.1 to 5.4 min, a phenomenon first described by Mikkers *et al.* [25]. Here too our computer model can predict and simulate fairly accurately such non-ideal behaviour.

We can summarize all the above observations by noting that, in CZE, nothing can be considered constant any more, as numerous phenomena affecting peak shape and transit time are strongly dependent on the molarity of sample present in a zone (and distortions are clearly visible already, for small analytes, at a level of 0.1 m*M*; see Fig. 3B). This is not surprising, and goes back to theories proposed at the turning of the century by Van't Hoff and Arrhenius and later developed by Debye and Hückel. The concentration of an analyte in solution affects both strong and weak electrolytes. In the former instance it changes the activity coefficient (γ); in the latter it alters the degree of dissociation (α, and ultimately the pK value of the substance). There are two ways to solve these problems: the first, as presented here, by proposing novel algorithms that can predict and model such phenomena, so that peak transit times and

shapes can be accurately described at any (reasonable) value of injected analyte. The second way is to exploit modern techniques labelling an analyte with a fluorescent tag (having a very high quantum yield) and induce such fluorescence by a laser beam: zeptomole sensitivity has been claimed; in fact, even as low as 500 yoctomol [28], which essentially would allow an almost infinite dilution of molecules in the sample peak. At such incredible dilutions, it is essentially guaranteed that the peak will have an ideal behaviour. Modern computer simulators should implement all such deviations from ideal behaviour, in order to serve as a user-friendly tool in laboratory practice. For example, also using immobilized pH gradients, where weak acids and bases are grafted on to a polyacrylamide matrix to create any pH gradient in the pH range 2.5–11 [29], Giaffreda *et al.* [30] have recently proposed a novel program that incorporates corrections to the degree of dissociation of such weak electrolytes as a function of the total prevailing ionic strength of the mixture according to the Debye–Hückel theory. We feel that the present version of our program has also evolved to such an extent to be a useful tool in laboratory work. It is a first approach at creating a "dry chemistry" (*e.g.*, computer modelling of the real CZE run) prior to the actual "wet chemistry" experiment.

6. Conclusions

Computer simulation in electrophoresis will become a more useful approach if in addition to the general pattern of the evolution it can predict the quantitative characteristics for a separation process. This work is an attempt to bring a new quantitative level to CZE modelling, when the experimental run is simulated with input data that are really used in everyday practice. The comparison of experimental and computer-simulated results was performed in terms of electropherograms displayed on the same scale as a temporary detector signal. This form of data presentation is the most natural way for experimenters, as it is usually implemented in commercial CZE units. Good coincidence of experimental and simulated concentration profiles and sample migration times gave one more validation for the mathematical model [8] underlying the computer code. We tried different substances, when their full and partial dissociation took place for samples consisting of one or more substances. The simulation data differed from those obtained in experiment by no more than a few per cent, which could be considered as satisfactory. At the same time the use of a simplified model with analytical solutions [11] gave much greater errors or even presented the wrong pattern of concentration profiles. Hence computer modelling confirmed again its power and usefulness.

Together with verification of the mathematical model for electrophoresis, the quantitative approach in computer simulation posed some questions that are of interest not only for modelling. Among them there are the problems of quantitative sample injection, the methods of recalculating the UV absorbance curves to concentration profiles and sample adsorption on the capillary walls. In this work we considered one of them. In order to quantify the UV absorbance electropherogram in terms of sample concentration two different methods were applied. They gave close but not coincident results. The reasons for the observed discrepancies should be the subject of separate studies, as also should the problem of interaction between the sample and the capillary wall. In this case the mathematical model needs modification to account for the sample adsorption.

7. Addendum

After this manuscript was accepted, we found an important review written by Hjertén [31] on the problem of quantitative analysis of peaks during electrophoresis in quartz tubes (I.D. 3 mm; O.D. 7.8 mm; present technology was not quite available in those days!). In pages 73–82 there is a thorough description on the problems of scanning a cylindrical object, on the relationship between absorbance and sample concen-

tration and on the accuracy of quantitative determinations, to which the reader is referred for additional information.

8. Acknowledgements

This work was supported in part by grants from the Agenzia Spaziale Italiana (ASI, Rome), the European Space Agency (ESA, Paris) and the Consiglio Nazionale delle Ricerche (CNR, Rome), Progetti Finalizzati Chimica Fine II and Biotecnologie e Biosensori. We thank Dr. M.S. Bello for helpful discussions and criticism.

9. References

[1] M. Bier, O.A. Palusinski, R.A. Mosher and D.A. Saville, *Science*, 219 (1983) 1281–1287.
[2] R.A. Mosher, W. Thormann and M. Bier, *J. Chromatogr.*, 320 (1985) 23–32.
[3] O.A. Palusinski, A. Graham, R.A. Mosher, M. Bier and D.A. Saville, *AIChE J.*, 32 (1986) 215–223.
[4] R.A. Mosher and W. Thormann, *Electrophoresis*, 11 (1990) 717–723.
[5] R.A. Mosher, D. Dewey, W. Thormann, D.A. Saville and M. Bier, *Anal. Chem.*, 61 (1989) 362–366.
[6] R.A. Mosher, P. Gebauer, J. Caslavska and W. Thormann, *Anal. Chem.*, 64 (1992) 2991–2997.
[7] R.A. Mosher, P. Gebauer and W. Thormann, *J. Chromatogr.*, 638 (1993) 155–164.
[8] R.A. Mosher, D.A. Saville and W. Thormann, *The Dynamics of Electrophoresis*, VCH, Weinheim, 1992.
[9] W. Thormann and R.A. Mosher, *Adv. Electrophoresis*, 2 (1988) 45–108.
[10] S.V. Ermakov, O.S. Mazhorova and Yu.P. Popov, *Informatica*, 3 (1992) 173–197.
[11] V. Šustáček, F. Foret and P. Boček, *J. Chromatogr.*, 545 (1991) 239–248.
[12] H. Poppe, *Anal. Chem.*, 64 (1992) 1908–1919.
[13] X. Huang, W.F. Coleman and R.N. Zare, *J. Chromatogr.*, 480 (1989) 95–110.
[14] S.E. Moring, in P.D. Grossman and J.C. Colburn (Editors), *Capillary Electrophoresis. Theory and Practice*, Academic Press, San Diego, 1992, Ch. 3, pp. 87–108.
[15] E.V. Dose and G. Guiochon, *Anal. Chem.*, 64 (1992) 123–128.
[16] S.V. Ermakov, O.S. Mazhorova and M.Yu. Zhukov, *Electrophoresis*, 13 (1992) 838–848.
[17] S.V. Ermakov, M.S. Bello and P.G. Righetti, *J. Chromatogr. A*, 661 (1994) 265–278.
[18] E. Grushka, R.M. McCormick and J.J. Kirkland, *Anal. Chem.*, 61 (1989) 241–246.
[19] A.E. Jones and E. Grushka, *J. Chromatogr.*, 466 (1989) 219–225.
[20] M.S. Bello and P.G. Righetti, *J. Chromatogr.*, 606 (1992) 103–111.
[21] M.S. Bello, E.I. Levin and P.G. Righetti, *J. Chromatogr.*, 652 (1993) 329–336.
[22] S. Hjertén, *Electrophoresis*, 11 (1990) 665–690.
[23] R.C. Weast (Editor), *CRC Handbook of Chemistry and Physics*, CRC Press, Boca Raton, FL, 67th ed., 1986–1987, pp. D159–D169.
[24] T. Hirokawa, M. Nishino and Y. Kiso, *J. Chromatogr.*, 252 (1982) 49–65.
[25] F.E.P. Mikkers, F.M. Everaerts and T.P.E.M. Verheggen, *J. Chromatogr.*, 169 (1979) 1–10.
[26] E. Grushka, in N. Catsimpoolas (Editor), *Methods of Protein Separation*, Vol. I, Plenum Press, New York, 1975, Ch. 6, pp. 161–192.
[27] W.J. Lambert and D.L. Middleton, *Anal. Chem.*, 62 (1990) 1585–1587.
[28] D.Y. Chen, H.P. Swerdlow, H.R. Harke, J.Z. Zhang and N.J. Dovichi, *J. Chromatogr.*, 559 (1991) 237–246.
[29] P.G. Righetti, *Immobilized pH Gradients: Theory and Methodology*, Elsevier, Amsterdam, 1990.
[30] E. Giaffreda, C. Tonani and P.G. Righetti, *J. Chromatogr.*, 630 (1993) 313–327.
[31] S. Hjertén, *Chromatogr. Rev.*, 9 (1967) 1–117.

ELSEVIER

Journal of Chromatography A, 666 (1994) 271–283

JOURNAL OF CHROMATOGRAPHY A

Capillary zone electrophoresis of synthetic opioid and tachykinin peptides

Huey G. Lee[a], Dominic M. Desiderio*[,a,b,c]

[a] *Charles B. Stout Neuroscience Mass Spectrometry Laboratory, University of Tennessee at Memphis, Memphis, TN 38163, USA*

[b] *Department of Neurology, College of Medicine, University of Tennessee at Memphis, 956 Court Avenue, Room A218, Memphis, TN 38163, USA*

[c] *Department of Biochemistry, University of Tennessee at Memphis, Memphis, TN 38163, USA*

(First received September 13th, 1993; revised manuscript received November 11th, 1993)

Abstract

Capillary zone electrophoresis was performed on fourteen synthetic opioid peptides and one tachykinin peptide (substance P = SP) at pH values of 2.5, 5.5 and 8.5 to rationalize the electrophoretic behavior of these neuropeptides. A plot of the theoretical $q/M_r^{2/3}$ values (where q = peptide charge) calculated across the pH range of 1 to 10 for these peptides was used to understand and to predict their separation. The experimentally determined electrophoretic mobilities (μ) were correlated to the estimate of the relative μ predicted by $q/M_r^{2/3}$ and by $[\ln (q+1)]/n^{0.43}$ (where n = number of constituent amino acids), where q values were calculated using amino acid pK_a values for an isolated amino acid and for an amino acid in a peptide. In general, relatively high correlations were obtained with either mathematical expression and with both sets of amino acid pK_a values for data at a single pH value. However, the combination of the former expression and the adjusted pK_a values gave the best prediction of electrophoretic behavior when data for the three pH values were correlated across these different separation conditions.

1. Introduction

Throughout the historical development of capillary zone electrophoresis (CZE), Jorgenson and Lukacs [1,2] were largely responsible for popularizing the technique in the early 1980s by demonstrating its high resolution capability using very narrow open-tubular glass capillaries (< 100 μm I.D.). Those narrow-I.D. capillaries have a high surface area-to-volume ratio that efficiently dissipate the heat (Joule heating) generated by the high voltage and by the buffer resistance. In addition to the important experimental parameter of high electrophoretic resolution that is achievable by CZE, other advantages include detection sensitivity, selectivity, rapid analyses, on-line detection, interfacing to mass spectrometry (MS), long column life, low sample/reagent consumption and automation.

In CZE, an analyte migrates in a capillary by its electrostatic attraction to an anode or cathode in the electric field gradient generated by high

* Corresponding author. Address for correspondence: Department of Neurology, College of Medicine, University of Tennessee at Memphis, 956 Court Avenue, Room A218, Memphis, TN 38163, USA

0021-9673/94/$07.00
SSDI 0021-9673(94)00044-A

voltage. Besides the electrostatic force, the analyte is also transported through the capillary by electroosmotic flow due to the ζ potential that exists between the analytes/electrolytes and the ionized silanols ($pK_a \approx 3.0$) on the inner wall of a glass or fused-silica capillary. The apparent electrophoretic mobility (μ_{app}) of an analyte is therefore equal to its inherent electrophoretic mobility (μ) plus the electroosmotic mobility (μ_{eo}), or,

$$\mu_{app} = \mu + \mu_{eo} \quad (1)$$

From an analyte's perspective, μ is predominantly a direct function of the analyte charge that is attracted by an electrostatic force and an inverse function of its mass, which retards electrophoretic migration due to frictional drag of the molecule against the medium and the silanols on the inner wall of the capillary. Understanding these two inherent physiochemical properties (charge and mass) of the analyte would aid in predicting and optimizing CZE separation. In fact, with various degrees of effort and different objectives, several research groups [3–13] have attempted to investigate this charge-to-mass relationship *vs.* peptide mobility in CZE.

Peptide charge (q) can be readily calculated from known amino acid pK_a values using the Henderson–Hasselbach equation (see ref. 14). In practice, the calculation of a charge on a peptide in a CZE capillary may not be possible, because not only do the pK_a values [9] of isolated amino acids differ from those pK_a values of amino acids in a peptide, but the microenvironment (solvent, dipoles, silanols, buffer) surrounding the peptide and other factors such as peptide hydrophobicity may also play a role in affecting a pK_a value through a change in the dielectric constant of the medium. Furthermore, temperature, viscosity, buffer composition and ionic strength can also affect the degree of ionization of the charged groups. Fortunately, many of these variables and their effects on peptide charge can be maintained nearly constant within an experiment, and thus, the charges calculated for a series of peptides become proportional to each other.

In this study, we investigated the CZE behavior of selected peptides as a function of the charge on the peptides calculated from isolated amino acid pK_a values and from adjusted amino acid pK_a values, using tabulated data from Rickard *et al.* [9]. The adjusted pK_a values were used to compensate for the amount of charge density of the amino acid at each terminus of a peptide because that density is diminished electrostatically by the presence of the first and last peptide bonds.

Because peptides have a limited secondary structure, parameters relative to their size/shape can often be simplified. Such simplifications allow the use of mathematical equations to correlate a peptide mass to peptide μ. Despite the existence of numerous peptide size/shape models, which are summarized by Rickard *et al.* [9], the Offord relationship [15] is the one that has been most studied and confirmed by many researchers [3–6,8–13]. Offord proposed that the retarding shear force that an analyte encounters in a conducting medium for paper electrophoresis is proportional to the analyte's surface area, assuming that the molecule is spherical and smooth. The molecular mass (M_r) of a peptide is used to estimate its size, and the 2/3 power accounts for the mathematical proportionality between area and volume. Thus, μ is correlated to this M_r model by the expression $q/M_r^{2/3}$. On the contrary, Grossman *et al.* [7] treated each peptide as a rod-shaped homopolymer whose size is determined by the number (n) of constituent amino acids, and they obtained high correlation ($r = 0.989$) between a peptide's μ and its charge-to-mass parameter $[\ln (q + 1)]/n^{0.43}$ for a series of synthetic peptides. Both theoretical approaches, with an emphasis on the former for the treatment of peptide size/shape, were used in this study.

Potential applications of CZE in biomedical research have been the subject of several recent reviews [16–18]. For many years, this laboratory has been involved in analyzing neuropeptides, and especially opioid and tachykinin neuropeptides, from biological sources including human tissues and fluids by using multi-dimensional reversed-phase high-performance liquid chroma-

tography (RP-HPLC) for sample preparation [19] and using radioimmunoassay (RIA) [20], MS [21] and tandem MS (MS–MS) [22] for qualitative and quantitative analyses [23]. CZE is an electrophoretic technique that may be used for substituting for, or for complementing, gel-permeation and RP-HPLC for the separation of and preparation of biological samples prior to RIA, MS and MS–MS detection. Fridland and Desiderio [24] have investigated the separation of synthetic opioid peptides by RP-HPLC based on peptide hydrophobicity. Those methods were used for analyzing peptides in human pituitaries [19,21–23].

In this present study, we investigated the separation of fourteen opioid peptides and one tachykinin peptide by CZE based on the physiochemical parameters of peptide charge and size/shape. Our investigation aims to better understand and to clarify the basic mechanisms involved in the new technique of CZE for analyzing neuropeptides in biological extracts.

2. Experimental

2.1. Reagents and materials

All synthetic opioid and tachykinin peptides were purchased from Sigma (St. Louis, MO, USA), and were used without any further purification. CZE buffers were prepared from ammonium formate (J.T. Baker, Phillipsburg, NJ, USA) or ammonium acetate (Mallinckrodt, Paris, KY, USA), and were titrated to the appropriate pH with trifluoroacetic acid (TFA; Pierce, Rockford, IL, USA) or ammonium hydroxide (Merck, Rahway, NJ, USA). Fused-silica capillary with 50 μm I.D. and 360 μm O.D. (155 μm wall thickness) was purchased from Polymicro Technologies (Phoenix, AZ, USA).

2.2. Instrumentation

CZE was performed on an ISCO Model 3140 Electropherograph (ISCO, Lincoln, NE, USA) outfitted with an IBM Personal System/2 Model 30 286 computer (IBM, Armonk, NY, USA). Peptide absorption was monitored at 200 nm using the built-in variable-wavelength UV detector. Operation of the instrument and data collection/analysis were controlled by the ISCO ICE 3.1.0 level software.

2.3. Methods

Charge calculations

The charge on each peptide was calculated using the Henderson–Hasselbach equation according to Skoog and Wichman [14]. The pK_a values for the amino and carboxyl groups of the peptide (*i.e.*, amino acids located at the N- and C-termini) and for each charged side-chain group within the peptide were obtained from a table that contained the isolated and adjusted amino acid pK_a values published by Rickard *et al.* [9]. The adjusted pK_a values were used mainly to account for the change in the electrostatic charge density that occurs on the amino acids at the N- and C-termini of a peptide. Theoretical charges were calculated across the pH range of 1 to 10 at an increment of 0.5 pH unit for each peptide using the isolated and adjusted pK_a values.

Capillary zone electrophoresis

The fused-silica capillary used was 98 cm long, with a 68 cm length from injection to the detector. The calculated surface area-to-volume ratio is 0.08. Prior to daily use, the column was preconditioned with the following sequence of solvents by applying 10 min of the electropherograph's "high vacuum" [25] from the outlet beaker for each solvent: water, 1 *M* NaOH, water, 0.1 *M* HCl, water, and finally the appropriate buffer for the experiment.

Volatile buffer systems similar to those described by others [26,27] were chosen so that samples could be further processed for MS detection. The buffers (all 20 m*M*) were ammonium formate (pH 2.5) and ammonium acetate (pH 5.5 and pH 8.5). Each individual peptide (*ca.* 1 μg; corresponding to 0.47–1.8 nmol) was dissolved in 10 μl of 1 m*M* of the appropriate buffer. The peptide mixture used in Fig. 3 also contained approximately 0.1 μg of

each peptide per μl of the 1 m*M* buffer (pH 2.5).

The applied voltage was 27 (± 1%) kV, and the temperature was regulated to 30 ± 0.5°C by the electropherograph's built-in air-circulating system. Injection was done by applying vacuum from the outlet buffer reservoir. This injection volume at 30°C was calculated to be *ca.* 8 nl using the Poiseuille equation [25,28].

Ionic strength

The CZE buffers were titrated to the appropriate pH with TFA or NH_4OH. The ionic strength of the buffers at pH 2.5, 5.5 and 8.5 was calculated, based on the charge contribution of each buffer component (including the acid or base components needed to reach the desired pH value), using the pK_a values of 3.75, 4.75, 9.25 and 0.70 (value for trichloroacetic acid) for formate, acetate, ammonium and TFA, respectively [29]. The ionic strengths were 29, 20 and 20 m*M* for the three buffers at pH 2.5, 5.5 and 8.5, respectively.

Electrophoretic mobility

The experimental μ was determined as described [7]. Electroosmotic mobility at pH 2.5 was determined by using the UV absorption (10.7 min) of the internal standard $DynA_{1-13}$ ($\mu = 3.42 \cdot 10^{-4}$ cm^2/V s) [7], which is detected at 10.7 min. At pH 5.5 and 8.5, μ_{eo} values were determined by using the negative dips at 24.2 min and 7.4 min, respectively, on the electropherograms due to the migration of water in the samples [8].

3. Results and discussion

3.1. Description of peptides

Table 1 lists several features (amino acid sequence, number of basic and acidic side-chains, and M_r) of the 14 synthetic opioid peptides and 1 tachykinin peptide that were investigated in this study. The peptides range in length from 5 to 17 amino acid residues, and in M_r from 556 to 2148. Five pentapeptides (ME,

Table 1
List of the synthetic opleid and tachykinin peptides investigated in this study

Peptide (No.)	Amino acid sequence[a]	Number of basic/acidic side-chain(s)	M_r [b]
ME (14)	YGGFM	0/0	573.7
ME-K (7)	YGGFM*K*	1/0	701.8
ME[O] (15)	YGGFM[sulfoxide]	0/0	589.7
ME-NH_2 (12)	YGGFM–NH_2	0/0	572.7
ME-RGL (9)	YGGFM*RGL*	1/0	900.1
ME-RF (8)	YGGFM*RF*	1/0	877.0
LE (13)	YGGFL	0/0	555.6
LE-R (10)	YGGFL*R*	1/0	711.8
LE-K (6)	YGGFL*K*	1/0	683.8
LE-NH_2 (11)	YGGFL–NH_2	0/0	554.6
$DynA_{1-17}$ (2)	YGGFL*RRIRPKLKWD*NQ	5/1	2147.5
DynB (4)	YGGFL*RR*QF*K*VVT	3/0	1570.9
PreproE (5)	GG*E*VLG*KR*YGGFM	2/1	1370.6
SP (3)	*RPK*PQQFFGLM–NH_2	2/0	1347.6
$DynA_{1-13}$ (1)	YGGFL*RRIRPKLK*	5/0	1604.0

ME = Methionine enkephalin; LE = leucine enkephalin; Dyn = dynorphin; PreproE = preproenkephalin; SP = substance P.
[a] The basic residues (K,R) and acidic residues (D,E) are italicized.
[b] Molecular mass is based on the chemical mass.

ME[O], ME-NH_2, LE and LE-NH_2) have no charged side-chain group. Three hexapeptides (ME-K, LE-R and LE-K), one heptapeptide (ME-RF) and one octapeptide (ME-RGL) contain one basic side-chain group, either arginine or lysine. Five larger peptides (DynB, SP, $DynA_{1-13}$, $DynA_{1-17}$ and PreproE) contain several basic residues, but only $DynA_{1-17}$ and PreproE have a combination of basic and acidic constituents. Three peptides (ME-NH_2, LE-NH_2 and SP) have an uncharged carboxamide group. Overall, these 15 peptides range from a near zero charge to multiple positive charges at physiological pH. The combination of charges and amino acid constituents also results in the differences in the hydrophilicity and hydrophobicity of these peptides. Most importantly, the peptides investigated are representative of those neuropeptides that are under study in biological preparations [19–24].

3.2. Titration curves

To rationalize and to predict the electrophoretic separation of these 15 peptides, theoretical titration curves (of the estimate of the relative μ calculated by $q/M_r^{2/3}$) across the pH range of 1 to 10 were obtained. The isolated and adjusted amino acid pK_a values (Fig. 1A and B, respectively) were used for these plots. The three vertical lines in Fig. 1 represent the three pH values studied here. A similar approach was taken by Van de Goor *et al.* [8] in predicting and in optimizing the CZE separation of adrenocorticotropic hormone (ACTH)-related fragments, and more recently by Langenhuizen and Janssen [30] for endorphin peptide fragments.

3.3. Mass–shape term

As mentioned above, the use of the mass–shape term ($M_r^{2/3}$) assumes that an analyte's mobility in an electric field is proportional to the analyte's surface area, with an estimated spherical volume representing its size or M_r [15]. Rickard *et al.* [9] obtained a high correlation coefficient ($r = 0.989$) between electrophoretic mobilities of a human growth hormone (hGH) trypsin digest and this charge-to-mass expression. Others [3–6,10,13] have also experimentally tested and confirmed this charge-to-size parameter. The rod-shaped homopolymer model of Grossman *et al.* [7] indicates that peptide μ values also correlate well with the charge-to-mass ratio expressed by $[\ln (q+1)]/n^{0.43}$. That homopolymer model was not used in this present study to predict electrophoretic separation, because fewer studies are available. However, it was tested with the experimental μ values. The Offord relationship was used to predict electrophoretic separation mainly because more confirmatory studies have been done, and thus more literature values are available for comparison to these present data.

Because the mass–shape parameter is assumed to be constant for each peptide across the entire pH range studied, the titration curves in Fig. 1 are solely dependent on the peptide charge across the pH range studied. As expected, the decrease in the amount of peptide charge as pH increases from acid to base is most apparent at the amino and carboxy pK_a regions, which are dominated by the C- and N-terminal amino acids for most of these peptides (Table 1). Furthermore, C- and N-terminal amino acid pK_a values are, on average, *ca.* 2.2 and 9.5, respectively, for isolated amino acids and *ca.* ten-fold less acid or base strength (3.2 and 8.1, respectively) in a peptide [9]. The shifts in the inflection points in Fig. 1A and B reflect that corresponding ten-fold decrease. Fig. 1A and B demonstrate these trends at each corresponding inflection point. The C-terminal amide peptides (ME-NH_2, LE-NH_2 and SP) do not exhibit any C-terminal amino acid ionization, and thus they maintain a constant charge until the pK_a of the N-terminal amino acid is reached.

3.4. Prediction of electrophoretic separation

The relationship between pH (and thus charge) *vs.* the $q/M_r^{2/3}$ parameter seems to be complicated, but can be rationalized readily by the ionization constants with the aid of the Henderson–Hasselbach equation. The importance of Fig. 1, however, is to predict the electrophoretic separation of these neuropep-

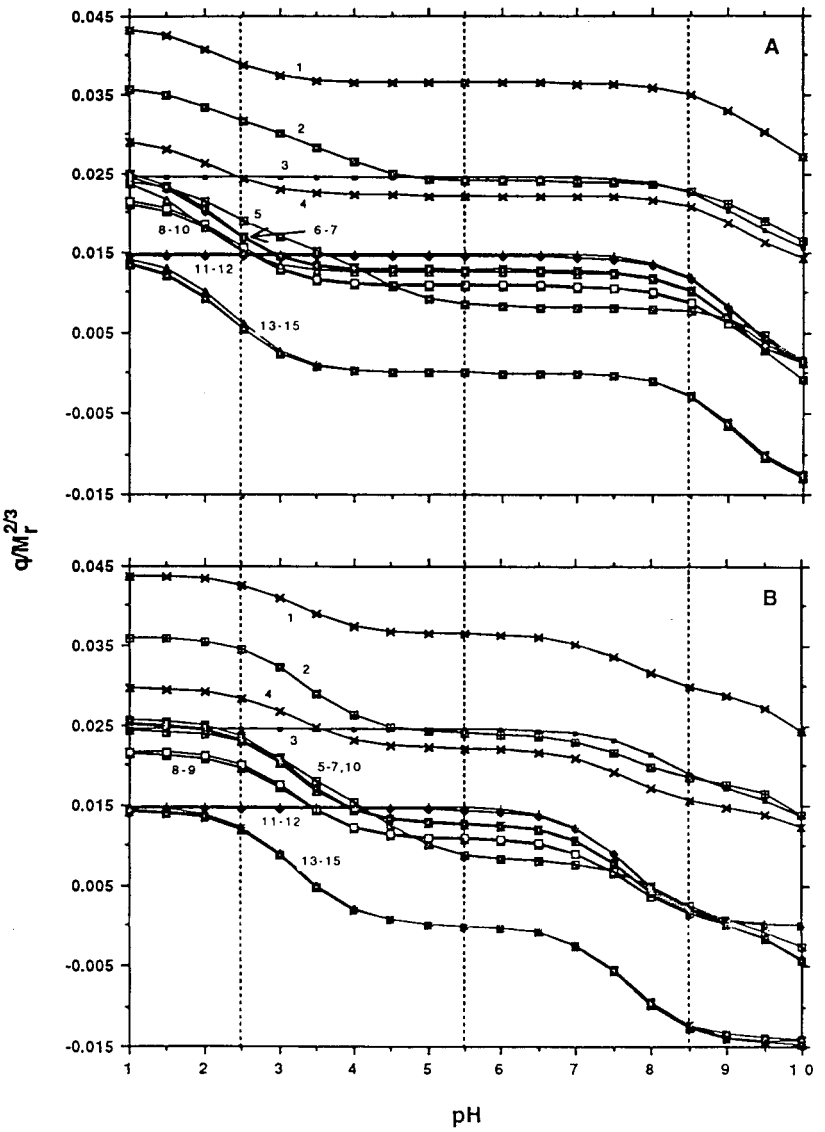

Fig. 1. The plot of $q/M_r^{2/3}$ *vs.* pH. The top figure (A) represents isolated amino acid pK_a values and the bottom (B) used adjusted pK_a values. For peptide numbering see Table 1. The vertical dashed lines indicate the three pH values (2.5, 5.5 and 8.5) studied for electrophoretic separation of these peptides.

tides. Within the three pH regions investigated (see vertical lines), the charge-to-mass differences among the peptides appear to be most diverse at pH 2.5, although differences in electrophoretic separation can be predicted from those data contained in Fig. 1A and B. For example, Fig. 1A predicts an earlier elution (*vs.* peptide 4) of peptide 3 (SP), whereas Fig. 1B predicts the opposite. Furthermore, peptides 8–9 and 11–12 are predicted to be isolated in pairs in Fig. 1B, but cluster near peptides 6–7 in Fig. 1A.

However, at pH 5.5, both plots predict a similar electrophoretic separation of all 15 peptides. [Though not very obvious from these

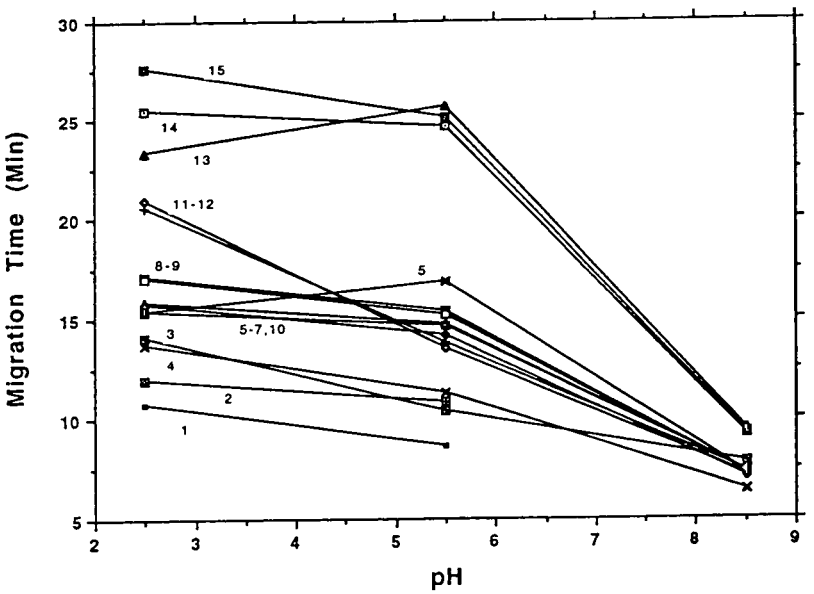

Fig. 2. Plot of electrophoretic migration time of the peptides *vs.* pH. The numbers in the figure represent the peptides listed in Table 1. $DynA_{1-13}$ (1) and $DynA_{1-17}$ (2) are missing in pH 8.5 because of analyte–wall interactions.

figures (but see later electropherogram in Fig. 3 and migration time data in Fig. 2), the electrophoretic separation of the peptides (electropherogram not shown) is less at pH 5.5.] Finally, at pH 8.5, Fig. 1A and B both predict the least electrophoretic separation (observe that the spread of the data within the 0.005–0.015 $q/M_r^{2/3}$ region is less at pH 8.5 *vs.* 5.5); Fig. 1B predicts even less separation than Fig. 1A because the amino terminus group is less ionized at that more basic pH value, according to the adjusted pK_a values. These data demonstrate that electrophoretic separation between peptides is predicted to occur when the parameter $q/M_r^{2/3}$ is $\geq ca.$ 0.004. For example, at pH 2.5, the peptides 5–7 are not predicted to separate; that prediction is correct (see Fig. 3 below).

It is also significant to correlate the sign of the charge on a peptide with pH. For example, at pH 8.5, only 3 of the 15 peptides studied could have a negative charge, and thus a negative $q/M_r^{2/3}$ parameter. Thus, ME, ME[O] and LE (peptides 13–15) are negatively charged at pH 8.5, and have a $q/M_r^{2/3}$ value of *ca.* −0.015 (see Fig. 1A and B).

3.5. Electrophoretic migration time

Fig. 2 shows the results of the electrophoretic migration times (uncorrected for electroosmosis) of the peptides individually determined at the pH values 2.5, 5.5 and 8.5. The reproducibility of the migration time of a peptide injection (fmol amounts of peptide) is typically high. For example, for the data in Fig. 2 that were obtained under these experimental conditions, the relative standard deviation (R.S.D.) is 0.13% ($n = 3$) for the multiply charged peptide SP and 0.44% ($n = 3$) for the near neutral peptide ME. This graph also demonstrates the resolution of these peptides at these pH values, and indicates that the electrophoretic migration times of any two peptides must differ by $\geq ca.$ 1 min to be resolved under these experimental conditions.

At pH 8.5, $DynA_{1-17}$ and $DynA_{1-13}$ were not detected within 30 min, presumably due to these multiply charged peptides binding to the negatively charged fused-silica wall at this pH. From Fig. 2, one can see that these 15 peptides can be best resolved at pH 2.5, because the migration times of these peptides range from *ca.* 11 to 28

min. The migration times of the peptides begin to merge (range decreases to *ca.* 8–25 min) at pH 5.5, and by pH 8.5, almost no resolution occurs (range is 7–9 min). Thus, an *ca.* 850% reduction occurred in the range of migration times of those peptides across the pH range 2.5–8.5.

Others [11,30,31] have also observed that an acidic pH is optimal for the separation of basic and neutral peptides. There are two experimental advantages of using an acidic pH to separate these peptides. First, electroosmosis is minimized, and thus the electrophoretic process is maximized; second, analyte–wall interactions are also minimized due to the protonation of silanol groups in the fused-silica wall, leading to better resolution and greater reproducibility. Thus, separation generally deteriorates more quickly than predicted (Fig. 1) as more basic pH values are used (Fig. 2).

3.6. Electropherogram data

When a mixture of all 15 peptides is injected into the capillary at pH 2.5, the electropherogram (Fig. 3) agrees very well to that separation predicted from the individual peptide migration times in Fig. 2 and with the $q/M_r^{2/3}$ parameter in Fig. 1B. All individual peptide peaks can be identified by their individual electrophoretic migration times, except for the peak that contains the mixture of ME-RF/ME-RGL (8–9) and for the peak that contains the mixture of peptides, PreproE, LE-K and ME-K (5–7).

Referring to the titration curves in Fig. 1, the observed separation of this complete mixture of the 15 peptides also agrees with the estimate of the relative μ calculated using the adjusted (Fig. 1B) *vs.* the isolated (Fig. 1A) amino acid pK_a values.

However, both titration curves in Fig. 1 fail to predict the excellent separation of peptides 13–15 at pH 2.5 shown in Figs. 2 and 3. This separation may be largely due to the fact that these peptides with a near-zero charge have undergone a significantly longer electrophoretic process, leading to greater separation. Also, specific structural features may play a role. For example, the sulfoxide group has a stronger

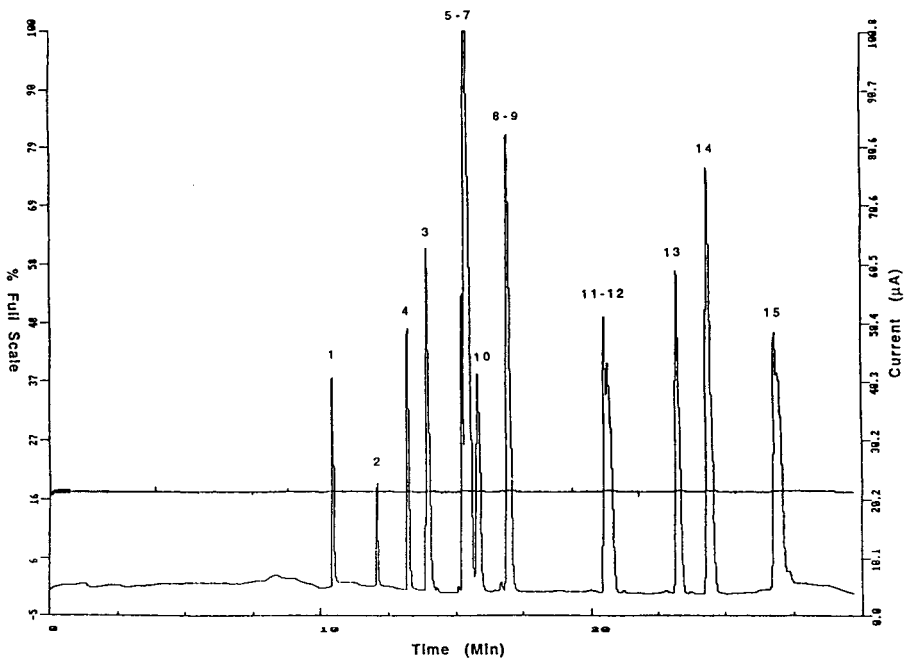

Fig. 3. Electropherogram of the peptide mixture. Numbers in the figure correspond to the peptides listed in Table 1. Separation was performed at pH 2.5. The horizontal line represents the monitored current (*ca.* 22 μA). AUFS = 0.02.

dipole than ME, ME has a polarizable sulfur atom, and LE contains neither.

3.7. Calculation of electrophoretic mobility

The migration time data collected in Fig. 2 are converted to their corresponding apparent electrophoretic mobility, based on the equation

$$\mu_{app} = v/E \quad (2)$$

where v = migration velocity (cm/s), and E = electrical field gradient (V/cm). Migration velocity is calculated by dividing the capillary length (cm) to the detector window by the migration time (s) of an analyte to reach that window. Electrical field strength is the applied voltage (V) divided by the total capillary length (cm). The calculated μ_{app} minus the μ_{eo} accounts for that portion of the peptide migration that is only due to the electrical attraction between analyte and cathode.

$$\mu = \mu_{app} - \mu_{eo} \quad (3)$$

Electroosmotic mobilities are calculated similar to peptide electrophoretic mobilities, using a small neutral molecule such as phenol or acetone [32]. Alternatively, an internal standard of known electrophoretic mobility could be included at that pH [7], or one could use the negative dip observed when the water that is contained in an injected sample migrates to the detector [8]. The measured μ_{eo} values are $4.10 \cdot 10^{-5}$ ($DynA_{1-13}$), $1.70 \cdot 10^{-4}$ (water) and $5.54 \cdot 10^{-4}$ (water) $cm^2/V\ s$ for pH 2.5, 5.5 and 8.5, respectively. As expected, the electroosmotic flow increases as pH increases to a more basic value due to the more complete ionization of the silanols on the fused-silica wall [32].

The two mass–shape parameters were tested *vs.* electrophoretic mobility. That test was done at the three pH values, and also with isolated and adjusted pK_a values. Although all of the plots that were used to test these relationships are not shown, the comparative results (linear correlation coefficients, y-intercepts and slopes) are summarized in Table 2. The results in Table 2 indicate that relatively high correlations (range: 0.928–0.997) are obtained with either mass–shape expression and with either set of amino acid pK_a values for data at any single pH value. Table 2 also provides the y-intercept and slope of each linear relationship. In general, the y-intercept is nearly zero (range: $+0.0000878$ to -0.000000340) in all cases in spite of the experimental difficulty in obtaining absolute electrophoretic mobilities due to the reasons discussed [9]. Only a minor variation in slopes was observed at the three pH values; however, the $q/M_r^{2/3}$ relationship gives a steeper slope (range: 0.00625–0.00882) than $[\ln (q+1)]/n^{0.43}$ (range: 0.000124–0.000643), indicating that μ is more sensitive to the $q/M_r^{2/3}$ parameter.

The degree of data scatter is least for the data set at pH 5.5 for both equations, in good agreement with the high r values obtained for that pH. That high correlation (and minimal data scatter) is readily rationalized by the titration curves in Fig. 1A and B. The greatest change in those curves obviously occurs near the inflection points (pH 2.5, 8.5), but no change at pH 5.5; thus, reproducibility is high.

Hilser *et al.* [12] performed a similar comparison at the single pH value of 2.5, using peptides obtained from the digestion with trypsin of rhIGF-I (human recombinant insulin-like growth hormone I), and reported a higher overall correlation coefficient with the homopolymer model (*e.g.* $r = 0.937$ using the adjusted amino acid pK_a values) than with the $M_r^{2/3}$ model ($r = 0.922$).

Other researchers have grouped their μ *vs.* mass–shape data that were measured within three similar pH ranges to provide a combined set of data [9]. That grouping is experimentally valid, because variables such as ionic strength, viscosity and temperature remain relatively constant over that pH range. For example, the ionic strength of the buffers used in this study at pH 2.5, 5.5 and 8.5 are 29, 20 and 20 mM, respectively. Of even greater importance is the fact that the ratio of buffer-to-analyte is *ca.* 200:1. Furthermore, μ_{eo} at pH 2.5 was determined by using $DynA_{1-13}$ (peptide 1); thus, the experimental parameters obtained at pH 2.5 (which has the highest ionic strength) are corrected for in these experiments. Thus, Table 2 also contains

Table 2
Correlation coefficients (r), y-intercepts and slopes of the electrophoretic mobility *vs.* two different equations of charge-to-mass ratio

	pH 2.5	pH 5.5	pH 8.5	Combined
$q/M_r^{2/3}$, isolated				
r^a	0.965	0.997	0.940	0.864
y-Intercept	0.0000878	−0.000000340	−0.0000699	−0.0000230
Slope	0.00685	0.00880	0.00758	0.0101
Data scatter[b]	++	+	++	+++
$q/M_r^{2/3}$, adjusted				
r^a	0.983	0.997	0.928	0.970
y-Intercept	0.0000444	−0.000000463	−0.00000916	−0.00000293
Slope	0.00751	0.00882	0.00625	0.00901
Data scatter[b]	++	+	++	++
$[\ln(q+1)]/n^{0.43}$, isolated				
r^a	0.958	0.976	0.980	0.857
y-Intercept	0.0000302	−0.0000242	−0.0000707	−0.0000473
Slope	0.000477	0.000480	0.000322	0.000539
Data scatter[b]	++	+	++	+++
$[\ln(q+1)]n^{0.43}$, adjusted				
r^a	0.984	0.976	0.985	0.857
y-Intercept	−0.0000742	−0.0000240	0.0000125	0.0000580
Slope	0.000643	0.000479	0.000124	0.000254
Data scatter[b]	++	+	++	+++

[a] Correlation coefficients of the linear least square lines.
[b] +, ++ and +++ indicate low, medium and high degree of data scatter, respectively.

the "combined" data, and Fig. 4 plots the combined data for μ *vs.* $q/M_r^{2/3}$ using adjusted pK_a values. That plot (Fig. 4) gives the best correlation ($r = 0.970$) and the least degree of data scatter *vs.* the other three combinations.

It is significant to note in Fig. 4 that three peptides, ME, ME[O] and LE, provide the three points at negative μ and negative charge ($q/M_r^{2/3}$). Those three peptides were shown above (Fig. 1) to be negatively charged at pH 8.5. These data demonstrate that μ_{eo} is greater than μ_{app} for these three peptides at pH 8.5. These three peptides are the only 3 of the 15 peptides studied (Table 1) that have a carboxylic group and no basic/acidic side-chain.

3.8. Electrophoretic mobility vs. pH

The correlation between μ and pH is shown by the very similar pattern obtained by compar-

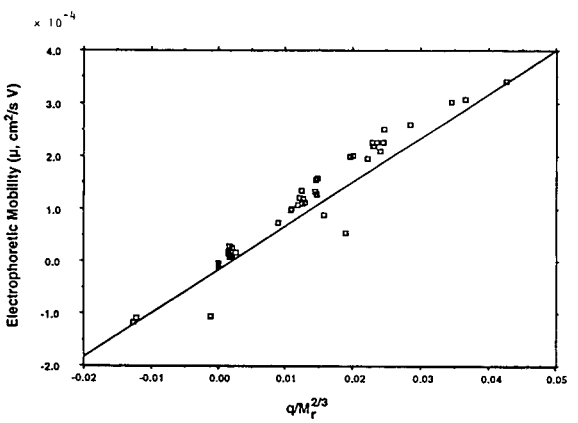

Fig. 4. Combined electrophoretic mobility measurements *vs.* $q/M_r^{2/3}$ using adjusted amino acid pK_a values over the pH range 2.5, 5.5 and 8.5. The equation of the best-fit line is $y = 0.009 - 0.000003x$ ($r = 0.970$).

ing the experimental μ (Fig. 5B) and the best-fit calculated estimate of the relative μ (Fig. 5A) plotted over the pH range studied. These μ *vs.* pH results suggest that Offord's relationship using the adjusted amino acid pK_a values of Rickard *et al.* [9] provides an additional dimension of correlation that the other three combinations fail to provide. For example, in Table 2, the combined data for rows 1 (isolated, $q/M_r^{2/3}$), and 3 and 4 (isolated and adjusted;

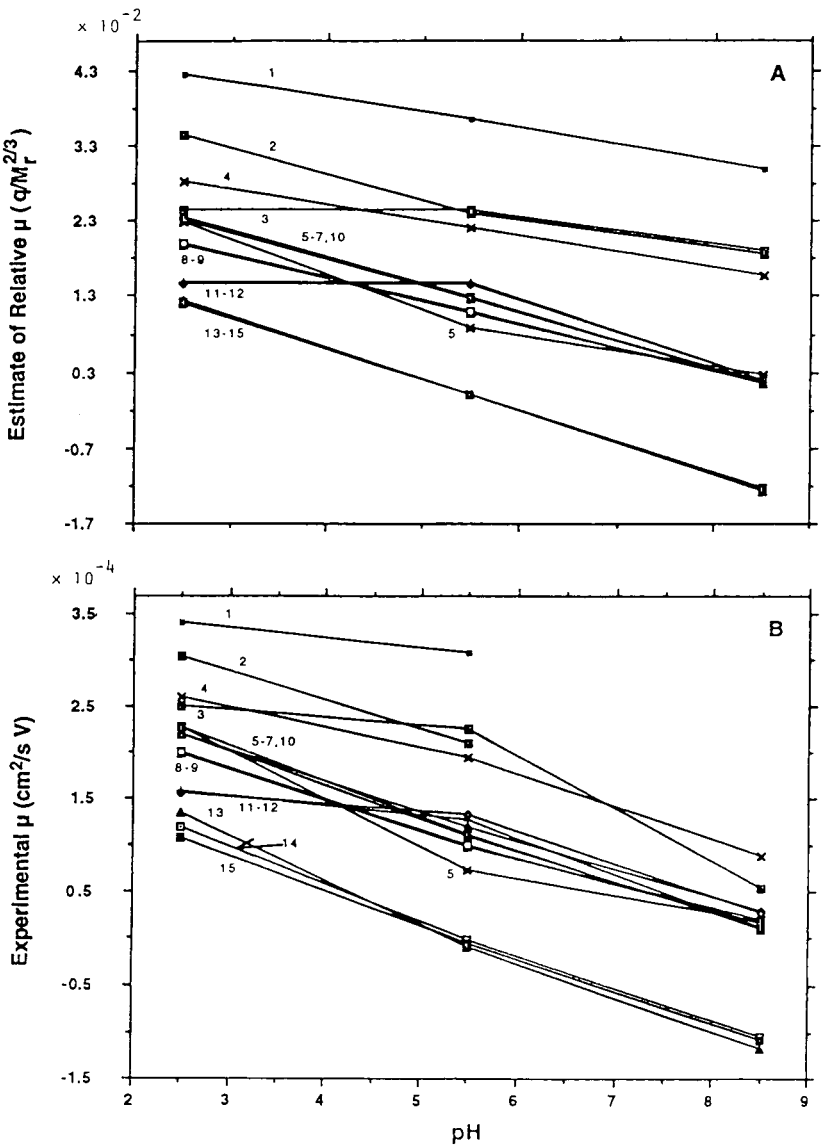

Fig. 5. Plot of experimental μ (B) and estimate of the relative μ (A) *vs.* pH. Fig. 5A correlates to Fig. 1B because only the calculations for the pH values of 2.5, 5.5 and 8.5 in Fig. 1B are shown in Fig. 5A. Fig. 5B is the experimentally determined μ at the same pH values. $DynA_{1-13}$ (1) and $DynA_{1-17}$ (2) are missing in pH 8.5 because of analyte–wall interactions.

$[\ln (q+1)]/n^{0.43}$) all have much lower r values (0.864, 0.857 and 0.857, respectively) compared to 0.970 (Fig. 4).

4. Conclusions

The separation of fourteen synthetic opioid peptides and one tachykinin peptide using CZE is demonstrated experimentally and the data are compared to several different theoretical models and factors. Data and experience derived from this study will be used to separate opioid and tachykinin peptides from human pituitary tissues and cerebrospinal fluid. A relatively wide range of pH values was investigated in this study to expand the comparison of theoretical predictions and experimental results. In general, we and others [11,28,29] conclude that neutral and basic peptides are well separated at acidic pH values such as pH 2.5, as predicted by the calculated titration curves. Furthermore, resolution is enhanced due to the low μ_{eo} and reduced analyte–wall interactions at pH 2.5. In comparing the correlation coefficient of the experimental μ *vs.* the two theoretical charge-to-mass models, one parameter, $q/M_r^{2/3}$, using adjusted amino acid pK_a values [9], provides the best overall predictable electrophoretic separation of these peptides across the wide pH range using three buffer systems. It was also demonstrated qualitatively that the titration curves obtained from the adjusted amino acid pK_a values (Fig. 1B) predict the relative electrophoretic behavior of these peptide migration times (Fig. 2) and electropherograms (Fig. 3) better than those obtained using isolated amino acid pK_a values (Fig. 1A). Although at any single pH value, the tabulated results of Table 2 suggest that $q/M_r^{2/3}$ and $[\ln (q+1)]/n^{0.43}$ both give a relatively well behaved linear relationship between the estimate of the relative μ and the experimental μ, using either set of amino acid pK_a values, the combined data indicate that $q/M_r^{2/3}$ with adjusted pK_a values provide the best correlation.

5. Acknowledgement

This work was supported by NIH GM 26666.

6. References

[1] J.W. Jorgenson and K.D. Lukacs, *Anal. Chem.*, 53 (1981) 1298.
[2] J.W. Jorgenson and K.D. Lukacs, *Science*, 222 (1983) 266.
[3] F. Nyberg, M.D. Zhu, J.L. Liao and S. Hjertén, in C. Shaefer-Nielsen (Editor), *Electrophoresis '88*, VCH, New York, 1988, p. 141.
[4] Z. Deyl, V. Rohlicek and R. Struzinsky, *J. Liq. Chromatogr.*, 12 (1989) 2515.
[5] Z. Deyl, V. Rohlicek and M. Adam, *J. Chromatogr.*, 480 (1989) 371.
[6] J. Frenz, S.-L. Wu and W.S. Hancock, *J. Chromatogr.*, 480 (1989) 379.
[7] P.D. Grossman, J.C. Colburn and H.H. Lauer, *Anal. Biochem.*, 179 (1989) 28.
[8] T.A.A.M. van de Goor, P.S.L. Janssen, J.W.V. Nispen, M.J.M.V. Zeeland and F.M. Everaerts, *J. Chromatogr.*, 545 (1991) 379.
[9] E.C. Rickard, M.M. Strohl and R.G. Nielsen, *Anal. Biochem.*, 197 (1991) 197.
[10] J.R. Florance, Z.D. Konteatis, M.J. Macielag, R.A. Lessor and A. Galdes, *J. Chromatogr.*, 559 (1991) 391.
[11] H.-J. Gaus, A.G. Beck-Sickinger and E. Bayer, *Anal. Chem.*, 65 (1993) 1399.
[12] V.J. Hilser, Jr., F.D. Worosila and S.E. Rudnick, *J. Chromatogr.*, 630 (1993) 329.
[13] H.J. Issaq, G.M. Janini, I.Z. Atamna, G.M. Muschik and J. Lukszo, *J. Liq. Chromatogr.*, 15 (1992) 1129–1142.
[14] B. Skoog and A. Wichman, *Trends Anal. Chem.*, 5 (1986) 82.
[15] R.E. Offord, *Nature*, 211 (1966) 591–593.
[16] B.L. Karger, A.S. Cohen and A. Guttman, *J. Chromatogr.*, 492 (1989) 585.
[17] Z. Deyl and R. Struzinsky, *J. Chromatogr.*, 569 (1991) 63.
[18] J.P. Landers, R.P. Oda, T.C. Spelsberg, J.A. Nolan and K.J. Ulfelder, *BioTech.*, 14 (1993) 98.
[19] J.L. Lovelace, J.J. Kusmierz and D.M. Desiderio, *J. Chromatogr.*, 562 (1991) 573.
[20] X. Zhu and D.M. Desiderio, *J. Chromatogr.*, 616 (1993) 175.
[21] J.J. Kusmierz, C. Dass, J.T. Robertson and D.M. Desiderio, *Int. J. Mass Spectrom. Ion Proc.*, 111 (1991) 247.
[22] D.M. Desiderio, J.J. Kusmierz, X. Zhu, C. Dass, D. Hilton, J.T. Robertson and H.S. Sacks, *Biol. Mass Spectrom.*, 22 (1993) 89.

[23] D.M. Desiderio, in D.M. Desiderio (Editor), *Mass Spectrometry of Peptides*, CRC Press, Boca Raton, FL, 1990.
[24] G. Fridland and D.M. Desiderio, *J. Chromatogr.*, 379 (1986) 251.
[25] H.G. Lee and D.M. Desiderio, *J. Chromatogr. B*, (1994) in press.
[26] I.M. Johansson, E.C. Huang, J.D. Henion and J. Zweigenbaum, *J. Chromatogr.*, 554 (1991) 311.
[27] M.A. Moseley, L.J. Deterding, K.B. Tomer and J.W. Jorgenson, *Anal. Chem.*, 63 (1991) 109.
[28] J. Harbaugh, M. Collette and H.E. Schwartz, *Technical Bulletin TIBC-103*, Beckman Instruments, Spinco Division, Palo Alto, CA, 1990.
[29] R.C. Weast (Editor), *CRC Handbook of Chemistry and Physics*, CRC Press, Boca Raton, FL, 70th ed., 1989, pp. D-163, D-164.
[30] M.H.J.M.L. Langenhuizen and P.S.L. Janssen, *J. Chromatogr.*, 638 (1993) 311.
[31] R.M. McCormick, *Anal. Chem.*, 60 (1988) 2322.
[32] K. Salomon, D.S. Burgi and J.C. Helmer, *J. Chromatogr.*, 559 (1991) 69.

ELSEVIER

Journal of Chromatography A, 667 (1994) 284–289

JOURNAL OF CHROMATOGRAPHY A

Short Communication

Reversed-phase high-performance liquid chromatography of functionalized dendritic macromolecules

Jean M.J. Fréchet*, Lubomir Lochman, Vladimir Šmigol, Frantisek Švec

Department of Chemistry, Baker Laboratory, Cornell University, Ithaca, NY 14853-1301, USA

(Received November 24th, 1993)

Abstract

Dendritic macromolecules substituted with various numbers of trimethylsilyl and dodecyl groups have been separated by reversed-phase HPLC. While size-exclusion chromatography only provides a rough picture of the composition of the mixture, reversed-phase chromatography allows the separation of individual components and estimation of the distribution of each component.

1. Introduction

Recently, macromolecules with architectures that differ significantly from those of classical linear and cross-linked polymers have emerged. Dendritic macromolecules are characterized by a tree-like structure with branches that converge to a single point. Each monomer unit is a branch point and, as a result, the molecule contains a large number of chain ends while adopting a globular shape due to steric considerations [1–5]. This is in contrast to the typical loose random coil of linear polymers in solution. The convergent method we use to prepare dendritic molecules allow the precise control of their chemistry as well as their sizes resulting in well defined architectures [3,4,6,7]. Other dendritic molecules such as carboxylated "Starburst" dendrimers appear to be excellent calibration standards for aqueous size-exclusion chromatography (SEC) [8].

Since the chain-ends have a great influence on ultimate properties of the dendritic macromolecules, we have developed precise methods that allow the replacement of one or more functionalities at the periphery of the globule [9–11]. More recently, a novel approach was developed to also substitute the internal sites of the dendrimers [12]. This involves metalation of the dendrimer by a superbase (SB) followed by reaction of the metalated dendrimer with an electrophile. The fourth generation dendrimer [G-4]-OH shown in Fig. 1 has a total of 46 activated sites (31 benzylic sites and 15 sites located on aromatic rings between two oxygen substituents) that can be metalated by the superbase. However, the simultaneous metalation of all of these reactive sites is not possible. For example, even the use of a two-fold excess of the SB with a molar ratio SB/[G-4]-OH = 92, only led to the incorporation of 34 deuterium atoms after reaction with ^2H_2O. Moreover, the reaction does not result in uniform products and a mixture of dendrimers with different numbers of substituents is formed. Therefore, a detailed analysis of the reaction products is essential for

* Corresponding author.

0021-9673/94/$07.00
SSDI 0021-9673(94)00056-F

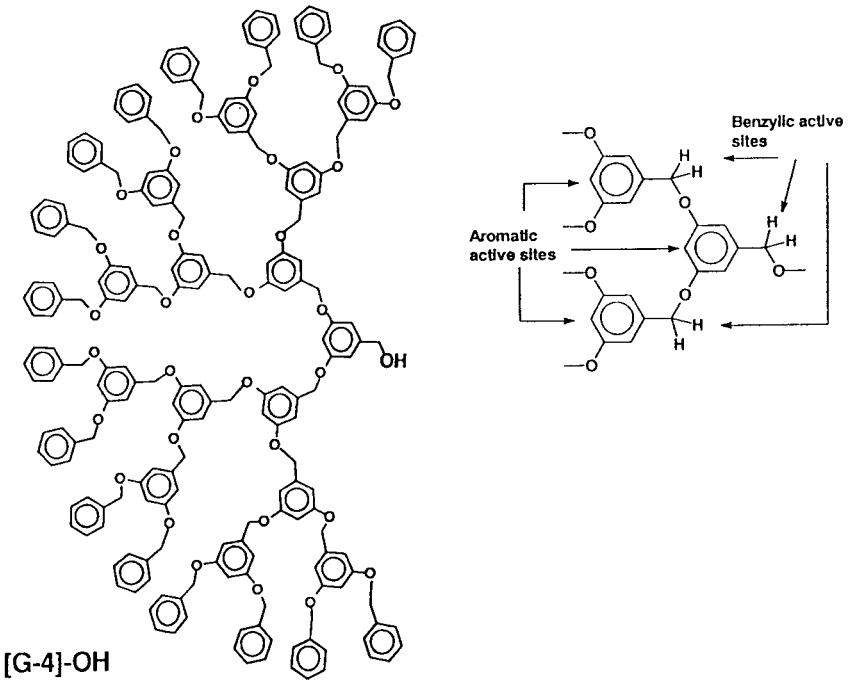

Fig. 1. Schematic representation of (G-4)-OH dendrimer.

optimization of this interesting functionalization reaction affecting "internal" sites of dendrimers.

This paper reports an application of reversed-phase HPLC to the characterization and separation of closely related functionalized dendritic macromolecules.

2. Experimental

2.1. Functionalized dendrimers

The functionalized dendrimers were prepared by metalation of dendrimer [G-4]-OH (Fig. 1), by SB prepared from butyllithium and potassium *tert.*-pentoxide [13,14], followed by reaction with electrophiles such as trimethylsilyl chloride and dodecyl chloride, according to the procedure described in detail elsewhere [12].

2.2. High-performance liquid chromatography

The SEC was performed with a Model 510 HPLC pump connected to a U6K injector (Millipore Waters Chromatography) to three 300 mm × 8 mm I.D. PL GEL columns (Mixed C, 100 Å and 500 Å, Polymer Labs.) thermostated at 30°C. The separation was monitored by a differential viscometer (Viscotek Corp.) and a differential refractometer Refractomonitor IV (Milton Roy).

The reversed-phase chromatographic separations were carried out in a commercial 150 mm × 3.9 mm I.D. stainless-steel column packed with Nova-Pak C_{18} 4 μm modified silica using an HPLC chromatograph comprised of two 501 HPLC pumps, an U6K injector and a 486 tunable absorbance UV detector. System control and data management was provided by a Millenium 2010 Chromatography Manager. All this equipment was from Millipore Waters Chromatography (Milford, MA, USA).

The isolated solid samples of functionalized dendrimers were dissolved in tetrahydrofuran, the solutions were then diluted with the highest amount of acetonitrile that did not induce precipitation prior to chromatography.

The mobile phase was a mixture of tetrafuran

(THF) and acetonitrile. The elutions were carried out at a flow-rate of 1 ml/min either in a gradient or in a combined isocratic and gradient mode at ambient temperature. The separations were monitored at 215 nm.

3. Results and discussion

Typically, the molecular mass distribution of a polymer is determined by SEC [15] while the interaction modes of HPLC are used less frequently for the separation of synthetic polymers, though the separation of oligomers and low molecular weight polymers can be achieved much faster. As the interactions of macromolecules depend on their composition, interactive HPLC is also an excellent tool for the determination of the chemical composition of copolymers in both reversed- and normal-phase mode [16,17].

The molecular mass of the starting [G-4]-OH is 3292. Substitution of a single activated site with a trimethylsilyl group increases the molecular mass by 72, for an increment of 2.25%, while modification with a dodecyl group (M_r 169) represents an increment of 5.13%. In theory, modification of half of all the potentially reactive sites should increase the average molecular mass of [G-4]-OH to 4944 upon functionalization with trimethylsilyl groups, and to 7129 upon modification with dodecyl groups. However, the reaction mixture may still contain the original unreacted [G-4]-OH, together with a variety of partly functionalized homologues and perhaps even a few fully substituted molecules with molecular masses as high as 6646 and 11 016, respectively. These molecular mass increases must be reflected in the hydrodynamic size of the dendrimers and produce a change of SEC trace. However, the increments are too small to allow precise monitoring of the individual components of the mixture. Therefore, the SEC analysis reveals only a peak covering all the species present in the sample. An example of such a SEC measurement is shown in Fig. 2.

The SEC data obviously fail to provide sufficient information about the composition of the

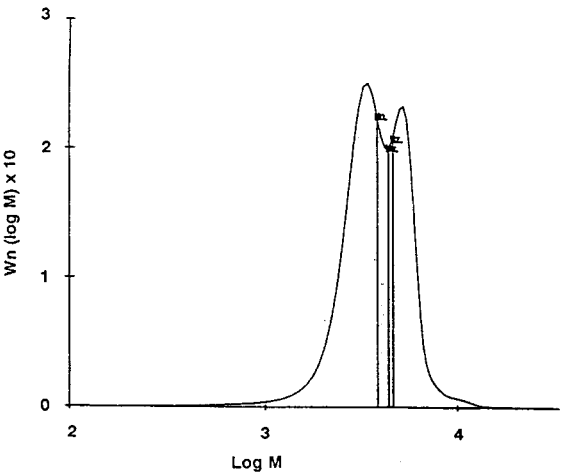

Fig. 2. Molecular mass distribution curve of dendrimer [G-4]-OH after metalation (SB/[G-4]-OH = 11) and reaction with trimethylsilyl chloride. Number-average molecular mass (M_n) = 3830; mass-average molecular mass (M_w) = 4370; *z*-average molecular mass (M_z) = 4610. M = Molecular mass; Wn = differential mass distribution function.

functionalized dendritic macromolecules. However, functionalization with trimethylsilyl and dodecyl groups changes not only the molecular size, but also the polarity of the dendrimers. Therefore, interactive modes of HPLC may be better suited to reflect these changes.

The size-exclusion chromatogram of a product prepared by metalation of [G-4]-OH with a twofold excess (92 equivalents) of SB, followed by reaction with trimethylsilyl chloride, reveals a relatively narrow distribution of hydrodynamic sizes. Injection of the same sample into a reversed-phase column also results in observation of only one peak that despite its breadth confirms the relative homogeneity of the sample (Fig. 3a). Fig. 3b shows the separation of a product resulting from metalation of [G-4]-OH with only half of the theoretical amount (23 equivalents) of SB followed by reaction with the same electrophile. This chromatogram reveals that the sample contains some amount of less substituted dendrimers that are only partly separated at the front of the main peak. The reversed-phase separation of the reaction mixture obtained using an even lower molar ratio of superbase to dendrimer (SB/[G-4]-OH = 11, which is less than 1/4th of the theoretical

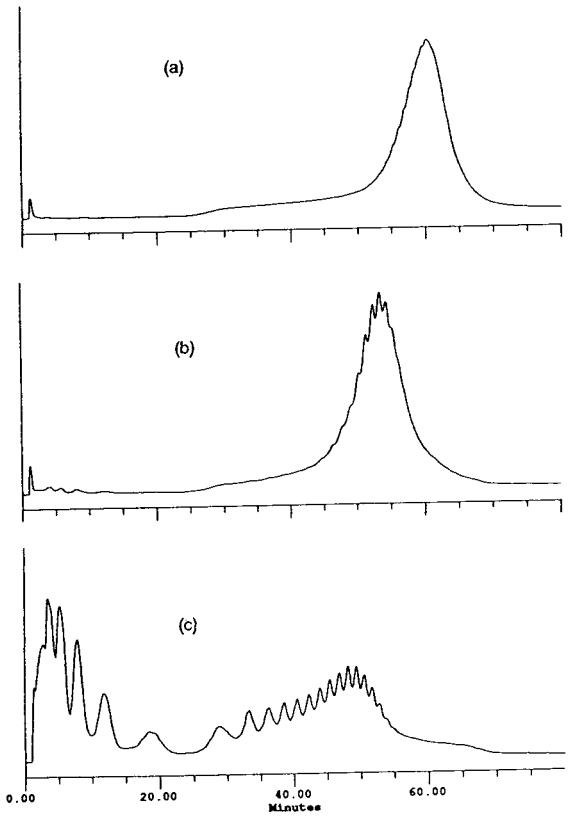

Fig. 3. Reversed-phase HPLC of dendrimer [G-4]-OH after metalation at a ratio SB/[G-4]-OH 92 (a), 23 (b) and 11 (c) and reaction with trimethylsilyl chloride. Conditions: Nova-Pak C_{18} column 150 mm × 3.9 mm I.D.; flow-rate 1 ml/min; isocratic elution with THF–acetonitrile (10:90) for 20 min followed by a linear gradient to THF–acetonitrile (50:50) within 40 min, detection at 215 nm.

amount) results in a chromatogram with 20 distinct peaks assigned to the original [G-4]-OH and 19 other species with different degrees of substitution (Fig. 3c). This chromatogram not only shows the composition of the sample, but it also serves as a reference for the assignment of peaks in chromatograms a and b. Because the last three peaks in Fig. 3c and the first three peaks in Fig. 3b overlap, the distinct peaks in Fig. 3b can be assigned to dendrimers substituted with 16 to 21 trimethylsilyl groups. Assuming that the peaks represent individual homologues with consecutively increasing number of sub-

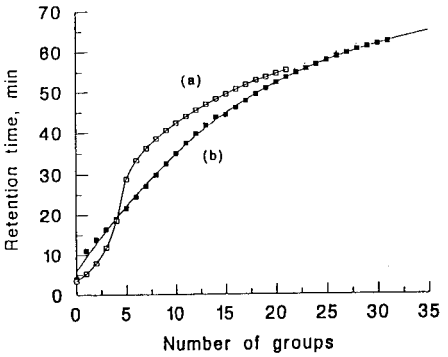

Fig. 4. Effect of degree of substitution of the [G-4]-OH dendrimer with trimethylsilyl (a) and dodecyl (b) groups on retention time of the homologues.

stituents, a curve showing the retention time as a function of number of substituents can easily be drawn (Fig. 4). Extrapolation of the data allows the assignment of the maximum in Fig. 3a to a dendrimer with 29 substituents. This is in good agreement with the finding of 31 substituents calculated from ^{1}H NMR measurements [13,14]. The S-shape of the calibration curve a in Fig. 4 is due to the change in the elution mode from an isocratic elution to a THF–acetonitrile gradient after 20 min.

An even better separation was observed for dendrimers substituted with dodecyl instead of trimethylsilyl groups (Fig. 5). Fig. 5b and c show the separation of products containing 26 and 21 different compounds prepared in the reaction of [G-4]-OH with 23 and 11 equivalents of SB per [G-4]-OH, respectively, followed by quenching with dodecyl bromide. The separation shown in Fig. 5c is an excellent baseline separation of 22 different compounds. As the dodecyl group is more hydrophobic, the separation is better and 17 peaks are detected (Fig. 5a) in the product prepared from an intermediate resulting from metalation with equimolar amounts of SB and reactive sites (SB/[G-4]-OH = 46). Using again the calibration diagram (Fig. 4b) constructed from the data reported in Fig. 5b and c, peaks are assigned to dendrimers containing from 15 to 32 dodecyl chains per dendritic macromolecule. As no isocratic elution precedes the gradient in

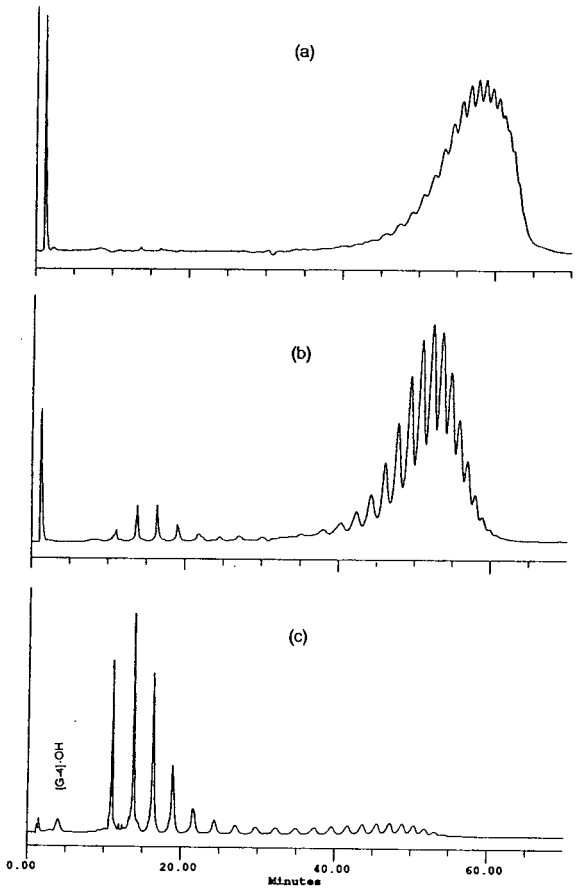

Fig. 5. Reversed-phase HPLC of dendrimer [G-4]-OH after metalation at a ratio SB/[G-4]-OH 46 (a), 23 (b) and 11 (c) and reaction with dodecyl chloride. Conditions: Nova-Pak C_{18} column 150 mm × 3.9 mm I.D.; flow-rate 1 ml/min; linear gradient of THF in acetonitrile from 50 to 80% within 60 min, detection at 215 nm.

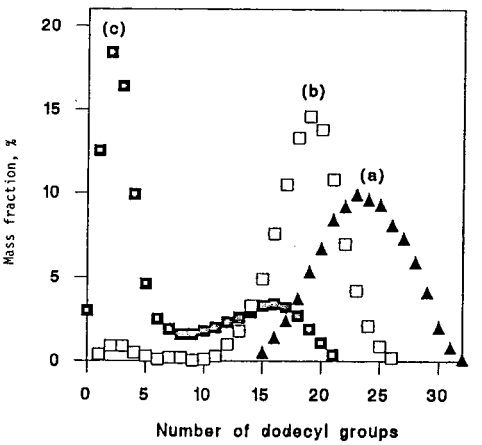

Fig. 6. Distribution diagram of dodecyl substituted homologues prepared from dendrimer metalated at a ratio SB/[G-4]-OH 46 (a), 23 (b) and 11 (c).

the chromatographic separation of the dodecyl derivatives, the calibration curve does not exhibit any inflection points.

The relative fraction of the homologues in the modified dendrimer mixtures can be easily calculated from the areas of peaks in the various chromatograms. For example, the relative fractions of dendrimers substituted with dodecyl groups are shown in Fig. 6. Unlike the substitution to a high degree of functionalization (curve a), the distribution curves of lesser substituted dendrimers (b and c) exhibit two clear maxima and suggest that the creation of some homologues is preferred. However, it must be emphasized that the distribution shown is not a continuous curve but only a schematic representation of the contents of discrete individual components in the sample.

With pure THF as solvent, the reversed-phase column used did not separate the homologues and no retention was observed. Therefore, a simple size exclusion mechanism is not operative in the reversed-phase separations shown in this paper. The solvophobic mechanism typical for very large molecules (polymers, proteins) which is based on contacts between the C_{18} hydrocarbon surface of the separation medium and the hydrophobic parts of the separated molecules [18,19] is also unlikely. The functionalization procedure used for the preparation of substituted dendrimers can occur on many sites. Each homologue is defined by its different number of substituents but these are attached at different points of the parent dendrimer molecule thus forming many possible isomers. For example, a homologue with 2 substituents has *theoretically* 820 isomers, while a homologue with 40 substituents has *theoretically* 41 isomers. Even if one takes into account the fact that many of the "theoretical" isomers are identical and that the

reactivity of all sites is not equal, the number of possible isomers remains high. Obviously, some isomers have the hydrophobic moiety more exposed on the outer surface of the globular dendritic macromolecule than others that have their hydrophobic component buried "inside" the globule. Therefore, if the solvophobic mechanism was operative, the strength of interaction of different isomers would depend on the accessibility of the hydrophobic patch rather than on the total number of hydrophobic groups and would result in an extensive overlap of the peaks. The chromatogram would be then an envelope covering all of the peaks and separation into distinct peaks would not be achieved.

Partition mechanisms are frequently encountered in the reversed-phase HPLC of small molecules [20]. The partition between the mobile phase and the organic modifier of the mobile phase which is adsorbed by the surface of the separation medium depends on the total hydrophobicity of the separated molecules and not on the extent of hydrophobic domains. Analysis of the chromatographic results achieved during this study supports the concept that the overall hydrophobicity of the individual moieties plays the most important role during the separation of dendrimers functionalized with hydrophobic substituents; the number of substituents rather than their location within the dendrimer is the key factor that determines the overall separation. This behavior is somewhat unexpected for molecules with molecular masses well over 3300. It implies that, owing to the dense globular character of the dendritic macromolecules, a partition mechanism is operative in the separation.

4. Acknowledgements

Support of this research by a grant of the National Science Foundation (DMR 9224421) and by a grant of the National Institutes of Health (GM 48364-01) is gratefully acknowledged. This work also made use of MRL Central Facilities (Polymer Characterization Facility) supported by the National Science Foundation under Award No. DMR-9121654.

5. References

[1] D.A. Tomalia, A.M. Naylor and W.A. Goddard, *Angew. Chem., Int. Ed. Engl.*, 29 (1990) 138.
[2] G.R. Newcome, Z. Yao, G.R. Baker and V.K. Gupta, *J. Org. Chem.*, 50 (1985) 2004.
[3] C.J. Hawker and J.M.J. Fréchet, *Chem. Commun.*, (1990) 2459.
[4] C.J. Hawker and J.M.J. Fréchet, *J. Am. Chem. Soc.*, 112 (1990) 7638.
[5] P. Hodge, *Nature*, 362 (1993) 18.
[6] C.J. Hawker and J.M.J. Fréchet, *J. Chem. Soc., Perkin Trans. I*, (1992) 2459.
[7] C.J. Hawker and J.M.J. Fréchet, *J. Am. Chem. Soc.*, 114 (1992) 8405.
[8] P.J. Dubin, S.L. Edwards, J.I. Kaplan, M.S. Mehta, D.A. Tomalia and J. Xia, *Anal. Chem.*, 64 (1992) 2344.
[9] C.J. Hawker and J.M.J. Fréchet, *Macromolecules*, 23 (1990) 4726.
[10] K.L. Wooley, C.J. Hawker and J.M.J. Fréchet, *J. Chem. Soc., Perkin Trans. I*, (1991) 1059.
[11] C.J. Hawker, K.L. Wooley and J.M.J. Fréchet, *J. Chem. Soc., Perkin Trans. I*, (1993) 1287.
[12] L. Lochman, K.L. Wooley, P.T. Ivanova and J.M.J. Fréchet, *J. Am. Chem. Soc.*, 115 (1993) 7043.
[13] L. Lochman and J. Trekoval, *Collect. Czech. Chem. Commun.*, 53 (1988) 76.
[14] L. Lochman and J. Petranek, *Tetrahedron Lett.*, 32 (1991) 1483.
[15] M. Potschka, *Macromolecules*, 18 (1991) 5023.
[16] G. Glockner, *Chromatographia*, 23 (1987) 517.
[17] R.W. Spiridans, H.A. Claessens, G.J.H. van Doremaele and A.M. van Herk, *J. Chromatogr.*, 508 (1990) 319.
[18] M.A. Quarry, M.A. Stadalius, H. Mourey and L.R. Snyder, *J. Chromatogr.*, 358 (1986) 1.
[19] M.A. Stadalius, M.A. Quarry, T.H. Mourey and L.R. Snyder, *J. Chromatogr.*, 358 (1986) 17.
[20] M.R. Bohmer, L.K. Koopal and R. Tijssen, *J. Phys. Chem.*, 95 (1991) 6285.

ELSEVIER

Journal of Chromatography A, 667 (1994) 290–297

JOURNAL OF CHROMATOGRAPHY A

Short Communication

Identification of flavan-3-ols and procyanidins by high-performance liquid chromatography and chemical reaction detection

D. Treutter*[,a], C. Santos-Buelga[a,☆], M. Gutmann[a], H. Kolodziej[b]

[a]*Institut für Pflanzenbau, Lehrstuhl für Obstbau, Technische Universität München, 85350 Freising-Weihenstephan, Germany*

[b]*Freie Universität Berlin, Fachbereich Pharmazie, Institut für Pharmazeutische Biologie, 14195 Berlin, Germany*

(First received November 30th, 1993; revised manuscript received January 13th, 1994)

Abstract

A method for characterizing flavan-3-ols and procyanidins by HPLC separation in connection with on-line UV detection and chemical reaction detection (CRD) is described. The post-column derivatization of the polyphenols with 4-dimethylaminocinnamaldehyde in the presence of sulphuric acid improves the sensitivity as compared to UV detection. The extent of improvement strongly depends on the structure of the procyanidin, hence resulting in characteristic absorbance ratios (CRD/UV) for the individual compounds under given reaction conditions. The ratios are further influenced by the solvent composition, by reaction time and by temperature.

1. Introduction

High-performance liquid chromatography (HPLC) is a valuable tool for the analytical separation of complex mixtures of naturally occurring phenolic compounds [1–4]. However, peak identification is often critical, even when the compounds are described in the literature to occur in a given plant or tissue. In many cases, HPLC analysis comprise more peaks than is expected from previous results obtained by TLC or column chromatography. Accordingly, photodiode array detection is frequently employed both for characterizing phenolic compounds and for checking the peak purity by their UV-absorbance spectra [5]. This approach appears convenient for the identification of simple phenols, hydroxycinnamic acids and most of the flavonoids, and even permits differentiation between flavan-3-ols possessing *o*-di- and trihydroxylated B-rings [6]. However, the UV-absorbance spectra of catechin, epicatechin and their oligomers, the variform procyanidins, do not exhibit any differences with respect to the usual UV-range from 250 to 400 nm.

This article deals with the characterization of flavan-3-ols and procyanidins using the selective post-column derivatization of flavan-3-ols by

* Corresponding author.

☆ Present address: Departamento de Química Analytica, Nutrición y Bromatologia, Facultad de Farmacia, Universidad de Salamanca, 37007 Salamanca, Spain.

0021-9673/94/$07.00
SSDI 0021-9673(94)00069-L

dimethylaminocinnamaldehyde as previously described [7] in combination with UV detection.

2. Experimental

The HPLC equipment consisted of two pumps T-414 (Kontron) and the gradient programmer 205 (Kontron). The column (250 × 4 mm I.D.) was prepacked in our laboratory with Shandon Hypersil ODS, 3 μm. The solvents were 5% formic acid (A) and gradient grade methanol (B) with a flow-rate of 0.5 ml/min.

The gradient profile used was: 0–5 min, isocratic, 5% B in A; 5–15 min, 5–10% B in A; 15–30 min, isocratic, 10% B in A; 30–50 min, 10–15% B in A; 50–70 min, isocratic, 15% B in A; 70–85 min, 15–20% B in A; 85–95 min, isocratic, 20% B in A; 95–110 min, 20–25% B in A; 110–140 min, 25–30% B in A; 140–160 min, 30–40% B in A; 160–175 min, 40–50% B in A; 175–190 min, 50–90% B in A.

Directly behind the column a Kontron filter detector (Uvikon 740 LC) was used for detection at 280 nm. Thereafter the eluent containing the phenols was mixed with the reagent in a simple T-connection. A Gynkotek HPLC pump (Model 300 C) moves the reagent at a flow-rate of 0.5 ml/min. For both the T-connection and the pump heads stainless steel is used. The reactors were knitted PTFE capillaries (0.5 mm I.D.) with different lengths. The PTFE capillaries have to be replaced after 4–5 months due to the occurrence of insoluble, blue to violet precipitations which can absorb phenolic compounds leading to peak tailing.

The blue reaction products were measured at 640 nm by a VIS-detector (Model SP6V, Gynkotek, Germany). The data of both chromatograms were evaluated simultaneously by a computer equipped with Gynkosoft chromatography software (Gynkotek).

For the heating experiments, a stainless-steel capillary (50 cm × 0.5 mm I.D.) was inserted between the T-connection and the PTFE-reactor. This short capillary was clamped between the open ends of the secondary coil of a laboratory-made low voltage/high current transformer and heated directly by an alternating current of approximately 20–30 A. The temperature was controlled electronically using a micro temperature probe attached to the capillary.

The reference compounds were either commercially available (catechin, Roth, Karlsruhe, Germany; epigallocatechin, epicatechin-3-O-gallate, epigallocatechin-3-O-gallate, Extrasynthèse, Lyon, France) or isolated from horse chestnut (epicatechin, procyanidins B2, B5, A2, C1, epicatechin-(4β → 8)-epicatechin-(4β → 6)-epicatechin, epicatechin-(4β → 8)-epicatechin-(4β → 8)-epicatechin-(4β → 8)-epicatechin, epicatechin-(4β → 8;2β → 7)-epicatechin-(4β → 8)-ent-epicatechin) after [8,9] and from Prunus spinosa (ent-epicatechin-(4α → 8; 2α → 7)-epicatechin, epicatechin-(4β → 8; 2β → 7)-epicatechin-(4β → 8)-ent-epicatechin) [10]. The procyanidins B3, B6 and C2 were synthesized according to ref. 11.

3. Results and discussion

3.1. Sensitivity of chemical reaction detection vs. UV-detection

Besides the advantage of high selectivity [7] which overcomes separation problems, the sensitivity after derivatization is generally better than that of UV-detection as can be seen in Fig. 1. This was verified for both peak area and peak height calculation. The maximal noise of 0.2 mAU for UV and 0.5 mAU for visible light detection gives an idea of the differences concerning the respective detection limits.

The calibration curves (Fig. 1) indicate the influence of the flavanoid structure on the absorbance of both UV (280 nm) and visible light (640 nm), before and after derivatization with 4-dimethylaminocinnamaldehyde (DMACA), respectively. At 280 nm, the molar extinction of epigallocatechin is much lower than that of catechin and epicatechin. This can be explained by the weak molar extinction of the pyrogallol-type B-ring of the former molecule, as compared to the analogous brenzcatechin element of the

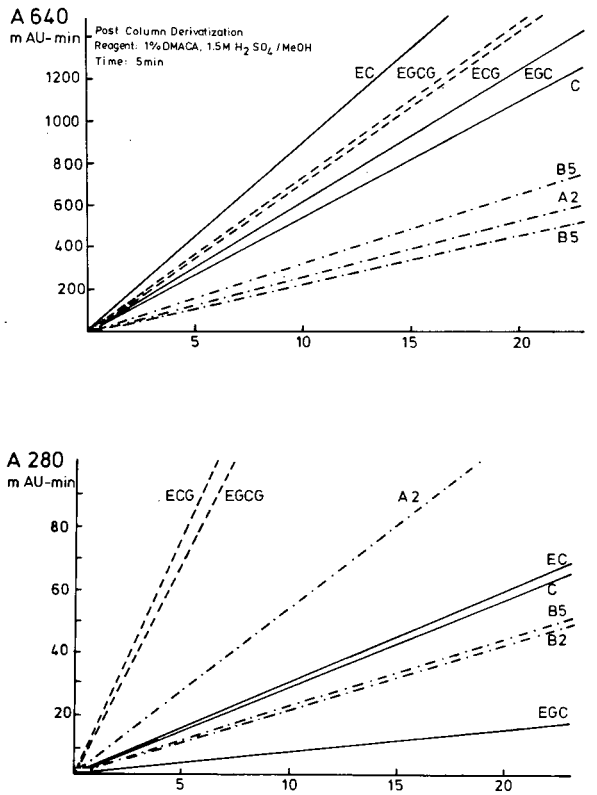

Fig. 1. Calibration curves of peak areas obtained at 280 nm and after derivatization with *p*-dimethylaminocinnamaldehyde at 640 nm. EC = epicatechin; EGCG = epigallocatechin-3-O-gallate; ECG = epicatechin-3-O-gallate; EGC = epigallocatechin; C = catechin. Units for *x*-axis: n*M*.

latter, exhibiting an absorbance about 4 times higher [12]. After derivatization, however, the absorbances of the reaction products of both phenols are quite similar.

Epicatechin and catechin show nearly identical curves at 280 nm. In contrast, the difference in absorbance at 640 nm is pronounced. This peculiar observation is only explicable in terms of the stereochemical difference of the 3-epimers despite of the fact that the chiral centre is relatively far removed from the site of reaction with the aldehyde.

The relatively high values of the epicatechin-3-O-gallate and the epigallocatechin-3-O-gallate at 280 nm are due to the gallic acid moiety which significantly contributes to the overall absorbances. This coincides with the observation of the strong UV-absorbance of both benzoic and hydroxycinnamic acids [13].

For the dimers, the doubly linked procyanidin A2 differs from the singly linked representatives B2 and B5 with respect to UV-absorption (Fig. 1). By contrast, all these procyanidins with their 2,3-*cis* constituent units show similar behaviour following post column derivatization with DMACA.

From these data it can be concluded that the ratio of the absorbance before and after derivatization is structurally related and is constant for each single structure under given conditions.

3.2. Influence of reaction time and solvent composition

As shown in Fig. 2, the reaction kinetics of various structures obtained in a conventional colorimetric assay are different and depend on the acid concentration. This may partially contribute to the results shown in Fig. 1. In order to transfer the reaction kinetics to HPLC-conditions, the flow injection mode was chosen using several reactors each with a different length (Table 1). Previously it was shown that the presence of methanol in the mobile phase accelerates the formation of the coloured product [7] resulting in higher ratios after 1.5 min reaction time. Replacement by a longer reactor chamber permitting 5 min reaction time leads to higher ratios only in instances of eluents containing 5% methanol, whereas a 15% methanol content already favours discoloration resulting in reduced ratios for all three compounds tested. However, if methanol in the reagent was replaced by glacial acetic acid, as proposed in ref. 14 for the vanillin reagent, the procyanidin A2 exhibits its maximum values after 5 min.

3.3. Influence of temperature

Instead of extending the reaction time, an increase in temperature appears to be an alternative for obtaining values characteristic for individual procyanidins (Table 2). The effect of temperature elevation on the CRD/UV ratio is most pronounced for the procyanidin A2. This

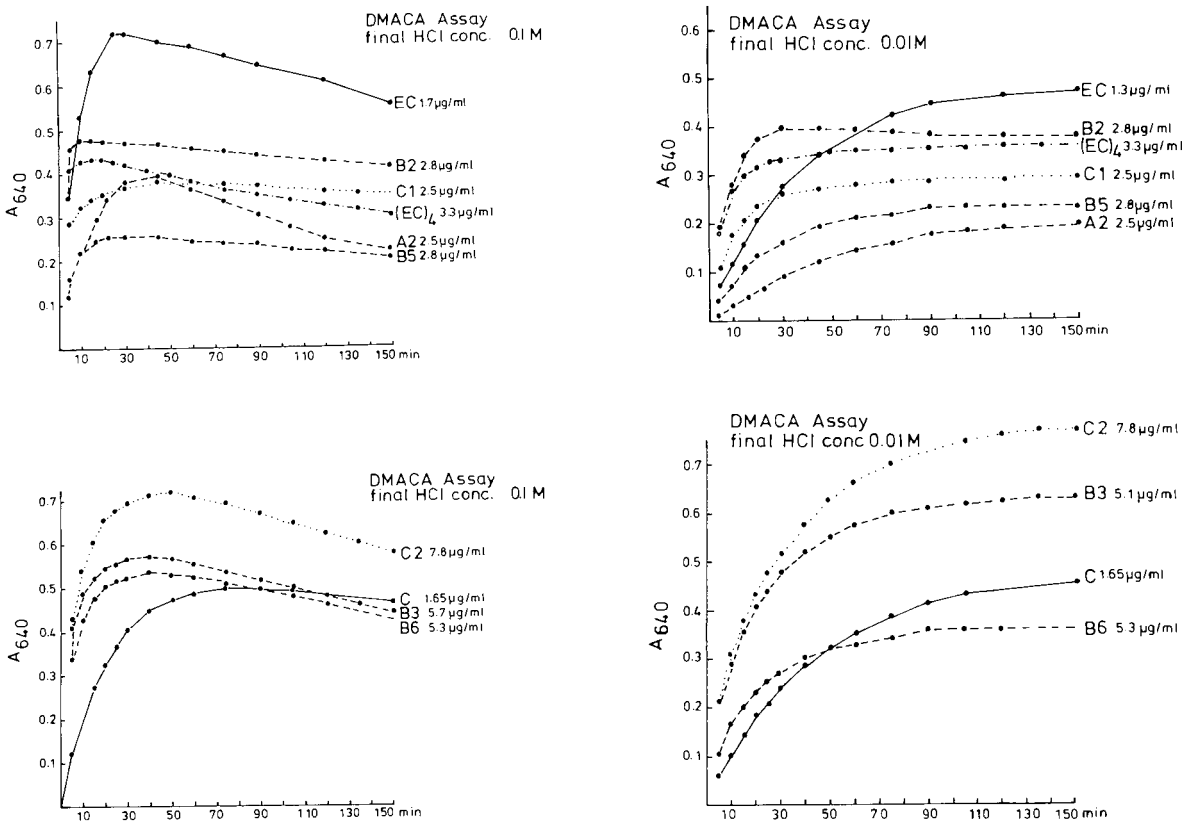

Fig. 2. Structure dependent kinetics of the aldehyde reaction at two acid concentrations using a colorimetric test. Reaction mixture: 1500 µl MeOH containing the flavanol, 300 µl reagent (2 mg DMACA per ml EtOH–6 *M* HCl, 9:1 or 99:1, respectively). Measurement at 640 nm in a Kontron spectrophotometer.

remains even true for the long reaction time of 5 min, *i.e.*, conditions under which the ratio for epicatechin already decreased. These observations can be interpreted as a synergistic effect of both prolonged reaction time and increased temperature. In general: the shorter the reaction time, the more significant is the effect of heating on the CRD/UV ratio.

3.4. Structural dependence of the CRD/UV ratio under HPLC conditions

Table 3 shows the ratio of the peak areas of a series of monomeric flavan-3-ols and oligomeric procyanidins obtained after and before derivatization. As mentioned above, the ratio for epigallocatechin is very high, due to its low UV-absorbance. On the other hand, galloylation enhances the UV-absorption resulting in reduced ratios for the 3-O-gallates (Table 3).

The degree of oligomerization generally decreases the ratio within a series of 4→8-linked oligoflavanoids, *e.g.* 2,3-*cis*, 2,3-*trans* and A-type procyanidins, respectively.

As compared to procyanidins with 4→8-linkages, those with 4→6-interflavanyl bonds show enhanced ratios, whereas doubly linked procyanidins such as A2 exhibit very low values.

The observation that the chain extending unit of a given procyanidin greatly influences the ratio is evident from procyanidins of mixed stereochemistry (B1 and B7) consisting of epicatechin and catechin constituent units. Here, the lower terminal catechin unit apparently does

Table 1
Influence of reaction time and solvent composition on the peak height ratio (CRD/UV)

Conditions	Peak height ratio		
	Epicatechin	Procyanidin B2 E(4β→8)E	Procyanidin A2 E(4β→8;2β→O→7)E
Reagent: 1% DMACA in 1.5 M sulphuric acid in methanol			
Reaction time: 1 min; solvent composition[a]: 5%	4.16	1.52	0.41
Reaction time: 1 min; solvent composition[a]: 15%	4.23	1.50	0.45
Reaction time: 1.5 min; solvent composition[a]: 5%	6.97	2.16	0.71
Reaction time: 1.5 min; solvent composition[a]: 15%	7.67	2.26	0.77
Reaction time: 5 min; solvent composition[a]: 5%	10.9	2.23	0.78
Reaction time: 5 min; solvent composition[a]: 15%	8.13	1.69	0.67
Reagent: 1% DMACA in 1.5 M sulphuric acid in glacial acetic acid			
Reaction time: 5 min; solvent composition[a]: 5%	10.3	1.83	0.91
Reaction time: 5 min; solvent composition[a]: 15%	9.5	1.4	0.9

The flow injection mode in combination with reactors of different tube lengths was employed. The apparatus and the reaction conditions are described in the Experimental section. Each value represents the mean of 3 to 5 replicates.
[a]Solvent composition: B (methanol) in A (5% formic acid).

Table 2
Influence of temperature on the peak height ratio after and before derivatization (640/280)

	Reaction time							
	1 min		1.5 min				5.0 min	
	30°C	90°C	30°C	50°C	70°C	90°C	30°C	90°C
Epicatechin	4.1	7.0	8.1	8.7	9.7	10.2	7.2	6.5
Procyanidin B2	1.4	1.6	2.2	2.3	2.3	2.3	1.5	1.6
Procyanidin A2	0.3	0.7	0.7	1.0	1.1	1.1	0.4	0.6

The apparatus is described in the Experimental section. The flow injection mode was employed.

not influence the ratio, compared to their homogeneous 2,3-*cis* analogues B2 and B5, respectively (Table 3).

The relative low ratios of 2,3-*trans* compounds as compared to those with 2,3-*cis*-configuration may at least in part be rationalized on the basis of kinetic differences, *i.e.* the somewhat delayed reaction of 2,3-*trans* procyanidins with the alde-

Table 3
Influence of the structure on peak area ratio (CRD/UV) and retention time

Common name	Structure	Ratio 640/280, reaction time 2 min	Retention time without CRD	Elution order (peak number in Fig.3)
2,3-cis Series				
Epigallocatechin		98.8	31.3	4
Epigallocatechin-3-O-gallate		3.2	49.5	6
Epicatechin-3-O-gallate		2.8	85.4	11
Epicatechin		20.9	55.6	7
Procyanidin B2	E(4β→8)E	10.9	41.2	5
Procyanidin C1	E(4β→8)E(4β→8)E	7.7	63.6	9
	E(4β→8)E(4β→8)E(4β→8)E	3.8	67.9	
Procyanidin B5	E(4β→6)E	14.5	112.0	14
	E(4β→8)E(4β→6)E	14.3	126.9	15
2,3-trans Series				
Catechin		12.4	28.5	3
Procyanidin B3	C(4α→8)C	5.5	20.7	1
Procyanidin C2	C(4α→8)C(4α→8)C	3.4	20.7	1
Procyanidin B6	C(4α→6)C	6.3	31.3	4
A-types				
Procyanidin A2	E(4β→8;2→O→7)E	2.9	100.5	13
	entE(4α→8;2α→O→7)E	2.0	94.2	12
	E(4β→8;2β→O→7)E(4β→8)entE	1.9	49.5	6
	entE(4α→8;2α→O→7)C	1.8	70.9	10
Stereochemically mixed procyanidins				
Procyanidin B1	E(4β→8)C	9.7	24.0	2
Procyanidin B7	E(4β→6)C	11.9	57.5	8

hyde reagent (Fig. 2). Additionally, the composition of the eluent has to be considered. For instance, the aqueous proportion of the reaction mixture decreases, while the amount of methanol increases with time and *vice versa*. Since the concentration of methanol strongly influences the reaction kinetics [7], all compounds which are retarded by the stationary phase find improved conditions for the derivatization as specified in the Experimental section.

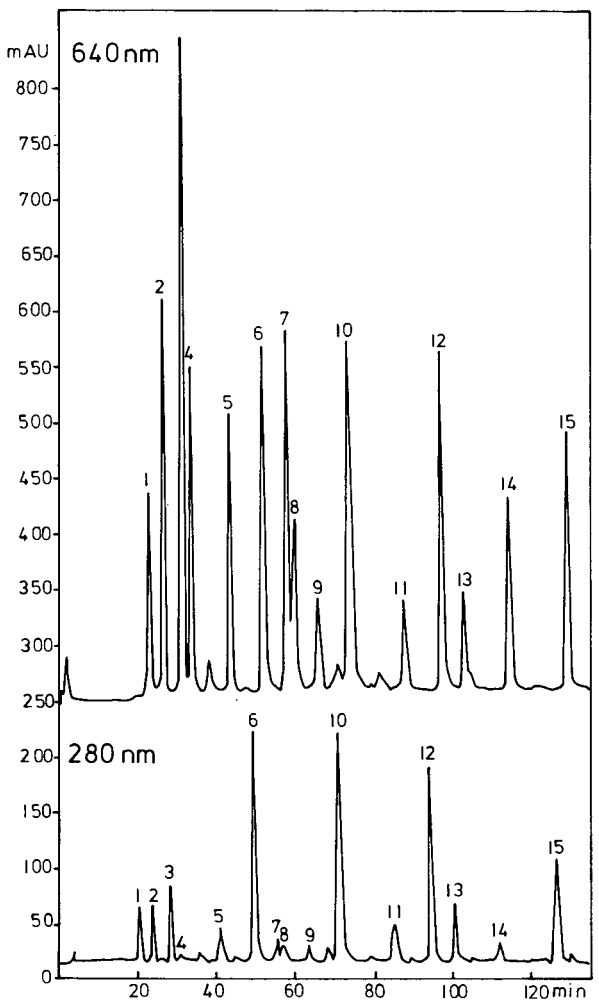

Fig. 3. HPLC separation of a synthetic mixture of catechins and procyanidins with UV-detection (280 nm) followed by derivatization with DMACA resulting in coloured products recorded at 640 nm. The method is described in the Experimental, for peak description *cf.* Table 3.

The presence of enantiomeric (2*S*) constituent units in A-type procyanidins has very weak influence on the CRD/UV ratio. Noteworthy is the marked effect on the retention time (Fig. 3). This may presumably be explained in terms of their overall configuration, associated with differences in the number of intramolecular hydrogen bridges. The elution sequence of the remaining oligomeric flavan-3-ols follows common rules observed by many authors [2,15–19]. Under the experimental conditions, flavan-3-ols and their oligomers possessing 2,3-*trans*-configuration elute earlier than their corresponding 2,3-*cis* analogues. Oligoflavanoids with 4→6 intramolecular linkages and doubly linked procyanidins (A-types) show relatively high t_R values when comparing structures with the same degree of oligomerization.

4. Conclusion

The method described assists in characterizing flavan-3-ol and procyanidin peaks in HPLC analysis, providing satisfactory resolution. Simultaneously, it may be applied for a purity check of compounds following various fractionation procedures. It should also prove helpful in unambiguous identification of procyanidins in plant extracts, even in complex mixtures.

5. Acknowledgements

The stay of C. Santos-Buelga was granted by Dirección General de Investigación Cientifica y Técnica (DGICYT, Ref. 93-021), Spain.

6. References

[1] K. Van de Casteele, H. Geiger and C.F. Van Sumere, *J. Chromatogr.*, 240 (1982) 81.
[2] K. Van de Casteele, H. Geiger, R. De Loose and C.F. Van Sumere, *J. Chromatogr.*, 259 (1983) 291.
[3] I. McMurrough and G.P. Hennigan, *J. Chromatogr.*, 258 (1983) 103.
[4] D. Treutter, *J. Chromatogr.*, 436 (1988) 490.

[5] K. Hostettmann, B. Domon, D. Schaufelberger and M. Hostettmann, *J. Chromatogr.*, 283 (1984) 137.
[6] D. Treutter, C. Santos-Buelga and W. Feucht, *Acta Horticulturae*, (1994) in press.
[7] D. Treutter, *J. Chromatogr.*, 467 (1989) 185.
[8] R.S. Thompson, D. Jacques, E. Haslam and R.J.N. Tanner, *J. Chem. Soc. Perkin Trans. I*, (1972) 1387.
[9] C. Santos-Buelga, H. Kolodziej and D. Treutter, (1994) in preparation.
[10] H. Kolodziej, M.K. Sakar, J.F.W. Burger, R. Engelshowe and D. Ferreira, *Phytochemistry*, 30 (1991) 2041.
[11] J.A. Delcour, D. Ferreira and R.G. Roux, *J. Chem. Soc. Perkin Trans. I*, (1983) 1711.
[12] Z. Czochanska, L.Y. Foo, R.D. Newman and L.J. Porter, *J. Chem. Soc.*, (1980) 2278.
[13] T. Swain and J.L. Goldstein, in J.B. Pridham (Editor), *Methods in Polyphenol Chemistry*, Pergamon Press, Oxford, 1964, p. 131.
[14] L.G. Butler, M.L. Price and J.E. Brotherton, *J. Agric. Food Chem.*, 30 (1982) 1087.
[15] T. Escribano-Bailon, Y. Gutierrez-Fernandez, J. Rivas-Gonzalo and C. Santos-Buelga, *J. Agric. Food Chem.*, 40 (1992) 1794.
[16] J. Jerumanis, *Proc. Eur. Brew. Conv. (Berlin)*, (1979) 309.
[17] J. Jerumanis, *J. Inst. Brew.*, 91 (1985) 250.
[18] H.A. Stafford and H.H. Lester, *Plant Physiol.*, 66 (1980) 1085.
[19] L.Y. Porter, in J.B. Harborne (Editor), *The Flavonoids. Advances in research since 1980*, Chapman and Hall, London, 1988, p. 21.

ELSEVIER

Journal of Chromatography A, 667 (1994) 298–303

JOURNAL OF CHROMATOGRAPHY A

Short Communication

Simultaneous analysis of hydroxylamine, N-methylhydroxylamine and N,N-dimethylhydroxylamine by ion chromatography

Alex M. Prokai, Ravi K. Ravichandran*

Research and Development, Boehringer Mannheim Corporation, 9115 Hague Road, Indianapolis, IN 46250, USA

(First received November 11th, 1993; revised manuscript received January 28th, 1994)

Abstract

Hydroxylamine and N-alkylhydroxylamines have been separated and analyzed using ion chromatography with conductivity and amperometric detectors. Conductivity detection is simple, but lacks selectivity. Amperometric detection provides good selectivity at modest working electrode operating potentials. However, in order to realize the selectivity, it is necessary to pretreat the working electrode which results in a significant reduction of the detector operating potential. While both conductivity and amperometric detectors have the capability to quantify nanomole amounts of hydroxylamines (absolute amount injected), amperometric detection possesses superior selectivity and sensitivity.

1. Introduction

Hydroxylamine and N-alkylhydroxylamines belong to an important class of reducing agents which are routinely used in industrial and pharmaceutical processes. Hydroxylamine has been identified as an intermediate in many biological processes [1]. Generally, hydroxylamines are mutagenic in nature. Simple derivatives of hydroxylamine, for example, hydroxamic acids or oximes which are important industrial raw materials, can be determined as hydroxylamine after initial hydrolysis [1]. Quantitative determination of hydroxylamines is therefore, very important both in studies of biological processes and for industrial purposes. A survey of the analytical procedures that exist in the literature reveals that volumetric and spectrophotometric methods are commonly used for the analysis of hydroxylamines [1]. A GC procedure with pre-column derivatization has been reported for trace level determination of hydroxylamine [2]. HPLC methods with UV detection (210 nm) [3] and potentiometric detection [4] have also been reported. However, to our knowledge, simultaneous analysis of hydroxylamine and its derivatives (N-alkylhydroxylamines) has not been performed. In this paper, we report the utility of both conductivity and amperometric detection following ion chromatographic (IC) separation for the simultaneous determination of hydroxylamine and N-alkylhydroxylamines, as well as the

* Corresponding author.

0021-9673/94/$07.00
SSDI 0021-9673(94)00108-L

selectivity and sensitivity aspects of both conductivity and amperometric detection schemes.

2. Experimental

2.1. Apparatus

Cyclic voltammetry experiments were performed using a Bioanalytical Systems (BAS) Model 100B instrument, glassy carbon working electrode, Pt counter electrode and Model RE-1 Ag/AgCl reference electrode. The chromatographic equipment used consisted of a Jasco Model 880 PU pump, Micromeritics Model 728 autosampler equipped with a Model 732 injector and 50-μl sample loop, Alltech Model 320 conductivity detector and PARC Model 400 electrochemical detector equipped with the BAS Model LC 17A thin-layer cell with a glassy carbon electrode. The post-column addition of base was achieved using a TimberLine Instruments reagent-delivery module, Model RDR-1. The chromatographic data were collected using a PE Nelson data system. All chromatography was performed using a 150 mm × 4.6 mm I.D. Alltech/Wescan Cation/R column. Unless otherwise stated, the mobile phase flow-rate was 1 ml/min. The post-column base (20 m*M* NaOH) was added at the rate of 1.5 ml/min.

2.2. Reagents

All solutions were prepared with Milli-Q water. The mobile phase for the chromatographic separation was prepared from Baker Ultrex-grade concentrated nitric acid by stepwise dilution to a final concentration of 10 m*M*. The mobile phase was filtered through a 0.45-μm nylon-66 membrane prior to use. The buffers used in the pH variation study were prepared according to Christian [5] using reagent-grade phosphate salts.

2.3. Electrode pretreatment

The glassy carbon electrode was polished three times with a 1-μm alumina slurry for 1 min and rinsed each time with Milli-Q water. The electrode was then sonicated using a Branson Model 1200 sonicator for 5 min in Milli-Q water to eliminate any adsorbed alumina particles. The electrochemical pretreatment itself consisted of holding the electrode at + 1.75 V *vs.* Ag/AgCl in a pH 7 buffer solution for 5 min and then at −1.2 V *vs.* Ag/AgCl for 10 s.

3. Results and discussion

3.1. Chromatography of hydroxylamines

Reversed-phase separation of hydroxylamine and hydroxyurea has been reported with water as the mobile phase [6]. The reported k' for hydroxylamine was large enough to suggest that N-alkylhydroxylamines could indeed be separated by RPLC. However, in our hands k' values for unsubstituted *vs.* substituted hydroxylamines were not significantly different. Therefore, another mode of separation was deemed necessary.

Alkanolamines have been successfully separated by IC [6]. A similar strategy should be applicable for the separation of hydroxylamines. Fig. 1 shows the chromatogram obtained for the separation of three hydroxylamines using single-column IC. The N,N-dimethylhydroxylamine peak tails somewhat, probably due to the hydrophobic nature of the column packing. The peak for hydroxylamine is preceded by a shoulder which is due to trace amounts of sodium ions. In a typical analytical situation, if the sample contained a significant amount of sodium ions, then one would observe a co-elution of both hydroxylamine and sodium ions. In order for this separation to be useful analytically, it is imperative that the separation be improved or a selective detector be used. Attempts to improve the resolution between sodium and hydroxylamines were not at all successful. Hydroxylamines do not absorb in the useful UV region significantly. The absorption maximum is in the more noise prone 190–215 nm UV region which does not facilitate selective detection. Hydroxylamines have been reported to be electroactive [7], which

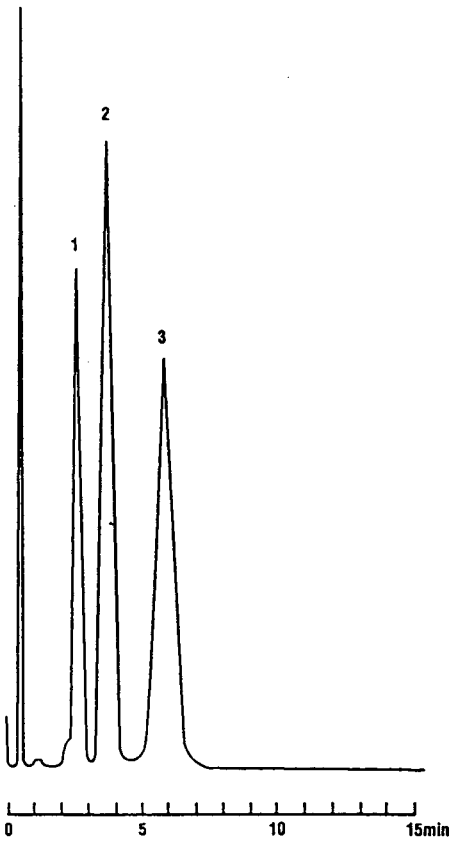

Fig. 1. Ion chromatogram of three hydroxylamines. Peaks: 1 = hydroxylamine $1 \cdot 10^{-4}$ *M*; 2 = N-methylhydroxylamine $2 \cdot 10^{-4}$ *M*; 3 = N,N-dimethylhydroxylamine $2 \cdot 10^{-4}$ *M*. Detector sensitivity 1 μS full scale.

raises the possibility of using LC with electrochemical detection (ED) for the selective detection of hydroxylamines.

3.2. Electrochemistry of hydroxylamines

N-Alkylhydroxylamines have been quantitatively determined by polarography [7]. There is very little information about the electrochemical behavior of hydroxylamines at solid electrodes such as glassy carbon which is commonly used in LC–ED. The electrochemical behavior of hydroxylamine at a glassy carbon electrode was first studied in 10 m*M* nitric acid, which was used as the mobile phase in the IC experiment. None of the hydroxylamines exhibited any electrochemical activity in 10 m*M* nitric acid. Organic oxidations are generally facile at alkaline pH conditions. The acidic pH (about 2.5) of the supporting electrolyte (10 m*M* nitric acid) might have inhibited the oxidation. To confirm this possibility, the effect of pH on the electrochemistry of hydroxylamine at the glassy carbon electrode was studied. It was found from the cyclic voltammetric (CV) studies that no significant electrochemical activity could be obtained until the pH of the supporting electrolyte was at or above pH 7. It was interesting to note that even at very alkaline pH levels, hydroxylamine underwent oxidation at substantial overpotentials. Similar results were obtained for N-methyl- and N,N-dimethylhydroxylamines. These observations indicated that in order to use ED for hydroxylamines, it becomes necessary to operate the electrochemical detector at very high potentials which would significantly decrease the detector selectivity and sensitivity by decreasing the *S/N* ratio. A simple electrochemical pretreatment has been shown to be very effective in enhancing the electrode response for many analytes [8]. Such a pretreatment has been successfully applied towards enhancement of LC–ED responses for several biologically important analytes in complex physiological matrices [9]. It is likely that a similar strategy could prove to be useful in enhancing the electrode response for hydroxylamines. Accordingly, the electrochemical behavior of hydroxylamines was studied at electrochemically pretreated electrodes. It was found that the electrochemical pretreatment of the electrode surface indeed resulted in increased electrochemical response. It was also observed that alkaline pH conditions were necessary to realize the diffusion-controlled oxidation of hydroxylamine. This observation is in agreement with the DME polarography work done by Iverson and Lund [7]. Fig. 2 shows the comparison of the electrochemical response for the three hydroxylamines at pH 9.0, before and after pretreatment. Clearly the electrode pretreatment does result in a reduction of the overvoltage needed to oxidize these species by 300–500 mV. It must be noted that the first scan in the CV exhibited a much higher response while the

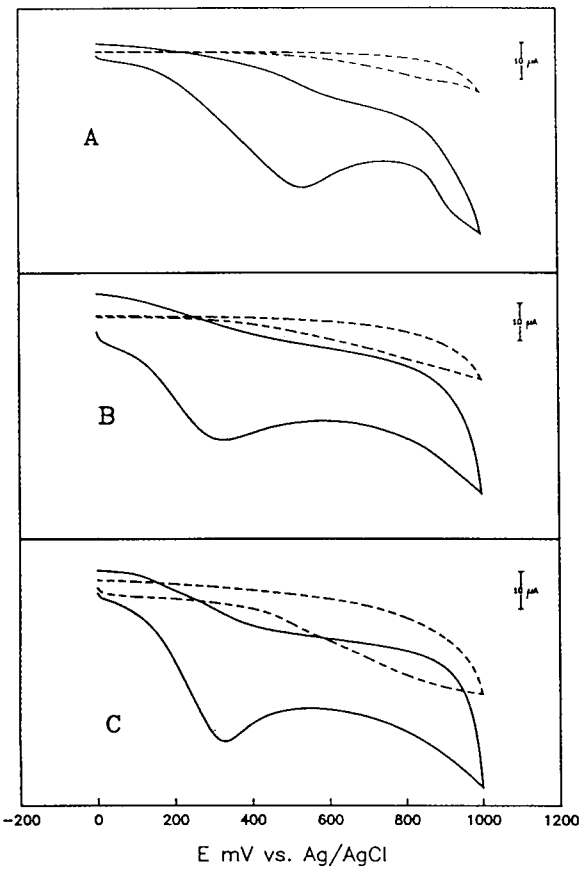

Fig. 2. Cyclic voltammograms of $2 \cdot 10^{-3}$ *M* of (A) hydroxylamine, (B) N-methylhydroxylamine and (C) N,N-dimethylhydroxylamine. Broken lines: untreated electrode response; solid lines: pretreated electrode response.

subsequent scans showed decreased response, possibly due to electrode surface fouling which is not likely to pose any problems in LC–ED. The electrochemical activity can be regained by polishing the electrode and reconditioning the surface electrochemically. These observations are very reproducible as long as the pretreatment procedure is followed as described in the Experimental section.

3.3. LC–ED of hydroxylamines

The electrochemical investigations described in the previous section indicated that in order to detect the hydroxylamines it is necessary to have the pH of the LC effluent at or above pH 7.0. However, the IC separation of the hydroxylamines requires 10 m*M* nitric acid which is obviously unsuitable for LC–ED. It is possible to achieve the neutral or alkaline pH of the effluent in two ways. The first method involves the use of chemical suppression of the acid. However, the resulting effluent has a low conductance rendering it almost useless for LC–ED. The second and simplest way to achieve the alkaline pH values is by post-column addition of a strong base to the effluent from the conductivity detector. It was determined by trial and error that addition of 20 m*M* sodium hydroxide to the conductivity detector effluent at a rate of 1.5 ml/min rendered the pH of the effluent to be around 10. Chromatograms obtained for a mixture of three hydroxylamines using LC–ED at both untreated and pretreated glassy carbon electrodes are provided in Fig. 3. In both cases, the electrode was maintained at 0.6 V *vs.* Ag/AgCl and the same hydroxylamine mixture was used to generate each chromatogram. At the modest working electrode potential used here, a very large re-

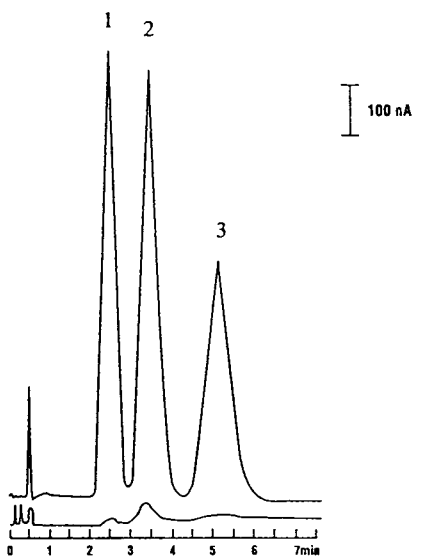

Fig. 3. Chromatograms of hydroxylamine mixture at 0.5 V *vs.* Ag/AgCl at (bottom curve) untreated and (top curve) electrochemically pretreated glassy carbon electrode. Peaks: 1 = hydroxylamine $1 \cdot 10^{-4}$ *M*; 2 = N-methylhydroxylamine $2 \cdot 10^{-4}$ *M*; 3 = N,N-dimethylhydroxylamine $2 \cdot 10^{-4}$ *M*.

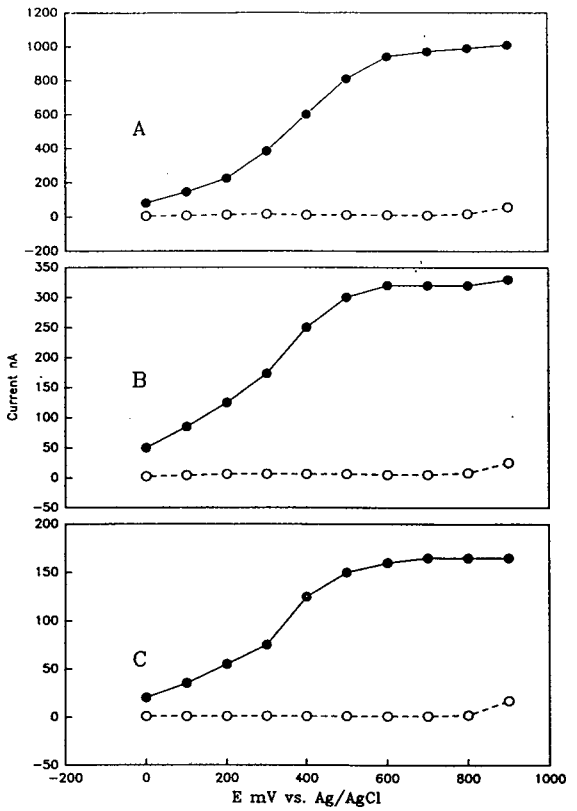

Fig. 4. Hydrodynamic voltammograms at untreated (○) and electrochemically pretreated (●) glassy carbon electrodes for equimolar mixture ($2 \cdot 10^{-4}$ *M*) of (A) hydroxylamine, (B) N-methylhydroxylamine and (C) N,N-dimethylhydroxylamine.

sponse was obtained for the pretreated electrode, while almost no signal was obtained at the untreated electrode. This behavior was exactly as expected based on the voltammetric data described in the previous section.

The hydrodynamic voltammograms (HDVs), peak current *vs.* potential profiles, for each of the three hydroxylamines at treated and untreated electrodes are shown in Fig. 4. These curves were obtained by plotting the detector response for a given concentration of each analyte at various applied electrode potentials under a given chromatographic condition. The HDV data for the untreated electrode was obtained first. The electrode was disconnected from the cell, pretreated as described in the Experimental section, reassembled and the HDV data was obtained. For the untreated electrode, an analytically useful signal could not be obtained even at 0.9 V. On the other hand, the pretreated electrode exhibited very well defined plateaus for all the three hydroxylamines in the vicinity of 0.6 V *vs.* Ag/AgCl. The calibration curves and detection limits for the three hydroxylamines were determined at 0.6 V. Calibration curves obtained over the concentration range examined were found to be linear with correlation coefficients greater than 0.99. The linear dynamic ranges in terms of the absolute amount injected were the following: hydroxylamine 0.05–2.5 nmol; N-methylhydroxylamine 0.25–5.0 nmol; and N,N-dimethylhydroxylamine 0.4–5.0 nmol. To the best of our knowledge, simultaneous analysis of hydroxylamines by HPLC techniques has not yet been reported. In the applications cited [3,4], no detection limits have been reported. The LOD value for hydroxylamine with conductivity detection reported in Table 1 com-

Table 1
Comparison of conductivity and electrochemical detector responses

Analyte	LC–conductivity detection		LC–ED	
	Linear range	LOD	Linear range	LOD
Hydroxylamine	1.0–25.0	0.5	0.05–2.5	0.01
N-Methylhydroxylamine	2.0–40.0	1.0	0.25–5.0	0.05
N,N-Dimethylhydroxylamine	2.5–50.0	1.0	0.40–5.0	0.08

All the amounts listed are absolute amounts injected on the column in nmol. LOD = Limit of detection (defined as the lowest detectable amount with *S/N* ratio of 3.0).

pares favorably with GC analysis with pre-column derivatization. The LOD value for hydroxylamine with ED is lower by at least an order of magnitude. The relative standard deviation of the response for all the three hydroxylamines for successive replicate injections ($n = 6$), was typically less than 5%, which supports the fact that surface fouling is not a problem in LC–ED. A comparison of the LC–ED detection limits with the conductivity detector is given in Table 1. The data demonstrate that ED does offer better sensitivity. It must be mentioned here that once the electrode surface has been pretreated, it can be used for over 10–12 h with no significant decrease in the signals for all the three hydroxylamines. Any signal change observed was within the 5% relative standard deviation and this observation is consistent with the work that has been previously reported [10].

One of our main interests in ED was prompted by the lack of selectivity associated with conductivity detection. The conductivity detector does not have the ability to quantify hydroxylamine accurately in the presence of excess sodium ions as evidenced by the shoulder in Fig. 1. The shoulder from the sodium ions is noticeably absent in the chromatograms obtained with the electrochemical detector (Fig. 3) which should not be surprising because of the electroinactive nature of sodium ions at the applied potential of 0.6 V *vs.* Ag/AgCl. In fact, we have observed in our laboratories that hydroxylamine can be quantified in the presence of excess of sodium ions using ED.

4. Conclusions

Our work has demonstrated that hydroxylamine and N-substituted hydroxylamines can be separated and analyzed by IC with both conductivity and ED schemes. Post-column addition of a strong base was deemed necessary to facilitate ED. The glassy carbon electrode must be electrochemically pretreated to obtain an LC–ED response. ED exhibits better selectivity and sensitivity than the conductivity detector although LC–ED requires the use of post-column reagent addition.

5. Acknowledgements

The authors wish to acknowledge the help of Eric Diebold and Steve Cunningham of Boehringer Mannheim Corporation for their help in the preparation of the manuscript.

6. References

[1] T. Kolasa and W. Wardencki, *Talanta*, 21 (1974) 845.
[2] F. Lombardi and T. Crolla, *J. Pharm. Sci.*, 77 (1988) 711.
[3] J. Pluscec and Y.-C. Yuan, *J. Chromatogr.*, 362 (1986) 298.
[4] P.R. Haddad, P.W. Alexander and M.Trojonowicz, *J. Liq. Chromatogr.*, 9 (1986) 777.
[5] G.D. Christian, *Analytical Chemistry*, Wiley, New York, 3rd ed., 1980, p. 186.
[6] *Application Note A0005*, Alltech Associates, Deerfield, IL, 1991.
[7] P.E. Iverson and H. Lund, *Acta Chem. Scand.*, 19 (1965) 2303.
[8] R.C. Engstrom, *Anal. Chem.*, 54 (1982) 2310.
[9] K. Ravichandran and R.P. Baldwin, *J. Liq. Chromatogr.*, 7 (1984) 2031.
[10] K. Ravichandran and R.P. Baldwin, *Anal. Chem.*, 55 (1983) 1782.

ELSEVIER

Journal of Chromatography A, 667 (1994) 304–310

JOURNAL OF CHROMATOGRAPHY A

Short Communication

Peptide mapping using combinations of size-exclusion chromatography, reversed-phase chromatography and capillary electrophoresis

Mats Strömqvist

Department of Protein Chemistry, Symbicom AB, P.O. Box 1451, S-901 24 Umeå, Sweden

(First received August 19th, 1993; revised manuscript received February 14th, 1994)

Abstract

Recombinant extracellular superoxide dismutase was proteolytically degraded by trypsin and the digest was thereafter separated using three different separation techniques. The size differences of the obtained fragments were exploited by size-exclusion chromatography (SEC) on a highly efficient column for peptide separation. Collected fractions representing different size groups of peptides were then separated on the basis of hydrophobicity on reversed-phase liquid chromatography (RPLC). This led to simplified RPLC-chromatograms where collected peaks were considerably more pure than if the digest was separated direct on RPLC and the identity of eluted peaks could easily be determined by amino acid analysis. Finally the digest was run on capillary electrophoresis for separation based on charge differences. For the identification of the different peaks in the electropherogram, the total digest was spiked with known peptides purified by the two other separation techniques. This technique proved to be very powerful for peak identification in an electropherogram from a digest composed of many fragments eluting closely together.

1. Introduction

Among the methods available for confirming the primary structure of proteins, peptide mapping is probably the most powerful. For recombinant proteins to be used as drugs it has become the most essential analysis for confirming identity between different batches to ascertain the quality of the product [1].

The protein is chopped into smaller pieces by means of a chemical or an enzymatic cleavage. The obtained peptides are thereafter separated on the basis of different properties such as size, charge and hydrophobicity (for a review see ref. 2). Since the introduction of peptide mapping the separation technique has been developed from slab-gel electrophoresis and thin-layer chromatography [3,4] to high-performance liquid chromatography [5–7] and capillary electrophoresis (CE) [8].

The outstanding method in recent years has been reversed-phase liquid chromatography (RPLC) separation which is an excellent method to detect small changes within a protein: a single amino acid difference in a peptide often gives rise to a change in the elution volume of that particular fragment. From the digest of a small protein with no or a few modifications, such as glycosylation, most peptides are usually well separated by RPLC and can be identified by amino acid analysis or mass spectrometry. However, when a protein is larger and more complex,

0021-9673/94/$07.00
SSDI 0021-9673(94)00145-Y

a single dimension analysis is usually not sufficient for a good exploration of the primary structure [7]. If the digest contains a large number of hydrophilic fragments, these might not be bound to the column and therefore elute unretarded and thus not separated. The option in that case is to use several different cleavage methods and/or use several different separation techniques to increase the knowledge of the structure.

Through the breakthrough of CE during the past five to six years (reviewed in refs. 9 and 10), this technique has been introduced and established as an excellent way of separating protein digests [11–13]. CE has the advantage of being very fast and the separating power is close to that of RPLC [14]. CE has fruitfully been combined with RPLC [15–17] and with SEC [18] to increase the information gained from peptide mapping.

In this paper it is shown how three different separation techniques separating on the basis of the size, hydrophobicity and charge of the generated peptides can be combined to reveal as much as possible of the structure of recombinant human extracellular superoxide dismutase (EC-SOD).

2. Experimental

2.1. Cleavage of EC-SOD

Recombinant EC-SOD produced in Chinese hamster ovary (CHO) cells was purified to more than 98% purity, carboxymethylated and cleaved with trypsin as described earlier [19].

2.2. Reversed-phase liquid chromatography

An Ultrasphere microbore C_{18} (250 × 2.0 mm I.D., Beckman Instruments, Palo Alto, CA, USA) coupled to a Beckman System Gold chromatography unit was used for all samples. The eluent system was 0.1% trifluoroacetic acid (TFA) in water–acetonitrile, the flow rate was 0.2 ml/min and temperature control (38°C) was achieved using a Waters (Milford, MA, USA) TCM temperature control unit.

2.3. Size-exclusion chromatography

For size separation of the peptides a polyhydroxyethyl aspartamide (200 × 9.4 mm I.D., 200 Å, Poly-lc Inc., Columbia, MD, USA) column was used. The buffer system was 0.2 *M* sodium sulfate–5 m*M* potassium phosphate, pH 3.0, containing 25% acetonitrile. The flow rate was 1 ml/min, the absorbance at 214 nm was recorded and the chromatography was performed at 22°C.

2.4. Capillary electrophoresis

A PACE 2100 (Beckman) was used for capillary electrophoresis. Samples were diluted in 10 m*M* H_3PO_4, pH 2.5, injected to the capillary (fused silica, 100 μm × 50 cm) by 10-s pressure injection, separated in 0.1 *M* H_3PO_4, pH 2.5 at 20 kV. Absorbance data at 214 nm was collected.

2.5. Amino acid analysis

The amino acid content was analyzed by PITC-derivatization and separation on an Ultrasphere ODS column (150 × 4.6 mm I.D., Beckman) as described earlier [19].

3. Results and discussion

Deduced from the amino acid sequence [20], EC-SOD should theoretically give 26 fragments upon cleavage with trypsin (Table 1). However, many of the fragments are too short to be identified by measuring the peptide bond at 214 nm. The composition of the digest is also complicated by the six adjacent cleavage sites at the C-terminus of the protein (T19–T24) and that some unspecific cleavage also occurs. Taken together this implies that it is difficult to separate all fragments by only one chromatographic step.

Reversed-phase liquid chromatography of the digest produces a chromatogram as shown in Fig. 1a. Many of the generated peptides could be identified in the chromatogram but most col-

Table 1

Theoretical tryptic fragments of EC-SOD

Fragment	Amino acid sequence
T1	WTGEDSAEPNSDSAEWIR
T2	DMYAK
T3	VTEIWQEVMQR
T4	R
T5	DDDGTLHAACQVQPSATLDAAQPR
T6	VTGVVLFR
T7	QLAPR
T8	AK
T9	LDAFFALEGFPTEPNSSSR
T10	AIHVHQFGDLSQGCESTGPHYNPLAVPHPQHPGDFGNFAVR
T11	DGSLWR
T12	YR
T13	AGLAASLAGPHSIVGR
T14	AVVVHAGEDDLGR
T15	GGNQASVENGNAGR
T16	R
T17	LACCVVGVCGPGLWER
T18	QAR
T19	EHSER
T20	K
T21	K
T22	R
T23	R
T24	R
T25	ESGCK
T26	AA

The fragment numbers start at the N-terminus of the intact protein.

lected fractions contained several fragments and the identity was therefore difficult to determine by total amino acid analysis. Amino acid composition analysis of the unretarded fraction from RPLC showed a high content of arginine which is not surprising since short fragments containing arginine could be expected both from the cluster of cleavage sites at the C-terminal part and from short internal fragments.

To improve the fingerprint, the digest was subjected to size-exclusion chromatography. The development of columns separating also short peptides with high resolution has improved this technique considerably as a tool for peptide mapping. Fig. 1b shows the result of SEC of the digest. The first peak eluted was a single fragment much larger than the other ones and was easily identified as the only glycosylated fragment, T9 plus an incompletely cleaved variant of it, T8 + 9. No other fragments could be directly identified from the size separation.

The separation of the EC-SOD digest on capillary electrophoresis (CE) is shown in Fig. 1c. The resolution is higher than in the SEC run, most fragments are well separated. No attempt to collect different fractions were made since the fragments eluted closely together in the electropherogram and were therefore difficult to collect as pure peaks.

To simplify the identification of the peaks within the RPLC-chromatogram and the CE-electropherogram, the different separation techniques were combined. First, the digest was separated on the basis of the fragment size on the SEC column. Six different fractions were collected from the SEC separation (as indicated

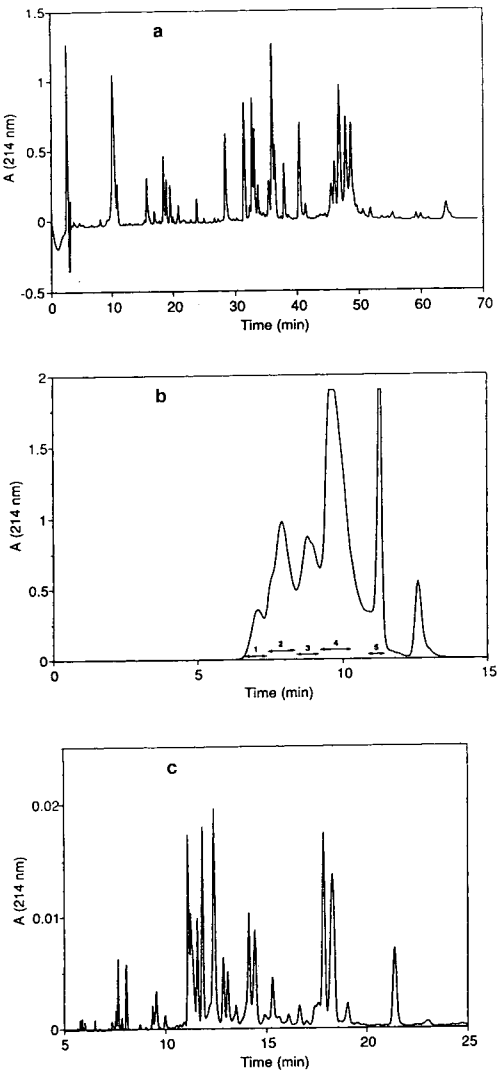

Fig. 1. (a) Tryptic digest of EC-SOD separated using reversed-phase chromatography. The gradient program started at 0.1% trifluoroacetic acid (TFA) in water, a linear gradient of 0–24% acetonitrile in 0.1% TFA from 5–30 min followed by a linear gradient from 24–36% acetonitrile over the next 30 min. The column was thereafter washed by a steep gradient up to 60% acetonitrile in 0.1% TFA and a 10-min wash at that acetonitrille concentration before re-equilibration to the starting conditions. The flow rate was 0.25 ml/min and 230 μg EC-SOD digest was loaded onto the column. (b) Size-exclusion chromatography of 400 μg EC-SOD digest, and (c) capillary electrophoresis of 10 μg EC-SOD digest. Fractions 1–5 collected from the SEC in (b) were further analyzed by RPLC (Fig. 2). The conditions for the chromatography in (b) and the electrophoresis in (c) are described under Experimental.

in Fig. 1b) and thereafter separated on the RPLC column (Fig. 2). The collected fractions from those RPLC runs were easily identified in most cases by amino acid composition analysis. Much help in the identification was gained from the information where this fragment eluted on SEC since this gives a useful hint on the size of the fragment.

Since there is no baseline resolution of the collected peaks from the SEC run, some fragments also appeared in the neighbouring peaks collected. After this two-dimensional separation all collected peaks were more than 80% pure according to analysis by CE (not shown) and their identity could be determined by amino acid analysis. When fractions were collected from a RPLC separation of the digest before it was separated on SEC, the dominating fragment in some fractions constituted only approximately 40% of the material even though the peak shape indicated that it was pure (not shown).

To identify the peaks in the electropherogram in Fig. 1c, the total digest was spiked with the purified and identified peaks from SEC–RPLC. Since the peaks of the electropherogram were so close together, running the purified individual fragments separately on CE gave not a certain identification. The amount of spiking fraction was chosen to give about twice the peak height of the particular peak. The spiking fraction was dissolved in 0.1% TFA in water and did not exceed 10% of the total sample volume when mixed with the total digest. The identity of the peak could therefore be obtained in only one run. Some of the spiked samples are shown in Fig. 3.

The best method for identification of peaks in an electropherogram is to use a mass spectrometer coupled to the CE instrument [21]. Alternatively peaks can be collected when eluted and thereafter subjected to mass spectrometry or amino acid sequencing. Collection techniques are dependent on a good resolution of the peaks because of a delay period between the time when the peak is detected and the time when it elutes from the capillary end. Another drawback with the collection technique is that the amount of digest that can be applied to the capillary at each

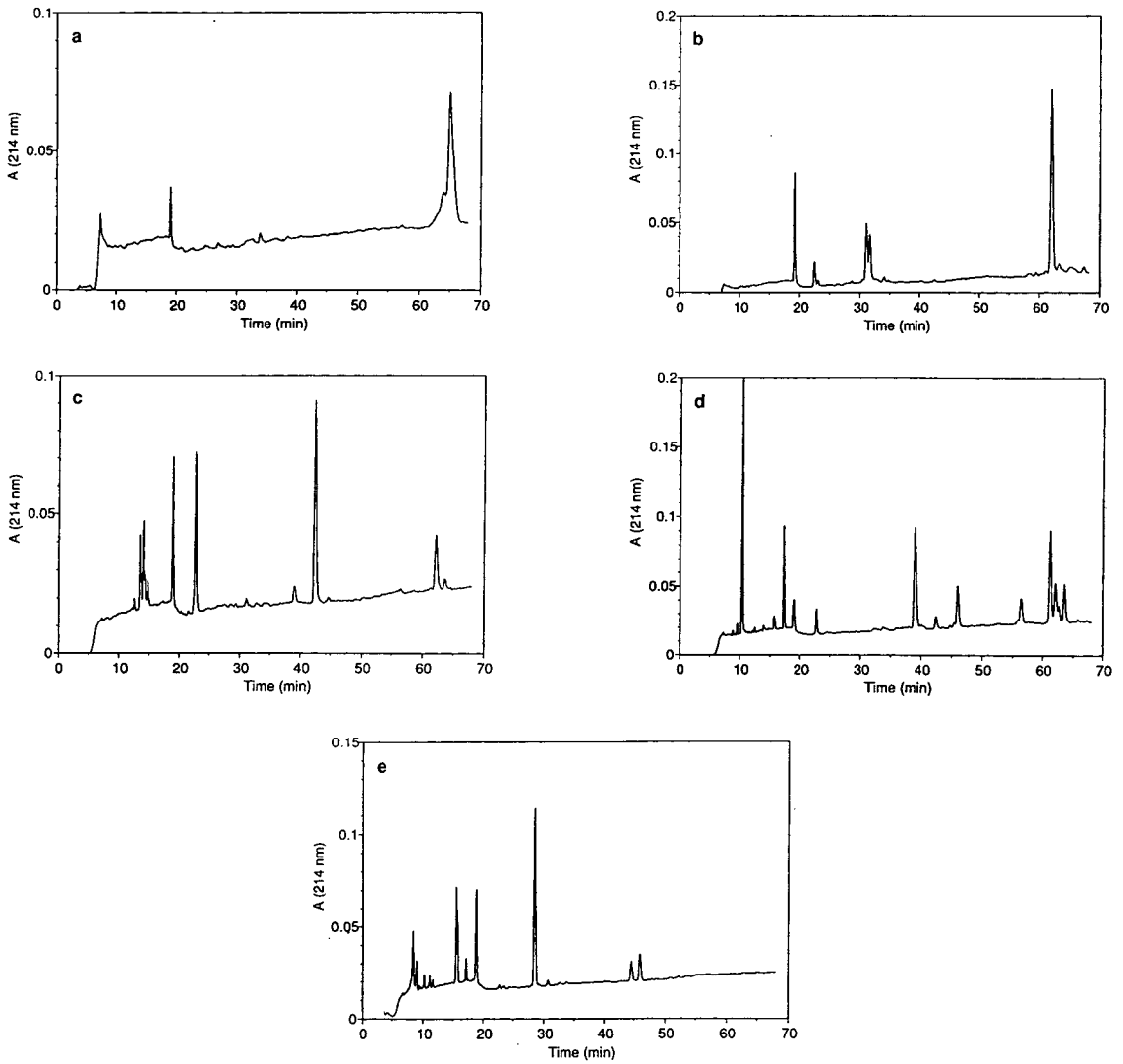

Fig. 2. RPLC of collected fractions 1–5 (a–e) from SEC of the tryptic digest of EC-SOD (Fig. 1b). Fractions collected in Fig. 1b were concentrated in a speed-vac and 20–50% of the pool was loaded onto the column. The gradient started by a linear increase from 0–15% acetonitrile in water in the first 15 min followed by a linear increase from 15–27% acetonitrile from 15–65 min and thereafter a steep increase up to 60% acetonitrile in one min. The column was thereafter washed and re-equilibrated. Both the water and the acetonitrile contained 0.1% TFA.

run is restricted. Therefore, it may be necessary to run the sample several times to collect amounts sufficient for analysis. The spiking technique used here is in many respects superior to the collection technique. The amount needed for this identification was minimal. This is a very powerful method that has also been used by others for the identification of peaks in electropherograms [22,23]. Fractions eluting very closely together can be identified, something which is very difficult otherwise, even if the reproducibility of the system is high. Since the

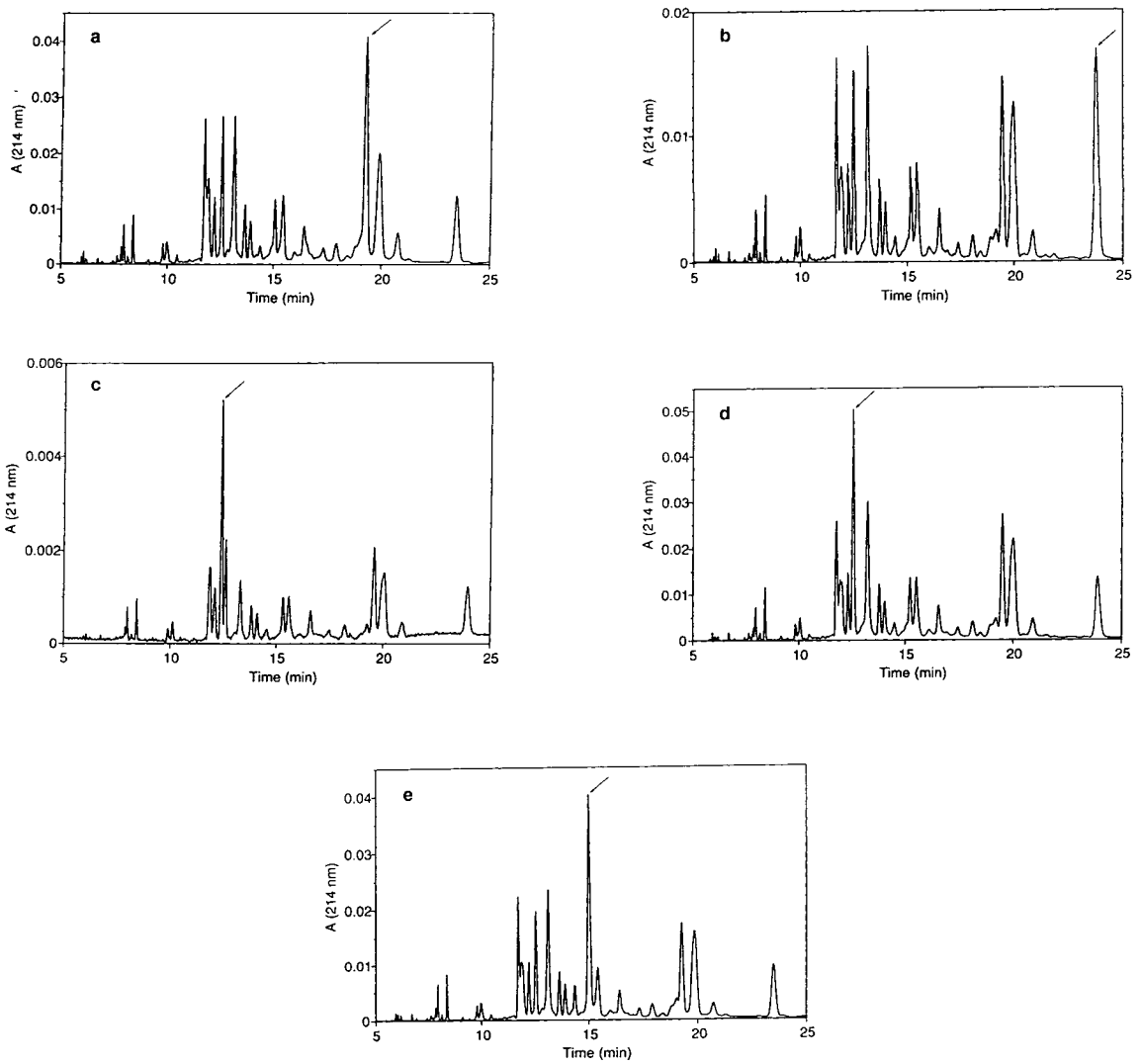

Fig. 3. Capillary electrophoresis of the tryptic digest of EC-SOD spiked with some of the identified peptides collected from the reversed-phase chromatographies described in Fig. 2. The EC-SOD digest (2–10 μg) was spiked with an amount of the purified peptide to obtain approximately twice the peak height of that particular peak in the chromatogram. The elution of the spiked peptide is indicated with an arrow. The digest was spiked with (a) fragment T1, (b) fragment T3, (c) fragment T6, (d) fragment T11 and (e) fragment T15.

particular fragment that is used for spiking is mixed with the total digest before electrophoresis, comigration is a very convincing evidence for identity, especially when only major fragments of the digest are used for spiking. In Fig. 3 the variation in the elution also can be seen. The elution time of the individual peaks varies too much between runs to make it possible to collect peaks with accuracy despite that the system was well equilibrated. By using the spiking technique

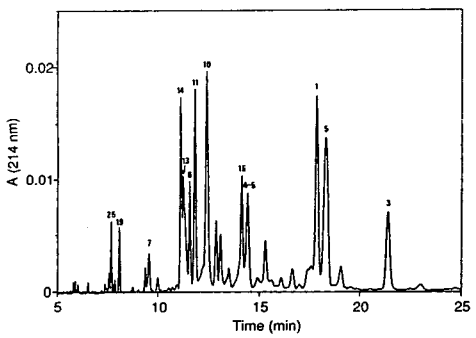

Fig. 4. The capillary electropherogram earlier shown in Fig. 1c with all identified peptides marked. The peptides were identified using the technique shown in Fig. 3 and are named according to the T-numbers they are given in Table 1.

this problem was overcome and most of the peptides could be identified in the electropherogram (Fig. 4).

4. Acknowledgements

The author acknowledges the excellent technical assistance of Helen Fält and Thord Johansson as well as the financial support of Symbicom AB.

5. References

[1] R.L. Garnick, N.J. Solli and P.A. Papa, *Anal. Chem.*, 60 (1988) 2546.
[2] E.A. Carrey, in T.E. Creighton (Editor), *Protein structure: a practical approach*, IRL Press, Oxford, 1989, p. 117.
[3] D.W. Cleveland, S.G. Fischer, M.W. Kirschner and U.K. Laemmli, *J. Biol. Chem.*, 252 (1977) 1102.
[4] R.E. Stephens, *Anal. Biochem.*, 84 (1978) 116.
[5] W.S. Hancock, C.A. Bishop, R.L. Prestidge and M.T.W. Hearn, *Anal. Biochem.*, 89 (1978) 203.
[6] F.E. Regnier, *LC·GC*, 5 (1987) 100.
[7] F.E. Regnier, *LC·GC*, 5 (1987) 230.
[8] J.W. Jorgenson and K.D. Lukacs, *J. High Resolut. Chromatogr. Chromatogr. Commun.*, 4 (1981) 230.
[9] Z. Deyl and R. Struzinsky, *J. Chromatogr.*, 569 (1991) 63.
[10] W.G. Kuhr and C.A. Monnig, *Anal. Chem.*, 64 (1992) 389R.
[11] K.A. Cobb and M. Novotny, *Anal. Chem.*, 61 (1989) 2226.
[12] R.G. Nielsen and E.C. Rickard, *J. Chromatogr.*, 516 (1990) 99.
[13] K.A. Cobb and M.V. Novotny, *Anal. Chem.*, 64 (1992) 876.
[14] J. Frenz, S.L. Wu and W.S. Hancock, *J.Chromatogr.*, 480 (1989) 379.
[15] M.M. Bushey and J.W. Jorgenson, *Anal. Chem.*, 62 (1990) 161.
[16] M.M. Bushey and J.W. Jorgenson, *Anal. Chem.*, 62 (1990) 978.
[17] J.P. Larmann Jr., A.V. Lemmo, A. W. Moore Jr. and J.W. Jorgenson, *Electrophoresis*, 14 (1993) 439.
[18] H. Yamamoto, T. Manabe and T. Okuyama, *J. Chromatogr.*, 515 (1990) 659.
[19] M. Strömqvist, J. Holgersson and B. Samuelsson, *J. Chromatogr.*, 548 (1991) 293.
[20] K. Hjalmarsson, S.L. Marklund, Å. Engström and T. Edlund, *Proc. Natl. Acad. Sci. U.S.A.*, 84 (1987) 6340.
[21] W.M.A. Niessen, U.R. Tjaden and J. van der Greef, *J. Chromatogr.*, 636 (1993) 3.
[22] T.E. Wheat, P.M. Young and N.E. Astephen, *J. Liq. Chromatogr.*,14 (1991) 987.
[23] M. Castagnola, L. Cassiano, R. Rabino, D.V. Rossetti and F.A. Bassi, *J. Chromatogr.*, 572 (1991) 51.

ELSEVIER

Journal of Chromatography A, 667 (1994) 311–315

JOURNAL OF CHROMATOGRAPHY A

Short Communication

Chromatographic evaluation of the binding of lysozyme to poly(dimethyldiallylammonium chloride)

Jiulin Xia[☆], Paul L. Dubin*

Department of Chemistry, Indiana University Purdue University at Indianapolis, Indianapolis, IN 46202-3274, USA

(First received September 29th, 1993; revised manuscript received January 5th, 1994)

Abstract

Size-exclusion chromatography on Superose columns was used to examine the binding of lysozyme to a strong polycation, poly(dimethyldiallylammonium chloride). A modified Hummel–Dreyer method was employed to determine the number of protein molecules bound per polymer chain as a function of protein concentration, in 0.325 *M* buffer, at pH 9.0. Even though this pH is smaller than the isoelectric point, the protein binds to this polycation. The binding data could be fit to Hill's equation, and the resulting fitting parameters indicate that the binding is cooperative.

1. Introduction

Proteins interact strongly with natural and synthetic polyelectrolytes mainly through electrostatic forces. These forces may lead to the formation of soluble complexes [1,2], complex coacervates [3–6] and amorphous precipitates [7–9]. The practical consequences of these phase changes may include (a) the use of polyelectrolytes for protein separation [10–12], (b) immobilization or stabilization of enzymes in polyelectrolyte complexes [13] and (c) the modification of protein-substrate affinity [14]. Such phenomena are also undoubtedly significant in the cell, where the Coulombic association of DNA with basic histones leads to the collapse of the nucleic acid and where basic polypeptides such as polylysine are thought to profoundly influence DNA behavior. Similar electrostatic interactions between proteins and nucleic acid are likely to play a role in the transcription process [15].

We have been investigating the interaction between polyelectrolytes and proteins [16–19] particularly in regard to the mechanism of the complex formation and complex composition. For the complexation of bovine serum albumin (BSA), ribonuclease and lysozyme with both polycations and polyanions, in solutions of moderate ionic strength, Dubin and co-workers [16,19] proposed formation of non-stoichiometric soluble complexes prior to phase separation. Kokufuta *et al.* [20], employed colloidal titration to study complexation between human serum albumin (HSA) and poly(dimethyldiallylammonium chloride) (PDMDAAC) and potassium poly(vinyl alcohol sulfate) (KPVSD) in pure water. Titrating the protein with the polyelectrolytes, they found turbidity maxima (referred to as end points) corresponding to conditions under which the mole numbers of quaternary

* Corresponding author.

☆ Present address: Life Technologies, Inc., P.O. Box 6009, Gaithersburg MD 20884-9980, USA.

0021-9673/94/$07.00
SSDI 0021-9673(94)00053-C

ammonium groups in PDMDAC and sulfates groups in KPVS were approximately identical to the contents of the acidic and basic groups in HSA. Therefore, it was concluded that complexation between HSA and PDMDAC and KPVS involves "stoichiometric" binding.

The stoichiometric structure of protein–polyelectrolyte complexes has been studied by methods such as sedimentation [14,21], X-ray scattering [14], light scattering [23] and size-exclusion chromatography (SEC) [17,24]. Among these methods, the former three are rather complicated with regard to both technique and the requirements of special equipment. In SEC, the relatively simple so-called Hummel–Dreyer (HD) method [25] may be used to determine the binding of one solute ("ligand") to a larger one, from which it is resolved chromatographically. However, the application of the HD method to the study of protein–polymer complexation is quite recent [17,24] and relatively underutilized. In this study, we use the HD method to study the association behavior of lysozyme with poly(dimethyldiallylammonium chloride).

2. Experimental

2.1. Materials

Poly(dimethyldiallylammonium chloride), a commercial sample "Merquat 100" with nominal molecular mass (M_r) of $2 \cdot 10^5$ and polydispersity of $M_w/M_n \approx 10$ (M_w = weight-average molecular weight, M_n = number-average molecular mass) was obtained from Calgon (Pittsburgh, PA, USA). The commercial sample was fractionated via SEC prior to use. The fractionation of PDMDAAC was carried out using a mobile phase of 0.5 *M* $NaNO_3$ buffered with 25 m*M* NaOAc of pH 6.5, which has been found to sufficiently repress adsorption effects. A 40.0-mg amount of polymer was applied to a Sephacryl S400 gel column via a 2.0-ml sample loop. The mobile phase was eluted through the column at a velocity of 2.0 ml/min, and the eluent was monitored using a R401 differential refractometer (Waters). The injected sample was separated into 30 fractions, collected at 4.8-ml intervals following the beginning of sample elution. The fraction with M_r of $1.97 \cdot 10^5$ and $M_w/M_n = 1.2$, characterized by light scattering and SEC, is used in this study. Lysozyme was obtained from Sigma as 95–99% pure with a p*I* of 11.0. All salts used in the present work were analytical-reagent grade and obtained from Sigma. Distilled and deionized water was used in all experiments.

2.2. Turbidimetric titration

Turbidimetric titrations were carried out at 22°C in solutions of the desired ionic strength. A 2-ml micro-buret (Gilmont) was used to deliver titrant (0.10 *M* NaOH) and the turbidity was followed with a Brinkmann PC600 probe colorimeter (420 nm, 2 cm pathlength). Solutions were always stirred, and turbidity values were obtained after several minutes of stabilization. In "type I" titrations NaOH was added to an initial solution of PDMDAAC, lysozyme and NaCl at a pH around 6. A pH electrode connected to Beckmann Φ34 pH meter was used to monitor pH change during the titration and the turbidity was recorded as a function of pH.

2.3. Size-exclusion chromatography

SEC was carried out on an apparatus comprised of a Minipump (Milton Roy), a Model 7012 injector (Rheodyne) equipped with a 100-μl sample loop, an R401 differential refractometer (Waters), and a Model 120 UV detector ($\lambda = 254$ nm) (Gilson). A Superose-6 column (30 cm × 1 cm OD) (Pharmacia) was eluted at 0.34 ml/min. Column efficiency, determined with acetone, was at least 12 000 plates/m.

Injections were performed in mobile phase of 0.325 *M* ionic strength (*I*) and pH 9.0, under which conditions PDMDAAC and lysozyme form soluble complexes. To determine complex stoichiometry, we have used the HD method. HD experiments were carried out employing 0.25 *M* NaOAc buffer as mobile phase, and the protein concentration in the mobile phase varied from 0.09 to 0.66 g/l. Higher protein concentrations could not be used because of a loss of detector sensitivity at high optical density. Poly-

mer samples (2.0 g/l) were filtered by Gelman 0.2-μm syringe filters before injection.

3. Results and discussion

Fig. 1 shows a Type 1 turbidimetric titration curve of PDMDAAC at polymer concentration of 0.06 g/l in 0.5 g/l lysozyme solution, in 0.325 *M* NaCl. The titration curve displays an abrupt increase in turbidity at pH 11.4, about 0.4 pH units above the isoelectric point of lysozyme, corresponding to colloidal complex formation. Prior to colloid formation, we observe a *ca.* 1% turbidity increase at pH 8.2 for the polymer–protein solution. This small turbidity increase is due to the initial formation of the soluble complex: particles with a size (35–46 nm) larger than either lysozyme (5 nm) or PDMDAAC (25 nm) are detected at this pH by quasielastic light scattering [19]. It is also interesting that the soluble complex is formed at conditions where the protein has the same charge sign as the polymer. This has been interpreted as arising from the existence of non-uniform charge distribution or "surface charge patches" on the protein [19].

The HD SEC method was used to evaluate the binding of lysozyme to PDMDAAC at $I = 0.325$ *M*, $8.5 < \mathrm{pH} < 10$, conditions under which soluble complexes are formed (see Fig. 1). PDMDAAC was injected onto an SEC column in which the mobile phase is a buffer, adjusted to the desired pH and ionic strength, and containing some appropriate concentration of lysozyme. As an example, a UV (254 nm) chromatogram resulting from the injection of PDMDAAC into a mobile phase of pH 9.20, 25 m*M* $Na_2B_4O_7$ and 0.25 *M* NaCl buffer, containing 0.093 g/l lysozyme, is displayed in Fig. 2. The initial UV-absorbing peak is observed at a smaller elution volume than that of protein alone, and must correspond to soluble complex. Its elution volume, 17.9 ml, is found to be independent of the protein concentration over the range studied. This result is consistent with highly cooperative binding (see below). Based on a calibration of the SEC column with pullulan standards, the apparent hydrodynamic radius $R_{SEC(pul)}$ of the complex is quite small, about twice the diameter of the protein. However, it is unlikely that the retention of the complex is free of solute-packing interaction effects; indeed, the very small $R_{SEC(pul)}$ observed for PDMDAAC (upper trace) is strong evidence for adsorption of the polycation. Interpretation of retention volumes in terms of size are therefore inappropriate.

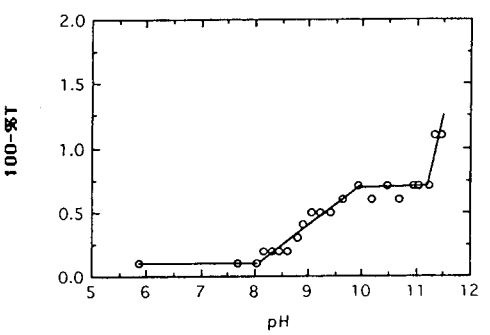

Fig. 1. Type I turbidimetric titration of 0.06 g/l PDMDAAC and 0.5 g/l lysozyme in 0.325 *M* NaCl, showing pH-dependence of % transmittance.

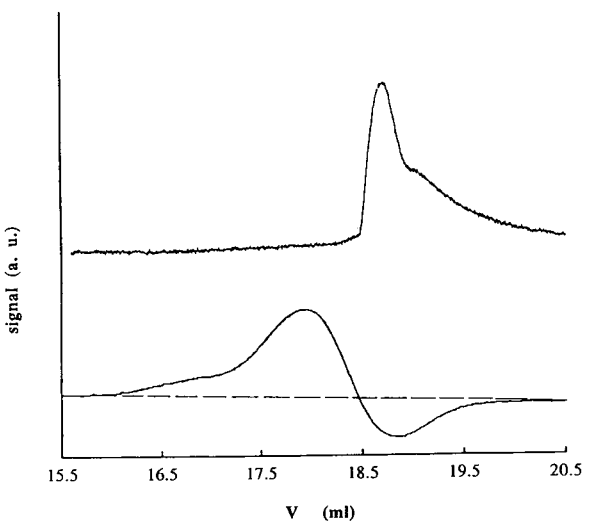

Fig. 2. UV (254 nm) chromatogram (Superose 6) of PDMDAAC in mobile phase comprised of 0.25 *M* NaCl + 25 m*M* $Na_2B_4O_7$, pH 9.2 buffer, containing 0.093 g/l lysozyme. Broken line shows baseline used for peak integration. For purposes of comparison, the chromatogram of PDMDAAC in protein-free mobile phase (monitored by refractive index) is shown above. Note that PDMDAAC itself is UV-inactive and so makes no contribution to the lower chromatogram.

In addition to the positive peak for the complex, one also sees the loss of protein from the mobile phase, as evidenced by the negative peak at the retention volume of lysozyme (*ca.* 18.9 ml). The area under this peak is proportional to the amount of protein bound to the injected polymer sample. The width of the two peaks may be in part a manifestation of some degree of adsorption of solutes on the column, as noted above, which at this pH surely bears some negative surface charge (although one cannot exclude the possible contribution of slow exchange between free and bound protein as a contributing effect). The moderate ionic strength of the mobile phase would be expected to diminish, but not eradicate such adsorptive band spreading. Even though the chromatographic peaks are larger than would be expected —at least for the unbound protein— the separation was sufficient to allow for quantitation of bound protein.

At $I = 0.325$ (25 m*M* $Na_2B_4O_7 + 0.25$ *M* NaCl), the amounts of protein corresponding to the negative peak area were determined from a calibration plot of peak area *vs.* protein concentration. The broken line in Fig. 2 illustrates the extrapolation of the baseline required for determination of the peak areas. Various detector level sensitivities were employed at different protein concentrations in order to optimize the accuracy of this measurement. Two injections were made for each protein concentration and the results were virtually identical in all cases. These results were used to calculate the degree of binding n, the molar ratio of bound lysozyme to polymer, *i.e.*, the number of protein molecules bound per polymer chain. Shown in Fig. 3 is n as a function of lysozyme concentration, obtained at $I = 0.325$ and pH 9.20.

In general, binding of ligands to macromolecules can be described by Hill's equation [22]

$$n = \frac{[L]_{bound}}{[P]} = \frac{c_1[L]^z}{1 + c_2[L]^z} \quad (1)$$

where n is the degree of binding, [L] is the free protein concentration, $[L]_{bound}$ is the bound protein concentration and [P] is the total polymer concentration, and c_1 and c_2 are constants related to the intrinsic binding constant and the number of sites. z is an empirical exponent, called Hill's coefficient. The quantity z is a measure of cooperativity; if $z = 1$, non-cooperativity is observed, *i.e.*, a single binding constant governs the independent binding of all ligands. If $z > 1$, the binding is cooperative, which means that the second ligand binds more readily than the first. If $z < 1$, then the binding is anti-cooperative.

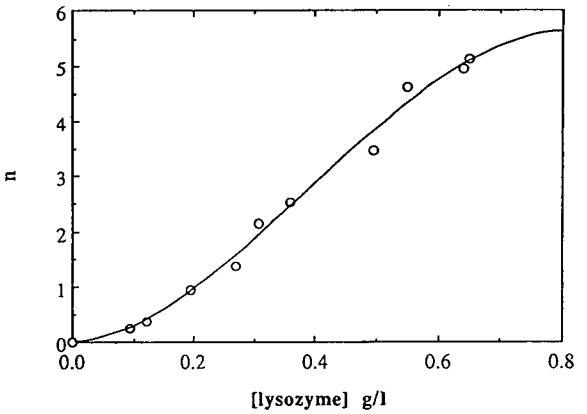

Fig. 3. Degree of binding n as a function of mobile phase lysozyme concentration ($I = 0.325$, pH 9.2, PDMDAAC concentration = 2.0 g/l). The solid line corresponds to Eq. 1 with $z = 2$.

In cooperative or anti-cooperative binding, the initial binding usually induces a conformation change in the macromolecule, thus affecting subsequent binding. For non-cooperative binding, c_1 and c_2 are identical to the binding constant. In the case of cooperative binding, c_1 and c_2 have no clear-cut physical definition because the overall cooperative binding constant is a function of both the intrinsic binding constant and the number of binding sites. The case dealt with here is of course more complicated than the model underlying Eq. 1 inasmuch as the polymer itself is capable of drastic conformational change accompanying the binding of the ligand —lysozyme— and the binding sites are not particularly well-defined. Nevertheless, the Hill equation may be considered a zeroth-order approach to analysis of the current binding results.

The binding data in Fig. 3 are fitted to Eq. 1, as shown by the solid curve, yielding $c_1 = 29.2$, $c_2 = 3.5$ and $z = 2$. The value of z suggests a cooperative association between lysozyme and PDMDAAC at the conditions of this study. On the other hand, the number of proteins bound per polymer chain at saturation conditions is only 6, which is considerably less than values found for other protein-polyelectrolyte pairs, such as BSA-PDMDAAC [23]. This may be a reflection of the strong repulsive electrostatic interactions that arise when lysozyme, at pH < pI, is complexed with a strong polycation. It is somewhat surprising that, despite these repulsive interactions, the binding is nevertheless cooperative. One possibility is that extension of the polymer chain upon binding enhances the binding of subsequence proteins. Such chain expansion during protein binding to a polyelectrolyte has been observed elsewhere [23].

In summary, we have shown, by both turbidimetric titration and HD SEC, the existence of stable, soluble complexes formed by lysozyme and PDMDAAC in pH 9.2 and $I = 0.325$ M supporting electrolyte. The binding of lysozyme to PDMDAAC to form soluble complexes is cooperative.

4. Acknowledgements

This research was supported by grants from the National Science Foundation (CHE-9021484); American Chemical Society (ACS-PRF 25532-AC7B); Eli Lilly Company, and the Exxon Education Fund.

5. References

[1] D. Sacco, F. Bonneaux and E. Dellacherie, *Int. J. Biol. Macromol.*, 10 (1988) 305.
[2] E. Dellacherie, *Am. Chem. Soc., Div. Polym. Chem. Prepr.*, 32 (1991) 602; and references cited therein.
[3] T. Lenk and C. Thies, in A. Eisenberg and F.E. Bailey (Editors), *Coulombic Interactions in Macromolecular Systems*, American Chemical Society, Washington, DC, 1987, Ch. 8.
[4] P. Dubin, T.D. Ross, I. Sharma and B. Yegerlehner, in W.L. Hinz and D.W. Armstrong (Editors), *Ordered Media in Chemical Separations*, American Chemical Society, Washington, DC, 1987, Ch. 8.
[5] A. Veis, *Am. Chem. Soc., Div. Polym. Chem. Prepr.*, 32 (1991) 596; and references cited therin.
[6] D.J. Burgess and J.E. Carless, *J. Colloid Interface Sci.*, 98 (1984) 1.
[7] T.Q. Nguyen, *Makromol. Chem.*, 187 (1986) 2567.
[8] M. Sternberg and C. Hershberger, *Biochim. Biophys. Acta*, 342 (1974) 195.
[9] E. Kokufuta, H. Shimizu and I. Nakamura, *Macromolecules*, 14 (1981) 1178.
[10] A.G. Bozzano, G. Andrea and C.E. Glatz, *J. Membr. Sci.*, 55 (1991) 181.
[11] K.M. Clark and C.E. Glatz, *Biotechnol. Prog.*, 3 (1987) 241.
[12] R.R. Fisher and C.E. Glatz, *Biotechnol. Bioeng.*, 32 (1988) 777.
[13] A. Margolin, S.F. Sheratyuk, V.A. Izumrudov, A.B. Zezin and V.A. Kabanov, *Eur. J. Biochem.*, 146 (1985) 625.
[14] K. Ruckpoul, H. Rein, G.R. Janig, W. Pfeil, O. Ristau, B. Damaschun, H. Damaschun, J.J. Muller, H.V. Purschel, J. Bleke and W. Scheler, *Stud. Biophys.*, 34 (1972) 81.
[15] S.L. Shaner, P. Melancon, K.S. Lee, R.R. Burgess and M.T. Record, Jr., *Cold Spring Harbor Symp. Quant. Biol.*, 47 (1983) 463.
[16] J.M. Park, B.B. Muhoberac, P.L. Dubin and J. Xia, *Macromolecules*, 25 (1992) 290.
[17] M.A. Stege, P.L. Dubin, J.S. West and C.D.D. Flinta, in M. Ladisch, R.C. Willson, C.C. Painton and S.E. Builder (Editors), *Protein Purification: from Molecular Mechanisms of Large-Scale Processes*, American Chemical Society, Washington, DC, 1990, Ch. 5.
[18] P.L. Dubin and J.M. Murrell, *Macromolecules*, 21 (1988) 2291.
[19] J. Xia, P. Dubin, B.B. Muhoberac, Y.S. Kim and V.J. Klimkowski, *J. Phys. Chem.*, 97 (1993) 4528.
[20] E. Kokufuta, H. Shimizu and I. Nakamura, *Macromolecules*, 15 (1982) 1618.
[21] V.A. Kabanov and A.B. Zezin, *Makromol. Chem. Suppl.*, 6 (1984) 259.
[22] A.V. Hill, *J. Physiol.*, 40 (1910) 190.
[23] J. Xia, P.L. Dubin and H. Dautzenberg, *Langmuir*, 9 (1993) 2015.
[24] V. Bargerousse, D. Sacco and E. Dellacherie, *J. Chromatogr.*, 369 (1986) 244.
[25] J.P. Hummel and W.J. Dreyer, *Biochim. Biophys. Acta*, 63 (1962) 530.

ELSEVIER

Journal of Chromatography A, 667 (1994) 316–321

JOURNAL OF CHROMATOGRAPHY A

Short Communication

Comparison of extraction procedures for high-performance liquid chromatographic determination of cellular deoxynucleotides

Sarah Palmer[a], Susan Cox*[,a,b]

[a]*Department of Clinical Virology, Karolinska Institute, S-141 86 Huddinge, Sweden*

[b]*Virology Department, Swedish Institute for Infectious Disease Control, Karolinska Institute, S-105 21 Stockholm, Sweden*

(First received October 8th, 1993; revised manuscript received January 18th, 1994)

Abstract

For the determination of cellular deoxynucleoside triphosphates (dNTPs) by high-performance liquid chromatography, the choice of extracting agent and periodate oxidation procedure is important for accurate results. Different extraction methods were compared using either cold methanol or trichloroacetic acid for extraction of dNTPs from lymphoblastoid cells. The recoveries of the dNTPs varied with the different extraction methods. A modification of the periodate oxidation procedure for degrading ribonucleoside triphosphates to their bases was also compared with the original method. Both methods gave accurate results when trichloroacetic acid was used as extracting agent, but when methanol was used interfering peaks were present on the chromatogram when the original method was used. These peaks were absent when the modified periodate procedure was used.

1. Introduction

The determination of cellular deoxynucleoside triphosphates (dNTPs) is important for the study of drugs interfering with DNA synthesis. Several anti-human immunodeficiency virus (anti-HIV) drugs are nucleoside analogues and compete with cellular deoxynucleosides for phosphorylation. The triphosphate form of the drug can be incorporated into the viral DNA strand and terminate viral replication [1]. The levels of cellular dNTPs and nucleoside analogue triphosphates are therefore crucial for the antiviral activity.

The levels of cellular dNTPs are usually measured by high-performance liquid chromatography (HPLC) [2–4]. The choice of extraction procedure for the HPLC of dNTPs from cell extracts is important for accurate quantification. Acid extraction of nucleotides using trichloroacetic acid (TCA) or perchloric acid and subsequent neutralization is often used [5–7]. However, some nucleoside analogues such as 2′,3′-dideoxyinosine (ddI) are acid labile, which makes TCA unsuitable as the extracting agent for determining intracellular levels of ddI nucleotides.

We compared different extraction methods based on cold 60% methanol (instead of TCA) for the extraction of cellular deoxynucleotides for HPLC analysis. The recoveries of standard dNTPs were compared with those obtained when TCA was used for extraction.

* Corresponding author. Address for correspondence: Swedish Institute for Infectious Disease Control, Karolinska Institute, S-105 21 Stockholm, Sweden.

0021-9673/94/$07.00
SSDI 0021-9673(94)00063-F

Before cellular deoxynucleotides can be determined by HPLC, the large amounts of ribonucleotides present in the cell extracts must be removed by selective degradation. Two different procedures for the degradation of ribonucleotides by periodate oxidation prior to HPLC analysis have been published [2,8]. We compared these two procedures with the different extraction methods. The procedure of Tanaka *et al.* [8] was superior when methanol was used as the extracting agent, but either procedure was suitable when TCA was used.

2. Experimental

2.1. Chemicals

Pure nucleotides were purchased from Sigma (St. Louis, MO, USA).

2.2. Chromatographic equipment

All HPLC analyses were done on a chromatograph from Gilson Medical Electronics equipped with a dual-wavelength spectrophotometer programmed to measure absorbance at 254 and 280 nm. All integration was performed on a Macintosh Classic II computer using Rainin Dynamax HPLC method manager software.

2.3. Chromatographic procedure

Nucleotides were separated on a strong anion-exchange column (Partisil 10 SAX, 250 × 4.6 mm I.D.) (Whatman, Clifton, NJ, USA) using phosphate buffer gradient elution. The two buffers used were 0.02 *M* potassium phosphate (pH 3.5) (buffer A) and 0.80 *M* potassium phosphate (pH 3.5) (buffer B). The gradient was completed in four steps. Step 1 was 100% buffer A for 5 min; step 2 was a 30-min linear increase in buffer B to 100%; step 3 was a constant isocratic 20-min delivery of 100% buffer B; and in step 4 buffer B was decreased to 0% in 10 min. A constant flow-rate of 1.3 ml/min was used throughout.

2.4. Cell harvesting procedure

CEM cells (a human CD4+ lymphoblastoid cell line) were grown at 37°C in a humidified atmosphere of 5% CO_2 in air in RMPI 1640 medium containing 10% heat-inactivated foetal calf serum, penicillin, streptomycin and pyruvate. Cells ($0.9 \cdot 10^8$–$1.3 \cdot 10^8$) were harvested by centrifugation at 1000 *g* for 10 min. The supernatant was decanted and the cell pellet was further drained by inverting the tube on tissue paper for 30 s. For comparison of extraction procedures, cells from the same batch were divided into aliquots for use with the different procedures.

2.5. Methanol extraction procedures

Four different methanol extraction methods were compared. To measure deoxynucleotide recoveries, the cell pellets ($0.9 \cdot 10^8$–$1.3 \cdot 10^8$ cells) were "spiked" with high concentrations (0.05 μmol) of deoxynucleoside triphosphate (dNTP) standards (dATP, dGTP, dCTP, dTTP) in a large excess of intracellular dNTP concentrations. The high concentrations of standards compared with cellular dNTPs is necessary to ensure that the cellular dNTPs present do not contribute significantly to the recoveries measured, thereby giving a falsely high recovery. Also, measuring the recovery of spiked cell extracts rather than of pure solutions of dNTPs gives an indication of losses due to protein binding.

In method 1, 1 ml of cold 60% methanol was added to the "spiked" cell pellet and this mixture was vortex mixed for 20 s. After a 5-min incubation on ice, the sample was mixed again. Cell matter was removed by centrifugation at 1000 *g* for 10 min. The supernatant was carefully removed with a Pasteur pipette and placed on ice. While maintaining the sample on ice, the methanol was reduced to half the volume by evaporation under nitrogen. The sample was then held at −86°C until frozen, followed by

freeze-drying at −50°C overnight. The dried sample precipitate was dissolved in 0.5 ml of cold distilled water and frozen at −20°C until use. The evaporation and freeze-drying steps were necessary to remove the methanol before ion-exchange HPLC could be performed.

Method 2 was the same as method 1 but instead of evaporation, the methanol was diluted by adding 500 μl of distilled water. The sample was then frozen and freeze-dried. This method was used to investigate whether large amounts of dNTPs were lost in the evaporation process.

We investigated whether using a larger volume of methanol for extraction would give a better recovery of dNTPs. In Method 3, 2.5 ml of cold 60% methanol was added to the "spiked" cell pellet and, after mixing, the pellet was left overnight in a freezer at −20°C. Mixing, centrifugation, evaporation and freeze-drying were then followed as in method 1.

Finally, we tried using a larger volume of methanol for extraction, but without evaporation. Method 4 used 2.5 ml of cold 60% methanol and overnight extraction as in method 3. After mixing and centrifuging, the methanol supernatant was removed and diluted by adding 1.5 ml of distilled water. The sample was then frozen and freeze-dried.

2.6. Trichloroacetic acid extraction procedure

For comparison of recoveries with those of the methanol procedures, the cell pellets ($0.9 \cdot 10^8$–$1.3 \cdot 10^8$) were "spiked" with the same concentration (0.05 μmol) of dNTP standards. To these "spiked" cell pellets an equal volume (800 μl) of 12% trichloroacetic acid was added [9] and this solution was vortex mixed for 20 s. The sample was placed on ice for a further 10 min and then remixed. The sample was then centrifuged at 1000 *g* for 10 min to remove the precipitate. The supernatant was removed to a new tube and its volume measured (*ca.* 1 ml). To neutralize the pH of the sample, 1 ml of a fresh 0.5 *M* solution of tri-*n*-octylamine in Freon was added [3,10]. The sample was vortex mixed for 20 s and then centrifuged for 2 min at 1000 *g* to separate the phases. After centrifugation, the neutralized top aqueous layer containing the nucleotides (*ca.* 1 ml) was carefully removed and frozen at −20°C.

2.7. Periodate oxidation procedures

Two different periodate oxidation procedures for the degradation of interfering rNTPs were compared. Procedure 1 was as developed by Garrett and Santi [2]. To each thawed sample tube, 40 μl of a 0.5 *M* aqueous sodium periodate solution were added, gently mixed and then incubated at 37°C for 3 min. After incubation, 50 μl of a 4 *M* aqueous solution of methylamine (adjusted to pH 7.0 with phosphoric acid) were added. The sample was incubated at 37°C for a further 30 min. Following this second incubation, the reaction was terminated by the addition of 10 μl of a 1 *M* aqueous solution of rhamnose. The samples were stored at −20°C until used.

Procedure 2 was a modification of the procedure developed by Tanaka *et al.* [8]. To each thawed sample, 20 μl of a 5 m*M* aqueous solution of deoxyguanosine and 30 μl of a 0.5 *M* aqueous solution of sodium periodate were added. The sample was gently mixed and incubated at 37°C for 5 min. After this incubation, 40 μl of a 4 *M* aqueous solution of methylamine (adjusted to pH 7.0 with phosphoric acid) and 10 μl of a 1 *M* aqueous solution of rhamnose were added. The sample was gently mixed and incubated at 37°C for a further 30 min. The samples were stored at −20°C until used.

2.8. HPLC analysis

A 100-μl volume of all 'spiked" cell extracts was injected into the HPLC system. For both "spiked" and "unspiked" cell extract samples, the dNTPs were identified by their retention times and the ratio of absorbance at 254 nm to that at 280 nm. Recoveries were calculated by comparisons of the peak areas of injected samples with those of pure dNTP standards with known concentrations.

3. Results and discussion

3.1. Comparison of extraction methods

We compared the four different extraction methods using cold 60% methanol and TCA for the extraction of standard dNTPs from spiked cell extracts. The recoveries of standard dNTPs from cells extracted using the different methods are given in Table 1. Comparison of the recoveries shows that the third methanol extraction method, using a larger volume of methanol for extraction and evaporation on ice, gave the highest recoveries of all dNTPs. This indicates that evaporation of the methanol on ice did not cause a loss of dNTPs, and was preferable to dilution of the sample with water (methods 2 and 4). Also, the larger volume of methanol used for extraction in method 3 gave better recoveries than the smaller volume used in method 1. Of the dNTPs, dCTP and dGTP were the most labile and gave the lowest recoveries.

Although the nucleotide pools of extracts of various cells and tissues have been analysed by HPLC, the recovery of nucleotides after extraction has not always been investigated [4–6]. In other instances, standard solutions of pure dNTPs in water have been used for recovery experiments with TCA and periodate, giving slightly higher recoveries than those shown here for TCA [3,8]. We chose to use spiked cell extracts instead of pure solutions for recovery experiments, to reveal whether non-specific binding to cellular proteins could affect the recovery of nucleotides. The results indicate that non-specific binding of nucleotides in cell extracts may result in a lower recovery compared with pure solutions in water [3,8].

3.2. Comparison of periodate oxidation methods

Two different methods for periodate oxidation of rNTPs after methanol extraction of unspiked cells were compared, and chromatograms from each of the methods are shown in Fig. 1. The original periodate oxidation method developed by Garrett and Santi [2] revealed two problematic peaks (Fig. 1a), as described previously [8], one eluting close to dTTP and the other appearing as a shoulder on the dGTP peak. These extra peaks interfered with accurate quantification of the cellular dNTPs.

Fig. 1b shows the results of the modified procedure for oxidation of rNTPs according to Tanaka *et al.* [8]. The two interfering peaks are absent, allowing accurate measurement of cellular dNTP levels. When TCA was used as the extracting agent, however, these interfering peaks were not seen, and the two periodate

Table 1
Comparison of the recoveries of deoxynucleotides using different extraction procedures

dNTP	Mean recovery ± S.E.M. (%)				
	Methanol				TCA method
	Method 1	Method 2	Method 3	Method 4	
dCTP	67 ± 3.8	58 ± 7.3	78 ± 7.0	66 ± 3.4	65 ± 1.8
dTTP	81 ± 0.9	75 ± 3.6	92 ± 2.2	76 ± 2.4	71 ± 3.8
dATP	94 ± 5.9	86 ± 5.8	102 ± 4.7	81 ± 1.7	75 ± 1.9
dGTP	66 ± 6.2	62 ± 3.2	72 ± 5.1	55 ± 9.1	58 ± 2.6

CEM lymphocytes were harvested by centrifugation, spiked with standard dNTPs and extracted using four different procedures based on methanol and one based on trichloroacetic acid. The recovery of dNTPs was determined after periodate oxidation by ion-exchange HPLC. Means of three different experiments ± standard error of the mean (S.E.M).

Table 2
dNTP levels in CEM cells extracted with methanol or TCA

Extraction method	dNTP content (pmol/10^6 cells ± S.E.M.)			
	dCTP	dTTP	dATP	dGTP
Methanol method 3[a]	9.7 ± 1.4	21.9 ± 1.1	55 ± 1.0	8.5 ± 1.4
Methanol method 3[b]	5.4 ± 0.7	19.8 ± 2.2	41.6 ± 1.6	8.0 ± 0.5
TCA method[a]	6.9 ± 0.7	21.7 ± 3.3	33.7 ± 5.1	8.3 ± 1.1

CEM lymphocytes were harvested by centrifugation, extracted with methanol or TCA and subjected to periodate oxidation as described under Experimental. dNTPs were determined by ion-exchange HPLC. Means of three experiments ± S.E.M.
[a] Periodate oxidation according to the method of Garrett and Santi [2].
[b] Periodate oxidation according to the method of Tanaka *et al.* [8].

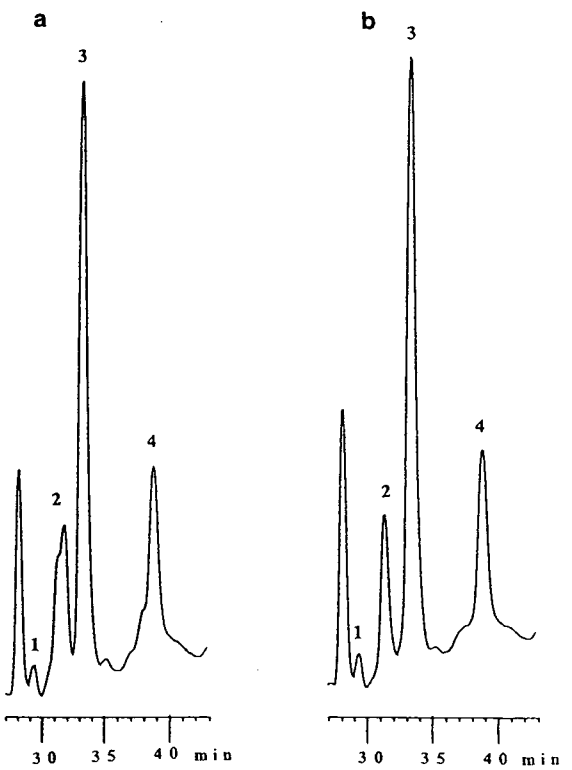

Fig. 1. Portion of the chromatogram showing absorbance at 254 nm obtained on HPLC of CEM cells extracted with methanol (method 3) after periodate oxidation according to (a) Garrett and Santi [2] or (b) Tanaka *et al.* [8]. Peaks: 1 = dCTP; 2 = dTTP and, in (a), an unknown compound; 3 = dATP; 4 = dGTP.

oxidation procedures gave identical chromatograms (data not shown).

3.3. Measurement of dNTPs in CEM cells

Following the results in Table 1, we compared the dNTP pools of unspiked CEM lymphoblastoid cells measured by HPLC after extraction with methanol or TCA, and the results are given in Table 2. Similar pools of dNTPs were measured with both extraction methods, indicating the methanol extraction of cells is a useful alternative to extraction with TCA.

In conclusion, we found that overnight extraction at −20°C with 2.5 ml of cold 60% methanol, followed by evaporation under nitrogen and freeze-drying, gave the best recoveries of dNTPs from CEM cell extracts. The modified periodate procedure of Tanaka *et al.* [8] gave superior results when methanol was used as extracting agent by removing interfering peaks, but did not confer advantages when TCA was used.

4. References

[1] J.-P. Sommadossi, *Clin. Infect. Dis.*, 16 (1993) S7.
[2] C. Garrett and D. Santi, *Anal. Biochem.*, 99 (1979) 268.

[3] S.-C. Chen, P. Brown and D. Rosie, *J. Chromatogr. Sci.*, 15 (1977) 218.
[4] C. Lim and T. Peters, *J. Chromatogr.*, 461 (1989) 259.
[5] M. Andersson, *Anal. Biochem.*, 174 (1988) 271.
[6] E. Brown, R. Newton and N. Shaw, *Anal. Biochem.*, 123 (1982) 378.
[7] J. Harmenberg, A. Karlsson and G. Gilljam, *Anal. Biochem.*, 161 (1987) 26.
[8] K. Tanaka, A. Yoshioka, S. Tanaka and Y. Wataya, *Anal. Biochem.*, 139 (1984) 35.
[9] J. Harmenberg, S. Cox and A. Åkesson Johansson, *J. Chromatogr.*, 508 (1990) 75.
[10] J. Khym, *Clin. Chem.*, 21 (1975) 1245.

ELSEVIER

Journal of Chromatography A, 667 (1994) 322–326

JOURNAL OF CHROMATOGRAPHY A

Short Communication

Application of centrifugal partition chromatography to the separation of Lauraceous alkaloids

Shoei-Sheng Lee

School of Pharmacy, National Taiwan University, 1 Jen-Ai Road Sec. 1, Taipei 100, Taiwan

(First received November 2nd, 1993; revised manuscript received January 17th, 1994)

Abstract

A thorough and facile separation of polar phenolic alkaloids from Lauraceous plants was achieved by application of centrifugal partition chromatography using $CHCl_3$–MeOH–H_2O (containing 0–1% HOAc) (2:2:1 or 5:5:3) as the delivery system, and subsequently in combination with conventional methods. This method solves the problems of low resolution and poor recovery in the application of general adsorption chromatography to the separation of polar phenolic alkaloids. The most polar alkaloid, laurolitsine, was isolated easily and several additional alkaloids were obtained from the investigation or reinvestigation of three Lauraceous plants.

Introduction

Lauraceous plants are widely distributed in Taiwan and it has been demonstrated that they are rich in isoquinoline alkaloids, especially of the aporphine type. The phenolic alkaloids are amphoteric natural products and hence are less stable and relatively polar. By using conventional adsorption chromatography to separate these compounds, two problems, poor resolution and poor recovery, are generally encountered. Reversed-phase liquid chromatography might be an alternative to solve the recovery problem. However, the low capacity, high cost and resolution problem need to be settled. Considering these, modern partition chromatographic techniques possessing the properties of high capacity and complete recovery were applied to resolve these problems. Among these, centrifugal partition chromatography (CPC) has the advantage of a high flow velocity, which greatly shortens the separation time [1]. We report here the results of the application of CPC to the separation and fractionation of the polar phenolic isoquinolines from three Lauraceous plants, *Litsea cubeba*, *Phoebe formosana* and *Neolitsea konishii*.

2. Experimental

2.1. Instrumentation and chemicals

The following instrumentation was used: for CPC, LLN Model, six preparative cartridges (Type 1000E, radius 11 cm), void volume 425 ml (Sanki Engineering, Nagaokakyo, Kyoto, Japan); for droplet counter-current chromatography) (DCCC), EYELA D.C.C.-A, 300 tubes (O.D. 0.5 cm, length 40 cm) (Tokyo Rikakikai, Tokyo, Japan); Chromatotron (a preparative centrifugally accelerated radial, thin-layer chromatograph), Model 7924T, coated with silica gel (Merck Kieselgel 60 PF_{254} gipshaltig, 2 mm thick) (Harrison Research, Palo Alto, CA,

0021-9673/94/$07.00
SSDI 0021-9673(94)00104-H

USA); TLC analytical system, silica gel TLC plate (Merck, 0.20 mm thick) with developing solvent systems (A) chloroform–methanol (9:1) and (B) acetone–toluene (3:2), both saturated with ammonia solution.

Ammonia solution (27%), glacial acetic acid, sodium hydroxide, bismuth subcarbonate and sodium iodide were purchased from Wako (Osaka, Japan). The last two reagents were used for preparing Dragendorff's reagent for detection of alkalodes. Other solvents were obtained locally and were distilled before use.

2.2. General procedure for extraction and separation of Lauraceous alkaloids

The dried and powdered plant material was extracted with MeOH or 95% EtOH. The alcoholic extract was triturated with citric acid (2%) or HOAc (2%). The combined acidic solution was partitioned with $CHCl_3$ to remove neutral or acidic components and was then adjusted to pH 9 with ammonia solution. In this process, the precipitate, if any, which generally contained laurolitsine (**1**) in several Lauraceous plants, was filtered. The filtrate was extracted with $CHCl_3$ and $CHCl_3$ layer, after drying over $MgSO_4$, was evaporated to give total free bases. The total alkaloids were divided into non-phenolic bases and phenolic bases by partitioning between $CHCl_3$ and NaOH (0.5 *M*).

By this procedure, the dried powdered stems of *Litsea cubeba* (Lour.) Persoon (8.50 kg) yielded non-phenolic bases (9.00 g) and phenolic bases (11.36 g) [2] and from 2.5 kg of roots 8.27 g of total free alkaloids were obtained. The dried, powdered roots of *Phoebe formosana* (Hayata) Hayata (10.5 kg) yielded non-phenolic bases (0.23 g), phenolic bases (15.5 g) and a precipitate (209 g, containing **1** as the major component) [3]. From the dried powdered stem woods (16.80 kg) of *Neolitsea konishii* (Hayata) Kanehira & Sasaki, non-phenolic alkaloids (0.58 g) and phenolic alkaloids (8.09 g) were obtained [4].

The phenolic fraction was subjected to CPC separation, 3.5–8.0 g in each run, using the upper layer (aqueous layer) and lower layer (organic layer) of chloroform–methanol–water (containing 0–1% of acetic acid) in the ratio of 2:2:1 or 5:5:3 (see Figs. 2–5) as mobile phase and stationary phase, respectively. The parameters set for optimum pressure (35–50 bar) were flow-rate 2.5–5.3 ml/min and centrifugal force 78.7–123.0 *g* (corresponding to 800–1000 rpm). The eluent was collected in 6.0–10.6-ml fractions. The fractions were monitored directly by TLC. The combined fractions were evaporated at 45°C under reduced pressure to remove the solvents and, if necessary, toluene or water was added to remove acetic acid azetropically. The fractions containing mixtures were further separated via a silica gel gravity column or flash column chromatography (Merck, 230–400 mesh) with sample–gel (1:40, w/w), or via preparative TLC plates (Merck, SiO_2, 1–2 mm thick, 20 × 20 cm) eluted with solvent A or B, or DCCC using the upper layer and lower layer of the solvent system $CHCl_3$–MeOH–1% HOAc (5:5:3) as mobile and stationary phase, respectively, at a flow-rate of 0.5 ml/min, or via the Chromatotron (2 mm thick) eluted with acetone–toluene (3:2) at a flow-rate of 4 ml/min. All the isolated alkaloids were characterized on the basis of spectral data and were found to be known bases.

3. Results and discussion

From the stem woods of *Litsea cubeba*, a novel phenanthrene alkaloid, litebamine, together with five known bases, liriotulipiferine, reticuline, boldine (**2**), N-methyllaurotetanine (**9**) and isocorydine (**10**), have been isolated [5–7]. *Phoebe formosana* is an abundant source of the aporphine laurolitsine [**1**, 0.84% (w/w) of the root] [8]. From the roots of *P. formosana*, two other phenolic bases, reticuline (**11**) and coreximine (**12**), were isolated [9]. Structures of all the compounds are shown in Fig. 1.

By using the reversed-phase partition model CPC with $CHCl_3$–MeOH–H_2O (containing 0–1% HOAc) (2:2:1 or 5:5:3; see Figs. 2–5) in the separation of phenolic alkaloids from *L. cubeba*, seven fractions from roots (Fig. 2) and eight fractions from stems (Fig. 3) were obtained.

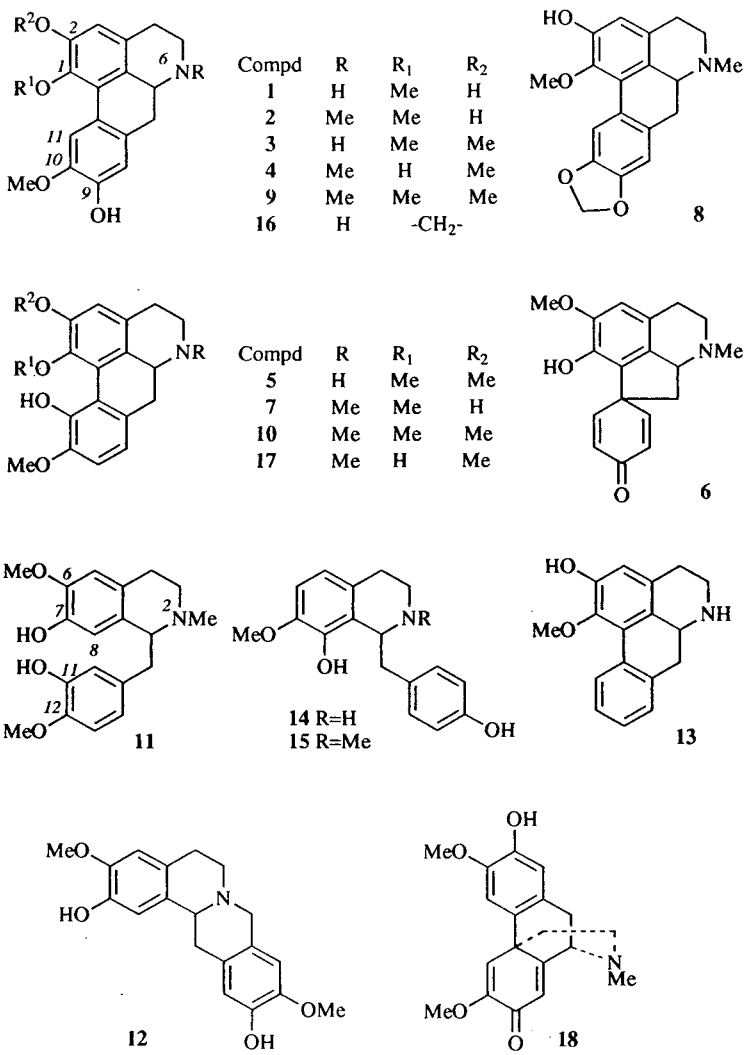

Fig. 1. Structures of compounds **1–18**.

Among these, **1** (fraction 1, Figs. 2 and 3), **2** (fraction 3, Fig. 3), norisocorydine (**5**) (fraction 6, Fig. 2) and **10** (fraction 8, Fig. 3) were directly obtained from these two separations as pure compounds. Similar treatment of the phenolic alkaloids from the roots of *P. formosana* yielded six fractions (Fig. 4). Of these, fraction 1 yielded the pure laurolitsine, appearing also as the major alkaloid.

From *L. cubeba*, six other known alkaloids, laurotetanine (**3**), isoboldine (**4**), glaziovine (**6**), N-methyllindcarpine (**7**), isodomesticine (**8**) and N-methyllaurotetanine (**9**), were isolated from the other fractions by the combination of flash column chromatography and preparative SiO_2 TLC [2]. Compounds **1** and **3–8** were isolated for the first time from this species. Similarly, four additional known phenolic bases, **3**, asimilobine (**13**), norjuziphine (**14**) and juziphine (**15**), in addition to the reported three, were separated from the root of *P. formosana* [3]. The last two benzylisoquinolines, **13** and **14**, were isolated for the first time from Lauraceous plants.

By application of this technique, we carried

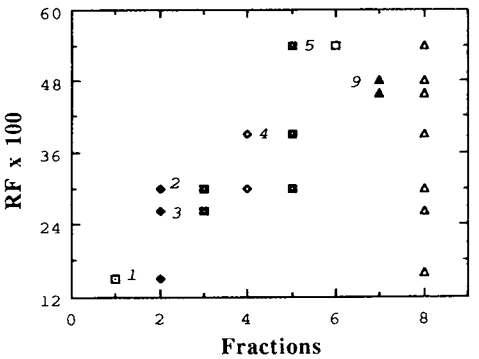

Fig. 2. TLC of fractions obtained by CPC separation of the phenolic alkaloids from the roots of *Litsea cubeba*. Sample: crude phenolic alkaloids (4.32 g). CPC conditions: $CHCl_3$–MeOH–0.5% HOAc (2:2:1); stationary phase, lower layer; mobile phase, upper layer; flow-rate, 4 ml/min; pressure, 40–42 bar; centrifugal force, 123.0 *g*; volume per tube, 10 ml. Fraction 1 (tubes 8–13), 407 mg; fraction 2 (tubes 14–23), 551 mg; fraction 3 (tubes 24–53), 2.63 g; fraction 4 (tubes 54–57), 445 mg; fraction 5 (tube 58), 82 mg; fraction 6 (tube 59), 73 mg; fraction 7 (tubes 60–69), 487 mg; 8 = sample. TLC developing system, solvent A; detection, Dragendorff's reagent.

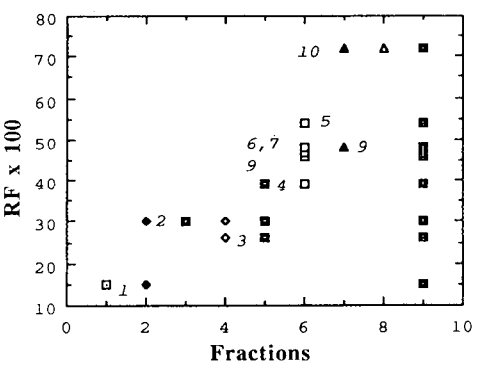

Fig. 3. TLC of fractions obtained by CPC separation of phenolic alkaloids from the stems of *Litsea cubeba*. Sample: crude phenolic alkaloids 3.78 g. CPC conditions: $CHCl_3$–MeOH–H_2O (pH 6.5) (2:2:1); stationary phase, lower layer; mobile phase, upper layer; flow-rate, 3 ml/min; centrifugal force, 123.0 *g*; volume per tube, 6 ml. Fraction 1 (tubes 22–94), 464 mg; fraction 2 (tubes 95–128), 360 mg; fraction 3 (tubes 129–140), 314 mg; fraction 4 (tubes 141–150), 552 mg; fraction 5 (tubes 151–162), 793 mg; fraction 6 (tubes 163–170), 297 mg; fraction 7 (tubes 171–180), 629 mg; fraction 8 (tube 181), 9 mg; 9 = sample. TLC developing system, solvent A; detection, Dragendorff's reagent.

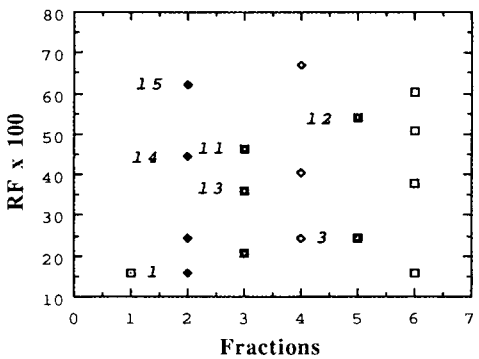

Fig. 4. TLC of fractions obtained by CPC separation of phenolic alkaloids from the root barks of *Phoebe formosana*. Sample: crude phenolic alkaloids, 7.00 g × 2. CPC conditions: $CHCl_3$–MeOH–1% HOAc (5:5:3); stationary phase, lower layer; mobile phase, upper layer; flow-rate, 2.5 ml/min; centrifugal force, 123.0 *g*; volume per tube, 10 ml; fraction 1, 9.018 g; fraction 2, 299 mg; fraction 3, 868 mg; fraction 4, 139 mg; fraction 5, 228 mg; fraction 6, 265 mg. TLC developing system, solvent A; detection, Dragendorff's reagent.

out the first chemical investigation of *Neolitsea konishii* (Hayata) Kanehira & Sasaki [4]. The CPC separation of the phenolic alkaloids from the woods (Fig. 5) resulted in the isolation of pure **1** (fraction 1), **11** (fraction 3) and **4** (fraction 7). Further separation of other fractions with DCCC, Chromatotron, flash column chromatography or preparative TLC gave **2**, **3**, actinodaphnine (**16**), corytuberine (**17**), pallidine (**18**) and N-methyllaurotetanine (**9**).

These results reveal that reversed-phase CPC is very useful for the separation of polar phenolic aporphine alkaloids. The results are reproducible under similar conditions. This technique not only separates the most polar constituent, laurolitsine (**1**), exclusively well, but also rearranges the elution order, which is not the reverse order of that given by the adsorption chromatography. The latter property facilitates to a great extent the further separation of the mixture in the same fraction because of their large R_F differences, such as between N-methyllaurotetanine (**9**, R_F 0.55, solvent B) and pallidine (**18**, R_F 0.30, solvent B) in fraction 9 (Fig. 5). The reason for this irregular elution order might be attributable to the protonation of the bases in the acidic

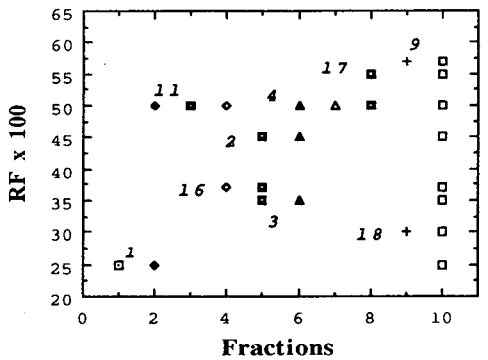

Fig. 5. TLC of fractions obtained by CPC separation of the phenolic alkaloids from the woods of *Neolitsea konishii*. Sample: crude phenolic alkaloids, 8.08 g. CPC conditions: $CHCl_3$–MeOH–1% HOAc (5:5:3); stationary phase, lower layer; mobile phase, upper layer; flow-rate, 5.3 ml/min; centrifugal force, 78.7 *g*; volume per tube, 10.6 ml. Fraction 1 (tubes 1–19), 2.09 g; fraction 2 (tubes 20–25), 393 mg; fraction 3 (tubes 26–49), 3.29 g; fraction 4 (tubes 50–52), 296 mg; fraction 5 (tube 53), 114 mg; fraction 6 (tube 54), 103 mg; fraction 7 (tubes 55–58), 351 mg; fraction 8 (tubes 59–61), 196 mg; fraction 9 (tubes 63–65), 99 mg; 10 = sample. TLC developing system, solvent B; detection, Dragendorff's reagent.

mobile phase, which increases the water solubility of alkaloids and plays a dominant role in polarity over those contributed by other functional groups. From the elution order, **1** > **11** > **16** > **2** > **3** > **4** > **17** > **18** > **5** ≈ **9** ≈ **7** > **10**, we observed that nor-aporphines (**1**, **3**, **5**) always eluted earlier than the corresponding aporphines (**2**, **9**, **10**). We also find that the elution of isomeric phenolic aporphines follows the order 2-OH (**2**) > 1-OH (**4**) > 11-OH (**17**) and 9-OH (**9** or **3**) > 11-OH (**10** or **5**). These elution properties will be of value for the purification of other related isoquinolines.

4. Conclusions

These studies demonstrate a good separation model for solving the conventional problems in dealing with complicated phenolic isoquinolines. With this approach, more thorough studies of alkaloidal contents in the Lauraceous plants will become more facile. We hope that these studies will lead to the establishment of a chemotaxonomy of Formosan Lauraceous plants.

5. Acknowledgement

We thank the National Science Council of the Republic of China for support of this research under Grant NSC 79-0412-B002-15 and NSC 80-0412-B002-22.

6. References

[1] W.D. Conway, *Countercurrent Chromatography*, VCH, New York, 1989.
[2] S.S. Lee, C.K. Chen, I.S. Chen and K.C.S. Liu, *J. Chin. Chem. Soc.*, 39 (1992) 453.
[3] S.S. Lee, F.Y. Tsai, I.S. Chen and K.C.S. Liu, *J. Chin. Chem. Soc.*, 40 (1993) 209.
[4] S.S. Lee and H.C. Yang, *J. Chin. Chem. Soc.*, 39 (1992) 189.
[5] Y.C. Wu, J.Y. Liou, C.Y. Duh, S.S. Lee and S.T. Lu, *Tetrahedron Lett.*, 32 (1991) 4169.
[6] M. Tomita, S.T. Lu, P.K. Lan and F.M. Lin, *J. Pharm. Soc. Jpn.*, 85 (1965) 593.
[7] S.T. Lu and F.M. Lin, *J. Pharm. Soc. Jpn.*, 87 (1967) 878.
[8] S.T. Lu and T.L. Su, *J. Chin. Chem. Soc.*, 20 (1973) 87.
[9] S.T. Lu, I.L. Tsai and S.P. Leou, *J. Taiwan Pharm. Assoc.*, 37 (1985) 179.

ELSEVIER

Journal of Chromatography A, 667 (1994) 327–333

JOURNAL OF CHROMATOGRAPHY A

Short Communication

Application of high-performance liquid chromatography to the determination of bitter principles of pharmaceutical relevance

O.P. Semenova*, A.R. Timerbaev☆, G.K. Bonn

Department of Analytical Chemistry, Johannes Kepler University, A-4040 Linz, Austria

(First received April 26th, 1993; revised manuscript received November 23rd, 1993)

Abstract

A rapid HPLC method for the determination of bitter principles of plant origin (BP) was developed. The reversed-phase systems with C_{18} columns and methanol–water mixtures with gradient concentrations used allow the complete separation of seven BP of different types to be achieved in less than 12 min. Several retention models are presented to describe the relationships between the capacity factors of BP and their hydrophobicities and/or the concentration of an organic modifier in the eluent, which are promising for the identification and evaluation of the chromatographic properties of new substances. Predictions of the retention models were found to agree well with the experimental data for different solute, mobile phase and column combinations in both isocratic and gradient elution modes. The method was applied to the determination of verbenalin in drug drops and found to be suitable for routine analysis.

1. Introduction

Bitter principles (BP), *e.g.*, iridoids, seco-iridoids and sesquiterpene lactones, are important natural products showing certain pharmacological properties [1–3]. Because of the growing interest in these substances by the phytopharmaceutical industry in recent years, the quality control of various phytomedicines and the investigation and exact determination of BP in different plant extracts have become important problems.

BP were first routinely separated by thin-layer chromatography [4–7]. However, in many instances the analysis was time consuming and insufficiently effective in detecting substances in small amounts of plant materials. Gas chromatographic analysis of BP is limited owing to their thermal unstability [8] or requires the preliminary derivatization [9]. Therefore, at present, high-performance liquid chromatography (HPLC) is one of the methods of choice for the rapid examination and separation of small amounts of BP. A number of HPLC procedures for determining BP have been reported [10–17], but all these methods are more or less restricted to the analysis of multi-component mixtures of BP, mainly owing to the use of the isocratic elution mode. Further, no attempts have been made to correlate the chromatographic retention of BP with their structure or mobile phase composition.

This paper reports the successful use of reversed-phase HPLC for the separation and de-

* Corresponding author.

☆ On leave from Mendeleev Russian University of Chemical Technology, Moscow, Russian Federation.

0021-9673/94/$07.00
SSDI 0021-9673(94)00115-P

termination of seven BP of different types. The applicability of the method for the rapid analysis of one of BP in a commercially used drug containing plant species is described. In order to establish a means for identifying new bitter substances and to approximate the retention as a function of the eluent composition, retention models based on a BP hydrophobicity parameter were also developed.

2. Experimental

2.1. Apparatus

The Waters (Milford, MA, USA) computer-controlled HPLC system used consisted of two Model 510 HPLC pumps, used as the solvent delivery system, a U6K injector, a Model 484 tunable absorbance detector monitoring at 254 nm and an interface module. A liquid chromatograph consisting of a Waters Model 600E programmable multi-solvent delivery system, a Waters Model 991 computer-controlled photodiode-array detector and a Waters Model 5200 printer–plotter was also used. The eluent flow-rate was 1 ml/min.

2.2. Columns

The columns used were a 250 × 4.6 mm I.D. stainless steel column slurry packed in the laboratory with 5-μm LiChrosorb RP-18 (Merck, Darmstadt, Germany) and an ODS-Hypersil (5 μm) column (250 × 4 mm i.d.) from Österreichisches Forschungszentrum (Seibersdorf, Austria).

2.3. Materials

BP standards were obtained from Sigma (St. Louis, MO, USA) and Carl Roth (Karlsruhe, Germany) and used as methanol solutions. Their structures are shown in Fig. 1. Methanol of analytical-reagent grade (J.T. Baker, Deventer, Netherlands) and doubly distilled water were used as solvents.

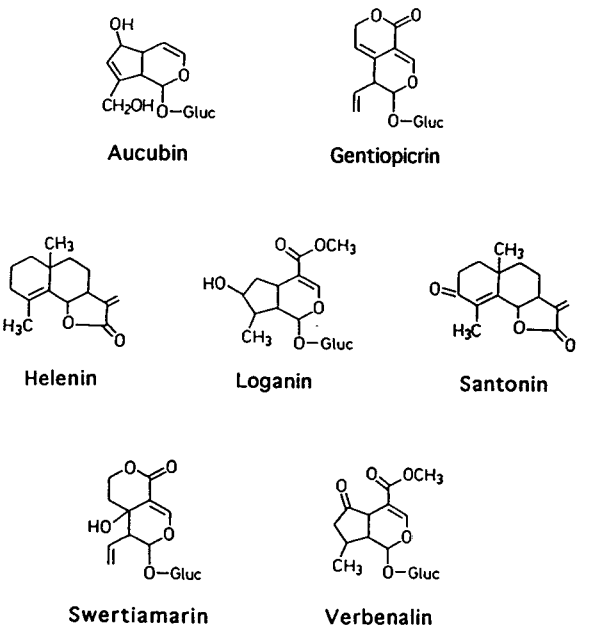

Fig. 1. Structures of the bitter principles examined. Gluc = glucose.

2.4. Procedure

A 20-μl aliquot of Sinupret drops (Bionorica, Neumarkt, Germany), based on a 19% aqueous ethanol solution, was injected directly into the column without any dilution.

3. Results and discussion

3.1. Retention behaviour of bitter principles and its model description

As shown in Fig. 1, the BP studied are related to three classes (iridoids, secoiridoids and sesquiterpene lactones) and differ in glucoside and non-glucoside nature, type of heterocyclic framework and number and position of polar functional groups (hydroxy, oxo, methoxycarbonyl, etc.). Accordingly, they show large differences in retention on reversed-phase columns, which makes their simultaneous separation difficult. For instance, the retention time of BP on the

LiChrosorb column with 50% methanol in the mobile phase varies from 7 to more than 30 min.

To determine the solute retentions and optimize the mobile phase composition in reversed-phase HPLC, calculation methods are widely used [18,19]. These methods can be based on models connecting the retention data with the parameters of solute hydrophobicity and eluent composition. Taking into account that the constituents of the phytochemical preparations under investigation represent different classes of natural substances, it was desirable for the corresponding retention models to be simple and universal.

Retention–structure model

As such a model, we offer here the model based on the simplified criterion of hydrophobicity, H, which was proposed by Shatz and Sakhartova [20] for describing the chromatographic behaviour of pharmaceutical substances with large structural differences:

$$H = n_h - 4n_f^{1/2} \quad (1)$$

where n_h and n_f are the numbers of elementary hydrophobic fragments (*i.e.*, carbon atoms) and polar functional groups of a molecule, respectively. For the BP investigated, the calculated H values are listed in Table 1.

It was found that H is linearly correlated with log k' values according to the equation

$$\log k' = a_0 + a_1 H \quad (2)$$

where k' is the capacity factor, and thereby reflects well the influence of the BP structure on their retention behaviour. For example, the experimental k' values and the k' values calculated from the hydrophobicity parameter are also given in Table 1; the resulting equation obtained by least-squares regression is $\log k' = -(0.269 \pm 0.099) + (0.122 \pm 0.018)H$; $n = 7$; $r = 0.952$; S.D. = 0.113 (r is the regression coefficient and S.D. is the standard deviation). When the retentions (log k') of three or four BP are known at a given eluent composition, Eq. 2 can be used to calculate a_0 and a_1 and approximate the capacity factors for other BP. Reasonably wide applicability of this retention model may be envisaged in the solution of an opposite problem, *viz.*, predicting the structure of an unknown BP from the experimentally obtained solute retention.

Retention–structure and eluent composition model

These combined models should describe the effect of BP structure and mobile phase composition on the capacity factors. The main chromatographic variable for controlling the solute retention is the eluent concentration of an organic modifier, while the simplest characteristic of binary water–organic eluents is the volume concentration of the organic component. Thus,

Table 1
Structural and retention parameters of bitter principals

Compound	Formula	Hydrophobicity parameter	Log k'	
			Exptl.[a]	Calc.[b]
Swertiamarin	$C_{15}H_{20}O_{10}$	2.35	0.055	0.018
Verbenalin	$C_{17}H_{24}O_{10}$	4.35	0.102	0.262
Loganin	$C_{17}H_{26}O_{10}$	4.35	0.138	0.262
Aucubin	$C_{15}H_{22}O_9$	3.00	0.207	0.097
Gentiopicrin	$C_{16}H_{20}O_9$	4.00	0.303	0.219
Santonin	$C_{15}H_{18}O_3$	8.07	0.766	0.716
Helenin	$C_{15}H_{20}O_2$	9.34	0.890	0.870

[a] Column, LiChrosorb RP-18; mobile phase, methanol–water (50:50, v/v).
[b] Log $k' = -(0.269 \pm 0.099) + (0.122 \pm 0.018)H$; $n = 7$; $r = 0.952$; S.D. = 0.113.

combining the parameters H and c (the volume percentage of methanol), we obtained a two-parametric model:

$$\log k' = a'_0 + a'_1 H - a'_2 c - a'_3 Hc \quad (3)$$

which is useful for the *a priori* calculations of organic modifier concentrations providing the desirable mobility of BP. Another important area of such calculations is the determination of initial mobile phase compositions for gradient elution, which could be accomplished with a limited number of isocratic chromatographic experiments (see below).

This model can also be applied to determine the magnitude of the retentions of BP than have not been studied chromatographically. The results of the corresponding calculations are compared with the experimental data in Fig. 2 ($a'_0 = -0.0053$; $a'_1 = 0.170$; $a'_2 = -0.0074$; $a'_3 = -0.0012$; $n = 26$). The error in the calculation of $\log k'$ values averages about 0.09.

Retention–gradient eluent composition model

Mathematical techniques for calculating solute retention parameters in gradient elution chromatography were considered in detail by Jandera and Churacek [19]. For the linear gradient function

$$c = A + Bt \quad (4)$$

where A is the initial concentration of an organic modifier, B is the gradient slope and t is the time after the start of the gradient, and the known coefficients a''_0 and a''_1 of the equation

$$\log k' = a''_0 - a''_1 c \quad (5)$$

the net retention volume V'_R is given by the relationship [21]

$$V'_R = (1/a''_1 B)\log[2.31 a''_1 B V_m \cdot (10^{a''_0} + 10^{a''_1 A})] - (A/B) \quad (6)$$

By using the experimentally obtained $\log k'$ values for 3–5 isocratic eluent compositions, we evaluated the optimal gradient parameters (Eq. 4), determined the coefficients of Eq. 5 and finally calculated by Eq. 6 the retention times of BP. These values are given in Table 2 in comparison with the corresponding experimental data. Hence the described retention model allows one to predict with fairly good accuracy the behaviour of BP in the gradient elution mode from a minimum of isocratic data.

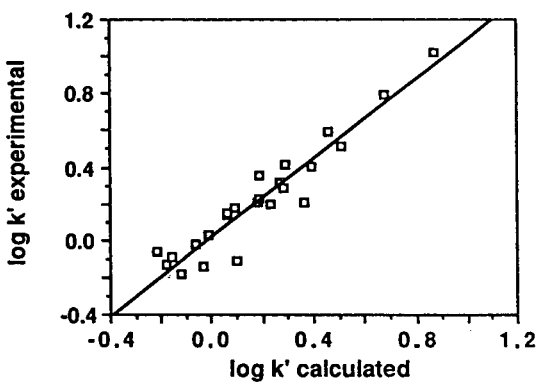

Fig. 2. Prediction of BP retention by Eq. 3. Column, ODS-Hypersil; mobile phase, 10–70% methanol.

3.2. Separation conditions

As mentioned above, it is virtually impossible to separate more than three BP under investigation within a reasonable analysis time using isocratic elution owing to the large differences in the retention. The linear gradients shown in Table 2 resulted in an increase in the number of separands, but the retention times observed were still long. Therefore, to minimize the analysis time and carry-over of long-retained BP, we further optimized gradient elution conditions.

The two main gradient compositions used were the following: (IV) 35% methanol from 0 to 4 min and 95% methanol from 4 to 15 min, and (V) 40% methanol from 0 to 4 min and 95% methanol from 4 to 15 min. Typical chromatograms obtained under the optimized conditions are shown in Fig. 3. Nearly baseline separations for all seven BP (with minimum resolution $R =$ 1.1 between verbenalin and loganin for gradient V) can be achieved in less than 12 min.

Table 2
Comparison of experimental and calculated retention times for BP

Compound	t_R (min)					
	Gradient I		Gradient II		Gradient III	
	Exptl.	Calc.	Exptl.	Calc.	Exptl.	Calc.
Aucubin	4.13	4.77	–	–	3.33	4.31
Verbenalin	5.33	4.69	5.66	4.81	4.34	4.16
Loganin	–	–	–	–	6.73	5.08
Gentiopicrin	8.26	8.62	–	–	8.70	7.34
Santonin	14.67	13.71	21.49	18.70	14.44	13.18
Helenin	19.27	19.70	28.68	29.81	21.00	21.80

Column, ODS-Hypersil. Mobile phase, linear variation from 20 to 70% methanol in 20 min (gradient I), from 30 to 60% methanol in 20 min (gradient II) and from 30 to 70% methanol in 30 min (gradient III). $t_0 = 1.65$ min.

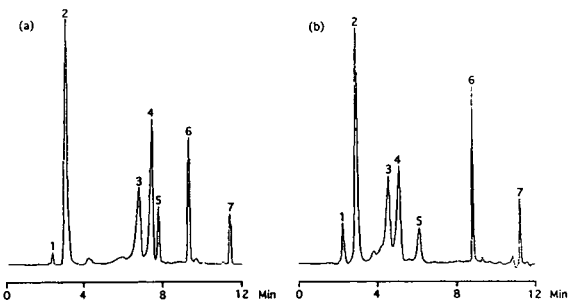

Fig. 3. Typical chromatograms of bitter principles. Column, ODS-Hypersil. Mobile phase: (a) gradient IV; (b) gradient V (for compositions, see text). Peaks (mg/l): 1 = aucubin (12); 2 = swertiamarin (6); 3 = verbenalin (94); 4 = loganin (90); 5 = gentiopicrin (226); 6 = santonin (20); 7 = helenin (136).

3.3. Linearity and detection limits

By plotting the peak heights against the amounts of BP injected, straight lines were obtained under the aforementioned conditions. Table 3 gives the parameters of the calibration graphs with the respective regression coefficients (note the poor correlation for swertiamarin, loganin and gentiopicrin, which might have resulted from insufficient purity of the corresponding standards). The minimum detectable amounts of BP were between 1.2 and 1.5 ng (with a 20-μl injection) at a signal-to-noise ratio of 3. The reproducibility of peak height was checked by six repeated determinations of swer-

Table 3
Parameters of calibration plots for BP

Compound	Interval of calibration (μg injected)	Intercept ×100	Slope $\times 10^3$	Correlation coefficient
Aucubin	1.5–70	10.4	0.07	0.99
Swertiamarin	0.1–0.8	2.4	4.9	0.90
Verbenalin	0.6–3	12.1	18.0	0.97
Loganin	0.5–8	10.0	16.3	0.91
Gentiopicrin	1.9–16	4.7	0.42	0.95
Santonin	0.5–3	0.5	21.8	0.98
Helenin	1.1–6	2.2	4.7	0.97

Chromatographic conditions as in Fig. 3 (gradient IV). $n = 4$–8.

tiamarin and loganin (sample size, 100 ng). The relative standard deviation was 1.4–2.2%.

3.4. Application to drug analysis

In order to evaluate the quantitative performance of the method, commercially used drug drops were analysed. Using a slightly modified gradient programme (25% methanol from 0 to 5 min and 95% methanol from 5 to 15 min), verbenalin was identified in Sinupret drops. This BP is present in *Herba verbenae* [22,23] as one of the main drug components of plant origin used for the preparation of this phytomedicine. Its identity was confirmed by the injection of a drug sample and a drug sample containing an additional small amount of verbenalin, which resulted in an increase in the height of the respective peak (Fig. 4). Additional confirmation was obtained from a UV spectrum of the corresponding peak recorded on-line with a photodiode-array detector and by capillary zone electrophoresis (the results will be presented in future papers).

The calibration graph for verbenalin of detector response (y) versus concentration (x, mg/l) was linear ($y = -0.0201 + 0.00012x$; $r^2 = 0.996$) in the concentration range 0.08–0.6 mg/l. The detection limit was found to be 51 μg/l. On the basis of triplicate analyses, the content of verbenalin in the drug was determined to be 148 ± 17 mg/l. From the results presented in Table 4, it can be seen that this technique produces satisfactory recovery results for the purpose of the determination of BP in phytotherapeutic products.

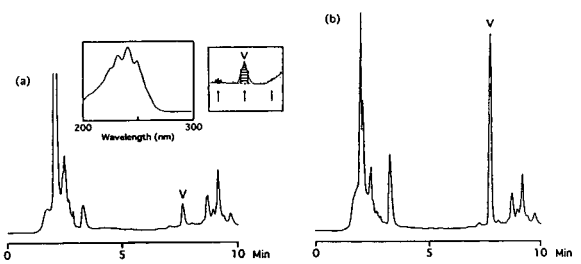

Fig. 4. Chromatograms of (a) a drug sample and (b) the drug spiked with 436 μg/ml of verbenalin (V). Column, ODS-Hypersil. Mobile phase as in text. Insets show the UV spectrum and peak purity recorded by the photodiode-array detector.

Table 4
Recovery of verbenalin added to a drug sample

Amount added (mg/l)	Amount found (mg/l)	Recovery (%)
155	150	96.8
390	412	105.6
436	429	98.4

5. Conclusions

HPLC allows the rapid determination of BP in phytotherapeutic products. Coupled with a photodiode-array detector, this method seems to be fairly promising for use in sophisticated phytopharmaceutical industry analyses. Investigations are in progress on the same application of high-performance capillary electrophoresis as a more efficient, economic and less sample-consuming alternative to HPLC.

6. Acknowledgements

We are grateful to Dr. Michael Popp of Bionorica (Neumarkt, Germany) for his interest in this work. Special thanks are due to Dr. Walter Zulehner, Johannes Kepler University, Linz, for his valuable assistance with the calculations.

7. References

[1] H. Wagner and P. Wolff (Editors), *New Natural Products and Plant Drugs with Pharmacological, Biological and Therapeutical Activity, Proceedings of Life Sciences*, Springer, Berlin, Heidelberg, New York, 1977.
[2] W.G. Van der Sluis, J.M. Van der Nat and R.P. Lebadie, *J. Chromatogr.*, 259 (1983) 522.
[3] K. Ishiguro, M. Yamaki and S. Takagi, *Yakugaku Zasshi*, 202 (1982) 755.
[4] H. Wagner and K. Vasirian, *Phytochemistry*, 13 (1974) 615.

[5] T. Hayashi, *Yakagaku Zasshi*, 96 (1976) 356.
[6] W.G. Van der Sluis and R.P. Labadie, *Planta Med.*, 32A (1977) 52.
[7] T.A. Van Beek, P.P. Lankhorst, R. Verpoorte and A. Baerheim Svendsen, *Planta Med.*, 44 (1982) 30.
[8] J.D. Weidenhamer, E.D. Jordan and N.H. Fisher, *J. Chromatogr.*, 504 (1990) 151.
[9] H. Inouye, K. Uobe, M. Hirai, Y. Masada and K. Hashimoto, *J. Chromatogr.*, 118 (1976) 201.
[10] B. Meier and O. Sticher, *J. Chromatogr.*, 138 (1977) 453.
[11] O. Sticher and B. Meier, *Pharm. Acta Helv.*, 53 (1978) 40.
[12] V. Quercia, G. Battaglino, N. Pierini and L. Turchetto, *J. Chromatogr.*, 193 (1980) 163.
[13] F. Ergun, S. Küsmenoglu and B. Sener, *J. Liq. Chromatogr.*, 7 (1984) 1685.
[14] D. Schäfelberger and K. Hostettmann, *J. Chromatogr.*, 346 (1985) 396.
[15] O. Spring, *Biochem. Syst. Ecol.*, 17 (1989) 509.
[16] W.A. Ayer and L.S. Trifonov, *J. Nat. Prod.*, 55 (1992) 1454.
[17] T.A. Van Beck, P. Maas, B.M. King, E. Leclercq, A.G.J. Voragen and A. de Groot, *J. Agric. Food Chem.*, 88 (1990) 1035.
[18] P.J. Schoenmakers, *Optimization of Chromatographic Selectivity—A Guide to Method Development*, Elsevier, Amsterdam, 1986.
[19] P. Jandera and J. Churacek, *J. Chromatogr.*, 91 (1974) 223.
[20] V. Shatz and O. Sakhartova, *Vysokoeffektivnaya zhidkostnaya kromatografiya; Osnovy teorii; Metodologiya; Primenenie v lekarstvennoj khimii*, Zinatne, Riga, 1988.
[21] P. Jandera, J. Churacek and L. Svoboda, *J. Chromatogr.*, 174 (1979) 35.
[22] R. Hegnauer, *Pharm. Acta Helv.*, 41 (1966) 577.
[23] R. Hänsel, *Planta Med.*, 14 (1966) 61.

ELSEVIER

Journal of Chromatography A, 667 (1994) 334–339

JOURNAL OF CHROMATOGRAPHY A

Short Communication

Application of a fused-silica column to the determination of very volatile amines by gas–solid chromatography

M. Mohnke*[,a], B. Schmidt[a], R. Schmidt[a], J.C. Buijten[b], Ph. Mussche[b]

[a]*Chrompack GmbH, R & D Laboratory Leipzig, Torgauer Strasse 114, 04347 Leipzig, Germany*

[b]*Chrompack International BV, Research and Development Column Technology Department, Herculesweg 8, 4338 PL Middelburg, Netherlands*

(First received October 6th, 1993; revised manuscript received January 31st, 1994)

Abstract

This paper reports the application of a PoraPLOT fused-silica column (PoraPLOT Amines) to the determination of very volatile amines such as monomethylamine, dimethylamine, trimethylamine and monoethylamine in aqueous, methanolic and pentane solutions. The column is also able to separate amines between C_1 and C_6 by using a temperature programme. A method for the trace determination of low-boiling amines using flame ionization detection and ammonia using an electrolytic conductivity detector for capillary GC is described. Examples of the determination of the purity of amines in the amine industry are given.

1. Introduction

The determination of volatile and very volatile amines by gas chromatography was exclusively done in the past using packed or micro-packed columns. Very volatile aliphatic amines such as mono-, di- and trimethylamine and monoethylamine have very low solubility in the usual liquid phases. Therefore, adsorption chromatography with partly deactivated sorbents is mostly preferred. Because of their high polarity and the strong basicity, aliphatic amines cause support effects (tailing) and a low separation efficiency results. Especially in the trace range and in the analysis of aqueous solutions quantitative determination is difficult. Moreover, well deactivated tubing material is important.

Di Corcia *et al.* [1] used 0.5% polyethyleneimine 40M + 0.3% KOH on graphitized carbon black (GCB A; Supelco, Bellafonte, PA, USA) in a 1.8-m packed column. The peak sequence was monomethylamine (MMA), dimethylamine (DMA), trimethylamine (TMA) and monoethylamine (MEA). Although there was good peak symmetry, the resolution was not complete.

Hollis [2] applied 10% tetraethylenepentamine (TEP) and 10% polyethyleneimine on Chromosorb 102. With a 1.8-m stainless-steel column, the separation of MMA and DMA was fairly good, but chromatograms for TMA and MEA were not shown.

Sze *et al.* [3] reported separations on a 2.7-m column packed with 15% diglycerol + 5% tetraethylenepentamine on Chromosorb W. The interesting peak sequence was TMA, DMA and MMA. We have found the same elution order with polyethyleneimine on a fused-silica column

* Corresponding author.

0021-9673/94/$07.00
SSDI 0021-9673(94)00107-K

but with very small k' values. It seems to be a complexation reaction of the aliphatic amines with an amino-containing stationary phase. The same workers could not fully separate TMA, NH_3, DMA and MMA in this sequence on a 4.5-m column packed with 5% tetrahydroxyethylethylenediamine.

Onuska [4], Dalene *et al.* [5] and Audunsson and Mathiasson [6] used columns packed with 28% Pennwalt 223 + 4% KOH on Gas-Chrom R for the determination of free amines with different detectors. Dunn *et al.* [7] compared the qualitative separation and the quantitative results in the trace range on ten different packed columns. They could not separate DMA from TMA and there was severe tailing on these phases.

With respect to the quantitative results, a number of papers have reported relatively successful determinations of very volatile amines on Chromosorb 102 or 103 [8–11], deactivated with either KOH or trimethylchlorosilane. The determination of DMA in air with Chromosorb 103 was carried out by Böhm *et al.* [12] under constant deactivation with some ammonia in the carrier gas.

A very inert support material for the separation of highly polar compounds is Carbopack B (Supelco) [13–16]. Carbopack B deactivated with 4% Carbowax 20M + 0.8% KOH in a 2-m packed column (glass or nickel) gave a nearly complete separation of MMA, DMA, MEA and TMA, but MEA eluted before TMA.

The work reported here was stimulated by the need to analyse, *e.g.*, pure aqueous amine solutions in industry and trace amines in medicine, the pharmaceutical industry, biology, food research and in the environment using modern fused-silica columns with high separation power and sensitivity and short analysis times.

2. Experimental

Porous layer open-tubular (PLOT) columns were introduced in the early days of capillary GC [17,18]. New coating techniques have made it possible also to coat a porous polymer on the inner wall of a fused-silica capillary column. This results in a highly efficient column that can be used for specific separations, especially those in which the liquid stationary phases do not provide sufficient retention such as with very volatile amines [19,20].

We have deactivated these PoraPLOT Q columns (Chrompack, Middelburg, Netherlands) by a proprietary technique in order to obtain gas–solid columns with higher retention and resolution for the very volatile amines above ambient separation temperatures and with satisfactory tailing-free peaks (PoraPLOT Amines, Chrompack). This is of special importance for the extremely high basicity and polarity of these compounds.

Table 1 gives the dissociation constants and dipole moments of different low-boiling amines in comparison with ammonia and water.

The amines MMA, DMA, TMA and MEA were obtained from Leuna Werke (Leuna, Germany).

All GC measurements were conducted on a CP 9001 gas chromatograph (Chrompack). Split injection was used and flame ionization detection (FID) and, in one case, electrolytic conductivity detection (ELCD) (with an instrument from Fraunhofer-Institut für Lebensmitteltechnologie und Verpackung, Munich, Germany) were applied.

The concentration of the normally used aque-

Table 1
Dissociation constants and dipole moments of very volatile amines compared with ammonia and water

Compound	Temperature (°C)	Dissociation constant in H_2O		Dipole moment (D)
		pK_a	K_a	
CH_3NH_2	25	10.657	$2.70 \cdot 10^{-11}$	1.31
$(CH_3)_2NH$	25	10.732	$1.85 \cdot 10^{-11}$	1.03
$(CH_3)_3N$	25	9.81	$1.55 \cdot 10^{-10}$	0.61
$C_2H_5NH_2$	20	10.81	$1.56 \cdot 10^{-11}$	1.22
$(C_2H_5)_2NH$	40	10.489	$3.24 \cdot 10^{-11}$	0.92
$C_3H_7NH_2$	20	10.708	$1.96 \cdot 10^{-11}$	1.17
NH_3	20	9.23	$5.89 \cdot 10^{-10}$	1.47
H_2O	20	14.167	$6.81 \cdot 10^{-15}$	1.85

ous test solution was in *ca.* 0.5 μg/μl, the absolute amount of sampling at a splitting ratio 1:100 being *ca.* 5 ng per amine. In all other instances the total amount is given in the figure captions.

The optimum working conditions for a PoraPLOT Amines column of dimensions 25 m × 0.32 mm I.D. and with a layer thickness $d_f = 10$ μm were as follows: sample size, 0.5–1 μl of solution; splitting ratio, 1:50 to 1:100; injector temperature, 200°C; detector temperature, 250°C; oven temperature, 130°C; GC sensitivity, 1×10^{-11} AUFS; carrier gas, hydrogen (45 kPa); and linear gas velocity, $u_{opt} = 27$ cm/s.

After each chromatographic run it is recommended to heat the column rapidly to 220°C using a temperature programme, *viz.*, 130°C (held for 10–15 min), increased at 20°C/min to 220°C (held for 15 min), for reactivation of the adsorbent. The maximum allowable operating temperature is 250°C.

3. Results and discussion

Fig. 1 shows a typical chromatogram with high resolution of the four very volatile amines MMA, DMA, TMA and MEA in aqueous solution. The peaks have a very good shape except for TMA, which is the most basic amine, comparable to ammonia (see Table 1).

Evaluation of the capacity factors between 369.0 and 393.7 K shows a typical behaviour of an adsorption column. This is illustrated in Fig. 2 by a plot of k' *versus* $1/T$.

Repetitive measurements of the separation factors α for MMA–DMA and DMA–TMA demonstrated the reproducibility of the selectivity for the different columns (Table 2).

Generally, a newly developed column has to be checked for quantitative trace analysis with respect to the linear range. Especially for the compounds considered here it is necessary to verify this down to detection limit. The results are illustrated in Fig. 3, which shows a linear range between 0.5 and 20 ng of amines.

Another qualitative observation was the fact that the prolonged use of calibration mixtures of

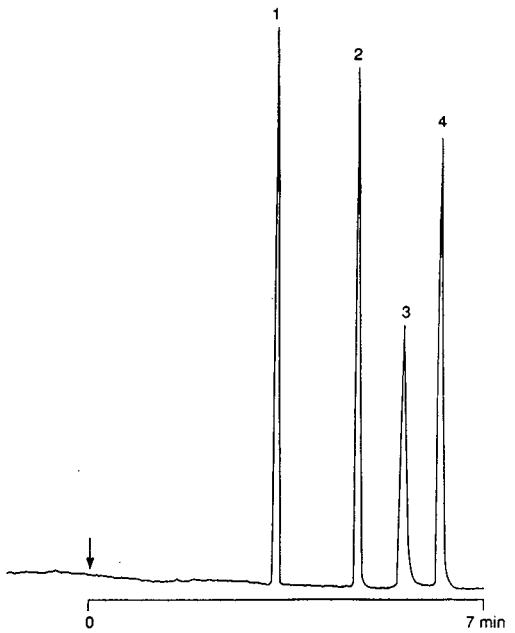

Fig. 1. Separation of very volatile amines. Column, 25 m × 0.32 mm I.D. PoraPLOT Amines; oven temperature, 130°C; detection, FID. Peaks: 1 = monomethylamine; 2 = dimethylamine; 3 = trimethylamine; 4 = monoethylamine in aqueous solution.

aqueous amine solutions generates double peaks on the chromatogram. This seems to be caused by chemical reactions (decomposition) due to sunlight and ambient temperature. It is therefore possible to conclude that only freshly prepared

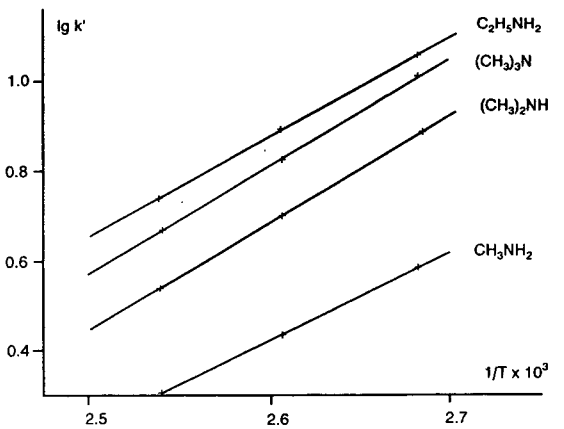

Fig. 2. Plots of capacity factors k' *versus* $1/T$ for very volatile amines.

Table 2
Column-to-column reproducibility with respect to selectivity

Column No.	α	
	MMA–DMA	DMA–TMA
462 117	1.76	1.20
462 257	1.76	1.22
462 364	1.72	1.20
462 452	1.76	1.21
462 521	1.80	1.25
462 637	1.75	1.20
462 721	1.75	1.20
Mean	1.76	1.21
Standard deviation	0.02	0.02

mixtures should be used or that they should be stored dark and cool.

Estel [21] used capillary column GC–ELCD to determine traces of ammonia in aqueous amine mixtures using a PoraPLOT Amines column. Fig. 4 shows the excellent separation and peak symmetry for ammonia and the amines in the nanogram range and high selectivity of ELCD.

Ewender and Piringer [22,23] analysed a pentane extract of C_1–C_6 amines using a PoraPLOT Amines column. The amine concentration was 80 ppm for each peak in pentane. The temperature-programmed separation is shown in Fig. 5. The use of methanol as a solvent for very volatile amines gave results comparable to those obtained with aqueous solution, but a methanol peak failed to appear.

For checking and controlling the production

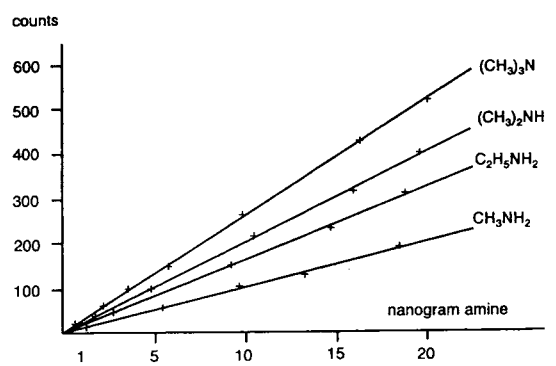

Fig. 3. Linearity of detection for very volatile amines.

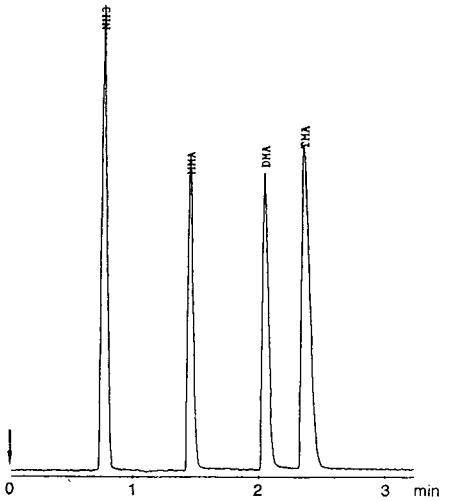

Fig. 4. Separation of ammonia, monomethylamine (MMA), dimethylamine (DMA) and trimethylamine (TMA) in aqueous solution. Column and oven temperature as in Fig. 1. Electrolytic conductivity detection (ELCD) according to Estel [21].

process in the amine industry, we used PoraPLOT Amines columns at higher linear gas velocities. It is possible to analyse pure aqueous

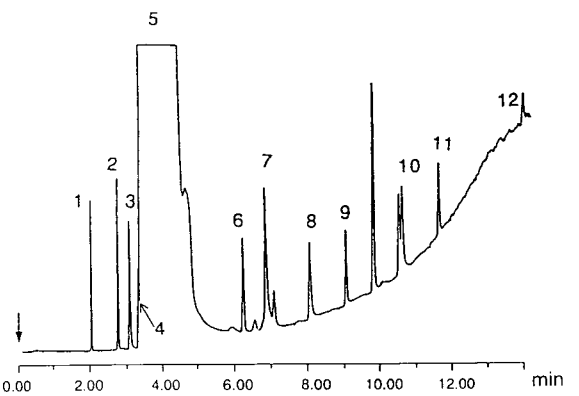

Fig. 5. Separation of C_1–C_6 amines in a pentane extract according to Ewender and Piringer [22,23]. Column and detector as in Fig. 1. Oven temperature programme, 140°C (held for 2 min), increased at 10°C/min to 250°C (held for 3 min); carrier gas, hydrogen (95 kPa). Peaks: 1 = monomethylamine; 2 = dimethylamine; 3 = trimethylamine; 4 = monoethylamine; 5 = pentane, 6 = 1-propylamine; 7 = diethylamine and *tert.*-butylamine; 8 = 2-butylamine; 9 = 1-butylamine; 10 = 2- and 3-pentylamine; 11 = *n*-pentylamine; 12 = 1-hexylamine. Concentration: 80 ppm per amine.

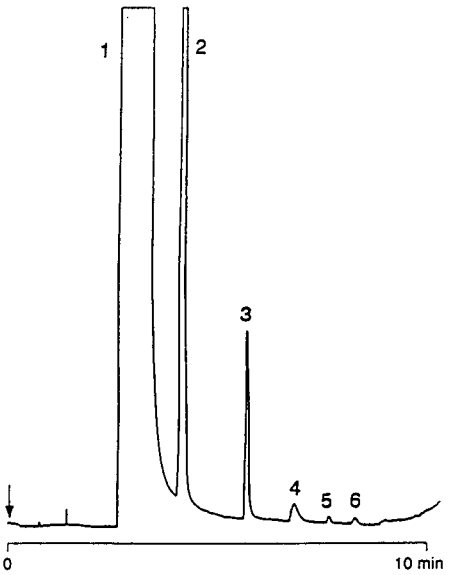

Fig. 6. Separation of impurities in technical-grade monomethylamine in aqueous solution. Column and detector as in Fig. 1. Oven temperature programme, 110°C (held for 8 min), increased at 15°C/min to 200°C (held for 10 min); carrier gas, hydrogen (100 kPa); $u = 56$ cm/s. Peaks: 1 = MMA; 2 = unknown; 3 = DMA; 4 = TMA; 5 = MEA; 6 = unknown.

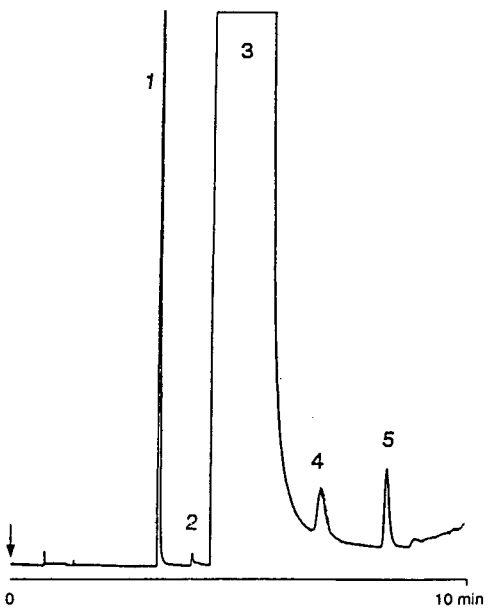

Fig. 7. Separation of impurities in technical-grade dimethylamine in aqueous solution. Conditions as in Fig. 6. Peaks: 1 = MMA; 2 = unknown; 3 = DMA; 4 = TMA; 5 = MEA.

solutions such as MMA (Fig. 6) and DMA (Fig. 7) within 10 min at $u = 56$ cm/s and a hydrogen inlet pressure of 100 kPa. The two chromatograms demonstrate the possible complete separation of the relevant trace amines. Such PoraPLOT Amines columns operated round the clock for 6 months, before the separation power decreased owing to sample impurities.

If it is necessary to determine very volatile amines by using wide-bore columns (0.53 I.D., length 25 or 50 m) with a layer thickness of $d_f = 20$ μm, such columns are also available. Wide-bore PoraPLOT Amines columns have a similarly good separation efficiency owing to the greater layer thickness.

4. Acknowledgements

We thank D. Estel, J. Ewender and Dr. O. Piringer for testing the columns and for permission to publish their chromatograms and Dr. Helga Dietrich, Leipzig, for revision of the English text.

References

[1] A. Di Corcia, A. Liberti and R. Samperi, *J. Chromatogr. Sci.*, 12 (1974) 710.
[2] O.L. Hollis, *Anal. Chem.*, 38 (1966) 309.
[3] Y.L. Sze, M.L. Borke and D.M. Ottenstein, *Anal. Chem.*, 35 (1963) 240.
[4] F.I. Onuska, *Water Res.*, 7 (1973) 835.
[5] M. Dalene, L. Mathiasson and J.A. Jönsson, *J. Chromatogr.*, 207 (1981) 37.
[6] G. Audunsson and L. Mathiasson, *J. Chromatogr.*, 315 (1984) 299.
[7] S.R. Dunn, M.L. Simenhoff and L.G. Wesson, Jr., *Anal. Chem.*, 48 (1976) 41.
[8] K. Kuwata, Y. Yamazaki and M. Uebori, *Anal. Chem.*, 52 (1980) 1980.
[9] K. Kuwata, E. Akiyama, Y. Yamazaki, H. Yamazaki and Y. Kuge, *Anal. Chem.*, 55 (1983) 2199.
[10] A. Tavakkol and D.B. Drucker, *J. Chromatogr.*, 274 (1983) 37.
[11] L. Grönberg, P. Lörkvist and J.A. Jönsson, *Chromatographia*, 33 (1992) 77.
[12] G. Böhm, G. Kainz, H. Witzani and W. Wliszak, *Mikrochim. Acta*, 3–4 (1983) 205.

[13] F. Bruner, P. Ciccioli, E. Brancaleoni and A. Longo, *Chromatographia*, 8 (1975) 503.
[14] F. Ferrari, J.P. Guenier and J. Muller, *Chromatographia*, 8 (1985) 5.
[15] M.E. Krzymien and J. Elias, *J. Food Sci.*, 55 (1990) 1228.
[16] X.H. Yang, C. Lee and M.I. Scranton, *Anal. Chem.*, 65 (1993) 572.
[17] M. Mohnke and W. Saffert, in *Preprints of the 4th International Gas Chromatography Symposium, Hamburg, 1962*, p. 214.
[18] M. Mohnke and W. Saffert, *Kernenergie*, 4/5 (1962) 434.
[19] J. de Zeeuw, R.C.M. de Nijs, J.C. Buijten, J.A. Peene and M. Mohnke, *Int. Lab.*, 17, No. 10 (1987) 52.
[20] J. de Zeeuw, R.C.M. de Nijs, J.C. Buijten, J.A. Peene and M. Mohnke, *J. High Resolut. Chromatogr. Chromatogr. Commun.*, 11 (1988) 162.
[21] D. Estel, Leuna Werke, Leuna, Germany, personal communication.
[22] J. Ewender, Fraunhofer-Institut für Lebensmitteltechnologie und Verpackung, Munich, personal communication.
[23] J. Ewender and O. Piringer, *Dtsch. Lebensm.-Rundsch.*, 87 (1991) 5.

ELSEVIER

Journal of Chromatography A, 667 (1994) 340–347

JOURNAL OF CHROMATOGRAPHY A

Short Communication

Influence of dissolved gases in the dynamic headspace analysis of styrene and other volatile organic compounds and improvement of their determination

J. Le Sech, V. Ducruet, A. Feigenbaum*

INRA, LNSA, 78352 Jouy en Josas Cedex, France

(First received September 14th, 1993; revised manuscript received December 27th, 1993)

Abstract

The on-line purge and trap dynamic headspace technique (PTI) was optimized for styrene. High-boiling volatiles such as styrene were efficiently desorbed from oil and from oil–water matrices. The effects governing the desorption were identified by comparison with an off-line procedure. The recovery of styrene depends dramatically on the amount of fat and on the desorption temperature. For oil–water systems, the aqueous phase had to be saturated with both sodium chloride and carbon dioxide; with PTI, no desorption occurs if the sample is initially degassed; regassing improved desorption, carbon dioxide giving the best results.

1. Introduction

Volatile organic compounds (VOCs) are usually determined by gas chromatography (GC). The main difficulty in their determination is their isolation from various matrices, especially for the higher boiling compounds. Styrene (b.p. 145°C) is a ubiquitous contaminant, which will be considered here as a model of these higher boiling VOCs. The isolation of styrene from solid, fatty or aqueous matrices has been carried out by azeotropic [1] and vacuum [2] distillation, and also by static [3] and dynamic headspace [4–8] methods. The latter can be either on-line or off-line. We report here a net improvement of the on-line method usually known as purge–trap–inject (PTI), mainly by paying attention to the influence of dissolved gases.

In off-line GC, styrene is swept from the matrix by a purge gas such as helium or nitrogen and trapped in a solvent [4] or on an adsorbent such as Tenax, from which it is then eluted [5]. In on-line GC, the preconcentration can be carried out on an adsorbent [6,9] or on a cryogenic trap. This is achieved on the head of the chromatographic column at room temperature [10,11] or, in the PTI method, on a coated capillary cooled well below room temperature, and connected to the column [12]. The cold trap usually contains a small amount of adsorbent [12]. The main advantage of the cold trap method is that if other volatiles are present, the efficiency of the trapping is not affected by their chemical structure [5] as with an adsorbent. The main difficulty associated with the PTI cold trap method is that when aqueous matrices are used,

* Corresponding author.

0021-9673/94/$07.00
SSDI 0021-9673(94)00103-G

the swept water must be selectively condensed before reaching the cryogenic trap, which would otherwise be blocked [12].

With the PTI technique, the recovery is governed by several processes, such as the removal of hydrocarbons from the liquid matrix, their discrimination from the condensed water or their condensation along the glass tubing of the device. In order to monitor separately the influence of these processes, we repeated the experiments with an alternative off-line purge and trap method, using Carbotrap, an adsorbent not sensitive to the presence of water vapour. This method consists of a purge sequence towards an adsorbent trap, followed by elution of the volatiles with hexane and finally a manual injection into the gas chromatograph. This procedure will be named here the [PAT,E,I] method.

2. Experimental

2.1. Chemicals

Hexane (RP grade, Prolabo, Paris) was distilled before use; styrene (Aldrich, Strasbourg, France) and ethylbenzene (Aldrich) were used without further purification. Peanut oil (Lesieur) was purchased in a retail store. The trap was Orbo 100 Carbotrap (Supelco, Bellefonte, PA, USA) containing two layers of 350 and 175 mg of graphitized carbon as adsorbent. NaCl and $(NH_4)_2SO_4$ were of analytical-reagent grade. Ultrapure water was obtained from a Milli-Q system (Millipore, Bedford, MA, USA).

2.2. Solutions of aromatic hydrocarbons

For the dissolution of the aromatic hydrocarbons, we used peanut oil rather than the official fatty food simulants (olive and sunflower oils), which naturally contain many volatile compounds.

2.3. Gas chromatography

In the [PAT,E,I] method, a Girdel 300 Delsi chromatograph equipped with a Jennings injector was used. The column was DBWax (0.5 μm) (30 m × 0.32 mm I.D.) (J&W Scientific, Folsom, CA, USA). Flame ionization detection (FID) was applied. An Enica 10 Delsi integrator was used.

For PTI, a Packard Model 427 gas chromatograph was equipped with a Chrompack purge and trap injector. The column was DBSil 5 (1 μm) (30 m × 0.32 mm I.D.) (J&W Scientific). FID was applied. A Spectra-Physics Model 4290 integrator was used.

2.4. Description of the [PAT,E,I] system (Fig. 1)

The purge gas flow was regulated with a valve and bubbled through a flask containing water to prevent clogging of the needle when using a saturated salt solution in the purge cell. This flask was connected to the purge cell via a stainless-steel Luer connection (Aldrich Z10,246-6) and a needle (Aldrich Z10,271-7), through a teflonized septum. We made the purge cell ourselves. It consists in a tube (15 mm I.D.) with a conical bottom, equipped with a lateral inlet (neck and septum adapted from a Varian 2-ml vial, ref. 03-906195-90) and an SVL No. 15 screw-stopper (Bibby Science), making adaptation of the Carbotrap tubes through an 8-mm SVL ring possible. Two different purge cell lengths were used: 5 cm for small samples (only oily solutions) and 11 cm when large volumes of saturated NaCl solution was added to the oily styrene solution.

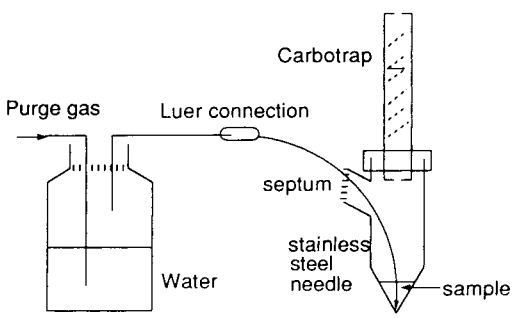

Fig. 1. The [PAT,E,I] procedure.

2.5. Analytical procedure with the [PAT,E,I] system

A solution of the VOCs in peanut oil was weighed into the purge cell and saturated NaCl solution (1 ml) was added in some experiments. The purge gas was admitted into the cell with a 150 ml min^{-1} flow. At the end of a purge period, the adsorbent tube was quickly replaced by a new one. The next purge period was started immediately. All the traps were analysed separately. The trapped volatiles were desorbed with hexane (5.0 ml). The elution time was adjusted between 2 and 5 min with the help of pressure at the top of the Carbotrap. A second elution with 1 ml of hexane was made in order to check that all the volatiles had been removed from the trap. A separate analysis was then carried out. Cumene (5.48 μg ml^{-1} in the eluent) was then added as an internal standard for the GC determination.

The method as used here had a sensitivity of 500 ng for styrene, with a signal-to-noise ratio of 5.

2.6. Analytical conditions for the PTI system (Fig. 2)

The Chrompack purge and trap injector was used as recommended by the manufacturer [12] under the following conditions: purge gas, hydrogen; purge gas flow-rate, 15 ml min^{-1}; purge gas time, 20 min; and clean-up flow-rate, 6 ml min^{-1}. The cryogenic trap was a fused-silica tube (30 cm × 0.53 mm I.D.) coated with Cp-Sil8CB (5 μm) (Chrompack).

As direct injection was not possible, the recovery yield could not be determined, and our results were expressed by the ratio:

$$\text{area ng}^{-1} = \frac{\text{area of the GC signal}}{\text{ng styrene introduced into the cell}}$$

A control of purge efficiency could be made with a second purge by checking whether there was still styrene which could be swept from the matrix. Each experiment was repeated 2–5 times. The variability was 20%.

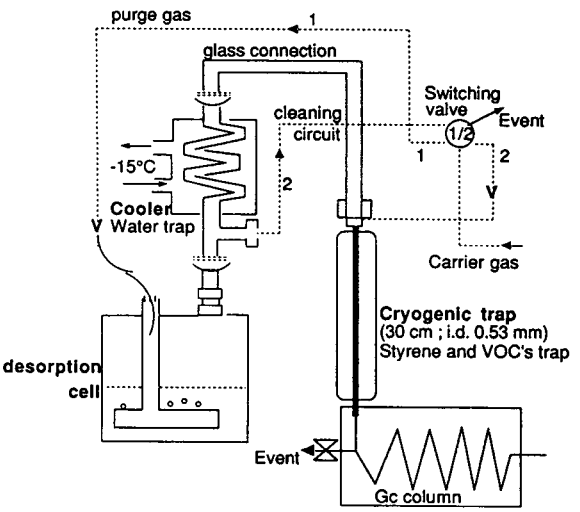

Fig. 2. The PTI system.

The method as used here had a sensitivity of 1 ng for styrene, with a signal-to-noise ratio of 5.

3. Results

3.1. Influence of the amount of oil for a given amount of styrene

Results with the PTI technique

With a constant amount of hydrocarbon (35 ng of styrene) introduced into the cell, and using a constant purge time, the area ng^{-1} values were measured for different amounts of oil in the cell, ranging from 1.1 to 91.3 mg. The results are reported in Fig. 3. Surprisingly, for very small amounts of oil, the area ng^{-1} value passes through a maximum at *ca.* 2.2 mg of oil. This was probably the result of a change in the evaporation mechanism [13], interface effects playing an important role for very small amounts.

Results with the [PAT,E,I] procedure

The results obtained using about 550 μg of styrene in the cell are presented in Fig. 4. Within a 30-min purge with nitrogen, 93% of the styrene

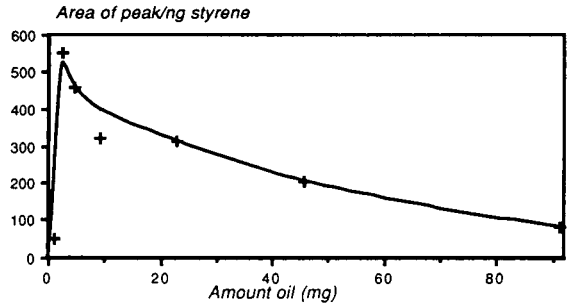

Fig. 3. Influence of the amount of peanut oil on the area ng^{-1} value for styrene (with 5 ml of water).

was desorbed from 26 mg of oil, but only 14% from 2185 mg of oil.

3.2. Influence of the temperature of the [PAT,E,I] cell

To decreases as much as possible the purge time required for a quantitative purge, whatever the concentration of styrene and the amount of oil, one approach consists in raising the temperature of the desorption cell. With *ca.* 500 μg of styrene in *ca.* 2000 mg of oil, the recovery in a 30-min purge increased with increasing temperature up to 80°C. Temperatures as high as 150°C, which corresponds more to distillation of styrene, have been reported in similar procedures [14], but they do not seem to be strictly necessary in view of our results. This result could certainly be extended to the PTI method.

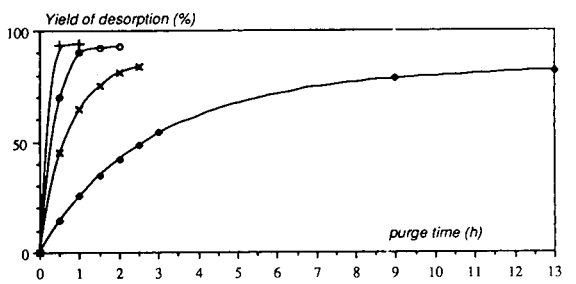

Fig. 4. Influence of the amount of oil (*ca.* 550 μg of styrene) in the cell in the [PAT,E,I] method. + = 26 mg of oil, 506 μg of styrene; ○ = 189 mg of oil, 647 μg of styrene; × = 353 mg of oil, 682 μg of styrene; ◇ = 2185 mg of oil, 510 μg of styrene.

3.3. Influence of the addition of aqueous solutions and of dissolved gas

Results with the PTI technique

It has been reported that adding water to the oil improved the GC determination of styrene by static headspace methods through the formation of a mixed vapour of water with the aromatic hydrocarbon [15]. We therefore added water to the analytical cell. With the PTI technique, this also permitted the immersion of the sintered glass (Fig. 2), thus allowing the purge gas to bubble through the solution. However, as shown in entries 1 (oil only) and 2 (oil + stock distilled water) in Table 1, this did not improve the area ng^{-1} value. This suggests that the effect of water in headspace methods might be more complex.

As this result could be due to the slight solubility of styrene in water (0.032% at 25°C) [16], the water was saturated with $(NH_4)_2SO_4$ or NaCl. When such solutions were freshly prepared, their use markedly enhanced the removal of styrene from the oil solution, as can be seen by comparing entries 2 (oil + water), 3 [oil + $(NH_4)_2SO_4$ saturated solution] and 7 (oil + NaCl saturated solution) in Table 1.

However, when the freshly prepared saturated salt solutions were reused the next day, the purge efficiency of styrene was disastrous (entries 4 and 8, Table 1). This difference in the behaviour of freshly prepared and "old" stock solutions could be linked to the decrease in solubility of the gases on going from pure water to the saturated solution, a hypothesis which was confirmed by the following experiments. A freshly prepared $(NH_4)_2SO_4$ saturated solution was thoroughly degassed by sonication for 10 min, then added to the PTI cell containing styrene in oil, then purged with hydrogen: no styrene was desorbed (entry 5, Table 1). When the same saturated salt solution was first sonicated, then regassed for 15 s by bubbling carbon dioxide immediately before use, the recovery of the hydrocarbons was excellent (entry 6, Table 1). A similar efficiency was obtained when a 1-day-old stock solution was regassed with CO_2 immediately before use (entry 9, Table 1). Bubbling nitrogen through the aqueous solution before

Table 1
Determination of ethylbenzene (40 ng) and styrene (35 ng) in oil (8 mg) by the PTI technique, using hydrogen as purge gas

Entry	Volume of aqueous solution added (ml)	Preparation and type of aqueous solution	Ethylbenzene (area ng^{-1})	Styrene (area ng^{-1})
1	None	–	393	453
2	5	Stock distilled water		190
3	5	Sat. $(NH_4)_2SO_4$ prepared just before use	327	334
4	5	Sat. $(NH_4)_2SO_4$ stock	–[a]	51
5	5	(1) Sat. $(NH_4)_2SO_4$ prepared just before use (2) Degassed by sonication	–[a]	–[a]
6	5	(1) Sat. $(NH_4)_2SO_4$ prepared just before use (2) Degassed by sonication (3) Regassed with CO_2 [b]	394	408
7	5	Sat. NaCl prepared just before use	217	233
8	5	Sat. NaCl 1-day-old solution	80	135
9	5	(1) Old sat. NaCl solution (2) Regassed with CO_2 [b]	550	485
10	5	(1) Old sat. NaCl solution (2) Regassed with N_2 [b]		214
11	5	(1) Distilled water (2) Regassed with N_2 [b]	241	284

[a] Only trace levels of the hydrocarbon were detected by GC.
[b] 100 ml min^{-1}, 15 s, just before use.

introduction of the hydrocarbons also increased the efficiency of the styrene purge, although the effect was less pronounced (entries 10 and 11, Table 1).

Dissolved gases seem to play a critical role in the efficiency of the added aqueous solutions. The poor efficiency of "old" stock solutions was the result of a slow release of the dissolved gases from the saturated solution after their preparation. Regassing the solution with carbon dioxide just before starting the purge turned out to enhance the purge efficiency of the hydrocarbons; in order to prevent the carbon dioxide from freezing in the cold trap, the temperature of the latter was raised from −150°C (recommended by the manufacturer) to −70°C.

Results with the [PAT,E,I] procedure

The use of aqueous solutions led to similar effects to those described above with the PTI procedure, but to a much lesser extent. The influence of the dissolved gases was far less than with the PTI technique: using the same purge gas, hydrogen, the sonication of the aqueous solution had only a slight effect on the desorption yield (entries 1 and 2, Table 2). With nitrogen as the purge gas, the desorption from solutions diluted in peanut oil was only slightly decreased by the use of an old stock saturated NaCl solution (Table 2, entries 4 and 5). Regassing this solution with carbon dioxide just before use gave an excellent recovery of styrene (Table 2, entries 5 and 6).

Considering the enhancement of the desorption of hydrocarbons by carbon dioxide with the PTI technique, this gas was adopted as the purge gas in the [PAT,E,I] method; however, the recovery of styrene decreased on replacing nitrogen with carbon dioxide. This was shown to be the result of an interaction of carbon dioxide with the Carbotrap, through the following experiment: styrene (150 μg) in solution in hexane (50 μl) was added directly on the top of two carbotrap columns; one of the columns was swept with nitrogen (150 ml min^{-1} for 1 h and the other was swept with carbon dioxide (150 ml min^{-1}) for the same time. The hydrocarbons still present on the adsorbent were then eluted with

Table 2
Influence of the purge gas on the recovery of styrene (500 μg) from peanut oil (30 mg) using a 30-min purge with the [PAT,E,I] procedure

Entry	Purge gas	Special features	Recovery (%) after 30-min purge		
			Styrene	Ethylbenzene	Propylbenzene
1	H_2	Old sat. NaCl solution[a]	85[c]	87	86
2	H_2	(1) Old sat. NaCl solution[a] (2) Sonicated before use	80[c]	87	79
3	H_2	Distilled water[a]	84[c]	94	84
4	N_2	No aqueous solution added	94[c]		
5	N_2	Old sat. NaCl solution[a]	79 89 after 1-h purge		
6	N_2	(1) Old sat. NaCl solution[a] (2) Regassed with CO_2 [b]	93[c]		
7	CO_2	Old sat. NaCl solution[a]	72[c]		
8	CO_2	Old sat. NaCl solution[a] (4 purges 7.5 min)	86		

[a] 1 ml.
[b] 100 ml min^{-1}, 15 s, just before use.
[c] No improvement in the recovery after a second purge period of 30 min.

hexane and analysed as usual. The recoveries thus determined were 100% for the tube swept with nitrogen and only 84% for the tube swept with carbon dioxide. It thus appeared that whereas carbon dioxide accelerates the purge of styrene from the matrix, it also induces the desorption of styrene from the Carbotrap. It should also be noted that ethylbenzene and styrene did not behave similarly. The behaviour of styrene was more similar to that of propylbenzene, which should be used as an internal standard for quantitative analyses when needed.

According to this result, high recoveries (88%) could be obtained using carbon dioxide as the purge gas in the [PAT,E,I] procedure with frequent replacement of the trap (every 7.5 min during 90 min).

4. Discussion and conclusion

4.1. Determination of volatile aromatic hydrocarbons by dynamic headspace analysis

In all our experiments, efficient purges were achieved with solutions of hydrocarbons in peanut oil, as long as the samples were small (less than *ca.* 50 mg). High-boiling volatile hydrocarbons such as styrene and propylbenzene can be determined efficiently by these dynamic headspace techniques [17]. Peanut oil appears to be a very convenient solvent for handling volatile compounds with dynamic headspace methods.

4.2. Determination of styrene in two-phase systems

The use of saturated salt solutions reduces the solubilities of the hydrocarbons in water and displaces the equilibrium towards the gas phase. The recoveries are thus higher than in the experiments where only distilled water is added; if the determination has to be achieved in aqueous media or in emulsions, it seems adequate to saturate the aqueous phases. In all instances, the preliminary bubbling of a gas through the aqueous solution enhances the recoveries.

Influence of the nature of the purge gas

The results with the PTI technique show that a

preliminary treatment of the matrix with carbon dioxide or, to a lesser extent, nitrogen enhances the purge efficiency. This might suggest that the nature of the purge gas could increase the sweeping efficiency of styrene, with the order $CO_2 > N_2 > H_2$, which seems to correlate with the solubilities of these gases in water at 20°C [18]: $1750 > 23 > 19$ ml l^{-1}. In fact, the experiments carried out with the [PAT,E,I] procedure showed that the nature of the purge gas has little effect on purge efficiency: nitrogen, carbon dioxide (with frequent replacement of the trap) and hydrogen gave similar recoveries (Table 2, entries 5, 8 and 1). It is therefore not the nature of the purge gas that accounts for the dramatic effects observed in PTI method. This is most likely the result of the preliminary saturation.

The results presented here could be explained consistently if one assumes that the volatile hydrocarbons can only be swept when the matrix is saturated by the purge gas. The time required to reach this saturation could then be a crucial parameter. The difference between the two techniques appears strikingly for the experiments using sonicated aqueous salt-saturated solutions (entry 5, Table 1 and entry 2, Table 2). In the PTI experiments, where both the purge flow and purge time are low (as recommended by the manufacturer), starting with a sonicated matrix and using hydrogen as the purge gas, this saturation would not be reached within the purge period (entry 5, Table 1). In the [PAT,E,I] experiments, the amount of matrix is five times smaller and the flow-rate ten times higher, resulting in the time required for saturation by the purge gas being 50 times lower than in PTI experiments. It could then in fact be reached within the purge period. This explains why the [PAT,E,I] experiment with sonication (entry 2, Table 2) showed little difference from those in which the matrix was not initially degassed.

The hypothesis that with the PTI method the system does not have the time to reach the required gas saturation, unless a preliminary purge is used, could also explain the poor reproducibility of the results usually reported with dynamic headspace techniques [19]. This could also explain why, in the volumetric dilution procedure, the use of a pipette (creating a depression above the liquid surface) is less suitable than the use of a burette [19], a fact which has been reported, but never coherently explained.

The best conditions for the desorption of the volatile aromatic hydrocarbons involve a short preliminary bubbling of carbon dioxide into a saturated NaCl solution, which is then added to the sample just before starting the purge (Table 1, entry 9; Table 2, entry 6). This procedure should be recommended for all dynamic headspace methods where rapid desorption of high-boiling organic volatiles is needed. The great efficiency of carbon dioxide could be linked to its high solubility in water, and probably also to its dissolution kinetics.

Among the factors governing the recovery, we found that the removal of hydrocarbons from the liquid matrix is essential, and greatly enhanced by the dissolved gases.

5. References

[1] S. Varner, C. Breder and T. Fazio, *J. Assoc. Off. Anal. Chem.*, 66 (1983) 1067–1073.
[2] J. Adda, J. Dekimpe, L. Vassal and H.E. Spinnler, *Lait*, 69 (1989) 115–120.
[3] J. Gilbert and R.A. Startin, *J. Sci. Food Agric.*, 34 (1983) 647–652.
[4] V. Ducruet, *Lebensm. Wiss. Technol.*, 17 (1984) 217–221.
[5] A. Venema, *J. High Resolut. Chromatogr. Chromatogr. Commun.*, 11 (1988) 128–131.
[6] J.W. Eichelberger, T.A. Bellar, J.P. Donelly and W.L. Budde, *J. Chromatogr. Sci.*, 28 (1990) 460–467.
[7] J.E. Matiella and T.C.Y. Hsieh, *J. Food Sci.*, 56 (1991) 387–390.
[8] X. Yan, K.R. Carney and E.B. Overton, *J. Chromatogr. Sci.*, 30 (1992) 491–496.
[9] J.S.Y. Ho, *J. Chromatogr. Sci.*, 27 (1989) 91–98.
[10] G.S. Fisher, M.G. Legendre, N.V. Lovgren, W.H. Schuller and J.A. Wells, *J. Agric. Food Chem.*, 27 (1979) 7–11.
[11] N.V. Lovegren, G.S. Fisher, M.G. Legendre and W.H. Schuller, *J. Agric. Food Chem.*, 27 (1979) 851–853.
[12] H. Kessels, W. Hoogerwerf and J. Lips, *J. Chromatogr. Sci.*, 30 (1992) 247.
[13] S. Kyosai and B. Rittmann, *Res. J. Water Pollut. Control Fed.*, 63 (1991) 887–894.

[14] P.G. Murphy, D.A. MacDonald and T.D. Lickly, *Food Chem. Toxicol.*, 30 (1992) 225–232.
[15] R.J. Steichen, *Anal. Chem.*, 48 (1976) 1398–1402.
[16] *Kirk Othmer Encyclopedia of Chemical Technology*, Vol. 21, Wiley, New York, p. 771.
[17] H.J. Ehret, V. Ducruet, J. Luciani and A. Feigenbaum, *Analusis*, in press.
[18] R.C. Weast (Editor), *CRC Handbook of Chemistry and Physics*, CRC Press, Boca Raton, FL, 17th ed., 1989, p. B112.
[19] T.A. Bellar and J.J. Lichtenberg, *J. Am. Water Works Assoc., December* (1974) 739–744.

ELSEVIER

Journal of Chromatography A, 667 (1994) 348–353

JOURNAL OF CHROMATOGRAPHY A

Short Communication

Rapid method for the determination of multiple pyrethroid residues in fruits and vegetables by capillary column gas chromatography

Guo-Fang Pang*[,a], Chun-Lin Fan[a], Yan-Zhong Chao[a], Tie-Sheng Zhao[b]

[a]*Qin Huangdao Import and Export Commodity Inspection Bureau, Qin Huangdao, Hebei 066002, China*

[b]*Qin Huangdao Health and Quarantine Bureau, Qin Huangdao, Hebei 066002, China*

(First received October 7th, 1993; revised manuscript received January 17th, 1994)

Abstract

A rapid and economical simplified multi-residue method is described for the determination of multiple pyrethroid insecticides in fruits and vegetables. The residues are extracted from crops with methanol and the crop co-extractives are removed by toluene partitioning and Florisil–charcoal minicolumn chromatography. The final extract is analysed by capillary column gas chromatography with electron-capture detection. The recoveries were determined by fortifying six different crops (apples, oranges, cabbages, pears, peppers and tomatoes) with eleven pyrethroids (Py-115, allethrin, biphenthrin, fenpropathrin, cyhalothrin, permethrin, cyfluthrin, flucythrinate, fluvalinate, fenvalerate and deltamethrin) at three levels, 0.01–0.07, 0.10–0.70 and 1.0–7.0 mg/kg. Three determinations were made at each level for each crop. Recoveries of the eleven pyrethroids ranged from 70.4 to 110.0% at the three different levels. The practical determination limit of the method was in the range 3.0–30.0 μg/kg for all the pyrethroid insecticides. The proposed method had major advantages that simplified steps were achieved for the extraction and the clean-up, the solvent consumption was reduced and the analysis time was shortened.

1. Introduction

Various pyrethroids are widely used as agricultural insecticides around the world. The development of a multi-residue method for the determination of these insecticides in crops is indispensable to routine work. Well known multi-residue approaches have been applied successfully to analyses for organohalogens [1], organophosphates [1,2] and carbamates [3,4] in agricultural products. The pyrethroid insecticides differ from the oganophosphates and the carbamates, as each of them is actually a mixture of more than one isomer, and some pyrethroids consist of eight possible isomers [5]. Therefore, it is more difficult to develop a multi-residue method for pyrethroids. However, several methods have been published for the multi-residue determination of pyrethroids in agricultural products [5–8].

Various methods for the extraction and clean-up of individual or several pyrethroids in crops have been described. The solvent systems included acetone–hexane [5,9,10], acetone–dichloromethane [6,11], acetone–light petroleum [7,8], acetonitrile–hexane [12], methanol–

* Corresponding author.

0021-9673/94/$07.00
SSDI 0021-9673(94)00080-S

toluene [13,14] and acetonitrile–light petroleum [15]. The different types of adsorbent used included Florisil [7,9,12,15], silica gel [5], alumina [6,16], Bio-Beads SX-3 [9,15], alumina–Florisil [10], Florisil–charcoal [13,14] and activated charcoal–magnesia–diatomaceous earth [6]. Most of these procedures for extraction and clean-up require large volumes of solvents and time-consuming evaporation of the organic solvents before further clean-up and analysis either to concentrate the residues or to remove solvents that interfere with selective detection.

Of the extraction and partitioning systems investigated, we found that methanol–toluene extraction and Florisil–charcoal minicolumn clean-up did not essentially have these drawbacks. It was originally used in a comprehensive multi-residue method for various compounds including two pyrethroids [13,14]. In this work, this technique for extraction and clean-up was appropriately modified, and it was successfully extended to the determination for multiple pyrethroid residues in fruits and vegetables.

2. Experimental

2.1. Instrumentation

A Hewlett-Packard Model 5890A gas chromatograph equipped with a ^{63}Ni electron-capture detector, a split–splitless capillary column injection port, a Model 7673A automatic sampler and a Model 3393A reporting integrator was used. The injection port temperature was 280°C and the detector temperature 300°C. Both the carrier gas and make-up gas were methane–argon (10:90).

Fused-silica capillary columns were supplied by Hewlett-Packard: (i) HP-1 (2.65 μm), 5 m × 0.53 mm I.D., as an analytical column, carrier gas flow-rate 5.0 ml/min, make-up gas flow-rate 60.0 ml/min, column temperature programme initially 230°C for 2 min and increased at 2°C/min to 260°C, held for 5 min; (ii) Ultra 2 (0.17 μm) (cross-linked 5% phenyl–methylsilicone), 25 m × 0.32 mm I.D., as a confirmation column, carrier gas flow-rate 1.2 ml/min, make-up gas flow-rate 54.0 ml/min, column temperature programme initially 50°C for 0.5 min, increased at 20°C/min to 210°C, held for 12 min, and increased at 1°C/min to 250°C, held for 8 min.

2.2. Reagents

Standard solutions of the insecticides in toluene (100 μg/ml) were prepared for deltamethrin (98.0%), cypermethrin (97.0%), fenpropathrin (92.3%), fenvalerate (94.1%), biphenthrin (94.3%), cyhalothrin (97.0%), permethrin (91.1%), flucythrinate (94.2%), fluvalinate (90.6%), cyfluthrin (93.8%), allethrin (92.3%) and Py-115 (93.7%). These insecticides were obtained from Roussel-Uclaf Nanjing Office (Nanjing, China), FMC Far East (Beijing, China), Shell China (Beijing, China), ICI China (Beijing, China) and Shanghai Midwest Pesticide Factory (Shanghai, China).

Methanol and toluene were redistilled in all-glass apparatus prior to use and procedural blanks were analysed by gas chromatography with electron-capture detection before sample analysis.

Charcoal (20–40 mesh), acid-washed and activated as described by Bolygŏ and Zakar [6], and Florisil (60–100 mesh), activated as described by Holland and McGhie [13], were used.

2.3. Extraction, clean-up and analysis

Place 50.0 g of chopped sample and 50 ml of methanol in a homogenizer jar and homogenize sample for 2 min at high speed. Vacuum filter the homogenate through a 12-cm perforated Büchner funnel containing filter-paper, collecting the filtrate in a 250-ml filter flask. Re-homogenize the filter cake with 50 ml of methanol and filter. Measure the volume of the combined filtrates. Transfer a portion of filtrate equivalent to 20 g of sample into a 250-ml separating funnel and add 10 ml of toluene followed by 60 ml of water containing 10% (w/v) NaCl. Shake well for 2 min and let the layers separate. Prepare a chromatographic minicolumn: on top of a glass-wool plug add 0.5 g of Florisil followed by 0.04 g of activated charcoal and 1.5 g of anhydrous

Table 1
Recoveries of pyrethroids from various crops

Compound	Added (ppm)	Average recovery ± S.D. (%)[a] and R.S.D. (%)[b]					
		Apples	Oranges	Pears	Peppers	Cabbages	Tomatoes
Py-115	0.01	107.2 ± 3.9 (3.6)	98.6 ± 4.2 (4.3)	89.1 ± 2.7 (3.0)	96.4 ± 5.6 (5.8)	101.1 ± 3.2 (3.2)	97.2 ± 1.6 (1.7)
	0.10	88.3 ± 2.8 (3.2)	96.7 ± 1.9 (2.0)	81.4 ± 3.2 (3.9)	86.2 ± 1.5 (1.7)	83.9 ± 2.7 (3.2)	97.5 ± 3.0 (3.1)
	1.00	92.6 ± 3.4 (3.7)	90.3 ± 4.0 (4.4)	83.2 ± 3.7 (4.5)	80.5 ± 2.9 (3.6)	91.6 ± 1.4 (1.5)	102.3 ± 3.9 (3.8)
Allethrin	0.01	95.4 ± 3.6 (3.8)	110.0 ± 3.1 (2.8)	98.4 ± 2.7 (2.7)	92.8 ± 4.3 (4.6)	89.7 ± 3.1 (3.5)	99.3 ± 3.0 (3.0)
	0.10	87.0 ± 1.5 (1.7)	81.9 ± 1.7 (2.1)	90.3 ± 2.3 (2.5)	86.4 ± 3.4 (3.9)	92.5 ± 3.1 (3.4)	89.3 ± 2.0 (2.2)
	1.00	88.4 ± 2.1 (2.4)	91.0 ± 3.5 (3.8)	80.1 ± 2.7 (3.4)	83.6 ± 1.9 (2.3)	92.1 ± 0.9 (1.0)	94.5 ± 3.3 (3.5)
Biphenthrin	0.02	80.3 ± 1.9 (2.5)	87.6 ± 2.5 (2.9)	85.0 ± 2.7 (3.2)	90.3 ± 4.6 (5.1)	96.1 ± 1.8 (1.9)	82.1 ± 3.9 (4.8)
	0.20	92.3 ± 3.5 (3.8)	89.0 ± 3.3 (3.7)	93.5 ± 2.4 (2.6)	107.5 ± 4.2 (3.9)	78.5 ± 1.9 (2.4)	79.0 ± 3.7 (4.7)
	2.00	83.2 ± 1.7 (2.0)	78.9 ± 2.1 (2.7)	97.0 ± 3.7 (3.8)	73.4 ± 2.6 (3.5)	81.4 ± 3.1 (3.8)	81.2 ± 0.9 (1.1)
Fenpropathrin	0.02	82.2 ± 2.0 (2.4)	79.8 ± 2.9 (3.6)	91.5 ± 0.7 (0.8)	75.3 ± 3.2 (4.3)	84.0 ± 1.6 (1.9)	96.4 ± 1.8 (1.9)
	0.20	80.7 ± 3.7 (4.6)	87.0 ± 1.9 (2.2)	77.4 ± 2.9 (3.9)	98.3 ± 1.7 (1.8)	83.8 ± 2.9 (3.5)	82.9 ± 1.9 (2.3)
	2.00	90.4 ± 1.2 (1.3)	101.1 ± 3.0 (3.0)	86.5 ± 0.7 (0.8)	85.8 ± 2.8 (3.3)	102.3 ± 1.6 (1.6)	81.4 ± 3.4 (4.2)
Cyhalothrin	0.01	95.6 ± 2.9 (3.1)	99.3 ± 1.7 (1.7)	89.6 ± 2.3 (2.6)	78.6 ± 2.4 (3.1)	85.7 ± 1.6 (1.9)	78.6 ± 2.2 (2.8)
	0.10	82.9 ± 1.6 (1.9)	106.7 ± 1.6 (1.5)	78.9 ± 0.8 (1.0)	96.4 ± 3.2 (3.3)	84.3 ± 3.1 (3.7)	82.9 ± 3.0 (3.6)
	1.00	79.6 ± 0.9 (1.1)	101.3 ± 3.1 (3.1)	85.7 ± 3.1 (3.6)	87.1 ± 1.8 (2.1)	96.4 ± 1.9 (2.0)	81.4 ± 4.5 (5.5)
Permethrin	0.07	80.9 ± 1.1 (1.4)	81.4 ± 1.7 (2.1)	82.9 ± 3.0 (3.6)	93.4 ± 2.3 (2.5)	92.9 ± 2.9 (3.1)	86.3 ± 1.3 (1.5)
	0.70	79.7 ± 1.7 (2.1)	102.3 ± 3.4 (3.3)	92.0 ± 1.9 (2.2)	106.5 ± 3.7 (3.5)	79.4 ± 1.9 (2.4)	80.7 ± 2.1 (2.6)
	7.00	83.6 ± 2.6 (3.1)	81.9 ± 2.6 (3.2)	98.4 ± 3.5 (3.6)	80.1 ± 1.5 (1.9)	81.3 ± 3.6 (4.4)	91.0 ± 1.7 (1.9)
Cyfluthrin	0.03	84.2 ± 3.5 (4.2)	83.3 ± 3.6 (4.3)	86.2 ± 1.5 (1.7)	78.0 ± 3.2 (4.1)	75.0 ± 3.4 (4.5)	86.3 ± 3.6 (4.2)
	0.30	80.0 ± 0.9 (1.1)	89.7 ± 1.9 (2.1)	87.9 ± 2.0 (2.3)	86.7 ± 1.7 (2.0)	82.1 ± 2.6 (3.2)	89.5 ± 1.5 (1.7)
	3.00	92.5 ± 2.9 (3.1)	77.0 ± 3.0 (3.9)	83.6 ± 3.3 (4.0)	82.1 ± 2.6 (3.2)	79.1 ± 2.7 (3.4)	97.9 ± 4.1 (4.2)
Flucythrinate	0.04	79.1 ± 2.5 (3.2)	93.3 ± 2.1 (2.3)	80.3 ± 3.1 (3.9)	81.0 ± 3.1 (3.8)	84.6 ± 2.5 (3.0)	80.0 ± 1.9 (2.4)
	0.40	89.5 ± 3.7 (4.1)	98.7 ± 3.6 (3.7)	82.4 ± 1.6 (1.9)	89.4 ± 2.4 (2.7)	90.0 ± 1.7 (1.9)	86.7 ± 2.3 (2.7)
	4.00	94.6 ± 1.1 (1.2)	87.9 ± 2.7 (3.1)	97.3 ± 2.7 (2.8)	90.3 ± 3.6 (4.0)	77.4 ± 2.8 (3.6)	81.1 ± 3.1 (3.8)

Table 1 (*continued*)

Compound	Added (ppm)	Average recovery ± S.D. (%)[a] and R.S.D. (%)[b]					
		Apples	Oranges	Pears	Peppers	Cabbages	Tomatoes
Fenvalerate	0.04	90.0 ± 4.1 (4.2)	76.9 ± 2.8 (3.6)	104.2 ± 4.3 (4.1)	80.4 ± 1.9 (2.4)	88.2 ± 3.3 (3.8)	106.3 ± 3.9 (3.7)
	0.40	95.2 ± 2.1 (2.2)	84.3 ± 1.7 (2.0)	91.0 ± 1.5 (1.7)	83.4 ± 0.8 (1.0)	85.4 ± 2.1 (2.5)	90.6 ± 2.1 (2.3)
	4.00	82.1 ± 3.0 (3.7)	82.1 ± 3.1 (3.8)	88.4 ± 2.6 (2.9)	91.3 ± 3.1 (3.4)	78.0 ± 3.6 (4.6)	83.2 ± 2.7 (3.3)
Fluvalinate	0.04	79.4 ± 1.8 (2.3)	79.4 ± 3.0 (3.8)	90.5 ± 3.1 (3.4)	83.0 ± 3.3 (4.0)	77.3 ± 4.2 (5.4)	81.6 ± 2.9 (3.6)
	0.40	96.9 ± 2.7 (2.8)	88.5 ± 2.3 (2.6)	79.3 ± 1.8 (2.3)	92.4 ± 1.5 (1.6)	83.6 ± 3.0 (3.6)	87.4 ± 0.8 (0.9)
	4.00	82.3 ± 3.4 (4.1)	83.2 ± 1.9 (2.3)	82.2 ± 3.6 (4.4)	80.0 ± 2.9 (3.6)	80.6 ± 2.9 (3.6)	109.4 ± 3.8 (3.5)
Deltamethrin	0.04	98.2 ± 2.3 (2.3)	72.3 ± 2.8 (3.9)	75.4 ± 2.9 (3.9)	92.1 ± 1.7 (1.8)	78.4 ± 2.7 (3.4)	81.0 ± 2.7 (3.3)
	0.40	94.3 ± 1.7 (1.8)	80.5 ± 1.2 (1.5)	88.6 ± 2.3 (2.6)	86.5 ± 1.1 (1.3)	88.1 ± 0.7 (0.8)	96.9 ± 1.1 (1.1)
	4.00	77.6 ± 2.9 (3.7)	89.2 ± 4.0 (4.5)	77.1 ± 3.2 (4.2)	90.3 ± 2.6 (2.9)	82.3 ± 1.9 (2.3)	85.4 ± 4.0 (4.7)

[a] $n = 3$.
[b] R.S.D.s in parentheses.

Na_2SO_4. Prewash the minicolumn with 20 ml of toluene. Add 5 ml of the toluene layer from the separating funnel and collect the eluate in a sample tube. Elute with an additional 5 ml of toluene and adjust the total eluate volume to a suitable level for gas chromatography. Tentatively identify the residue peaks according to the retention times. Measure peak areas or peak heights and determine the residue content by comparison with that obtained from a known content of appropriate reference material.

3. Results and discussion

The efficiency of extraction and clean-up of the modified procedure was satisfactory, as no interfering peaks were observed on the chromatogram of the different samples under the selected conditions. However, organochlorine compounds such as HCB, BHC, heptachlor, aldrin, heptachlor epoxide and DDT would also be extracted together with the pyrethroid insecticides, if present in the sample. We found that the retention times of the pyrethroids on the capillary columns described as above were considerably longer than those of organochlorines. It took *ca.* 3 min for the organochlorines to be eluted from the column before the pyrethroid insecticides, except for Py-115 and allethrin, which has almost the same retention times as isomers of BHC and DDT, respectively. This problem could be resolved by the confirmatory method described below.

The proposed method validation was based on the recovery of different insecticides from the selected crops. Six fruits and vegetables were fortified with eleven pyrethroids at 0.01–0.07, 0.10–0.70 and 1.0–7.0 mg/kg levels, using 50 g

of each sample and adding *ca.* 1 ml of methanol containing an appropriate amount of each of the insecticides. One unfortified portion and three fortified portions of each sample were analysed at one time. The recovery data obtained are given in Table 1. A chromatogram of these compounds is shown in Fig. 1. Linear calibration graphs were obtained from 0.005 to 3.0 ng for the eleven insecticides. The practical determination limit of the method was in the range 3.0–30.0 μg/kg for all the insecticides.

In order to increase the reliability of peak identification on the basis of wide-bore capillary gas chromatographic data, especially in the presence of interferents originating from crop samples or possible cross-interference from either some pyrethroids or organochlorine compounds present together, we also examined separations on a high-resolution narrow-bore capillary column. An example of the analysis of an apple sample spiked with 12 pyrethroids is given in Fig. 2. As can be seen in Figs. 1 and 2, all isomers of each insecticide appeared as a single peak on the chromatogram from the wide-bore column, except for flucythrinate, whereas they were all separated as isomeric peaks on the narrow-bore column. This should not only enhance the resolution but also confirm the presence of various pyrethroids. For example, biphenthrin and fenpropathrin had the same retention time on the wide-bore column but were completely resolved with the narrow-bore column.

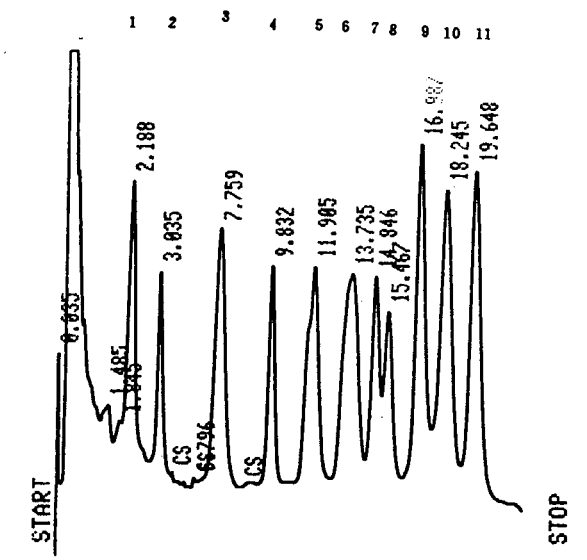

Fig. 1. Chromatogram of a spiked apple extract using the wide-bore capillary column. Peaks: 1 = Py-115 (0.10 mg/kg); 2 = allethrin (0.10 mg/kg); 3 = biphenthrin (0.12 mg/kg) + fenpropathrin (0.12 mg/kg); 4 = cyhalothrin (0.15 mg/kg); 5 = permethrin (0.70 mg/kg); 6 = cyfluthrin (0.35 mg/kg); 7, 8 = flucythrinate (0.40 mg/kg); 9 = fenvalerate (0.40 mg/kg); 10 = fluvalinate (0.40 mg/kg); 11 = deltamethrin (0.40 mg/kg). For chromatographic conditions, see text; injection volume, 1 μl. Values at peaks indicate retention times in min.

Cyfluthrin, cypermethrin and flucythrinate consist of four, four and two isomers, respectively. They can be eluted separately as one, one and two peaks with the wide-bore capillary column. However, cyfluthrin and cypermethrin were not resolved and the peak of cypermethrin and the first isomeric peak of flucythrinate overlapped when present together in the samples. The three insecticides were eluted separately as four, four and two peaks with the narrow-bore capillary column, and their isomeric peaks were well resolved, except for the last isomeric peak of cypermethrin and the first isomeric peak of fluthrinate, which overlapped. However, these problems have no effect on the identifications of the various pyrethroids. Therefore, the wide-bore capillary column was used as the analytical column and the narrow-bore capillary as the confirmation column. By this means it was easy to determine multiple residues of the pyrethroids in fruits and vegetables.

In conclusion, the method described is relatively simple, rapid and economical, and is suitable for multi-residue analyses for pyrethroid insecticides in non-fatty samples.

4. Acknowledgements

The authors gratefully thank ICI China, FMC Far East and Shell China for providing reference pesticides.

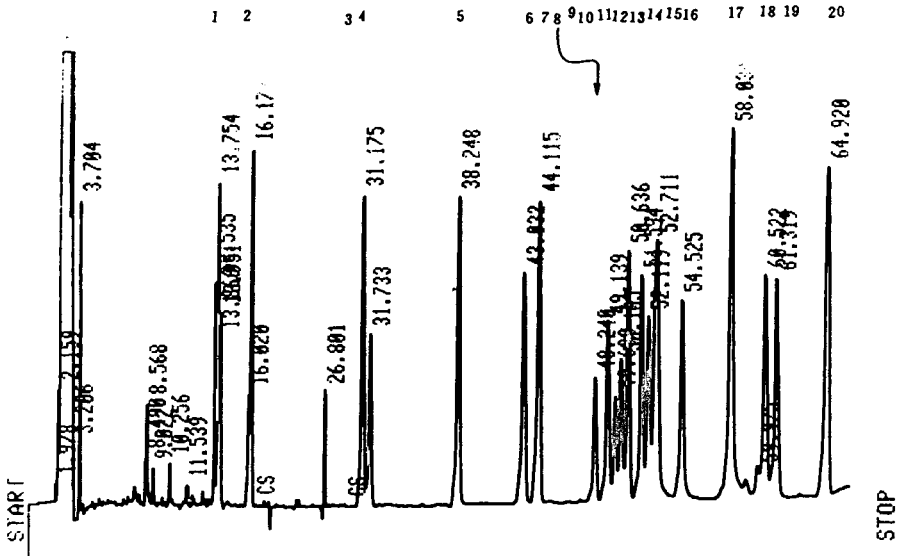

Fig. 2. Chromatogram of a spiked apple extract using the narrow-bore capillary column. Peaks: 1 = Py-115; 2 = allethrin; 3 = biphenthrin; 4 = fenpropathrin; 5 = cyhalothrin; 6, 7 = permethrin; 8, 9, 10, 11 = cyfluthrin; 12, 13, 14 = cypermethrin; 15 = cypermethrin + flucythrinate; 16 = flucythrinate; 17 = fenvalerate; 18, 19 = fluvalinate; 20 = deltamethrin. For chromatographic conditions, see text; injection volume, 1 μl. Spiked sample concentrations as in Fig. 1, plus cypermethrin (0.40 mg/kg). Values at peaks indicate retention times in min.

5. References

[1] *Official Methods of Analysis of the Association of Official Analytical Chemists*, AOAC, Arlington, VA, 15th ed., 1990, p. 274.
[2] *Official Methods of Analysis of the Association of Official Analytical Chemists*, AOAC, Arlington, VA, 15th ed., 1990, p. 287.
[3] *Official Methods of Analysis of the Association of Official Analytical Chemists*, AOAC, Arlington, VA, 15th ed., 1990, pp. 291 and 292.
[4] D. Chaput, *J. Assoc. Off. Anal. Chem.*, 71 (1988) 542.
[5] P.G. Baker and P. Bottomley, *Analyst*, 107 (1982) 206.
[6] E. Bolygó and F. Zakar, *J. Assoc. Off. Anal. Chem.*, 66 (1983) 1013.
[7] J.X. Ming, C.F. Qina and Z.L. Liu, *Acta Agric. Univ. Pekinensis*, 15 (1989) 181.
[8] G.F. Pang, C.L. Fan, Y.Z. Chao and T.S. Zhao, *J. Assoc. Off. Anal. Chem.*, in press.
[9] *Pesticide Analytical Manual*, Vol. II, Food and Drug Adminstration, Washington, DC, 1986, Sect. 180.418.
[10] M.D. Awasthi, *J. Food Technol.*, 22 (1985) 4.
[11] Y. Ishii, N. Adachi, J. Taniuchi and T. Sakamoto, *J. Pestic. Sci.*, 15 (1990) 225.
[12] H.E. Braun and J. Stanek, *J. Assoc. Off. Anal. Chem.*, 65 (1982) 685.
[13] P.T. Holland and T.K. McGhie, *J. Assoc. Off. Anal. Chem.*, 66 (1983) 1003.
[14] Y. Ishii, T. Sakamoto, K. Asukura, N. Adachi and J. Taniuchi, *J. Pestic. Sci.*, 15 (1990) 205.
[15] W. Dicke, H.D. Ocker and H.P. Thier, *Z. Lebensm.-Unters.-Forsch.*, 186 (1988) 125.
[16] P. Bottomely and P.G. Baker, *Analyst*, 109 (1984) 85.

ELSEVIER

Journal of Chromatography A, 667 (1994) 354–360

JOURNAL OF CHROMATOGRAPHY A

Short Communication

Molar mass determination of oligomeric ethylene oxide adducts using supercritical fluid chromatography and matrix-assisted laser desorption–ionization time-of-flight mass spectrometry

Ulrich Just*[,a], Hans-Rainer Holzbauer[b], Martin Resch[c]

[a]*Federal Institute for Material Research and Testing (BAM), Unter den Eichen 87, 12205 Berlin, Germany*
[b]*Centre for Macromolecular Chemistry, Rudower Chaussee 5, 12484 Berlin, Germany*
[c]*Shimadzu Europa GmbH, Albert-Hahn-Str. 6–10, 47269 Duisburg, Germany*

(Received November 15th, 1993)

Abstract

Supercritical fluid chromatography (SFC) and matrix-assisted laser desorption–ionization time-of-flight mass spectrometry [MALDI-MS (TOF)] are suitable, mutually complementary methods for characterizing oligomeric ethylene oxide adducts. While SFC is successfully applicable in the low-molecular-size range up to molar masses of *ca.* 1000 g/mol, MALDI-MS facilitates proper differentiation also in higher molar mass ranges. In the lower molar mass ranges down to approximately degree of polymerization $n = 6$, the problem of discrimination arises when MALDI-MS is applied; this problem is reduced considerably through the addition of lithium chloride instead of sodium or potassium ions, a measure which also eases identification of the molar peak. Provided that the ethylene oxide chain is known, it is also possible to definitely determine substituents in the molecule (*e.g.*, alkyl or arylalkyl chains). By-products, which may arise, for example, when water is split off during the reaction or during storage, can be detected.

1. Introduction

Oligomeric ethylene oxide adducts are of great significance in the chemistry of both surfactants and polymers. From scientific and economic points of view, it is necessary to know the composition and the oligomer distribution of these compounds and mixtures.

In the low-molecular-size range, gas chromatography (GC) can be applied as a method of analysis. High-temperature GC (HTGC) facilitates high-resolution analysis in the shortest of times; further, its use in conjunction with various detection and other methods such as GC–MS, GC–IR and GC–LC is both well tested and easy to implement [1].

Supercritical fluid chromatography (SFC) extends the molar mass range. An essential advantage over GC is that the compounds can be eluted at lower temperatures. This is of particular significance with respect to thermolabile components or compounds. Capillary SFC is the method of choice for the molar mass range 500–1000 g/mol [2]; reversed-phase high-perform-

* Corresponding author.

0021-9673/94/$07.00
SSDI 0021-9673(94)00101-E

ance liquid chromatography (RP-HPLC, gradient elution) can be applied for higher molar mass ranges, *e.g.*, for separating polyethylene glycols up to a molar mass of 4500 g/mol [3].

Separation of substances with comparably high molar masses has also been achieved with capillary SFC by increasing the density (pressures up to 560 bar at 120°C) [4]. Hitherto, however, commercially available equipment has permitted pressures only up to *ca.* 400 bar. Unknown samples can be identified by coupling SFC with mass spectrometry (MS).

In order to facilitate the analysis of polar compounds using SFC, the addition of modifiers, *e.g.*, methanol or acetone, to the supercritical fluid carbon dioxide is recommended. In this instance detection can be implemented through the use of an evaporative light-scattering detector. In this work on the composition and purity of oligomeric ethylene oxide adducts, the chromatographic technique used was SFC with supercritical carbon dioxide and flame ionization detection (FID).

During the past few years, matrix-assisted laser desorption–ionization mass spectrometry (MALDI-MS) has proved a valuable complement to chromatography. This method is based on the principle that the dissolved specimen is mixed with a matrix and then crystallizes. The specimen is desorbed and ionized by laser incidence. The molar mass is determined by the time of flight (TOF) [5–11]. The aim of this investigation was to compare the information obtained through MALDI-MS (TOF) with that obtained by SFC with respect to the composition and purity of oligomeric ethylene oxide adducts.

2. Experimental

2.1. SFC

A Lee Scientific 602-D system with a fused-silica separation column (10 m × 50 μm I.D.) was used with SB-Biphenyl-30 as the stationary phase and CO_2 (SFC grade; Scott, Plumsteadville, PA, USA) as the mobile phase. FID at 380°C was applied. An integral restrictor was used and the injection system was a switching valve with an internal loop (Valco) and timed split.

For the chromatograms shown in Fig. 1a–f the oven temperature was initially 100°C (5 min isothermal), then programmed at 1.6°C/min to 200°C. The pressure was initially 100 bar (5 min isobaric), then increased at 10 bar/min to 300 bar and at 5 bar/min to 400 bar, with 30 min isobaric at 400 bar. For the chromatograms shown in Fig. 1g–i the oven temperature was 130°C and the density was programmed from 0.25 to 0.55 g/ml in 42.86 min and from 0.55 to 0.7 g/ml in 27.27 min.

2.2. MALDI-MS

A Kratos Compact MALDI III system was used in the positive-ion mode with reflectron time-of-flight, and a 20 kV accelerating voltage. The matrix was dihydroxybenzoic acid (10 mg/ml in acetone).

2.3. Reference substances

The following series of substances were chosen for this study: defined polyethylene glycols (degree of hydroxyethylation $n = 4, 6, 8$); defined *n*-octylpolyethylene glycol ethers ($n = 3, 4, 6$); and defined *p*-isononylphenylpolyethylene glycol ethers ($n = 2, 6, 9$). These defined substances were prepared either by specific synthesis or by distillative isolation from homologeous mixtures [2].

3. Results and discussion

For the molar mass range of the oligomeric ethylene glycols, alkylethylene glycol ethers and alkylarylethylene glycol ethers studied, SFC has shown itself to be the method of choice. The reference substances facilitate a precise assignment of the peaks in the distribution chromatogram (Fig. 1a–i). This is fundamental for the calculation of the molar masses for oligomeric mixtures [2]. In the case of hydroxyethylated *p*-isononylphenols, SFC provides not only for a separation according to the degree of hydroxy-

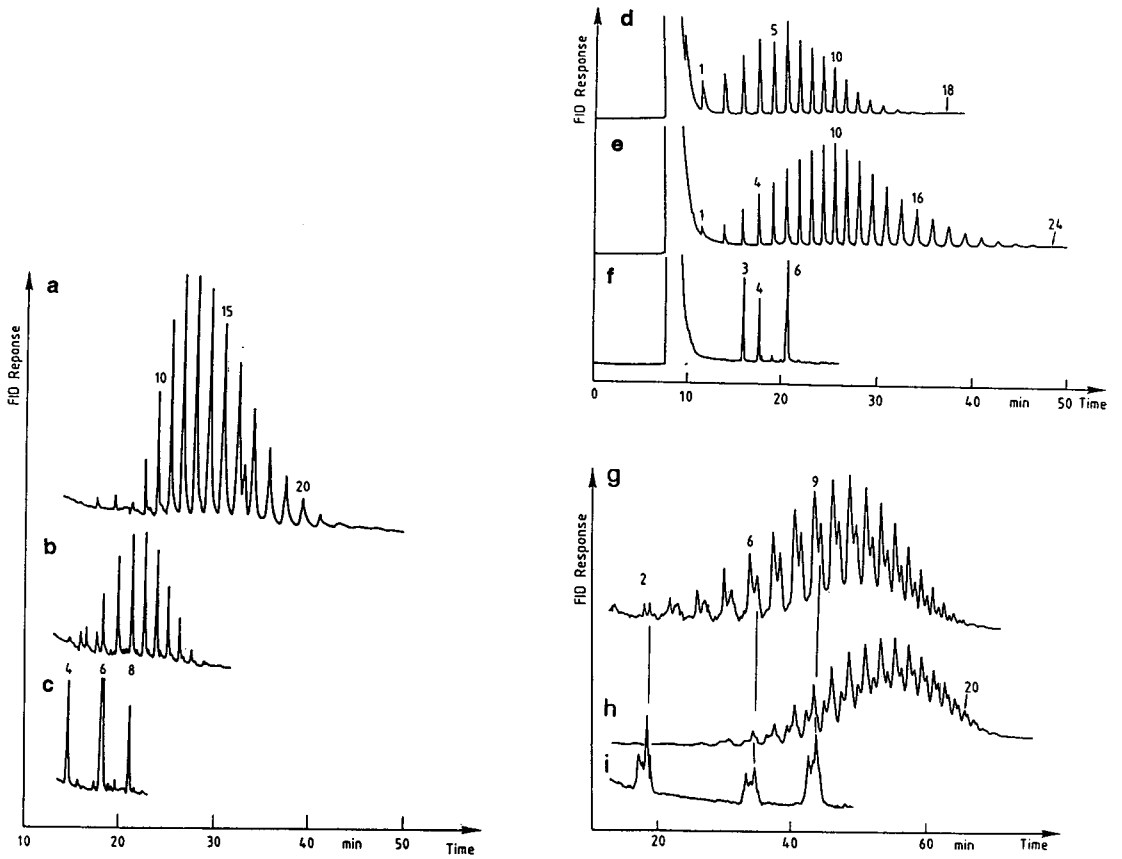

Fig. 1. SFC of (a) polyethylene glycol (PEG 600) (Polymer Laboratories, Church Stretton, UK), (b) polyethylene glycol (PEG 440) (Polymer Laboratories), (c) a mixture of reference substances (defined polyethylene glycols, $n = 4$, 6, 8), (d) *n*-octylpolyethylene glycol ether ($n = 5_{\text{statistical}}$), (e) *n*-octylpolyethylene glycol ether ($n = 10_{\text{statistical}}$), (f) a mixture of reference substances (defined polyethylene glycol ethers, $n = 3$, 4, 6), (g) *p*-isoalkylphenylpolyethylene glycol ether ($n = 10_{\text{statistical}}$), (h) *p*-isononylphenylpolyethylene glycol ether ($n = 13_{\text{statistical}}$) and (i) a mixture of reference substances (defined *p*-isononylphenylpolyethylene glycol ethers, $n = 2$, 6, 9).

ethylation but also according to the alkyl residues on the benzene ring. However, differentiations of this type become difficult where a branched nonylphenyl ethoxylate in the presence of, for example, octylphenyl ethoxylate is involved (Fig. 1g–i). Here MALDI-MS provides decisive information; it permits the exact determination of the lengths of the alkyl chains in the compound. Of course, branched chains cannot be differentiated from the corresponding linear chains, because the method only separates by mass. Both methods, SFC and MALDI-MS, complement each other to provide a solution to this analysis problem.

MALDI-MS provides outstanding differentiation in the higher molar mass range. While SFC for polyethylene glycol (PEG) 600, for example, facilitates the detection of components up to a degree of polymerization $n = 24$, MALDI-MS can differentiate up to a $n = 30$. In this molar mass range MALDI-MS is therefore superior to SFC. The reduced time required in comparison with an analysis by capillary SFC is also noteworthy.

A different picture is obtained in the molar mass range below *ca.* 500 g/mol. On application of MALDI-MS, a clear discrimination of the low-molar-mass components can be noted. In the

mass spectrum of the reference mixture tetra-, hexa- and octaethylene glycol (1:1:1), the peak for degree of polymerization $n = 6$ (molar mass 282 g/mol) shows only *ca.* 45% of the peak height to be expected in accordance with the mixture components as compared with $n = 8$ (molar mass 370 g/mol), and $n = 4$ (molar mass 194 g/mol) only shows *ca.* 4% as compared with $n = 8$ (Fig. 2a). The spectra show the molar peaks plus the mean molar mass of lithium (*ca.* 7 g/mol).

A similar result is obtained for a reference mixture of *n*-octyl(tri-, tetra- and hexa)ethylene glycol ethers (1:0.8:1). The peak for degree of polymerization $n = 4$ (molar mass 306 g/mol) shows only *ca.* 75% of the peak height to be expected in accordance with the mixture components as compared with $n = 6$ (molar mass 394 g/mol), and $n = 3$ (molar mass 262 g/mol) shows only *ca.* 20%. As in SFC, so too the MALDI mass spectrum shows a small portion of $n = 5$ (molar mass 350 g/mol) (Fig. 2c).

The spectra usually show the molar peaks plus the molar mass of sodium (23 g/mol) and potassium (39 g/mol). Unless they have been specifically added, the sodium and potassium ions come from contaminants in the specimen and/or the matrix. Alternatively, the quality of the result can be influenced by adding a suitable salt [12]. The addition of lithium chloride suppresses the discrimination of the low-molar-mass components in the oligomeric mixture. While the mass spectrum of the octylpolyethylene glycol ether ($n = 5_{\text{statistical}}$) only begins at $n = 6$, the addition of lithium chloride makes it possible to also discern $n = 5$, 4 and 3. However, even in this preparation of the specimen, $n = 2$, 1 and 0, which are distinctly separated in SFC, are miss-

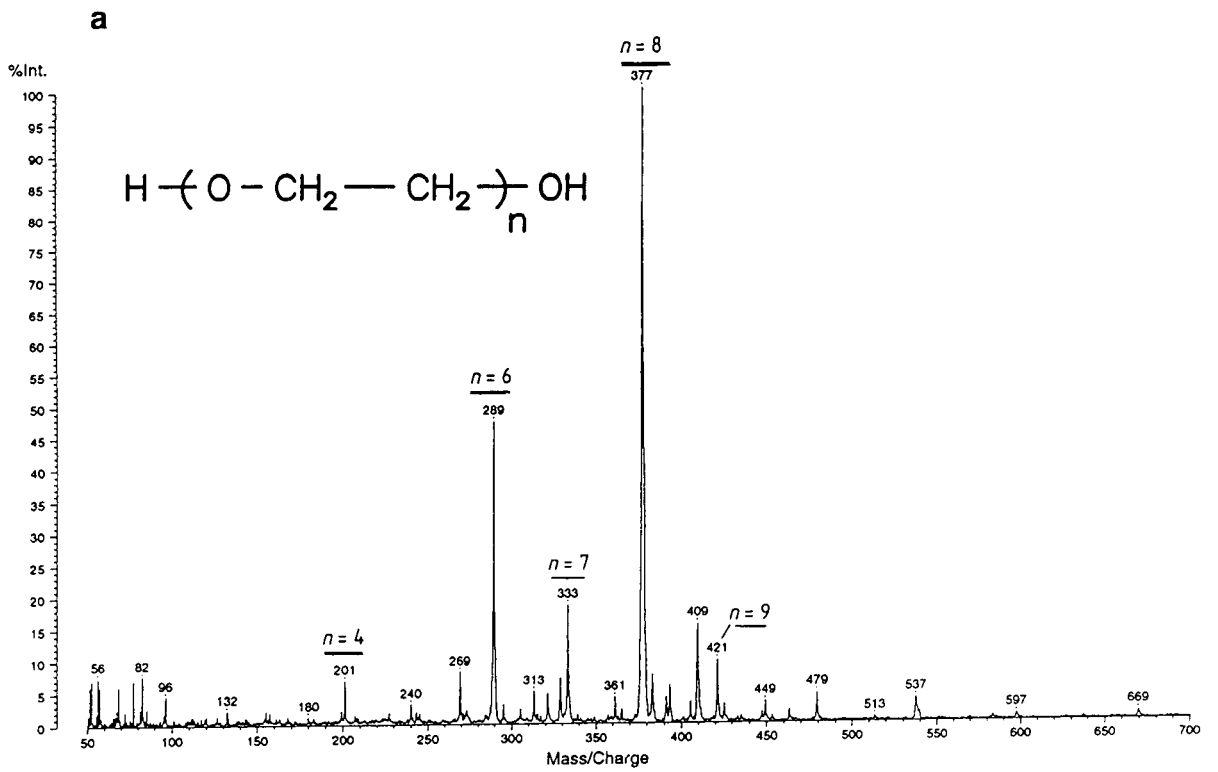

Fig. 2.

(*Continued on p. 358*)

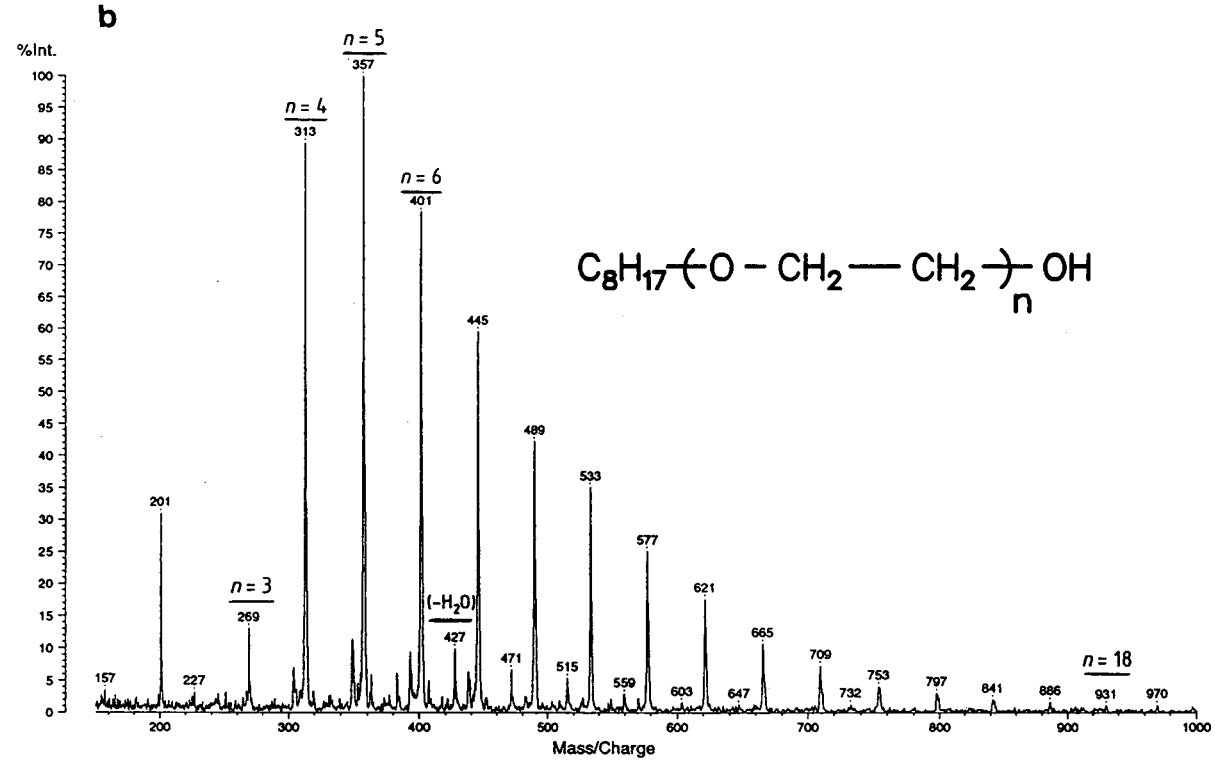
b
%Int.
n = 5
357
n = 4
313
n = 6
401
445
489
533
577
621
665
709
753
797
841
886
931
970
201
n = 3
269
(-H2O)
427
471
515
559
603
647
732
157
227
n = 18
C8H17-(-O-CH2-CH2-)n-OH
Mass/Charge

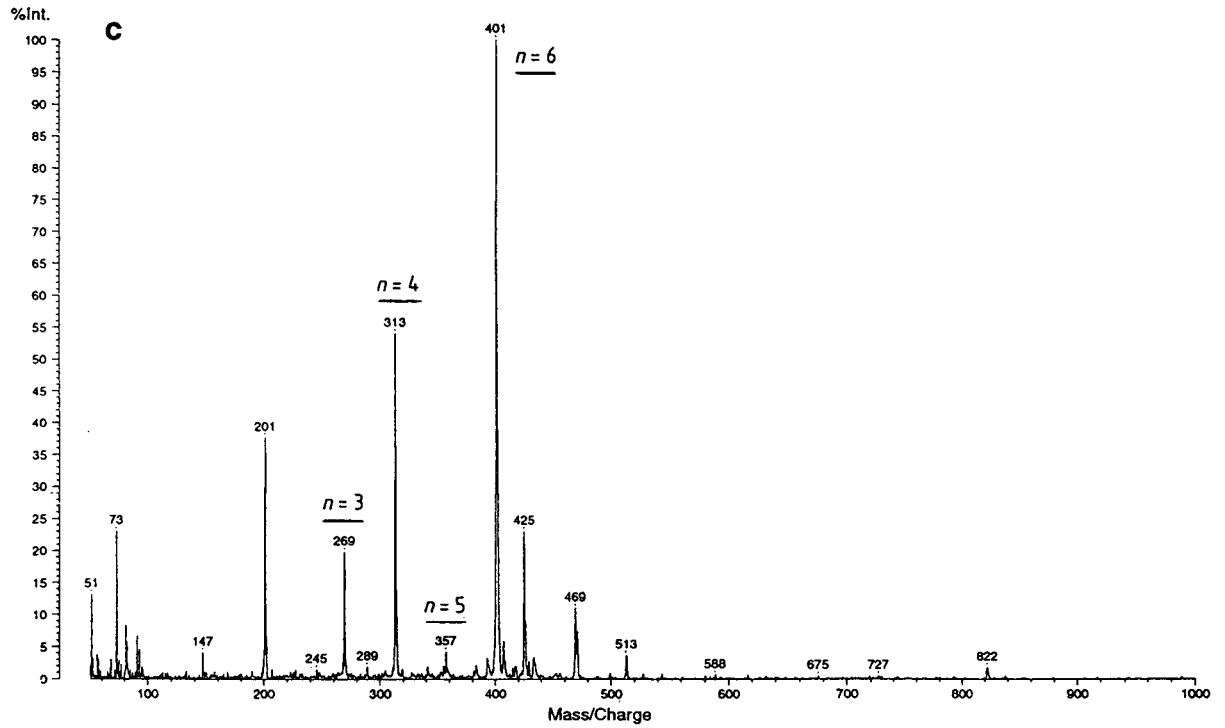
c
%Int.
401
n = 6
n = 4
313
201
n = 3
269
73
51
425
469
513
n = 5
357
147
245
289
588
675
727
822
Mass/Charge

Fig. 2.

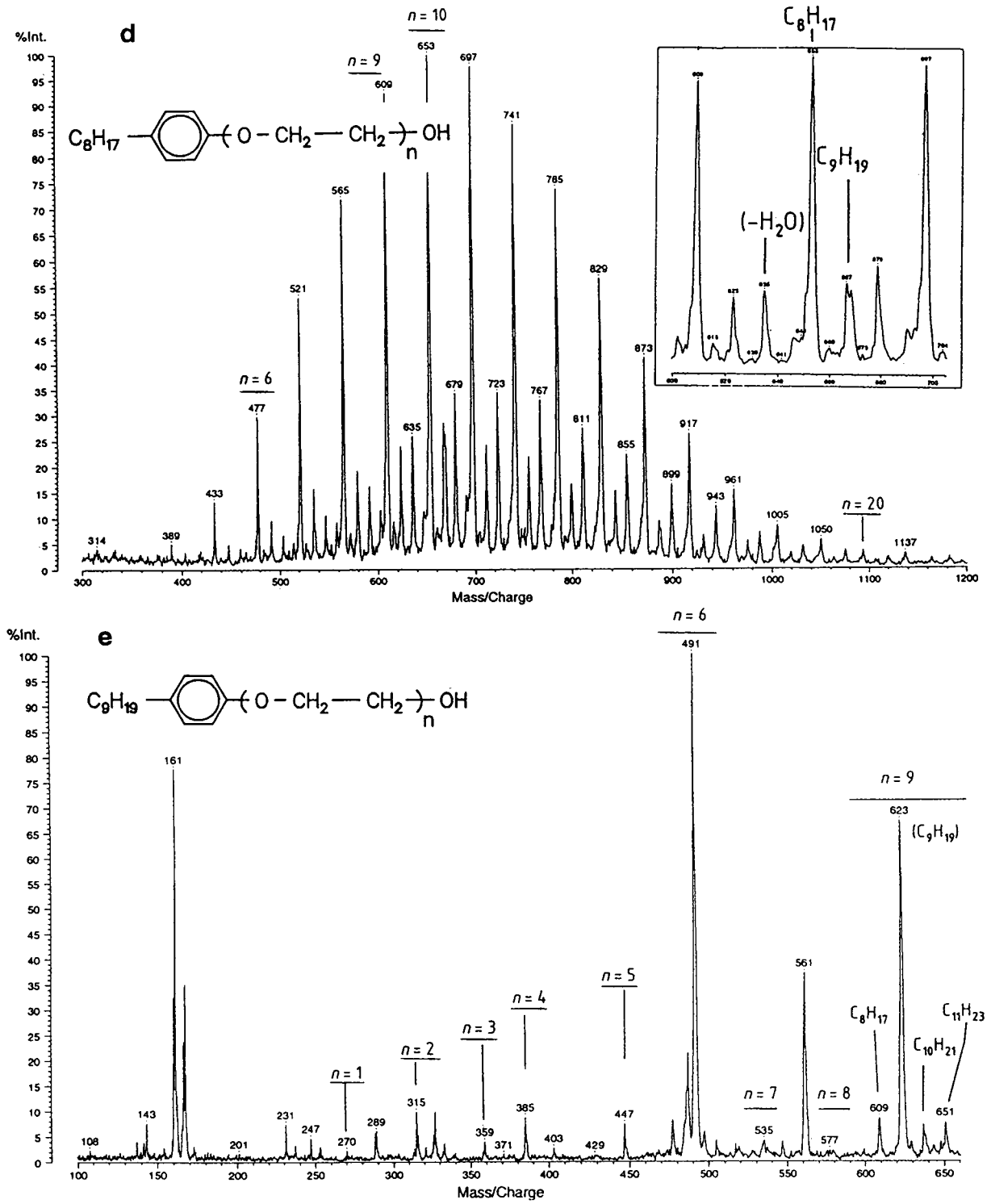

Fig. 2. MALDI mass spectra of (a) a mixture of reference substances (defined polyethylene glycols, $n = 4$, 6, 8), (b) *n*-octylpolyethylene glycol ether ($n = 5_{\text{statistical}}$), (c) a mixture of reference substances (defined *n*-octylpolyethylene glycol ethers, $n = 3$, 4, 6), (d) *p*-isoalkylphenylpolyethylene glycol ether ($n = 10_{\text{statistical}}$) and (e) a mixture of reference substances (defined *p*-isononylphenylpolyethylene glycol ethers, $n = 2$, 6, 9).

ing in the MALDI mass spectrum, as a comparison between Fig. 2b with Fig. 1d shows. An essential advantage provided by the addition of lithium chloride is that sodium and potassium ions hardly appear, so that the spectra can be more easily interpreted. In the spectrum for octylpolyethylene glycol ether ($n = 5_{\text{statistical}}$), when lithium chloride is added a second distribution is identifiable, the molar masses of which are respectively 18 u per degree lower than for the regular n-degrees; this can be explained through mutual reactions with each other resulting in water splitting off (Fig. 2b). The maximum of this distribution is shown for molar mass 420 g/mol.

Through the application of MALDI-MS, it can be further shown that the mixture of the reference substances nonylphenyl ethoxylate with n = 2, 6 and 9 also contains components of all degrees $n = 1$–9; further, for example, for $n = 9$, it is found that the alkyl residue not only consists of a nonylic residue, but that there are also small portions of octyl, decyl and undecyl residues (Fig. 2e).

The mass spectrum of the p-isoalkylphenylethoxylate ($n = 10_{\text{statistical}}$) clearly shows octylphenyl ethoxylate as the main component; a second distribution shows nonylphenyl ethoxylate with a 14 g/mol higher molar mass per degree. With addition of LiCl, the molar peak can be clearly interpreted. When LiCl is not used and sodium and potassium ions are present, the presence of the latter hampers identification. The third distribution, on the other hand, again shows water split off (Fig. 2d). With MALDI-MS, this reaction can be clearly seen in specimens PEG 440 and p-isononylphenyl ethoxylate ($n = 14_{\text{statistical}}$).

4. References

[1] P. Sandra and F. David, *J. High Resolut. Chromatogr.*, 13 (1990) 414–417.
[2] H.R. Holzbauer and U. Just, *Tenside Detergents*, in press.
[3] R.E. Escott and N. Mortimer, *J. Chromatogr.*, 553 (1991) 423–432.
[4] T.L. Chester, D.J. Bowling, D.P. Innis and J.D. Pinkston, *Anal. Chem.*, 62 (1990) 1299–1301.
[5] J. Grotemeyer and E.W. Schlag, *Angew. Chem.*, 100 (1988) 461–474.
[6] M. Karas and F. Hillenkamp, *Anal. Chem.*, 60 (1988) 2299.
[7] K.O. Börnsen, M. Schär and E. Gassmann, *Biol. Mass Spectrum.*, 20 (1991) 471.
[8] F. Hillenkamp, M. Karas, B.T. Chait and R.C. Beavis, *Anal. Chem.*, 63 (1991) 1193A.
[9] R.J. Cotter, *Anal. Chem.*, 64 (1992) 1027–1039.
[10] U. Bahr, A. Deppe, M. Karas, F. Hillenkamp and U. Giessmann, *Anal. Chem.*, 64 (1992) 2866–2869.
[11] U. Pieles, W. Zürcher, M. Schär, H. Moser and H.M. Widmer, presented at the *17th International Symposium on Liquid Column Chromatography, Hamburg, May 17–21, 1993.*
[12] *Additional Techniques in Synthetic Polymer Analysis*, Kratos Application Note, Shimadzu Europa GmbH, Duisburg.

ELSEVIER

Journal of Chromatography A, 667 (1994) 361–366

JOURNAL OF CHROMATOGRAPHY A

Short Communication

Thin-layer chromatographic determination of β-carotene, cantaxanthin, lutein, violaxanthin and neoxanthin on Chromarods

A.J. Rosas Romero*,[a], J.C. Herrera[a], E. Martinez De Aparicio[a], E.A. Molina Cuevas[b]

[a]*Departamento de Química, Universidad Simón Bolívar, Apartado 89000, Caracas 1080A, Venezuela*
[b]*Departamento de Matemáticas Puras y Aplicadas, Universidad Simón Bolívar, Apartado 89000, Caracas 1080A, Venezuela*

(First received June 9th, 1993; revised manuscript received November 29th, 1993)

Abstract

The separation and the simultaneous determination of β-carotene, cantaxanthin, lutein, violaxanthin and neoxanthin was accomplished using thin-layer chromatography on Chromarods, flame ionization detection and a two-stage development technique. Data were transformed through an unweighted straight-line regression of the logarithm of peak area ratios on the logarithm of the mass ratios. The determinations are highly reproducible and all statistical estimates are highly significant. The linear concentration range for each compounds is reported. No evidence of degradation of the carotenoids during the analyses was found. Up to ten samples can be analysed simultaneously in less than 2 h.

1. Introduction

Open-column chromatography (OCC) is the traditional method most frequently used to perform the separation of carotenoids [1,2]. It is generally employed for preparative separations and has also received quantitative applications, which includes separation using magnesium oxide followed by photometric determination [3]. Analysis using this method requires a long time and consumes considerable amounts of solvents and chromatographic materials. At the same time it has the disadvantage of not allowing the separation of the individual carotenoids; instead, the elutions are made according to the polarity in the three main groups, carotenes and mono- and dihydroxyxanthophylls.

In the last few years, OCC has been progressively displaced by high-performance liquid chromatography (HPLC) in the analysis of carotenoids [2]. Both normal-phase [2,4] and reversed-phase systems [5–7] can be used for the separation of carotenoids. The optimum conditions for maximum recovery and selectivity, using different C_{18} columns, have been reported [8].

Historically, thin-layer chromatography (TLC) is the method most often used for the separation of carotenoids [1,2]. There are many reports on the applications of silica gel TLC to the separation of this family of compounds [9–14]. TLC separations with magnesium oxide [15] and with a chemically bonded C_{18} stationary phase [16,17]

* Corresponding author.

0021-9673/94/$07.00
SSDI 0021-9673(93)E0017-O

have also been employed in the separation of individuals carotenoids. Recent work [17] pointed out the degradation of β-carotene during multiple-development TLC as a major difficulty for the separation and analysis of these compounds.

The Iatroscan chromatograph combines the capability of TLC with the quantification power of the flame ionization detector, (TLC–FID) [18,19]. Different aspects related to the quantitative application of the technique have been reviewed [20,21]. This paper presents a description of the application of TLC–FID to the determination of the five major carotenoids, β-carotene, lutein, violaxanthin, neoxanthin and cantaxanthin.

2. Experimental

2.1. Apparatus and experimental conditions

The equipment consisted of an Iatroscan TH-10 MK II TLC–FID analyser (Iatron Labs., Tokyo, Japan), Waters (Milford, MA, USA) 745/745B data module integrator and silica gel SIII Chromarods (Iatron Labs.). The Iatroscan was operated under the following conditions: hydrogen flow-rate, 160 ml/min; air flow-rate, 2000 ml/min; and scanning speed, 0.42 cm/s.

2.2. Materials

β-Carotene was obtained from BDH Biochemicals (Poole, UK), lutein, cantaxanthin, violaxanthin and neoxanthin from Hoffmann-La Roche (Basle, Switzerland), methyl tetracosanoate from Analabs (North Haven, CT, USA) and the fatty alcohol cholesterol from Polyscience (Niles, IL, USA). All organic solvents were of the highest purity available and used as received. Light petroleum (b.p. 55–70°C) was used. Sep-Pak silica cartridges (Waters) were used for the purification of oxidized β-carotene solution.

2.3. Chromatographic procedure

Chromarods were activated by passing them through the FID flame just before application of the sample. Each rod was spotted with 1 μl of sample solution. After being spotted, the rods were placed in a constant-humidity chamber (65%) for 30 min. This chamber was one of the developing tanks containing 35.8% sulphuric acid. Development was carried out in glass chambers, wrapped in black paper, with three of their internal faces covered with filter-paper. After development in the appropriate mobile phase, the rods were left to dry at room temperature for 5 min and immediately scanned in the TLC–FID system.

A constant volume of developing solvent was used, sufficient to cover the first 3 mm of the rods. Developing solutions were freshly prepared each day. After 20–30 runs the rods were immersed overnight in 10% sulphuric acid, and washed thoroughly with deionized water.

The analysis is carried out by a double development technique. In the first stage, β-carotene, the internal standard and the non-saponifiable neutral lipid fraction were separated in light petroleum–chloroform–acetone (89.5:10:0.5), while the xanthophylls did not move from the injection point. The developing time for this stage was kept constant at 30 min. After development, the rods were taken to the Iatroscan and burnt down to 0.5 cm from the injection point.

In the second stage, the xanthophylls were separated by developing the rods in light petroleum–chloroform–2-propanol (50:40:10) for 45 min and burning the whole length of the rod.

All handling of the samples was carried out under dim, diffuse artificial light.

2.4. Calibration

For each of the carotenoids, chloroform solutions were prepared in concentrations ranging from 0.3 to 10 mg/ml. All solutions contained 4

mg/ml of methyl tetracosanoate as internal standard. Ten different concentrations were analysed simultaneously for each compound in each run. Calibration graphs were constructed by plotting the peak-area ratio (carotenoid/methyl tetracosanoate) against their mass ratio (carotenoid/methyl tetracosanoate). From the calibration graphs, the linear range for each of the analyses and the statistical parameters were calculated.

3. Results and discussion

In addition to improving the reproducibility, it proved easier to keep the developing time constant rather than trying to develop the rods until the solvent had reached a certain, pre-established height. Moreover, this procedure avoided the difficulty of visually localizing the solvent front.

To ensure reproducibility, the rods were matched according to the speed of solvent migration during development. Throughout this study, only those rods which did not present appreciable differences were employed.

In a study on the instability of plant carotenoids during their separation by multiple developments [17], evidence was presented of degradation of the carotenoids through photolytic and/or oxidatives processes. It was found that when β-carotene was subjected to multiple development on silica gel TLC plates, a decrease in the absorbance of the β-carotene peak was observed following each development, together with the formation of a considerably more polar compound that remained at the origin. When β-carotene was spotted on octadecylsilanized silica gel, the same decrease in response was found after each development, without the obvious formation of a new product. The phenomenon was found to be time dependent, particularly the time spent on the dried layer during sample application, solvent evaporation and scanning densitometry.

In view of those results, we performed the same kind of experiments on silica gel SIII Chromarods. Following the procedure explained under Experimental, we spotted, developed and scanned β-carotene on ten Chromarods. We found no decrease in the FID response or the formation of new products after a second development. The same results were obtained when the spotted Chromarods were left in the constant-humidity chamber for 1 h instead of 30 min. The whole procedure was repeated for each of the other compounds under study. Again, no evidence of a decrease in signal or of the formation of new products was found. In another experiment we worked with an intentionally oxidized β-carotene solution, and in this instance we observed a new peak that remained at the injection point. This peak disappeared when the polar compounds were previously removed from the oxidized β-carotene solution in light petroleum by filtration through a Sep-Pak silica cartridge.

We believe that the difference among our results and those reported previously [17] maybe due to differences between the TLC plates and the SIII Chromarods, along with the differences imposed by the scanning techniques employed in each instance.

3.1. Determination of β-carotene

A typical chromatogram of this first stage of the analysis is shown in Fig. 1A. Peaks a and b correspond to β-carotene and the internal standard, respectively.

The neutral lipid fraction appears separate from those two peaks. Fig. 1B depicts the chromatogram of a sample that contained β-carotene, the internal standard and a mixture of fatty alcohols and sterols, which are the types of compounds that would remain after extraction of the carotenoids and removal of the saponifiables from, for example, green leaves [18,19].

For β-carotene, the working concentration range lies between 0.6 and 5 mg/ml. For concentrations greater than 5 mg/ml, the β-carotene peak broadens and overlaps with the peak of the internal standard, and consequently the detector

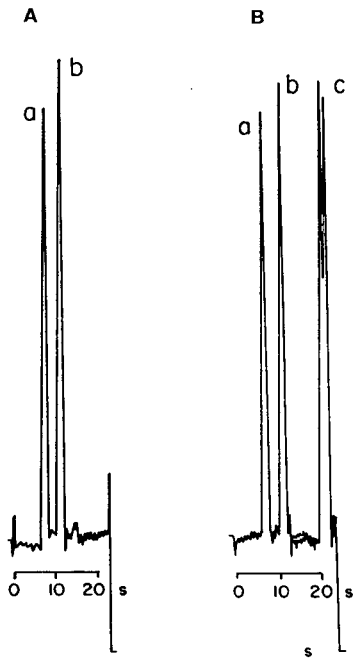

Fig. 1. (A) TLC of β-carotene and the internal standard. For experimental conditions, see text. First development with light petroleum–chloroform–acetone (89.5:10:0.5). β-Carotene (peak a) appears at 7.8 s and the internal standard (peak b) at 11.4 s. (B) TLC of a solution containing β-carotene, internal standard and sterols and fatty alcohols (as an example of non-saponifiable lipids). Developing system, light petroleum–chloroform–acetone (89.5:10:0.5). Non-saponifiable lipids (peak c) appear at 21 s, well resolved from β-carotene (peak a) and the internal standard (peak b).

response is smaller than expected and the slope progressively diminishes.

3.2. Determination of xanthophylls

Fig. 2 shows a typical chromatogram of the separation of the xanthophylls in the second development of the samples. Peaks a, b, c and d correspond to cantaxanthin, lutein, violaxanthin and neoxanthin, respectively.

As in the analysis of β-carotene, outside the working concentration range the peaks broaden and the FID response progressively decreases. This range is 0.3–9 mg/ml for cantaxanthin, 1.2–8 mg/ml for lutein, 0.5–8 mg/ml for violaxanthin and 1–10 mg/ml for neoxanthin.

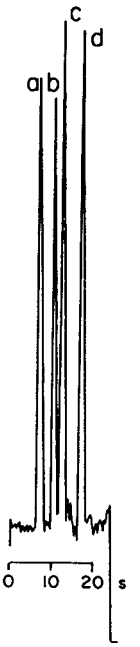

Fig. 2. Chromatographic separation of xanthophylls in light petroleum–chloroform–2-propanol (50:40:10) for 45 min. Peaks: a = cantaxanthin (6 s), b = lutein (9.6 s), c = violaxanthin (12.6 s) d = neoxanthin (16.8 s). For experimental conditions, see text.

3.3. Statistical analysis

The data consisted of several measurements of peak areas at different mass levels, *i.e.*, a repeated measurements analysis. A scatter plot of peak-area ratios against mass ratios revealed a nearly linear relationship, with a slight curvature towards the lower and higher mass ratio levels. A plot of standard deviations against mass ratio showed an increasing relationship. This behaviour of both the trend and the standard deviations, which has been reported previously [22,23], suggests the need for a stabilizing transformation, a weighted analysis or a combination of both.

A simple linear regression was performed in order to make a residual analysis. The residual analysis shows influential observations at the lower and higher mass ratio levels. The normal probability plot emphasizes the need to adjust the analysis for the non-homogeneity of the

variances. A simple straight-line fit is inadequate, giving too much weight to the middle range of the data. A weighted analysis improves the non-homogeneity of the variances but gives too much weight to the lower range of the data. This residual analysis reveals the need to include a second-order term. Therefore, a second-degree polynomial was fitted by weighted least squares; this stabilizes the variance and takes into account the slight curvature in the trend, at the expense of having to deal with an extra parameter.

As a second step, a Box–Cox transformation analysis was performed [24]. This second analysis favours a power transformation of the peak area ratios ($Y^{0.7}$) over the logarithmic transformation. However, an unweighted straight-line regression of the logarithm of peak-area ratios on the logarithm of the mass ratios renders a similar fit, with a simpler model:

$$\log(\text{peak-area ratio}) = a + b \log(\text{mass ratio}) \quad (1)$$

For all the compounds, the residual normal probability plot for eq. 1 does not show important departures from normality, while the residual analysis is satisfactory, showing that the model allows for the slight curvature in the trend, and stabilizes the variances at the same time.

Taking into consideration that the main objective of the analysis is to find a calibration graph for interpolation, we decided in favour of eq. 1. This model renders a simple interpolation procedure without sacrificing either precision or goodness of fit.

Table 1 summarizes the results of the regression analysis of eq. 1 for each of the compounds studied. As can be seen, all determinations are precise and accurate. For all the compounds studied the detector response increases significantly with increasing mass ratio, *i.e.*, the observed values for the slope are significantly different from zero (for $p < 0.05$). Table 1 shows that eq. 1 provides an excellent goodness of fit, as indicated by the values of the coefficient of determination, R^2, which measures the proportion of total variation explained by the model [25].

Table 1
Linear regression analysis for the calibration graphs, using the logarithm of peak-area ratios on the logarithm of mass ratios

Compound	Slope	Intercept	R^2
β-Carotene	1.40 ± 0.02	−0.26 ± 0.02	98.41
Cantaxanthin	1.56 ± 0.02	0.07 ± 0.02	99.16
Lutein	1.98 ± 0.02	−0.88 ± 0.02	99.40
Violaxanthin	2.15 ± 0.02	0.57 ± 0.02	99.08
Neoxanthin	0.98 ± 0.01	0.589 ± 0.007	99.37

Results are expressed as the mean ± standard error. Each mass was measured ten times. All values are statistically significant at $p < 0.05$.

4. Acknowledgements

These studies were supported by a grant from the Decanato de Investigaciones y Desarrollo of the Universidad Simón Bolívar (Venezuela).

5. References

[1] B.H. Chen, S.H. Yang and L.H. Han, *J. Chromatogr.*, 543 (1991) 147.
[2] R.F. Taylor, *Adv. Chromatogr.*, 22 (1983) 157.
[3] W. Horwitz (Editor), *Official Methods of Analysis of the Association of Official Analytical Chemists*, AOAC, Washington, DC, 13rd ed., 1980, p. 738.
[4] S.H. Rhodes, A.G. Netting and B.V. Milborrow, *J. Chromatogr.*, 442 (1988) 412.
[5] G. Britton, *Nat. Prod. Rep.*, 8 (1991) 223.
[6] F. Granado, B. Olmedilla, I. Blanco and E. Rojas-Hidalgo, *J. Liq. Chromatogr.*, 14 (1991) 2457.
[7] F.W. Quackenbush, *J. Liq. Chromatogr.*, 10 (1987) 643.
[8] K.S. Epler, L.C. Sander, R.G. Ziegler, S.A. Wise and N.E. Craft, *J. Chromatogr.*, 595 (1992) 89.
[9] G. Britton, R.K. Singh, T.W. Goodwin and A. Ben-Aziz, *Phytochemistry*, 14 (1975) 2427.
[10] P.M. Bramley and B.H. Davis, *Phytochemistry*, 14 (1975) 463.
[11] G. Britton and T.W. Goodwin, *Phytochemistry*, 14 (1975) 2530.
[12] U. Leuenberger and I. Steward, *Phytochemistry*, 15 (1976) 227.
[13] K. Iryama, M. Yoshiura, M. Shiraki, S. Yano and S. Saito, *Anal. Biochem.*, 106 (1980) 322.
[14] M.N. Merzlyak, V.A. Kovrizhnih and Y.N. Kaurov, *J. Chromatogr.*, 262 (1983) 331.
[15] R. Sadowski and W. Wojcik, *J. Chromatogr.*, 262 (1983) 455.

[16] M. Isaksen and G.W. Francis, *J. Chromatogr.*, 355 (1986) 358.
[17] M.J. Cikalo, S.K. Poole and C.F. Poole, *J. Planar Chromatogr.*, 5 (1992) 200.
[18] J.K.G. Kramer, R.C. Fouchard and E.R. Farnworth, *J. Chromatogr.*, 198 (1980) 74.
[19] R. Thomas Crane, S.C. Goheen, E.C. Larkin and G. Ananda, *Lipids*, 18 (1983) 74.
[20] R.G. Ackman, C.A. McLeod and A.K. Banerjee, *J. Planar Chromatogr.*, 3 (1990) 450.
[21] R.G. Ackman, *Methods Enzymol.*, 72 (1981) 205.
[22] C.C. Parrish and R.G. Ackman, *Lipids*, 20 (1985) 521.
[23] C.C. Parrish, *Can. J. Fish. Aquat. Sci.*, 44 (1987) 722.
[24] A.C. Atkinson, *Plots, Transformations and Regression*, Oxford University Press, Oxford, 1985, pp. 85–90.
[25] N.R. Drapper and H. Smith, *Applied Regression Analysis*, Wiley, New York, 1966, p. 26.

ELSEVIER

Journal of Chromatography A, 667 (1994) 367–370

JOURNAL OF CHROMATOGRAPHY A

Short Communication

Separation of chiral isomers of *p*-nitrophenyl-2-amino-3-hydroxypropanone by capillary zone electrophoresis using cyclodextrins as chiral selector

Junling Gu, Ruonong Fu*

Department of Chemical Engineering, Beijing Institute of Technology, Beijing 100081, China

(First received August 23rd, 1993; revised manuscript received December 7th, 1993)

Abstract

Chiral isomers of *p*-nitrophenyl-2-amino-3-hydroxypropanone (NPAP) were separated by capillary zone electrophoresis in a background electrolyte containing β-cyclodextrin as stereospecific selector. In order to improve the resolution, three soluble cellulose derivatives as modifiers of the background electrolyte were studied. The operating conditions of capillary zone electrophoresis, such as concentrations of β-cyclodextrin and Tris, pH of buffer solution and applied voltage, were investigated. Under the optimized condition the NPAP optical isomers could be successfully separated.

1. Introduction

In recent years capillary zone electrophoresis (CZE) has become a powerful technique for the separation of a variety of complex mixtures. Micellar electrokinetic capillary chromatography (MECC) [1], which combines the advantages of HPLC and CZE, permits the separation of neutral compounds. One important area of CZE application is enantiomer separations, owing to the high separation power and the use of some chiral selectors. Cyclodextrins (CDs) and their derivatives have been successfully used in HPLC as stationary phases or mobile phase additives [2] for many years and more recently in capillary GC as stationary phases [3]. There are many examples of the use of CDs and their derivatives as chiral selectors for the separation of optical isomers, such as drugs, amino acids and plant growth regulators [4–8].

p-Nitrophenyl-2-amino-3-hydroxypropanone (NPAP) (Fig. 1) is one of the metabolites of chloramphenicol (CAP) in human blood and may play a significant role in CAP-induced hematotoxicity [9–11]. CAP metabolites have been separated by HPLC but the separation of NPAP optical isomers has not been reported. The L-isomer of NPAP is a raw material for producing L-CAP and therefore the separation of the optical isomers of NPAP is an important task.

In this work, a CZE method was developed for the separation of NPAP optical isomers. The operating conditions are discussed.

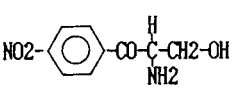

Fig. 1. Structure of NPAP.

* Corresponding author.

0021-9673/94/$07.00
SSDI 0021-9673(93)E0087-B

2. Experimental

2.1. Apparatus

The capillary used for electrophoresis was a fused-silica capillary tube of 60 cm × 50 μm I.D. with a 40-cm effective length (Hebei Yongnian Optical Fibre Factory, Hebei, China). The experiments were carried out on a high-performance capillary electrophoresis apparatus obtained from Beijing Institute of New Technology Application, with UV detection at 254 nm.

2.2. Reagents

Standard D- and L-*p*-nitrophenyl-2-amino-3-hydroxypropanone (NPAP) were donated by the Centre of Material Science, Beijing Institute of Technology. β-Cyclodextrin (β-CD) was purchased from Guangdong Yunang Glutamate Factory (Guangdong Yunang, China) and recrystallized several times. Tris(hydroxymethyl)aminomethane (Tris) was obtained from Sichuan Chengdu Chemicals Factory (Sichuan Chengdu, China). Methylcellulose (MC) hydroxypropylmethylcellulose (HPMC), and carboxymethylcellulose (CMC) were provided by the Sichuan Luzhou Chemical Factory (Sichuan Luzhou, China). Citric acid obtained from Beijing Chemicals Factory (Beijing, China) was of analytical-reagent grade. Other chemicals used were of reagent grade. The buffer solution was prepared from citric acid and Tris. The samples were injected by the hydrodynamic or electrodynamic method.

3. Results and discussion

3.1. Effect of CD concentration on the separation of optical isomers

Optical isomers are not easily separated from each other by common methods. CDs are cyclic oligosaccharides consisting of six, seven or eight glucopyranose units corresponding to α-, β- and γ-cyclodextrin. These compounds have been successfully used as chiral separation selectors.

Table 1
Effect of β-CD concentration on the resolution of NPAP optical isomers

Parameter	Isomer	β-CD concentration (m*M*)		
		10	20	30
R_h (%)[a]	–	22.3	59.0	76.1
Migration time (min s)	L	6 03	6 24	6 50
	D	6 08	6 29	6 55

Operating conditions: buffer, 20 m*M* Tris–citric acid; pH, 3.5; applied voltage, 25 kV; current, 12–13 μA.
[a] $R_h = (H - H')/H$, where H and H' are the heights of the lower isomer peak and of the valley between the two peaks, respectively.

In this work, β-CD was used as a chiral selector for the separation of NPAP optical isomers. The separation data are given in Table 1, where it can be seen that the resolution of the optical isomers increases with increasing β-CD concentration. This relationship has been reported by other workers [12]. The optimum concentration of β-CD is 30 m*M*, at which the migration time of isomers is longer than that at lower β-CD concentrations. Because the solubility of β-CD in water is lower, it is difficult to use concentrations of β-CD higher than 40 m*M*.

3.2. Effect of cellulose derivatives on the separation of optical isomers

It is clear that even though β-CD can improve the separation of NPAP optical isomers, baseline resolution was not obtained. Snopek *et al.* [13] used soluble alkylhydroxycellulose derivatives to modify the background electrolytes, improving the separation of chloramphenicol drug optical isomers. Therefore, three cellulose derivatives were added to the buffer in order to improve the separation of NPAP optical isomers (Fig. 2). Of the three cellulose derivatives tried, hydroxypropylmethylcellulose (HPMC) is the best one for modifying the background electrolyte for the separation of NPAP optical isomers. In this instance, complete baseline separation of the optical isomers was achieved, because HPMC in the buffer decreases the electroosmotic flow,

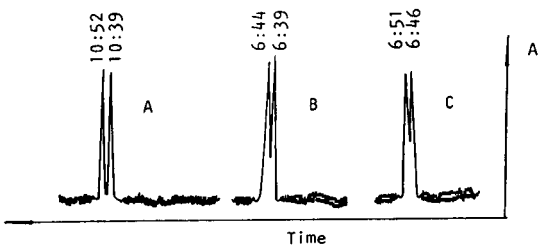

Fig. 2. Influence of the type of methylcellulose on the separation of NPAP optical isomers. Conditions as in Table 1. (A) background electrolyte (BE) + 0.1% HPMC, (B) BE + 0.1% MC, (C) BE + 0.1% CMC. Time at peaks indicated in min:s.

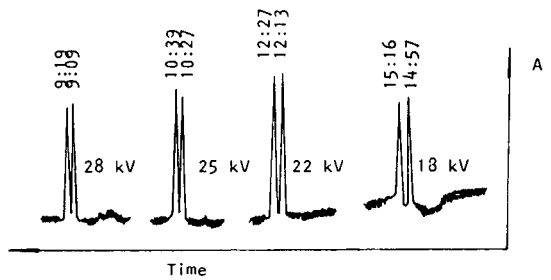

Fig. 3. Influence of applied voltage on the separation of NPAP optical isomers. Conditions as in Fig. 2A. Time at peaks indicated in min:s.

giving more time for the interaction between β-CD and the optical isomers investigated. Fig. 2 shows that the migration time of D-NPAP using HPMC as additive is 10 min 52 s, whereas using the others the migration times are less than 7 min. Table 2 gives the electroosmotic flow-rates (EOF) in 20 m*M* Tris–citric acid and 20 m*M* β-CD solution containing 0.1% cellulose derivatives, using dimethyl sulphoxide (DMSO) as a tracer. The data clearly show that HPMC possesses the highest EOF and CMC the lowest; CMC does not assist the separation.

3.3. Effect of applied voltage on the separation

In general, the higher the applied voltage over the two sides of capillary tube for electrophoresis, the higher is the efficiency obtained. On the other hand, the migration time of a solute is inversely proportional to the applied voltage. For these reasons, under a higher applied voltage the high column efficiency will provide a separation, but it can shorten the migration time, which lowers the resolution, as mentioned above. Therefore, the applied voltage does not notably influence the separation, as shown in Fig. 3.

Table 2
Effect of type of methylcellulose derivatives on u_{EOF} (time over the 60 cm length)

Type of MC derivatives	u_{EOF} (min s)
None	20 54
HPMC	>70
CMC	19 15
MC	30 04

3.4. Effect of acidity on the separation

In CZE, pH is an important parameter for the separation, with a large influence on the EOF and the migration times of solutes. Fig. 4 illustrates the influence of the pH of the background electrolyte on the separation of NPAP optical isomers. It shows that at pH 3.5–6 the separation of isomers is perfect. In this pH range the EOF is lower and NPAP possesses a positive charge.

3.5. Effect of ionic strength on the separation

In order to test the influence of the ionic strength of the buffer solution on the separation,

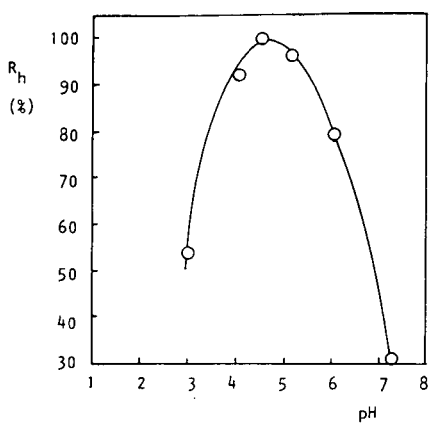

Fig. 4. Influence of pH of background electrolyte on the separation of NPAP optical isomers. Conditions as in Fig. 2A, except pH of buffer.

Table 3
Effect of ionic strength of buffer on the separation of NPAP optical isomers

Parameter	Ionic strength (m*M* Tris)			
	10	20	30	40
R_h (%)[a]	81.5	100	100	100
Migration time (min)	10.17	10.22	10.40	10.18
	10.28	10.38	10.62	10.37

[a] See Table 1.

concentrations of 10–40 m*M* Tris were added to the background electrolytes. The separation of NPAP optical isomers is depicted in Table 3. The results clearly show that with concentrations of Tris above 20 m*M* a perfect separation can be achieved.

4. Conclusions

Chiral isomers of *p*-nitrophenyl-2-amino-3-hydroxypropanone (NPAP) can be separated by CZE. The background electrolyte contains β-CD as a stereospecific selector and hydropropylmethylcellulose as an electroosmotic flow reducer. The optimized operating conditions are as follows: background electrolyte containing 0.2–0.4 m*M* Tris, 0.2 m*M* citric acid, 0.2–0.3 m*M* β-CD and 0.1% HPMC; applied voltage, *ca.* 25 kV; and pH, 3.5–6.

5. Acknowledgement

This work was kindly supported by the National Science Foundation of China.

6. References

[1] S. Terabe, K. Otsuka, K. Ichikawa, A. Tsuchiya and T. Ando, *Anal. Chem.*, 556 (1984) 111.
[2] T.J. Ward and D.W. Armstrong, *J. Liq. Chromatogr.*, 9 (1986) 407.
[3] R. Fu, *SePu*, 10 (1992) 14.
[4] S. Fanali, *J. Chromatogr.*, 474 (1989) 441.
[5] M. Tanaka, S. Asano, M. Yoshinago, Y. Kawaguchi, T. Tetsumi and T. Shono, *Fresenius' J. Anal. Chem.*, 339 (1991) 63.
[6] S. Fanali, *J. Chromatogr.*, 545 (1991) 437.
[7] T. Ueda, R. Mitchell, F. Kitamura, T. Metcalf, T. Kuwana and A. Nakamoto, *J. Chromatogr.*, 593 (1992) 2655.
[8] S.K. Yeo, H.K. Lee and S.F.Y. Li, *J. Chromatogr.*, 594 (1992) 335.
[9] S. Abou-Khalil, W.H. Abou-Khalil, A.N. Masoud and A.A. Yunis, *J. Chromatogr.*, 417 (1987) 111.
[10] W.H. Abou-Khalil, A.A. Yunis and S. Abou-Khalil, *Pharmacology*, 36 (1988) 272; *C.A.*, 108 (1988) 142766b.
[11] J.J. Jimenez, G.K. Arimura, W.H. Abou-Khalil, M. Isilder and A.A. Yunis, *Blood*, 70 (1987) 1180; *C.A.*, 108 (1988) 15835y.
[12] R. Kuhn and S. Hoffstetter-Kuhn, *Chromatographia*, 34 (1992) 505.
[13] J. Snopek, H. Soini, M. Novotny, E. Smolkova-Keulemansova and I. Jelinek, *J. Chromatogr.*, 559 (1991) 215.

ELSEVIER

Journal of Chromatography A, 667 (1994) 371–376

JOURNAL OF CHROMATOGRAPHY A

Short Communication

Ionophoretic technique in the study of Cu(II), Ni(II), Co(II) and Mn(II)–hydrazine–nitrilotriacetate mixed-ligand complexes

Urmila Mishra*, R.K.P. Singh

Electrochemical Laboratories, Department of Chemistry, University of Allahabad, Allahabad-211002, India

(First received October 18th, 1993; revised manuscript received January 17th, 1994)

Abstract

A method involving the use of paper electrophoresis is described for the study of equilibria in mixed-ligand complex systems in solution. The method is based on the migration of a spot of a metal ion (M) with the complexants added to the background electrolyte (0.1 *M* sodium perchlorate). For the study of ternary complexes, the concentration of one of the complexants, hydrazine, is kept constant, while that of the second ligand, nitrilotriacetate (NTA), is varied. A graph of mobility against −log [NTA] is used to obtain information on the formation of the mixed-ligand complex and to calculate the stability constants. The overall stability constants of M–hydrazine and M–hydrazine–NTA complexes were found to be $10^{5.6}$, $10^{2.7}$ and $10^{4.7}$ for Cu(II), $10^{2.7}$, $10^{1.8}$ and $10^{5.5}$ for Ni(II), $10^{2.0}$, $10^{1.7}$ and $10^{4.7}$ for Co(II) and $10^{4.9}$, $10^{1.7}$ and $10^{6.1}$ for Mn(II) complexes at $\mu = 0.1$ and 35°C.

1. Introduction

Paper electrophoresis has previously been applied to the study of metal complexes in solution and attempts have been made to determine the stability constants of the complex species [1,2]. In previous work a method was developed for the study of stepwise complex formation [3–5]. Although the use of paper electrophoresis for the study of metal complex systems with a single ligand seems to be well established, there has been no systematic study of mixed-ligand complexes. However, Czakis Sulikowska [6] made some observations on the formation of mixed halide complexes of Hg(II), but the studies were only qualitative and did not throw light either on the nature of the species or on their stabilities.

In previous papers [7,8] a method was described for the study of mixed-ligand complexes. This work represents an extension of that technique and this paper reports our observations on the Cu(II), Ni(II), Co(II) and Mn(II)–hydrazine–nitrilotriacetate (NTA) mixed-ligand-system.

2. Experimental

Horizontal–vertical-type electrophoresis equipment (Systronics Model 604) was used together with various accessories. In each instance electrophoresis was carried out for 60 min at 200 V at 35°C. Whatman No. 1 paper strips (25 × 1 cm) were used. pH measurements were made with an Elico Model L_{1-10} pH meter using a glass electrode.

* Corresponding author.

0021-9673/94/$07.00
SSDI 0021-9673(94)00065-H

Metal perchlorates were prepared by an appropriate method and the final concentrations were kept at 5.0×10^{-3} *M*. 1-(2-Pyridylazo)-2-naphthol (PAN) [0.1% (w/v) in ethanol] was used for detecting Cu(II) Mn(II) and Co(II) ions and dimethylglyoxime for detecting Ni(II) ions. A saturated solution of silver nitrate in acetone was sprayed on the paper, which was subsequently fumed with ammonia to detect glucose spots.

The background electrolyte for the study of binary complexes was 0.1 *M* perchloric acid, 0.02 *M* hydrazine or $3.3 \cdot 10^{-3}$ *M* NTA with sodium hydroxide added to produce the desired pH and for the study of ternary complexes it was 0.1 *M* perchloric acid–0.02 *M* hydrazine with various amounts of NTA, maintained at pH 9.0 by addition of sodium hydroxide solution.

2.1. Procedure for binary complexes

Whatman No. 1 paper strips (25×1 cm) in duplicate are spotted in the middle with metal ion solutions. An extra strip is marked with glucose. The strips are sandwiched between two insulated hollow metal plates and the temperature of the system is maintained by water supplied within the plates at a fixed temperature. The plates are then mounted on the electrophoresis equipment with the end of the paper strips dipping in the tank solutions on both sides of the instrument. Electrophoresis is carried out for 60 min. The strips are then removed from the tank and dried and the migrated spots are detected with specific reagents. The movement of a metal spot towards the negative electrode is taken as positive mobility and in the reverse direction as negative mobility. Duplicate strips always recorded less than a 5% variation in the distance travelled and the mean of the two was taken for calculation of mobility. The movement of glucose is used as a correction factor for electroosmosis. The electrophoretic migration of metal spots on the paper was observed at different pH values of the background electrolyte. Division of movements by the potential gradient yields mobilities, which are plotted in Figs. 1 and 2.

2.2. Procedure for ternary complexes

Strips are marked with metal ion solutions in duplicate along with an additional strip marked with glucose. After drenching the strips with the background electrolyte, electrophoresis is carried out for 60 min at the same potential difference as for binary complexes. For subsequent observations, the NTA solution (pH 9.0) is added progressively and the ionophoretic mobility is recorded. Mobility is plotted against $-\log[\text{NTA}]$ (Fig. 3).

3. Results and discussion

3.1. M–hydrazine system

The plot of the overall electrophoretic mobility of a metal spot against pH gives a curve with three plateaux, as shown in Fig. 1. A plateau is an indication of the pH range where the speed is virtually constant. This is possible only when a particular complex is overwhelmingly formed. Thus every plateau indicates the formation of a certain complex species. The first plateau corresponds to the region in which metal ions are non-complexed. Beyond the first plateau the metal ion spots have progressively decreasing velocities and hence complexation of metal ions should be taking place with non-protonated species of the hydrazine ligand, whose concentration increases with increasing pH of the background electrolyte. The decrease in mobility continues until a second plateau in the positive range of mobility is reached. The second plateau corresponds to the overwhelming formation of a 1:1 complex. The region between first and second plateaux corresponds to the progressive conversion of non-complexed metal ion into a binary complex with the ligand (hydrazine). On further increasing the pH beyond the second plateau, the concentration of unprotonated species of the ligand increases further and adduction of another molecule to 1:1 binary complex takes place. The mobility registers a downward trend, ultimately resulting in a third plateau which tends to have zero mobility. The third

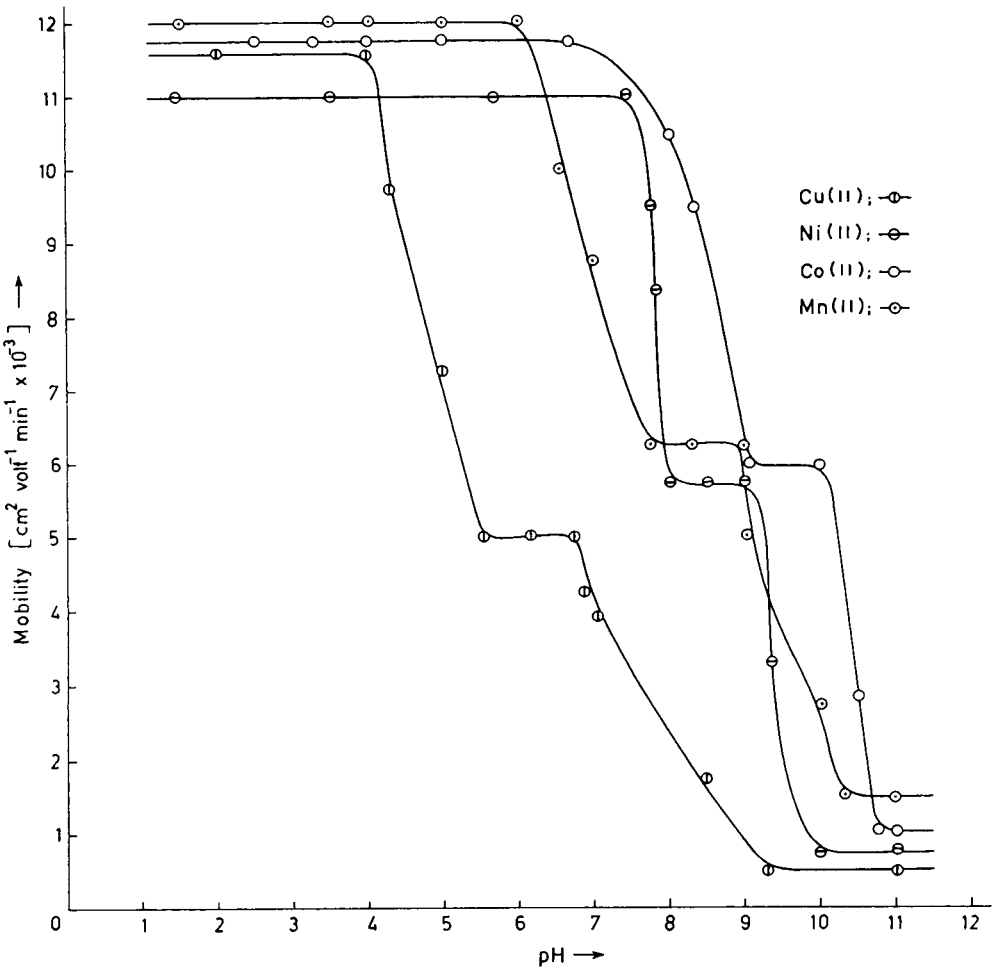

Fig. 1. Plots of mobility *versus* pH for the metal–hydrazine system.

plateau corresponds to the overwhelming formation of a 1:2 complex of the metal ion with the unprotonated species. Further increase in pH does not lead to any change in mobility, ruling out the formation of any other higher mononuclear complex.

The metal spot on the paper is thus a combination of uncomplexed metal ions and 1:1 and 1:2 complexes. This spot is moving under the influence of the electric field, its overall mobility being given by the equation

$$U = \sum U_n f_n \qquad (1)$$

where U_n and f_n are the mobility and mole fraction of a particular complex species, respectively. This equation is transformed into the following form on taking into consideration different equilibria:

$$U = \frac{U_0 + U_1 K_1[\mathrm{L}] + U_2 K_1 K_2[\mathrm{L}]^2}{1 + K_1[\mathrm{L}] + K_1 K_2[\mathrm{L}]^2} \qquad (2)$$

where U_0, U_1 and U_2 are the mobilities of the uncomplexed metal ion and 1:1 and 1:2 complexes, respectively, [L] is the concentration of the unprotonated ligand, which takes part in com-

plex formation, and K_1 and K_2 are stability constants of the 1:1 and 1:2 complexes, respectively, which are expressed as

$$K_1 = \frac{[ML]}{[M][L]} \quad (3)$$

$$K_2 = \frac{[ML_2]}{[ML][L]} \quad (4)$$

Using the principle of average mobility, K_1 can be calculated with the help of the mobilities of the first and second plateaux. Similarly, K_2 can be calculated with the help of the mobilities of the second and third plateaux. The concentration of unprotonated ligands at different pH values for the calculation of stability constants can be calculated with the assistance of the equilibria of protonated and deprotonated species of the ligands. Protonation constants help in the assessment of the unprotonated species at any pH with the relevant equation:

$$[L] = \frac{[L_t]}{1 + k/[H^+]}$$

where [L] is the concentration of the unprotonated species, $[L_t]$ is the total ligand concentration and k is the protonation constants for (hydrazine $k = 10^{8.3}$) [9,10]. The calculated values of the stability constants of 1:1 and 1:2 complexes are given in Table 1.

3.2. M–NTA system

The overall mobilities of the metal spots in the presence of NTA at different pH values are presented in Fig. 2. It is evident that with all the metal ions two plateaux are obtained, the mobility of the second plateau lying in the negative region, showing the negatively charged nature of the complex. Hence only one NTA anion is assumed to combine with one bivalent metal ion to give a 1:1 M–NTA complex, which is in conformity with the findings of other workers [13,14]. The stability constants of complexes with NTA were calculated as described for the M–hydrazine system and are given in Table 2.

Table 1
Stability constants of M–hydrazine complexes at 35°C and ionic strength = 0.1

Metal ion	Calculated values		Literature values		Ref.
	Log K_1	Log K_2	Log K_1	Log K_2	
Cu(II)	5.6	2.7	–	–	–
Ni(II)	2.7	1.8	2.8	2.4	11
Co(II)	2.0	1.7	1.6	0.6	12
Mn(II)	4.9	1.7	–	–	–

3.3. M–hydrazine–NTA system

This system was studied at pH 9.0 with a specific purpose. It was observed from the mobility curves for M–hydrazine and M–NTA binary systems that binary complexes are formed

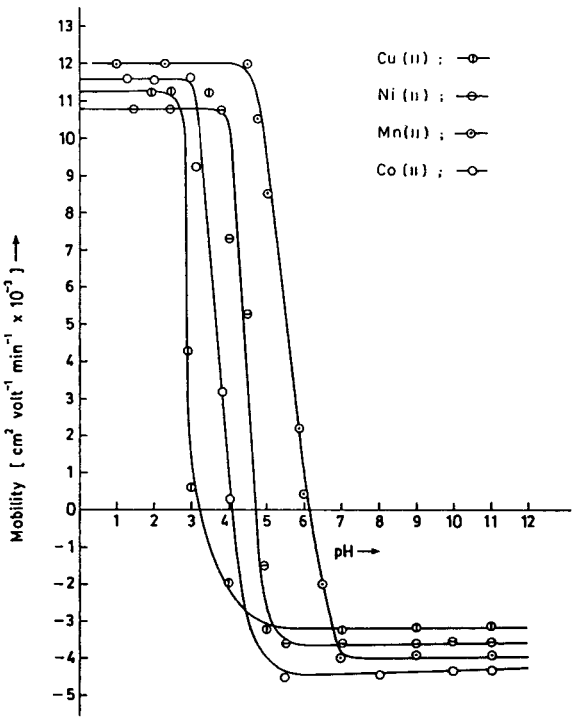

Fig. 2. Plots of mobility *versus* pH for the metal–NTA system.

Table 2
Stability constants of M–NTA complexes at 35°C and ionic strength = 0.1

Metal ion	Log K_{M-NTA}	
	Calculated values	Literature values [15]
Cu(II)	11.5	13.0
Ni(II)	11.4	11.5
Co(II)	10.5	10.4
Mn(II)	8.9	7.5

up to 9.0 pH. Fig. 3 illustrates the transformation of ML_2 into the M–L–NTA complex on progressive addition of NTA. There are two plateaux. At the first plateau the constant value of the mobility obviously corresponds to the mobility of M–hydrazine complexes, whereas the mobility of second complex corresponds to the mobility of a new complex.

This new complex may be a binary complex of M–NTA, as $ML_2 + NTA \rightleftharpoons M\text{–}NTA + 2L$, where the two ligand, units of the complex have been completely replaced with one NTA. The new complex may also be a mixed complex in accordance with the reaction $M\text{–}L_2 + NTA \rightleftharpoons ML\text{–}NTA + L$.

Obviously the final plateau will correspond to the mobility of M–NTA or M–L–NTA, whichever is formed in the interaction. Both the complexes will carry one negative charge, but as the mixed complex is bulkier than the pure M–NTA complex the latter will have greater mobility in the negative direction than the former. The higher mobility for the binary M–NTA complex confirms the formation of mixed complexes in the interaction. From Fig. 3, the total concentration of NTA at which the overall mobility is the mean of the mobilities of the two plateaux was determined. For this the concentration of $[NTA^{3-}]$ anion at pH 9.0 was calculated and log K is obviously = $1/[L]$. These values of the

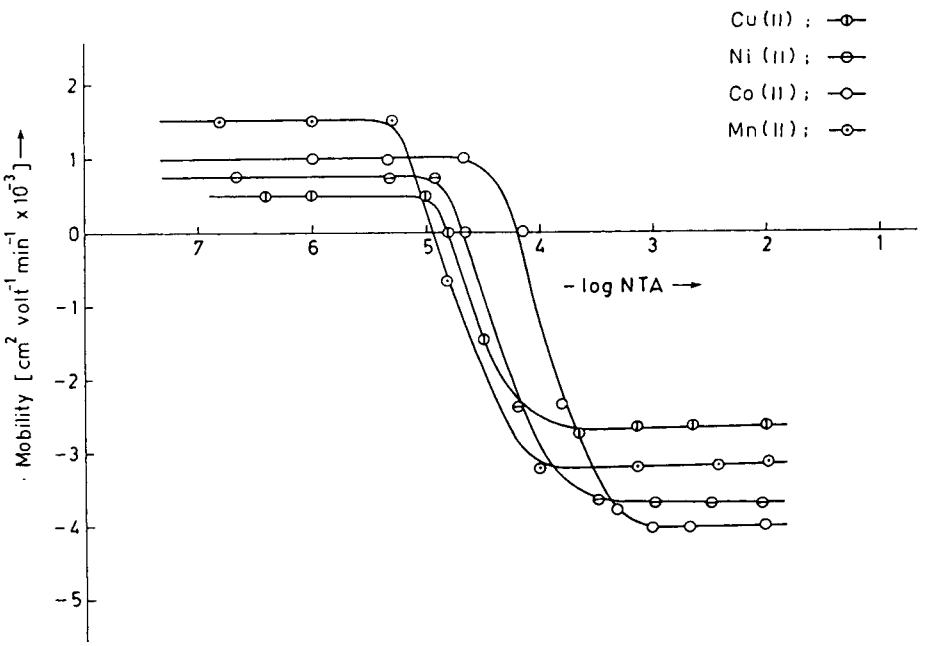

Fig. 3. Plots of mobility *versus* −log [NTA] for the metal–hydrazine system.

Table 3
Stability constants of M–NTA–hydrazine complexes at 35°C and ionic strength = 0.1

Metal ion	Calculated Log K
Cu(II)	4.7
Ni(II)	5.5
Co(II)	4.7
Mn(II)	6.1

stability constants of the mixed-ligand complexes are reported in Table 3.

4. References

[1] V. Jokl, *J. Chromatogr.*, 14 (1964) 71.
[2] J. Biernat, *Rocz. Chem.*, 38 (1964) 343; C.A., 61 (1964) 6456b.
[3] R.K.P. Singh, J.K. Sircar, J.R. Yadav, P.C. Yadav and K.L. Yadava, *Electrochim. Acta*, 26 (1980) 305.
[4] R.K.P. Singh, J.K. Sircar, R. Khelawan and K.L. Yadava, *Chromatographia*, 13 (1980) 709.
[5] R.K.P. Singh, J.R. Yadava, P.C. Yadava and K.L. Yadava, *Z. Phys. Chem. (Leipzig)*, 264 (1983) 464.
[6] M. Czakis Sulikowska, *Zesz. Nauk. Politech. Lodz., Chem.*, 6 (1967) 2038; *C.A.*, 65 (1966) 1746e.
[7] P.C. Yadava, A.K. Ghosh, K.L. Yadava and A.K. Dey, *Chromatographia*, 9 (1976) 410.
[8] J.R. Yadava, J.K. Sircar and K.L. Yadava, *Electrochim. Acta*, 26 (1981) 391.
[9] G.W. Ware, J.B. Sulnik and E.C. Gilbert, *J. Am. Chem. Soc.*, 58 (1936) 1605.
[10] G. Schwarzenbach, *Helv. Chim. Acta*, 19 (1936) 178.
[11] G. Schwarzenbach and A. Zobrist, *Helv. Chim. Acta*, 35 (1952), 1291.
[12] M. Sieprawski, J. Said and R. Cohen-Adad, *J. Chim. Phys.*, 70 (1973) 1417.
[13] M.M. Taquikhan and A.E. Martell, *J. Am. Chem. Soc.*, 89 (1967) 5585.
[14] C.M. Fray and J.E. Stuehr, *J. Am. Chem. Soc.*, 94 (1972) 8898.
[15] A.E. Martell and R.M. Smith, *Critical Stability Constants. Amino Acids*, Vol. 1, Plenum Press, New York, 1974, p. 141.

Author Index

PUBLICATION SCHEDULE FOR THE 1994 SUBSCRIPTION

Journal of Chromatography A and *Journal of Chromatography B: Biomedical Applications*

MONTH	O 1993	N 1993	D 1993	J	F	M	A	
Journal of Chromatography A	652/1 652/2 653/1	653/2 654/1 654/2 655/1	655/2 656/1 + 2 657/1 657/2	658/1 658/2 659/1 659/2	660/1 + 2 661/1 + 2 662/1 662/2	663/1 663/2 664/1	664/2 665/1 665/2 666/1 + 2 667/1 + 2	The publication schedule for further issues will be published later.
Bibliography Section						681/1		
Journal of Chromatography B: Biomedical Applications				652/1	652/2 653/1	653/2 654/1	654/2 655/1	

INFORMATION FOR AUTHORS

(Detailed *Instructions to Authors* were published in *J. Chromatogr. A*, Vol. 657, pp. 463–469. A free reprint can be obtained by application to the publisher, Elsevier Science B.V., P.O. Box 330, 1000 AH Amsterdam, Netherlands.)

Types of Contributions. The following types of papers are published: Regular research papers (full-length papers), Review articles, Short Communications and Discussions. Short Communications are usually descriptions of short investigations, or they can report minor technical improvements of previously published procedures; they reflect the same quality of research as full-length papers, but should preferably not exceed five printed pages. Discussions (one or two pages) should explain, amplify, correct or otherwise comment substantively upon an article recently published in the journal. For Review articles, see inside front cover under Submission of Papers.

Submission. Every paper must be accompanied by a letter from the senior author, stating that he/she is submitting the paper for publication in the *Journal of Chromatography A* or *B*.

Manuscripts. Manuscripts should be typed in **double spacing** on consecutively numbered pages of uniform size. The manuscript should be preceded by a sheet of manuscript paper carrying the title of the paper and the name and full postal address of the person to whom the proofs are to be sent. As a rule, papers should be divided into sections, headed by a caption (*e.g.*, Abstract, Introduction, Experimental, Results, Discussion, etc.). All illustrations, photographs, tables, etc., should be on separate sheets.

Abstract. All articles should have an abstract of 50–100 words which clearly and briefly indicates what is new, different and significant. No references should be given.

Introduction. Every paper must have a concise introduction mentioning what has been done before on the topic described, and stating clearly what is new in the paper now submitted.

Experimental conditions should preferably be given on a *separate* sheet, headed "Conditions". These conditions will, if appropriate, be printed in a block, directly following the heading "Experimental".

Illustrations. The figures should be submitted in a form suitable for reproduction, drawn in Indian ink on drawing or tracing paper. Each illustration should have a caption, all the *captions* being typed (with double spacing) together on a *separate sheet*. If structures are given in the text, the original drawings should be provided. Coloured illustrations are reproduced at the author's expense, the cost being determined by the number of pages and by the number of colours needed. The written permission of the author and publisher must be obtained for the use of any figure already published. Its source must be indicated in the legend.

References. References should be numbered in the order in which they are cited in the text, and listed in numerical sequence on a separate sheet at the end of the article. Please check a recent issue for the layout of the reference list. Abbreviations for the titles of journals should follow the system used by *Chemical Abstracts*. Articles not yet published should be given as "in press" (journal should be specified), "submitted for publication" (journal should be specified), "in preparation" or "personal communication".

Vols. 1–651 of the *Journal of Chromatography*; *Journal of Chromatography, Biomedical Applications* and *Journal of Chromatography, Symposium Volumes* should be cited as *J. Chromatogr.* From Vol. 652 on, *Journal of Chromatography A* (incl. Symposium Volumes) should be cited as *J. Chromatogr. A* and *Journal of Chromatography B: Biomedical Applications* as *J. Chromatogr. B*.

Dispatch. Before sending the manuscript to the Editor please check that the envelope contains four copies of the paper complete with references, captions and figures. One of the sets of figures must be the originals suitable for direct reproduction. Please also ensure that permission to publish has been obtained from your institute.

Proofs. One set of proofs will be sent to the author to be carefully checked for printer's errors. Corrections must be restricted to instances in which the proof is at variance with the manuscript.

Reprints. Fifty reprints will be supplied free of charge. Additional reprints can be ordered by the authors. An order form containing price quotations will be sent to the authors together with the proofs of their article.

Advertisements. The Editors of the journal accept no responsibility for the contents of the advertisements. Advertisement rates are available on request. Advertising orders and enquiries can be sent to the Advertising Manager, Elsevier Science B.V., Advertising Department, P.O. Box 211, 1000 AE Amsterdam, Netherlands; courier shipments to: Van de Sande Bakhuyzenstraat 4, 1061 AG Amsterdam, Netherlands; Tel. (+31-20) 515 3220/515 3222, Telefax (+31-20) 6833 041, Telex 16479 els vi nl. *UK*: T.G. Scott & Son Ltd., Tim Blake, Portland House, 21 Narborough Road, Cosby, Leics. LE9 5TA, UK; Tel. (+44-533) 753 333, Telefax (+44-533) 750 522. *USA and Canada*: Weston Media Associates, Daniel S. Lipner, P.O. Box 1110, Greens Farms, CT 06436-1110, USA; Tel. (+1-203) 261 2500, Telefax (+1-203) 261 0101.

Announcing...

International Ion Chromatography Symposium 1994

19-22 September , 1994
Turin, Italy

Program Chairman:
Corrado Sarzanini
Analytical Chemistry
University of Turin
Via Giuria 5
I - 10125 Turin, Italy
Telephone: +39-11-670-7628
Fax: +39-11-670-7615

Session Topics

- Separation Selectivity and Column Technology
- Developments in Separation Methodology
- Advances in Detection
- Special Sample Treatment Procedures
- Novel Applications
- Process Monitoring and Control
- Separation of Metal Ions
- Pharmaceutical Applications
- Environmental Applications
- Ion analysis in the Electrical Generating Industry
- Standard Methods and Data Processing

For more information, contact:

Century International, Inc.
P.O.Box 493 • 25 Lee Road
Medfield, MA 02052-0493 USA
508/359-8777 • 508/359-8778 (FAX)